Preparation for Implementation of the Mechanistic-Empirical Pavement Design Guide in Michigan Part 2: Evaluation of Rehabilitation Fixes

Final Report

Michigan Department of Transportation
Office of Research Administration
8885 Ricks Road
Lansing MI 48909

By

Neeraj Buch, Karim Chatti, Syed W. Haider,
Gilbert Baladi, Wouter Brink, and Iman Harsini

Report # RC-1594

Michigan State University
Department of Civil and Environmental Engineering
3546 Engineering Building
East Lansing, MI 48824

August 2013

Technical Report Documentation Page

1. Report No. Research Report RC-1594	**2. Government Accession No.**	**3. MDOT Project Manager** Mike Eacker
4. Title and Subtitle Preparation for Implementation of the Mechanistic-Empirical Pavement Design Guide in Michigan Part 2: Evaluation of Rehabilitation Fixes		**5. Report Date** **6. Performing Organization Code**
7. Author(s) Neeraj Buch, Karim Chatti, Syed W. Haider, Gilbert Baladi, Wouter Brink, and Iman Harsini		**8. Performing Org. Report No.**
9. Performing Organization Name and Address Michigan State University Department of Civil and Environmental Engineering 428 S. Shaw Lane, 3546 Engineering Building East Lansing, MI 48824 Tel: (517) 355-5107, Fax: (517) 432-1827		**10. Work Unit No. (TRAIS)** **11. Contract No.** **11(a). Authorization No.**
12. Sponsoring Agency Name and Address Michigan Department of Transportation Office of Research Administration 8885 Ricks Road Lansing MI 48909		**13. Type of Report & Period Covered** Final Report **14. Sponsoring Agency Code**
15. Supplementary Notes		

16. Abstract

The main objectives of Task 2 of the project were to determine the impact of various input variables on the predicted pavement performance for the selected rehabilitation design alternatives in the MEPDG/DARWin-ME, and to verify the pavement performance models for MDOT rehabilitation design practice. In general, for HMA over HMA, the overlay thickness and HMA volumetrics are the most significant inputs for the overlay layer while the existing thickness and pavement condition rating have a significant effect on pavement performance among the inputs related to the existing pavement. For composite pavements, overlay thickness and HMA air voids are significant inputs for the overlay layer. In addition, among the inputs related to the existing intact PCC pavement, the existing thickness and PCC layer modulus have a significant effect on pavement performance. For rubblized pavements, the HMA air voids and effective binder content are the most significant inputs for the overlay layer. Furthermore, for longitudinal cracking and IRI, existing PCC thickness is more important as compared to the existing PCC layer modulus. However, existing PCC layer modulus is more significant for alligator cracking and rutting. For unbonded overlays, all overlay related inputs significantly impact the cracking performance while the PCC elastic modulus is the most important among inputs related to existing layers. The interaction between overlay air voids and existing pavement thickness significantly impacts all performance measures among HMA rehabilitation options. The interaction between overlay thickness and existing PCC layer modulus is the most significant effect on unbonded overlay performance. It should be noted that all analyses were conducted using the inputs ranges reflecting Michigan practices. The verification of the performance prediction models based on the selected projects for different rehabilitation options show the need for local calibration.

17. Key Words MEPDG, DARWin-ME, Rehabilitation fixes, Sensitivity analysis, Verification, and Calibration		**18. Distribution Statement** No restrictions. This document is available to the public through the Michigan Department of Transportation.	
19. Security Classification - report Unclassified	**20. Security Classification - page** Unclassified	**21. No. of Pages**	**22. Price**

TABLE OF CONTENTS

CHAPTER 1 - INTRODUCTION....1
1.1 PROBLEM STATEMENT....1
1.2 BACKGROUND AND SIGNIFICANCE OF WORK....1
1.3 RESEARCH OBJECTIVES....2
1.4 BENEFITS TO MDOT....2
1.5 RESEARCH PLAN....2
1.5.1 Task 2-1: Literature Search....2
1.5.2 Task 2-2: Review MDOT's Rehabilitation Fixes and Design Methods....3
1.5.3 Task 2-3: Sensitivity Analysis of Rehabilitation Options....4
1.5.4 Task 2-4: Project Selection....7
1.5.5 Task 2-5: Verification of Rehabilitation Performance Models....8
1.5.6 Task 2-6: Deliverables....8
1.6 OUTLINE OF REPORT....8

CHAPTER 2 - LITERATURE REVIEW....9
2.1 INTRODUCTION....9
2.2 SUMMARY OF PREVIOUS SENSITIVITY STUDIES....10
2.2.1 MDOT Sensitivity Study....10
2.2.2 NCHRP 1-47 Study....11
2.2.3 Traffic Inputs in Michigan....15
2.2.4 Unbound Material Inputs in Michigan....16
2.3 OVERVIEW OF DIFFERENCES BETWEEN NEW AND REHABILITATION DESIGN....17
2.3.1 Rehabilitation Options in MEPDG/DARWin-ME....17

CHAPTER 3 - CHARACTERIZING THE EXISTING PAVEMENT LAYERS....29
3.1 INTRODUCTION....29
3.2 EXISTING PCC ELASTIC MODULUS LIMITATIONS....29
3.3 DESIGN SUBGRADE MODULUS....30
3.4 EQUIVALENT THICKNESS CONCEPT....31
3.5 UNBONDED OVERLAY THICKNESS LIMITATIONS....33
3.6 LAYER STRUCTURE IN COMPOSITE PAVEMENTS....34
3.7 USE OF FWD IN THE MEPDG/DARWIN-ME....34
3.7.1 Flexible Pavements....34
3.7.2 Rigid Pavements....35
3.7.3 Composite Pavements....36
3.7.4 Summary of FWD Data Usage in the MEPDG/DARWin-ME....36
3.8 LABORATORY VERSUS BACKCALCULATED MODULI....38
3.9 SELECTION OF APPROPRIATE FREQUENCY FOR BACKCALCULATED MODULUS....39
3.10 FWD TESTING GUIDELINES....39

CHAPTER 4 - REHABLITATION SENSITIVITY ANALYSES 41
4.1 INTRODUCTION....41
4.2 PRELIMINARY SENSITIVITY ANALYSIS 42
4.2.1 HMA over HMA Analysis and Results 42
4.2.2 Composite (HMA over JPCP) Analysis and Results....45
4.2.3 Rubblized (HMA over Fractured PCC) Pavement Analysis and Results....47
4.2.4 Unbonded PCC overlay Analysis and Results....48
4.2.5 CRCP over HMA....50
4.2.6 CRCP over JPCP....52
4.2.7 CRCP over CRCP....54
4.2.8 Summary of Results....55
4.3 DETAILED SENSITIVITY ANALYSIS....57
4.3.1 HMA over HMA Analysis and Results 57
4.3.2 Composite (HMA over JPCP) Pavement Analysis and Results 64
4.3.3 Rubblized (HMA over Fractured PCC) Pavement Analysis and Results....67
4.3.4 Unbonded PCC Overlay Analysis and Results....68
4.3.5 Summary Results 72
4.4 GLOBAL SENSITIVITY ANALYSIS....73
4.4.1 GSA Methodology....73
4.4.2 Global Sensitivity Analysis Results....86
4.5 SATELLITE STUDIES 107
4.5.1 Effect of different HMA Gradations on Predicted Pavement Performance 107
4.5.2 Impact of Binder G* Variations on Predicted Pavement Performance 110
4.5.3 Impact of Unbound Layer Gradations on Predicted Performance....111

CHAPTER 5 - VERIFICATION OF REHABILITATION DESIGN.... 114
5.1 INTRODUCTION.... 114
5.2 PROJECT IDENTIFICATION & SELECTION 114
5.2.1 Project Selection Criteria and Design Matrix 115
5.2.2 Project Information by Rehabilitation Option 116
5.3 PROJECT FIELD PERFORMANCE 124
5.3.1 Selected Distresses and Conversion.... 124
5.3.2 Measured Field Performance 127
5.4 PROJECT INPUTS FOR VERIFICATION 133
5.4.1 Unbonded Overlays 133
5.4.2 Rubblized Overlays.... 135
5.4.3 Composite Overlays.... 136
5.4.4 HMA over HMA.... 136
5.5 VERIFICATION RESULTS.... 142
5.5.1 Unbonded Overlays 142
5.5.2 Rubblized Overlays.... 143
5.5.3 Composite Overlays.... 146
5.5.4 HMA over HMA.... 147
5.6 SUMMARY 150

CHAPTER 6 - CONCLUSIONS AND RECOMMENDATIONS....151
6.1 SUMMARY 151
6.2 CONCLUSIONS....152

6.2.1 The MEPDG/DARWin-ME Software Issues 152
6.2.2 Sensitivity Analyses.....152
6.2.3 Verification of the Rehabilitation Performance Models.....158
6.3 RECOMMENDATIONS 158
6.4 IMPLEMENTATION 159

REFERENCES 161

Appendix A Preliminary and Detailed Sensitivity Analysis Results
Appendix B Global Sensitivity Analysis Results
Appendix C Verification
Appendix D MDOT PMS Distress Manual

LIST OF TABLES

Table 2-1 Impact of input variables on rigid pavement performance....11
Table 2-2 Impact of input variables on flexible pavement performance....11
Table 2-3 Ranking of new HMA design inputs by maximum NSI values (9)....12
Table 2-4 Ranking of HMA/stiff foundation design inputs by maximum NSI values (9)....13
Table 2-5 Ranking of new JPCP design inputs by maximum NSI values (9)....13
Table 2-6 Ranking of JPCP/stiff foundation design inputs by maximum NSI values (9)....14
Table 2-7 Ranking of New CRCP design inputs by maximum NSI values (9)....14
Table 2-8 Conclusions and recommendations for traffic input levels....16
Table 2-9 Average roadbed soil MR values (7)....16
Table 2-10 Structural condition of rigid pavements (11)....20
Table 2-11 Rigid pavement rehabilitation hierarchical levels for the elastic modulus of the existing pavement....21
Table 2-12 Summary of distress computation locations for flexible overlay designs (11)....25
Table 2-13 Summary of distress computation locations for existing pavement in HMA overlay of flexible and stabilized pavements....25
Table 2-14 Summary of distress computation location for existing pavement in HMA overlay of fractured slabs....25
Table 2-15 Summary of distress computation locations for existing pavement in HMA overlay of intact PCC pavements....26
Table 2-16 Damage based on pavement condition rating (11)....28
Table 2-17 Description of existing pavement condition rating (13)....28
Table 3-1 Comparison between the subgrade modulus input value and the value used internally....31
Table 3-2 Use of deflection data in the MEPDG/DARWin-ME (5)....37
Table 3-4 Recommended FWD testing guidelines (5)....40
Table 4-1 MDOT Rehabilitation options....41
Table 4-2 Design inputs for HMA over HMA....43
Table 4-3 HMA over HMA base case....43
Table 4-4 Summary of NSI values for each design input for HMA overlay....44
Table 4-5 Input variable values for composite pavements....45
Table 4-6 Composite pavement base case....46
Table 4-7 Summary of NSI values for each design input for composite pavement....46
Table 4-8 Input variable values for rubblized pavement....47
Table 4-9 Base case values for rubblized pavement analysis....47
Table 4-10 Summary of NSI values for each design input for rubblized pavements....47
Table 4-11 List of input variables for unbonded overlay option....49
Table 4-12 Base case values for unbonded overlay....49
Table 4-13 Summary of NSI values for each design input for unbonded overlay....50
Table 4-14 Input variable values for CRCP over HMA pavement....51
Table 4-15 Base case values for CRCP over HMA pavement analysis....51
Table 4-16 Summary of NSI values for each design input for CRCP over HMA pavements....51
Table 4-17 Base case values for CRCP over JPCP pavement analysis....52
Table 4-18 Input variable values for CRCP over JPCP pavement....53
Table 4-19 Summary of NSI values for each design input for CRCP over JPCP pavements....53
Table 4-20 Input variable values for CRCP over CRCP pavement....54

Table 4-21 Base case values for CRCP over CRCP pavement analysis....54
Table 4-22 Summary of NSI values for each design input for CRCP over CRCP pavements....55
Table 4-23 List of significant inputs from preliminary sensitivity analysis....56
Table 4-24 Inputs levels for characterizing existing pavement....56
Table 4-25 List and range of design inputs for HMA over HMA....58
Table 4-26 HMA over HMA longitudinal cracking ANOVA Results....59
Table 4-27 Pavement performance criteria after 20 years – flexible pavements....61
Table 4-28 Summary of significant interactions (HMA over HMA) – existing....62
Table 4-29 Summary of significant interactions (HMA over HMA) – within existing and within overlay layers....64
Table 4-30 List and range of design inputs for composite pavement....65
Table 4-31 Summary of significant interactions composite pavement....65
Table 4-32 Summary of significant interactions (Composite) – Within existing and within overlay layers....66
Table 4-33 Input variable ranges for HMA over fractured JPCP....67
Table 4-34 Summary of significant interactions (HMA over fractured JPCP)....68
Table 4-35 Summary of significant interactions (Rubblized) – Within existing and within overlay layers....68
Table 4-36 Input variable ranges for JPCP over JPCP (unbonded overlay)....69
Table 4-37 Pavement performance criteria after 20 years – Rigid pavements....70
Table 4-38 Interaction summary table (unbonded overlay)....71
Table 4-39 Summary of significant interactions (Unbonded overlay) – Within existing and within overlay layers....71
Table 4-40 Base cases for global sensitivity analysis....73
Table 4-41 List of design inputs for HMA over HMA....77
Table 4-42 List of design inputs for composite....77
Table 4-43 List of design inputs for HMA over fractured JPCP (Rubblized)....78
Table 4-44 List of design inputs for JPCP over JPCP (unbonded overlay)....78
Table 4-45 Required number of simulations....80
Table 4-46 Generated samples for HMA over JPCP fractured....80
Table 4-47 Recommended threshold values for performance measures—NCHRP 1-47....84
Table 4-48 Recommended threshold values for performance measures—AASHTO....84
Table 4-49 Distress threshold values used in this study based on discussion with MDOT....84
Table 4-50 The MEPDG inputs ranking for HMA over HMA....103
Table 4-51 The MEPDG inputs ranking for composite pavement....104
Table 4-52 The MEPDG inputs ranking for rubblized PCC pavement....104
Table 4-53 The MEPDG inputs ranking for unbonded PCC overlay....105
Table 4-54 Interaction ranking for HMA over HMA....105
Table 4-55 Interaction ranking for composite pavement....106
Table 4-56 Interaction ranking for rubblized PCC pavement....106
Table 4-57 Interaction ranking for unbonded PCC overlay....106
Table 4-58 Typical flexible pavement cross-section....107
Table 4-59 Volumetric properties of the selected mixtures....108
Table 4-60 Design matrix for sensitivity analysis....112
Table 4-61 Cross-section information....112
Table 5-1 Selection matrix displaying selected projects....115
Table 5-2 Complete project matrix for unbonded overlays....117
Table 5-3 Unbonded overlay cross-section information....117

Table 5-4 Complete project matrix for rubblized overlays 119
Table 5-5 Rubblized overlay cross-section information 119
Table 5-6 Complete project matrix for composite overlays 121
Table 5-7 Composite overlay cross-section information 121
Table 5-8 Complete project selection matrix for HMA over HMA 123
Table 5-9 HMA over HMA cross-section information 123
Table 5-10 Flexible pavement distresses 124
Table 5-11 Rigid pavement distresses 125
Table 5-12 Unbonded overlay input data 138
Table 5-13 Rubblized overlay input data 139
Table 5-14 Composite overlay input data 140
Table 5-15 HMA overlay input data 141
Table 6-1 List of significant inputs from preliminary sensitivity analysis 153
Table 6-2 List of significant inputs from detailed sensitivity analysis 154
Table 6-3 List of significant inputs — HMA over HMA 155
Table 6-4 List of significant inputs — Composite pavement 155
Table 6-5 List of significant inputs — Rubblized PCC pavement 156
Table 6-6 List of significant inputs — Unbonded PCC overlay 156
Table 6-7 Significant interaction between inputs — HMA over HMA 156
Table 6-8 Significant interaction between inputs — Composite pavement 157
Table 6-9 Significant interaction between inputs — Rubblized pavement 157
Table 6-10 Significant interaction between inputs — Unbonded PCC overlay 157
Table 6-11 Flexible pavement distresses 159
Table 6-12 Rigid pavement distresses 160
Table 6-13 Testing needs for significant input variables for rehabilitation 160

LIST OF FIGURES

Figure 2-1 Typical cross-sections of PCC rehabilitation strategies. (a) Unbonded PCC overlays, (b) Bonded PCC overlays, (c) PCC overlays of HMA pavements (1) 20
Figure 2-2 Rigid rehabilitation design process (11) 22
Figure 2-3 Flexible rehabilitation design process (11) 24
Figure 2-4 Overlay design strategies available for flexible pavement rehabilitation 24
Figure 2-5 Existing HMA layer damaged E* mastercurve computation (*11*) 27
Figure 3-1 Comparison between DARWin-ME and MEPDG for time to failure by varying the elastic modulus of the existing PCC pavement 30
Figure 3-2 Equivalent slab thickness base case structure 32
Figure 3-3 Sensitivity analysis based on modified equivalent slab calculations (a) effect of existing PCC elastic modulus, (b) effect of existing PCC thickness, (c) effect of HMA interlayer elastic modulus, (d) effect of HMA interlayer thickness on equivalent thickness 33
Figure 3-4 Effect of pavement thickness on distress when analyzed until failure 34
Figure 4-1 NSI plots for HMA overlay 44
Figure 4-2 Overlay distresses for HMA over HMA based on different levels of existing pavement condition rating at 20th year 45
Figure 4-3 NSI plots for composite pavements 46
Figure 4-4 NSI plots for rubblized 48
Figure 4-5 Typical unbonded overlay cross section (*5*) 48
Figure 4-6 NSI plots for unbonded overlay 50
Figure 4-7 NSI plots for CRCP over HMA 52
Figure 4-8 NSI plots for CRCP over JPCP 53
Figure 4-9 NSI plots for CRCP over CRCP 55
Figure 4-10 Interaction plots (a) overlay thickness and existing condition rating, (b) overlay PG and existing HMA thickness 60
Figure 4-11 Pavement performance criteria for fatigue cracking (*6*) 60
Figure 4-12 Pavement performance criteria for rutting (*6*) 60
Figure 4-13 Performance criteria for IRI (*6*) 61
Figure 4-14 Interpretation of interactions for rutting 63
Figure 4-15 Adopted performance criteria for JPCP (*7*) 70
Figure 4-16 Summary of climatic properties by location within Michigan (*1*) 74
Figure 4-17 Comparison between levels 1 and 3 rehabilitation for longitudinal cracking 76
Figure 4-18 Comparison between levels 1 and 3 rehabilitation for fatigue cracking 76
Figure 4-19 Comparison between Monte Carlo and LHS simulations 79
Figure 4-20 Example of sampling in LHS method 80
Figure 4-21 Effect of different threshold values on NSI calculation 85
Figure 4-22 Network diagram (*11*) 86
Figure 4-23 Relative importance of design inputs for HMA over HMA 88
Figure 4-24 Sensitivity of alligator cracking to HMA overlay air voids 89
Figure 4-25 Summary of NSI curves for HMA over HMA 91
Figure 4-26 Interaction between HMA overlay thickness and existing thickness 92
Figure 4-27 Interaction between HMA overlay effective binder and existing thickness 92
Figure 4-28 Interaction between HMA overlay air voids and existing thickness 93
Figure 4-29 Relative importance of design inputs for composite pavement 95

Figure 4-30 Summary of NSI curves for composite pavement 96
Figure 4-31 Relative importance of design inputs for rubblized PCC pavement 98
Figure 4-32 Summary of NSI curves for rubblized PCC pavement 99
Figure 4-33 Relative importance of design inputs for unbonded PCC overlay 101
Figure 4-34 Summary of NSI curves for unbonded PCC overlay 102
Figure 4-35 Alligator cracking predictions 108
Figure 4-36 Rutting predictions 109
Figure 4-37 IRI predictions 109
Figure 4-38 The G* master curves for two binders with same PG 110
Figure 4-39 The effect of G* variation on predicted HMA over HMA pavement performance .111
Figure 4-40 Coarse, fine and default gradations 112
Figure 4-41 Impact of aggregate gradation on rigid pavement performance 113
Figure 4-42 Impact of aggregate gradation on HMA over HMA pavement performance 113
Figure 5-1 Geographic location of the eight unbonded overlay projects 116
Figure 5-2 Geographic location of the eleven rubblized overlay projects 118
Figure 5-3 Geographical location of the seven composite overlay projects 120
Figure 5-4 Geographical location of 14 HMA over HMA projects 122
Figure 5-5 Current pavement distress and condition of unbonded overlay projects 127
Figure 5-6 Performance of unbonded overlay project 37997 128
Figure 5-7 Current pavement distress and condition for rubblized overlays 129
Figure 5-8 Performance of rubblized overlay project 28115 130
Figure 5-9 Current pavement distress and condition of composite overlay projects 131
Figure 5-10 Performance of composite overlay project 29586. 131
Figure 5-11 Current pavement distress and conditions of the selected of HMA over HMA projects 132
Figure 5-12 Performance of HMA over HMA project 28155. 133
Figure 5-13 Example of time-series verification results for an unbonded overlay project based on different distresses 142
Figure 5-14 Predicted vs. measured results for all unbonded overlay projects. 143
Figure 5-15 Example of time-series verification results for an rubblized overlay project based on different distresses 144
Figure 5-16 Predicted vs. measured results for rubblized overlay projects using backcalculated subgrade MR 145
Figure 5-17 Predicted vs. measured results for rubblized overlay projects using design MR 145
Figure 5-18 Example of time-series verification results for a composite overlay project based on different distresses 146
Figure 5-19 Predicted vs. measured results for all composite overlay projects 147
Figure 5-20 Example of time-series verification results for a HMA over HMA project 148
Figure 5-21 Predicted vs. Measured performance for HMA over HMA with poor existing condition. 148
Figure 22 Predicted vs. Measured performance for HMA over HMA with fair existing condition. 149
Figure 23 Predicted vs. Measured performance for HMA over HMA with good existing condition. 149

EXECUTIVE SUMMARY

The main objectives of Task 2 of the project were to determine the impact of various input variables on the predicted pavement performance for the selected rehabilitation design alternatives in the MEPDG/DARWin-ME, and to validate the pavement performance models for MDOT rehabilitation design practice. Therefore, the significant inputs related to material characterization, existing pavement condition, and structural design for the selected rehabilitation options were identified. Subsequently, the accuracy of the rehabilitation performance models was evaluated by comparing measured and predicted performance.

In general, for HMA overlays, the overlay thickness and HMA volumetrics are the most significant inputs for the overlay layer while the existing thickness and pavement condition rating have a significant effect on pavement performance among the inputs related to the existing pavement. For composite pavements, overlay thickness and HMA air voids are significant inputs for the overlay layer. In addition, among the inputs related to the existing intact PCC pavement, the existing thickness and PCC layer modulus have a significant effect on pavement performance. For rubblized pavements, the HMA air voids and effective binder content are the most significant inputs for the overlay layer. Furthermore, for longitudinal cracking and IRI, existing PCC thickness is more important as compared to the existing PCC layer modulus. However, existing PCC layer modulus is more significant for alligator cracking and rutting. For unbonded overlays, all overlay related inputs significantly impact the cracking performance while the PCC elastic modulus is the most important among inputs related to existing layers. The interaction between overlay air voids and existing pavement thickness significantly impacts all performance measures among HMA rehabilitation options. The interaction between overlay thickness and existing PCC layer modulus is the most significant effect on unbonded overlay performance. It should be noted that all analyses were conducted using the inputs ranges reflecting Michigan practices.

The verification of the performance prediction models based on the selected projects for different rehabilitation options show the need for local calibration. All of the identified projects used for verification will be utilized in Task 3 for local calibration. Based on the results of the analyses, various conclusions and recommendations were made and are presented in the next sections.

CHAPTER 1 - INTRODUCTION

1.1 PROBLEM STATEMENT

There are apprehensions on the part of State Highway Agencies (SHAs) towards the adoption of the MEPDG/DARWin-ME because of (i) the complex nature of the design software (numerous inputs and their hierarchical nature); (ii) perceived needs to collect more laboratory and/or field data; (iii) necessity to retool the PMS for making it compatible with the outputs of the design guide and the required inputs for the guide; (iv) the need for the calibration of the performance equations to local conditions; (v) the need to employ or train pavement professionals at the regional level; and (vi) shrinking manpower and funds. The successful completion of this project will go a long way in reducing some of the uncertainties associated with the implementation of the MEPDG/DARWin-ME. Guidance with respect to practical ranges of significant inputs for flexible and rigid pavement designs, calibration coefficients for the transfer functions reflecting local conditions and hot mix asphalt (HMA) mixture characteristics |E*| will demonstrate to Michigan Department of Transportation (MDOT) pavement engineers the viability of implementing the MEPDG/DARWin-ME in the near future. An extensive test (for rehabilitation designs) of the software will add evidence on the viability and accuracy of the software. Identifying the list of input variables for rehabilitation designs that significantly impact pavement performance would assist MDOT in determining the types of new data elements needed. The technology transfer packages to be developed in this timely and significant project will serve as invaluable training tools that would enhance the capability of MDOT.

The research study has three distinct tasks: (1) characterization of asphalt mixtures for the MEPDG/DARWin-ME in Michigan, (2) evaluation of the MEPDG/DARWin-ME for pavement rehabilitation design in Michigan, and (3) calibration and validation of the MEPDG/DARWin-ME performance models for Michigan conditions. Therefore, the study was divided into three separate tasks. The HMA mixtures in Michigan were characterized in Task 1 and the final report was submitted to MDOT in December 2012. This report contains the details for Task 2 of the study. In Task 3, the calibration and validation of performance models will be executed and a separate report will be submitted at the end of the project.

1.2 BACKGROUND AND SIGNIFICANCE OF WORK

The MEPDG/DARWin-ME is becoming the state-of-the-practice for flexible and rigid pavement designs in some states. While several design inputs are identical for both new and rehabilitation design processes, there are variations in how some inputs are selected for use in rehabilitation design. The material properties to characterize existing pavement play a vital role in the MEPDG/DARWin-ME rehabilitation analysis and design process. In this study, material characterization needs for pavement rehabilitation are addressed and the results are used in evaluating the rehabilitation analysis and design process of the MEPDG/DARWin-ME. By adopting the MEPDG/DARWin-ME, MDOT can achieve the most cost-effective and sound rehabilitation strategies for repairing flexible and rigid pavements.
MDOT has already laid the foundation for the adoption of the MEPDG/DARWin-ME by supporting several studies in the last five years. The key deliverables of these studies

included: (a) critical/sensitive inputs for the design of new flexible and jointed plain concrete pavements, (b) Levels 2 and 3 traffic inputs for the design of new and rehabilitated flexible and rigid pavements, (c) Catalog of level 2 inputs for coefficient of thermal expansion (CTE) of typical paving concrete mixtures, and (d) Ranges for levels 2 and 3 resilient moduli for subgrade and unbound materials. It should be noted that results from all these previous studies were utilized in Task 2 of this study wherever applicable.

1.3 RESEARCH OBJECTIVES

The objectives of the research in Task 2 were to: (a) determine the sensitivity of various input variables to the predicted performance for each of the rehabilitation design alternatives in the MEPDG/DARWin-ME, and (b) validate the current globally calibrated performance models for different rehabilitation types in Michigan

1.4 BENEFITS TO MDOT

The outcomes of research conducted in Task 2 of the study will have several short-term and long-term benefits in implementing the MEPDG/DARWin-ME in Michigan. The short-term benefits include:

- Recommendations on the application of the MEPDG/DARWin-ME for Michigan specific rehabilitation fixes.
- A list of the most important inputs and typical values needed for using the MEPDG/DARWin-ME rehabilitation design of both flexible and rigid pavements.
- Ranking of the important inputs based on their level of impact on the predicted performance.
- Recommendations for falling weight deflectometer (FWD) procedures and practices in support of the MEPDG/DARWin-ME implementation.

The long-term benefits will emerge by knowing the following:

- A set of recommendations for the type of data needed in MDOT Pavement Management System (PMS) to support use of the MEPDG/DARWin-ME in the future. The recommendations will be made at the conclusion of Task 3 of the study.
- A set of recommendations regarding a comprehensive and systematic database that houses project construction data (materials, layer properties and thicknesses, costs), design information and PMS pavement condition data. The recommendations will be made at the conclusion of the Task 3 of the study.

1.5 RESEARCH PLAN

Task 2 of the study was accomplished through six subtasks described below:

1.5.1 Task 2-1: Literature Search

Over the last five years, the pavement group at MSU has been working with MDOT to explore the various attributes of the MEPDG/DARWin-ME and to assist with its

implementation process. As a result of this effort the following final reports have been published:

- Quantifying Coefficient of Thermal Expansion Values of Typical Hydraulic Cement Concrete Paving Mixtures (*1*). The principal investigator (PI) for this project was Dr. Neeraj Buch
- Evaluation of the 1-37A Design Process for New and Rehabilitated JPCP and HMA Pavements (*2*). The PIs for this project were Drs. Buch, Chatti and Haider
- Characterization of Traffic for the New M-E Pavement Design Guide in Michigan (*3*). The PIs for this project were Drs. Buch, Chatti and Haider
- Pavement Subgrade MR Design Values for Michigan's Seasonal Changes (4): the PI for this project was Dr. Baladi
- Backcalculation of Layer Moduli of Unbound Granular Layers for both Rigid and Flexible Pavements (5). The PI for this project was Dr. Baladi.

In addition to this work, the team has conducted a 1-1/2 day technology transfer workshop designed for MDOT pavement professionals highlighting the salient features of the MEPDG software. The results from these projects have also been highlighted in MDOT's Research Administration newsletters. As a result of these efforts the research team is very familiar with the MEPDG.

The project team also reviewed national literature to benchmark the efforts made by other state DOTs in this area. The sources for collecting such information include (i) National Cooperative Highway Research Program (NCHRP) and Federal Highway Administration (FHWA) reports and research circulars; (ii) papers published in the journal of the Transportation Research Record; and (iii) project reports published by the various state DOTs on the subject.

1.5.2 Task 2-2: Review MDOT's Rehabilitation Fixes and Design Methods

The commonly used rehabilitation fixes in Michigan that can be designed using the MEPDG/DARWin-ME software include (i) HMA overlay placed on top of rubblized portland cement concrete (PCC) pavements; (ii) HMA overlays constructed over HMA and PCC pavements; (iii) Crush and shape (pulverize the existing HMA followed by new HMA surfacing) (iv) Unbonded concrete overlays and (v) PCC overlay constructed over HMA pavements. It should be noted that only a few PCC overlays over HMA experimental projects have been constructed in Michigan. *Currently MDOT does not use bonded concrete overlays, continuously reinforced concrete pavement (CRCP), and crack and seat techniques to rehabilitate the pavement network; therefore these fixes were not considered in the analyses for Tasks 2 and 3.*

At the initiation of this part, the project team met with the MDOT research advisory panel (RAP) to better understand the pavement rehabilitation design practices. The applicability and usefulness of the MEPDG/DARWin-ME process for rehabilitation designs hinges on what type of design and construction information are (or can be) collected by MDOT and on the availability and compatibility of performance (distress and roughness)

data in the MDOT PMS database and other sources such as the long-term pavement performance (LTPP) database.

An important part of the evaluation process is the use of non-destructive testing (NDT) to characterize existing pavements to establish Level 1 inputs. Two important tests should be included in this process: The ground penetrating radar (GPR) test to determine layer thicknesses and the FWD test to characterize in-situ layer moduli. The GPR testing has been effectively used in conjunction with FWD testing in rehabilitation projects by several DOT's (for example Texas). FWD usage is imperative for cost effective mechanistic rehabilitation design. MDOT has been using the FWD test on a selective basis depending on the region. A more systematic use of FWD testing is envisioned if/when the MEPDG/DARWin-ME is adopted by MDOT for rehabilitation design. The MEPDG/DARWin-ME requires FWD testing only for level 1 analysis. The MEPDG recommends ratios of lab to field moduli based on LTPP data. However, these were obtained from fairly weak statistical correlations, and depend on the existing pavement cross-section. Dr. Baladi has looked at this issue as part of two MDOT projects on estimating resilient moduli for subgrade and base/subbase unbound materials. In these studies both back-calculated in-situ and laboratory MRs are reported. Drs. Chatti and Kutay have also been working on relating FWD derived to laboratory measured HMA moduli as part of a FHWA funded project FHWA DTFH61-08-R-00032 "Relationships Between Laboratory-Measured and Field-Derived Properties of Pavement Layers". The issue there is that MEPDG requires the E^* curve for each HMA layer as an input, while standard back-calculation only gives one "effective" modulus. To circumvent this problem, the MEPDG/DARWin-ME rehabilitation design procedure calls for using the back-calculated modulus to calculate a damage index, which is then used to shift the undamaged E^* curve (using volumetric information obtained from cores) to get a damaged E^* curve. Also related to this, Dr Chatti was involved in the FHWA project DTFH61-06-C-00046 "Using FWD data with M-E Design and Analysis", which reviewed various pavement deflection testing procedures and commonly used deflection analysis approaches and back-calculation programs for flexible, rigid, and composite pavement structures. The relevance of the different procedures and approaches to the current MEPDG/DARWin-ME were explored in this study.

1.5.3 Task 2-3: Sensitivity Analysis of Rehabilitation Options

For rigid pavements the MEPDG/DARWin-ME considers the design of the following rehabilitation fixes: (1) concrete pavement restoration (CPR) for jointed concrete pavements, (2) unbonded jointed plain concrete pavement (JPCP) or CRCP overlays over existing rigid or composite pavements, (3) bonded JPCP or CRCP overlays over existing JPCP or CRCP pavements, and (4) conventional JPCP or CRCP on existing flexible. For flexible pavements, the rehabilitation fixes include: (1) HMA overlay of existing HMA surfaced pavements, both flexible and semi-rigid, (2) HMA overlay of existing PCC pavement that has received fractured slab treatments; crack and seat, break and seat, and rubblization, and (3) HMA overlay of existing intact PCC pavement (JPCP and CRCP), including composite pavements or second overlays of original PCC pavements. Given that Michigan does not support CRCP, only preliminary sensitivity analysis was performed for CRCP in this study. Also, fractured slab treatments was limited to rubblization of JPCP and jointed reinforced concrete pavement (JRCP), since MDOT practice does not allow for crack and seat and break and seat techniques. The input parameters considered for the design of the various rehabilitation

strategies are summarized below**.** A significant number of these inputs are independent of the type of design, i.e. new versus rehabilitation. The input parameters that are unique to the rehabilitation design process are *italicized* for easy identification.

A. General and Project Information: Project identities, construction dates of the existing pavement and the new overlay, restoration date, traffic opening date, and type of rehabilitation strategy
B. Analysis Parameters: Initial smoothness, IRI (post rehabilitation), and performance criteria (IRI, cracking and faulting)
C. Climate Data: Weather station close to the selected project or interpolation of multiple weather stations if a weather station is not available at the project site
D. Traffic: ADTT, percent trucks, vehicle speed, traffic volume and axle adjustment factors, wheel location, traffic wander and others
E. Drainage and Surface Properties: Pavement cross-slope and length of drainage path, and surface absorptivity
F. Layer Definition and Material Properties: Number of layers, description and material type, pavement cross-section details, PCC mechanical and thermal properties, HMA material properties, traffic opening date, and type of rehabilitation strategy
G. Design Features: Transverse and longitudinal joint design parameters, reinforcing details (CRC pavements only), load transfer efficiency (LTE) details and edge support type, and traffic opening date
H. Rehabilitation: Existing distress (CPR), percent of slabs with repairs after restoration (CPR), and foundation support

Differences between the analyses of new pavements and pavement rehabilitation strategies are due to two possible sources: (1) performance prediction models, and (2) inputs to characterize the existing pavement structure and materials. For flexible overlays, all the performance prediction models are the same as those for new flexible pavement analysis and design. Only the roughness model changes when an HMA overlay is placed over existing PCC pavement. Also, an additional reflective cracking model is added for rehabilitation design. For rigid pavement restoration and unbonded overlays, only the faulting model coefficients are different than that used for new rigid pavements. Additional inputs that need to be considered in the sensitivity analysis are as follows:

- For flexible overlays, rehabilitation levels need to be considered. For level 1, back-calculation of layer moduli from FWD testing is required; measured rutting in the existing pavement layers are needed along with the thickness of existing HMA layer to be milled. For level 2, only estimates of layer moduli are needed (based on correlations); estimated rutting in the existing layers and cracking in the existing HMA layers along with HMA milling thickness are required. For level 3, pavement rating (excellent to very poor) to represent pavement condition and total surface rutting are needed. All other material-related inputs are similar to those of a new flexible pavement.
- For HMA overlays of existing JPCP, the information of percent slabs with transverse cracking before and after restoration of existing JPCP and dynamic modulus of subgrade reaction (back-calculated using FWD data, or internally calculated based on MR) are required.

- For HMA overlays of fractured concrete, the resilient modulus of the fractured concrete and type of fracture (crack/seat or rubblization) are needed.
- For JPCP restoration, the information of percent slabs with transverse cracking before and after restoration and dynamic modulus of subgrade reaction are required.
- For PCC overlays of JPCP/CRCP, the resilient modulus, the existing thickness, the thermal properties of the existing concrete layer, type of fracture (crack/seat or rubblization) and dynamic modulus of subgrade reaction are required. In addition, the properties of the bond-breaker asphalt layer are required which are similar to the HMA properties mentioned above in the flexible pavement section.

The multi-step process presented below will be utilized to identify the most critical/sensitive input parameters for use in the MEPDG/DARWin-ME for pavement rehabilitation designs.

FIRST STEP - Determination of the mathematical viability and "reasonableness" of the performance models for rehabilitated HMA and JPC pavements. To conduct the "reasonableness" analyses of the performance models, it is essential to determine practical ranges of the input variables listed above. The primary sources for the magnitudes of input parameters (material characteristics and pavement structure) are, but not limited to, (i) typical design inputs used by MDOT for flexible and rigid rehabilitation designs; (ii) General Pavement Studies (GPS) and Specific Pavement Studies (SPS) in the LTPP database, these pavement sections are located in various climatic regions in the US and (iii) default input variable ranges recommended in the MEPDG/DARWin-ME software for inputs where data are not available from the LTPP or MDOT. To evaluate the significance of input variables from both a practical and statistical point of view, there is a need to assess their effect rationally based on some performance criteria which are more acceptable by the pavement community. Therefore, to determine the consequence of various levels of each input variable, rather than using subjective criteria based on the visual inspection of the performance curves, a more coherent criterion was adopted in this study. It is proposed that two different approaches be investigated to determine the significant effects:

- Performance threshold, and
- Age threshold

For performance threshold, acceptable failure criteria at national/local (MDOT) levels can be considered for various performance measures. Performance(s) threshold may be used to determine ages, at which the performance threshold is exceeded, for each input level for the same variable. From these ages significance (statistical and practical) will be determined. For example, if the difference in ages is more than 5 years, one can consider this variable has a practically significant effect. On the other hand if the difference is less than 5 years, one can assume practically insignificant effect. For the age threshold, the performance for each input level of a variable can be determined based on distress magnitude at a pre-specified age. The difference in performances at a particular age (10, 15 or 20 years) can be compared to the national common characteristics of good and poorly performing pavements. The acceptable thresholds were determined after discussion with the RAP.

SECOND STEP - Cataloging the various performance parameters associated with the flexible and rigid rehabilitation designs based on the MEPDG/DARWin-ME "runs." A

preliminary assessment of the input sensitivity will be made based on visual trend, engineering judgment, and performance thresholds identified in step 1.

THIRD STEP - Designing the full-cell factorial matrix consisting of the sensitive input variables identified in the second step. The performance magnitudes based on performance thresholds or age thresholds will be cataloged and subjected to an analysis of variance (ANOVA). This analysis will assist in highlighting the significant main effects and possible two-way interactions. At the end of this three step process, the research team will be able to identify input variables that have a significant impact on the performance of flexible and rigid pavement rehabilitation designs and recommend appropriate ranges of these input variables. The results of this process will assist MDOT in customizing the use of the software by focusing on the most important input variables and their levels.

1.5.4 Task 2-4: Project Selection

Information was collected to select pavement sections (rehabilitation design) to compare measured and predicted performance histories. The measured performance data was obtained from MDOT PMS. The collected data included the following:

A. Rehabilitation type: unbonded concrete overlay, HMA over existing HMA, existing PCC or rubblized PCC. Maintenance type and history over the performance life of the overlay
B. Site factors: The site factors will address the various regions in the state, climatic zones and subgrade soil types.
C. Traffic: The various levels of traffic will assist in distinguishing between Michigan routes, US routes and Interstate routes.
D. Overlay thicknesses: The range of constructed overlay thicknesses.
E. Open to traffic date: This information determines the performance period.
F. As built cross-section details (existing and overlay structure)
G. Pre-overlay repairs performed on the existing pavement (such as partial and/or full depth repairs, dowel bar retrofit)
H. Material properties of both the existing and new structure

Based on this list, the project team populated (in consultation with the RAP) a test matrix which was used in Task 2-5. The research team selected projects that have been subjected to FWD tests in prior years and for which inventory and laboratory test data were available. The pool of projects in the test matrix corresponded to the two recent MDOT projects “Pavement Subgrade MR Design Values for Michigan’s Seasonal Changes” and “Back-calculation of Resilient Modulus Values for Unbound Pavement Materials”. This database included over 4000 and 2500 FWD tests for rigid and flexible pavement projects, respectively. The data fields included regions, county, control section and beginning mile post, location, pavement type and cross-section. However, no fix type information is available. Additional projects were identified in order to include rehabilitation strategies that may not be covered in the above mentioned projects.

1.5.5 Task 2-5: Verification of Rehabilitation Performance Models

Based on the inputs identified as a result of Task 2.3 and projects selected in Task 2.4, MEPDG/DARWin-ME runs will be executed. The predicted results will be compared with the field performance of the projects. It is recommended that 5 projects per rehabilitation strategy be used for the comparative analysis. For the selected projects the data needs will include (i) inventory (as constructed wherever possible or at the bid stage); (ii) falling weight deflectometer data for establishing layer moduli; (iii) traffic; and (iv) pavement condition. Each project will constitute a case study where MEPDG will be run at the different input levels (1, 2 and 3).

The comparison will be done with the understanding that differences can be attributed to the performance models in the MEPDG/DARWin-ME (these will be the subject of verification/calibration in Part 3 of the study) or the input values for the various variables used in the MEPDG/DARWin-ME analysis (these will be investigated as part of tasks 2-2 and 2-3). Recommendations will be made on rehabilitation design inputs, including back-calculation results, and their effects on predicted MEPDG performance curves.

1.5.6 Task 2-6: Deliverables

Several types of reports will be submitted, quarterly, draft final and final report, according to the format specified in the Research & Implementation Manual. A PowerPoint presentation showing the basis and results of the study will also be submitted. The draft final report documenting the findings of Part 2 will be submitted to the MDOT RAP no later than March 31, 2013 and the revised (based on the comments of the project panel) will be submitted to MDOT no later than June 20, 2013.

1.6 OUTLINE OF REPORT

The report consists of the following five chapters:

1. Introduction
2. Literature Review
3. Sensitivity Analysis
4. Validation of Performance Models
5. Conclusions and Recommendations

Chapter 1 outlines the problem statement, research objectives and the outline of the final report. Chapter 2 documents the review of literatures from the previous studies related to sensitivity analysis and aspects of the MEPDG/DARWin-ME related to pavement rehabilitation types for rigid and flexible pavements. The review of MDOT pavement rehabilitation practice is also presented in this chapter (Tasks 2-1 and 2-2). Chapter 3 entails sensitivity analysis and results for different rehabilitation options (Task 2-3). Chapter 4 summarizes the project selection process for validation of the rehabilitation models and discusses the validation results by comparing the observed pavement performance to the predicted performance for all the selected projects (Tasks 2-4 and 2-5). Chapter 6 includes the conclusions and detailed recommendations for each rehabilitation option.

CHAPTER 2 - LITERATURE REVIEW

2.1 INTRODUCTION

The MEPDG/DARWin-ME software was made public in mid-2004. Since the release of the software, many State Highway Agencies (SHA's) have worked on exploring several aspects of the design and analysis procedures. Most of the efforts focused on (a) determining significant input variables through sensitivity studies, (b) evaluating local calibration needs, and, (c) implementation issues. To support the MEPDG/DARWin-ME implementation process in the state of Michigan, the pavement researchers at Michigan State University (MSU) have been working with MDOT to explore the various attributes of the design and analysis software. As a result of these efforts over the last five years, the following reports have been published:

- Quantifying Coefficient of Thermal Expansion Values of Typical Hydraulic Cement Concrete Paving Mixtures (Report No. RC-1503)
- Evaluation of the 1-37A Design Process for New and Rehabilitated JPCP and HMA Pavements (Report No. RC-1516)
- Characterization of Traffic for the New M-E Pavement Design Guide in Michigan (Report No. RC-1537)
- Pavement Subgrade MR Design Values for Michigan's Seasonal Changes (Report No. RC-1531)
- Backcalculation of Unbound Granular Layer Moduli (Report No. RC-1548)

Furthermore, the NCHRP 1-47 (Sensitivity Evaluation of MEPDG Performance Prediction) project performed a similar study to determine the sensitive input variables for newly designed rigid and flexible pavements. Since very limited literature is available for sensitivity analysis of rehabilitation options in the MEPDG/DARWin-ME, the literature review will consist of the following topics:

a. Summary of findings from the previous MDOT studies (*1-8*), and the NCHRP 1-47 (*9*) study, and
b. Overview of the differences between new and the rehabilitation models in the MEPDG/DARWin-ME.

It is anticipated the former information on the sensitive inputs related to material characterization, pavement design, and site conditions will also assist the pavement designer in understanding their role in the rehabilitation analysis and design using the MEPDG/DARWin-ME. It should be noted that previous findings will be valid for an overlay layer. On the other hand, the latter knowledge of unique differences in the pavement analysis and design between new and rehabilitation modules of the MEPDG/DARWin-ME will enhance and assist in basic understanding about the rehabilitation design process.

2.2 SUMMARY OF PREVIOUS SENSITIVITY STUDIES

2.2.1 MDOT Sensitivity Study

The MSU research team conducted a study entitled "Evaluation of the 1-37A Design Process for New and Rehabilitated JPCP and HMA pavements"(*3*). The main objectives of the study were to:

a. Evaluate the MEPDG pavement design procedures for Michigan conditions
b. Verify the relationship between predicted and observed pavement performance for selected pavement sections in Michigan and
c. Determine if local calibration is necessary

The report outlined the performance models for JPCP and HMA pavements. Two types of sensitivity analyses were performed namely, a preliminary one-variable-at-a-time (OAT), and a detailed analysis consisting of a full factorial design. Both analyses were conducted to reflect MDOT pavement construction, materials, and design practices. For both new rigid and flexible pavement designs, the methodology contained the following steps:

1. Determine the input variables available in the MEPDG/DARWin-ME and the range of values which MDOT uses in pavement design,
2. Determine the practical range for each input variable based on MDOT practice and Long Term Pavement Performance (LTPP) data,
3. Select a base case and perform the OAT
4. Use OAT results to design the detailed sensitivity analysis
5. Determine statistically significant input variables and two-way interactions
6. Determine practical significance of statistically significant variables
7. Draw conclusions from the results

Tables 2-1 and 2-2 show the impact of input variables on different pavement performance measures for rigid and flexible pavements, respectively.

Table 2-1 Impact of input variables on rigid pavement performance

Design/Material Variable	Impact on distress/smoothness		
	Transverse joint faulting	Transverse cracking	IRI
PCC thickness	High	High	High
PCC modulus of Rupture	None	High	Low
PCC coefficient of thermal expansion	High	High	High
Joint spacing	Moderate	High	Moderate
Joint load transfer efficiency	High	None	High
PCC slab width	Low	Moderate	Low
Shoulder type	Low	Moderate	Low
Permanent curl/warp	High	High	High
Base type	Moderate	Moderate	Low
Climate	Moderate	Moderate	Moderate
Subgrade type/modulus	Low	Low	Low
Truck composition	Moderate	Moderate	Moderate
Truck volume	High	High	High
Initial IRI	NA	NA	High

Table 2-2 Impact of input variables on flexible pavement performance

Fatigue cracking	Longitudinal cracking	Transverse cracking	Rutting	IRI
HMA thickness HMA effective binder content HMA air voids Base material type Subbase material type	HMA thickness HMA air voids HMA effective binder content Base material Subbase material Subgrade material	HMA binder grade HMA thickness HMA effective binder content HMA air voids HMA aggregate gradation	HMA thickness Subgrade material Subgrade modulus HMA effective binder content HMA air voids Base material Subbase material Base thickness Subbase thickness	HMA thickness HMA aggregate gradation HMA effective binder content HMA air voids Base material type Subbase thickness Subbase material type Subgrade material type

Note: The input variables are listed in order of importance.

2.2.2 NCHRP 1-47 Study

The NCHRP 1-47 study investigated the impacts of different input variables on pavement performance. The study quantified the importance of inputs by using a sensitivity index by using a range for a particular input. The sensitivity metric adopted in the study is referred to as normalized sensitivity index (NSI) which is defined as the percentage change of predicted distress relative to its design limit caused by a given percentage change in the design inputs. The NSI is calculated based on Equation (1):

$$NSI = S_{ijk}^{DL} = \frac{\Delta Y_{ji}}{\Delta X_{ki}} \frac{X_{ki}}{DL_j} \quad (1)$$

where:

S_{ijk}^{DL} = sensitivity index for input *k*, distress *j*, at point *i* with respect to a given design limit (DL)

ΔY_{ji} = change in distress j around point i $\left(Y_{j,i+1} - Y_{j,i-1}\right)$

X_{ki} = value of input X_k at point i

ΔX_{ki} = change in input X_k around point i $\left(X_{k,i+1} - X_{k,i-1}\right)$

DL_j = design limit for distress j

The largest *NSI* was determined based on mean and standard deviation $\left(NSI_{\mu\pm2\sigma}\right)$ as the measure for ranking and comparing the sensitivity for different design inputs. The following categories for NSI were used to gauge the sensitivity of each design input:

- Hypersensitive: $NSI_{\mu\pm2\sigma} > 5$
- Very sensitive: $1 < NSI_{\mu\pm2\sigma} < 5$
- Sensitive: $0.1 < NSI_{\mu\pm2\sigma} < 1$
- Non-sensitive: $NSI_{\mu\pm2\sigma} < 0.1$

The sensitivity analyses were performed for five pavement types: new HMA, HMA over stiff foundation, new JPCP, JPCP over stiff foundation, and CRCP. The new HMA and JPCP over stiff foundation represented either stabilized base/subgrade condition or flexible/rigid overlay on the existing pavement. The summary of Global Sensitivity Analysis (GSA, further details in Chapter 4) results for different pavement types are shown in Tables 2-3 to 2-7.

Table 2-3 Ranking of new HMA design inputs by maximum NSI values (9)

Design Input	Maximum $NSI_{\mu\pm2\sigma}$ Values (ANN RSMs)[1]							
	Long. Crack	Alligator Crack	Thermal Crack	AC Rut Depth	Total Rut Depth	IRI	Max	OAT[2]
HMA E* Alpha Parameter[3]	-29.52	-15.94	-0.58	-24.40	-8.98	-3.58	-29.52	HS
HMA E* Delta Parameter[3]	-23.87	-13.18	2.41	-24.43	-8.99	-2.80	-24.43	HS
HMA Thickness	-10.31	-7.46	-0.86	-4.21	-1.58	-1.11	-10.31	HS
HMA Creep Compliance m Exponent	*N.A.*	*N.A.*	*-4.85*	*N.A.*	*N.A.*	*N.A.*	*-4.85*	*VS*
Base Resilient Modulus	*-4.72*	*-2.73*	*-0.17*	*0.14*	*-0.15*	*-0.36*	*-4.72*	*VS*
Surface Shortwave Absorptivity	*4.32*	*1.28*	*-0.20*	*4.65*	*1.67*	*0.67*	*4.65*	*VS*
HMA Air Voids	*4.47*	*3.39*	*1.33*	*-0.05*	*0.03*	*0.29*	*4.47*	*VS*
HMA Poisson's Ratio	*-2.38*	*-1.01*	*0.23*	*-4.33*	*-1.46*	*-0.43*	*-4.33*	*VS*
Traffic Volume (AADTT)	*3.72*	*3.94*	*0.02*	*1.87*	*0.66*	*0.51*	*3.94*	*VS*
HMA Effective Binder Volume	*-3.88*	*-2.93*	*-0.17*	*0.05*	*0.06*	*-0.24*	*-3.88*	*VS*
Subgrade Resilient Modulus	*-2.07*	*-3.41*	*0.15*	*0.08*	*-0.28*	*-0.44*	*-3.41*	*VS*
Base Thickness	*-2.40*	*-1.02*	*-0.03*	*0.22*	*0.04*	*-0.09*	*-2.40*	*VS*
Subgrade Percent Passing No. 200	*-1.71*	*-0.68*	*0.08*	*-0.10*	*-0.10*	*-0.12*	*-1.71*	*S*
HMA Tensile Strength at 14°F	*N.A.*	*N.A.*	*-1.59*	*N.A.*	*N.A.*	*N.A.*	*-1.59*	*S*
Operational Speed	*-1.26*	*-0.83*	*-0.04*	*-1.06*	*-0.39*	*-0.15*	*-1.26*	*S*
HMA Creep Compliance D Parameter	*N.A.*	*N.A.*	*-1.03*	*N.A.*	*N.A.*	*N.A.*	*-1.03*	*S*
HMA Unit Weight	*-0.88*	*0.97*	*-0.76*	*-0.88*	*-0.30*	*-0.08*	*0.97*	*S*
Base Poisson's Ratio	*0.91*	*0.90*	*0.18*	*-0.19*	*-0.05*	*0.09*	*0.91*	*S*
HMA Heat Capacity	*-0.76*	*-0.55*	*-0.77*	*-0.81*	*-0.28*	*-0.14*	*-0.81*	*S*
Subgrade Liquid Limit	*-0.67*	*-0.79*	*-0.10*	*-0.10*	*0.07*	*0.03*	*-0.79*	*S*
Binder Low Temperature PG	*0.56*	*0.09*	*-0.74*	*0.25*	*0.09*	*0.02*	*-0.74*	*S*
HMA Thermal Conductivity	*-0.53*	*-0.40*	*-0.67*	*0.20*	*0.04*	*0.02*	*-0.67*	*S*
Binder High Temperature PG	*-0.60*	*-0.48*	*0.00*	*-0.66*	*-0.25*	*-0.09*	*-0.66*	*S*
Subgrade Poisson's Ratio	*0.44*	*-0.59*	*0.16*	*0.08*	*0.07*	*0.04*	*-0.59*	*S*
Groundwater Depth	*0.20*	*-0.16*	*0.08*	*0.01*	*-0.02*	*-0.02*	*0.20*	*S*
Subgrade Plasticity Index	*-0.15*	*0.11*	*0.03*	*0.01*	*0.02*	*0.00*	*-0.15*	*S*
Aggregate Coef. Of Thermal Contraction	N.A.	N.A.	-0.07	N.A.	N.A.	N.A.	-0.07	NS

[1]Maximum sensitivity over all baseline cases and distresses. Note: The ranking is based on absolute NSI value.
[2]HS=Hypersensitive; VS=Very Sensitive; S=Sensitive; NS=Non-Sensitive.
[3]See Equation (4)

Table 2-4 Ranking of HMA/stiff foundation design inputs by maximum NSI values (9)

Design Input	Maximum $NSI_{\mu\pm2\sigma}$ Values (ANN RSMs)[1]							
	Long. Crack	Alligator Crack	Thermal Crack	AC Rut Depth	Total Rut Depth	IRI	Max	OAT[2]
HMA E* Delta Parameter[3]	-19.60	9.00	3.52	-43.25	-12.76	-3.49	-43.25	HS
HMA E* Alpha Paramater[3]	-22.02	-3.91	-2.82	-39.33	-13.12	-3.67	-39.33	HS
HMA Unit Weight	10.77	3.69	-1.02	-1.70	-0.65	-0.38	10.77	VS
HMA Air Voids	*-8.12*	*-2.53*	*1.84*	*0.62*	*-0.26*	*-0.08*	*-8.12*	*VS*
Surface Shortwave Absorptivity	*-4.90*	*-1.86*	*-0.38*	*7.43*	*2.50*	*0.86*	*7.43*	*HS*
HMA Poisson's Ratio	*-6.93*	*-2.11*	*-0.30*	*-5.57*	*-1.96*	*-0.61*	*-6.93*	*HS*
Subgrade Liquid Limit	*6.76*	*2.47*	*0.18*	*0.97*	*0.19*	*-0.16*	*6.76*	*S*
HMA Creep Compliance m Exponent	*N.A.*	*N.A.*	*-6.65*	*N.A.*	*N.A.*	*N.A.*	*-6.65*	*VS*
Sub Resilient Modulus	*5.82*	*0.94*	*0.37*	*1.85*	*-1.72*	*-0.29*	*5.82*	*S*
HMA Effective Binder Volume	*-5.61*	*0.90*	*-0.70*	*-1.98*	*-0.40*	*-0.16*	*-5.61*	*VS*
Base Poisson's Ratio	*5.55*	*2.26*	*-0.46*	*-2.78*	*-0.56*	*-0.16*	*5.55*	*S*
HMA Heat Capacity	*-5.24*	*-1.88*	*-0.68*	*-1.36*	*-0.38*	*-0.24*	*-5.24*	*S*
Base Thermal Conductivity	*-5.05*	*-1.42*	*-0.84*	*-1.13*	*-0.42*	*-0.18*	*-5.05*	*HS*
Base Thickness	*3.25*	*1.67*	*0.22*	*2.00*	*0.32*	*0.10*	*3.25*	*VS*
HMA Thickness	*2.73*	*1.82*	*-0.70*	*3.11*	*0.87*	*0.30*	*3.11*	*VS*
Operational Speed	*3.09*	*0.56*	*-0.14*	*-1.62*	*-0.58*	*-0.16*	*3.09*	*VS*
Traffic Volume (AADTT)	*0.74*	*0.56*	*-0.06*	*2.94*	*0.91*	*0.26*	*2.94*	*VS*
Subgrade Percent Passing No. 200	*2.78*	*0.53*	*-0.35*	*0.57*	*-0.23*	*0.10*	*2.78*	*S*
Base Resilient Modulus	*-1.84*	*0.58*	*-0.47*	*-2.23*	*-0.33*	*0.22*	*-2.23*	*S*
Base Heat Capacity	*-2.18*	*-0.50*	*-0.40*	*-0.86*	*-0.45*	*-0.23*	*-2.18*	*S*
Subgrade Plasticity Index	*1.66*	*0.49*	*-0.07*	*0.70*	*0.09*	*0.02*	*1.66*	*S*
HMA Tensile Strength at 14°F	*N.A.*	*N.A.*	*-1.65*	*N.A.*	*N.A.*	*N.A.*	*-1.65*	*VS*
Base Resilient Modulus	*-1.63*	*-0.25*	*-0.09*	*0.94*	*0.30*	*-0.13*	*-1.63*	*S*
Groundwater Depth	*-1.30*	*-0.24*	*0.09*	*0.34*	*-0.06*	*-0.02*	*-1.30*	*S*
Binder High Temperature PG	*-0.68*	*-0.23*	*0.00*	*-1.15*	*-0.38*	*-0.11*	*-1.15*	*VS*
HMA Creep Compliance D Parameter	*N.A.*	*N.A.*	*-1.10*	*N.A.*	*N.A.*	*N.A.*	*-1.10*	*VS*
Binder Low Temperature PG	*-0.51*	*-0.09*	*-0.92*	*0.38*	*0.15*	*0.07*	*-0.92*	*S*
HMA Thermal Conductivity	*0.83*	*-0.60*	*-0.56*	*0.62*	*0.24*	*0.15*	*0.83*	*S*
Aggregate Coef. Of Thermal Contraction	N.A.	N.A.	-0.16	N.A.	N.A.	N.A.	-0.16	NS

[1]Maximum sensitivity over all baseline cases and distresses. Note: The ranking is based on absolute NSI value.
[2]HS=Hypersensitive; VS=Very Sensitive; S=Sensitive; NS=Non-Sensitive.[3]See Equation (4), [4]20-year strength ratio values not considered explicitly in OAT analyses

Table 2-5 Ranking of new JPCP design inputs by maximum NSI values (9)

Design Input	Maximum $NSI_{\mu\pm2\sigma}$ Values (ANN RSMs)[1]				
	Faulting	Transverse Cracking	IRI	Maximum	OAT[2]
Slab Width	-17.97	-5.04	-8.81	-17.97	HS
PCC 28-Day Modulus of Rupture	***0.92***	***-4.21***	***-0.63***	***-4.21***	***HS***
PCC Thickness	***0.51***	***-3.88***	***-0.50***	***-3.88***	***HS***
Design Lane Width	***1.58***	***-3.78***	***0.65***	***-3.78***	***HS/NS***[3]
PCC Unit Weight	***-2.33***	***3.13***	***-1.19***	***3.13***	***VS***
PCC Coef. of Thermal Expansion	***2.16***	***2.81***	***1.25***	***2.81***	***VS***
PCC Ratio of 20-year to 28-day Modulus of Rupture	***0.50***	***-2.69***	***-0.26***	***-2.69***	-[4]
PCC 28-Day Elastic Modulus	***0.21***	***2.57***	***0.37***	***2.57***	***HS***
Surface Shortwave Absorptivity	***0.68***	***2.27***	***0.55***	***2.27***	***HS***
Joint Spacing	***0.66***	***1.79***	***0.36***	***1.79***	***HS***
PCC Water-to-Cement Ratio	***0.62***	***1.62***	***0.82***	***1.62***	***S***
PCC Thermal Conductivity	***-0.21***	***-1.12***	***-0.21***	***-1.12***	***HS***
Subgrade Resilient Modulus	*-0.20*	*-0.34*	*-0.99*	*-0.99*	*S*
Dowel Diameter	*-0.69*	*0.98*	*-0.37*	*0.98*	*VS*
PCC Poisson's Ratio	*0.26*	*-0.75*	*0.19*	*-0.75*	*VS*
Traffic Volume (AADTT)	*0.63*	*0.56*	*0.37*	*0.63*	*VS*
PCC Cement Content	*0.30*	*0.55*	*0.18*	*0.55*	*S*
Base Resilient Modulus	*0.33*	*0.40*	*0.22*	*0.40*	*VS*
Groundwater Depth	*0.08*	*-0.37*	*-0.06*	*-0.37*	*S*
Base Thickness	*-0.12*	*0.35*	*-0.08*	*0.35*	*S*
Edge Support – Load Transfer Efficiency	*-0.13*	*-0.26*	*-0.07*	*-0.26*	*NS*
Erodibility Index	*0.25*	*-0.19*	*0.16*	*0.25*	*S*
Construction Month	*0.11*	*0.22*	*0.07*	*0.22*	*S*

[1]Maximum sensitivity over all baseline cases and distresses. Note: The ranking is based on absolute NSI value.
[2]HS=Hypersensitive; VS=Very Sensitive; S=Sensitive; NS=Non-Sensitive, [3]See Equation (4).

Table 2-6 Ranking of JPCP/stiff foundation design inputs by maximum NSI values (9)

Design Input	Maximum $NSI_{\mu\pm2\sigma}$ Values (ANN RSMs)[1]				
	Faulting	Transverse Cracking	IRI	Maximum	OAT[2]
Slab Width	**-16.34**	**-4.74**	**-9.63**	**-16.34**	**HS**
PCC 28-Day Modulus of Rupture	**0.49**	**-5.52**	**-0.62**	**-5.52**	**HS**
PCC Thickness	**0.40**	**-5.05**	**-0.51**	**-5.05**	**HS**
PCC Unit Weight	***-4.16***	***2.68***	***-2.63***	***-4.16***	***HS***
Design Lane Width	***1.67***	***-3.23***	***-0.74***	***-3.23***	***HS/NS***[3]
PCC Coef. of Thermal Expansion	***2.54***	***3.10***	***1.42***	***3.10***	***VS***
PCC Ratio of 20-year to 28-day Modulus of Rupture	***0.31***	***-3.02***	***-0.29***	***-3.02***	***-***[4]
PCC 28-Day Elastic Modulus	***0.47***	***2.40***	***0.45***	***2.40***	***HS***
PCC Water-to-Cement Ratio	***0.28***	***2.23***	***0.78***	***2.23***	***S***
Joint Spacing	***0.70***	***1.98***	***0.33***	***1.98***	***HS***
Surface Shortwave Absorptivity	***0.67***	***1.97***	***0.58***	***1.97***	***HS***
PCC Thermal Conductivity	***-0.54***	***-1.29***	***-0.33***	***-1.29***	***HS***
Dowel Diameter	***-0.44***	***1.13***	***-0.36***	***1.13***	***VS***
Subgrade Resilient Modulus	***-0.38***	***0.24***	***-1.06***	***-1.06***	***VS***
PCC Poisson's Ratio	*0.26*	*0.72*	*0.24*	*0.72*	*VS*
Traffic Volume (AADTT)	*0.47*	*0.72*	*0.35*	*0.72*	*VS*
Base Thickness	*-0.32*	*-0.51*	*-0.17*	*-0.51*	*VS*
Edge Support – Load Transfer Efficiency	*-0.12*	*-0.47*	*-0.10*	*-0.47*	*S*
Erodibility Index	*0.27*	*-0.12*	*0.15*	*0.27*	*S*
Loss of Friction	*0.03*	*-0.26*	*-0.02*	*-0.26*	*S*
PCC Cement Content	*0.21*	*0.22*	*0.12*	*0.22*	*S*
Groundwater Depth	*-0.07*	*-0.21*	*-0.05*	*-0.21*	*S*
Stabilized Base Resilient Modulus	*0.06*	*-0.19*	*-0.06*	*-0.19*	*NS*
Construction Month	*0.10*	*0.14*	*0.06*	*0.14*	*VS*

[1]Maximum sensitivity over all baseline cases and distresses. Note: The ranking is based on absolute NSI value.
[2]HS=Hypersensitive; VS=Very Sensitive; S=Sensitive; NS=Non-Sensitive.
[3]20-year strength ratio values not considered explicitly in OAT analyses

Table 2-7 Ranking of New CRCP design inputs by maximum NSI values (9)

Design Input	Maximum $NSI_{\mu\pm2\sigma}$ Values (ANN RSMs)[1]					
	Punchout	Crack Width	Crack LTE	IRI	Max	OAT[2]
PCC 28-Day Indirect Tensile Strength	**11.13**	**61.48**	**-1.33**	**2.37**	**61.48**	**-**[3]
PCC 28-Day Modulus of Rupture	**-40.29**	**-47.80**	**2.35**	**-7.37**	**-47.80**	**HS**
PCC Thickness	**-44.43**	**-10.47**	**1.57**	**-8.94**	**-44.43**	**HS**
PCC Water-to-Cement Ratio	**8.42**	**36.09**	**-0.82**	**1.88**	**36.09**	**HS**
PCC Unit Weight	**-17.22**	**-35.27**	**0.53**	**-3.22**	**-35.27**	**HS**
Bar Diameter	**11.41**	**23.29**	**-1.49**	**1.93**	**23.29**	**HS**
Base Slab Friction	**-4.17**	**-21.62**	**0.35**	**-0.78**	**-21.62**	**HS**
PCC Cement Content	**7.56**	**21.55**	**-0.65**	**1.38**	**21.55**	**HS**
PCC Ratio 20-year to 28-day Modulus of Rupture	**-18.81**	**7.88**	**-0.50**	**-3.48**	**-18.81**	**-**[3]
Percent Steel	**-15.41**	**-18.00**	**1.04**	**-2.99**	**-18.00**	**HS**
PCC 28-Day Elastic Modulus	**10.90**	**15.97**	**-0.61**	**2.13**	**15.97**	**HS**
Steel Depth	**6.43**	**13.39**	**-0.61**	**1.51**	**13.39**	**HS**
Traffic Volume (AADTT)	**8.47**	**1.03**	**-0.42**	**1.61**	**8.47**	**HS**
Base Resilient Modulus	**-6.39**	**-4.71**	**0.10**	**-1.16**	**-6.39**	**VS**
PCC Coef. of Thermal Expansion	**6.19**	**5.54**	**-0.06**	**1.19**	**6.19**	**VS**
PCC Ratio 20-year to 28-day Indirect Tensile Strength	**1.62**	**-5.81**	**0.14**	**-0.29**	**-5.81**	**-**[3]
Surface Shortwave Absorptivity	**3.32**	**-5.44**	**0.20**	**0.74**	**-5.44**	**HS**
Base Thickness	***-1.79***	***4.71***	***-0.10***	***-0.42***	***4.71***	***S***
Subgrade Resilient Modulus	***-3.23***	***-4.64***	***0.06***	***-1.17***	***-4.64***	***VS***
Edge Support – Load Transfer Efficiency	***-3.26***	***2.16***	***0.30***	***-0.59***	***-3.26***	***S***
PCC Poisson's Ratio	***1.79***	***-2.44***	***0.04***	***0.34***	***-2.44***	***S***
Construction Month	***1.62***	***2.33***	***-0.08***	***0.25***	***2.33***	***S***
Groundwater Depth	***0.43***	***-1.19***	***0.03***	***-0.09***	***-1.19***	***S***

[1]Maximum sensitivity over all baseline cases and distresses. Note: The ranking is based on absolute NSI value.
[2]HS=Hypersensitive; VS=Very Sensitive; S=Sensitive; NS=Non-Sensitive.
[3]20-year strength ratio values not considered explicitly in OAT analyses

The results in above tables show the ranking of significant input variables. The variables located in the top portion are hypersensitive while the portions below show input variables that are very sensitive and sensitive, respectively. The shaded cells represent the top three sensitive variables (based on absolute NSI values) for each performance measure. The results in Tables 2-3 and 2-4 show that HMA master curve parameters have the most significant impact on flexible pavement distresses. On the other hand, among the design inputs, slab width and thickness have significant impact of rigid pavement performance. In addition, among the material properties, PCC modulus of rupture (MOR) has very important impact on predicted performance in rigid pavements (see Tables 2-5 to 2-7).

Another study related to the implementation of the MEPDG was performed in Tennessee (*10*). The State of Tennessee validated the MEPDG models using their typical pavement designs. The study analyzed 19 highway pavement sections for validation. The predicted performance was compared to the measured performance for each project. The analysis considered asphalt concrete overlays on PCC and HMA pavements. The pavements were analyzed using the new/reconstruct pavement design procedures in the MEPDG instead of rehabilitation design options. The roughness (IRI) and rutting predicted performance was determined and compared to the measured values. It was found that the initial IRI value needs to be determined before calculation. The MEPDG predicted rutting values gave satisfactory results for level 1, and over-predicted AC rutting for level 3 analyses. Over predictions also occurred for base and subgrade rutting. Traffic was found to be an important variable. Finally, local calibration of the MEPDG performance models was recommended.

2.2.3 Traffic Inputs in Michigan

The research team has extensively worked on the traffic characterization for the MEPDG/DARWin-ME in Michigan (*5*, *6*). The following traffic characteristics were investigated:

1. Monthly distribution factors
2. Hourly distribution factors
3. Truck traffic classifications
4. Axle groups per vehicle
5. Axle load distributions for different axle configurations

The data was collected from 44 Weigh-in-motion (WIM) sites distributed in the entire state of Michigan. The data were used to develop Level 1 (site specific) traffic inputs for the WIM locations. Cluster analysis was conducted to group similar sites with similar characteristics for development of Level 2 (regional) inputs. Statewide (Level 3) averages were also determined. The inputs and their recommended input levels are summarized in Table 2-8.

Table 2-8 Conclusions and recommendations for traffic input levels

Traffic Characteristic	Impact on pavement Performance		Suggested Input Levels	
	Rigid Pavement	Flexible Pavement	Rigid Pavement	Flexible Pavement
TTC	Significant	Moderate	Level II	
HDF	Significant	Negligible	Level II	Level III
MDF	Negligible		Level III	
AGPV	Negligible		Level III	
Single ALS	Negligible		Level III	
Tandem ALS	Significant	Moderate	Level II	
Tridem ALS	Negligible	Negligible	Level III	
Quad ALS	Negligible	Moderate	Level III	

2.2.4 Unbound Material Inputs in Michigan

Two studies to characterize unbound material in Michigan were carried out in the last few years(*7*, *8*). The first study outlined the importance of the resilient modulus (MR) of the roadbed soil and how it affects pavement systems. The study focused on developing reliable methods to determine the MR of the roadbed soil for inputs in the MEPDG/DARWin-ME. The study divided the state of Michigan into fifteen clusters based on the similar soil characteristics. Lab tests were performed to determine moisture content, grain size distribution, and Atterberg limits. Furthermore, another aspect of the study was to determine the differences between laboratory tested MR values and back-calculated MR. Based on the analysis it was concluded that the values between laboratory tested MR and back-calculated MR are almost equal if the stress boundaries used in the laboratory matched those of the FWD tests. Table 2-9 summarizes the recommended MR values for design based on different roadbed types in Michigan. The study suggests that the design recommended value should be used for design.

Table 2-9 Average roadbed soil MR values (*7*)

Roadbed Type		Average MR			
USCS	AASHTO	Laboratory determined (psi)	Back-calculated (psi)	Design value (psi)	Recommended design MR value (psi)
SM	A-2-4, A-4	17,028	24,764	5,290	5,200
SP1	A-1-a, A-3	28,942	27,739	7,100	7,000
SP2	A-1-b, A-2-4, A-3	25,685	25,113	6,500	6,500
SP-SM	A-2-4, A-4	21,147	20,400	7,000	7,000
SC-SM	A-2-6, A-6, A-7-6	23,258	20,314	5,100	5,000
SC	A-4, A-6, A-7-6	18,756	21,647	4,430	4,400
CL	A-4, A-6, A-7-6	37,225	15,176	4,430	4,400
ML	A-4	24,578	15,976	4,430	4,400
SC/CL/ML	A-2-6, A-4, A-6, A-7-6	26,853	17,600	4,430	4,400

The second study focused on the backcalculation of MR for unbound base and subbase materials and made the following recommendations (*8*):

1. In the design of flexible pavement sections using design levels 2 or 3 of the MEPDG, the materials beneath the HMA surface layer should consist of the following two layers:
   a. Layer 1 - An aggregate base whose modulus value is 33,000 psi
   b. Layer 2 - A sand subbase whose modulus is 20,000 psi
2. In the design of rigid pavement sections using design levels 2 or 3 of the MEPDG, the materials beneath the PCC slab could be either:
   a. An aggregate base layer whose modulus value is 33,000 psi supported by sand subbase whose modulus value is 20,000 psi
   b. A granular layer made up of aggregate and sand mix whose composite modulus value is 25,000 psi
   c. A sand subbase whose modulus value is 20,000 psi
3. For the design of flexible or rigid pavement sections using design level 1 of the MEPDG, it is recommended that:
   - For an existing pavement structure where the PCC slabs or the HMA surface will be replaced, FWD tests be conducted every 500 feet along the project and the deflection data be used to backcalculate the moduli of the aggregate base and sand subbase or the granular layer. The modulus values to be used in the design should correspond to the 33rd percentile of all values. The 33rd percentile value is the same as the average value minus half the value of the standard deviation.
   - For a total reconstruction or for a new pavement section, the modulus values of the aggregate base and the sand subbase or the granular layer could be estimated as twice the average laboratory determined modulus value.
4. Additional FWD tests and backcalculation analyses should be conducted when information regarding the types of the aggregate bases under rigid and flexible pavements becomes known and no previous FWD tests were conducted.
5. MDOT should keep all information regarding the various pavement layers. The information should include the mix design parameters of the HMA and the PCC, the type, source, gradation and angularity of the aggregate and the subbase material type, source, gradation and angularity. The above information should be kept in easily searchable electronic files.

2.3 OVERVIEW OF DIFFERENCES BETWEEN NEW AND REHABILITATION DESIGN

2.3.1 Rehabilitation Options in MEPDG/DARWin-ME

It is important to determine the effect of input variables on the pavement performance specific to the rehabilitation models in the MEPDG/DARWin-ME.
The different rehabilitation options in the MEPDG/DARWin-ME are divided into two categories—rigid and flexible rehabilitation. Within each category, several different rehabilitation design options are available as shown below:

Rigid pavement rehabilitation options

- JPCP over JPCP/CRCP (unbonded)
- CRCP over JPCP/CRCP (unbonded)
- PCC over JPCP/CRCP (bonded)
- JPCP over HMA

Flexible pavement rehabilitation options

- HMA over HMA
- HMA over JPCP
- HMA over CRCP
- HMA over fractured JPCP/CRCP (Rubblized, crack and seat)

None of the previous studies investigated the rehabilitation options of the MEPDG/DARWin-ME. However, to investigate the impact of input variables, it is important to highlight some important differences between new and rehabilitation pavement analysis and performance prediction models in the MEPDG/DARWin-ME.

While distress prediction models (transfer functions) in new and rehabilitation designs are similar, there are some basic differences in the way the damage is calculated in the pavement layers. These differences between new and rehabilitation designs using MEPDG/DARWin-ME include the:

1. Location with the pavement layers where damage is calculated for flexible rehabilitation options,
2. Hardening of the existing HMA layers due to aging, and
3. Characterization of the existing pavement damage.

Since the location of fatigue calculation is different in rehabilitation and new flexible pavement design, the percent alligator cracking is different. Also, the reflective cracking is only considered in rehabilitation analyses but not in the new pavement design. On the other hand, due the reduction in existing modulus because of the age hardening of the asphalt layer over time, rutting and longitudinal cracking and hence IRI are different for the rehabilitation options.

2.3.1.1. Rigid Pavement Rehabilitation

The approach for rigid pavement rehabilitation design follows a similar procedure to the new designs. In addition, the performance models (transfer functions) used to predict pavement performance for each rigid rehabilitation option do not change. The main difference between new and rehabilitated pavement design corresponds to characterizing the existing pavement structure damage. The typical pavement structure layout for all the available rigid rehabilitation designs are shown in Figure 2-1.

The overlay input variables are identical to new rigid pavement designs in the MEPDG/DARWin-ME, and therefore will not be discussed in detail. For a full description on new rigid pavement design using the MEPDG/DARWin-ME refer to the previous MDOT study (*3*). For unbonded overlays, the asphalt interlayer is unique to rigid pavement rehabilitation and is used to ensure that that no bond exists between the existing pavement structure and the overlay. The interlayer separates the existing PCC slab from the overlay to prevent distresses from propagating to the overlay slab. The interlayer material input values are also identical to new HMA layer properties. The existing PCC pavement properties differ compared to new rigid designs. The following input variables are used to characterize the existing PCC layer:

- PCC thickness
- PCC unit weight
- PCC Poisson's ratio
- Is the slab fractured? (if yes: specify fracture technique)
- PCC elastic modulus (in-tact or fractured)
- Thermal conductivity
- Heat capacity

Another input parameter unique to rehabilitation design is the option to input the dynamic modulus of subgrade reaction (*k*) directly, which overrides the internal calculation of *k* established considering base, subbase and subgrade soil information. For rigid pavement rehabilitation, the existing PCC elastic modulus is the only way to classify the condition of the existing PCC pavement.

The existing PCC pavement elastic modulus should be determined either by testing cores taken from the field or by using back-calculation techniques. Once the elastic modulus value is obtained from testing, Equation (2) should be used to calculate the value to be used in the MEPDG/DARWin-ME.

$$E_{base/design} = C_{BD} \times E_{Test} \quad (2)$$

where:

$E_{base/design}$ = Elastic modulus of the existing layer used in the software

E_{Test} = Static elastic modulus obtained from coring and laboratory testing or back-calculation of an intact slab

C_{BD} = Factor based on the overall condition of the existing PCC pavement, recommended range based on the existing pavement condition are given below (*11*).

- 0.42 – 0.75 for pavements in "good" structural conditions
- 0.22 – 0.42 for pavements in "moderate" structural conditions
- 0.042 – 0.22 for pavements in "severe" structural conditions

Table 2-10 summarizes characterization of the existing pavement (all hierarchical Levels) based on measured cracking performance. Once, a pavement condition is determined based on the distress data (percent slab cracked), the value of C_{BD} is estimated. Subsequently, the C_{BD} and the elastic modulus (E_{Test}) are used in Equation (2) to determine $E_{base/design}$. However, for $E_{base/design}$, the software recommends a maximum value of 3,000,000 psi to account for existing joints even if few cracks exist. To characterize the existing pavement structural capacity, the software specifies three different input levels with varying data needs (see Table 2-11).

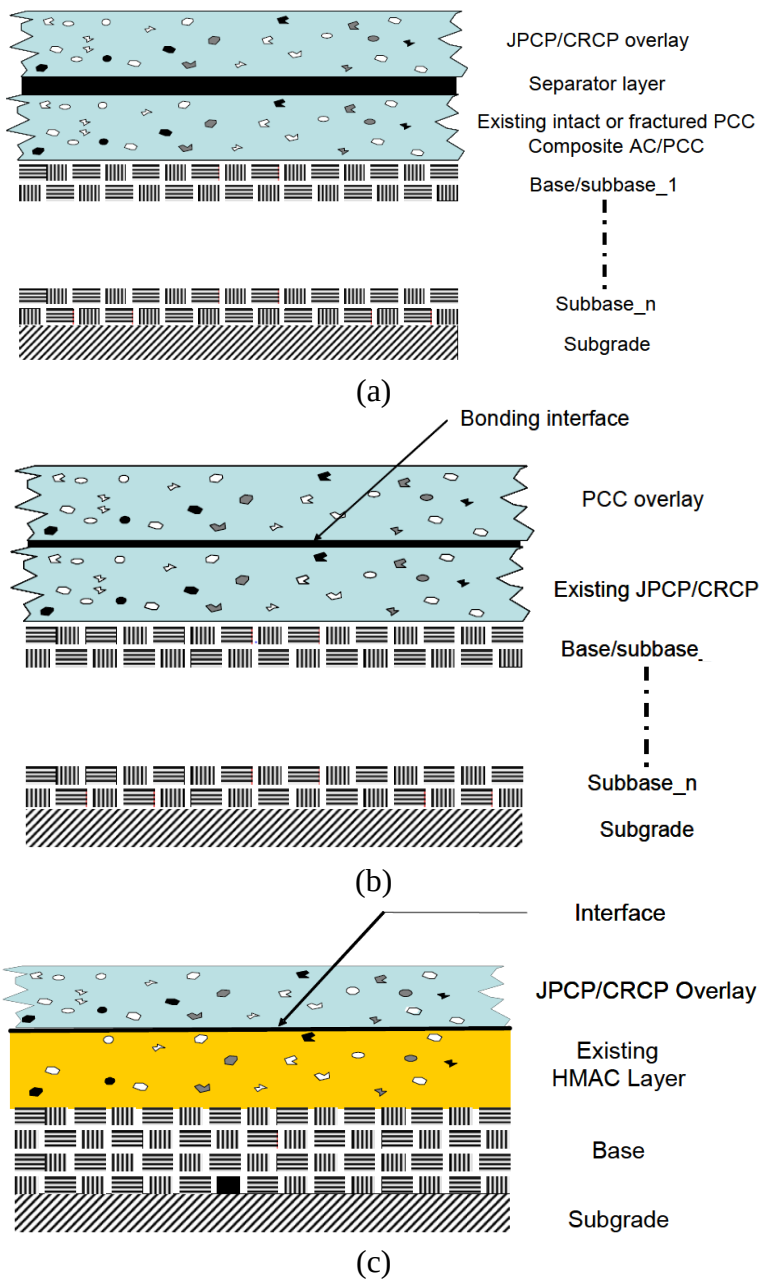

Layer Numbers:

1. JPCP or CRCP overlay
2. Separator Layer (HMA) – considered the base in structural and non-structural analysis
3. Existing JPCP/CRCP – considered the base in structural analysis
4. Stabilized or unstabilized subbase
5. Subbase (if applicable)
6. Subgrade

Layer Numbers:

1. JPCP or CRCP overlay (bonded to the existing layer)
2. Existing JPCP/CRCP
3. Stabilized or unstabilized subbase – considered the base in structural analysis
4. Stabilized or unstabilized subbase (if applicable)
5. Subgrade

Layer Numbers:

1. JPCP or CRCP overlay (bonded to the existing layer)
2. Existing HMA layer – considered the base in structural and non-structural analysis
3. Stabilized or unstabilized subbase
4. Stabilized or unstabilized subbase (if applicable)
5. Subgrade

Figure 2-1 Typical cross-sections of PCC rehabilitation strategies. (a) Unbonded PCC overlays, (b) Bonded PCC overlays, (c) PCC overlays of HMA pavements (1)

Table 2-10 Structural condition of rigid pavements (*11*)

Existing pavement type	Structural condition		
	Good	Moderate	Severe
JPCP (percent slabs cracked)	<10	10 to 50	>50
JRCP (percent area deteriorated)	< 5	5 to 25	> 25
CRCP (percent area deteriorated)	< 3	3 to 10	>10

Table 2-11 Rigid pavement rehabilitation hierarchical levels for the elastic modulus of the existing pavement

Input data	Hierarchical level		
	1	2	3
Existing PCC slab design elastic modulus	Determine the elastic modulus of the existing pavement (E_{test}) from coring, or through FWD back-calculation techniques. Determine the $E_{base/design}$ by using Equation 2	Determine the compressive strength of the existing pavement from PCC cores and convert to elastic modulus. Determine $E_{base/design}$ as described for level 1	Estimate $E_{base/design}$ from historical agency data and local experience for the existing project under design

2.3.1.2. The MEPDG/DARWin-ME Analysis for Rigid Pavement Rehabilitation

The performance prediction for rehabilitation analysis and design based on the structural response models is the same as new JPCP designs. Figure 2-2 illustrates the analysis and design selection process for rigid rehabilitation design. More details about the response models and performance prediction can be found in the NCHRP 1-37A Report (*11*). As an overview, the internal steps necessary to determine various distresses for rigid pavement rehabilitation in the software are presented below:

- Transverse joint faulting is estimated by determining the differential elevation across a joint. Faulting can vary significantly from joint to joint; therefore, the mean faulting across all transverse joints in a pavement section is predicted. The faulting model uses an incremental approach and accumulates over the entire analysis period. The procedure for predicting JPCP transverse joint faulting consists of the following steps:

  1. Tabulate input data needed for predicting JPCP faulting,
  2. Process the traffic input to determine the equivalent number of single, tandem and tridem axles produced by each passing of tandem, tridem, and quad axles,
  3. Process the pavement temperature profile data by converting the temperature profiles generated using the EICM to an effective nighttime difference by calendar month,
  4. Process the monthly relative humidity data to account for the monthly deviations in slab warping,
  5. Calculate the initial maximum faulting,
  6. Evaluate the joint load transfer efficiency,
  7. Determine the critical pavement responses for each increment,
  8. Evaluate the loss of shear capacity and dowel damage,
  9. Calculate the faulting increment,
  10. Calculate the cumulative faulting over the analysis period.

- Transverse cracking is estimated by calculating the fatigue damage at the top and bottom of the concrete slab for each month over the entire analysis period. The

software internally uses the following steps to estimate fatigue damage and subsequently, transverse cracking:

1. Tabulate input data needed for predicting JPCP cracking,
2. Process the traffic input to determine the equivalent number of single, tandem and tridem axles produced by each passing of tandem, tridem, and quad axles,
3. Process the pavement temperature profile data by converting the temperature profiles generated using the EICM to a distribution of equivalent linear temperature differences (temperature gradient) in each month,
4. Process the monthly relative humidity data to account for the monthly deviations in slab warping,
5. Calculate the stress corresponding to each load configuration, load level, load position, and temperature difference for each month,
6. Calculate fatigue damage for both bottom-up and top-down damage over the design life,
7. Calculate bottom-up and top-down cracking based on the fatigue damage,
8. Calculate total cracking by combining both bottom-up and top-down cracking.

- The calculation of smoothness (IRI) is related to the development of joint faulting and transverse cracking and other distresses.

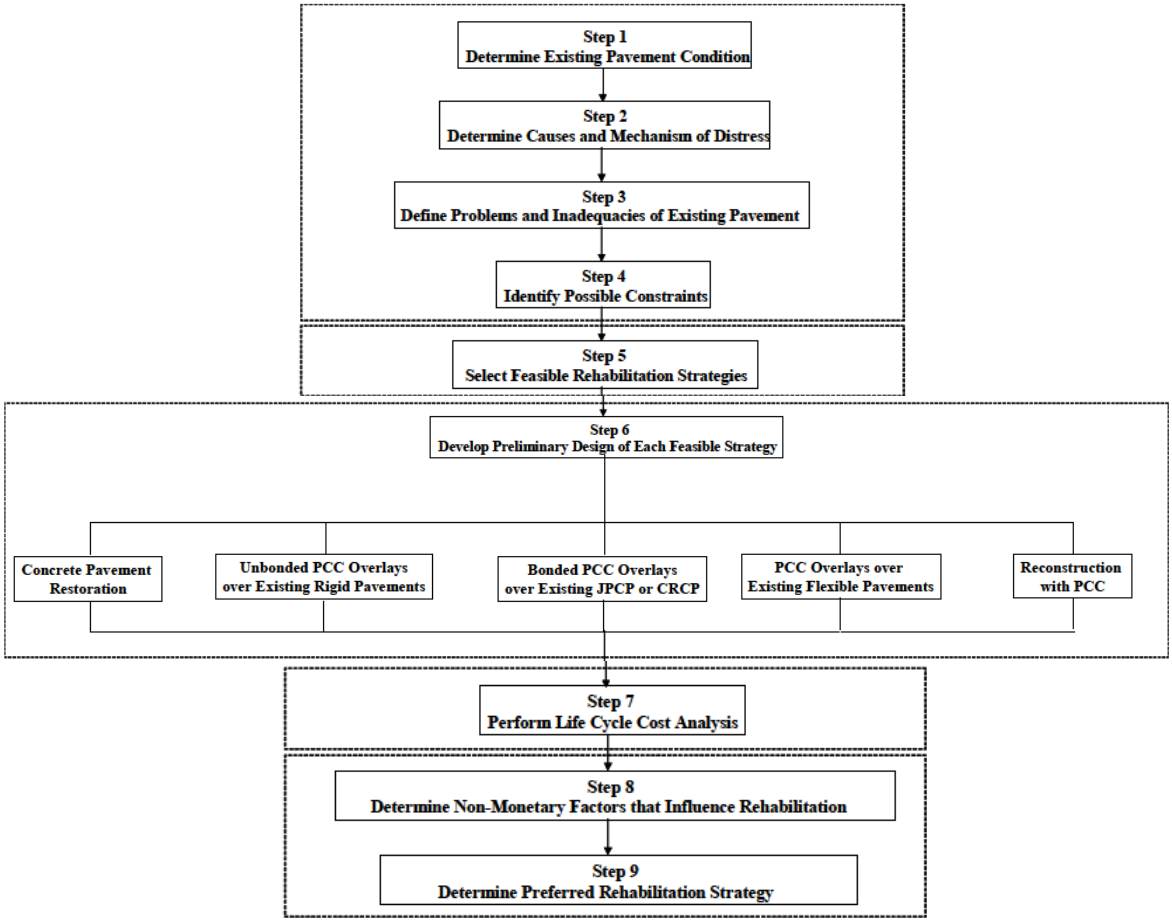

Figure 2-2 Rigid rehabilitation design process (*11*)

2.3.1.3. Flexible Pavement Rehabilitation

Figure 2-3 illustrates the flowchart for HMA rehabilitation analysis and design selection procedure. The focus of this study is the structural rehabilitation design, which starts from step 6 of the flowchart. The procedure for distress prediction in the overlay analyses is the same as for new flexible pavements. The following distresses are considered:

- Load associated fatigue damage
    - HMA layers
        - Top-down cracking
        - Bottom-up cracking
        - Reflective cracking
    - Any chemically stabilized layer
- Permanent deformation
    - HMA layers
    - Unbound layers
- Thermal fracture in HMA surface layers
- IRI

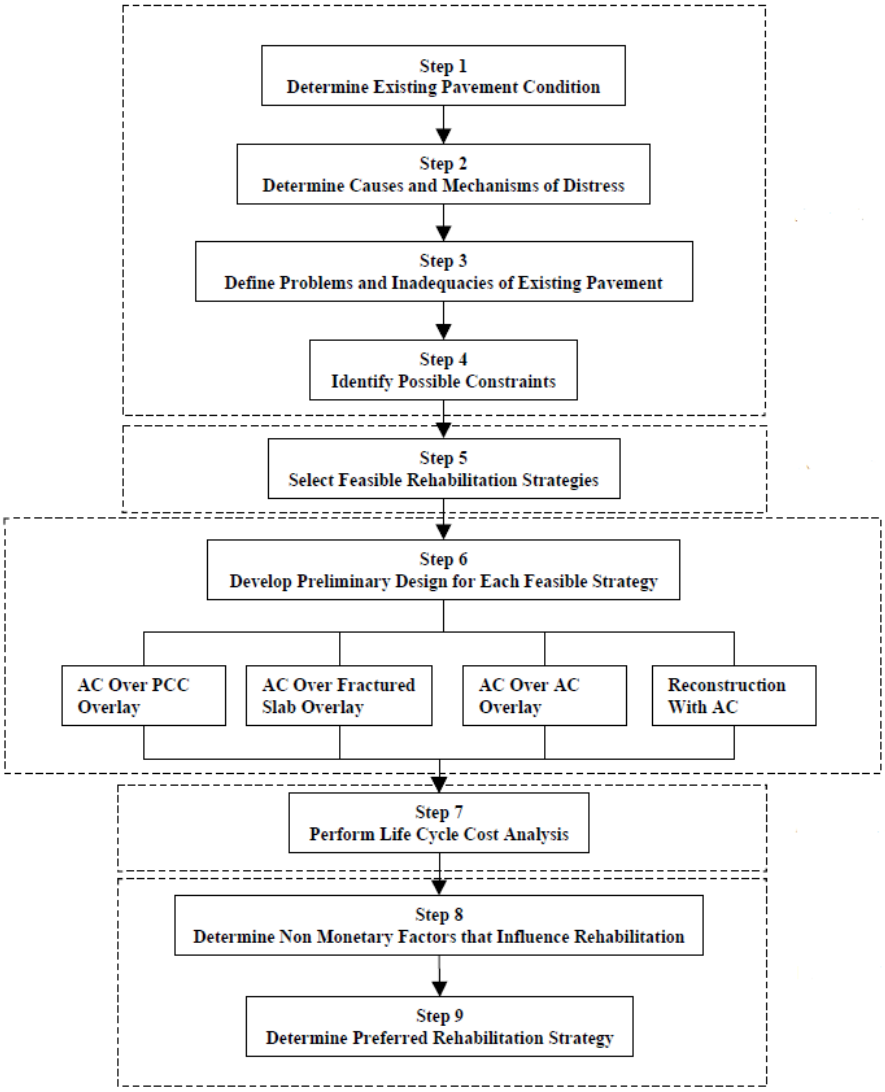

Figure 2-3 Flexible rehabilitation design process (*11*)

For the rehabilitation option, distresses can be analyzed for four general overlay structures shown in Figure 2-4. However, in the case of multiple layers, those may need to be combined to keep the number of layers and evaluation locations within the limits of the MEPDG/DARWin-ME.

Case 1	Case 2	Case 3	Case 4
AC 1	AC 1	AC 1	AC 1
AC 2	AC 2	AC 2	AC 2
AC 3/ATB	AC 3/ATB	GB	AC 3/ATB
Existing Pavement	GB	AC 3/ATB	CTB
	Existing Pavement	Existing Pavement	Existing Pavement

ATB: Asphalt treated base, GB: Granular base, CTB: Cement treated base

Figure 2-4 Overlay design strategies available for flexible pavement rehabilitation

Case 1 is a representation of a conventional HMA overlay. This case can also be used to represent the in-place recycling of existing HMA layers. Cases 2 and 3 represent an overlay where an unbound granular layer is used to control reflection cracking of an underneath PCC layer. These cases may also be used to convert an existing flexible pavement into a sandwich type pavement. Case 4 represents an example of in-place recycling (i.e., full-depth reclamation, FDR) of HMA surface and granular base using cement stabilization. Tables 2-12 through 2-15 summarize the distress prediction locations in the overlay and the existing pavement for the cases shown in Figure 2-4.

Table 2-12 Summary of distress computation locations for flexible overlay designs (*11*)

Distress	Case 1	Case 2	Case 3	Case 4
Longitudinal cracking	Top layer	Top layer	Top layer	Top layer
Alligator cracking	Bottom HMA layer	Bottom HMA layer	1st HMA layer above granular layer; bottom HMA layer	Bottom HMA layer
Thermal cracking	Top layer	Top layer	Top layer	Top layer
Rutting in HMA layers	All HMA layers	All HMA layers	All HMA layers	All HMA layers
Rutting in unbound layers	NA	Granular layer	Granular layer	NA
CSM* modulus reduction	NA	NA	NA	CTB layer
CSM* fatigue cracking	NA	NA	NA	CTB layer
Reflection cracking	Top layer	Top layer	Top layer	Top layer

*CSM: Chemically stabilized material

Table 2-13 Summary of distress computation locations for existing pavement in HMA overlay of flexible and stabilized pavements

Distress	Flexible	Stabilized pavements
Alligator cracking	Existing HMA layer	Existing HMA layer
Rutting in HMA layers	Existing HMA layer	Existing HMA layer
Rutting in unbound layers	All unbound layers	All unbound layers
CSM modulus reduction	NA	CSM layer

Table 2-14 Summary of distress computation location for existing pavement in HMA overlay of fractured slabs

Distress	Fractured slab
Rutting in HMA layers	HMA base if present
Rutting in unbound layers	All unbound layers

Table 2-15 Summary of distress computation locations for existing pavement in HMA overlay of intact PCC pavements

Distress	PCC	Composite
Alligator cracking	NA	Top of existing JPCP layer
Rutting in HMA layers	NA	Existing HMA layer
CTB modulus reduction	CTB layer if present	CTB if present
PCC damage	JPCP and CRCP	JPCP and CRCP

2.3.1.4. The MEPDG/DARWin-ME Analysis for Flexible Pavement Rehabilitation

One of the critical factors in the design of an HMA overlay is the characterization of the existing pavement structure. Based on the available data, the designer has options to consider a three-level hierarchy for inputs for rehabilitation in the MEPDG/DARWin-ME. Three levels are available for the characterization of the existing pavement (*11, 12*). Each level depends on the available data. In this section, the different rehabilitation levels are described followed by the discussion of their impact on overlay performance.

Each of the three rehabilitation levels requires different inputs for estimating the existing pavement damage. It should be noted that regardless of the selected rehabilitation level, there are always three levels for characterizing the HMA mixture and binder. The Level 1 characterization requires in-situ field cores to obtain the undamaged dynamic modulus master curve for the existing HMA layer. Nondestructive deflection testing (NDT) data are needed for estimating the layer back-calculated modulus to characterize damage for the existing HMA layer. The back-calculated dynamic modulus from NDT is used to obtain the initial damage level and damaged modulus master curve. From standard forensic tests on field cores (in-situ properties), the parameters needed for the dynamic modulus predictive equation are (*11*):

- Air void content
- Asphalt content
- Gradation
- A and VTS parameters for the ASTM viscosity temperature susceptibility relationship as determined from recovered binder.

These in-situ HMA volumetric properties and recovered binder parameters are then used in the dynamic modulus predictive equation to establish the undamaged master curve for the existing HMA layer. The damaged modulus is obtained directly from NDT analysis. Knowing the damaged and undamaged dynamic modulus values, fatigue damage is calculated using Equation (3) (*11*) and the process is shown schematically in Figure 2-5.

$$E^*_{dam} = 10^{\delta} + \frac{E^* - 10^{\delta}}{1 + e^{-0.3+5*\log(d_{AC})}} \quad (3)$$

where:

E^*_{dam} = damaged modulus, psi.

δ = regression parameter, representative of minimum value of E^*
E^* = undamaged modulus for a specific reduced time
d_{AC} = fatigue damage in the HMA layer

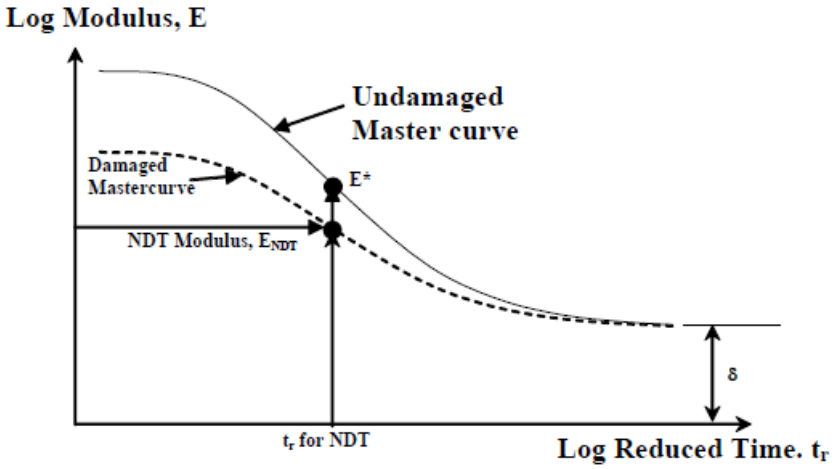

Figure 2-5 Existing HMA layer damaged E* mastercurve computation (*11*)

In level 2 rehabilitation, characterization for an existing asphalt layer uses field cores to obtain the undamaged modulus similar to rehabilitation level 1. The level 2 rehabilitation combine the use of correlations between modulus and measured material characteristics with pavement surface condition data (% cracking and rutting). The initial damage and the damaged modulus master curve are then developed from an estimate of fatigue damage obtained from pavement surface condition data. The amount of alligator cracking measured at the pavement surface is used to solve for the HMA damage using Equation (4).

$$C_{AC} = \frac{100}{1+e^{c+d(d_{AC})}} \quad (4)$$

where:
C_{AC} = percent alligator cracking in the existing HMA layer
d_{AC} = damage computed in the existing HMA layer
c, d = field calibration fitting parameters

Having the undamaged dynamic modulus master curve and field damage, the damaged modulus master curve is calculated from Equation (3). The level 3 rehabilitation uses typical published or recommended values for modulus and information from pavement condition ratings for estimating damage. For level 3 rehabilitation, no HMA and binder testing are required. The undamaged modulus is obtained from the dynamic modulus predictive equation using typical HMA volumetric and binder properties for the existing pavement mixture type. The current damage,d_{AC}, is obtained from the pavement surface condition rating as shown in Table 2-16 (*11*). Pavement condition can also be represented by the pavement surface cracking area as shown in Table 2-17. Having the undamaged modulus master curve and current damage known, the damaged modulus master-curve is obtained from Equation (3).

Table 2-16 Damage based on pavement condition rating (*11*)

Category	Damage
Excellent	0.00-0.20
Good	0.20-0.40
Fair	0.40-0.80
Poor	0.80-1.20
Very Poor	>1.20

Table 2-17 Description of existing pavement condition rating (*13*)

Category	Percent cracked area
Excellent	<5%
Good	5-15%
Fair	15-35%
Poor	35-50%
Very Poor	>50%

CHAPTER 3 - CHARACTERIZING THE EXISTING PAVEMENT LAYERS

3.1 INTRODUCTION

Several issues were encountered while running the MEPDG/DARWin-ME rehabilitation options. These concerns were related to certain structural and material properties. In addition, reasonableness of certain inputs was investigated whenever some unusual results were encountered during the analyses. These concerns are related to the following topics:

- Existing concrete elastic modulus to characterize damage
- Design subgrade modulus
- Impact of interlayer thickness and modulus on the existing PCC slab equivalent thickness
- Discrepancy in performance prediction for thin PCC unbonded overlay
- Layer structure in composite pavement

3.2 EXISTING PCC ELASTIC MODULUS LIMITATIONS

As mentioned in Chapter 2, the maximum value of the existing PCC slab modulus is recommended to be 3,000,000 psi in the MEPDG/DARWin-ME. Based on the existing backcalculated results from LTPP database (General Pavement Studies, GPS-9), where the existing PCC elastic modulus ranged between 3,000,000 psi and 10,000,000 psi with most of the sections around 5,000,000 psi. To verify that the maximum value entered in the MEPDG/DARWin-ME should not exceed 3,000,000, a trial analysis was performed by varying the existing PCC slab elastic modulus to determine its impact on the predicted pavement performance. A sensitivity analysis was performed and the time to reach 20 percent slabs cracked was determined. Figure 3-1 shows the results for different existing PCC elastic moduli for both MEPDG and DARWin-ME. It can be seen that a concrete pavement with a E_{PCC} greater than 3,000,000 psi reaches the distress threshold limit faster. These results are counterintuitive because PCC with higher elastic modulus should perform better than PCC with a lower elastic modulus. Therefore, the recommended maximum limit of 3,000,000 psi for the elastic modulus was used in all analyses in the study.

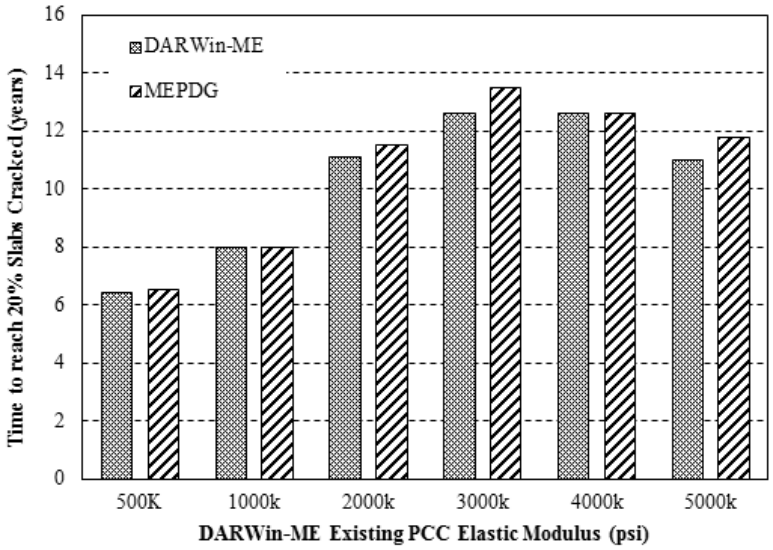

Figure 3-1 Comparison between DARWin-ME and MEPDG for time to failure by varying the elastic modulus of the existing PCC pavement

3.3 DESIGN SUBGRADE MODULUS

MDOT inquired about the use of appropriate MR values to represent soils resilient moduli in Michigan. In general, the values recommended by the MEPDG/DARWin-ME are significantly larger than those being used in MDOT practice. It should be noted that the subgrade moduli values used in the MEPDG/DARWin-ME are based on back-calculated subgrade modulus values from the LTPP database. However, the subgrade modulus values are internally reduced by a factor of 0.55 or 0.67 (*1*) depending on whether the soil type is fine or coarse grained in order to convert the moduli values from field to laboratory. Table 3-1 shows the backcalculated MR (from the Subgrade MR Study) and the DARWin-ME internally reduced MR values. This investigation shows that even though a higher MR value is used as the input for design in the MEPDG/DARWin-ME, the software reduces the values by a fixed factor. Thus, the MEPDG/DARWin-ME factored MR values reflects laboratory determined MR. For level 1 rehabilitation , the reduction factor can be specified by the user. The internal reduction factor cannot be adjusted for levels 2 and 3 analyses. Furthermore, at a project level the backcalculated subgrade MR is recommended for use in rehabilitation design. If backcalculated MR is not available for an overlay or a new project, the unadjusted laboratory MR value from the MDOT subgrade MR study should be used as an input to characterize subgrade.

It should be noted that the MR values reported by Baladi et.al (Subgrade MR Study) were recommended to be used in the AASHTO 93 and the MEPDG designs. However, at the time when the subgrade study was conducted, the information regarding the subgrade modulus internal reduction in the MEPDG was not known and was not considered. Therefore, the MR values suggested in that report should only be considered for AASHTO 93 design procedure. The DARWin-ME design methodology is entirely different from an empirical design approach such as AASHTO 93. The DARWin-ME performance models were nationally calibrated using backcalculated subgrade MR values from the LTPP

database. Those backcalculated values are much greater than typical AASHTO 93 design MR values. However, further investigation will be conducted during the local calibration of the performance models (Part 3 of the study) to evaluate the appropriateness of both backcalculated and design subgrade MR values.

Table 3-1 Internal MR reduction factors for various soil types in DARWin-ME

Roadbed Type		Average MR			DARWin-ME Reduced MR	
USCS	AASHTO	Back-calculated (psi)	Design value (psi)	Recommended design MR value (psi)	Reduced MR (psi)	Factor
SM	A-2-4, A-4	24,764	5,290	5,200	17,261	0.70
SP1	A-1-a, A-3	27,739	7,100	7,000	18,724	0.68
SP2	A-1-b, A-2-4, A-3	25,113	6,500	6,500	16,198	0.65
SP-SM	A-2-4, A-4	20,400	7,000	7,000	13,586	0.67
SC-SM	A-2-6, A-6, A-7-6	20,314	5,100	5,000	8,552	0.42
SC	A-4, A-6, A-7-6	21,647	4,430	4,400	9,113	0.42
CL	A-4, A-6, A-7-6	15,176	4,430	4,400	6,389	0.42
ML	A-4	15,976	4,430	4,400	5,384	0.34
SC/CL/ML	A-2-6, A-4, A-6, A-7-6	17,600	4,430	4,400	7,157	0.41

3.4 EQUIVALENT THICKNESS CONCEPT

In unbonded overlays for rigid pavement, a thin HMA interlayer is generally used to separate the two PCC slabs (i.e., existing and overlay slabs). The research team investigated the impact of interlayer thickness and modulus on the equivalent thickness of the existing PCC slab. The main objective was to verify the impact of interlayer thickness on the predicted performance. For both new PCC design and unbonded overlay design, the MEPDG uses the concept of equivalent thickness to reduce the multilayer system into one equivalent slab. The equivalent slab is then analyzed as a slab on grade. Equation (1) is used within the software to calculate the equivalent thickness for a newly designed PCC pavement where the PCC slab is above the granular base (*2, 3*).

$$h_{eff} = \sqrt[3]{h_{PCC}^3 + \frac{E_{base}}{E_{PCC}} h_{base}^3} \quad (1)$$

where:
h_{eff} = equivalent slab thickness
E_{PCC} = PCC slab modulus of elasticity
E_{base} = base modulus of elasticity
h_{PCC} = PCC slab thickness
h_{base} = base thickness

The equation was modified to incorporate the structural aspects of the asphalt interlayer and the existing PCC layer to determine its impact on the equivalent thickness. Equation (2) was used to account for the existing PCC and the asphalt interlayer.

$$h_{eff} = \sqrt[3]{h_{PCC}^3 + \frac{E_{existingPCC}}{E_{PCC}} h_{existingPCC}^3 + \frac{E_{asphalt}}{E_{PCC}} h_{asphalt}^3} \quad (2)$$

where:
H_{eff} = equivalent slab thickness
E_{PCC} = PCC overlay modulus of elasticity
$E_{existingPCC}$ = existing PCC modulus of elasticity
$E_{asphalt}$ = asphalt interlayer elastic modulus
h_{PCC} = PCC overlay thickness
$h_{existingPCC}$ = existing PCC thickness
$h_{asphalt}$ = asphalt interlayer thickness

One-at-a-time sensitivity analysis was performed on the existing PCC elastic modulus, existing PCC thickness, asphalt interlayer modulus and the asphalt interlayer thickness. The following ranges were used for each input variable:

- PCC elastic modulus:
  - 1,000,000 – 10,000,000psi
- PCC thickness:
  - 5 – 13 inches
- Asphalt interlayer elastic modulus:
  - 100,000 – 600,000 psi
- Asphalt interlayer thickness:
  - 0 – 5 inches

The pavement structure for the sensitivity analysis is illustrated in Figure 3-2.

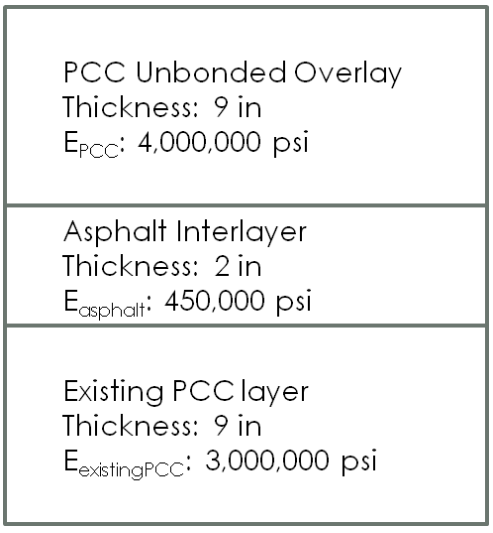

Figure 3-2 Equivalent slab thickness base case structure

The results from the equivalent slab thickness calculations can be seen in Figure 3-3. It is observed that the greatest effect comes from the existing PCC layer properties, while the

asphalt interlayer has very little effect on the equivalent thickness. The reason for such a trend is that the PCC elastic modulus is much greater compared to the asphalt interlayer elastic modulus. Therefore, the interlayer modulus and thickness have insignificant impact on the equivalent thickness. This also implies the interlayer thickness and stiffness will not have much impact on the predicted performance. These results regarding the impact of the asphalt interlayer on the equivalent thickness are intuitive and follow the conventional wisdom in rigid pavement overlay designs.

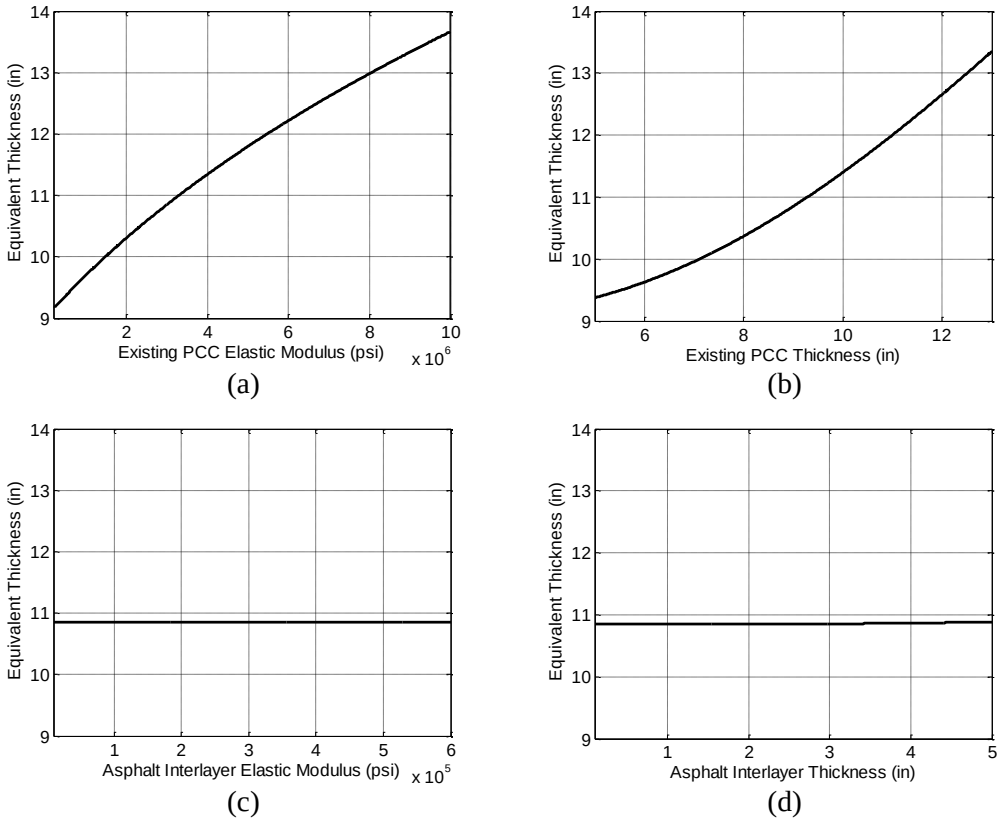

Figure 3-3 Sensitivity analysis based on modified equivalent slab calculations (a) effect of existing PCC elastic modulus, (b) effect of existing PCC thickness, (c) effect of HMA interlayer elastic modulus, (d) effect of HMA interlayer thickness on equivalent thickness

3.5 UNBONDED OVERLAY THICKNESS LIMITATIONS

During the sensitivity analysis, it was found that the MEPDG (version 1.1) software does not allow the user to input any PCC design thickness less than 7 inches. While the DARWin-ME allows for thickness inputs less than 7 inches, caution is advised when running the software beyond a practical design life (i.e. 40+ years) for unbonded overlays thinner than 7 inches. As an example, one unbonded pavement section was analyzed with different thicknesses. A design life of 80 year was chosen in the DARWin-ME in order to ensure failure (i.e., 15% slabs cracked) of the unbonded overlays. The cracking prediction results in Figure 3-4 shows

that a 6 inch unbonded overlay yields less cracking than an 8 inch unbonded overlay at 80 years design life. However, within the practical range of design life (20-40 years), the transverse cracking trends are as one would expect.

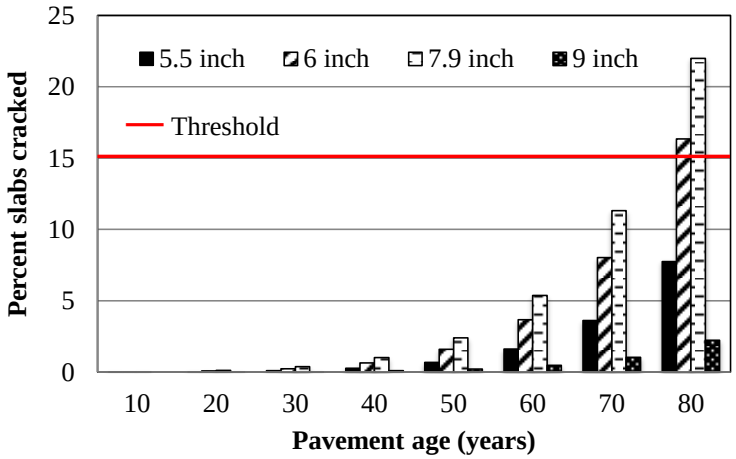

Figure 3-4 Effect of pavement thickness on distress when analyzed until failure

3.6 LAYER STRUCTURE IN COMPOSITE PAVEMENTS

The MSU research team encountered several issues when performing the validation of composite pavements. The MEPDG (version 1.1) software would stop working when the existing base and subbase layers were beyond a certain thickness. It is critical that the most representative section needs to be used in order to provide the most accurate validation results. However, this issue did not occur in the DARWin-ME and the actual pavement cross-sections were used.

3.7 USE OF FWD IN THE MEPDG/DARWIN-ME

The rehabilitation options available in the MEPDG/DARWin-ME suggest using falling weight deflectometer (FWD) deflection data to backcalculate the existing pavement layer moduli. The FWD information is used to characterize the existing condition of both flexible and rigid pavements. This section outlines the needs for FWD testing in the MEPDG/DARWin-ME.

3.7.1 Flexible Pavements

3.7.1.1. HMA

For new HMA pavements, the various input levels used to characterize the properties of the HMA layer is documented in the literature review. The dynamic modulus (E^*) is the most important parameter to characterize the HMA pavement layer. While FWD testing is not necessary for newly designed HMA pavements, such testing is highly recommended for rehabilitation design because it provides a better estimate of the existing in-situ conditions.

Based on backcalculated modulus, the damaged *E** master curve for rehabilitation design is determined for various input levels as mentioned below (*4*):

- For level 1 input, the MEPDG/DARWin-ME requires the following procedure:
    1. Conduct FWD tests in the outer wheelpath and determine the backcalculated HMA modulus. Record the HMA layer temperature at the time of testing and determine the layer thickness from coring or ground penetrating radar testing.
    2. Determine HMA mix volumetric and asphalt viscosity parameters from cores.
    3. Develop an undamaged *E** mastercurve using the modified Witczak equation and the data from step 2 at the same temperature recorded in the field and at an equivalent frequency corresponding to the FWD pulse duration.
    4. Estimate the fatigue damage in the HMA layer using the damaged *E** obtained from step 1 and the undamaged *E** from step 3.
    5. Calculate $\alpha' = (1 - d_{ac})\alpha$; where α is a function of mix gradation parameters.
    6. Determine the field-damaged *E** mastercurve using α' instead of α.
- For levels 2 and 3 inputs, FWD testing is not required.

It should be noted that based on steps 1 and 2, the MEPDG/DARWin-ME software determines the damaged *E** mastercurve using steps 3 through 6.

3.7.1.2. Unbound materials

The DARWin-ME flexible pavement rehabilitation design characterizes the unbound material as follows:

- For level 1 Rehabilitation
    - The backcalculated resilient modulus for each unbound layer (including the subgrade) is used as a direct input
- Otherwise
    - Level 2 input consists of correlations with strength data
    - Level 3 input consists of typical modulus values for different soil classifications

3.7.2 Rigid Pavements

The input parameters needed for the design of an overlay on top of a PCC pavement using the MEPDG/DARWin-ME that can be determined from FWD data. These inputs are: (a) elastic modulus of the existing PCC and base layers, (b) the subgrade k-value, and (c) the PCC flexural strength. The following recommendations need to be considered when determining these inputs based on FWD data.

Effective k-Value

As previously discussed, the suggested method for characterizing the in-situ subgrade condition in the MEPDG/DARWin-ME is by backcalculating the effective k-value, which represents the stiffness of all layers beneath the base. It is important to correctly enter in the

other material characterization properties, such as the gradations of these layers, because this information is used along with the EICM to estimate the seasonal effects on the k-value. When entering the k-value, the designer must also enter the month in which the k-value was measured. Seasonal corrections are then applied to the k-value based on the moisture conditions predicted through the EICM.

It is important to note that the subgrade k-value determined from backcalculation of FWD data is a dynamic k-value, which may be two to three times higher than a static value (*4*).

PCC Elastic Modulus

The elastic modulus of the existing slab must be determined for overlay designs. The elastic modulus can be determined by taking a core and measuring the chord modulus based on ASTM C 469 or by using FWD data to backcalculate the modulus. A backcalculated modulus must be multiplied by 0.8 to convert from a dynamic to a static elastic modulus (*4*).

For an unbonded overlay, the static elastic modulus of the PCC pavement that is determined using backcalculation or laboratory testing must be adjusted to reflect the overall condition of the pavement. The modulus is adjusted based on the condition of the pavement by multiplying it by the appropriate condition factor. Condition factors for a range of pavement conditions are provided in the explanation of Equation (2) in Chapter 2.

3.7.3 Composite Pavements

The MEPDG evaluates HMA/PCC pavements in two steps. First, the pavement system is analyzed as a rigid pavement to model continued cracking of the underlying PCC pavement. The HMA distresses are then modeled, including thermal cracking, fatigue cracking, and rutting, as well as IRI. For a HMA overlay on existing PCC, the key input parameters for this analysis obtained from FWD data are the subgrade *k*-value, E_{PCC}, and PCC modulus of rupture. Although, the PCC modulus of rupture can be estimated from backcalculated E_{PCC} using an empirical correlation (*4*), limited core testing is highly recommended to verify the values.

The backcalculation results for HMA/PCC pavements may contain greater variability than those for other pavement types, largely because the data may contain the results for tests conducted over joints or cracks in the underlying PCC pavement. For valid results, the locations of the joints in the underlying pavement should be identified and the testing conducted should be performed at mid-slab. Any significant deviations from the representative values may be an indication that the testing was conducted too close to underlying cracks or joints, and those results should be excluded in determining the average *k* and *E* values. For the evaluation of the structural adequacy of the underlying PCC pavement, the elastic modulus determined over the intact portion of the slab is needed.

The composite pavements in the MEPDG/DARWin-ME include: (a) HMA over PCC, and (b) PCC over HMA. In the first case when PCC is the existing pavement, the MEPDG/DARWin-ME allows the dynamic backcalculated *k*-value to be entered directly. Both the representative *k*-value and month of testing are needed. However, the backcalculated *k*-value is an optional input; the user is still required to enter resilient moduli for all unbound layers and subgrade. The MEPDG/DARWin-ME processes the input as usual (similar to new design) and determines the seasonal *k*-values based on EICM results and

using the E-to-*k* conversion procedure. For the second case when HMA is the existing pavement, the seasonal resilient moduli are used, but no adjustment is made to account for any difference between the *k*-value from the E-to-*k* conversion process and the backcalculated *k*-value.

3.7.4 Summary of FWD Data Usage in the MEPDG/DARWin-ME

Table 3-2 summarizes the use of deflection data for different existing pavements in the rehabilitation option for the MEPDG/DARWin-ME. The procedure outlines information necessary to determine the measure outside/inside of the MEPDG/DARWin-ME for all existing pavement types.

Table 3-2 Use of deflection data in the MEPDG/DARWin-ME (*5*)

Existing Pavement Layer	Measure	Procedure
All pavement types	Determine pavement condition uniformity.	• Evaluate deflections (e.g., using center deflection or deflection basin parameter) over length of project to determine if subsection is necessary subsections may require different overlay thicknesses based on level of deflection/distress).
HMA	Dynamic modulus, E_{HMA}	• Backcalculate existing (damaged) layer moduli (E_{dam}) from deflection testing. • Determine undamaged layer moduli (E^*) through laboratory testing of field cores. • ***Calculate damage factor (d_{ac}).*** • ***Determine α'.*** • ***Determine field master curve for existing layer, adjust for rate of loading and surface temperature at time of NDT testing.***
PCC	Elastic modulus, $E_{BASE/DESIGN}$	• Backcalculation of PCC-layer modulus (E_{TEST}). • Multiply E_{TEST} by 0.8 to convert from a dynamic to a static elastic modulus. • Determine condition of existing pavement and select a pavement condition factor (C_{BD}) • Calculate $E_{BASE/DESIGN} = (C_{BD})(E_{TEST})$.
	PCC flexural strength, E_c	• MEPDG highly recommends laboratory testing of field obtained beams or correlation with splitting tensile strength from cores for JPCP; and indirect tensile strength for CRCP.
	Effective k-value	• Use backcalculation procedures that directly produce the effective dynamic k-value. k-value determination by rehabilitation strategy • HMA over HMA – not used in MEPDG. • Bonded PCC overlay – backcalculated k-value can be used directly if existing PCC is on a stabilized base. For PCC over unstabilized base, use PCA method to negate the effects of the unstabilized base (PCA 1984). In addition, select a typical value for the base elastic modulus if unstabilized, and if stabilized, use the method proposed by Ioannides and Khazanovich (1994). • Unbonded PCC overlay – use same procedure as outlined for bonded PCC overlay. • PCC overlay of HMA – determine existing layer moduli as described for HMA pavements.

Table 3-2 Use of deflection data in the MEPDG/DARWin-ME (*5*) (Continued…)

PCC	Joint (LTE)	• LTE is not an MEPDG input; however, it can be used for determining the need for retrofit dowels in JPCP and controlling punchout-related longitudinal cracking.
	Loss of support under corner (void detection)	• The presence of voids is not a direct input for the MEPDG; however, the MEPDG assumes that voids are addressed prior to overlay placement.
Chemically stabilized materials (lean concrete, cement stabilized base, lime/cement/flyash stabilized soils)	Modulus E_{CTB}	• Backcalculate existing (damaged) layer moduli (E_{CTB}) from deflection testing. If layer is less than 150 mm (6 in) in depth, backcalculation may be problematic and laboratory testing to determine layer moduli may be required. • Determine intact modulus (E_{max}) of intact (undamaged) cores from compressive strength testing. • Determine damage level (d_{CTB}). • Adjust E_{CTB} for layer and surface condition.
Unbound Materials	Resilient modulus, M_R	• Backcalculate existing layer modulus (E_R) from deflection testing. • Apply modulus ratio (M_R/E_R) to adjust backcalculated to laboratory-obtained values. MEPDG suggests adjustment factors of 0.40 for subgrade soils and 0.67 for granular bases and subbases

3.8 LABORATORY VERSUS BACKCALCULATED MODULI

In terms of potential compatibility between field derived and laboratory measured parameters for the HMA material, it can be stated that fundamentally, field FWD test results and the indirect tensile test (IDT) results under haversine pulse loading should be similar. In addition, assuming that the boundary conditions are appropriately defined, the moduli values from lab and field testing should be similar, provided that (*6*):

1. The pulse duration is the same in both tests;
2. The effective temperature of the HMA mix is the same;
3. The effect of confinement is minimal;
4. The effect of anisotropy is minimal;
5. The effect of loading mode (compression versus tension) is minimal.
6. The effect of the backcalculation technique (in terms of the effect of error propagation in the inverse problem from other backcalculated layer moduli, namely, subgrade and base/subbase layers) is minimal.

The first two issues (pulse duration and temperature) are believed to be the most important in explaining the difference between laboratory and field derived HMA moduli using the current test protocols: (1) the pulse duration in the field is typically 0.035 sec to 0.050 sec, whereas it is 0.1 sec in the standard resilient modulus (MR) test (AASHTO P31, NCHRP 1-28A, and ASTM 4123); (2) the HMA temperature in the field is variable, and is therefore generally different from the standard MR test temperature in the laboratory.

Based on the current practices used to characterize the existing pavement materials, there is a need to determine fundamental material properties. These are the relaxation modulus, *E(t)*, for the HMA and the stress-dependent elastic moduli for base and subgrade layers.

3.9 SELECTION OF APPROPRIATE FREQUENCY FOR BACKCALCULATED MODULUS

It should be noted that since the MEPDG/DARWin-ME uses the dynamic modulus (as opposed to the resilient modulus), it assumes that the ratio of backcalculated to laboratory-measured HMA modulus is one as long as the HMA mixture is identical and the equivalent loading frequency is the same. The equivalent frequency is essentially the dominant frequency imposed by a loading pulse of certain duration. In reality, a transient pulse contains a spectrum of frequencies, so the equivalent frequency is an attempt to determine the one frequency that would best represent the frequency spectrum or the dominant range of frequencies. This equivalent loading frequency is taken as the inverse of the FWD load pulse duration, or 1/t; i.e., for a 33 ms FWD pulse load, the equivalent frequency is taken as 30 Hz. It has been reported that this equivalency frequency is incorrect, and that a more reasonable equivalent frequency should be about 1/2t, or 15 Hz in this example (*4*). For level 1 rehabilitation in flexible rehabilitation options, the software needs direct user input for the backcalculated modulus, temperature and frequency. Therefore, the load pulse of the MDOT FWD equipment should be used to calculate the frequency based on the $f = \frac{1}{2t}$.

3.10 FWD TESTING GUIDELINES

The guidelines discussed in the following section are related to the physical testing equipment configuration (such as sensor locations and load levels) as well as the type and location of deflection data that are obtained during FWD testing (*5*). A recent FHWA study outlined the overall testing procedures and guidelines for flexible and rigid pavements. These guidelines are related to the following aspects of FWD testing:

- Sensor configuration
- Number of drops and load levels
- Testing locations
- Testing increments
- Temperature measurements
    - Air and surface temperature
    - Temperature gradient
- Joint/Crack opening
- Safety guidelines

Table 3-3 summarizes the recommended FWD testing guidelines for both HMA and PCC pavements.

Table 3-3 Recommended FWD testing guidelines (*5*)

Testing Component	Recommendation								
Sensor Configuration (mm):	0	207	305	457	610	914	1219	1524	-305
(in):	0	8	12	18	24	36	48	60	-12
Load level, kN (kips)	Seating			26.7 (6)		40 (9)		53.4 (12)	
Number of drops									
HMA	1			1		1		1	
PCC	1			---		1		1	
Testing locations	Testing in outer traffic lane on multiple lane facilities. Possible directionally staggered testing on two-lane facilities								
HMA	Mid-lane and outer wheelpath								
PCC	Mid-lane, outer wheelpath and transverse joint								
Testing increments	12 to 15 tests per uniform pavement section								
General testing	30 to 150 m (100 to 500 ft)								
Project level	7.6 to 15.2 m (25 to 50 ft)								
Temperature measurements									
Air and surface	Measured at each test location								
Gradient	Measured during testing at 1-hour intervals								
Depth, mm (in)	25 (1)		50 (2)		100 (4)		200 (8)		300 (12)

CHAPTER 4 - REHABILITATION SENSITIVITY ANALYSES

4.1 INTRODUCTION

As outlined in Chapter 2, the MEPDG/DARWin-ME offers several different design options for flexible and rigid pavement rehabilitation. Based on discussions with the MDOT Research Advisory Panel (RAP), rehabilitation fixes used by MDOT were identified and are summarized in Table 4-1. Currently, MDOT does not construct any continually reinforced concrete pavement (CRCP); however, the CRCP options in the MEPDG/DARWin-ME are considered in the preliminary sensitivity analysis only.

Table 4-1 MDOT Rehabilitation options

Asphalt Concrete Overlay	PCC Overlay
AC over AC	JPCP over JPCP (unbonded)
AC over JPCP	
AC over JPCP (Fractured)	

This chapter summarizes the sensitivity analyses for the rehabilitation design options in the MEPDG according to Task 2-3 of the approved work plan. The main objective of this task was to evaluate the impact of inputs specific to various rehabilitation options on the predicted pavement performance. To accomplish this goal, the following analyses techniques were performed:

1. Preliminary sensitivity
2. Detailed sensitivity
3. Global sensitivity

Each methodology has a unique contribution to the overall understanding in determining the impact of design inputs on the predicted pavement performance. The outcome of the preliminary sensitivity is the identification of the significant inputs related to the existing pavement layers. Subsequently, these inputs were combined with the significant inputs for the new pavement layer (overlay) identified in the previous MDOT study (*1*) to conduct the detailed sensitivity. The outcome from the detailed sensitivity analyses include the significant main and interactive effects between the inputs related to the existing and overlay layers.

Finally, the global sensitivity analysis was performed based on the results from the detailed sensitivity analysis. The GSA is more robust because of the following reasons:

a. Main and interaction results are based on the entire domain of each input variable.
b. The importance of each input can be quantified using the Normalized Sensitivity Index (NSI).
c. Relative importance of each design input can be determined.

The details of each sensitivity type are presented in this chapter.

4.2 PRELIMINARY SENSITIVITY ANALYSIS

While the AASHTO 1993 Design Guide requires limited data information for the structural design of pavements, the MEPDG pavement analysis and design procedure requires a large number of design inputs related to layer materials, environment, and traffic. Ideally all the input variables should be studied together to determine their impacts on the predicted pavement performance (*2*). However, performing such an analysis including all these input variables is not efficient. Therefore, in this study the inputs specific to rehabilitation options in the MEPDG were considered along with some important inputs related to the new pavement layer.

In order to further reduce the list of important input variables, a preliminary sensitivity analysis was performed. Results of the analysis were used to identify sensitive and non-sensitive inputs for various rehabilitation options and predicted pavement performance types. Subsequently, the significant input variables identified through preliminary analysis are included in detailed and global sensitivity analyses for further evaluations. The MEPDG design inputs in rehabilitation modules can be divided into two categories:

a. Inputs that are specific to rehabilitation modules and are not part of new design, and
b. Inputs that are similar to new pavement design and are addressed in previous studies (*1, 3*).

The preliminary sensitivity analysis was performed for the current Michigan rehabilitation practices as presented above. The methodology and the results are discussed below for each rehabilitation option.

4.2.1 HMA over HMA Analysis and Results

Only level 3 design inputs specific to rehabilitation for HMA overlays were considered in this analysis (see section 4.4.1.2 to see reasons for using level 3 design inputs):

- milled thickness,
- total rutting in the existing pavement, and
- existing pavement condition rating

The design inputs for characterizing the existing HMA pavement are shown in Table 4-2. Practical ranges for the inputs were needed for the sensitivity analysis and these ranges were determined in consultation with MDOT and the Long-term Pavement Performance (LTPP) experiments as shown in Table 4-2.

Table 4-2 Design inputs for HMA over HMA

Input	Min	Base case	Max
Existing thickness (in)	2.5	6	12
Existing rating	Very poor	Fair	Excellent
Milled thickness (in)	1.5	2	3.5
Total rutting in existing (in)	0	0.5	1
Binder type	Mix 24	Mix 37 & 44	Mix 204
Asphalt mix aggregate gradation	Type 1	Type 2	Type 3

It should be noted that the inputs used in this analysis correspond to MDOT practices. For example, mixtures 24, 37 and 44 in Table 4-2 are surface courses while mixture 204 is a leveling course. The properties of these mixture numbers are explained in the Part 1 final report (*4*). The aggregate mix gradations were plotted, and the extreme bands (i.e. the upper and lower band) of the gradations were selected as the minimum and maximum of the range.

The base traffic and pavement structure for analysis are presented in Table 4-3. More details about aggregate gradation, and mix types are presented in Appendix A.

Table 4-3 HMA over HMA base case

Traffic		
AADTT	3500	20.18 million ESALS*
Other traffic data	Level 3 Statewide averages	
Climate	Lansing	
Layer properties		
Structure (layers)	Material	Thickness
1-Asphalt layer	HMA	6
2-Existing asphalt layer	HMA (existing)	6
3-Granular base	A-1-b	10
4-Subgrade	A-4	semi-infinite

* Internally estimated 20 years ESAL by the MEPDG using the default axle load spectra. The higher AADTT was used to ensure some level of distresses for sensitivity analysis.

To evaluate the effect of the design inputs on the predicted pavement distresses, the inputs were varied one at a time over their ranges. Based on the predicted distress (longitudinal cracking, alligator cracking, total rutting, and IRI), the Normalized Sensitivity Index (NSI) was calculated for each input-distress combinations using Equation (1) in Chapter 2. The inputs were ranked based on the NSI (absolute) magnitude. Table 4-4 shows the calculated NSI values and Figure 4-1 presents NSI values for all inputs. An input variable with absolute NSI value greater than one was identified as a significant input. It can be seen from the results in Table 4-4, that existing pavement condition rating and existing pavement thickness are important inputs for longitudinal cracking prediction.

In addition, to verify the effect of the existing pavement condition rating, the predicted distresses at the end of pavement life were evaluated as shown in Figure 4-2. Results were compared with the threshold values shown with red dotted line. It should be noted that all distresses must be compared to the performance threshold to evaluate the significance of an input. Figure 4-2 visually shows the impact of significant inputs on the predicted performance.

Table 4-4 Summary of NSI values for each design input for HMA overlay

Input	Longitudinal cracking	Alligator cracking	Total rutting	IRI
	Maximum NSI	Maximum NSI	Maximum NSI	Maximum NSI
Existing gradation	0.04	0.01	0	0
Milling thickness	0.01	0	0.01	0
Binder type	0.08	0.01	0	0
Existing condition rating	1.69	0.34	0.01	0.01
Existing HMA thickness	5.56	0.32	0.15	0.05
Total surface rutting	0	0	0.21	0.049

Note: Highlighted cells indicate the significant design inputs (|NSI| >1). The absolute NSI values are reported in the table.

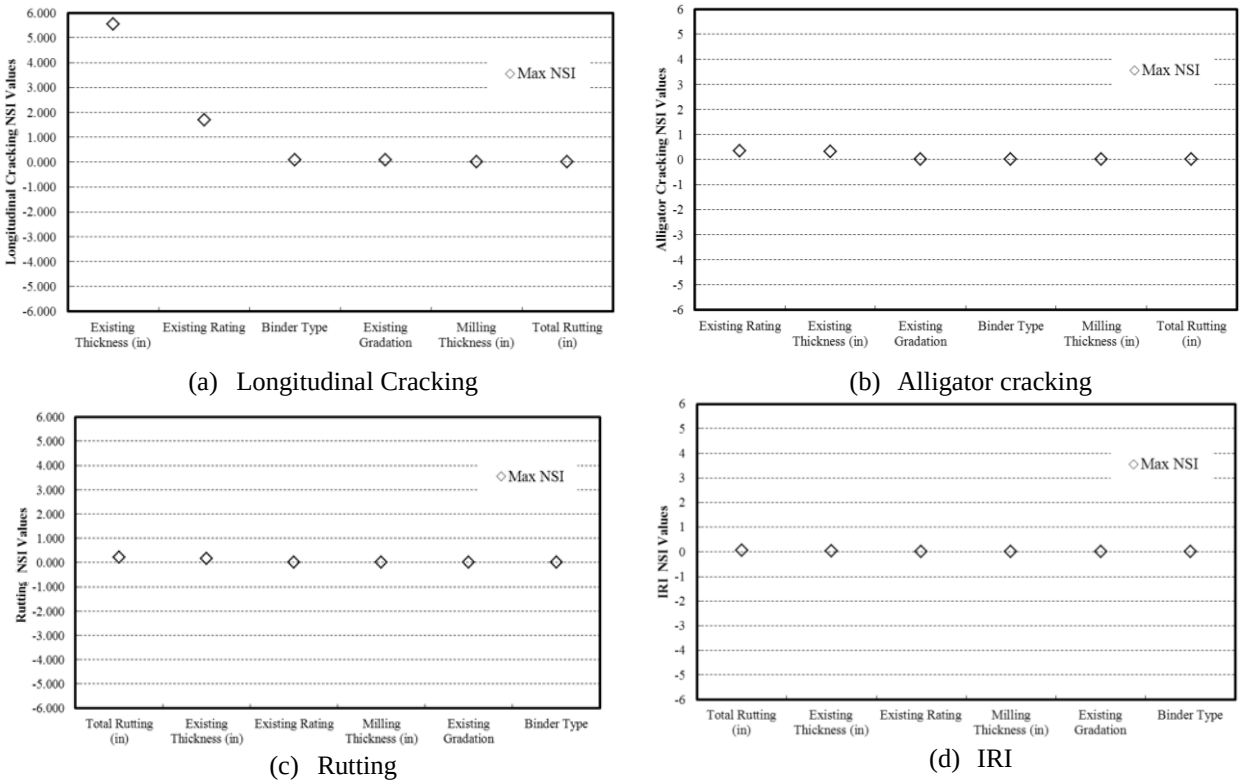

(a) Longitudinal Cracking

(b) Alligator cracking

(c) Rutting

(d) IRI

Figure 4-1 NSI plots for HMA overlay

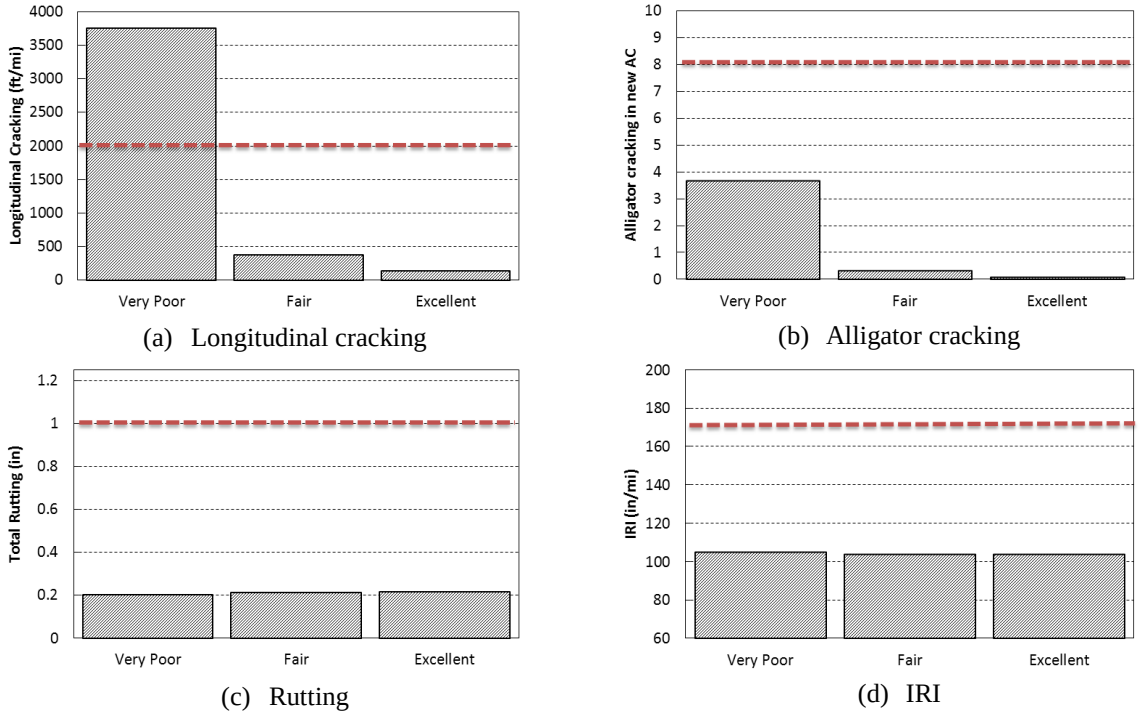

(a) Longitudinal cracking

(b) Alligator cracking

(c) Rutting

(d) IRI

Figure 4-2 Overlay distresses for HMA over HMA based on different levels of existing pavement condition rating at 20th year

It should be noted that reflective cracking was not included in the results. In the MEPDG software, the empirical reflective cracking model is not accessible. For example, the software does not allow the user to define a design limit (or threshold) for reflective cracking. Additionally, the transverse cracking model predicts minimal cracking when the appropriate binder grade is selected. The binder types for the analyses were selected based on MDOT practices. In order to induce more transverse cracking, binders 2 to 3 grades warmer should be used in the sensitivity analysis (*3*). In this study no thermal cracking was observed because of appropriate PG binder grade selection. Therefore, thermal cracking was not predicted by the model and no further analysis could be conducted on thermal cracking.

4.2.2 Composite (HMA over JPCP) Analysis and Results

Table 4-5 presents the list of inputs needed to characterize the existing pavement for the composite rehabilitation option in the MEPDG. Input ranges were determined in consultation with MDOT and using LTPP databases. Table 4-6 shows the traffic and pavement structure for the base case.

Table 4-5 Input variable values for composite pavements

Input variable	Min	Base case	Max
PCC existing thickness (in)	7	9	11
PCC existing strength (psi)	450	550	900
PCC CTE (per °F x 10^{-6})	4	5.5	7
Cement content (lb/yd^3)	402	556	686
Water/cement ratio	0.3	0.47	0.7

Table 4-6 Composite pavement base case

Traffic		
AADTT	15000	86.49 million ESALs*
Other traffic data	Level 3 Statewide averages	
Climate	Lansing	
Layer properties		
Structure (layers)	Material	Thickness (in)
1 - Surface layer	HMA	6
2 - Existing pavement	PCC	9
3 - Base	Crushed stone	7
4 - Subgrade	A-4	semi-infinite

* Internally estimated 20 years ESAL by the MEPDG using the default axle load spectra. The higher AADTT was used to ensure some level of distresses for sensitivity analysis.

Table 4-7 summarizes the calculated NSI for different performance measures. Figure 4-3 illustrates the calculated NSI values for various inputs and different distresses. The data in the figure indicate that only the existing PCC slab has a significant effect on predicted longitudinal cracking. The existing PCC thickness and PCC flexural strength (MOR) were considered for use in the subsequent analysis. It should be noted that no alligator cracking was predicted in this case. This is consistent with expectations, given the stiff underlying PCC base.

Table 4-7 Summary of NSI values for each design input for composite pavement

Input	Longitudinal cracking	Rutting	IRI
	Maximum NSI	Maximum NSI	Maximum NSI
Existing PCC thickness	3.40	0.37	0.04
Existing PCC flexural strength	0.90	0.14	0.01
PCC CTE	0	0	0
Cement content	0	0	0
Water/cement ratio	0	0	0

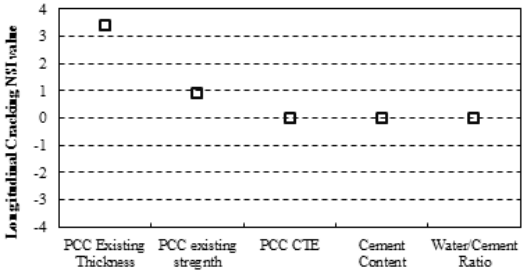

(a) Longitudinal Cracking

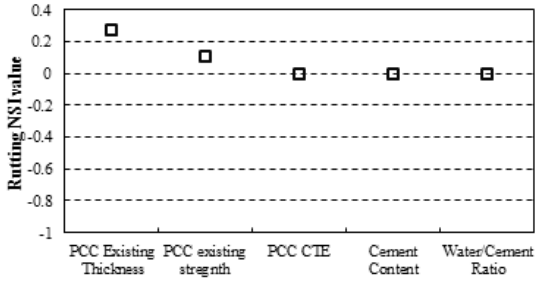

(b) Rutting

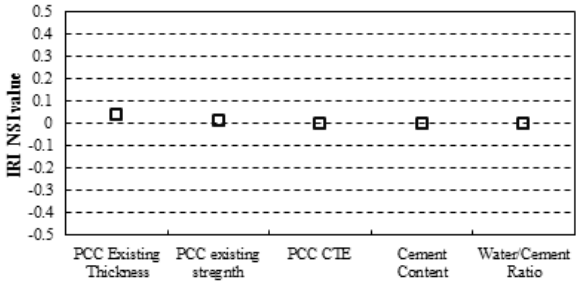

(c) IRI

Figure 4-3 NSI plots for composite pavements

4.2.3 Rubblized (HMA over Fractured PCC) Pavement Analysis and Results

Table 4-8 presents the range of existing pavement inputs that are specific to this rehabilitation option. The base case traffic and pavement structure information are presented in Table 4-9. As mentioned before, the inputs for the overlay layer will be held constant in order to determine the significant inputs specific to the existing pavement layers.

Table 4-8 Input variable values for rubblized pavement

Input Variable	Min	Base case	Max
Existing rubblized PCC thickness (in)	7	9	11
Existing rubblized PCC elastic modulus (psi)	200,000	400,000	1,500,000

Table 4-9 Base case values for rubblized pavement analysis

Traffic		
AADTT	15,000	86.49 million ESALs*
Other traffic data	Level 1: Statewide averages	
Climate	Lansing	
Layer properties		
Structure (layers)	Material	Thickness (in)
1 - Surface layer	AC	6
2 - Existing pavement	PCC (fractured)	9
3 - Base	Crushed stone	7
4 - Subgrade	A-4	semi-infinite

* Internally estimated 20 years ESAL by the MEPDG using the default axle load spectra. The higher AADTT was used to ensure some level of distresses for sensitivity analysis.

For this rehabilitation option, no input variable related to the existing pavement condition is needed. Therefore, only input variables for characterization of the existing materials and thickness were included in the analysis. Table 4-10 shows the NSI values for different performance measures and these values were plotted in Figure 4-4. Similar to composite pavements, no alligator cracking was predicted. Based on the NSI values, it was determined that the existing fractured PCC thickness and elastic modulus don't significantly affect the predicted performance. Nevertheless, they were still considered for subsequent analysis to study their interactions with overlay design inputs.

Table 4-10 Summary of NSI values for each design input for rubblized pavements

Input	Longitudinal cracking	Rutting	IRI
	Maximum NSI	Maximum NSI	Maximum NSI
PCC Existing thickness	0.04	0.01	0.01
PCC Existing strength	0.03	0.05	0.02

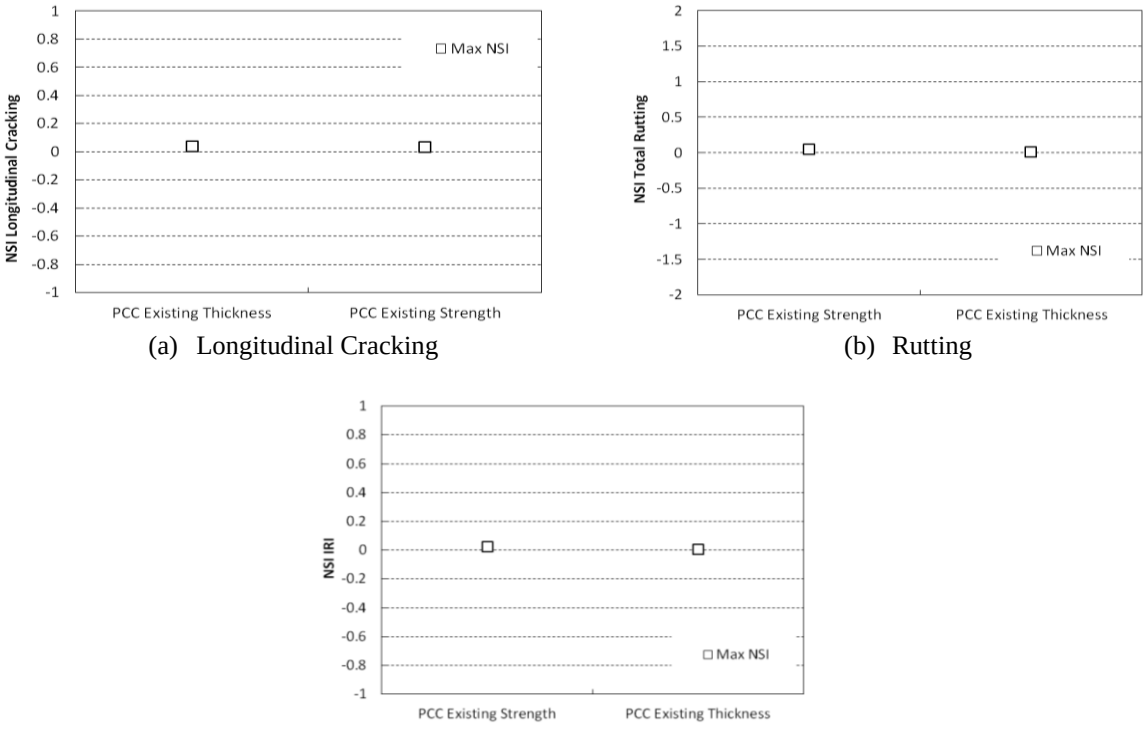

(a) Longitudinal Cracking (b) Rutting

(c) IRI

Figure 4-4 NSI plots for rubblized

4.2.4 Unbonded PCC overlay Analysis and Results

The basic structure of an unbonded overlay cross-section is shown in Figure 4-5. For unbonded overlay design, an interlayer needs to be considered. The separator (or interlayer) layer consists of an asphalt material that breaks the bond between the existing PCC layer and the new overlay.

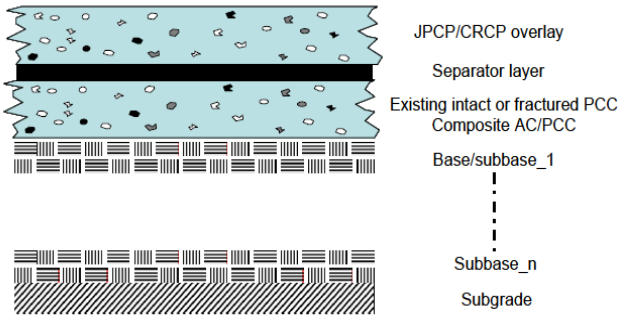

Figure 4-5 Typical unbonded overlay cross section (*5*)

The inputs specific to the asphalt interlayer include:

- Interlayer asphalt mixture data
  - Level 1: Complete dynamic modulus data (E*)
  - Level 2 & 3: Aggregate gradation
- Asphalt Binder data

    - Level 1 & 2: G* and δ values at specific temperatures and angular frequencies
    - Level 3: Select the high and low temperature PG grade
- General asphalt properties
    - Reference temperature
    - Effective binder content
    - Air voids
    - Total unit weight
    - Poisson's ratio
    - Thermal conductivity
    - Heat capacity

Another input specific to rehabilitation design is the foundation support. The dynamic modulus of subgrade reaction (k-value) can be selected as a standalone input within the unbonded overlay rehabilitation option. To characterize the existing pavement, the existing PCC elastic modulus, and PCC thickness were included in the analysis. For existing PCC modulus and thickness, the software gives a range from 200,000 to 5,000,000 psi and 1.5 to 20 inch, respectively. However, due to the software issues discussed in Chapter 3, the inputs and their range used for the analysis were limited to the minimum and maximum values that the software allows, and are shown in Table 4-11. The inputs in Table 4-11 are only related to pavement structure and strength properties of the existing PCC layer and asphalt interlayer in the MEPDG. The base case traffic and pavement structure are presented in Table 4-12.

Table 4-11 List of input variables for unbonded overlay option

Main input	Min	Base case	Max
Interlayer thickness (in)	1	2	3
Interlayer PG grade	Mix 37	Mix 24	Mix 204
Existing thickness (in)	7	9	11
Existing elastic modulus (psi)	500000	1000000	3000000

Table 4-12 Base case values for unbonded overlay

Site Factors		
AADTT	3500	20.18 Million ESALS*
Other traffic data:	Level 1: Statewide averages	
Climate	Lansing	
Layer Properties		
Structure (layers)	Material	Thickness (in)
1-PCC	PCC	9
2-Asphalt interlayer	HMA	1.5
3-Existing PCC	JPCP (existing)	9
4-Granular base	Crushed stone	7
5-Subgrade	A-4	semi-inf

* Internally estimated 20 years ESAL by the MEPDG using the default axle load spectra. The higher AADTT was used to ensure some level of distresses for sensitivity analysis.

Table 4-13 summarizes the maximum calculated NSI for all of the distresses. The NSI values close or larger than 1 in Table 4-13 show the significant inputs. The NSI values

are graphically displayed in Figure 4-6 for all inputs related to both existing and overlay layers.

Table 4-13 Summary of NSI values for each design input for unbonded overlay

Input	Cracking	Faulting	IRI
	Maximum NSI	Maximum NSI	Maximum NSI
Existing thickness	1.41	0.07	0.16
Existing elastic modulus	0.68	0.04	0.09
Interlayer thickness	0.14	0.01	0.08
Interlayer PG grade	0.01	0	0

Note: Inputs related to existing pavements are only shown in the table.

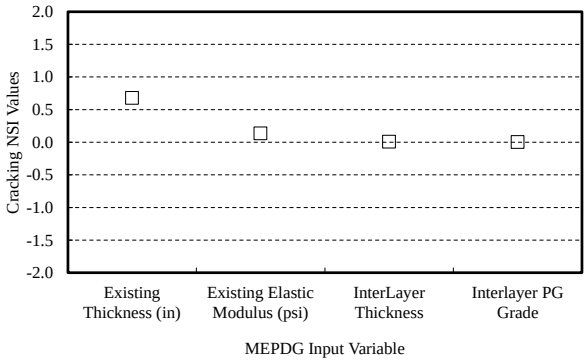

(a) Cracking

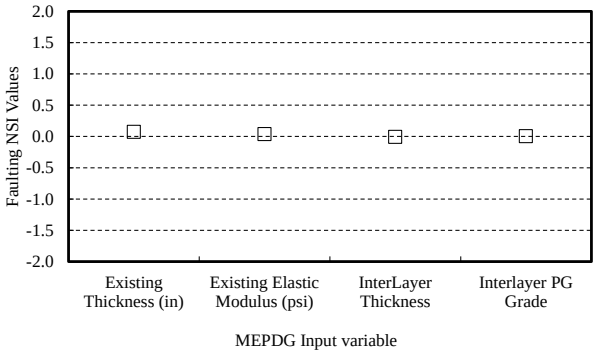

(b) Faulting

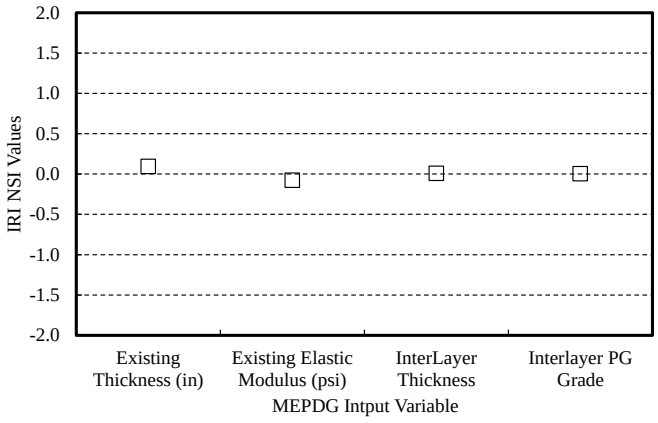

(c) IRI

Figure 4-6 NSI plots for unbonded overlay

4.2.5 CRCP over HMA

Table 4-14 presents the range of existing pavement inputs for this rehabilitation option. The base case traffic and pavement structure information are presented in Table 4-15. As mentioned before, the inputs for the overlay layer were held constant in order to determine the significant inputs specific to the existing pavement layers. Again, mixtures 24, 37 and 44

in Table 4-14 are surface courses. The properties of these mixture numbers are explained in the Part 1 final report (*4*) .

Table 4-14 Input variable values for CRCP over HMA pavement

Input variable	Min	Base case	Max
Existing Gradation	Type 1	Type 2	Type 3
Milling Thickness (in)	0	3	4
Binder Type	Mix 37	Mix 24	Mix 44
Existing Rating	Very Poor	Fair	Excellent
Existing Thickness (in)	2	6	12
Ultimate Shrinkage (days)	30	35	50

Table 4-15 Base case values for CRCP over HMA pavement analysis

Site Factors		
AADTT	3,500	20.18 million ESALs*
Other traffic data	Level 1: Statewide averages	
Climate	Lansing	
Layer properties		
Structure (layers)	Material	Thickness (in)
1 - PCC	PCC (CRCP)	7
2 - Asphalt interlayer	AC	6
3 - Base	Crushed gravel	5
4 - Subgrade	A-7-6	semi-infinite

* Same as Table 4-3

Table 4-16 shows the NSI values for different performance measures and these values were plotted in Figure 4-7. Based on the NSI values, it was determined that the existing HMA thickness affects the predicted performance significantly.

Table 4-16 Summary of NSI values for each design input for CRCP over HMA pavements

Input	Crack width	Crack LTE	Punchout	IRI
	Max NSI	Max NSI	Max NSI	Max NSI
Existing gradation	0.50	0.00	0.21	0.02
Milling thickness (in)	0.00	0.00	0.00	0.00
Binder type	0.50	0.00	0.18	0.02
Existing rating	0.50	0.00	0.72	0.08
Existing thickness (in)	4.00	0.00	2.45	0.28

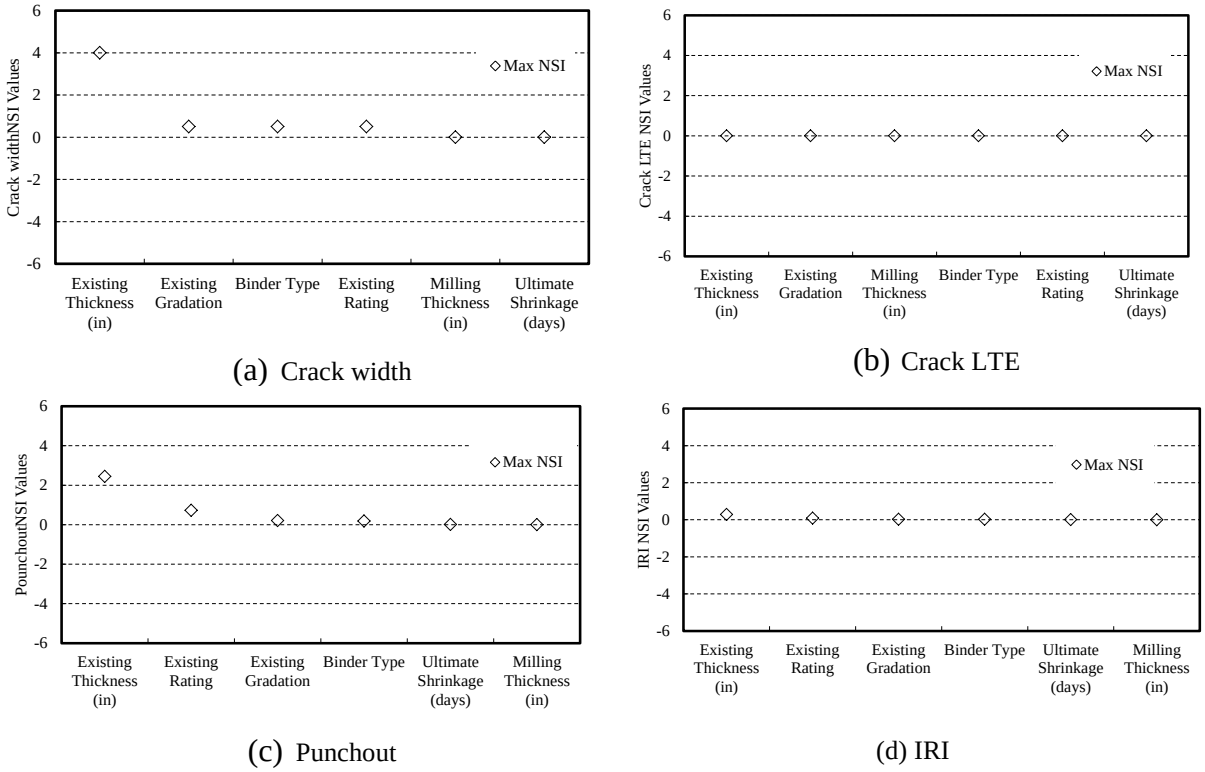

(a) Crack width (b) Crack LTE

(c) Punchout (d) IRI

Figure 4-7 NSI plots for CRCP over HMA

4.2.6 CRCP over JPCP

Table 4-18 presents the range of existing pavement inputs for CRCP over JPCP. The base case traffic and pavement structure information are presented in Table 4-17. As mentioned before, the inputs for the overlay layer were held constant in order to determine the significant inputs specific to the existing pavement layers.

Table 4-17 Base case values for CRCP over JPCP pavement analysis

Site factors		
AADTT	10000	
Other Traffic Data	Level 1: Statewide Averages	
Climate	Lansing	
Layer properties		
Structure (layers)	Material	Thickness (in)
1 - Surface Layer	CRCP	7
2 - AC Interlayer	AC	2
3 - Existing Pavement	PCC JPCP	9
4 - Base	Crushed Stone	7
5 - Subgrade	A-4	semi-inf

Table 4-18 Input variable values for CRCP over JPCP pavement

Input Variable	Min	Base case	Max
PCC Existing Strength (psi)	500000	1000000	3000000
PCC Existing Thickness (in)	7	9	11
AC Interlayer Thickness (in)	1	2	4
AC Interlayer Binder	52-10	PG 58-22	64-28
Subgrade K value (psi/in)	100	250	400

Table 4-19 shows the NSI values for different performance measures and these values were plotted in Figure 4-8. Based on the NSI values, it was determined that the existing PCC thickness and modulus, and subgrade *k*-value affect the predicted performance significantly.

Table 4-19 Summary of NSI values for each design input for CRCP over JPCP pavements

Input Value	Crack Width	Crack LTE	Punchouts	IRI
	Max NSI	Max NSI	Max NSI	Max NSI
PCC existing strength	0.00	0.36	6.28	0.72
PCC existing thickness	0.00	0.00	4.68	0.55
AC interlayer thickness	0.00	0.00	0.08	0.01
AC interlayer binder	0.00	0.00	0.00	0.00
Subgrade k- value	0.00	0.00	2.50	0.29

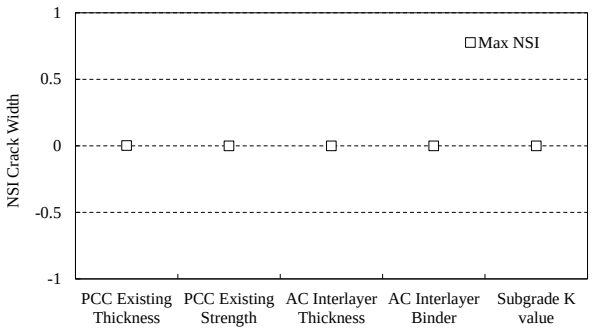

(a) Crack width

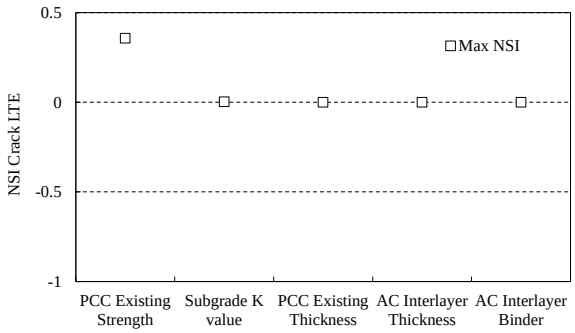

(b) Crack LTE

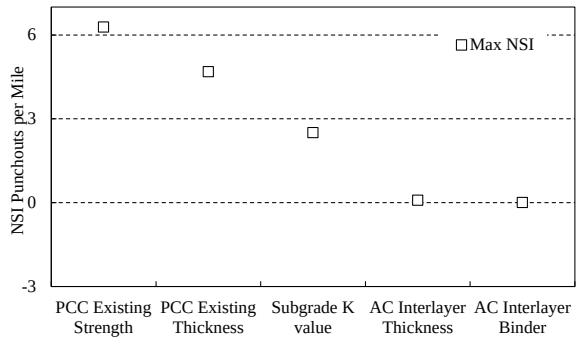

(c) Punchout

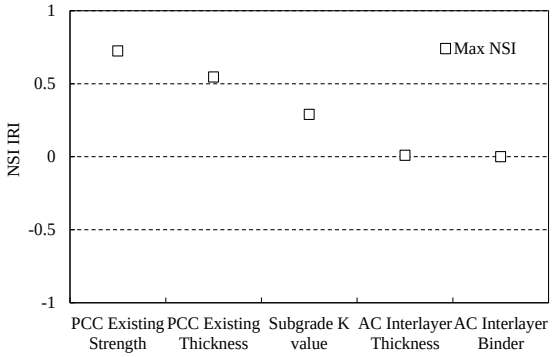

(d) IRI

Figure 4-8 NSI plots for CRCP over JPCP

4.2.7 CRCP over CRCP

Table 4-20 presents the range of existing pavement inputs specific to this rehabilitation option. The base case traffic and pavement structure information are presented in Table 4-21.

Table 4-20 Input variable values for CRCP over CRCP pavement

Input variable	Min	Base case	Max
Existing thickness (in)	7	8	10
Existing strength (psi)	2,000,000	3,000,000	5,000,000
Base thickness (in)	2	5	10
Base Poisson's ratio	0.25	0.35	0.4
Base resilient modulus (psi)	20000	25000	30000
Subgrade modulus (psi)	8000	13000	13500
Rehab k-value (psi/in)	50	200	300

Table 4-21 Base case values for CRCP over CRCP pavement analysis

Site factors		
AADTT	20,000	
Other traffic data	Level 1: Statewide averages	
Climate	Lansing	
Layer properties		
Structure (layers)	Material	Thickness (in)
1 - Surface layer	CRCP	8
2 - HMA interlayer	HMA	2
3 - Existing pavement	PCC CRCP	8
4 - Base	Crushed stone	5
5 - Subgrade	A-4	semi-inf

Table 4-22 shows the NSI values for different performance measures and these values were plotted in Figure 4-9. Based on the preliminary analysis, none of the existing pavement inputs affect the predicted performance significantly based on the NSI values. More detailed analysis is required to analyze the effect the existing pavement has on the predicted performance of the rehabilitated pavement because of the probable interaction between different inputs.

Table 4-22 Summary of NSI values for each design input for CRCP over CRCP pavements

Input Value	Crack With	Crack LTE	Punchouts	IRI
	Max NSI	Max NSI	Max NSI	Max NSI
Existing Thickness	0.01	0.00	0.01	0.00
Existing Strength	0.00	0.06	0.01	0.00
Base thickness	0.00	0.00	0.00	0.00
Base Poisson's Ratio	0.00	0.00	0.00	0.00
Base Resilient Modulus	0.00	0.00	0.00	0.00
Subgrade Modulus	0.02	0.00	0.00	0.00
Rehab k-value	0.04	0.01	0.00	0.00

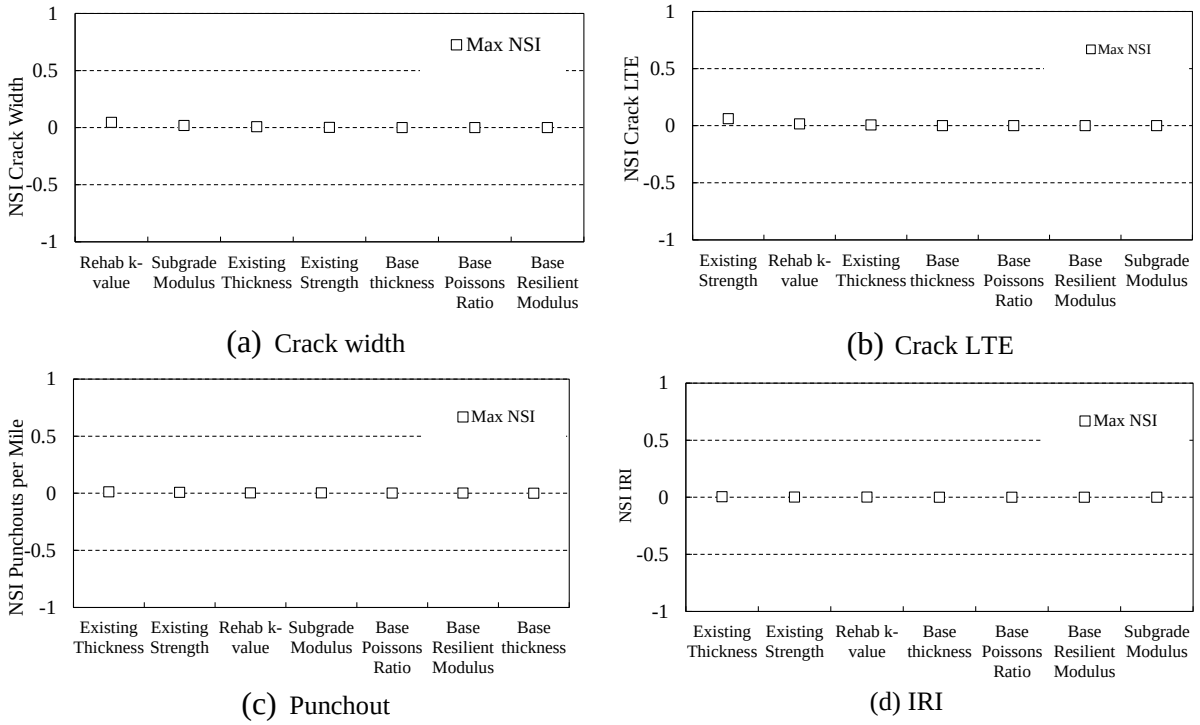

(a) Crack width (b) Crack LTE

(c) Punchout (d) IRI

Figure 4-9 NSI plots for CRCP over CRCP

4.2.8 Summary of Results

Table 4-23 summarizes the significant inputs from the preliminary sensitivity analyses for each rehabilitation option. These inputs only characterize existing pavement. The results show that existing surface layer thickness and existing pavement structural capacity are the most important inputs for all rehabilitation options. Table 4-24 presents the input levels to characterize the existing surface layer structural capacity. It should be noted that only level 3 inputs were used in the preliminary sensitivity analysis. Further, some of these inputs related to existing layer were not significant based on the preliminary sensitivity; however, those were retained in the analysis for investigating interactions in the subsequent analyses. Since, the preliminary sensitivity was conducted only for inputs related to the existing layers, it is

necessary to investigate their potential interactions with inputs related to the overlay layer. The following insignificant input variables were retained for the detailed sensitivity analysis:

- Rubblized (existing PCC thickness and elastic modulus)
- Composite (Existing PCC flexural strength)
- Unbonded overlay (existing PCC modulus)

Table 4-23 List of significant inputs from preliminary sensitivity analysis

Rehabilitation option	Significant inputs
HMA over HMA	Existing HMA condition rating Existing HMA thickness
Composite	Existing PCC thickness
Unbonded overlay	Existing PCC thickness
CRCP over HMA	Existing HMA thickness
CRCP over JPCP	Existing PCC thickness Existing PCC strength Subgrade k-value

Note: For rubblized rehabilitation option, no input was significant based on the preliminary sensitivity

Table 4-24 Inputs levels for characterizing existing pavement

Rehabilitation option	Input levels for characterizing existing condition
HMA over HMA	Existing HMA condition • Level 1: NDT Modulus, frequency, temperature • Level 2: Milled thickness, fatigue cracking, rut depth • Level 3: Pavement condition rating, milled thickness, total rut depth
Composite	Strength inputs • Level 1: Existing PCC modulus of rupture or elastic modulus • Level 2: Compressive strength • Level 3: MOR, or compressive strength or elastic modulus from historical records Percent of distressed slabs before restoration Percent of distressed slabs after restoration
Rubblized	Existing rubblized PCC elastic modulus
Unbonded overlay	Existing PCC thickness

4.3 DETAILED SENSITIVITY ANALYSIS

Section 4.2 presented the results and findings of the preliminary sensitivity analyses for various rehabilitation options. The main purpose of the analyses was to identify significant input variables related to the existing pavement layers materials and condition. Since the performance prediction models for rehabilitation module are similar to those for new designs, it can be concluded that the significant input variables related to the overlay (i.e. the new layer) are similar to those for a new pavement design. Such significant inputs were identified in the previous MDOT study (*1*) for both flexible and rigid pavements. Therefore, in the detailed sensitivity both types of input variables (for existing and new (overlay) pavements) were considered to identify the important main and interaction effects.

In the detailed sensitivity analysis, a full factorial design matrix was considered and includes several inputs related to existing and overlay layers for each rehabilitation option. The factorial matrices were used to generate pavement scenarios for various MEPDG runs. These runs were executed to capture pavement performance curves .The predicted performance measures at 20 years were used to conduct Analysis of Variance (ANOVA). In this analysis all main effects and possible two-way interactions were considered between input variables. Once all the desired MEPDG runs were accomplished, a database was prepared to evaluate the impact of input variables on various pavement performance measures. The detailed statistical analyses were conducted for each predicted performance measure. Two levels (values) were considered for each input and these levels were based on the ranges from the preliminary sensitivity analysis and the previous MDOT study (*1, 2*).

ANOVA was performed on the performance data at 20 years for each distress to: (a) obtain the design inputs main effects with some level of confidence, (b) explore the interactive effects between various input variables, (c) provide conclusions to distinguish between practical and statistical significance. The results of these for each rehabilitation option are discussed next.

4.3.1 HMA over HMA Analysis and Results

The input variables for HMA over HMA factorial matrix are summarized in Table 4-25. The full factorial matrix for HMA over HMA consists of 11 input variables at 2 levels each and a total of 2048 MEPDG runs (see Table A-3 in Appendix A). This list consists of the potential significant design inputs from preliminary sensitivity analysis as well as the significant inputs for new pavement design. Generally, full-factorial experiments such as the one considered in this study can be analyzed using fixed-effect models employing ANOVA. This type of statistical analyses can help identify the main and the interactive effects between variables. However, it should be noted that if certain variables are interacting with each other, their main effect alone should not be considered while making conclusions. Therefore, conclusions in this case will be based on the interactive effects. As an example, the summary results from ANOVA for longitudinal cracking at 20 years are given in Table 4-26. A *p-value* less than 0.05 (i.e. a confidence level of 95%) is used to identify a statistically significant effect. The highlighted rows are significant main or interactive effects of input variables. The ANOVA results for other distresses are presented in Appendix A.

The results show that for HMA over HMA, most of the main effects are significant while significant interactions differ for different distress types. It should be noted that interaction effects are critical in such analysis since the impact of one input variable can be

highly dependent on the value of another input variable. In addition, the significant interactions identified by ANOVA are based on statistics. However, in order to verify the practical significance of an effect, visual inspection combined with FHWA criteria (*6*) and engineering judgment was employed. For example, Figure 4-10 shows two interactions that are statistically significant based on ANOVA. However, as the plots indicate, only the interaction shown in Figure 4-10a is of practical significance. The results in the figure show that for a thin overlay, existing pavement condition has a significant effect on surface rutting while it may not be important in the case of a thick overlay. On the other hand Figure 4-10b shows no interaction between existing pavement thickness and overlay binder PG grading. In other words, existing thickness controls the difference in surface rutting irrespective of overlay binder PG.

Table 4-25 List and range of design inputs for HMA over HMA

No.	Input variables		Lower limit	Upper limit	Comments
1	Overlay thickness (inch) (OLTH)		2	8	This range might be larger than the typical overlay thickness used in Michigan; however a wider range is used for sensitivity purposes.
2	Overlay effective binder (% by volume) (OLEB)		7	14	Based on the report, "Evaluation of the 1-37A Design Process for New and Rehabilitated JPCP and HMA Pavement"
3	Overlay PG (OLPG)		PG 58-22	PG 76-28	Based on the MDOT mix types (tested in the Part 1 of this study), largest and smallest range is chosen
4	Overlay AV (%) (OLAV)		5	12	Based on the report, "Evaluation of the 1-37A Design Process for New and Rehabilitated JPCP and HMA Pavement"
5	Overlay aggregate gradation (%) (OLAGG)	3/4" sieve	100	100	Based on the MDOT mix types (tested in the Part 1 of this study)
		3/8" sieve	86.8	88.6	
		#4 sieve	79.2	73.2	
		passing # 200	5.6	4.9	
6	Existing condition rating (EXCON)		Very poor	Excellent	Two possible extremes of the MEPDG are selected
7	Existing HMA thickness (inch) (EXTH)		4	12	Considering the overlay thickness and previous MDOT study, this range is chosen
8	Existing base modulus (psi) (BMOD)		15000	40000	Based on the report, "Evaluation of the 1-37A Design Process for New and Rehabilitated JPCP and HMA Pavement"
9	Existing Sub-base modulus (psi) (SBMOD)		15000	30000	Based on the report, "Evaluation of the 1-37A Design Process for New and Rehabilitated JPCP and HMA Pavement"
10	Subgrade modulus (psi) (SGMOD)		2500	25000	Based on the report, "Evaluation of the 1-37A Design Process for New and Rehabilitated JPCP and HMA Pavement"
11	Climate		Pellston	Detroit	Based on the report, "Evaluation of the 1-37A Design Process for New and Rehabilitated JPCP and HMA Pavement"

Note: The shaded cells show the inputs related to the overlay layer.

Figures 4-11 to 4-13 show the FHWA criteria based on different performance measures. This criterion documents the analysis and findings of a study to identify the site conditions and design/construction features of flexible pavements that lead to good and poor pavement performance. Data from the Long-Term Pavement Performance (LTPP) pavement sections were used. Separate criteria were developed for each performance measure including roughness (IRI), rutting, and fatigue cracking. These criteria were used to obtain the practical significance of inputs for different performance measures. It should be noted that these

criteria are not available for longitudinal cracking. Table 4-27 summarizes performance criteria developed by the FHWA (*6*).

Table 4-26 HMA over HMA longitudinal cracking ANOVA Results

Source	Type III Sum of Squares	df	Mean Square	F	Sig.
Corrected Model	33374980919.535	56	595981802.135	221.480	.000
Intercept	23091314591.350	1	23091314591.350	8581.248	.000
OLTH	15332796877.727	1	15332796877.727	5698.010	.000
OLEB	368936830.134	1	368936830.134	137.105	.000
OLPG	3252647.869	1	3252647.869	1.209	.272
OLAV	1983679431.092	1	1983679431.092	737.180	.000
OLAG	2479152.113	1	2479152.113	.921	.337
EXCON	4477631784.047	1	4477631784.047	1663.988	.000
EXTH	3487966887.913	1	3487966887.913	1296.206	.000
BMOD	133832100.750	1	133832100.750	49.735	.000
SBMOD	236874.143	1	236874.143	.088	.767
SGMOD	878139393.840	1	878139393.840	326.336	.000
Climate	2752504.654	1	2752504.654	1.023	.312
EXCON * BMOD	60543223.968	1	60543223.968	22.499	.000
EXTH * BMOD	272603632.116	1	272603632.116	101.306	.000
OLAG * BMOD	474.686	1	474.686	.000	.989
OLAV * BMOD	1224265.290	1	1224265.290	.455	.500
OLEB * BMOD	2806218.200	1	2806218.200	1.043	.307
OLPG * BMOD	425157.258	1	425157.258	.158	.691
OLTH * BMOD	20966345.571	1	20966345.571	7.792	.005
BMOD * SBMOD	87689.129	1	87689.129	.033	.857
BMOD * SGMOD	1023030.126	1	1023030.126	.380	.538
EXCON * EXTH	535687513.647	1	535687513.647	199.073	.000
OLAG * EXCON	107406.276	1	107406.276	.040	.842
OLAV * EXCON	100875494.134	1	100875494.134	37.488	.000
OLEB * EXCON	10145350.215	1	10145350.215	3.770	.052
OLPG * EXCON	80696.258	1	80696.258	.030	.863
OLTH * EXCON	2796705580.783	1	2796705580.783	1039.318	.000
EXCON * SBMOD	9590125.087	1	9590125.087	3.564	.059
EXCON * SGMOD	389200.176	1	389200.176	.145	.704
OLAG * EXTH	345354.255	1	345354.255	.128	.720
OLAV * EXTH	323975489.726	1	323975489.726	120.397	.000
OLEB * EXTH	21408876.072	1	21408876.072	7.956	.005
OLPG * EXTH	20016069.524	1	20016069.524	7.438	.006
OLTH * EXTH	962088193.870	1	962088193.870	357.533	.000
EXTH * SBMOD	4405402.445	1	4405402.445	1.637	.201
EXTH * SGMOD	502947530.966	1	502947530.966	186.907	.000
OLAV * OLAG	32218.166	1	32218.166	.012	.913
OLEB * OLAG	1766.817	1	1766.817	.001	.980
OLPG * OLAG	26521.348	1	26521.348	.010	.921
OLTH * OLAG	231816.235	1	231816.235	.086	.769
OLAG * SBMOD	14.841	1	14.841	.000	.998
OLAG * SGMOD	6690.281	1	6690.281	.002	.960
OLEB * OLAV	140439906.866	1	140439906.866	52.191	.000
OLPG * OLAV	48273651.829	1	48273651.829	17.940	.000
OLTH * OLAV	420262650.377	1	420262650.377	156.179	.000
OLAV * SBMOD	1166039.157	1	1166039.157	.433	.510
OLAV * SGMOD	3038505.372	1	3038505.372	1.129	.288
OLEB * OLPG	36442959.078	1	36442959.078	13.543	.000
OLTH * OLEB	302338706.749	1	302338706.749	112.356	.000
OLEB * SBMOD	1017.653	1	1017.653	.000	.984
OLEB * SGMOD	4593425.563	1	4593425.563	1.707	.192
OLTH * OLPG	48360207.191	1	48360207.191	17.972	.000
OLPG * SBMOD	22047.638	1	22047.638	.008	.928
OLPG * SGMOD	15622114.522	1	15622114.522	5.806	.016
OLTH * SBMOD	73283.472	1	73283.472	.027	.869
OLTH * SGMOD	33878122.174	1	33878122.174	12.590	.000
SBMOD * SGMOD	16450.146	1	16450.146	.006	.938

Note: Shaded cells indicate a statistical significant effect.

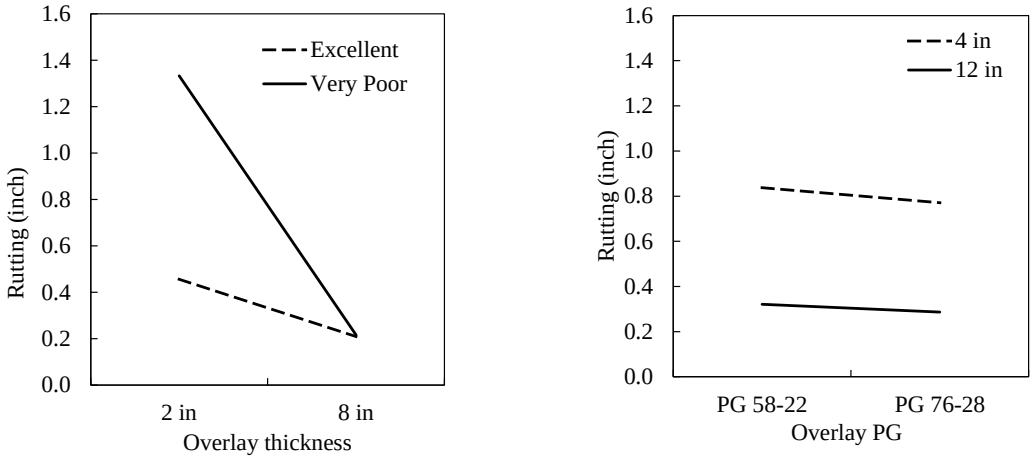

(a) Overlay thickness vs. existing pavement condition (↓)

(b) Overlay PG vs. existing pavement thickness

Figure 4-10 Interaction plots (a) overlay thickness and existing condition rating, (b) overlay PG and existing HMA thickness

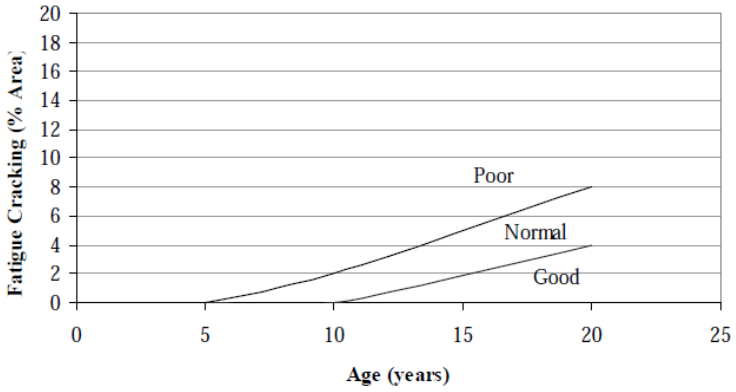

Figure 4-11 Pavement performance criteria for fatigue cracking (*6*)

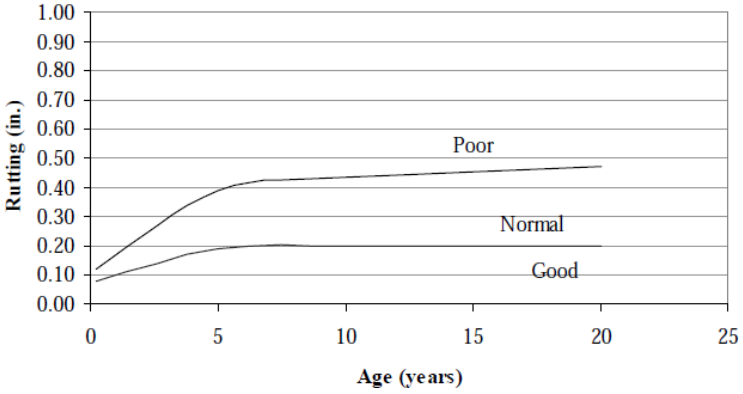

Figure 4-12 Pavement performance criteria for rutting (*6*)

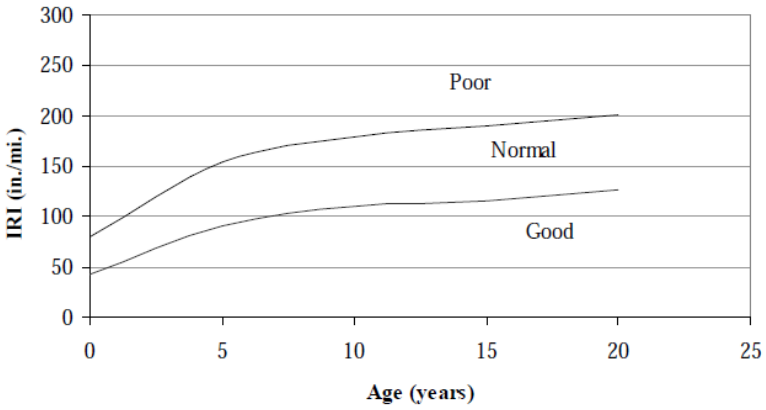

Figure 4-13 Performance criteria for IRI (*6*)

Table 4-27 Pavement performance criteria after 20 years – flexible pavements

Performance measure	Criteria after 20 years
Longitudinal cracking	500 ft/mile
Alligator cracking	4%
Rutting	0.3 in
IRI	75 in/mile

Table 4-28 summarizes the interactions that are of statistical and practical significance for HMA over HMA pavements. These interactions only involve existing pavement and overlay related inputs. Several important interactions were identified for HMA over HMA designs; however, this interdependence between variables varies among different distress types. The results of the sensitivity analyses show that the existing pavement condition rating and thickness for the HMA over HMA rehabilitation option are critical for all performance measures. In addition, several overlay layer related inputs interact with existing pavement properties. These interactions will have significant impact on the predicted pavement performance. Figure 4-14 shows examples for interpreting the interactions for any performance measure. Appendix A contains similar plots for all other performance measures within different rehabilitation options.

For example, higher percent air voids in the HMA overlay causes higher longitudinal and alligator cracking, and higher rutting and IRI, especially when the existing pavement condition is poor. The interaction between existing pavement condition and overlay effective binder content indicates that higher effective binder may reduce alligator cracking difference between poor and excellent existing pavement conditions. However, as expected, increases in the effective binder content cause an increase in surface layer rutting, especially when the existing pavement condition is poor. The overlay thickness will assist in reducing all the pavement distresses; this effect for the thicker HMA overlay is independent of the existing conditions.

The interaction between existing pavement thickness and overlay effective binder content indicates that higher effective binder may reduce both longitudinal and alligator cracking difference between thin and thick existing pavement. However, as expected, such increase in effective binder content will increase surface rutting, especially when the existing

pavement is thinner. A higher overlay thickness will assist in reducing all the pavement distresses.

Table 4-28 Summary of significant interactions (HMA over HMA) – Existing and overlay layers

Existing pavement inputs	Overlay inputs	Longitudinal cracking	Alligator cracking	Rutting	IRI
Existing pavement condition *(Very poor and excellent)*	Overlay air voids *(5% and 12%)*	↑	↑	↑	↑
	Overlay effective binder *(7% and 14%)*		↓	↑	↓
	Overlay PG *(PG 58-22 and PG 76-28)*		↑		
	Overlay thickness *(2in and 8in)*	↓	↓	↓	↓
Existing pavement thickness *(4in and 12in)*	Overlay air voids *(5% and 12%)*	↑		↑	
	Overlay effective binder *(7% and 14%)*	↓	↓	↑	
	Overlay PG *(PG 58-22 and PG 76-28)*	↑			
	Overlay thickness *(2in and 8in)*	↓	↓	↓	
Base modulus *(15000 psi and 40000 psi)*	Overlay thickness *(2in and 8in)*	↓			
Subgrade modulus *(2500 psi and 25000 psi)*	Overlay PG *(PG 58-22 and PG 76-28)*	↑			
	Overlay thickness *(2in and 8in)*	↓			

Note:

↓ Interaction is statistically and practically significant, and the difference in distress magnitude is higher at the lower level than the difference at the higher level of the input variables (see Figure 4-10).

↑ Interaction is statistically and practically significant, and the difference in distress magnitude is lower at the lower level than the difference at the higher level of the input variables.

The blank cell means no practically interaction exists. All interaction are shown graphically in Appendix A

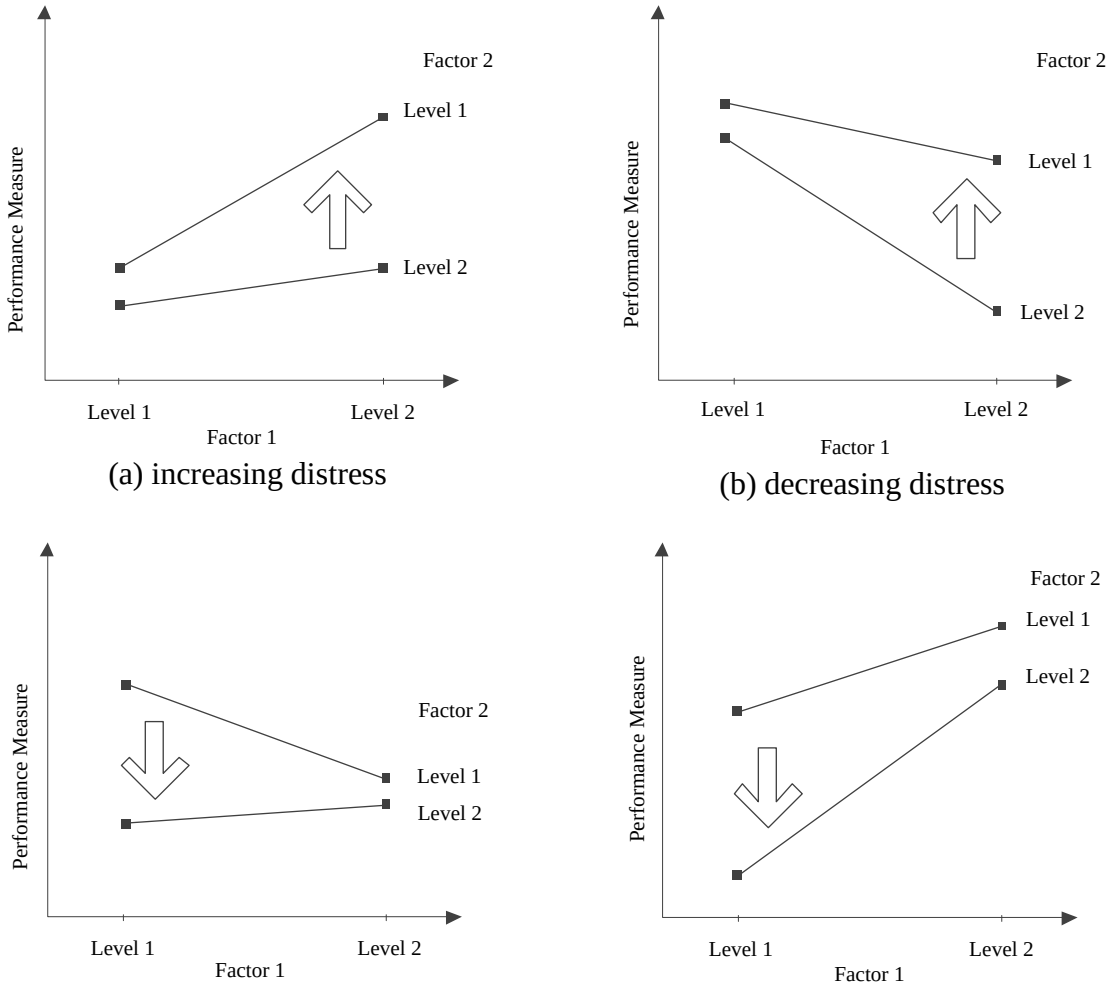

(a) increasing distress (b) decreasing distress

(c) decreasing distress (d) increasing distress

Figure 4-14 Interpretation of interactions for rutting

The interactions between the existing and overlay layer inputs were investigated and presented above. The interactions between the overlay design inputs are identical to the inputs for new pavement (as addressed in the previous MDOT study). In addition, the interactions between the existing pavement layer inputs may not be of practical importance because designer may not have a control on these inputs. However, possible interaction between inputs related to all layers (i.e., within overlay and within existing) were evaluated and are summarized in Table 4-29. For interaction between the inputs within existing layers, the results show that higher base modulus will reduce the impacts of existing condition and thickness on longitudinal cracking. Also, for thicker existing HMA layers, existing conditions will have higher impact on longitudinal cracking while for thinner existing HMA, existing conditions will have higher impact on alligator cracking and surface rutting. The higher subgrade modulus with thinner existing HMA layer has higher longitudinal cracking.

For interactions between the inputs within overlay layer, higher effective binder will have higher effect on longitudinal cracking for different air void levels while it has lower

effect on alligator cracking for different air void levels. Stiffer binder PG will have higher effect on longitudinal cracking for different overlay air voids and effective binder. Thicker overlay will have lower effect on longitudinal cracking for different overlay air void or effective binder. Thicker overlay will also have lower effect on alligator cracking and IRI for various effective binder levels. Finally, thicker overlay will have higher effect on longitudinal cracking for different levels of binder PG.

Table 4-29 Summary of significant interactions (HMA over HMA) – Within existing and within overlay layers

Interaction type	Longitudinal cracking	Alligator cracking	Rutting	IRI
Existing - Existing	BMOD * EXCON (↓)	BMOD * EXCON	BMOD * EXCON	EXCON * BMOD
	BMOD * EXTH (↓)	BMOD * EXTH	BMOD * EXTH	EXTH * BMOD
	EXCON * EXTH (↑)	EXCON * EXTH (↓)	EXCON * EXTH (↓)	EXCON * EXTH
	EXTH * SGMOD (↑)	EXCON * SGMOD	EXCON * SGMOD	
			EXTH * SBMOD	
			EXTH * SGMOD	
Overlay - Overlay	OLAV * OLEB (↑)	OLAV *OLEB (↓)	OLAV * OLEB	OLAV*OLEB (↓)
	OLAV * OLPG (↑)	OLAV * OLPG	OLEB * OLPG	OLAV * OLTH
	OLAV * OLTH (↓)	OLAV * OLTH	OLEB * OLTH	OLEB * OLTH (↓)
	OLEB * OLPG (↑)	OLEB * OLPG		
	OLEB * OLTH (↓)	OLEB * OLTH (↓)		
	OLPG * OLTH (↑)			

Note:
The interactions with an arrow are statistically and practically significance. The interactions without an arrow are only statistically significance. Blank cells indicate no statistically significant interaction exists.

4.3.2 Composite (HMA over JPCP) Pavement Analysis and Results

The input variables for composite factorial matrix are summarized in Table 4-30. The full factorial matrix consists of a total of 9 input variables at 2 levels each and a total of 512 MEPDG runs. The factorial matrix and the ANOVA tables for all the distresses are presented in Appendix A.

Based on the existing back-calculated results from LTPP database, an existing PCC elastic modulus of 3,000,000 psi is very low compared to the observed elastic moduli values for existing concrete pavements. However, as mentioned in Chapter 2, the maximum value of the existing PCC slab modulus is recommended to be 3,000,000 psi in the M-E PDG (MEPDG predictions become erratic when using a higher PCC modulus).

In order evaluate the operational (practical) importance; statistical significant interactions from ANOVA are assessed using the FHWA pavement performance criteria listed in Table 4-27. The performance difference within the levels of each input was compared with the values shown in the table. For example, in Figure 4-10a, the rutting difference between poor and excellent condition at 2-inch overlay thickness is 0.85-inch while for 8-inch overlay the difference is zero. Therefore, the total difference is 0.85-inch which is more than 0.3-inch as suggested in Table 4-27. Table 4-31 summarizes the interactions that are of statistical and practical significance for HMA over JPCP. Existing

PCC elastic modulus and thickness are important in determining the performance of an HMA overlay over an intact JPCP. For a given existing condition of the existing pavement, HMA overlay volumetric properties, binder type and amount, and thickness may play an important role. Also HMA volumetrics, binder type and amount, and thickness can be carefully selected for the overlays to mitigate various distresses when the existing pavement is an intact JPCP.

Table 4-30 List and range of design inputs for composite pavement

No.	Input variables		Lower limit	Upper limit	Comments
1	Overlay thickness (inch) (OLTH)		2	8	This range might be larger than the typical overlay thickness used in Michigan; however a wider range is used for sensitivity purposes
2	Overlay effective binder (% by volume) (OLEB)		7	14	Based on the report, "Evaluation of the 1-37A Design Process for New and Rehabilitated JPCP and HMA Pavement"
3	Overlay PG (OLPG)		PG 58-22	PG 76-28	Based on the MDOT mix types (being tested in this study), largest and smallest range is chosen
4	Overlay AV (%) (OLAV)		5	12	Based on the report, "Evaluation of the 1-37A Design Process for New and Rehabilitated JPCP and HMA Pavement"
5	Overlay aggregate gradation (%) (OLGRAD)	3/4" sieve	100	100	Based on the PG, the corresponding MDOT mix type and aggregate gradation are used
		3/8" sieve	86.8	88.6	
		#4 sieve	79.2	73.2	
		passing # 200	5.6	4.9	
6	Existing PCC thickness (inch) (EPCCTH)		7	11	Based on previous MDOT study
7	Existing PCC elastic modulus (psi) (EMOD)		500,000	3,000,000	The MEPDG limits the value of the existing pavement elastic modulus to ensure reliable results at 3,000,000 psi.
8	Subgrade reaction modulus (psi/in) (EK)		50	300	This input over-rides the calculation of the modulus of subgrade reaction. The lower bound value within the MEPDG is 50 and an upper value of 300 psi/in was selected
9	Climate		Pellston	Detroit	Based on previous MDOT study

Note: The shaded cells show the inputs related to the overlay layer

Table 4-31 Summary of significant interactions composite pavement

Existing pavement inputs	Overlay inputs	Longitudinal cracking	Alligator cracking	Rutting	IRI
Existing pavement modulus *(500000 psi to 3000000 psi)*	Overlay air voids *(5% and 12%)*	↑			
	Overlay thickness *(2in and 8in)*	↑			
Existing pavement thickness *(7 in to 11 in)*	Overlay air voids *(5% and 12%)*	↑			
	Overlay PG *(PG 58-22 and PG 76-28)*	↑			
	Overlay thickness *(2in and 8in)*	↑			
Climate *(Pellston and Detroit)*	Overlay air voids *(5% and 12%)*	↑			
	Overlay thickness *(2in and 8in)*	↑			

Note:

↓ Interaction is statistically and practically significant, and the difference in distress magnitude is higher at the lower level than the difference at the higher level of the input variables (see Figure 4-10).

↑ Interaction is statistically and practically significant, and the difference in distress magnitude is lower at the lower level than the difference at the higher level of the input variables.

The blank cell means no practically interaction exists. All interaction are shown graphically in Appendix A

Possible interactions between inputs related to all layers (i.e., within overlay and within existing) were evaluated and are summarized in Table 4-32. No practically significant interaction was found within the existing layer. Within the overlay layer, higher overlay air voids will have higher effect on longitudinal cracking for different overlay thicknesses. Also thicker overlay will have higher effect for different binder PGs. Finally, stiffer binder will have lower effect for different overlay air void levels.

Table 4-32 Summary of significant interactions (Composite) – Within existing and within overlay layers

Interaction type	Longitudinal cracking	Alligator cracking	Rutting	IRI
Existing - Existing	EXCON * BMOD		EMOD * EPCCTH	EMOD * EPCCTH
	EXTH * BMOD			
	EXCON * EXTH			
Overlay - Overlay	OLEB * OLAV		OLEB * OLAV	OLEB * OLAV
	OLTH * OLAV (↑)		OLGRAD * OLAV	OLGRAD * OLAV
	OLTH * OLEB		OLTH * OLAV	OLTH * OLAV
			OLPG * OLAV	OLPG * OLAV
	OLPG * OLTH (↑)		OLGRAD * OLEB	OLGRAD * OLEB
			OLTH * OLEB	OLTH * OLEB
	OLAV * OLPG (↓)		OLPG * OLEB	OLPG * OLEB
			OLTH * OLGRAD	OLTH * OLGRAD
			OLPG * OLGRAD	OLPG * OLGRAD
			OLTH * OLPG	OLTH * OLPG

Note:
The interactions with an arrow are statistically and practically significance. The interactions without an arrow are only statistically significance. Blank cells indicate no statistically significant interaction exists.

4.3.3 Rubblized (HMA over Fractured PCC) Pavement Analysis and Results

The input variables for the factorial matrix of HMA over fractured (rubblized) PCC pavement are summarized in Table 4-33. The full factorial matrix for rubblized designs contains a total of 8 input variables at 2 levels each and a total of 256 MEPDG runs. The factorial matrix and the ANOVA tables for all the distresses are presented in Appendix A.

Table 4-33 Input variable ranges for HMA over fractured JPCP

No	Input variables		Lower limit	Upper limit	Comments
1	Overlay thickness (inch) (OLTH)		2	8	This range might be larger than the typical overlay thickness used in Michigan; however a wider range is used for sensitivity purposes
2	Overlay effective binder (% by volume) (OLEB)		7	14	Based on the report, "Evaluation of the 1-37A Design Process for New and Rehabilitated JPCP and HMA Pavement"
3	Overlay PG (OLPG)		PG 58-22	PG 76-28	Based on the MDOT mix types (being tested in this study), largest and smallest range is chosen
4	Overlay AV (%) (OLAV)		5	12	Based on the report, "Evaluation of the 1-37A Design Process for New and Rehabilitated JPCP and HMA Pavement"
5	Overlay aggregate gradation (%) (OLAG)	3/4" sieve	100	100	Based on the PG, the corresponding MDOT mix type and aggregate gradation are used
		3/8" sieve	86.8	88.6	
		#4 sieve	79.2	73.2	
		passing # 200	5.6	4.9	
6	Existing PCC thickness (inch) (EPCCE)		7	11	Based on previous MDOT study
7	Existing PCC elastic modulus (psi) (EPCCTH)		35,000	1,500,000	The MEPDG limits the value of the existing pavement elastic modulus to ensure reliable results at 3,000,000 psi.
8	Climate		Pellston	Detroit	Based on previous MDOT study

Note: The shaded cells show the inputs related to the overlay layer

Table 4-34 summarizes the interactions that are of statistical and practical significance for the rubblized rehabilitation option. The existing PCC rubblized modulus and thickness are important in determining the performance of HMA overlay over rubblized JPCP. HMA volumetrics, binder type and amount, and thickness can be selected for the overlays to mitigate various distresses when the existing pavement is rubblized JPCP.

As shown in Table 4-34 and Appendix A, the results show that higher air voids in the HMA overlay will produce higher longitudinal and alligator cracking, especially for the weaker existing rubblized pavement. While higher rutting should be expected with higher air voids in the HMA layer, the impact of existing rubblized layer moduli is lower for rutting performance relative to other pavement performance measures. The overlay thickness will assist in reducing all the pavement distresses; this effect for the thicker HMA overlay is independent of the existing conditions.

Table 4-34 Summary of significant interactions (HMA over fractured JPCP)

Existing pavement inputs	Overlay inputs	Longitudinal cracking	Alligator cracking	Rutting	IRI
Existing pavement modulus *(35000 psi to 1500000 psi)*	Overlay air voids *(5% and 12%)*	↑	↑	↓	↑
	Overlay effective binder *(7% and 14%)*		↓	↓	↓
	Overlay PG *(PG 58-22 and PG 76-28)*	↑		↑	
	Overlay thickness *(2in and 8in)*	↓	↓	↓	↓
Existing pavement thickness *(7 in to 11 in)*	Overlay thickness *(2in and 8in)*	↑			

Note:

↓ Interaction is statistically and practically significant, and the difference in distress magnitude is higher at the lower level than the difference at the higher level of the input variables (see Figure 4-10).

↑ Interaction is statistically and practically significant, and the difference in distress magnitude is lower at the lower level than the difference at the higher level of the input variables.

The blank cell means no practically interaction exists. All interaction are shown graphically in Appendix A

Possible interactions between inputs related to all layers (i.e., within overlay and within existing) were evaluated and are summarized in Table 4-35. No practically significant interaction was found within overlay or within the existing layers.

Table 4-35 Summary of significant interactions (Rubblized) – Within existing and within overlay layers

Interaction type	Longitudinal cracking	Alligator cracking	Rutting	IRI
Existing - Existing	EPCCE * EPCCTH		EPCCE * EPCCTH	
Overlay - Overlay	OLTH * OLAV		OLTH * OLAG	OLEB * OLAV
	OLTH * OLPG		OLEB * OLAV	OLTH * OLAV
			OLPG * OLAV	OLTH * OLEB
			OLTH * OLAV	
			OLPG * OLEB	
			OLTH * OLEB	
			OLTH * OLPG	

Note:

The interactions with an arrow are statistically and practically significance. The interactions without an arrow are only statistically significance. Blank cells indicate no statistically significant interaction exists.

4.3.4 Unbonded PCC Overlay Analysis and Results

The input variables for unbonded PCC overlay factorial matrix are summarized in Table 4-36. The full factorial matrix for unbonded PCC overlay contains 9 input variables at 2 levels each and a total of 256 MEPDG runs. The factorial matrix and the ANOVA tables for all the distresses are presented in Appendix A.

Table 4-36 Input variable ranges for JPCP over JPCP (unbonded overlay)

No.	Input variable	Lower limit	Upper limit	Comments
1	Overlay PCC thickness (inch) (OLTH)	7	10	The minimum thickness for an unbonded concrete overlay within MEPDG is 7 inches. The upper bound was selected based on LTPP unbonded overlay thicknesses and to ensure that it is lower than the existing pavement layer
2	Overlay PCC CTE (per °F x 10^{-6}) (OLCTE)	4	7	The overlay PCC CTE was selected based on the values from the previous MDOT study
3	Overlay joint spacing (feet) (OLJS)	10	15	Joint spacing was selected based on MDOT's unbonded overlay joint spacing of 12 feet. 10 and 15ft were selected for the lower and upper bound values.
4	Overlay PCC MOR (psi) (OLMOR)	550	900	Based on typical values
5	Modulus of subgrade reaction, *k* (psi/in) (SGMOD)	50	300	This input over-rides the calculation of the modulus of subgrade reaction. The lower bound value within the MEPDG is 50 and an upper value of 300 psi/in was selected
6	Existing PCC thickness (inch) (EXTH)	7	11	Based on previous MDOT study
7	Existing PCC elastic modulus (psi) (EXMOD)	500,000	3,000,000	The MEPDG limits the value of the existing pavement elastic modulus to ensure reliable results at 3,000,000 psi.
8	Climate (CL)	Pellston	Detroit	Based on previous MDOT study

Note: The shaded cells show the inputs related to the overlay layer

For PCC overlay in this investigation, performance criteria developed by the FHWA (*7*), were modified to reflect MDOT practices and were used to ascertain the practical significance of an effect on cracking, faulting, and IRI. The details of modifying the performance criteria can be found elsewhere (*1*). Figure 4-15 shows the performance criteria for the PCC overlay performance measures and Table 4-37 summarizes the performance thresholds for practical significance.

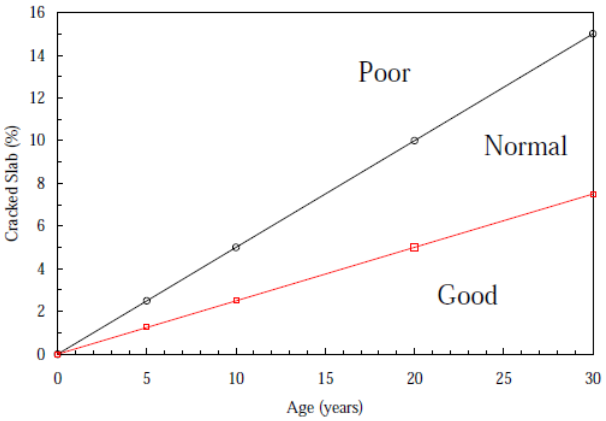

(a) Percent slab cracked

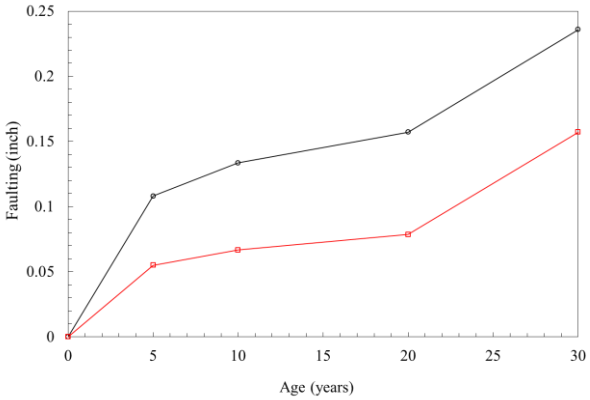

(b) Joint or crack faulting

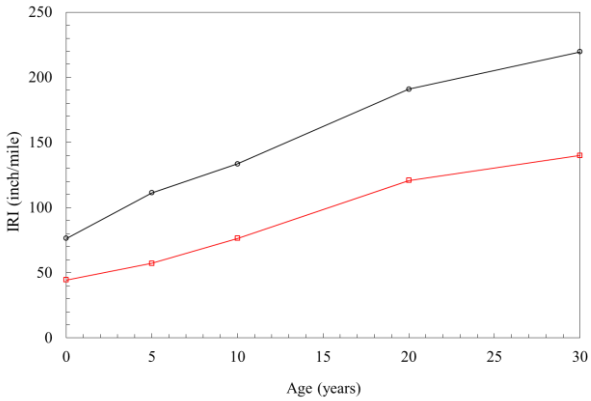

(c) Roughness in terms of IRI

Figure 4-15 Adopted performance criteria for JPCP (*7*)

Table 4-37 Pavement performance criteria after 20 years – Rigid pavements

Performance measure	Threshold after 20 years
Percent slabs cracked	5%
Faulting	2 mm
IRI	70 in/mile

The predicted performance data were analyzed using ANOVA and only the interactions between existing and overlay pavement layers were further investigated. The statistically significant results were further analyzed to determine the practical significance of the interaction. Table 4-38 summarizes the practically significant interactions for unbonded PCC overlay rehabilitation option.

The results of the sensitivity analyses show that the existing pavement condition (in terms of *E*) for unbonded overlays is critical for their cracking performance. Higher MOR and thickness of overlay will limit the cracking. However, if the existing foundation is weak, a better strategy to improve the unbonded overlay cracking performance would be to increase MOR and thickness and use concrete with lower CTE within the practical range used in Michigan.

Table 4-38 Interaction summary table (unbonded overlay)

Interactions and input values		Cracking	Faulting	IRI
Existing elastic modulus *(500,000 and 3,000,000 psi)*	Overlay MOR *(550 and 900 psi)*	↓		
	Overlay thickness *(7 and 9 in)*	↓		
	Overlay CTE *(4 and 7 per °F x 10^{-6})*			
	Overlay joint spacing *(10 and 15 ft)*			
Existing thickness *(9 and 11 in)*	Overlay MOR *(550 and 900 psi)*	↓		
	Overlay thickness *(7 and 9 in)*			
	Overlay CTE *(4 and 7 per °F x 10^{-6})*			
	Overlay joint spacing *(10 and 15 ft)*			
Modulus of subgrade reaction *(50 and 300 psi/in)*	Overlay MOR *(550 and 900 psi)*	↓		
	Overlay thickness *(7 and 9 in)*	↓		
	Overlay CTE *(4 and 7 per °F x 10^{-6})*	↓		
	Overlay joint spacing *(10 and 15 ft)*			

Note:
↓ Interaction is statistically and practically significant, and the difference in distress magnitude is higher at the lower level than the difference at the higher level of the input variables.
↑ Interaction is statistically and practically significant, and the difference in distress magnitude is lower at the lower level than the difference at the higher level of the input variables.

Possible interactions between inputs related to all layers (i.e., within overlay and within existing) were evaluated and are summarized in Table 4-39. Within the existing layer, for cracking, thicker existing PCC will have higher effect for various existing PCC moduli values while higher subgrade modulus will have lower effect in interacting with existing PCC modulus. Thicker overlays will lessen the effect of joint spacing, MOR and CTE on transverse cracking in unbonded overlays. The same effect can be verified while MOR is interacting with CTE and joint spacing. Finally, higher joint spacing will have higher effect on cracking for different levels of CTE.

Table 4-39 Summary of significant interactions (Unbonded overlay) – Within existing and within overlay layers

Interaction type	Cracking	Faulting	IRI
Existing - Existing	EXMOD * EXTH (↑)	EXMOD * EXTH	
	EXMOD * SGMOD (↓)	EXMOD * SGMOD	
Overlay - Overlay	OLCTE * OLJS (↑)	OLCTE * OLJS	OLCTE * OLJS
	OLCTE * OLMOR (↓)	OLCTE * OLMOR	OLTH * OLCTE
	OLCTE * OLTH (↓)	OLCTE * OLTH	OLJS * OLMOR
	OLJS * OLMOR (↓)	OLJS * OLMOR	OLTH * OLMOR
	OLJS * OLTH (↓)	OLJS * OLTH	
	OLMOR * OLTH (↓)	OLMOR * OLTH	

Note:
The interactions with an arrow are statistically and practically significance. The interactions without arrow are only statistically significance. Blank cells indicate no statistically significant interaction exists.

4.3.5 Summary Results

Only four of the seven rehabilitation options considered in preliminary sensitivity analysis were considered in the detailed sensitivity analyses based on the MDOT practices. This section evaluated the impact of various design inputs on the predicted performance for the three flexible pavement rehabilitation options. The detailed sensitivity analyses included the significant variables identified in OAT analyses in addition to the significant inputs previously identified for new pavement layers *(1)*. Full factorials were designed to determine statistically significant main and two-way interaction effects. The results of the sensitivity analyses show that the existing pavement condition rating and existing thickness for HMA over HMA overlays is critical for all performance measures. On the other hand, existing PCC modulus and thickness are important in determining the performance of HMA overlay over intact and rubblized JPCP. For a given condition of the existing pavement, HMA overlay volumetric properties, binder type and amount, and thickness may play an important role. In addition, HMA volumetrics, binder type and amount, and thickness can be carefully selected for the overlays to mitigate various distresses whether the existing pavement is intact or rubblized JPCP.

For unbonded overlays, the results of the sensitivity analyses show that the existing pavement condition (in terms of *E*) is critical for their cracking performance. Higher MOR and thickness of overlay will limit the cracking. However, if the existing foundation is weak, a better strategy to improve the unbonded overlay cracking performance would be to increase MOR, thickness and concrete with lower CTE.

The detailed sensitivity produced a list of important inputs for different rehabilitation options. However, more rigorous analysis was conducted in the next section; therefore, a list of significant inputs will be presented subsequently.

4.4 GLOBAL SENSITIVITY ANALYSIS

The overall goal of Global Sensitivity Analysis (GSA) is to determine sensitivity of pavement performance prediction models to the variation in the design input values. The main difference between GSA and detailed sensitivity analyses is the way the levels of an input are considered. While extreme values (only two levels) of the input ranges are considered in the detailed sensitivity analysis, GSA utilizes the entire domain for the input ranges. In this section, the details of the GSA process are presented first followed by the findings and discussion of results for the four rehabilitation options.

4.4.1 GSA Methodology

The process for GSA analysis involves various steps.

1. The first step is to define a base case for all the rehabilitation options. The base cases consist of the pavement cross-section, material properties and climate information. These base cases should cover the design practices and climatic conditions in the State of Michigan.
2. The second step is to determine the ranges of input variables in order to cover the entire problem domain.
3. The third step is to sample input combinations from the problem domain.
4. The fourth step includes generating the predicted performance to the sampled inputs from the third step.
5. The fifth step involves fitting response surface models (RSM) to the generated data in step four.
6. Finally, the sensitivity metric is determined for the fitted RSM to quantify the impact of input variables on predicted performance measures.

The details of the analysis related to all the above steps are presented next.

4.4.1.1. Base cases

Similarly to the previously described analyses, the GSA analysis was conducted on the rehabilitation options currently used in Michigan DOT practice; i.e., HMA over HMA, HMA over PCC (composite), HMA over rubblized PCC, and unbonded PCC overlay. Also two different weather stations (Pellston and Detroit) were used to represent the effect of climate in Michigan. The effect of traffic was evaluated in the previous MDOT studies (*2*, *8*, *9*); hence in this analysis, the traffic was held constant at a typical interstate traffic level. The eight base cases evaluated in this study are shown in Table 4-40.

Table 4-40 Base cases for global sensitivity analysis

Rehabilitation type	Climate
HMA over HMA	Pellston Detroit
Composite (HMA over PCC)	
HMA over Rubblized PCC	
Unbonded PCC overlay	

Figure 4-16 shows the climatic data for the two locations considered in the State of Michigan. It can be observed that these climates cover different ranges of temperatures and freezing indices.

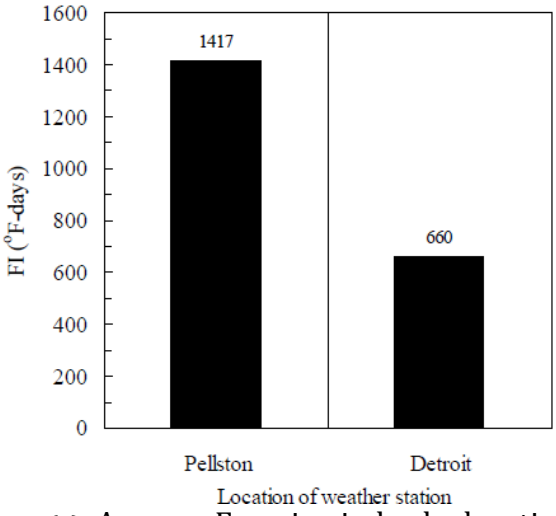

(a) Average Freezing index by location

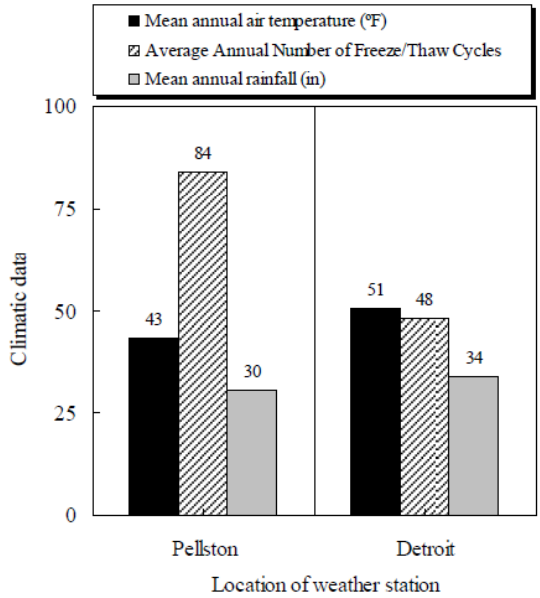

(b) Mean annual air temperature, number of F/T cycles and average precipitation by location

Figure 4-16 Summary of climatic properties by location within Michigan (*1*)

4.4.1.2. Design inputs

The MEPDG inputs represent a wide range of categories including traffic characterization, climatic data, and pavement structural and material information. Some of the inputs related to material characterization need special considerations. For example, characterizing existing pavement damage involves different input levels for the HMA over HMA rehabilitation option. Therefore, some decisions are needed to determine the specific input for the selected

level. The following section presents some of such cases for HMA over HMA rehabilitation option.

Characterizing HMA over HMA layer

HMA dynamic modulus (*E**) of the asphalt mixture is an input for level 1 characterization of the asphalt mixtures in the MEPDG. Details of *E** were presented and discussed in the Task 1 report of this study. In the *E** equation, α and δ are fitting parameters that determine the minimum and maximum values of *E**[δ represents the minimum value (lower shelf) for dynamic modulus and ($\alpha + \delta$) represents the maximum value (upper shelf)]. The level 1 characterization of *E** is preferred because it is a direct way of evaluating E*; i.e., no prediction or correlation is involved. However, several issues were encountered, which led the research team to use level 3 for HMA mixture characterization. This is explained below.

Equations 1 to 3 show the *E** prediction model in the MEPDG (*5*).

$$log(E^*) = \delta + \frac{\alpha}{1 + e^{\beta + \gamma \log(t_r)}} \quad (1)$$

$$\alpha = 3.871977 - 0.0021\rho_4 + 0.003958\rho_{38} - 0.000017\rho^2_{38} + 0.005470\rho_{34} \quad (2)$$

$$\delta = 3.750063 + 0.02932\rho_{200} - 0.001767\rho^2_{200} - 0.002481\rho_4 - 0.058097V_a - 0.802208\left[\frac{Vb_{eff}}{V_{beff} + V_a}\right] \quad (3)$$

where,

ρ_4 = cumulative % retained on No. 4 sieve.

ρ_{200} = % passing the No. 200 sieve.

ρ_{38} = cumulative % retained on 3/8 in sieve.

ρ_{34} = cumulative % retained on ¾ in sieve.

V_{beff} = effective bitumen content, % by volume.

V_a = air void content, %

From Equation 3 it can be seen that there is a strong correlation between δ , % air voids and % binder content. In GSA, an Artificial Neural Network (ANN) is used to predict the pavement performances. However, having independent variables which are correlated should not be considered together because of collinearity concerns. In addition, it is not possible to run ANN without including % air voids and % effective binder because these variables are further used in the cracking transfer function to predict cracking. Therefore, to characterize the asphalt mixture, level 3 inputs (aggregate gradation and asphalt volumetric properties) were used instead of mixture master-curves.

Characterizing the existing HMA layer

For level 1 input for characterizing the existing pavement structural capacity, HMA back-calculated modulus is required to measure the current damage. The overall procedure for damage calculations and existing pavement characterization for different rehabilitation levels is summarized in Chapter 2. However, to clarify the possible relationship between level 1 and

level 3 rehabilitation levels, the amount of overlay cracking was obtained using the MEPDG for these levels. In this exercise, the permanent deformation input was kept constant while the pavement condition rating was varied to determine the corresponding back-calculated modulus to produce the same amount of cracking. Thin (3 in) and thick (6 in) overlays were used for the comparison and the results are shown in Figures 4-17 and 4-18. The results show that each pavement condition rating corresponds to a specific range of the existing HMA back-calculated moduli. For example, very poor condition rating for an existing pavement corresponds to 250 ksi modulus as both rehabilitation levels exhibited the same amount of longitudinal and alligator cracking regardless of the overlay thickness. On the other hand, a modulus of 600 ksi for existing HMA yielded the same amount of cracking similar to excellent pavement condition rating. Based on these results, it is possible to relate the level 3 existing pavement condition ratings with the level 1 back-calculated moduli of the existing HMA layer. Therefore, in this study level 3 rehabilitation was utilized in all analyses. Also, if there is a fair estimate of the existing pavement modulus, level 3 (pavement condition rating) can be used instead of the level 1 (back-calculated modulus).

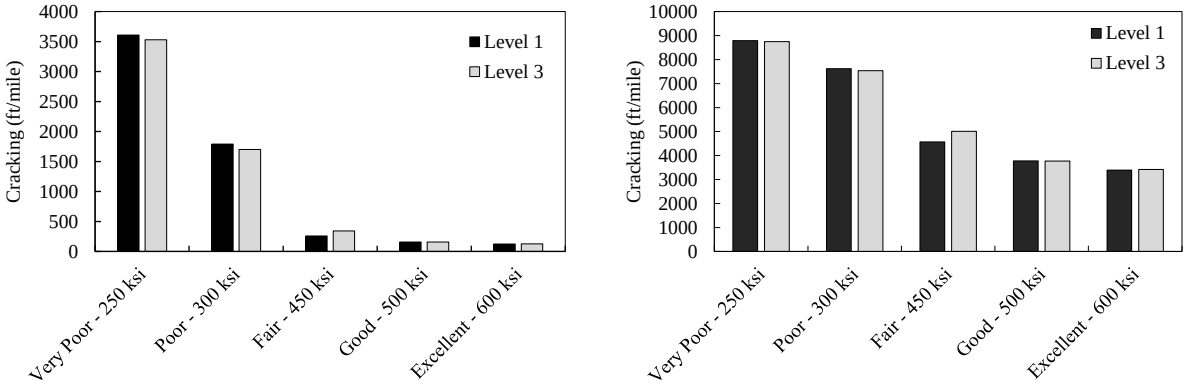

(a) Longitudinal cracking for 6 in overlay (b) Longitudinal cracking for 3 in overlay

Figure 4-17 Comparison between levels 1 and 3 rehabilitation for longitudinal cracking

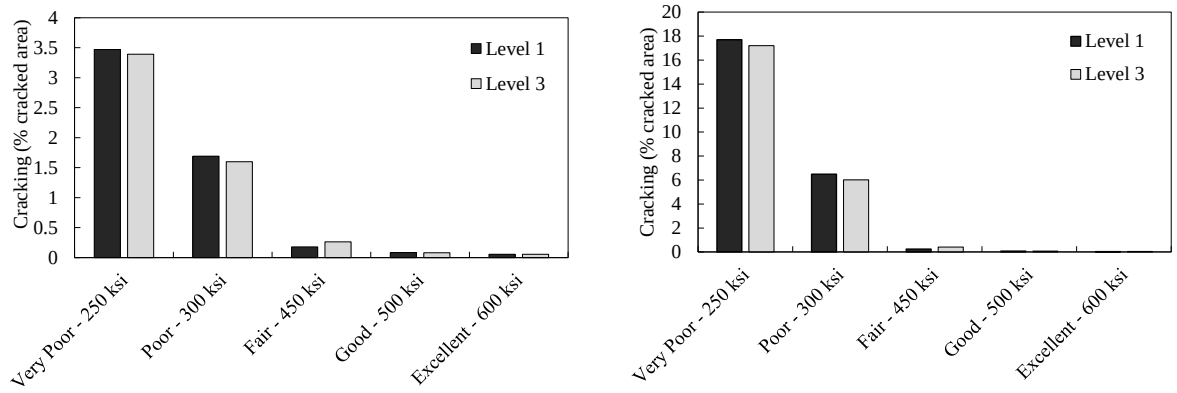

(a) Fatigue cracking for 6 in overlay (b) Fatigue cracking for 3 in overlay

Figure 4-18 Comparison between levels 1 and 3 rehabilitation for fatigue cracking

Rehabilitation options design inputs and ranges

The results of the preliminary sensitivity analysis were used here to determine the potentially significant inputs for different rehabilitation options. The final list of design inputs and their ranges were finalized with MDOT. Tables 4-41 to 4-44 summarize the design inputs, their ranges, and the baseline values for all rehabilitation options considered in this study. For the one-at-a-time (OAT) sensitivity analysis, the value of each input variable was varied over its entire range (from lower to upper limits) while all other input variables were held constant at their baseline values.

Table 4-41 List of design inputs for HMA over HMA

No.	Input variables		Baseline values	Lower limit	Upper limit
1	Overlay thickness (inch)		5	2	8
2	Overlay effective binder (% by volume)		10.5	7	14
3	Overlay PG		PG 58-22[1]	PG 58-22	PG 76-28
4	Overlay AV (%)		8.5	5	12
5	Overlay aggregate gradation (%)	3/4" sieve	100	100	100
		3/8" sieve	88.6	86.8	88.6
		#4 sieve	73.2	79.2	73.2
		passing # 200	4.9	5.6	4.9
6	Existing condition rating		Poor	Very poor	Excellent
7	Existing HMA thickness (inch)		8	4	12
8	Existing base modulus (psi)		27500	15000	40000
9	Existing Sub-base modulus (psi)		20000	15000	30000
10	Subgrade modulus (psi)		13750	2500	25000
11	Climate		Pellston[2]	Pellston	Detroit

Table 4-42 List of design inputs for composite

No.	Input variables		Baseline values	Lower limit	Upper limit
1	Overlay thickness (inch)		5	2	8
2	Overlay effective binder (% by volume)		10.5	7	14
3	Overlay PG		PG 76-28	PG 58-22	PG 76-28
4	Overlay AV (%)		8.5	5	12
5	Overlay aggregate gradation (%)	100	100	100	100
		88.6	86.8	86.8	88.6
		73.2	79.2	79.2	73.2
		4.9	5.6	5.6	4.9
6	Existing PCC thickness (inch)		9	7	11
7	Existing PCC MOR (psi)		650	550	900
8	Subgrade reaction modulus (psi/in)		175	50	300
9	Climate		Detroit	Pellston	Detroit

[1] Only two levels for PG were considered; therefore, the baseline value is identical to the lower limit.
[2] Pellston was used as a baseline in this case.

Table 4-43 List of design inputs for HMA over fractured JPCP (Rubblized)

No.	Input variables		Baseline values	Lower limit	Upper limit
1	Overlay thickness (inch)		5	2	8
2	Overlay effective binder (% by volume)		10.5	7	14
3	Overlay PG		PG 76-28	PG 58-22	PG 76-28
4	Overlay AV (%)		8.5	5	12
5	Overlay aggregate gradation (%)	3/4" sieve	100	100	100
		3/8" sieve	86.8	86.8	88.6
		#4 sieve	79.2	79.2	73.2
		passing # 200	5.6	5.6	4.9
6	Existing PCC thickness (inch)		9	7	11
7	Existing PCC elastic modulus (psi)		100000	35,000	1,500,000
8	Climate		Detroit	Pellston	Detroit

Table 4-44 List of design inputs for JPCP over JPCP (unbonded overlay)

No.	Input variable	Baseline values	Lower limit	Upper limit
1	Overlay PCC thickness (inch)	9	7[1]	10
2	Overlay PCC CTE (per °F x 10^{-6})	5.5	4	7
3	Overlay joint spacing (feet)	15	10	15
4	Overlay PCC MOR (psi)	650	550	900
5	Modulus of subgrade reaction, *k* (psi/in)	175	50	300
6	Existing PCC thickness (inch)	9	7	11
7	Existing PCC elastic modulus (psi)	3000000	500,000	3,000,000
8	Climate	Detroit	Pellston	Detroit

[1]The minimum thickness for an unbonded concrete overlay within MEPDG is 7 inches. The upper bound was selected based on LTPP unbonded overlay thicknesses and to ensure that it is lower than the existing pavement layer.

4.4.1.3. Sampling from the problem domain

The Latin Hypercube Sampling (LHS) method is a powerful technique that can be used to generate stratified random samples within the range of all design inputs covering the entire problem domain. The LHS is a statistical method for generating samples of plausible collections of parameter values from a multidimensional distribution. Generally, the method is commonly used to reduce the number of runs necessary for a Monte Carlo simulation to achieve a reasonably accurate random distribution as shown graphically in Figure 4-19. In this Figure, x_1 and x_2 are two input parameters which form a two dimensional problem domain. In order to cover the entire domain shown in Figure 4-19a, Monte Carlo and LHS are used separately. For this example, Monte Carlo needs 100 samples (Figure 4-19b) while the LHS requires 25 samples (Figure 4-19c) to cover the same problem domain thus LHS significantly improves the efficiency yet maintaining similar accuracy. The LHS can be incorporated into an existing Monte Carlo model fairly easily, and works with variables having any probability distribution.

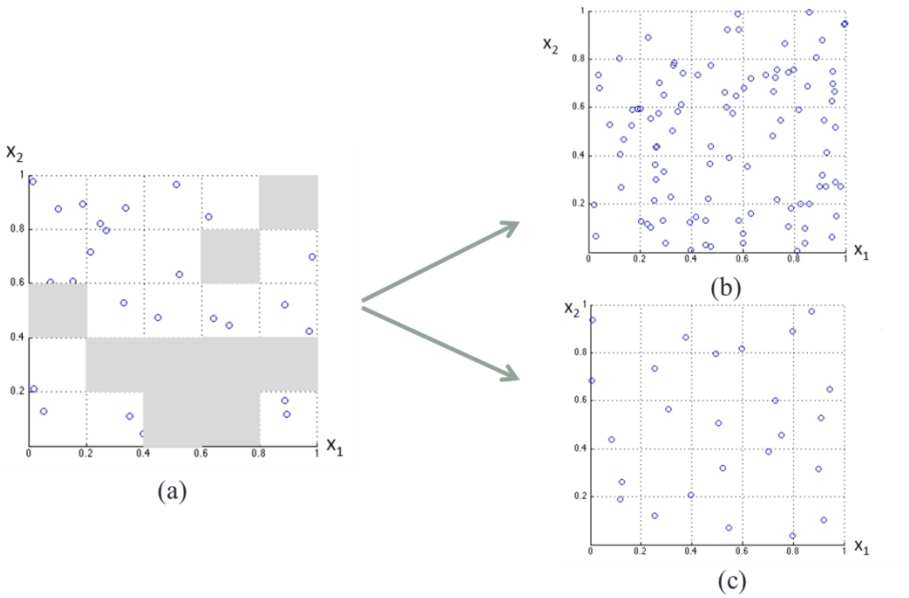

Figure 4-19 Comparison between Monte Carlo and LHS simulations

Figure 4-20 shows two design inputs (x_1 and x_2) with minimum value of zero and maximum value of a and b, respectively. For example if 3 samples are required, each input parameter range is divided into 3 equal intervals forming a square grid containing sample positions if (and only if) there is only one sample in each row and each column (which is referred as Latin Square as shown in Figure 4-20a). The concept can be extended for more design inputs by generalizing of Latin Square to an arbitrary number of dimensions (for e.g., 3 inputs as shown in Figure 4-20b), whereby each sample is the only one in each axis-aligned hyper-plane. By using this method, a fewer number of simulations are needed to adequately cover the domains of all inputs.

Once LHS sample combinations of all input variables are determined, they can be used as inputs in the MEPDG to obtain the predicted pavement performance over time. The number of required MEPDG runs is dependent on the number of design inputs used to generate LHS samples. Based on a limited parametric investigation performed in the NCHRP report 1-47 (*3*), the sufficient number of MEPDG runs to obtain stable results for GSA should be at least 20K (where K is the number of design inputs for each rehabilitation option). However, in this study, to increase the reliability of the networks predictions and accuracy, 30K simulations were used. These simulations cover the entire range of the problem domain, which means all the possible inputs combinations are considered. Table 4-45 shows the total number of the MEPDG runs needed for different rehabilitation options. As an example, Table 4-46 shows a portion of the randomly generated sample using LHs for the HMA over JPCP fractured.

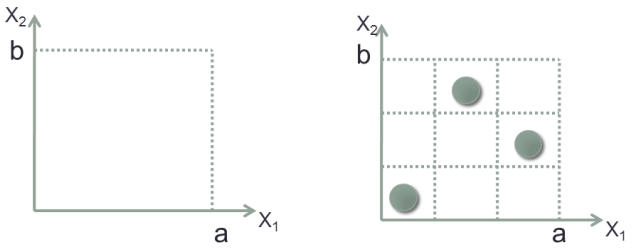

(a) Latin Square

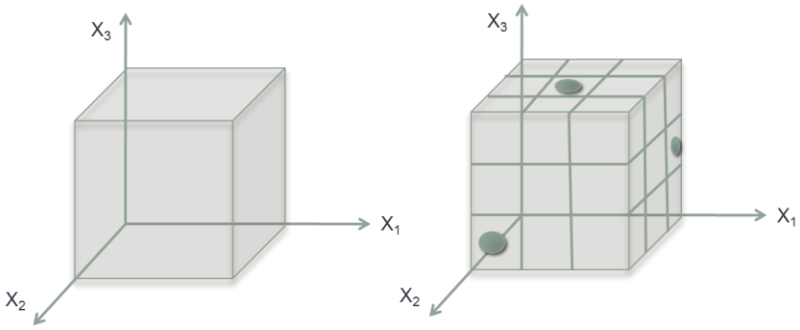

(b) Latin Cube

Figure 4-20 Example of sampling in LHS method

Table 4-45 Required number of simulations

Rehabilitation type	Number of inputs	Number of runs
HMA over HMA	11	330
HMA over PCC (Composite)	9	270
HMA over Rubblized PCC	8	240
Unbonded PCC overlay	8	240

Table 4-46 Generated samples for HMA over JPCP fractured

Run	Overlay Thickness	Overlay Effective Binder	Overlay PG	Overlay Air Voids	Overlay Aggregate	Existing Thickness	Existing Thickness	Climate
1	3.188	12.952	PG 76-28	6.489	Coarse	9.636	50924	Pellston
2	5.585	10.358	PG 76-28	11.371	Coarse	10.903	683920	Detroit
3	7.118	10.002	PG 76-28	5.864	Coarse	10.794	412611	Pellston
.	.	.	.	.	.	.	.	.
.	.	.	.	.	.	.	.	.
236	7.587	13.136	PG 58-22	7.946	Coarse	7.498	949310	Pellston
237	3.933	10.191	PG 76-28	5.298	Coarse	9.244	499617	Pellston
238	3.634	11.373	PG 58-22	10.032	Fine	7.691	475511	Detroit
239	6.086	7.794	PG 76-28	6.936	Coarse	8.153	142600	Pellston
240	7.703	11.393	PG 76-28	8.179	Coarse	9.332	1249368	Pellston

4.4.1.4. Response surface models (RSM)

The LHS generated input combinations (which are essentially random MEPDG design input scenarios) were used to make the MEPDG input files. The pavement performance prediction results were obtained after executing these input files using the MEPDG (version1.1). These results were used to provide a continuous surface of pavement performance at discrete locations in the problem domain. However, to obtain continuous performance measures other than the predefined discrete locations, a continuous surface should be fitted on these discrete points. Therefore, Artificial Neural Network (ANN) fitting tools were used to fit continuous surfaces. ANN consists of an interconnected group of artificial neurons, and it processes information using a connectionist approach for computation. Neural networks are used to model complex relationships between inputs and outputs or to find patterns in data. The ANN can be viewed as a nonlinear regression model except that the functional form of the fitting equation does not need to be specified necessarily (*3*). Subsequently, the RSMs estimated by using ANN were utilized to calculate sensitivity of different design inputs using the sensitivity metric called Normalized Sensitivity Index (NSI).

4.4.1.5. Sensitivity metric

The NSI can be used for a point estimation of sensitivity across a problem domain. The point-normalized sensitivity index S_{ijk} is defined as:

$$S_{ijk} = \left.\frac{dy_j}{dx_k}\right|_i \frac{x_{ki}}{y_{ji}} \tag{4}$$

where,

x_{ki} is the value of input *k* at point *i*

y_{ji} is the value of distress *j* at point *i*

$\left.\frac{dy_j}{dx_k}\right|_i$ is change of distress j with respect to change in input k at point i

Equation (4) can be simplified to:

$$S_{ijk} = \left.\frac{\frac{dy_j}{y_j}}{\frac{dx_k}{x_k}}\right|_i \tag{5}$$

Equation (5) shows that the sensitivity index is a ratio between rates of change in performance measure and design input. In some cases, predicted distress, y_{ji} is close to zero resulting in an artificially large sensitivity. Therefore, to overcome this problem S_{ijk} can be

normalized with the design limit for a distress. The final formula for sensitivity index is as follows (*3*):

$$NSI = S_{ijk}^{DL} = \frac{\Delta y_{ji}}{\Delta x_{ki}} \times \frac{x_{ki}}{DL_j} \tag{6}$$

where,

NSI is normalized sensitivity index for design limit at point i for distress j and input k

Δy_{ji} is change in distress *j* about point *i*

Δx_{ki} is change in input *k* about point *i*

x_{ki} is the value of input *k* at point *i*

DL_j is the design limit for distress *j*

The NSI was calculated using Equation (6) for most of the cases. However, for discrete design inputs (for e.g., climate, condition rating, PG grade etc.), a modified equation was implemented to determine the sensitivity index. Equation (7) still considers the design limit as reference for predicted distress; it normalizes the change in the performance with respect to the specified design limit for a certain distress if the design input is changed by one category. For example, if by changing PG grade from PG 58-22 to PG 76-28 rutting changes by 0.7 inches while all other inputs are held constant, the NSI for rutting will be 0.7/0.5=1.4. It should be noted that the difference in the predicted performance between categories should be higher than the threshold to obtain NSI greater than 1 to consider the input as significant.

$$NSI = \left. \frac{\Delta y_{ji}}{DL_j} \right|_{\Delta X_{ki} = 1 category} \tag{7}$$

The NSI for IRI also needs special attention because the lower bound for IRI is non-zero. The NSI formula for IRI when the design limit is 172 inch/mile and the initial IRI is 63 inch/mile is expressed in Equation (8). This equation was proposed in the NCHRP 1-47 study for performing the sensitivity analysis.

$$NSI = \frac{IRI - 63}{172 - 63} \tag{8}$$

The NSI can be interpreted as:

- If NSI=0, then there is no change in performance with respect to the change in input,
- If NSI=1, then the rates of change in performance and input are the same,
- If NSI >1, the performance rate of change is faster than the rate of change in the input.

The NSI interpretation is for OAT analysis, and only explains the main effect of an input on a given distress measure. Therefore, there was a need to explain the interactive effect of two variables for evaluating the joint effect of variables. Equations (9) and (10) were developed to evaluate NSI of an interaction where Equation (11) shows the numerical solution for Equation (10).

$$S_{ijklm}\Big|_{(i,j)} = \frac{\partial^2 y^m}{\partial x^k \partial x^l} \times \frac{x^k x^l}{y^m}\Bigg|_{(i,j)} \tag{9}$$

$$NSI^{DL}_{ijklm}\Big|_{(i,j)} = \frac{\partial^2 y^m}{\partial x^k \partial x^l} \times \frac{x^k x^l}{DL^m}\Bigg|_{(i,j)} \tag{10}$$

$$NSI = S^{DL}_{ijklm}\Big|_{(i,j)} = \frac{x_i^k \times x_j^l}{\Delta x_i^k \times \Delta x_j^l} \times \frac{y^m{}_{x^k{}_{i+1},x^l{}_{j+1}} - y^m{}_{x^k{}_{i},x^l{}_{j+1}} - y^m{}_{x^k{}_{i+1},x^l{}_{j}} + y^m{}_{x^k{}_{i},x^l{}_{j}}}{DL^m} \tag{11}$$

where,

$S^{DL}_{ijklm}\Big|_{(i,j)}$ = sensitivity index for input *k* and *l*, distress *m*, at point (*i,j)* with respect to design limit (DL)

x_i^k = value of input x^k at point *i*

x_j^l = value of input x^l at point *j*

Δx_i^k = change in input x^k around point *i* $\left(x^k{}_{i+1} - x^k{}_{i-1}\right)$

Δx_j^l = change in input x^l around point *j* $\left(x^l{}_{j+1} - x^l{}_{j-1}\right)$

$y^m{}_{x^k{}_i,x^l{}_j}$ = value of distress *m*, for input x^k at point *i* and input x^l at point *j*

DL^m = design limit for distress *m*

4.4.1.6. Distress thresholds for GSA

The NSI calculation involves the design limit (threshold value) for each distress type. Tables 4-47 and 4-48 summarize recommended threshold values for various performance measures from the NCHRP Report 1-47(*3*) and MEPDG manual of practice (*10*), respectively . It should be noted that practically, the distress threshold values depend on the road class, and may vary among agencies based on their practices. Finally, Table 4-49 summarizes the threshold values adopted in this study based on discussions with MDOT (January 7, 2013).

Table 4-47 Recommended threshold values for performance measures—NCHRP 1-47

Pavement type	Performance measure	Threshold	Reference
Flexible	Alligator cracking	25%	1-47 NCHRP
	Longitudinal cracking	2000 ft/mile	
	Surface rutting	0.75 in	
	IRI	172 in/mile	
Rigid (JPCP)	% Slab cracked	15%	
	Faulting	0.12 in	
	IRI	172 in	
Rigid (CRCP)	Crack width	20 mils	
	Crack LTE	75%	
	Punchouts	10/mile	
	IRI	172 in/mile	

Table 4-48 Recommended threshold values for performance measures—AASHTO

Pavement type	Distress	Threshold	Reference
Flexible (New & Overlay)	Alligator cracking	I=10% P=20% S=35%	AASHTO manual of practice
	Surface rutting	I=0.4 inch P=0.5 inch S=0.65 inch	
	IRI	I=160 inch/mile P=200 inch/mile S=200 inch/mile	
Rigid (JPCP) (New & Overlay)	% Slab cracked	I=10% P=15% S=20%	
	Faulting	I=0.15 inch P=0.2 inch S=0.25 inch	
	IRI	I=160 inch/mile P=200 inch/mile S=200 inch/mile	

Note: I= interstate, P=primary, and S=secondary

Table 4-49 Distress threshold values used in this study based on discussion with MDOT

Pavement type	Distress	Threshold
Flexible (New & Overlay)	Alligator cracking	20%
	Longitudinal cracking	2000 ft/mi
	Thermal cracking	1000 ft/mi
	Surface rutting	0.5 in
	IRI	172 in/mi
Rigid (JPCP) (New & Overlay)	% Slab cracked	15%
	Faulting	0.25 in
	IRI	172 in/mi

As mentioned above, the point-normalized sensitivity index defined in Equation (6) is normalized with the design limit (threshold). Equation (6) shows that changing the threshold value will change the NSI value proportionally. The effect of the threshold value on the calculated NSI was investigated. Figure 4-21 shows the NSI curves for three different

threshold values. The results show that the change in threshold value will proportionally increase or decrease the NSI value for a given performance measure.

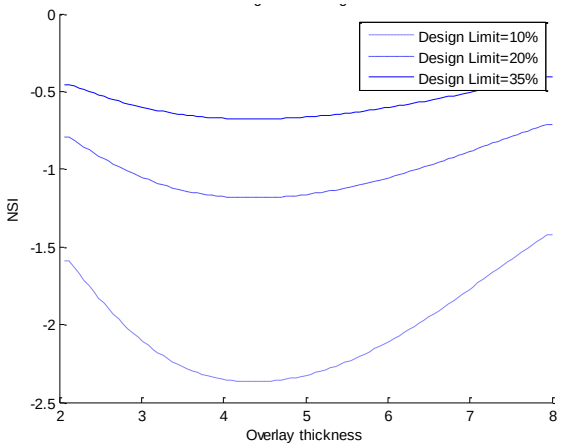

(a) Alligator cracking for HMA over HMA

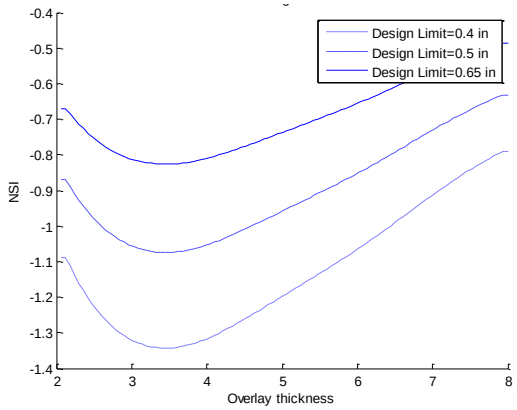

(b) Surface rutting for HMA over HMA

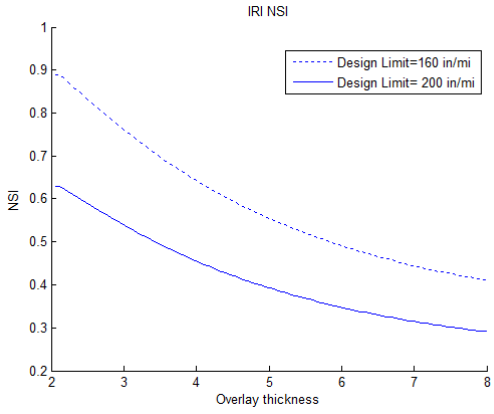

(c) Roughness (IRI) for HMA over HMA

Figure 4-21 Effect of different threshold values on NSI calculation

4.4.2 Global Sensitivity Analysis Results

In GSA, for each rehabilitation option both main and interactive effects of inputs on pavement distresses were investigated. More than 1000 ANN RSMs were performed for each input-distress combination and the RSMs were averaged to obtain an expected RSM to improve the accuracy of performance predictions. Subsequently, those RSMs were utilized to evaluate the NSI. Due to the variation in the ANN predictions for 1000 RSMs, a 95% confidence interval was provided for distress and NSI predictions. The GSA included the following components for each rehabilitation option:

1. The relative importance of design inputs were determined by using the Garson algorithm.
2. The main effects of each design input were evaluated by using NSI values.
3. The interaction effects of important design inputs were evaluated by using two-variable NSI values.

The results for each rehabilitation option are presented next.

4.4.2.1. HMA over HMA

Relative importance of design inputs

In order to obtain the overall relative significance of design inputs, all the inputs should be changed simultaneously to cover their entire possible combinations. Therefore, in this case despite an OAT analysis (where all results are based on a base case), no base case or baseline values for design inputs are needed. However, it should be noted that such methodology only determines the relative ranking of inputs among each other. Garson algorithm was implemented to get the relative importance of the design inputs. Garson (*11*) proposed a method for partitioning the neural network connection weights in order to determine the relative importance of each input variable in the network. An example showing the application of Garson's algorithm in a single hidden layer feed forward multi-layer perceptron (MLP) with two processing elements (PEs) is shown in Figure 4-22.

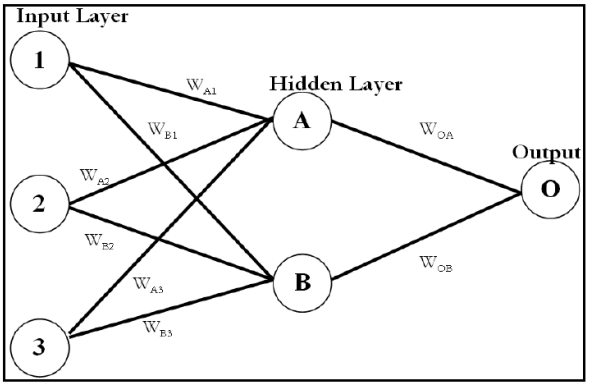

Figure 4-22 Network diagram (*11*)

The dataset used in this analysis are the LHS inputs generated for GSA. The LHS inputs cover the entire range of problem domain hence it takes into account all the possible input combinations. The relative importance of the design inputs is shown in Figure 4-23 for all pavement performance measures. The relative importance of an input can also be expressed as the percent participation of design inputs in the distress prediction models (i.e. for a given pavement distress each design input will have a percent contribution to the predicted distress). The results show that overlay thickness is the most important input and has the highest contribution in all predicted performance measures. The volumetric parameters for overlay HMA mixture (effective binder and air voids) are important for cracking, especially for alligator cracking. Existing condition rating for alligator cracking and existing HMA thickness for longitudinal cracking and rutting have important overall contributions.

The height of each bar graph shows the percent contribution of the input parameters (which adds up to 100%). In general, these numbers can be used to compare and quantify the contributions of each input for a specific performance measure.

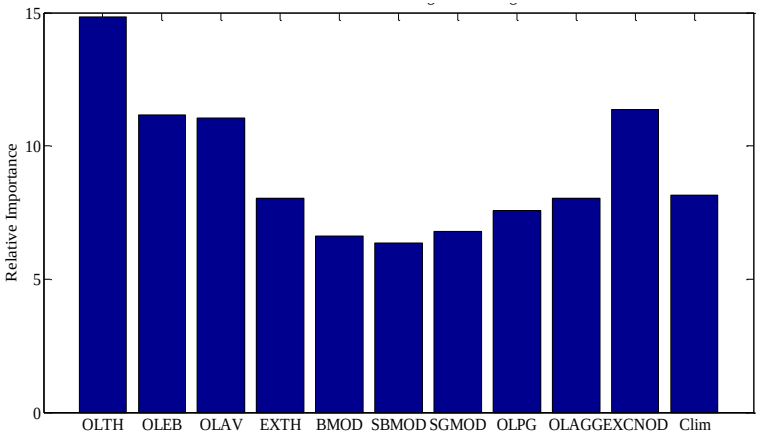

(a) Relative importance of design inputs for alligator cracking

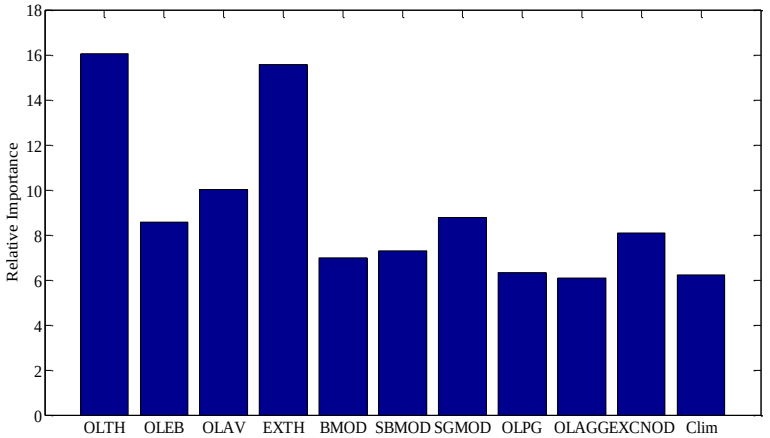

(b) Relative importance of design inputs for longitudinal cracking

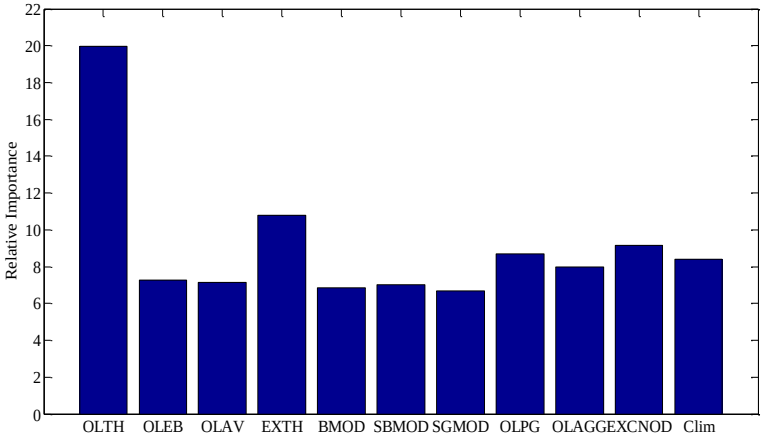

(c) Relative importance of design inputs for rutting

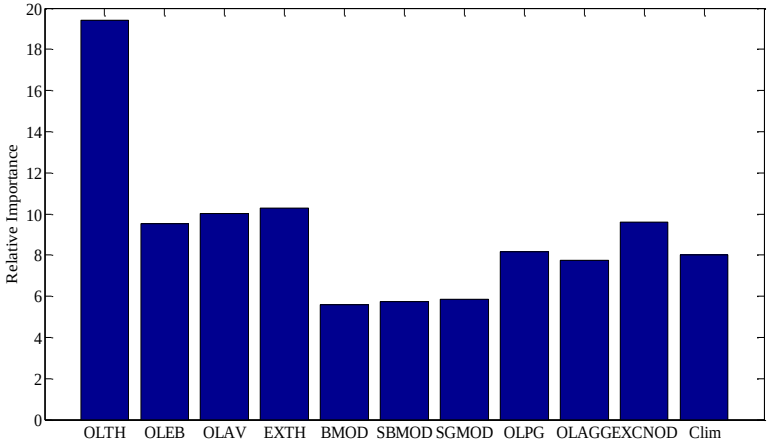

(d) Relative importance of design inputs for IRI

Figure 4-23 **Relative importance of design inputs for HMA over HMA**

Main effect of design inputs

As mentioned above, the relative importance of inputs can be used for determining their overall contribution to predicted pavement performance. In order to investigate the impact of the input variables with respect to a standard, a base case should be specified. In this scenario, each input variable of interest should vary over its range while other variables are held constant at their base values. The base cases, input ranges, and baseline values were presented before.

The neural networks were trained to fit the best surface on the discrete points from LHS simulations for each pavement performance measure. As the fitted surfaces cover the entire problem domain, those allow the evaluation of each variable over its entire range. Figure 4-24 shows an example of predicted alligator cracking for overlay thickness using the ANN RSM. Due to the variability in the ANN predictions, a 95% confidence interval is provided. This variability is a function of sampling process for the training of ANN. In each ANN run, 70% of the data set is sampled randomly for training and remaining is used for validation and testing. Using Equation (6) the NSI was calculated for overlay air void - alligator cracking combination. A 95% confidence interval is also provided for the NSI curve. The wider confidence interval band means an increase in the variability of ANN predictions.

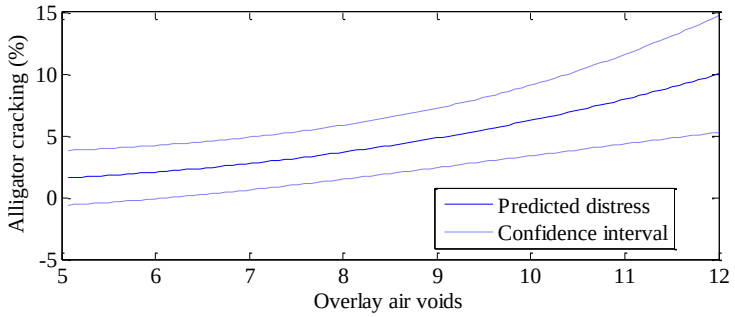

(a) Predicted alligator cracking

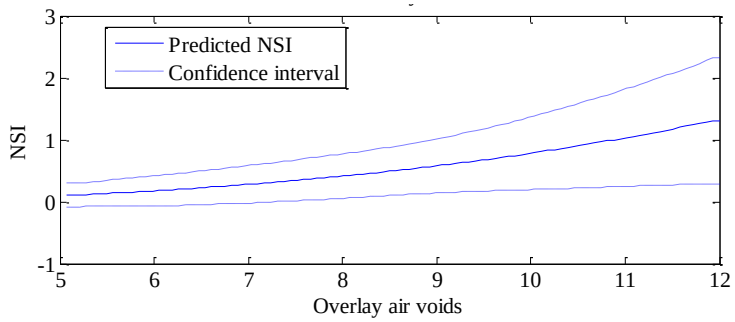

(b) Calculated NSI

Figure 4-24 Sensitivity of alligator cracking to HMA overlay air voids

The main effects of all the input variables on all predicted distresses were investigated. The distress and NSI plots for all of the inputs and distresses are presented in Appendix B. Figure 4-25 summarizes the main effects of all input variables on each pavement performance

measure by box plots. The results show that overlay air void percentage has a significant impact on cracking (NSI>1). An increase in air voids is associated with higher cracking. For longitudinal cracking; overlay and existing HMA thickness, effective binder content, unbound layer moduli and existing conditions all have a significant impact. The effect of a particular input on pavement performance measure can be interpreted as follows:

- If a NSI is positive, the distress magnitude will increase by increasing the input value.
- If a NSI is negative, the distress magnitude will decrease by increasing the input value.

For rutting and IRI, the NSI results show that all inputs have relatively lower impact as compared to cracking.

Interactive effect of design inputs

The detailed sensitivity analysis identified some practically significant interactions between input variables. Those interactions were further investigated in detail in this part. An interactive effect means that one input can amplify or reduce the effect of another input on the predicted pavement performance. Therefore, it is vital to consider the interactive effect of given design input variables when such interaction exists. It should be noted that only interactions between overlay design and existing design inputs were considered. Similar to the NSI for one variable, a NSI for interaction was developed as shown in Equation (11). Figures 4-26 to 4-28 show the significant interactions for alligator cracking and the corresponding NSI plots. The results shown in Figure 4-26a indicates that higher overlay thicknesses lower the impact of existing thickness on alligator cracking. For example, for an 8-inch overlay thickness, regardless of the existing HMA thickness, the predicted cracking will be negligible over the design life. On the other hand, for a thin overlay depending on the existing HMA thickness, the rehabilitation strategy will exhibit 10 to 20% alligator cracking over the design life. Figure 4-26b shows that the rate of change in cracking with respect to overlay thickness will increase as the existing thickness increases.

Other interactions in Figures 4-27 and 4-28 can be interpreted similarly. The maximum NSI for interactions can be used to rank the interactions. The results for alligator cracking of HMA over HMA as shown in Figure 4-26 to Figure 4-28 manifests that the interaction between overlay air voids and existing HMA thickness has the most important effect. The interaction between existing thickness and overlay thickness, and existing thickness and overlay effective binder content have somewhat similar effects on alligator cracking. It should be noted that in the interaction sensitivity plots, the magnitude of the NSI should be consider rather than the surface colors.

On each boxplot, the central mark (red line) is the median of the distribution; the lower and upper edges of the box are the 25th and 75th percentiles, respectively. The whiskers extend to the most extreme data points without considering outliers, and outliers are plotted individually as the red plus signs in the graph. It should be noted that box plots are used for continuous variables to represent a continuous distribution and do not apply to discrete variables.

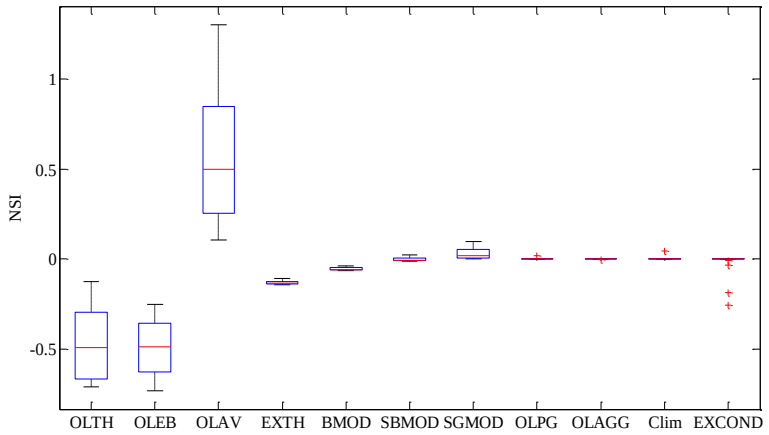

(a) Alligator cracking

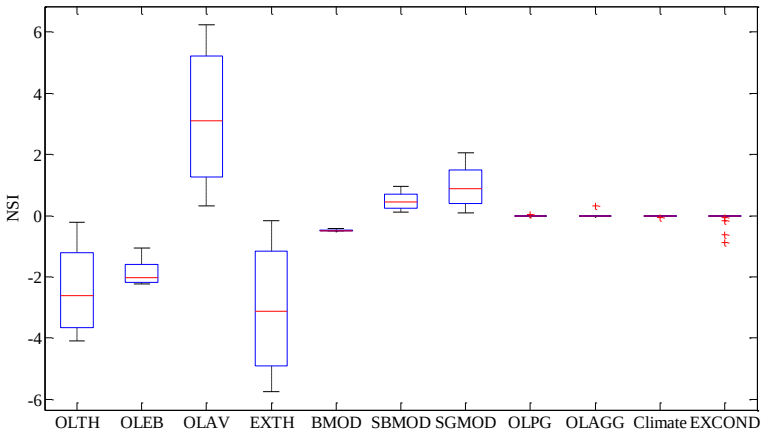

(b) Longitudinal cracking

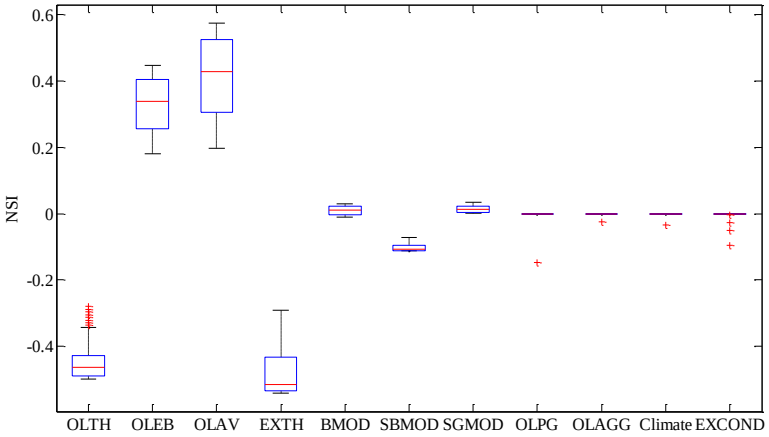

(c) Rutting

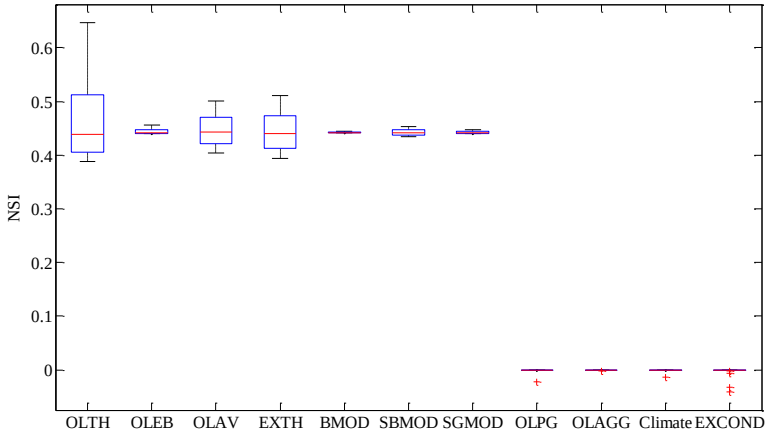

(d) IRI

Figure 4-25 Summary of NSI curves for HMA over HMA

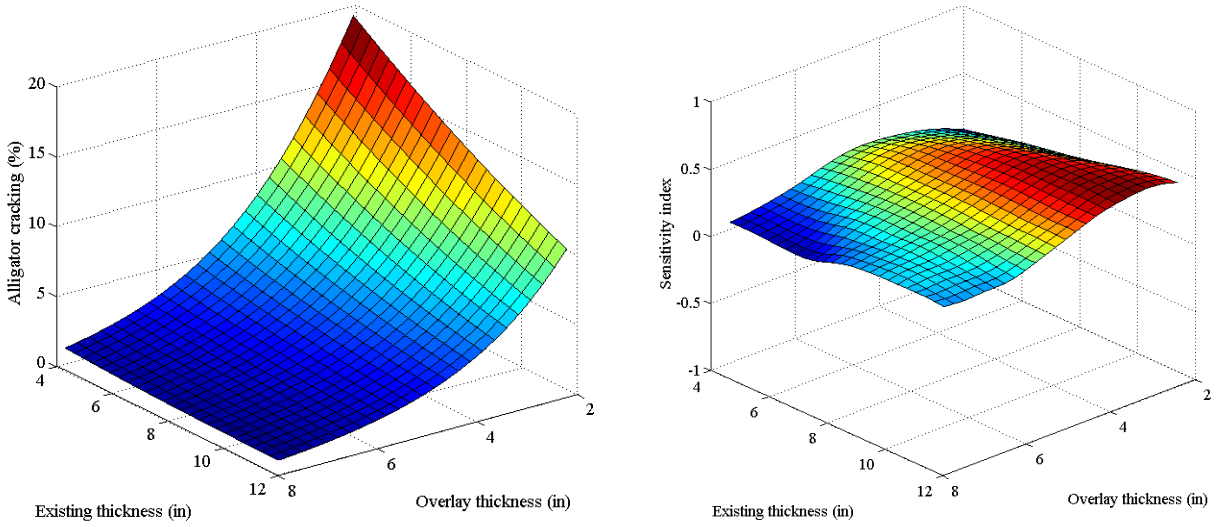

(a) Predicted alligator cracking (b) Calculated NSI

Figure 4-26 Interaction between HMA overlay thickness and existing thickness

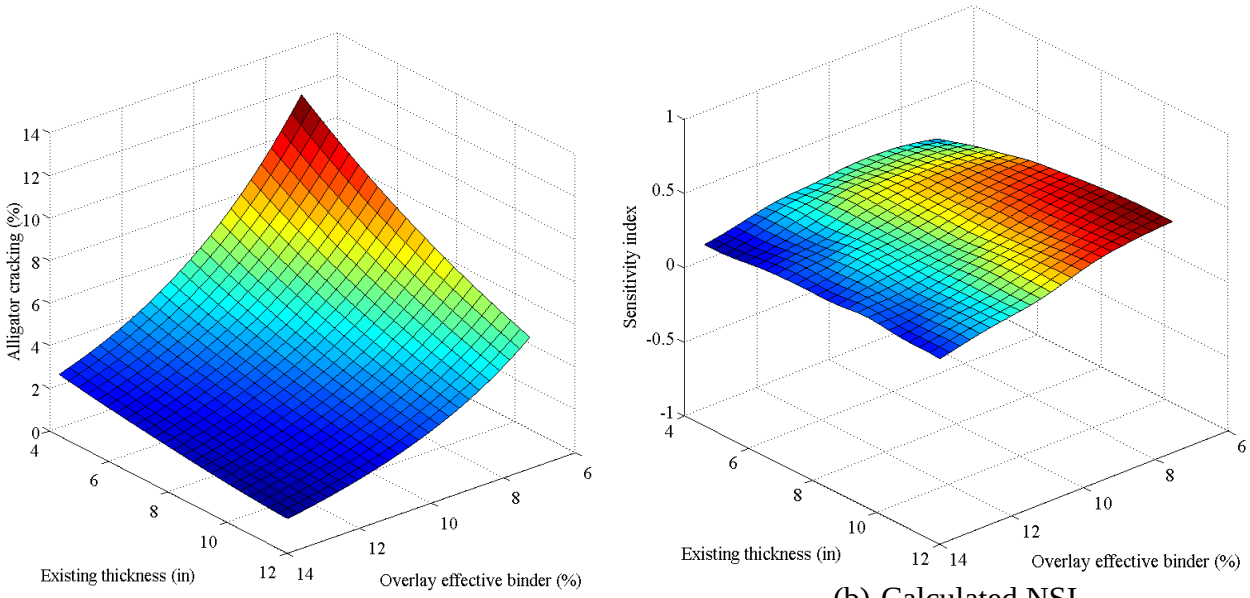

(a) Predicted alligator cracking (b) Calculated NSI

Figure 4-27 Interaction between HMA overlay effective binder and existing thickness

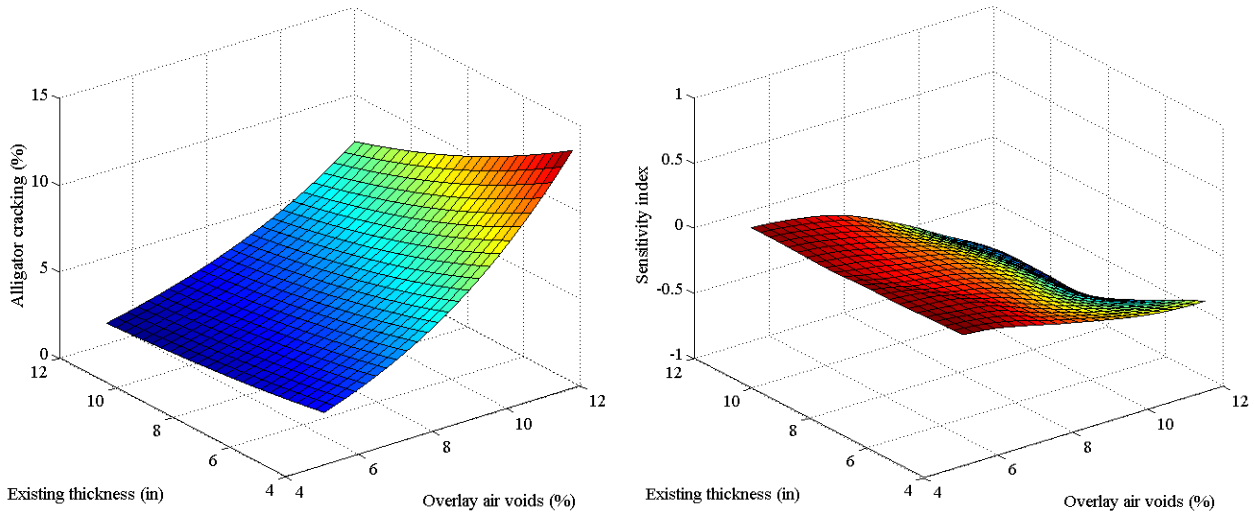

(a) Predicted alligator cracking (b) Calculated NSI

Figure 4-28 Interaction between HMA overlay air voids and existing thickness

4.4.2.2. Composite pavement

Relative importance of design inputs

Similar to HMA overlay, the relative importance of design inputs for this rehabilitation option is determined as shown in Figure 4-29. Since no alligator cracking was predicted by the MEPDG, the results are only shown for the remaining distresses. The results demonstrate the overlay thickness and overlay air voids have the highest contribution to all the predicted pavement performance measures. The volumetric parameters for overlay HMA mixture (effective binder content, air voids, and aggregate gradation) and PG grade are important for rutting and have somewhat similar contributions.

Main effect of design inputs

The summary of NSI plots for composite pavements is presented in Figure 4-30. The results show that the overlay thickness and overlay air voids have the highest impact on all predicted distress among design inputs. Existing PCC thickness has an important effect on longitudinal cracking. The NSI results show that all inputs have relatively lower impact on IRI as compared to cracking and rutting. The plots were generated using more than 100 points within the ranges of the design inputs; therefore, some of the inputs (e.g., OLAV) might show a noticeable number of outliers. However, such outliers were much less than the total number of data point for generating these plots. It should be noted that box plot summarizes a NSI curve for each design input range. In some cases if there is a rapid change in NSI due to a specific input value, the point will be shown as an outlier in the box plot (see Figure B-59 for overlay air voids NSI). Therefore, the maximum value of NSI was used as the criteria for identifying a significant input variable.

Interactive effect of design inputs

Interaction effects between input variables and NSI for this rehabilitation option are presented in Appendix B. Figures B-66 and B-67 show significant interactions for longitudinal cracking. The results show that thinner overlay will lower the impact of existing thickness on longitudinal cracking. For example, for a 2-inch overlay, regardless of the existing PCC slab thickness, the predicted cracking will be negligible over the design life. On the other hand, for a thick overlay depending on the existing PCC thickness, longitudinal cracking may vary from low to very high (2000 ft/mile), which is the threshold for longitudinal cracking. Figure B-66 for NSI interaction shows that the rate of change in cracking with respect to overlay thickness will increase as the existing thickness increases. Other interactions can be interpreted similarly. The maximum NSI for interactions can be used to rank the interactions. The results for longitudinal cracking for composite rehabilitation option show that the interaction between overlay air voids and existing PCC thickness has the most significant effect among other interactions (see Figure B-67). The interaction between existing thickness and overlay thickness, and existing thickness and overlay air voids have somewhat similar effects on rutting.

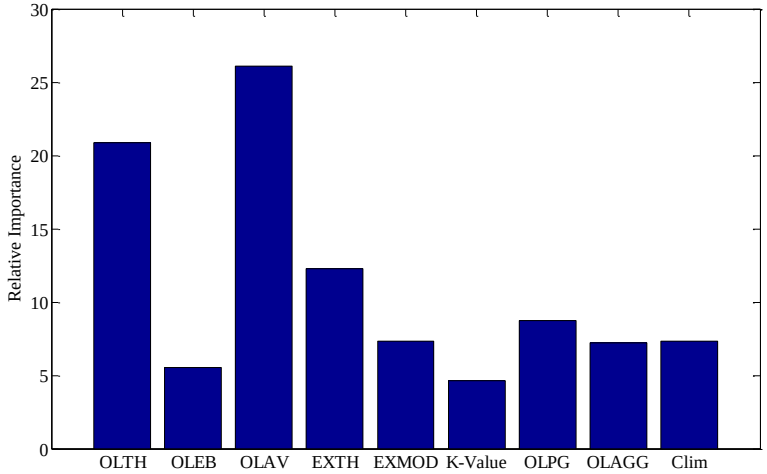

(a) Relative importance of design inputs for longitudinal cracking

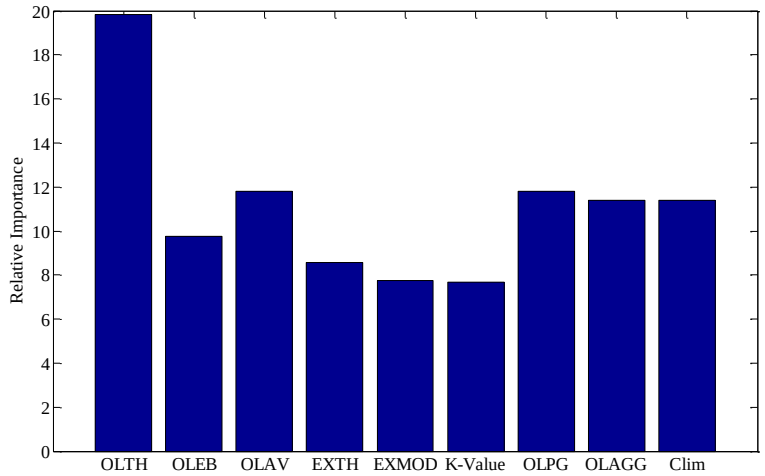

(b) Relative importance of design inputs for rutting

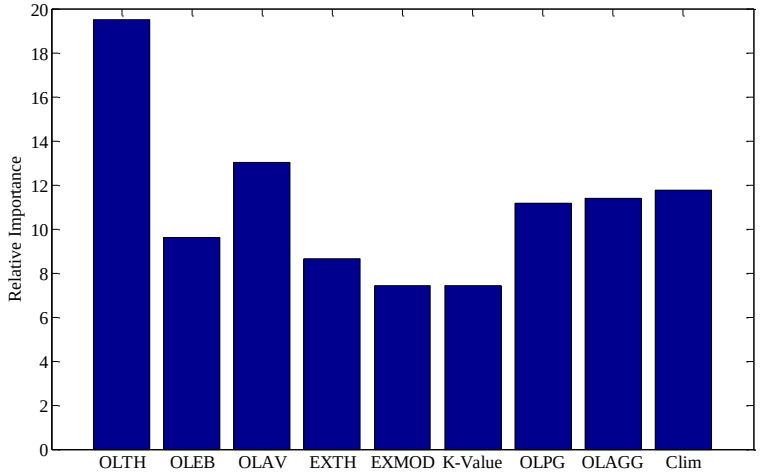

(c) Relative importance of design inputs for IRI

Figure 4-29 Relative importance of design inputs for composite pavement

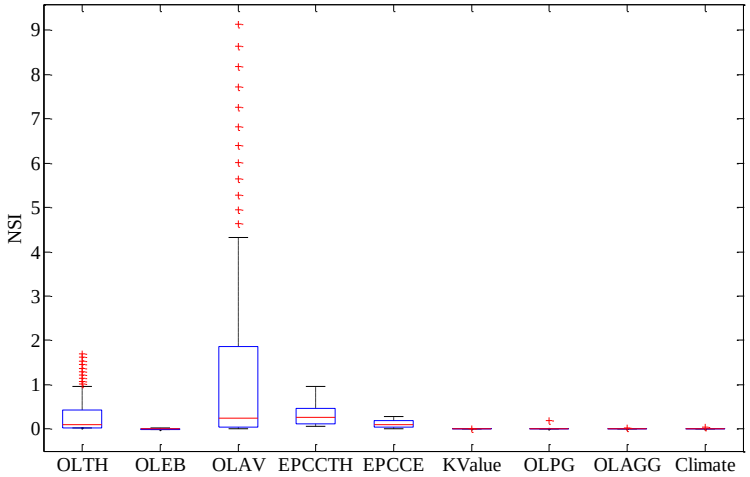

(a) Relative importance of design inputs for longitudinal cracking

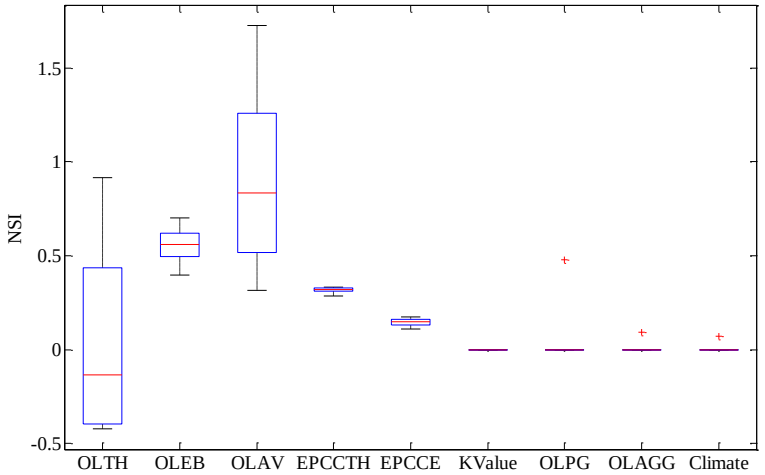

(b) Relative importance of design inputs for rutting

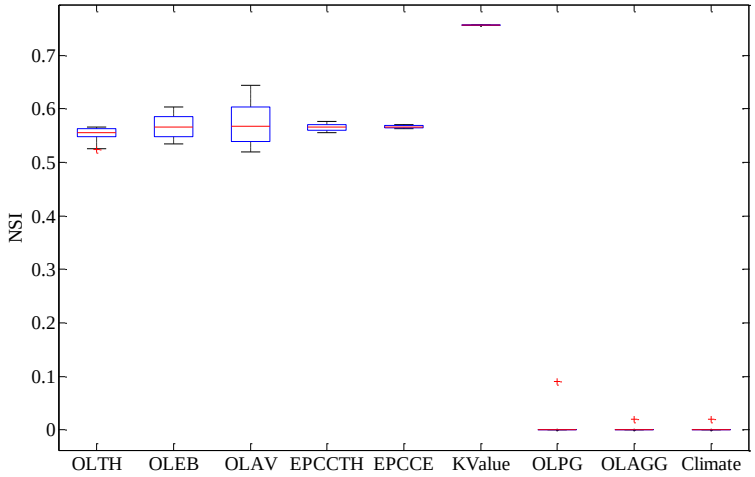

(c) Relative importance of design inputs for IRI

Figure 4-30 Summary of NSI curves for composite pavement

4.4.2.3. Rubblized pavement

Relative importance of design inputs

Figure 4-31 illustrates the relative importance of design inputs for HMA over rubblized PCC pavement. The results show that the existing PCC fractured modulus has the highest impact on the pavement distresses except for rutting. Overlay thickness has the most significant effect on the rutting prediction. Overlay HMA mixture volumetric parameters (overlay air voids and aggregate gradation) and PG grade have important contributions to rutting besides overlay thickness.

Main effect of design inputs

The main effects of all the input variables on all predicted distresses were investigated, as shown in Figure 4-32. The distress and NSI plots for all of the inputs and distresses are presented in Appendix B. The results show that overlay air voids has a significant impact on all the pavement performance measures (NSI>1 for all cases). Overlay thickness, effective binder content, and existing PCC modulus all have a significant impact on alligator cracking. In the case of rutting, overlay effective binder content shows a significant impact. For IRI all design inputs except overlay air voids show relatively lower contribution. It should be noted that box plot summarizes a NSI curve for each design input range. In some cases if there is a rapid change in NSI due to a specific input value, the point will be shown as an outlier in the box plot. Therefore, the maximum value of NSI was used as the criteria for identifying a significant input variable.

Interactive effect of design inputs

Interaction between input variables for distress and NSI for this rehabilitation option are presented in Appendix B. Figures B-96 to B-98 show the significant interactions for alligator cracking and the corresponding NSI plots. The results in Figure B-96 show that lower overlay air voids will reduce the impact of existing modulus on alligator cracking. For example, for low overlay air voids and fair to high existing rubblized PCC modulus, the predicted cracking will be negligible over the design life. On the other hand, for high overlay air voids depending on the existing rubblized PCC modulus; the HMA layer may exhibit 0 to 50% alligator cracking over the design life. Figure B-96 also shows that the rate of change in cracking w.r.t overlay air voids will increase as the existing rubblized PCC modulus decreases. The maximum NSI for interactions can be utilized to rank the interactions. The interactions are compared based on the maximum NSI later in the summary of this section.

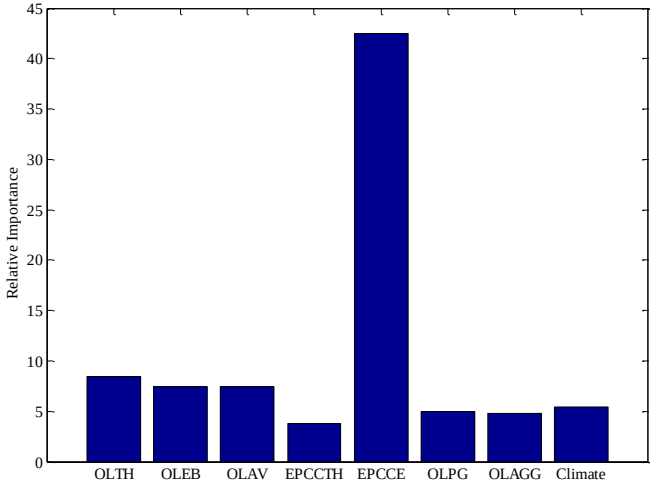

(a) Relative importance of design inputs for alligator cracking

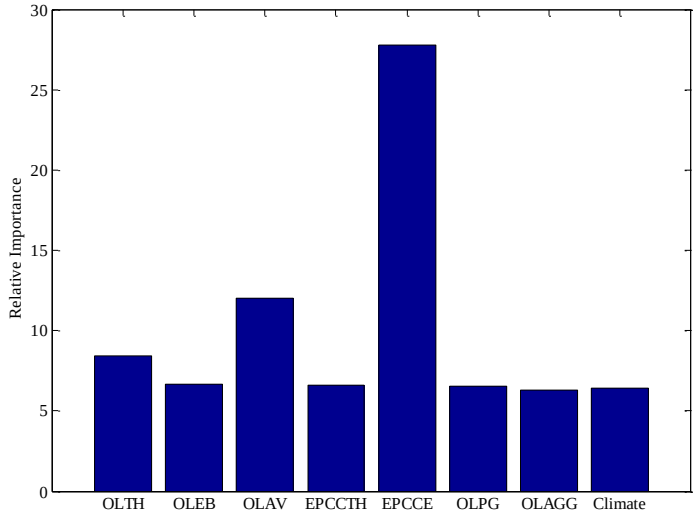

(b) Relative importance of design inputs for longitudinal cracking

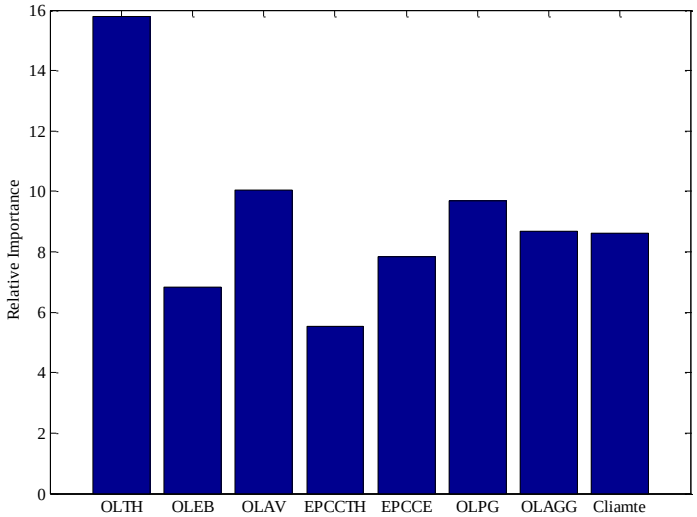

(c) Relative importance of design inputs for rutting

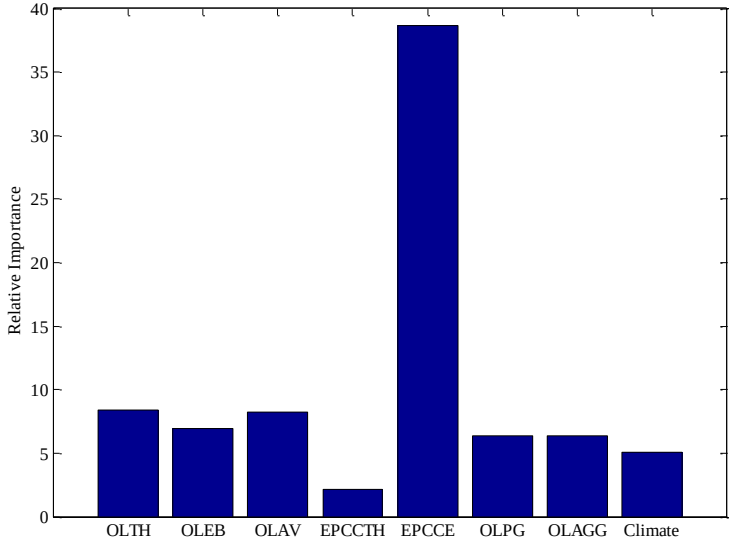

(d) Relative importance of design inputs for IRI

Figure 4-31 Relative importance of design inputs for rubblized PCC pavement

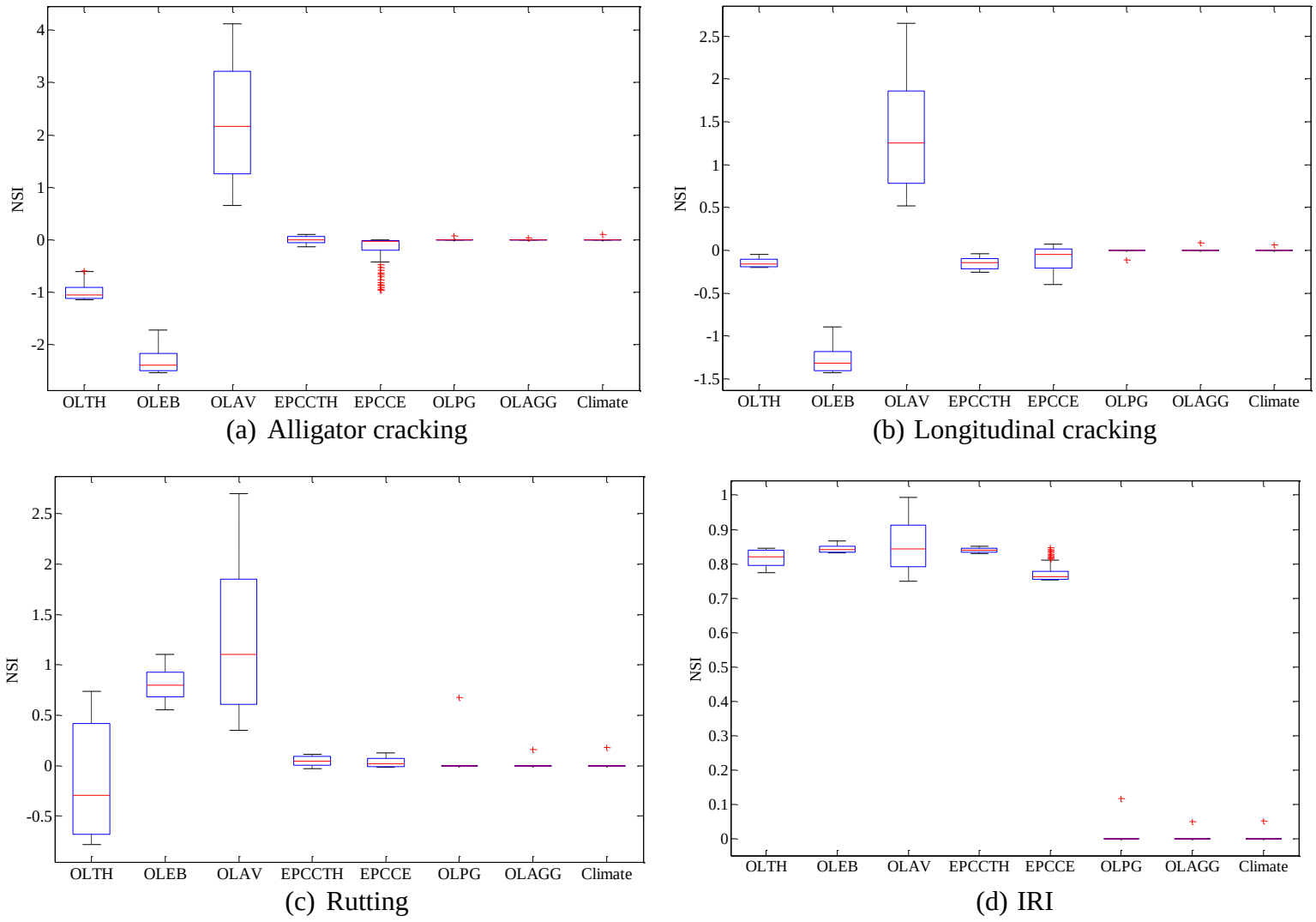

(a) Alligator cracking

(b) Longitudinal cracking

(c) Rutting

(d) IRI

Figure 4-32 Summary of NSI curves for rubblized PCC pavement

4.4.2.4. Unbonded PCC overlay

Relative importance of design inputs

Figure 4-33 presents the relative importance of input variables for different pavement performance measures. The results show that for cracking, overlay thickness, overlay MOR, and subgrade modulus of reaction (*k*-value) have the most significant contributions. For faulting, overlay CTE and climate are the major contributors. For IRI, overlay CTE, *k*-value, and climate have important but somewhat similar contributions in predicted roughness.

Main effect of design inputs

The summary of NSI plots for unbonded PCC overlay is presented in Figure 4-34. The main effects of all the design inputs on all predicted distresses were investigated similarly to other rehabilitation options and are presented in Appendix B. The results demonstrate that overlay CTE has a significant impact on all pavement performance measures. For cracking, overlay thickness has the highest effect followed by overlay MOR, CTE and joint spacing. Faulting and IRI showed lower sensitivity to design inputs compared to cracking. However, overlay thickness and existing PCC modulus show relatively large impact on IRI.

Interactive effect of design inputs

Figures B-140 to B-142 show the significant interactions for cracking and the corresponding NSI interaction plots. Figure B-141 shows that higher overlay MOR will lower the impact of existing PCC modulus on cracking. For example, for 900 psi overlay MOR, regardless of the existing PCC modulus, the predicted cracking will be close to zero over the design life. On the other hand, for low overlay MOR depending on the existing PCC modulus, the unbonded PCC overlay will exhibit 20-40% cracking over the design life. Figure B-141 also shows that the rate of change in cracking with respect to overlay MOR will decrease as the existing PCC modulus increases. The interaction between existing modulus and overlay thickness has a significant effect on cracking. The interaction between design inputs for faulting and IRI showed lower effects. The maximum NSI for interactions can be used to rank the interactions.

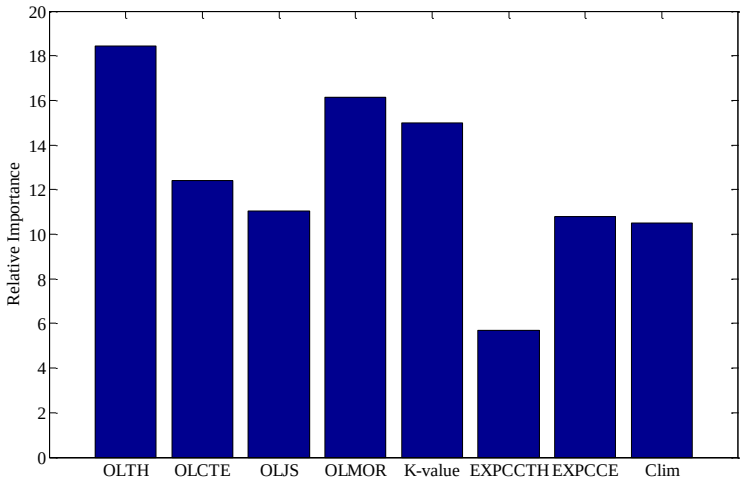

(a) Relative importance of design inputs for cracking

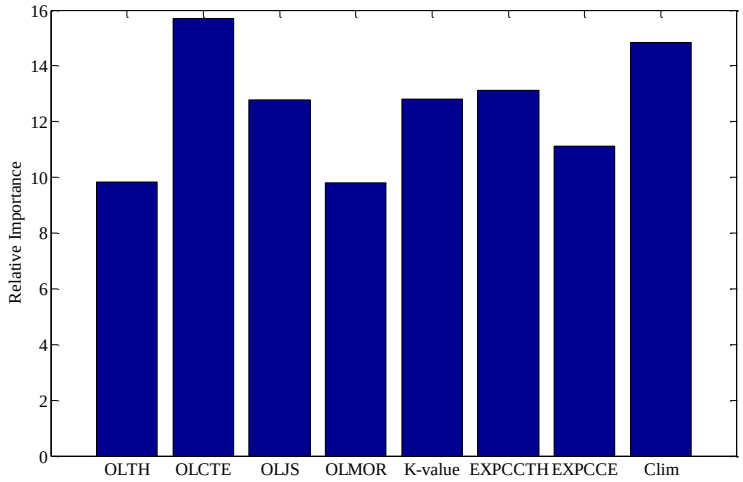

(b) Relative importance of design inputs for faulting

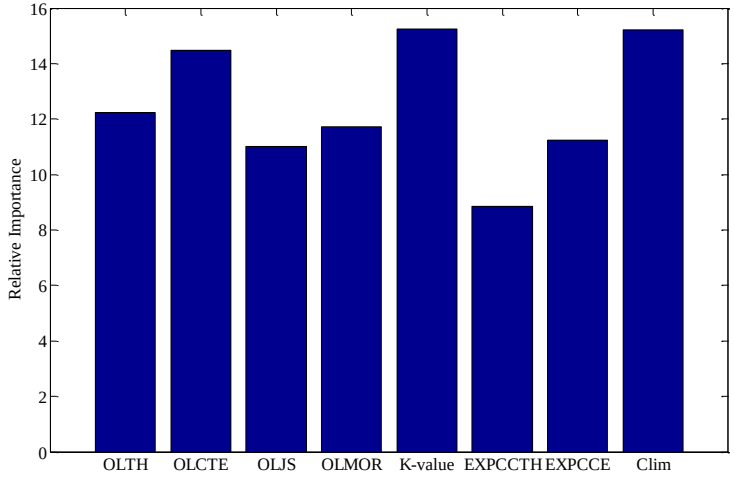

(c) Relative importance of design inputs for IRI

Figure 4-33 Relative importance of design inputs for unbonded PCC overlay

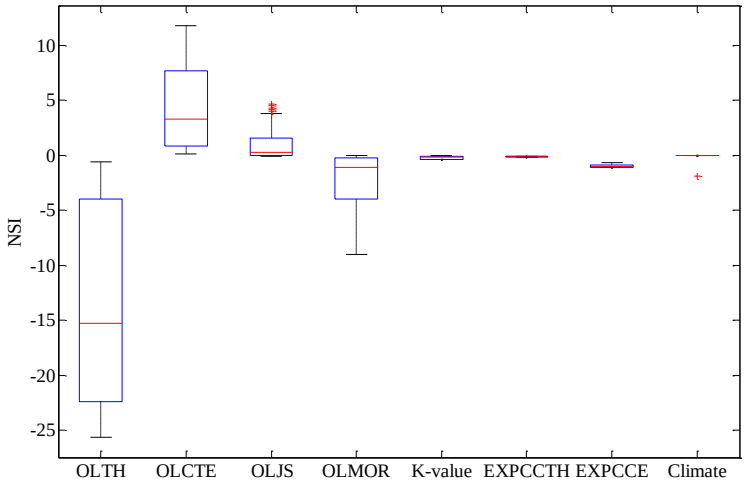

(a) Relative importance of design inputs for cracking

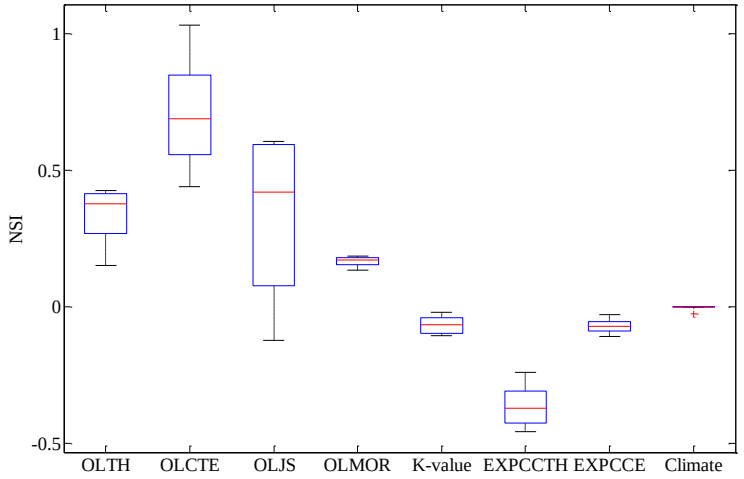

(b) Relative importance of design inputs for faulting

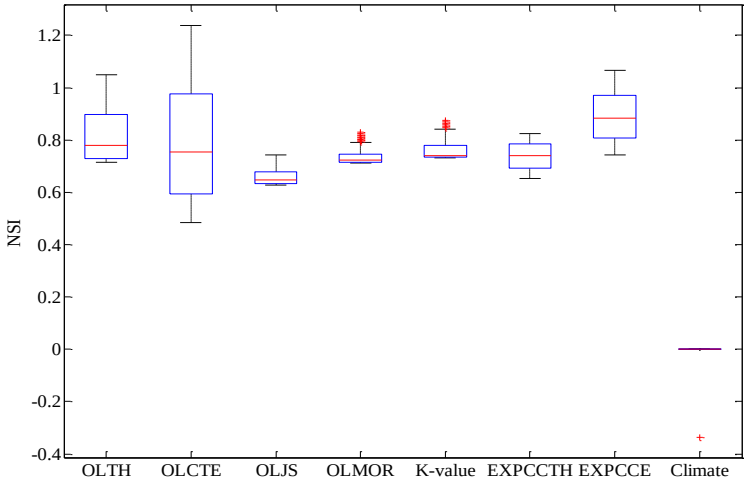

(c) Relative importance of design inputs for IRI

Figure 4-34 Summary of NSI curves for unbonded PCC overlay

4.4.2.5. Summary Results

The four rehabilitation options were considered in GSA similarly to the preliminary and the detailed sensitivity analyses. First, the relative contributions of the design inputs for various pavement performance measures were identified and discussed. Second, the main effect of design inputs for a base case was investigated. Finally the interactive effect of the design inputs was studied for all pavement performance measures within each rehabilitation option.

The results are summarized based on the main effects determined through the maximum NSI values from GSA. The input variables are ranked based on NSI which indicates their impact on the difference in pavement performance measures. Table 4-50 shows the inputs for HMA over HMA. The results can be summarized as follows:

- In general, the overlay thickness and HMA volumetrics are the most significant inputs for the overlay layer.
- The existing thickness and condition rating have an important effect among the existing pavement inputs.

Table 4-50 The MEPDG inputs ranking for HMA over HMA

Input variables	Alligator cracking ranking (NSI)	Longitudinal cracking ranking (NSI)	Rutting ranking (NSI)	IRI ranking (NSI)
Overlay thickness	3 (0.6)	3 (4)	2 (0.5)	1 (0.65)
Overlay air voids	1 (1.2)	1 (6)	1 (0.52)	2 (0.51)
Overlay effective binder	2 (0.7)	5 (2)	3 (0.47)	4 (0.51)
Existing thickness	5 (0.15)	2 (5)	4 (0.47)	3 (0.51)
Base modulus	9 (0.05)	8 (0.4)	7 (0.05)	6 (0.44)
Subbase modulus	8 (0.05)	7 (1)	5 (0.35)	5 (0.45)
Subgrade modulus	6 (0.1)	6 (2)	9 (0.05)	7 (0.44)
Existing pavement condition rating	4 (0.5)	4 (3.8)	6 (0.2)	10 (0.05)
Overlay aggregate gradation	10 (0)	9 (0.25)	10 (0.05)	8 (0.05)
Overlay PG	11 (0)	11 (0)	8 (0.05)	11(0.05)
Climate	7 (0.1)	10 (0.05)	11 (0.05)	9 (0.05)

Note: The shaded cells show the most important input variables (|NSI|>1)

Table 4-51 shows the inputs for HMA over PCC composite rehabilitation option. The results can be summarized as follows:

- The overlay thickness and HMA air voids are the most significant inputs for the overlay layer.
- The existing thickness has an important effect among the existing pavement inputs.

Table 4-51 The MEPDG inputs ranking for composite pavement

Inputs	Longitudinal cracking ranking (NSI)	Rutting ranking (NSI)	IRI ranking (NSI)
Overlay thickness	2 (1.8)	2 (1)	6 (0.56)
Overlay air voids	1 (8.5)	1 (1.75)	3 (0.61)
Overlay effective binder	7 (0)	3 (0.7)	2 (0.64)
Overlay PG	5 (0.2)	4 (0.6)	7 (0.5)
Overlay aggregate gradation	9 (0)	7 (0.1)	8 (0.5)
Existing PCC thickness	3 (1)	5 (0.3)	4 (0.58)
Existing PCC modulus	4 (0.25)	6 (0.2)	5 (0.57)
Subgrade reaction modulus	8 (0)	9 (0)	1 (0.75)
Climate	6 (0.1)	8 (0.05)	9 (0.5)

Note: The shaded cells show the most important input variables (|NSI|>1)

Table 4-52 shows the inputs for HMA over rubblized PCC rehabilitation option. The results can be summarized as follows:

- The HMA thickness, air voids and effective binder content are the most significant inputs for the overlay layer.

Table 4-52 The MEPDG inputs ranking for rubblized PCC pavement

Inputs	Alligator cracking ranking (NSI)	Longitudinal cracking ranking (NSI)	Rutting ranking (NSI)	IRI ranking (NSI)
Overlay thickness	3 (1)	5 (0.1)	3 (0.8)	3 (0.85)
Overlay air voids	1 (4)	1 (6)	1 (2.8)	1 (1)
Overlay effective binder	2 (2.1)	2 (1.2)	2 (1.1)	2 (0.87)
Overlay PG	6 (0.05)	7 (0.05)	4 (0.4)	6 (0.84)
Overlay aggregate gradation	7 (0.05)	8 (0.05)	5 (0.2)	8 (0.84)
Existing PCC thickness	5 (0.05)	4 (0.1)	8 (0.1)	4 (0.85)
Existing PCC modulus	4 (0.8)	3 (0.4)	6 (0.15)	5 (0.85)
Climate	8 (0.05)	6 (0.05)	7 (0.1)	7 (0.84)

Note: The shaded cells show the most important input variables (|NSI|>1)

Table 4-53 presents the inputs for unbonded PCC overlay rehabilitation option. The results can be summarized as follows:

- All overlay related inputs seem to significantly impact the cracking performance.
- The existing PCC elastic modulus is the most important input among all inputs related to existing layers.

Table 4-53 The MEPDG inputs ranking for unbonded PCC overlay

Design inputs	Cracking ranking (NSI)	Faulting ranking (NSI)	IRI ranking (NSI)
Overlay PCC thickness (inch)	1 (23)	4 (0.4)	2 (1.05)
Overlay PCC CTE (per °F x 10-6)	2 (12)	1 (1.1)	1 (1.2)
Overlay joint spacing (ft)	4 (5)	2 (0.55)	8 (0.75)
Overlay PCC MOR (psi)	3 (8)	5 (0.2)	5 (0.82)
Modulus of subgrade reaction (psi/in)	5 (0.5)	8 (0.1)	4 (0.88)
Existing PCC thickness (inch)	8 (0.1)	3 (0.45)	6 (0.81)
Existing PCC elastic modulus (psi)	6 (1)	7 (0.1)	3 (1.05)
Climate	7 (1)	6 (0.1)	7 (0.8)

Note: The shaded cells show the most important input variables (|NSI|>1)

Tables 4-54 to 4-57 rank the interactions between input variations from overlay and existing layer for all the rehabilitation options based on the maximum NSI. The results can be summarized as follows:

- The interaction between overlay air voids and existing pavement thickness seems to be the most important in impacting all pavement performance measures among HMA rehabilitation options. A higher air void in the overlay layers on a thin existing layer seems to be the worst combination for predicted cracking.
- The interaction between overlay thickness and existing PCC layer modulus seems to have the most significant effect on unbonded PCC overlay performance. A thicker overlay may hide the impact of weak existing PCC layer on pavement predicted performance.

All the interactions studied here are practically and statistically significant. Therefore all of them should be considered in the design and analysis.

Table 4-54 Interaction ranking for HMA over HMA

Interaction	Alligator cracking ranking (NSI)	Longitudinal cracking ranking (NSI)	Rutting ranking (NSI)	IRI ranking (NSI)
Overlay air voids and existing thickness	1 (0.8)	1 (15)	3 (0.3)	3 (0.1)
Overlay effective binder and existing thickness	2 (0.5)	3 (7)	2 (0.3)	2 (0.1)
Overlay thickness and existing thickness	3 (0.5)	2 (10)	1 (0.4)	1 (0.2)

Table 4-55 Interaction ranking for composite pavement

Interaction	Longitudinal cracking ranking (NSI)	Rutting ranking (NSI)
Overlay thickness and existing thickness	2 (25)	2 (1.5)
Overlay air voids and existing thickness	1 (44)	1 (1.7)

Table 4-56 Interaction ranking for rubblized PCC pavement

Interaction	Alligator cracking ranking (NSI)	Longitudinal cracking ranking (NSI)	Rutting ranking (NSI)	IRI ranking (NSI)
Overlay air voids and existing thickness	1 (3.7)	1 (2.4)	2 (0.8)	2 (0.1)
Overlay effective binder and existing thickness	2 (2.1)	2 (1.1)	1 (1)	1 (0.1)
Overlay thickness and existing thickness	3 (0.8)	3 (0.5)	3 (0.8)	3 (0.1)

Table 4-57 Interaction ranking for unbonded PCC overlay

Interaction	Cracking ranking (NSI)	Faulting ranking (NSI)	IRI ranking (NSI)
Overlay thickness and existing modulus	1 (28.5)	1 (0)	1 (1.5)
Overlay MOR and existing thickness	3 (6)	2 (0)	3 (0.7)
Overlay MOR and existing modulus	2 (14.5)	3 (0)	2 (0.7)

4.5 SATELLITE STUDIES

Several additional clarification studies were performed to evaluate the sensitivity of input variables in the MEPDG/DARWin-ME. These investigations were important to understand intricate details about the following topics:

1. Impact of HMA gradation on the predicted performance of flexible pavement
2. Effect of binder's *G** on predicted performance of HMA over HMA
3. Influence of unbound layers gradation on predicted performance of flexible and rigid pavements

4.5.1 Effect of different HMA Gradations on Predicted Pavement Performance

The main objective for this investigation was to evaluate the impact of HMA gradations (level 3) on the predicted pavement performance based on the specification limits. Different HMA gradations were obtained for the specific MDOT mixtures from Part 1 of the study. The process for the selection of the HMA mixtures included the following steps:

a. Evaluate all HMA mixtures used in Part 1 of the project
b. Sort the mixtures by course type i.e., top, leveling, and base
c. Plot the aggregate gradation for each HMA mixture
d. Select a coarse, fine and intermediate gradation based on step c
e. Perform DARWin-ME analysis using the specific volumetric properties of the selected HMA mixtures in step d
f. Compare the predicted pavement performance measures to evaluate the effect of gradation.

A typical pavement cross-section used in this investigation is shown in Table 4-58. Table 4-59 presents the volumetric properties of different MDOT mixtures selected for this evaluation. The base case consisted of mid gradations for all HMA layers. The HMA gradations were changed one-at-a-time while all others were held constant.

Table 4-58 Typical flexible pavement cross-section

Layer Type	Thickness (in)	Modulus (psi)	Type
HMA Top	2	N/A	PG 58-28
HMA Leveling	2		
HMA Base	2		
Base	4	30,000	A-1-A
Subbase	10	20,000	A-3
Subgrade	semi inf	17,000	A-4

Figures 4-35 to 4-37 show the predicted alligator cracking, surface rutting and IRI, respectively. Based on the results, it can be seen that only HMA base course gradation has some effect on the predicted bottom-up alligator cracking. The base case values lie directly under one of the other curves indicating no performance differences. Therefore, it can be

concluded that for level 3 inputs, HMA gradation doesn't significantly impact the predicted pavement performance. In addition, the average gradation from the specification limits can be used for initial pavement design. However, it should be noted that these findings are valid for the range of HMA gradations obtained in this study.

Table 4-59 Volumetric properties of the selected mixtures

Course type	Gradation	MDOT HMA mixture types		
		Mid (base case)	Fine	Coarse
Top	3/4"	100	100	100
	3/8"	95.7	99.5	99.7
	No. 4	80.1	76.2	84.1
	No. 200	5.8	5.4	6
	Eff AC	12.58	11.4	12.06
Leveling	3/4"	100	100	100
	3/8"	87.6	89.9	87.1
	No. 4	66.5	69.3	76.4
	No. 200	5.7	5.6	5.3
	Eff AC	10.62	10.9	10.58
Base	3/4"	100	100	99.9
	3/8"	76.1	72.3	82.6
	No. 4	56.9	47.3	65
	No. 200	3.5	5	5.1
	Eff AC	9.78	9.8	10.4

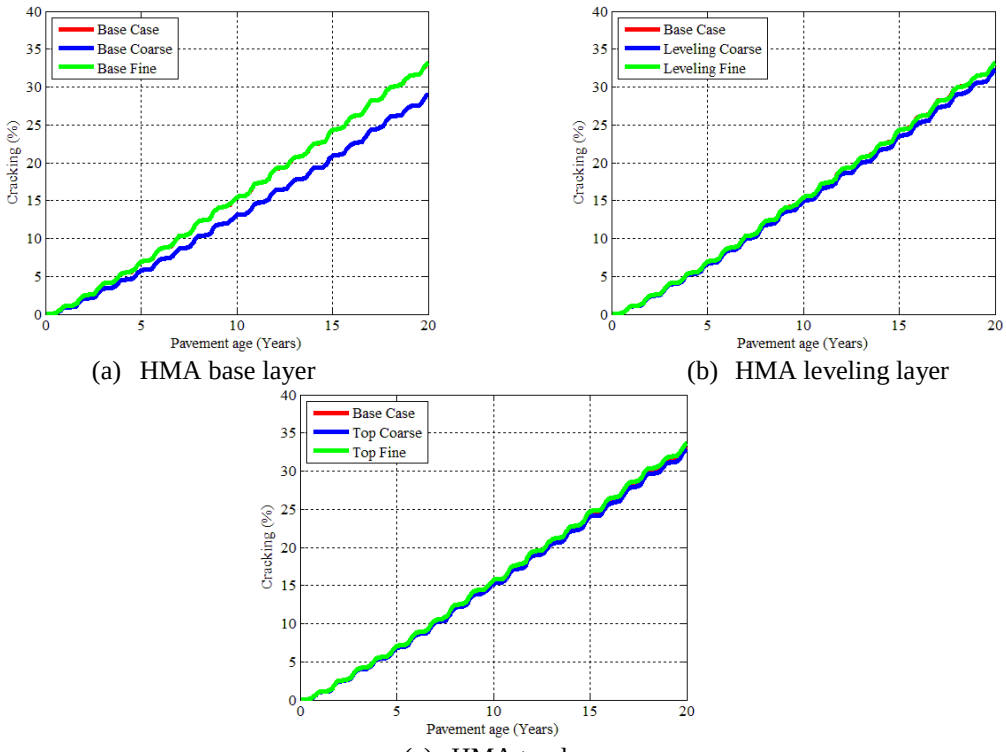

(a) HMA base layer

(b) HMA leveling layer

(c) HMA top layer

Figure 4-35 Alligator cracking predictions

(a) HMA base layer

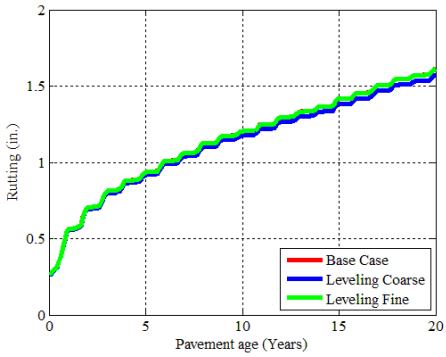

(b) HMA leveling layer

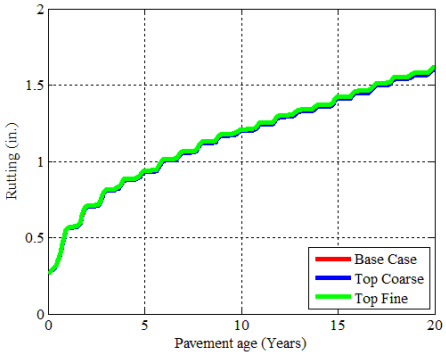

(c) HMA top layer

Figure 4-36 Rutting predictions

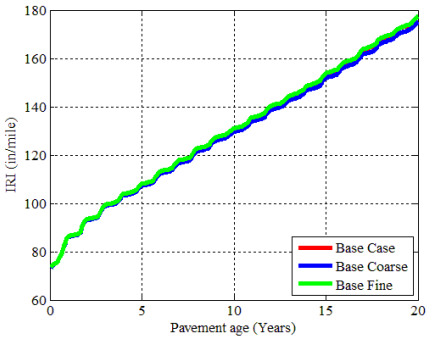

(a) HMA base layer

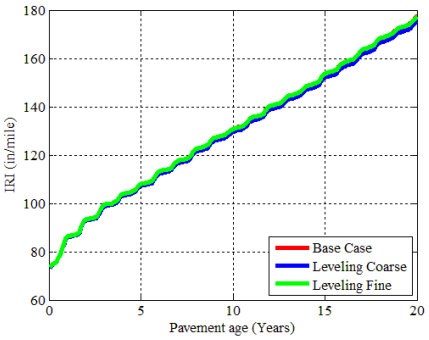

(b) HMA leveling layer

(c) HMA top layer

Figure 4-37 IRI predictions

4.5.2 Impact of Binder *G** Variations on Predicted Pavement Performance

In Part 1 of the study, several binders being used by MDOT were tested and characterized. It was observed that multiple binders with similar PG can have significantly different rheological behavior; i.e., master curves for dynamic shear modulus (*G**). The main objective of this investigation was to assess the variations in the MEPDG pavement performance predictions due to multiple binders having the same PG but different *G** master curves. Figure 4-38 shows the *G** master curves for two binders with the same PG grading (PG 64-28). The two binders have different G* magnitude at different frequencies.

In order to evaluate the effect of *G** on predicted performance of HMA over HMA, a typical cross-section was selected. All inputs were held constant while *G** data was used to characterize the binder at level 1. Figure 4-39 shows the predicted pavement performance. The results show that the effect of *G** variation is only important for rutting prediction. Therefore, it is recommended that *G** master curve (level 1) should be used if available, especially if rutting is a dominant distress. The variations in *G** master curve could be attributed to different binder sources for the same PG. However, it is anticipated that if a binder from the same source is utilized for mix design at a specific location, the level 1 *G** master curve should not vary significantly. Therefore, an average can be used for multiple G* master curves. Part 1 of this study addressed this issue in more detail.

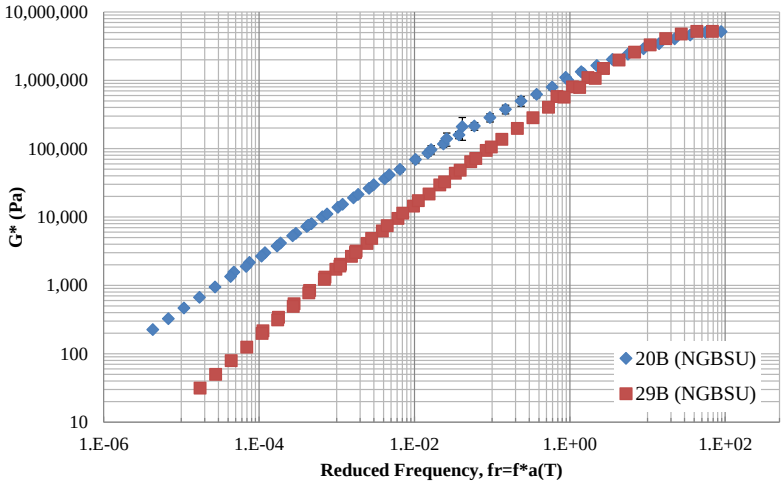

Figure 4-38 The G* master curves for two binders with same PG

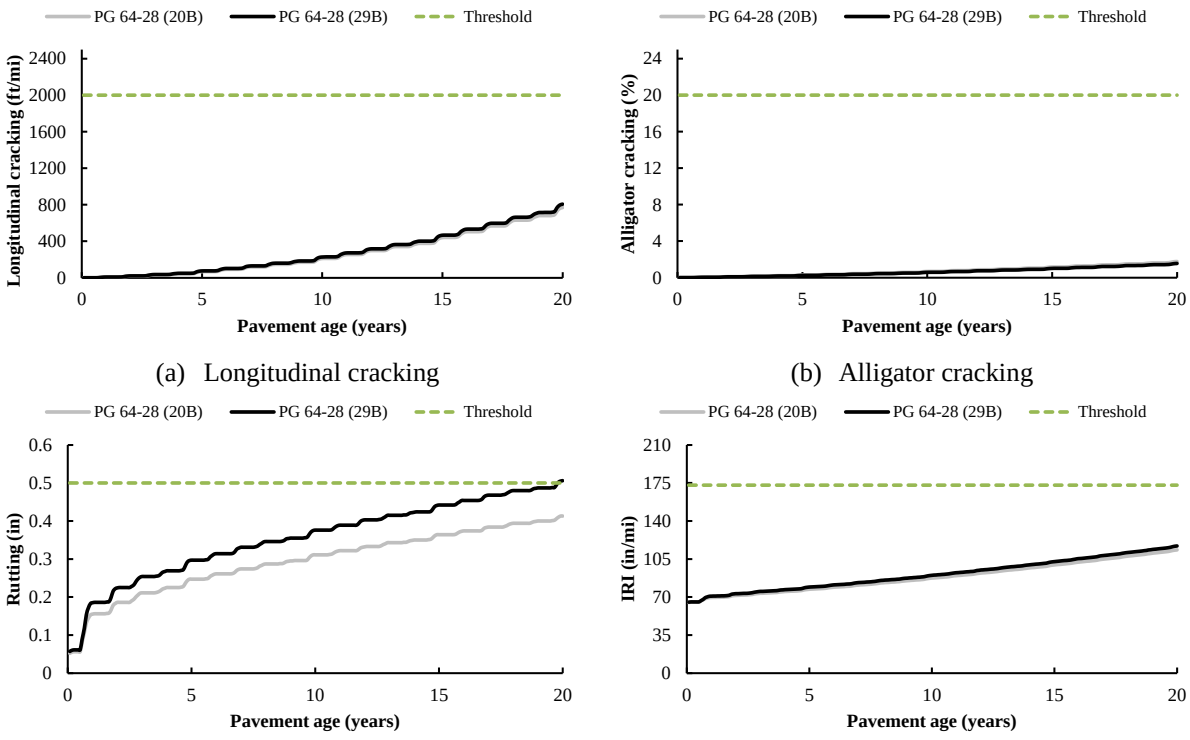

(a) Longitudinal cracking

(b) Alligator cracking

(c) Rutting

(d) IRI

Figure 4-39 The effect of G* variation on predicted HMA over HMA pavement performance

4.5.3 Impact of Unbound Layer Gradations on Predicted Performance

The main objective of this investigation is to study the impact of aggregate base and subbase gradations on the predicted performance. A sensitivity analysis was performed to study the effects. Three gradations each were selected for base and subbase materials. The gradations were selected for fine and coarse aggregates for each material type from the MDOT specifications. In addition, the default gradation based on A-3 and A-1-a in the DARWin-ME was considered for base and subbase materials, respectively. It should be noted that a pavement structure can be designed based on several combinations of these materials with different gradations. The design matrix for the sensitivity study is shown in Table 4-60. The following procedure was used to select the coarse, and fine aggregate gradations:

1. Determine materials used for base and subbase from MDOT specifications
    a. Base course – 22A, 21AA,
    b. Subbase – Class II materials
2. Determine gradations from the MDOT specifications
    a. Table 902-1 and 902-2 for base materials
    b. Table 902-4 for subbase materials
3. Perform DARWin-ME analysis for both new JPCP and HMA pavements with coarse (lower) and fine (upper) specification limits for base and subbase materials.

Table 4-60 Design matrix for sensitivity analysis

Material type	Pavement scenario							
	1	2	3	4	5	6	7	8
Base material (A-3)	Coarse	Fine	Default	Default	Coarse	Coarse	Fine	Fine
Subbase material (A-1-a, A-1-b)	Default	Default	Coarse	Fine	Coarse	Fine	Coarse	Fine

Figure 4-40 shows the gradations for the selected base and subbase layers. The analyses were performed for new JPCP and flexible pavements. The cross-section information is summarized in Table 4-61. For each pavement type the time to reach a threshold for a specific distress was determined. Figure 4-41 shows the pavement performance predictions and time to reach threshold for new rigid pavement. The results show that the difference in time to failure for transverse cracking is less than 2 years for any combination shown in Table 4-60. The faulting and IRI predictions did not reach the threshold limit in the 20 year design life and therefore are not shown. Similar analysis for unbonded overlay showed no difference in the predicted performance for all combinations. Figure 4-42 shows the results for alligator and reflective cracking as well as for surface rutting. Longitudinal cracking and IRI did not reach the threshold limit in the 20 year design and therefore are not shown. Based on these results it is recommended that for the same material type and climate, the base and subbase aggregate gradations can be selected within the limits of the specifications or just use the default values.

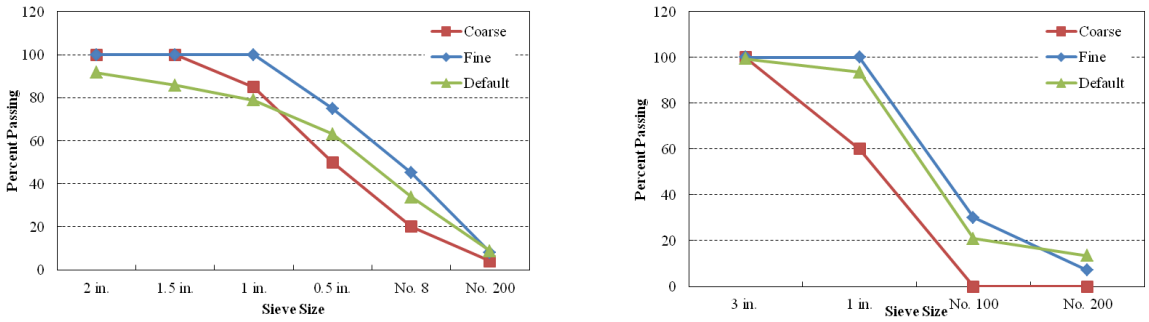

(a) base (b) subbase

Figure 4-40 Coarse, fine and default gradations

Table 4-61 Cross-section information

Pavement type	Layer type	Thickness (inches)
Rigid	JPCP	9
	Base	4
	Subbase	10
Flexible	HMA	6
	Base	8
	Subbase	15

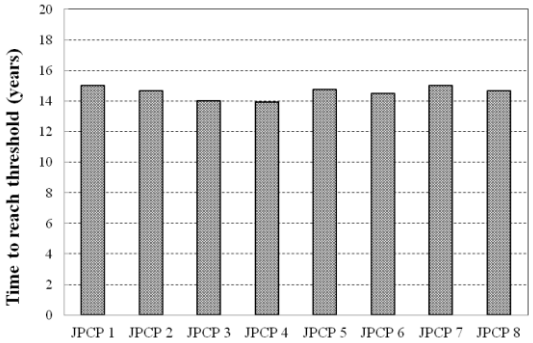

(a) Time to threshold

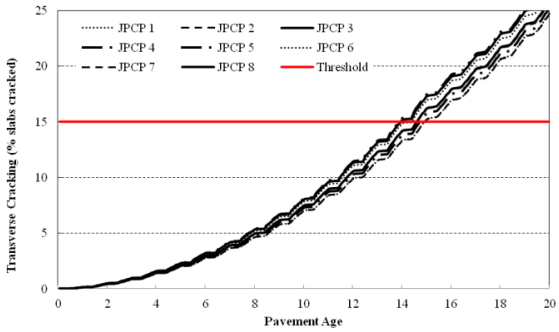

(b) Transverse cracking

Figure 4-41 Impact of aggregate gradation on rigid pavement performance

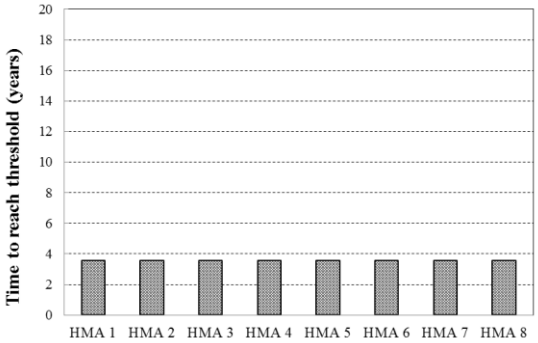

(a) Time to threshold

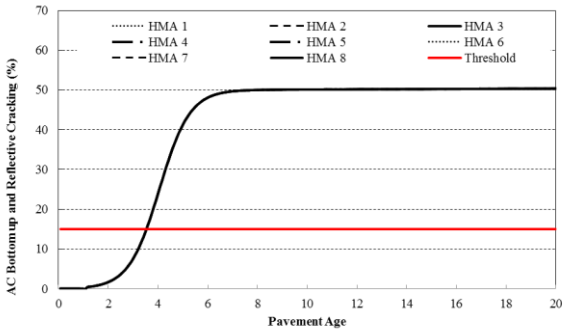

(b) Alligator and reflective cracking

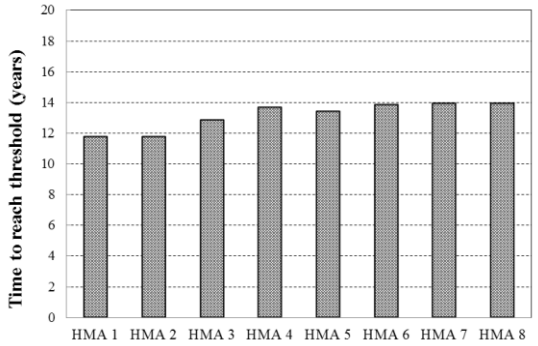

(c) Time to threshold

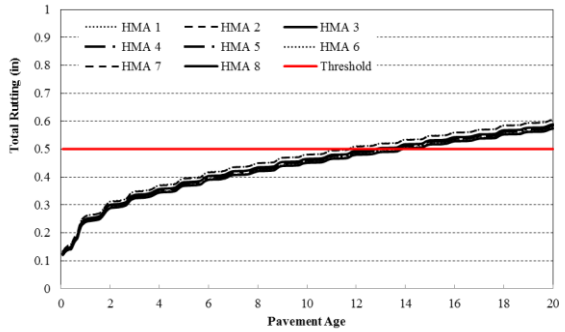

(d) Surface rutting

Figure 4-42 Impact of aggregate gradation on HMA over HMA pavement performance

CHAPTER 5 - VERIFICATION OF REHABILITATION DESIGN

5.1 INTRODUCTION

Validation of the MEPDG/DARWin-ME performance models is necessary to determine how well the models predict measured pavement performance in the State of Michigan. The first step in the verification process is to identify projects across different regions in the State based on local pavement design and construction practices. The second step involves extraction of the measured pavement performance data for each project from the MDOT Pavement Management System (PMS) and Sensor (laser measured IRI, rutting and faulting) database. The third step entails documentation of all input data related to pavement materials, cross-section, traffic and climatic conditions for the identified projects. The accuracy of these input data is important in determining the true predictability of the performance models in the MEPDG/DARWin-ME. Finally, measured and predicted performances are compared for each project to evaluate the existing performance models and to identify the local calibration needs. It should be noted, that only DARWin-ME was used for the verification of the rehabilitation models. In this chapter, the work related to the following tasks as outlined in Chapter 1 is presented:

- Task 2-4: Project identification and selection
    - Project selection criteria and matrix
    - Project information by rehabilitation option
- Task 2-5: Verification of rehabilitation performance models
    - Project performance
        - Available distresses in MDOT's PMS and conversion to match DARWin-ME
        - Project field performance
    - Project Inputs for verification
    - Verification results
        - Predicted vs. measured
        - Model accuracy
        - Need for local calibration

5.2 PROJECT IDENTIFICATION & SELECTION

In-service pavement projects were identified and selected to determine the validity of the performance prediction models for Michigan. It should be noted that some identified pavement projects may not be selected because they lack sufficient performance data or adequate construction records. The project selection criteria, design matrix, and a summary of the selected projects are discussed in the subsequent sections.

5.2.1 Project Selection Criteria and Design Matrix

MDOT identified and provided rehabilitation projects (unbonded, rubblized and composite overlays) for the verification of the rehabilitation models. The MSU research team identified HMA over HMA projects and MDOT provided the needed inputs. The HMA over HMA pavement projects to be included in the study were selected based on the following criteria:

- Site factors: The site factors will address the various regions in the state, climatic zones and subgrade soil types.
- Traffic: Three traffic levels were selected; level 1, less than 1000 AADTT, level 2, 1000 to 3000 AADTT; and level 3 more than 3000 AADTT. The three levels were selected based on pavement class, trunk routes, US routes and Interstate routes.
- Overlay thicknesses: The range of constructed overlay thicknesses.
- Open to traffic date: The information is needed to determine the performance period.
- As built cross-section: Includes details of the existing structure and the overlay.
- Pre-overlay repairs performed on the existing pavement (such as partial and/or full depth repairs, dowel bar retrofit)
- Material properties of both the existing and the new structure

Table 5-1 summarizes the number of selected pavement projects based on the selection criteria presented above. A total of 42 projects were selected representing various rehabilitation options. It can be seen that each rehabilitation option contains more than 5 projects.

Table 5-1 Selection matrix displaying selected projects

Rehabilitation type	Traffic level*	Overlay thickness level*	Age (years)			Total
			<10	10 to 20	>20	
Composite overlay	1	2		1	1	7
	2	2		2	2	
	3	2			1	
HMA over HMA	1	1			8	16
		2	1	5		
	2	2	1		1	
Rubblized overlay	1	2		4	2	11
		3		2		
	2	2			1	
	3	2			1	
		3		1		
Unbonded overlay	2	2		1		8
		3		1		
	3	3	1	5		
*Levels		1	2	3		
Traffic (AADTT)		<1000	1000-3000	>3000		
Overlay thickness (in)		<3	3-6	>6		

5.2.2 Project Information by Rehabilitation Option

Pavement cross-section and material related information for each selected pavement project are essential to generate the most representative project in the DARWin-ME. In addition, the validity of the performance predictions using the software depends on how well the overlay and existing pavement layers are defined. This section outlines the overlay, existing pavement cross-section, and the geographical location information of the selected projects.

5.2.2.1. Unbonded Overlays

Figure 5-1 presents the locations of the eight unbonded concrete overlay pavement projects selected for this study. Geographically, the eight projects are located on the east and west sides of the Lower Peninsula of Michigan. Since there are no unbonded JPCP pavements built prior to 1998 in the State of Michigan, the selected projects were constructed between 1998 and 2004. Table 5-2 provides a detailed summary of the selected projects based on traffic, overlay thickness, and pavement age. Table 5-3 summarizes the cross-section information for each selected project. The data in the table indicate that:

- The overlay thickness ranges from 6 to 8 inches
- The existing PCC pavement thickness for all projects is 9 inches.
- The existing base and subbase thicknesses ranged from 3 to 4 inches and from 10 to 14 inches, respectively.
- The asphalt interlayer thickness for all unbonded overlay projects is 1-inch, except for one project that had a variable interlayer thickness from 1- to 2.5-inch because crown correction was done with the separator layer.
- The average annual daily truck traffic (AADTT) for each project is greater than 1000.

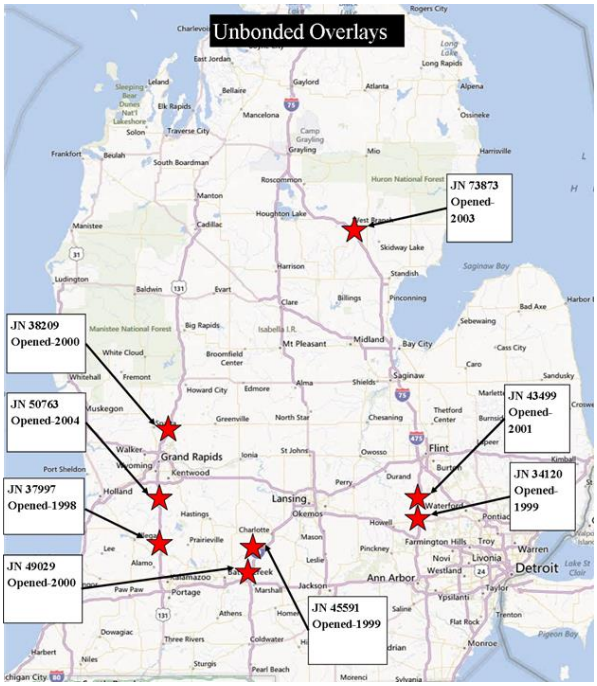

Figure 5-1 Geographic location of the eight unbonded overlay projects

Table 5-2 Complete project matrix for unbonded overlays

Rehab type	Traffic (AADTT)	Age (years)	OL thickness (in)	No. of projects
Unbonded overlays	<1000	<10	<3	
			3 to 6	
			>6	
		10 to 20	<3	
			3 to 6	
			>6	
		>20	<3	
			3 to 6	
			>6	
	1000 to 3000	<10	<3	
			3 to 6	
			>6	
		10 to 20	<3	
			3 to 6	1
			>6	1
		>20	<3	
			3 to 6	
			>6	
	>3000	<10	<3	
			3 to 6	
			>6	1
		10 to 20	<3	
			3 to 6	
			>6	5
		>20	<3	
			3 to 6	
			>6	
Total				8

Table 5-3 Unbonded overlay cross-section information

Job number	Control section	Overlay thickness (in)	Existing thickness (in)	Base thickness (in)	Subbase thickness (in)	Interlayer thickness (in)	Interlayer PG Grade
37997	3111	7.1	9 (1960)	3	11	1	PG 58-28
34120	47014	7.9	9 (1960)	3	14	1	PG 58-28
49029	13074	7.1	9 (1969/1972)	4	10	1	PG 58-28
45591	13074 23061	7.1	9 (1972)	4	10	1	PG 58-28
38209	41132 41133	6.3	9 (1970/1973)	4	10	1	PG 58-28
43499	47014	7.1	9 (1960)	3	14	1	PG 70-28
73873	65041	6	9 (1974)	4	10	1	PG 64-28
50763	39014 3111	6.5	9 (1963)	4	10	1-2.5	PG 58-28

5.2.2.2. Rubblized Overlays

Figure 5-2 shows the locations of the 11 selected rubblized projects. Geographically, all projects are located in the Lower Peninsula of Michigan. The projects were constructed between 1989 and 2000. The existing JRCP pavement was rubblized prior to applying an HMA surface. Table 5-4 presents a detailed summary of the selected projects based on traffic, overlay thickness, and pavement age. Table 5-5 lists the cross-section information for each project. The data in the table indicate that:

- The overlay thickness ranges from 4 to 9.5 inches.
- The existing PCC pavement thicknesses ranged from 8 to 9 inches.
- The existing base and subbase thicknesses range from 0 to 4 inches and from 0 to 18 inches, respectively.

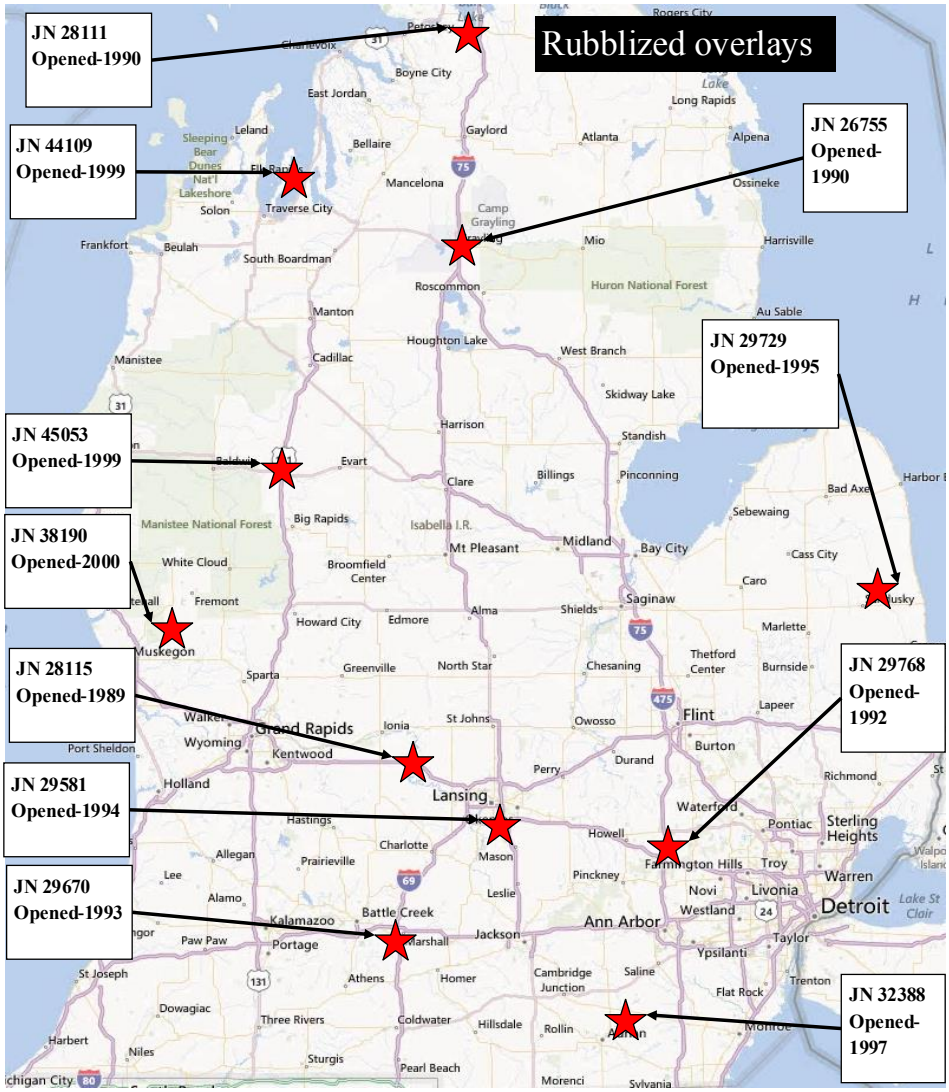

Figure 5-2 Geographic location of the eleven rubblized overlay projects

Table 5-4 Complete project matrix for rubblized overlays

Rehab type	Traffic (AADTT)	Age (years)	OL thickness (in)	No. of projects
Rubblized overlays	<1000	<10	<3	
			3 to 6	
			>6	
		10 to 20	<3	
			3 to 6	4
			>6	2
		>20	<3	
			3 to 6	
			>6	
	1000 to 3000	<10	<3	
			3 to 6	
			>6	
		10 to 20	<3	
			3 to 6	
			>6	
		>20	<3	
			3 to 6	3
			>6	
	>3000	<10	<3	
			3 to 6	
			>6	
		10 to 20	<3	
			3 to 6	
			>6	1
		>20	<3	
			3 to 6	1
			>6	
Total				11

Table 5-5 Rubblized overlay cross-section information

Job Number	Overlay thickness (in)	Existing thickness (in) (construction. date)	Base thickness (in)	Subbase thickness (in)	Penetration or PG Grade
28115	5	9 (1959)	3	9	120-150
26755	4.25	8 (1955)	0	0	120-150
29768	5.25	9 (1962)	4	14	85-100
29670	6.25 @ Center Line, 5.5 @ rt edge	9 (1960)	3	9	85-100
29581	7.5 min to 9.5(crown correction.)	9 (1963/64)	4	10	85-100
28111	4	9-7-9 (1936/37)	0	0	200-250
29729	5 @ edge; 7.2” @ Center Line	9-7-9 (1939)	0	18 average; (8 min)	120-150
45053	5.5 minimum	9 (1958)	3	12	64-28 (T)
44109	7.5	8 (1954)	0	9	58-28
38190	5.5	9 (1963)	4	14	58-28
32388	6 @ Center Line; 7 @ edge	8 (1953)	0	6 min, up to 12	58-28

5.2.2.3. Composite Overlays

Figure 5-3 shows the location of the 7 composite overlay projects selected for this study. Geographically, the seven projects are located in the Lower Peninsula of Michigan. The projects were constructed between 1987 and 2000. The composite overlay projects are built over an intact JRCP. Table 5-6 presents a detailed summary of the selected projects based on traffic, overlay thickness, and pavement age. Table 5-7 summarizes the cross-section information for each project. The data in the table indicate that:

- The overlay thickness ranges from 3.5 to 4.5 inches.
- The existing PCC pavement thicknesses are between 7 and 9 inches.
- The existing base and subbase thicknesses range from 0 to 4 inches and from 0 to 15 inches, respectively.

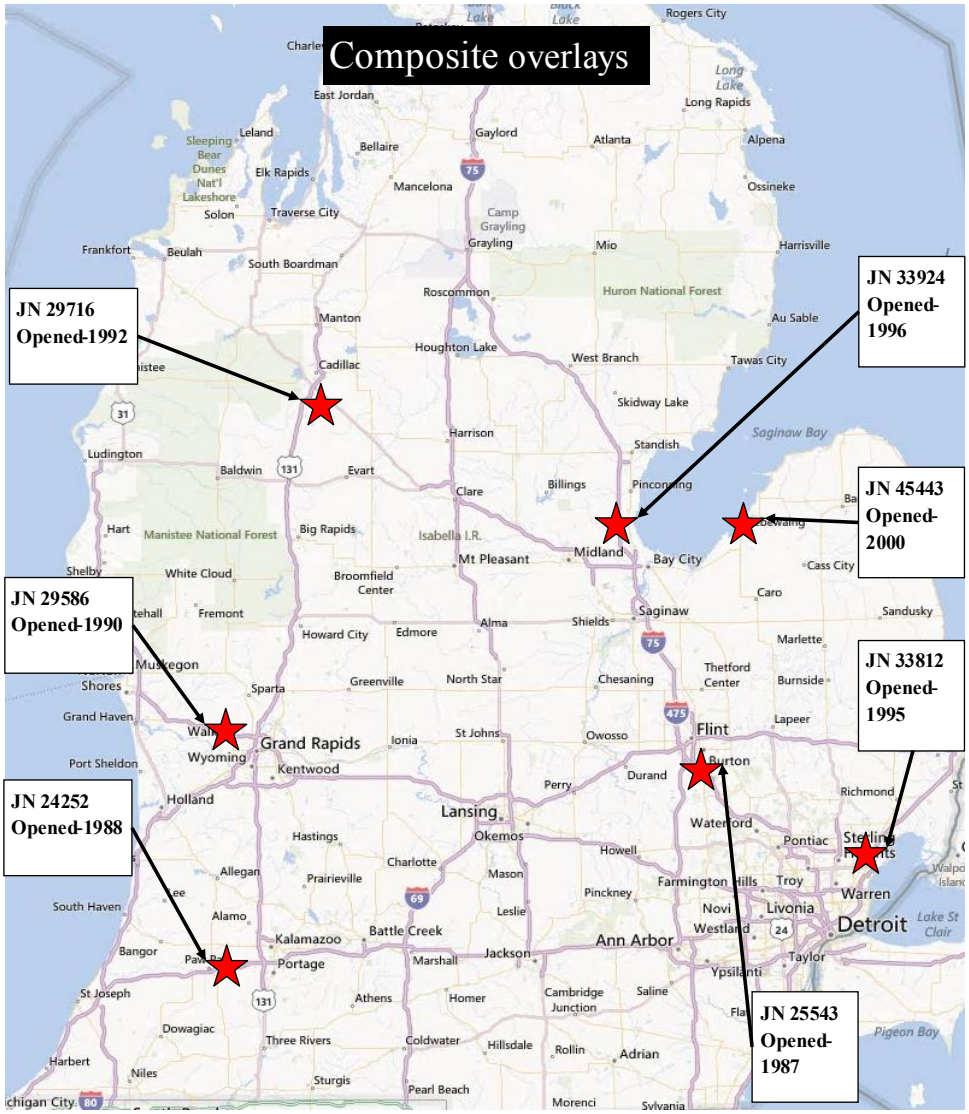

Figure 5-3 Geographical location of the seven composite overlay projects

Table 5-6 Complete project matrix for composite overlays

Rehab type	Traffic (AADTT)	Age (years)	OL thickness (in)	No. of projects
Composite	<1000	<10	<3	
			3 to 6	
			>6	
		10 to 20	<3	
			3 to 6	1
			>6	
		>20	<3	
			3 to 6	1
			>6	
	1000 to 3000	<10	<3	
			3 to 6	
			>6	
		10 to 20	<3	
			3 to 6	2
			>6	
		>20	<3	
			3 to 6	2
			>6	
	>3000	<10	<3	
			3 to 6	
			>6	
		10 to 20	<3	
			3 to 6	
			>6	
		>20	<3	
			3 to 6	1
			>6	
Total				7

Table 5-7 Composite overlay cross-section information

Job number	Overlay thickness (in)	Existing thickness (in) (construction date)	Base thickness (in)	Subbase thickness (in)	Penetration or PG Grade
25543	4	9 (1963)	4	10	85-100
24252	4.5	9 (1959)	3	9	85-100
29586	3	9 (1961)	3	12 minimum	85-100
29716	3.5	9-7-9 (1938)	0	0	120-150
33812	3	9 (1959)	3	14 min	85-100
33924	4	8 (1964/67)	4	Sloped Lt to Rt 3-10	120-150
45443	3.5 min	8 (1949)	0	15	64-28

5.2.2.4. HMA over HMA

Figure 5-4 shows the location of 14 out of 15 HMA over HMA pavement projects selected for this study. One of the projects did not meet all criteria and was excluded from the verification study. Geographically, 14 projects are located in the Lower Peninsula and one project in the Upper Peninsula of Michigan. In the Lower Peninsula, six projects are located in the South West, five in the North West, and three projects are located in the Southern part of the State. All projects were constructed between 1983 and 2005. The HMA over HMA projects are built over existing flexible pavements. Table 5-8 presents a detailed summary of the selected projects based on traffic, overlay thickness, and pavement age, while Table 5-9 summarizes the cross-section information. The data in the latter table indicate that:

- The overlay thickness ranges from 2 to 3.5 inches.
- The existing HMA pavement thicknesses range between 1.5 and 7.5 inches.
- The existing base and subbase thicknesses range from 4 to 11 inches and from 0 to 28 inches respectively.

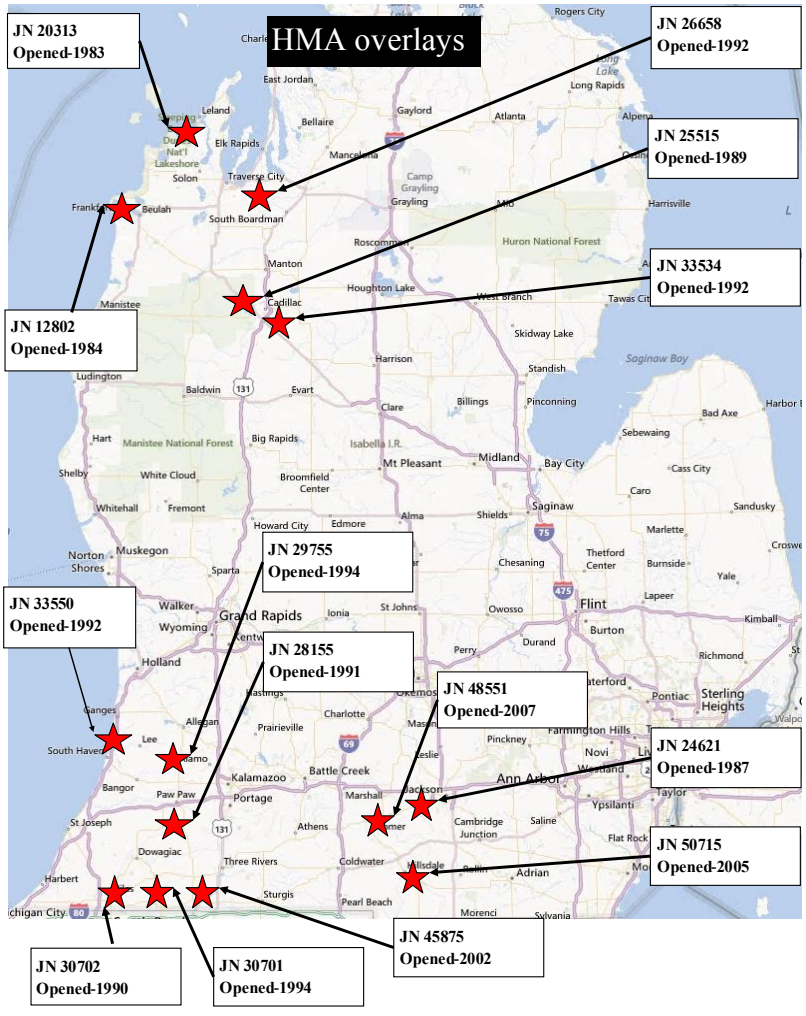

Figure 5-4 Geographical location of 14 HMA over HMA projects

Table 5-8 Complete project selection matrix for HMA over HMA

Rehab type	Traffic (AADTT)	Age (years)	OL thickness (in)	No. of projects
HMA over HMA	<1000	<10	<3	
			3 to 6	1
			>6	
		10 to 20	<3	
			3 to 6	5
			>6	
		>20	<3	7
			3 to 6	
			>6	
	1000 to 3000	<10	<3	
			3 to 6	
			>6	
		10 to 20	<3	
			3 to 6	
			>6	
		>20	<3	
			3 to 6	2
			>6	
	>3000	<10	<3	
			3 to 6	
			>6	
		10 to 20	<3	
			3 to 6	
			>6	
		>20	<3	
			3 to 6	
			>6	
Total				15

Table 5-9 HMA over HMA cross-section information

Job number	Overlay thickness (in)	Existing thickness	Base thickness (in)	Subbase thickness (in)	PG Grade
33534	2.5	3.25	11	25	85-100 ex, 120-150 OL
33550	3	6.4	11	28	85-100
28155	2.5	5.2	7	12	120-150
26658	2.5				120-150
29755	3	4-5.5	4 or 5 stabilized	0 or 15	120-150
30701	3	4.5	7 or 7+3 select	0 or 18	85-100
31047	3	3.3	10	13.7	120-150
32361	3	3.7	5-7-5	0 or 15	120-150
45875	2	4.5	6-11	8	64-28
50715	3.5	7.59	6		64-28
20313	2.25	1.5	5	0 or 12	120-150
12802	2.5	2.25 or 4.75	7		120-150
24621	2.5	3.75	8		120-150
25515	2.5	2.25	10		120-150
30702	2.5	7.1	5		85-100

5.3 PROJECT FIELD PERFORMANCE

Once all the projects were selected, the next step was to determine the measured time series performance for each project. MDOT collects distress and laser based measurement (sensor) data on their pavement network every other year. The distress data in the MDOT PMS are represented by different principle distress codes (PD's). Each PD corresponds to a visually measured surface distress observed in the field. Certain distress types collected by MDOT are expressed in a form that is not compatible with the DARWin-ME; therefore, conversions were necessary to make the data comparable. The distress types collected by MDOT and the necessary conversion process are discussed in this section. Furthermore, the current condition of each pavement section is also presented.

5.3.1 Selected Distresses and Conversion

The necessary distress information was identified and extracted from the MDOT PMS and sensor database. The extraction process of all the necessary distress and sensor data needed assistance from MDOT. The MDOT PMS Current Distress Manual was used to determine all the PD's corresponding to predicted distresses in the DARWin-ME. The latest version of the document outlining all the different distress calls can be found in Appendix D. It should be noted that, all PD's were included since MDOT began collecting this data (1992), earlier versions of the PMS manual were consulted to ensure that the correct data was extracted for all years.

The necessary steps for PMS data extraction include:

1. Identify the PD's that corresponds to the MEPDG/DARWin-ME predicted distresses,
2. Convert (if necessary) MDOT PD's to units compatible with the MEPDG/DARWin-ME
3. Extract PD's, and sensor data for each project
4. Summarize time-series data for each project

The identified and extracted pavement distresses and conditions for flexible and rigid pavements are summarized in Tables 5-10 and 5-11. A detailed discussion of the conversion process is detailed for both, flexible and rigid overlays.

Table 5-10 Flexible pavement distresses

Flexible pavement distresses	MDOT principle distresses	MDOT units	DARWin-ME units	Conversion needed?
IRI	Directly measured	in/mile	in/mile	No
Top-down cracking	204, 205, **724, 725**	miles	ft/mile	Yes
Bottom-up cracking	234, 235, **220, 221, 730, 731**	miles	% area	Yes
Thermal cracking	**101,** 103, 104, 114, **701, 703, 704,** 110	No. of occurrences	ft/mile	Yes
Rutting	Directly measured	in	in	No
Reflective cracking	No specific PD	None	% area	No

*Bold numbers represent older PD's that are not currently in use

Table 5-11 Rigid pavement distresses

Rigid pavement distresses	MDOT principle distresses	MDOT units	DARWin-ME units	Conversion needed?
IRI	Directly measured	in/mile	in/mile	No
Faulting	Directly measured	in	in	No
Transverse cracking	112, 113	No. of occurrences	% slabs cracked	Yes

5.3.1.1. Distresses conversion for HMA designs

It should be noted that only the distress types predicted by the DARWin-ME were considered for the verification exercise. The corresponding MDOT PD's were determined and compared to distress types predicted by the DARWin-ME to determine if any conversions were necessary. The MDOT measured pavement distresses that are related to HMA overlays are listed in Table 5-10. The conversion process (if necessary) for all distress types is as follows:

IRI: The IRI measurements in the MDOT sensor database are compatible to those in DARWin-ME. Therefore, no conversion or adjustments was need and the data were used directly.

Top-down cracking: Top-down cracking is defined as load related cracking in the wheel-path (longitudinal cracking). The PD's 204, 205, 724, and 725 are assumed to correspond to top down cracking in the MDOT PMS database because those may not have developed an indication of alligator cracking; however, these cracks could be bottom-up. The PD's are recorded in miles and needs conversion to feet/mile. Data from the wheel-paths were summed into one value and divided by the total project length.

Bottom-up cracking: The bottom up cracking is defined as alligator cracking in the wheel-path. The PD's 234, 235, 220, 221, 730 and 731 match this requirement in the MDOT PMS database. The PD's have units of miles; however, to make those compatible with the DARWin-ME alligator cracking units, conversion to percent total area is needed. This can be achieved by using the following Equation (1):

$$\%AC_{bottom-up} = \frac{\text{Length of cracking} \times \text{width of wheelpaths}}{\text{Length of project} \times \text{Lane width}} \quad (1)$$

Thermal cracking: Thermal cracking corresponds to transverse cracking in flexible pavements. The DARWin-ME predicts thermal cracking in feet/mile. The PD's 101, 103, 104, 114, 701, 703 and 704 were utilized to extract transverse cracking in flexible and rubblized pavements. For the composite pavement, PD's 101, 110, 114 and 701 were used. The transverse cracking is recorded as the number of occurrences. In order to convert transverse cracking in feet/mile, the number of occurrences was multiplied by the lane width for PD's 101, 103 and 104. For the PDs 114 and 701, the number of occurrences was multiplied by 3 feet because these PD's are defined as "tears" (short cracks) that are less than

half the lane width. All transverse crack lengths are summed and divided by the project length to get feet/mile.

Rutting: This is the total amount of surface rutting contributed by all the pavement layers. The average rutting (left & right wheel-paths) was determined for the entire project length. No conversion was necessary. It is assumed that the measured rutting corresponds to total surface rutting, and was compared to the total rutting in the DARWin-ME.

Reflective cracking: MDOT does not have any specific PDs for reflective cracking. It is difficult to determine the difference between a thermal and a reflective crack at the surface. Therefore, the total transverse cracking observed can be compared to the total combined thermal and reflective cracking. Reflective cracking was not included in verification for this reason and due to the limitations in the prediction model.

5.3.1.2. Distress conversion for JPCP Designs

As mentioned before, only the distresses that are predicted in the DARWin-ME were considered for verification. The corresponding MDOT PD's were determined and necessary conversions were made if needed. Table 5-11 summarizes the distresses related to JPCP overlays and the conversion process is discussed below:

IRI: The IRI in the MDOT sensor database does not need any conversion; the values were used directly

Faulting: The faulting is predicted as average joint faulting by the DARWin-ME. The faulting values reported in the MDOT sensor database corresponds to the average height of each fault for both cracks and joints. However, the DARWin-ME faulting prediction does not distinguish between faulting at cracks or joints and only predicts faulting at the joints. Therefore, only measured average joint faulting should be compared with the predicted faulting by DARWin-ME. However, because MDOT's data does not discern between faults at cracks and faults at joints, no conversions were made and the measured faulting at joints and cracks was directly compared to the predicted faulting from DARWin-ME.

Transverse cracking: The transverse cracking distress is predicted as % slabs cracked in the DARWin-ME. However, MDOT measures transverse cracking as the number of transverse cracks. PD's 112 and 113 correspond to transverse cracking. The measured transverse cracking needs conversion to percent slabs cracked by using Equation (2).

$$\%\ \text{Slabs Cracked} = \frac{\sum PD_{112,113}}{\left(\frac{\text{Project Length(miles)} \times 5280\ ft}{\text{Joint Spacing (ft)}}\right)} \times 100 \qquad (2)$$

5.3.2 Measured Field Performance

A customized PMS and sensor databases were created in order to query the selected PD's. The databases include all the distress and sensor data for multiple years in respective

Microsoft Access databases. These databases allowed the research team efficient performance data extraction for any project length. The databases included measured PMS performance data from 1992 to 2011 and the sensor data from 1996 to 2011, respectively. The sensor data prior to 1996 were not in a consistent format and could not be included in the custom database. The time series condition data were extracted for each selected project. The divided highway can have an increasing and a decreasing direction to indicate north/south or east/west bounds directions. Therefore, for such projects, both directions are included in the time-series data. Distress data for undivided highways are collected in one direction only. The threshold value of each distress and condition type is indicated by the horizontal straight line on each figure. The distress threshold values were discussed in Chapter 4.

5.3.2.1. Unbonded Concrete Overlays

The current performance of each unbonded overlay project is summarized in Figure 5-5. The magnitude represents the latest distress amount of each project regardless of maintenance fixes performed throughout the project life. The overlay pavement age is displayed in parentheses below the project number. It can be seen that none of the projects reached the distress thresholds for percent slabs cracked, IRI and faulting. It should be noted that all the project ages are below the design life of 20 years.

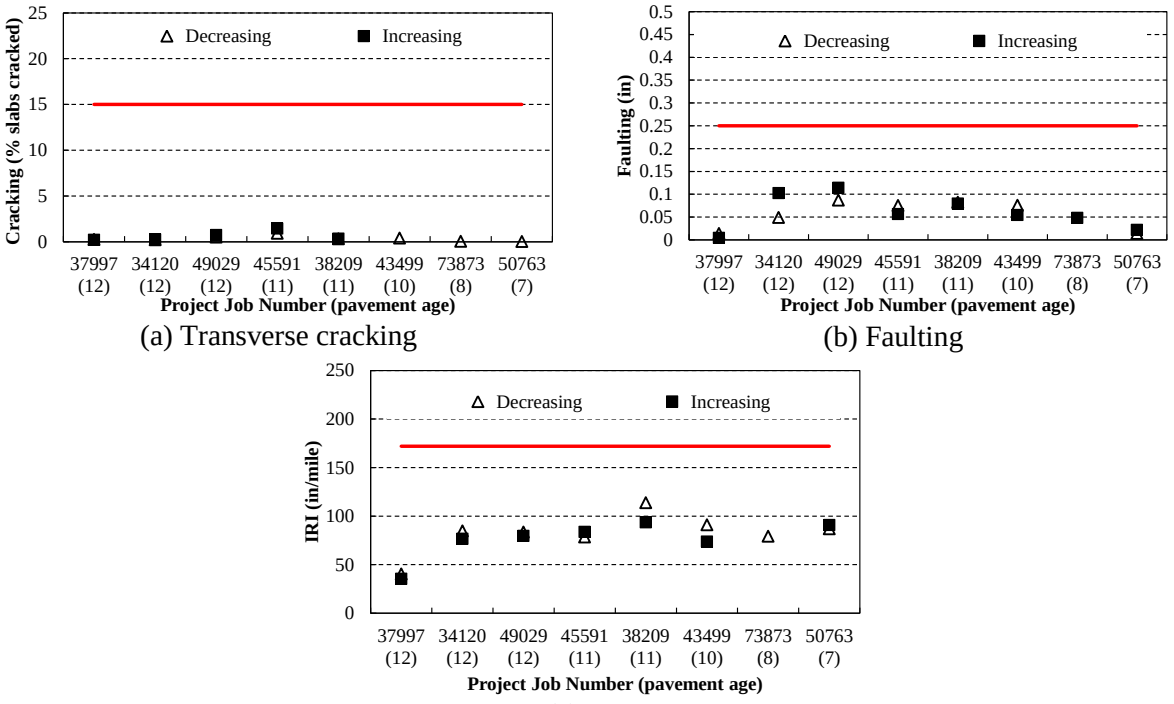

(a) Transverse cracking

(b) Faulting

(c) IRI

Figure 5-5 Current pavement distress and condition of unbonded overlay projects

Figure 5-6 shows an example of the extracted time-series data for Job number 37997. The distress data is plotted versus age for both the increasing and decreasing direction depending on the project. The divided highway can have increasing and decreasing direction to indicate north/south or east/west bounds. The vertical dashed lines indicate a maintenance action

performed on the pavement. For this particular pavement project, diamond grinding was performed in 2001, 2 years after construction, and joint sealing and concrete pavement restoration (CPR) were performed in 2006, 7 years after construction. It can be seen from the figure, that the maintenance fixes did not affect the magnitude of percent slabs cracked, but did affect IRI over time. It is possible that the IRI measurements were performed prior to the diamond grinding. However, it is reported for the same year as a fix. The time-series distress figures (in the same format) for all unbonded overlay projects can be found in Appendix C.

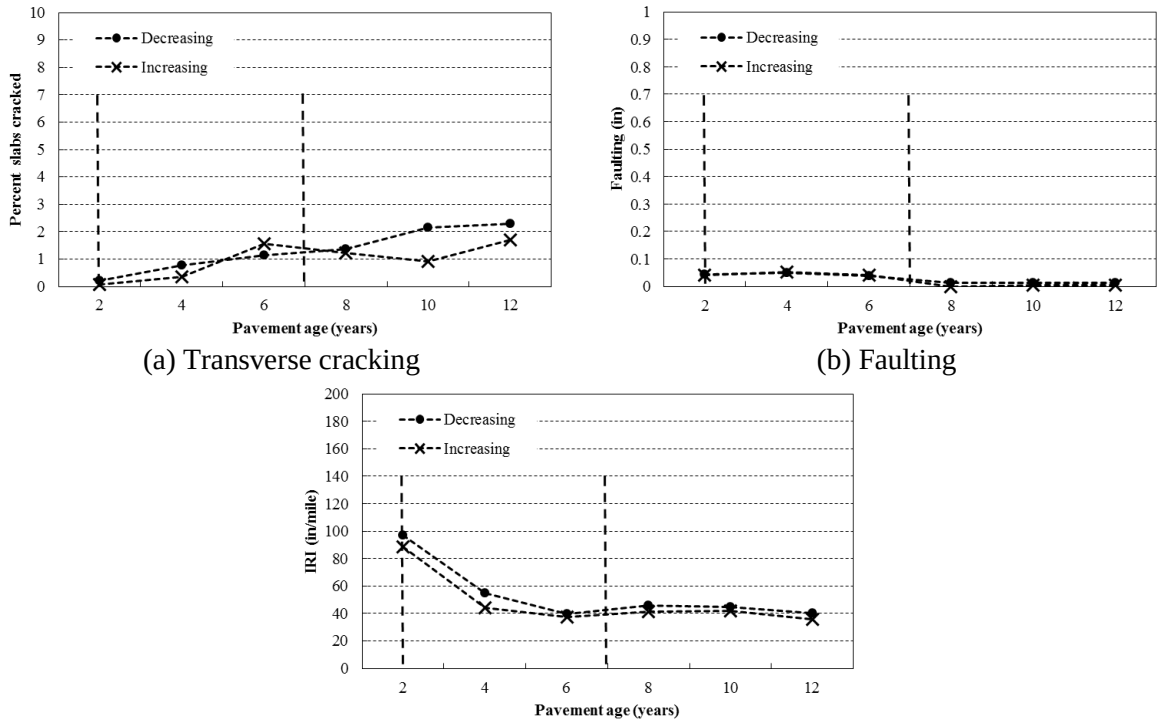

(a) Transverse cracking (b) Faulting

(c) IRI

Figure 5-6 Performance of unbonded overlay project 37997

5.3.2.2. Rubblized Overlays

The current performance of each rubblized overlay project is summarized in Figure 5-7. The distress magnitudes represent the latest distress value of each project regardless of maintenance fixes. The pavement age is displayed in parentheses below the project number. It can be seen that only thermal cracking exceeded the distress threshold value. It should be noted that it is not possible to determine the differences between thermal and reflective cracking from MDOT's PD's as they do not represent reflective cracking directly. Depending on the rubblization techniques used (badger or sonic breaker), joints could still be intact, and could cause reflective cracking in rubblized overlays.

As an example, Figure 5-8 shows the extracted time-series data for Job number 28115. The extracted distress data is plotted versus age for both the increasing and decreasing directions. The vertical dashed lines indicate a maintenance action performed on the pavement. For this particular pavement project, a chip seal was performed in 1998, 9 years after construction and an overband crack fill was performed in 2000, 11 years after construction. The figure

also shows that the number of distress points for both directions are not always equal. Both directions were included if the information was available. The IRI and rutting data were only available beyond 1996, and since this particular project was constructed prior to 1996, no data were available prior to the 9th year of the project. The time-series distress figures for all rubblized overlay projects can be found in Appendix C.

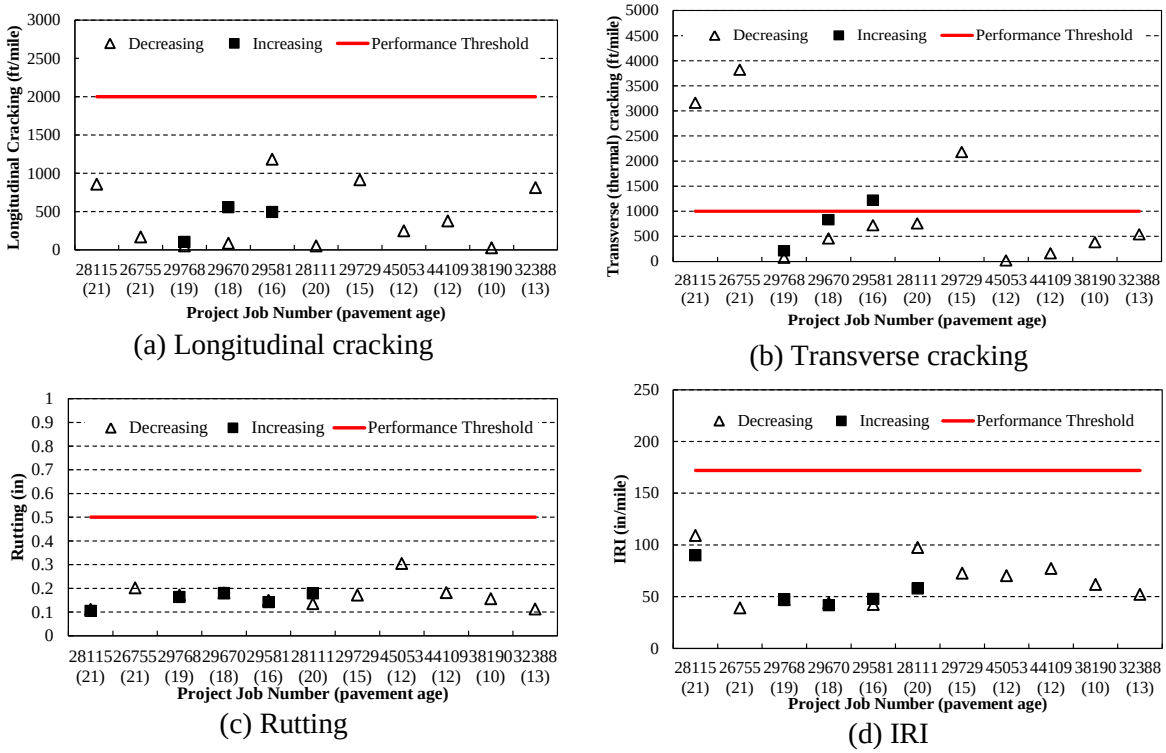

(a) Longitudinal cracking

(b) Transverse cracking

(c) Rutting

(d) IRI

Figure 5-7 Current pavement distress and condition for rubblized overlays

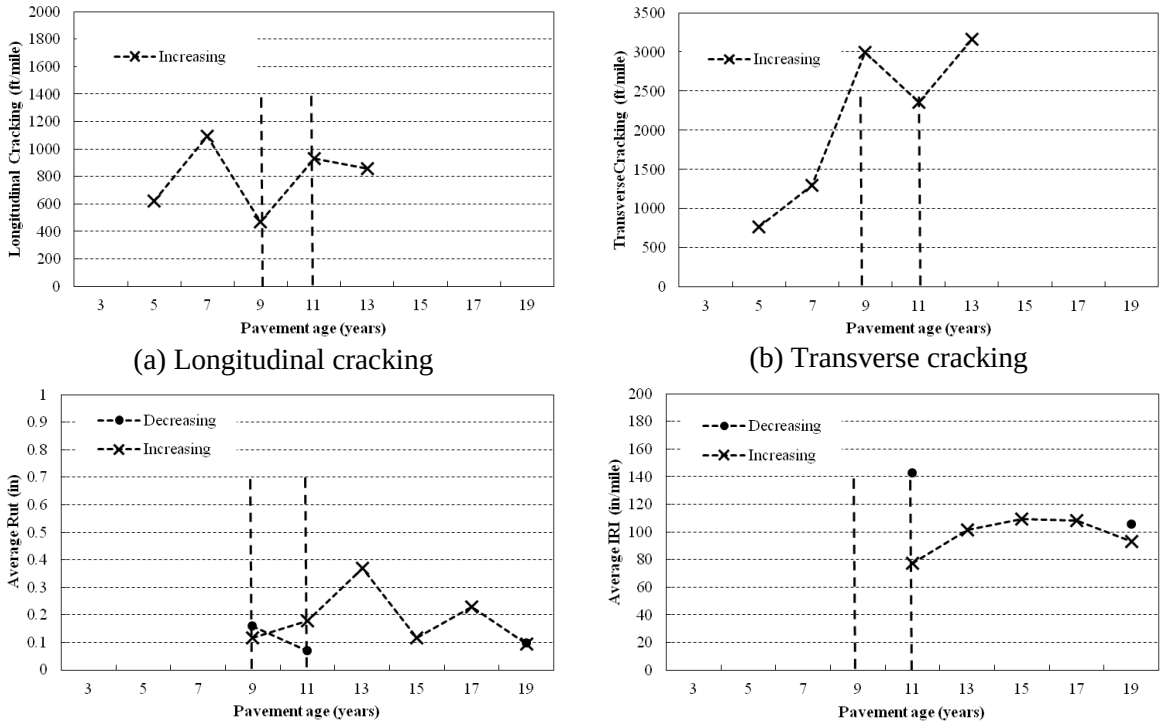

(a) Longitudinal cracking (b) Transverse cracking

(c) Rutting (d) IRI

Figure 5-8 Performance of rubblized overlay project 28115

5.3.2.3. Composite Overlays

The current performance of each composite overlay project is summarized in Figure 5-9. The distress magnitudes represent the latest distress value of each project regardless of the maintenance fixes. It can be seen that only thermal transverse cracking exceeded the distress threshold. Similar to rubblized overlays, it is not possible to distinguish between reflective cracking and thermal cracking in MDOT's PMS database. It is possible that some of the thermal cracking is actually reflective cracking.

Figure 5-10 shows the extracted time-series data for Job number 29586. The extracted distress data is plotted versus age for both the increasing and decreasing directions. The vertical dashed lines indicate if a maintenance action has been performed on the pavement. For this particular pavement project, a cold mill and resurfacing was performed in 1999, 9 years after construction. As mentioned for rubblized overlays, the missing IRI and rutting data is due to the age of the project. The time-series distress figures for all composite overlay projects can be found in Appendix C.

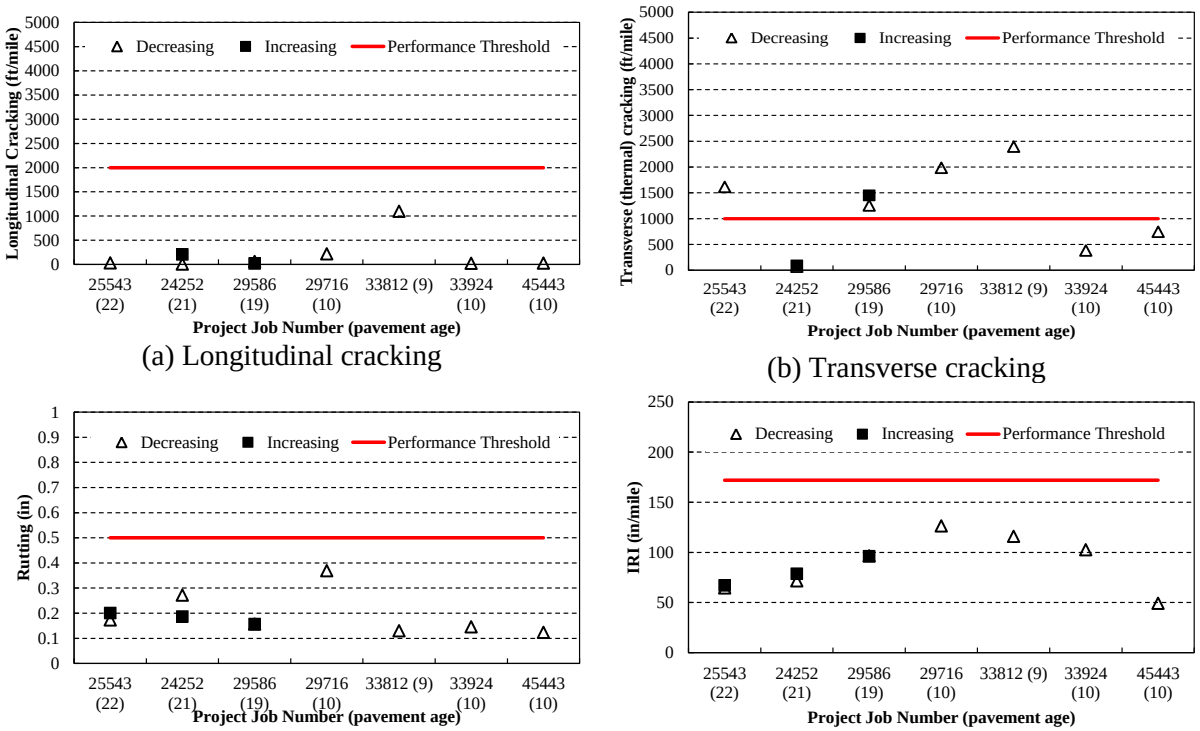

(a) Longitudinal cracking

(b) Transverse cracking

(c) Rutting

(d) IRI

Figure 5-9 Current pavement distress and condition of composite overlay projects

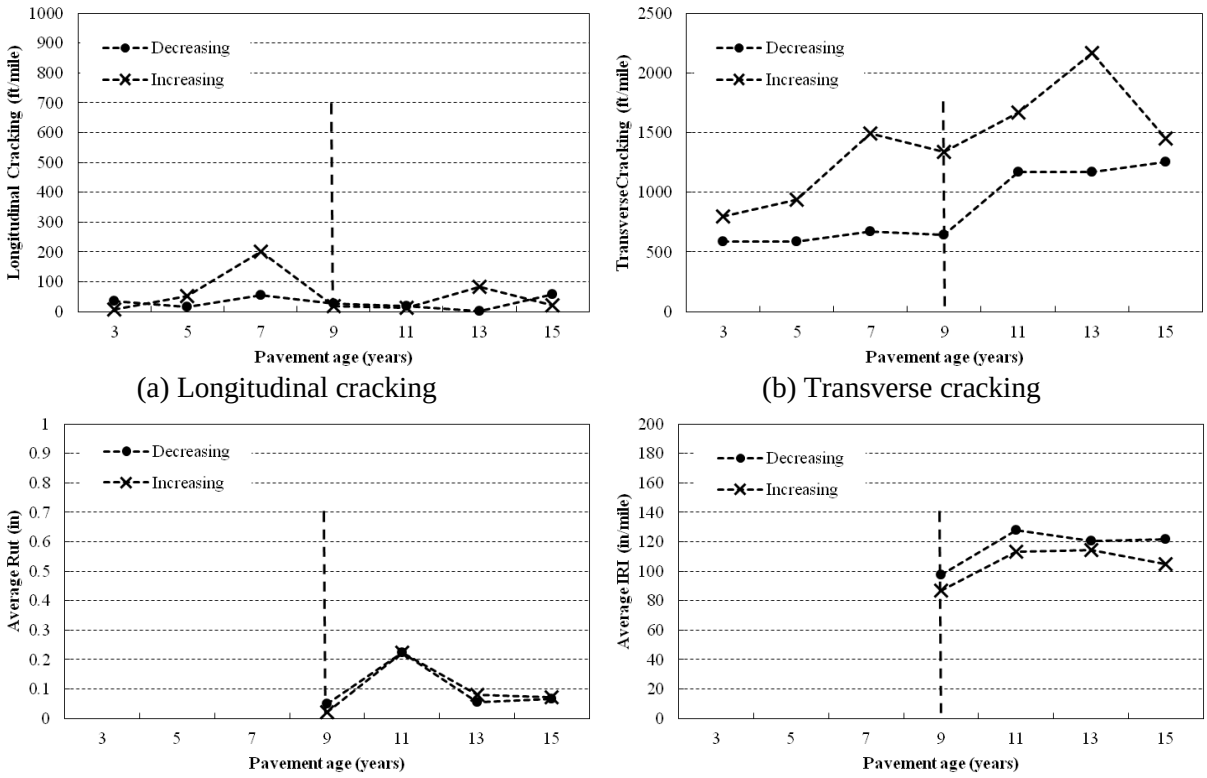

(a) Longitudinal cracking

(b) Transverse cracking

(c) Rutting

(d) IRI

Figure 5-10 Performance of composite overlay project 29586.

5.3.2.4. HMA over HMA

The current performance of each HMA over HMA project is summarized in Figure 5-11. The values represent the latest distress magnitude for each project regardless of maintenance fixes. It can be seen that one project exceeds the threshold for IRI and four projects exceeded the thermal transverse cracking distress threshold. As with rubblized and composite overlays, it is not possible to distinguish between thermal and reflective cracking.

Figure 5-12 shows the extracted time-series data for Job number 28155. The vertical dashed lines indicate the maintenance performed. For this particular project, crack treatments were performed in 1997 (5 years after construction) and 2000 (8 years after construction), a cold mill and resurfacing was performed in 2006 (14 years after construction). The time-series distress figures for all composite overlay projects can be found in Appendix C.

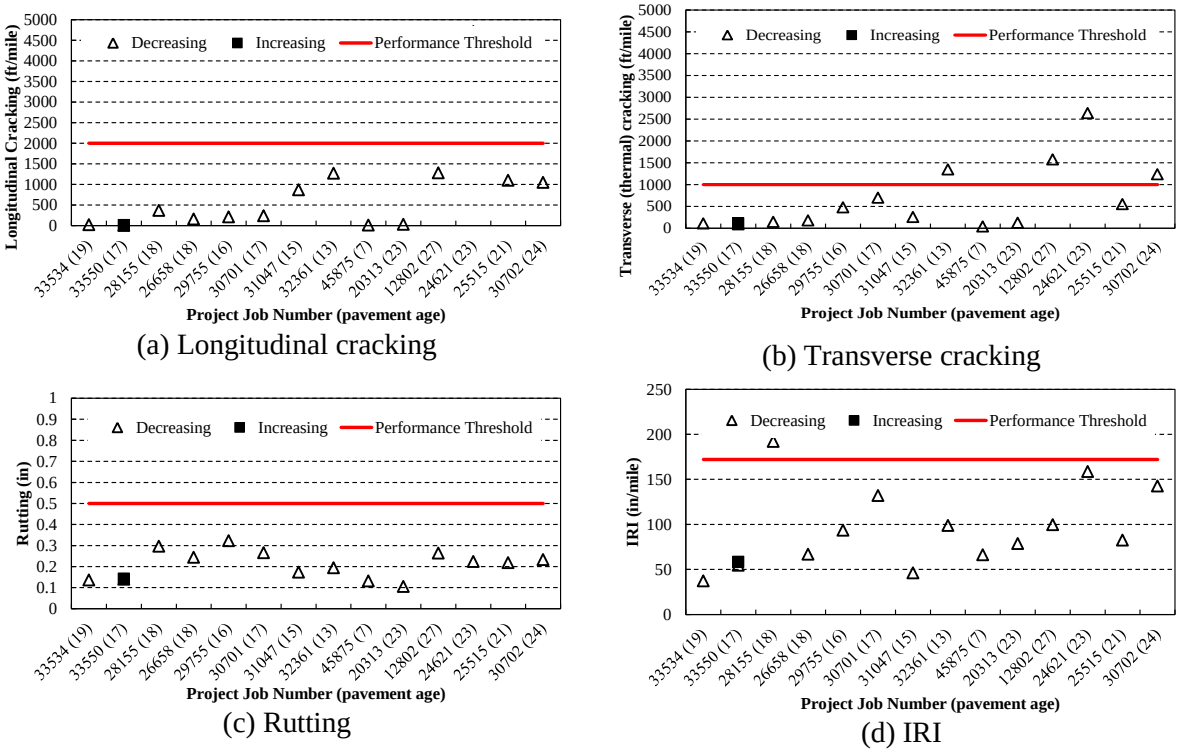

(a) Longitudinal cracking

(b) Transverse cracking

(c) Rutting

(d) IRI

Figure 5-11 Current pavement distress and conditions of the selected HMA over HMA projects

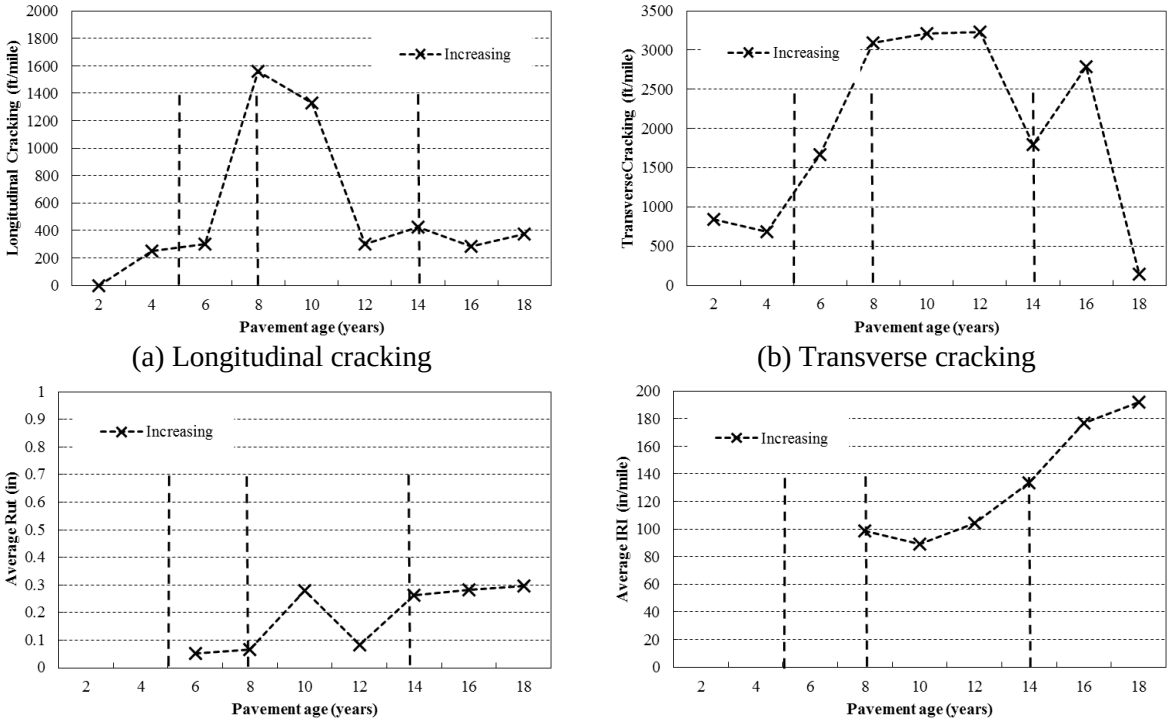

(a) Longitudinal cracking (b) Transverse cracking

(c) Rutting (d) IRI

Figure 5-12 Performance of HMA over HMA project 28155.

The time-series plots presented here show the results of the extraction process from the customized MDOT PMS and Sensor database. The magnitudes of the measured performance data are critical for comparing the measured and predicted performance. The next section discusses the process for identifying and collecting all the necessary input data to create the most representative pavement project in DARWin-ME.

5.4 PROJECT INPUTS FOR VERIFICATION

The next step of the validation process consists of identifying and documenting input variables for each selected project. The material, cross-section, climate, traffic, and existing pavement condition information are essential to create the most representative project to be analyzed in the DARWin-ME. The collection of required inputs needed extensive collaboration with the MDOT RAP to ensure the appropriateness of the selected values. The inputs for each project were obtained from MDOT historical records (project plans, material records), the previous MDOT studies (Report numbers: RC-1516, RC-1531, and RC-1537), and geographical location to select climate conditions.

5.4.1 Unbonded Overlays

The inputs for all unbonded overlay projects are summarized in Table 5-12. The inputs needed to represent the as-constructed designs are discussed below.

Cross-section information

The pavement cross-section information was collected from the project design drawings provided by MDOT. The cross-section for unbonded overlays consisted of thickness of overlay layer, asphalt interlayer, existing PCC, base and subbase. Some projects did not have all the necessary layer thicknesses; however, the missing pavement layer thicknesses were determined after consultation with the RAP, or a typical design values for the time period of project construction (new and existing) were recommended by MDOT.

Material related information

The material related information necessary for each pavement layer consisted of the following:

- Overlay PCC modulus of rupture (MOR)
- Asphalt interlayer binder type and volumetric properties
- Existing PCC elastic modulus
- Base/subbase material type and resilient modulus
- Subgrade soil type and resilient modulus

The overlay PCC modulus of rupture values were selected from the previous MDOT study, RC-1516 because the study included typical values agreed upon by MDOT. The asphalt interlayer binder type was determined from the mix design information extracted from the MDOT historical records for each project. The existing PCC elastic modulus value is the only way to characterize the condition of the underlying PCC pavement. The value of 3,000,000 psi was assumed because it is the upper limit suggested by the software as discussed in Chapter 3. The base/subbase type and modulus values were also obtained from a previous MDOT study (RC-1516) because the values were agreed upon by MDOT. The subgrade soil type and resilient moduli values were obtained from a previous MDOT study (RC-1531) which outlined the subgrade soil type and moduli values for the entire State of Michigan.

Climate information

The climate information for each project was determined by their geographical location. The DARWin-ME has a database for specific weather stations across the State of Michigan. The closest weather station to the actual project was selected. If none of the pre-loaded weather stations were located near the project, an interpolation was performed by selecting two or more weather stations in the vicinity of the project.

Traffic information

The traffic information is essential and one of the most important inputs to analyze pavements using the DARWin-ME. The annual average daily truck traffic (AADTT) was determined from as-constructed project design drawings and by collaboration with the RAP.

When such information was not available, current traffic values were obtained from the traffic maps specific to the project location which are available on MDOT's website (<http://www.michigan.gov/mdot/0,4616,7-151-9622_11033-22141--,00.html>). The AADTT values obtained from the website were back-casted to reflect the traffic at the time of construction using a growth rate of two percent.

5.4.2 Rubblized Overlays

The inputs for all rubblized overlay projects are summarized in Table 5-13. The inputs needed to represent the as-constructed projects as much as possible and are discussed below.

Cross-section information

The pavement cross-section information was collected from the project design drawings provided by MDOT. The cross-section for rubblized overlays consisted of thickness of the HMA overlay layer, existing fractured PCC layer, base and subbase. Some projects did not have all the necessary layer thicknesses; however, the missing pavement layer thicknesses were determined after consultation with the RAP, or typical design values for the time period of project construction (new and existing) were recommended by MDOT.

Material related information

The material related information necessary for each pavement layer consisted of the following:

- Asphalt overlay binder type, mixture gradation, effective binder content, and air voids
- Fractured PCC slab elastic modulus
- Base/subbase material type and resilient modulus
- Subgrade soil type and resilient modulus

The asphalt overlay layer properties were determined from the project job mix formula information extracted from the historical data provided by MDOT. The HMA volumetric properties were obtained from the job mix formula data sheets. The existing rubblized PCC elastic modulus is the only way to classify the existing condition of the rubblized layer. It was difficult to estimate this value; therefore, a value of 70,000 psi was assumed based on discussions with MDOT. The base/subbase and subgrade soil types and moduli values were obtained using the same procedure as for unbonded overlays.

Climate information

The climate information for each project was determined as discussed in the unbonded overlay section.

Traffic information

The traffic information for each project was determined similar to unbonded overlay section.

5.4.3 Composite Overlays

The inputs for all composite overlay projects are summarized in Table 5-14. The inputs that are needed to represent the as-constructed projects are discussed below.

Cross-section information

The pavement cross-section information was collected from the project design drawings provided by MDOT. The cross-section for composite overlays consisted of thickness for the overlay layer, existing intact PCC layer, base and subbase. Some projects did not have all the necessary layer thicknesses; however, the missing pavement layer thicknesses were determined after consultation with the RAP, or a typical design values for the time period of project construction (new and existing) were recommended by MDOT.

Material related information

The material related information necessary to characterize each layer consisted of the following:

- Asphalt overlay binder type, mixture gradation, effective binder content, and air voids
- Existing PCC MOR or elastic modulus
- Base/subbase material type and resilient modulus
- Subgrade soil type and resilient modulus

The asphalt overlay layer volumetric properties were determined from the project job mix formulas obtained from the historical project data provided by MDOT. The existing pavement is classified by the measured cracking, and how much of the measured cracking was fixed during pre-overlay repairs. The PCC MOR was used to characterize the strength of the existing layer similar to the unbonded overlay layer MOR. The base/subbase and subgrade soil types and moduli values were obtained using the same procedure as for unbonded overlays discussed previously.

Climate information

The climate information for each project was determined as discussed in the unbonded overlay section.

Traffic information

The traffic information for each project was determined in a similar method as discussed in the unbonded overlay section.

5.4.4 HMA over HMA

The inputs for all HMA over HMA projects are summarized in Table 5-15. The inputs needed to represent the as-constructed projects are discussed below.

Cross-section information

The pavement cross-section information was collected from the project design drawings provided by MDOT. The cross-section for HMA over HMA projects consisted of thickness for the overlay layer, existing HMA layer, base and subbase. Some projects did not have all the necessary layer thicknesses; however, the missing pavement layer thicknesses were determined after consultation with the RAP, or a typical design values recommended by MDOT were used.

Material related information

The material related information necessary to characterize each layer consisted of the following:

- Asphalt overlay binder type, mixture gradation, effective binder content, and air voids
- Existing HMA pavement binder type, mixture gradation, effective binder content, and air voids
- Base/subbase material type and resilient modulus
- Subgrade soil type and resilient modulus

The asphalt overlay layer properties were determined from the project historical data provided by MDOT. The HMA volumetric properties of the overlay were obtained from the job mix formula data sheets. The existing pavement was characterized by selecting the condition rating of each project consisting of poor, fair and good conditions. Since the existing condition is difficult to determine, the verification was performed for all three conditions ratings. The HMA mixture properties for the existing pavement were obtained from the job mix formula data sheets if available, otherwise, the values were assumed based on projects in a similar climate, or by selecting properties from the MDOT specifications. The specifications in effect during the time of original construction were used. The base/subbase and subgrade soil types and moduli values were obtained using the same procedure as for unbonded overlays discussed previously.

Climate information

The climate information for each project was determined as discussed in the unbonded overlay section.

Traffic information

The traffic information for each project was determined in a similar method as discussed in the unbonded overlay section.

Table 5-12 Unbonded overlay input data

Unbonded Overlay Projects								
Project Number	37997	34120	49029	45591	38209	43499	73873	50763
Year opened	1998	1999	1999	2000	2000	2001	2003	2004
Traffic								
Two way AADTT	4250	4279	5700	5595	2744	5004	1458	3185
ESALs (millions) (DARWin-ME)	19.14	25.44	36.73	36.06	14.4	29.75	7.43	14.34
Lanes in design direction	2	2	2	2	2	2	2	2
Climate	Kalamazoo	Ann Arbor	Kalamazoo	Battle Creek	Grand Rapids	Ann Arbor	Houghton Lake	Kalamzoo
Overlay Layer								
PCC Thickness (in)	7.1	7.9	7.1	7.1	6.3	7.1	6	6.5
PCC Modulus of Rupture (psi)	650	650	650	650	650	650	650	650
AC Interlayer								
AC Thickness (in)	1	1	1	1	1	1	1	1
AC PG or Penetration Grade	PG 58-28	PG 58-28	PG 58-28	PG 58-28	PG 58-28	PG 70-28	PG 64-28	PG 58-28
Existing PCC								
PCC Thickness (in)	9	9	9	9	9	9	9	9
PCC Elastic Modulus (ksi)	3000	3000	3000	3000	3000	3000	3000	3000
Base Layer								
Thickness (in)	3	3	4	4	4	3	4	4
Material type	Crushed Stone	Crushed Stone	Crushed Stone	Crushed Stone	Crushed Stone	Crushed Stone	Crushed Stone	Crushed Stone
Modulus (psi)	30000	30000	30000	30000	30000	30000	30000	30000
Subbase Layer								
Thickness (in)	11	14	10	10	10	14	10	10
Material type	A-3	A-3	A-3	A-3	A-3	A-3	A-3	A-3
Modulus (psi)	13500	13500	13500	13500	13500	13500	13500	13500
Subgrade								
Material type (by loc.)	SP1-A-3	SP2-A-3	SP1-A-3	SP1-A-3	A-4	SP2-A-3	SP2-A-3	SP1-A-3
Modulus (psi) (backcalc /design-Baladi project)	27739/ 7000	25113/ 6500	27739/ 7000	27739/ 7000	20314/ 5000	25113/ 6500	25113/ 6500	27739/ 7000

Note: Gray cells represent assumed values

Table 5-13 Rubblized overlay input data

Rubblized Projects											
Project Number	28115	26755	29768	29670	29581	28111	29729	45053	44109	38190	32388
Year opened	1989	1990	1992	1993	1994	1990	1995	1999	1999	2000	1997
Traffic											
Two way AADTT	490/340	1550	3390	856	3707	280	370	675	279	575	455
ESALs (millions) (DARWin-ME)	3.11	8.9	19.44	4.51	23.51	1.87	2.47	4.51	1.86	3.84	3.04
Lanes in design direction	2	2	2	2	2	1	1	1	1	1	1
Climate	Grand Rapids	Houghton Lake	Ann Arbor	Battle Creek	Lansing	Pellston	Flint	Reed City	Traverse City	Muskegon	Adrian
Overlay Layer											
HMA Thickness (in)	5	4.25	5.25	6.25	7.5	4	5 Edge, 7.2 Center Line	5.5	7.5	5.5	6 Center Line, 7 Edge
HMA binder type	Pen 120-150	Pen 120-150	Pen 85-100	Pen 85-100	Pen 85-100	Pen 200-300	Pen 120-150	PG 64-28 (T) PG 58-28(B+L)	PG 58-28	PG 58-28	Pen 85-100
Existing PCC (fractured)											
PCC Thickness (in)	9	8	9	9	9	9	9	9	8	9	8
PCC Fractured Elastic Modulus (psi)	70000	70000	70000	70000	70000	70000	70000	70000	70000	70000	70000
Base Layer											
Thickness (in)	3		4	3	4			3		4	
Material type	Crushed Stone		Crushed Stone	Crushed Stone	Crushed Stone			Crushed Stone		Crushed Stone	
Modulus (psi)	30000		30000	30000	30000			30000		30000	
Subbase Layer											
Thickness (in)	9		14	9	10		18	12	9	14	12
Material type	A-3		A-3	A-3	A-3		A-3	A-3	A-3	A-3	A-3
Modulus (psi)	13500		13500	13500	13500		13500	13500	13500	13500	13500
Subgrade											
Material type	A-4	SP2-A-3	SP2- A-3	SP1-A-3	CL - A-6	SP1-A-3	SM - A-4	SP1- A-3	SP1-A-3	SP1-A-3	CL-A-6
Modulus (psi) (backcalc/design -Baladi project)	20314/ 5000	25113/ 6500	25113/ 6500	27739/ 7000	17600/ 4400	27739/ 7000	24764/ 5200	27739/ 7000	27739/ 7000	27739/ 7000	17600/ 4400

Note: Gray cells represent assumed values

Table 5-14 Composite overlay input data

Composite Overlay Projects							
Project Number	25543	24252	29586	29716	33812	33924	45443
Year opened	1987	1988	1990	1992	1995	1996	2000
Traffic							
Two way AADTT	2250	6064	2882	672	1380	1000	512
ESALs (millions)	15.66	43.49	20.05	4.68	9.6	6.96	3.56
Lanes in design direction	2	2	2	2	2	2	2
Climate	Flint	Kalamazoo	Grand Rapids	Reed City	Detroit	Bay City	Bay City
Overlay Layer							
HMA Thickness (in)	4	4.5	3	3.75	3	4	3.5
HMA binder type	85-100	85-100	85-100	120-150	85-100	120-150	PG 64-28
HMA aggregate Gradation	Top course	Top course	Top course		Top course	Top course	Top course
Cumulative % Retained 3/4	0	0	0	0	0	0	0
Cumulative % Retained 3/8	11.4	12	11.6	13	38.3	14.4	15.5
Cumulative % Retained #4	31.7	31.9	36.2	40	56	51.5	23.3
% Passing 200	6.5	5.4	6.5	6	5.6	5.4	5.3
Existing PCC							
PCC Thickness (in)	9	9	9	9	9	8	8
PCC Compressive Strength (psi)	5000	5000	5000	5000	5000	5000	5000
Base Layer							
Thickness (in)	4	3	3		3	4	
Material type	Crushed Stone	Crushed Stone	Crushed Stone		Crushed Stone	Crushed Stone	
Modulus (psi)	30000	30000	30000		30000	30000	
Subbase Layer							
Thickness (in)	10	9	12		14	10	15
Material type	A-3	A-3	A-3		A-3	A-3	A-3
Modulus (psi)	13500	13500	13500		13500	13500	13500
Subgrade							
Material type	SM - A-4	SP1-A-3	A-4	SP1- A-3	SP1-A-3	SC - A-6	SC - A-6
Modulus (psi) (backcalc/design - Baladi project)	24764/ 5200	27739/ 7000	20314/ 5000	27739/ 7000	27739/ 7000	17600/ 4400	17600/ 4400

Note: Gray cells represent assumed values

Table 5-15 HMA over HMA input data

HMA over HMA Projects															
Project Number	33534	33550	28155	26658	29755	30701	31047	32361	45875	50715	20313	12802	24621	25515	30702
Year opened	1992	1992	1991	1992	1994	1994	1996	1997	2002	2005	1983	1984	1987	1989	1990
Traffic															
Two way AADTT	450	1564	185	130	185	408	260	3900 ADT	805	350	300	3800 ADT	238	315	365
ESALs (millions)	3.09	10.75	1.27	0.89	1.27	2.8	1.79	1.37	5.53	2.41	3.88	1.37	3.08	4.08	4.73
Lanes in design direction	2	2	2	1	1	1	1	1	1	1	1	1	1	1	1
Climate	Reed City	Kalamzaoo	Kalamazoo	Traverse City	Traverse City	Kalamazoo	Marquette/ Iron Mountain	Flint	South Bend	Jackson/ Battle Creek	Traverse City	Traverse City	Battle Creek	Cadillac/ Gaylord	South Bend
Overlay Layer															
HMA Thickness (in)	2.5	3	2.5	2.5	3	3	3	3	4	3.5	2.25	2.5	2.5	2.5	2.5
HMA binder type	120-150	85-100	120-150	120-150	120-150	85-100	120-150	120-150	PG 64-28	PG 64-28	120-150	120-150	120-150	120-150	85-100
HMA aggregate Gradation	3b	3c	1100T	1100T	1100T	3c	1100T	1100T	5E3	5E3	1100T	1100L	1100T	1100T	1500T
Mixture Air Voids (as const)	6	6.6	7	5	4.8	6.6	4.8	4.8	8	8	6	7	7	7	7
HMA Effective binder	9.4	10	12	12	12	10	12	12	12	12	12	11.2	11.2	11	11.2
Cumulative % Retained 3/4	0	0	0	0	0	0	0	0	0	0	0	0	0	0	0
Cumulative % Retained 3/8	28.6	36	36	18.6	18.6	36	18.6	18.6	2.5	2.5	15.4	15	14.2	10.2	11.2
Cumulative % Retained #4	50.2	45.6	45.6	40.4	40.4	45.6	40.4	40.4	32.8	32.8	32.9	36	36.4	38.4	32.2
% Passing 200	4.8	6.5	6.5	5.4	5.4	6.5	5.4	5.4	5.4	5.4	7.4	6.4	6.9	5.6	6
Existing HMA															
Existing HMA Thickness (in)	3.25	4.5	5.2	5	4-5.5	4.5	3	3.7	4.5	7.5	1.5	2.25 or 4.75	3.75	2.25	7.1
HMA binder type	85-100	85-100	120-150	120-150	120-150	85-100	120-150	120-150	PG 64-28	PG 64-28	120-150	120-150	120-150	120-150	85-100
HMA aggregate Gradation	3b	3c	1100L	1100L	1100L	3C	1100L		4E3	4E3		1100L			
Mixture Air Voids (as const)	7	7	7	7	7	7	7	7	7	7	7	7	7	7	7
HMA Effective binder	11.6	12	11	11.4	11	11	11	11	11	11	11	11	11	11	11
Cumulative % Retained 3/4	0	0	0	0	0	0	0	0	0	0	0	0	0	0	0
Cumulative % Retained 3/8	28.6	36	10.6	18.6	17.3	36	17.3	17.3	13.2	13.2	13.4	15	13.3	12	11.2
Cumulative % Retained #4	50.2	45.6	31.5	40.4	37.4	45.6	37.4	37.4	35.1	35.1	37	36	34.1	35.2	32.2
% Passing 200	4.8	6.5	5.4	5.4	5.7	6.5	5.7	5.7	4.6	4.6	5.8	6.4	8.5	5.6	6
Base Layer															
Thickness (in)	11	8	7	7	4/5 stabilized	7	10	7	11	6	5	7	8	10	5
Material type	Crushed Stone	Crushed Stone	Crushed Stone	Crushed Stone		Crushed Stone	Crushed Stone	Crushed Stone	Crushed Stone	Crushed Stone	Crushed Stone	Crushed Stone	Crushed Stone	Crushed Stone	Crushed Stone
Modulus (psi)	30000	30000	30000	30000		30000	30000	30000	30000	30000	30000	30000	30000	30000	30000
Subbase Layer															
Thickness (in)	25	28	12	12		15	18	13.7	15	8		0 or 12			
Material type	A-3	A-3	A-3	A-3		A-3	A-3	A-3	A-3	A-3		A-3			
Modulus (psi)	13500	13500	13500	13500		13500	13500	13500	13500	13500		13500			
Subgrade															
Material type	SP1- A3	SP1-A-3	SP1-A-3	SP1-A-3	SP1-A-3	SP1-A-3	SP-SM	SM - A-4	SP1-A-3	SP-SM	SP1-A-3	SP1-A-3	SP1- A-3	SP1-A-3	SP1-A-3
Modulus (psi) (backcalc/design - Baladi project)	27739/ 7000	27739/ 7000	27739/ 7000	27739/ 7000	27739/ 7000	27739/ 7000	20400/ 7000	24764/ 5200	27739/ 7000	20400/ 7000	27739/ 7000	27739/ 7000	27739/ 7000	27739/ 7000	27739/ 7000

Note:Gray cells represent assumed values

5.5 VERIFICATION RESULTS

The verification process entails the comparison between the measured and predicted pavement performance of each selected project using DARWin-ME. The results for unbonded, rubblized, composite, and HMA over HMA pavements are presented in this section. The results include an example of the time-series comparison between the predicted and the measured performance. In addition, the predicted distresses for all projects within each rehabilitation strategy were plotted against the measured distresses. These plots give a clear indication if the software over or under predicts the measured performance. Finally, the comparison of the predicted with the measured distresses highlights the need for local calibration of the DARWin-ME performance prediction models. In addition, conclusions can be made regarding the accuracy of the rehabilitations models for use in design.

5.5.1 Unbonded Overlays

The verification results for unbonded overlay projects are summarized in this section. Figure 5-13 shows an example of the time-series distresses for the project JN34120. The predicted performance values are superimposed on the measured distresses. For all the projects, limited distress magnitudes were observed. None of the projects were close to the performance threshold value. It should be noted, that for projects with multiple directions, only one DARWin-ME project file was created because for this study, it was assumed that the as constructed input values were the same for both directions. The time-series results from both directions are compared to the DARWin-ME predicted distresses. The time-series comparison between predicted and measured performance for all unbonded overlay projects are included in Appendix C.

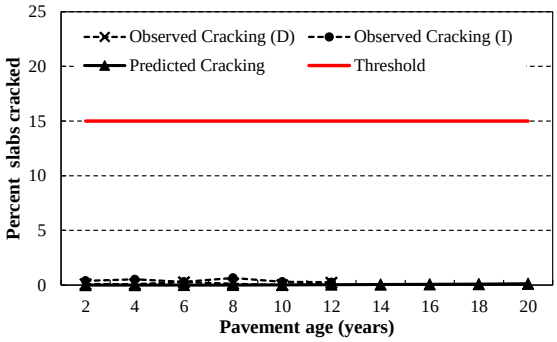

(a) Transverse cracking

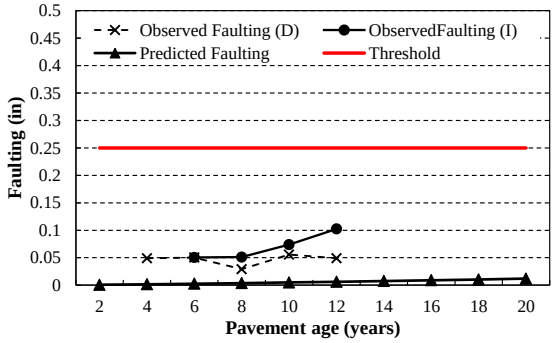

(b) Faulting

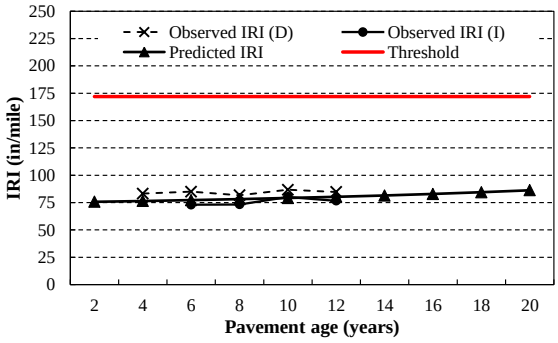

(c) IRI

Figure 5-13 Example of time-series verification results for an unbonded overlay project based on different distresses

Figure 5-14(a) shows that DARWin-ME under predicts the measured cracking for the unbonded overlay projects. The faulting model also under predicts the measured faulting as shown in Figure 5-14(b). The measured and predicted faulting values are minimal and do not reach the threshold limit. It is expected that minimal faulting should be predicted in DARWin-ME because dowels (1.25 inch in diameter) were included in the design for load transfer at the joint. The IRI predicted values (Figure 5-14c) are closer to the measured performance. Based on these results, calibration of all the performance models for unbonded overlay is necessary to improve the accuracy of DARWin-ME for the Michigan conditions.

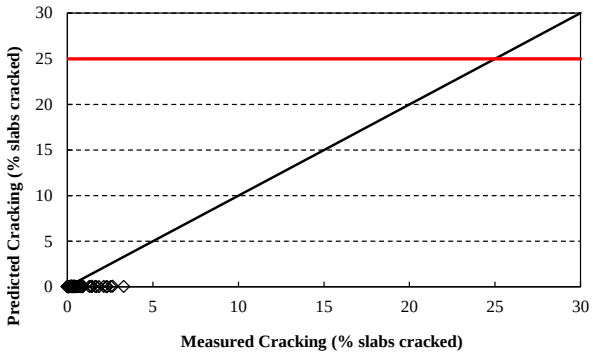

(a) Transverse cracking

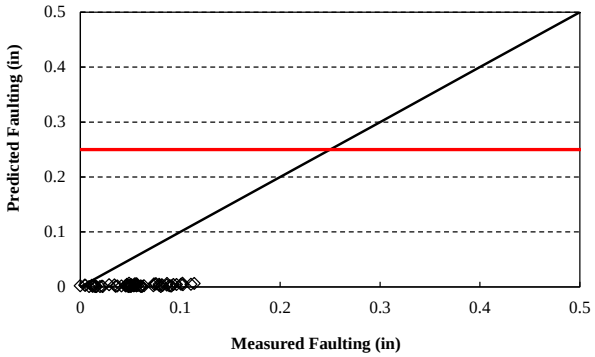

(b) Faulting

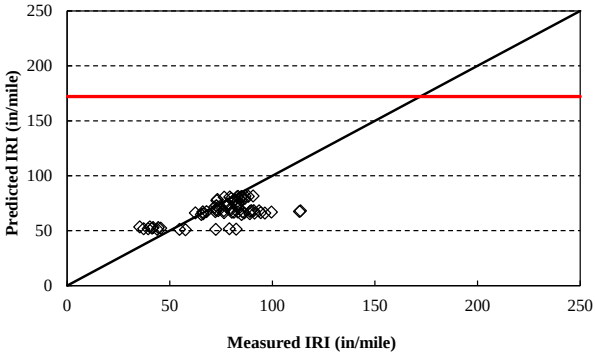

(c) IRI

Figure 5-14 Predicted vs. measured results for all unbonded overlay projects.

5.5.2 Rubblized Overlays

The verification results for rubblized overlay projects are summarized in this section. The verification was performed using two different subgrade moduli (see the back-calculated and design MR values in Table 2-9 which are from MDOT Report Number RC-1531). The back-calculated values were not determined in this study. The subgrade modulus has significant effect on rutting performance. Figure 5-15 shows an example of the time-series comparison between predicted and measured performance for the project JN44109. Figure 5-16 summarizes the predicted vs. measured performance for all rubblized projects using the back-calculated subgrade moduli. Figure 5-17 illustrates the same results with the adjusted recommended design subgrade modulus values. The time-series comparison between predicted and measured performance for all rubblized overlay projects are included in Appendix C

The results in Figure 5-16 and Figure 5-17 illustrate that the predictions are not close to the line of equality. It can be concluded that the design software under-predicts longitudinal cracking for most of the pavement sections. The thermal transverse cracking model under-predicts the measured performance. The minimal amount of thermal transverse cracking predicted by the software could be due to appropriate binder selection for a specific climate. However, this is not observed in the field as each selected project has significant amounts of measured transverse cracking. It should be noted that several of the selected projects were constructed prior to Superpave binder specification were adopted for design. Thus, climatic considerations were not taken into account during binder selection. It is observed that the software over predicts the measured distresses for both rutting and IRI. The design value subgrade MR over predicted rutting more than the backcalculated MR. Therefore, calibration of all the performance models is necessary to improve the accuracy of DARWin-ME for the Michigan conditions. Based on the results, it is also recommended to use backcalculation to determine the subgrade soil condition.

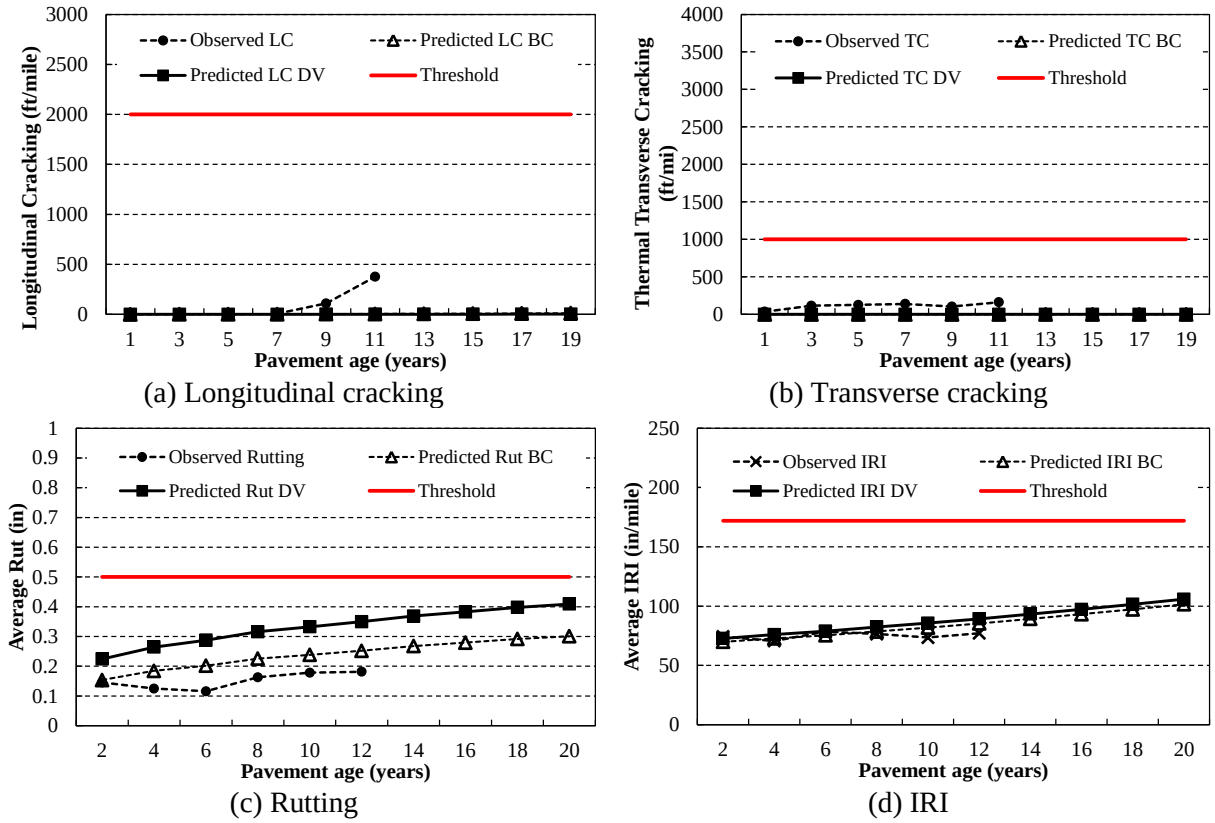

(a) Longitudinal cracking (b) Transverse cracking

(c) Rutting (d) IRI

Figure 5-15 Example of time-series verification results for a rubblized overlay project based on different distresses

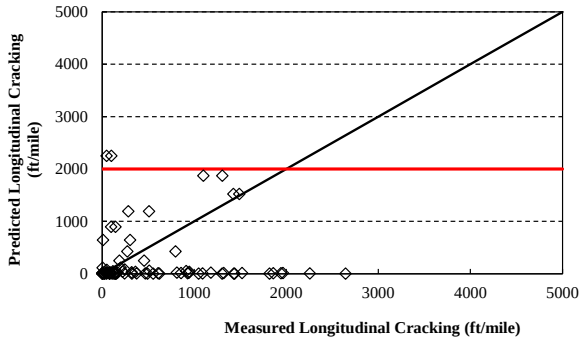

(a) Longitudinal cracking

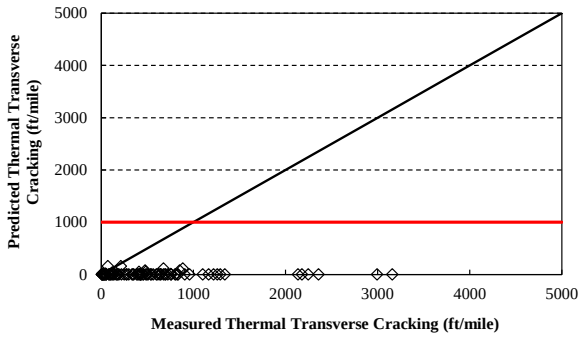

(b) Thermal transverse cracking

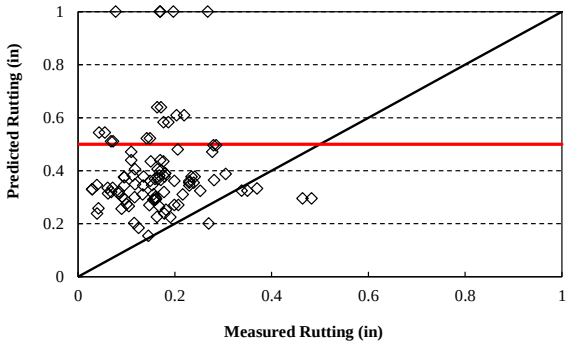

(c) Rutting

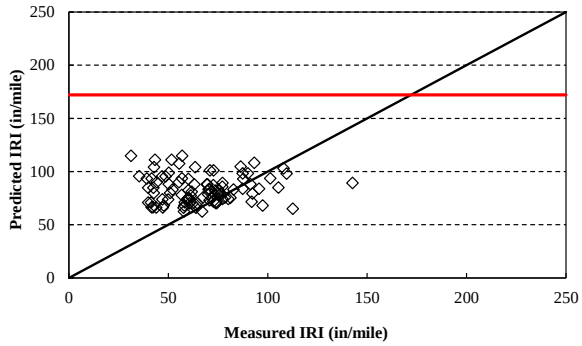

(d) IRI

Figure 5-16 Predicted vs. measured results for rubblized overlay projects using backcalculated subgrade MR

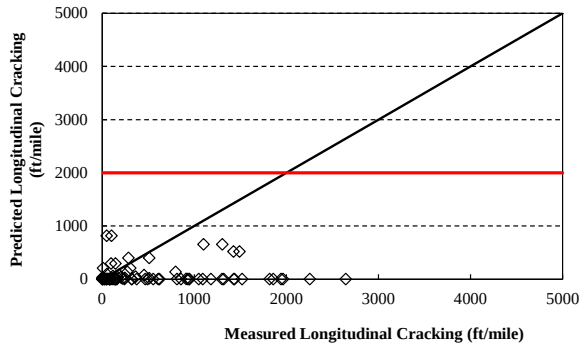

(a) Longitudinal cracking

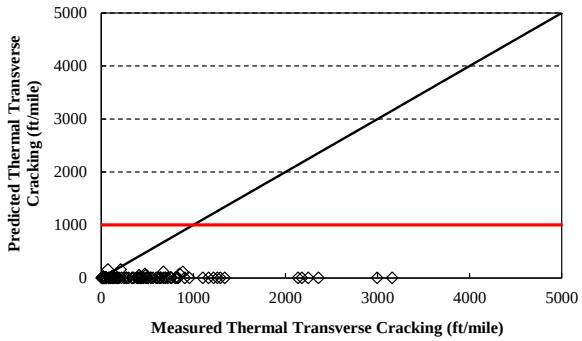

(b) Thermal transverse cracking

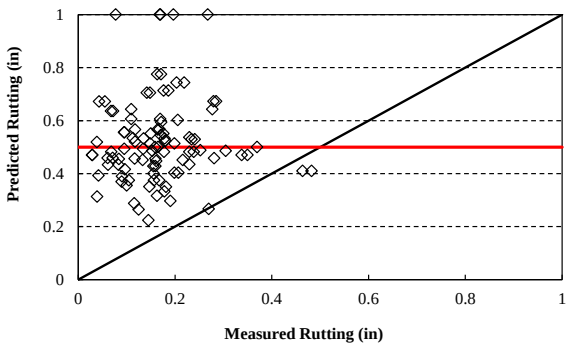

(c) Rutting

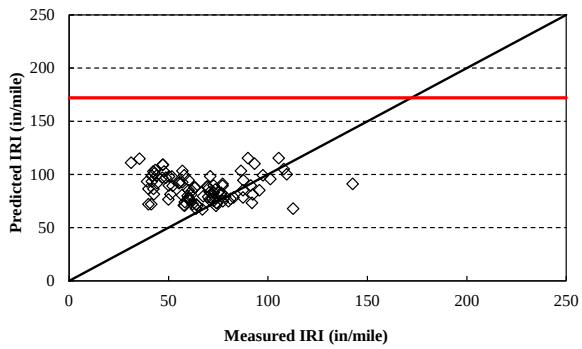

(d) IRI

Figure 5-17 Predicted vs. measured results for rubblized overlay projects using design MR

5.5.3 Composite Overlays

The verification results for composite overlay projects are summarized in this section. Figure 5-18 shows an example of the time-series distresses for the project JN45443. The predicted time series distress values are superimposed on the measured values. Figure 5-19 summarizes the predicted vs. measured performance to determine how well the predictions match measured distress for all selected projects. The time-series comparison between predicted and measured performance for all composite overlay projects are included in Appendix C.

The results in Figure 5-19 illustrate that the predicted performance is not close to the line of equality. It is observed that a bias exists between the predicted and measured performance for both rutting and IRI. The software under-predicts longitudinal cracking. The thermal transverse cracking values were not included for composite pavements because the software predicted values that were identical for all projects. Therefore, calibration of all the models is necessary to improve the accuracy of DARWin-ME for the Michigan conditions.

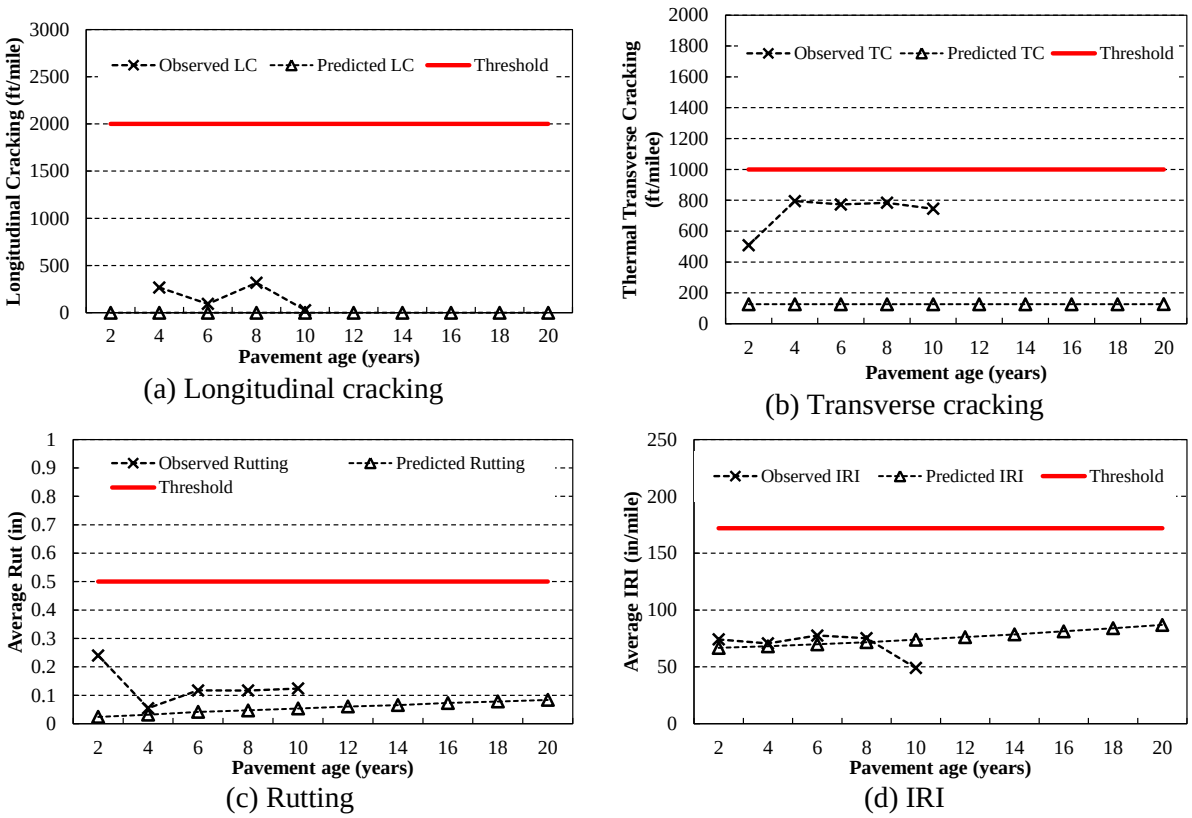

(a) Longitudinal cracking

(b) Transverse cracking

(c) Rutting

(d) IRI

Figure 5-18 Example of time-series verification results for a composite overlay project based on different distresses

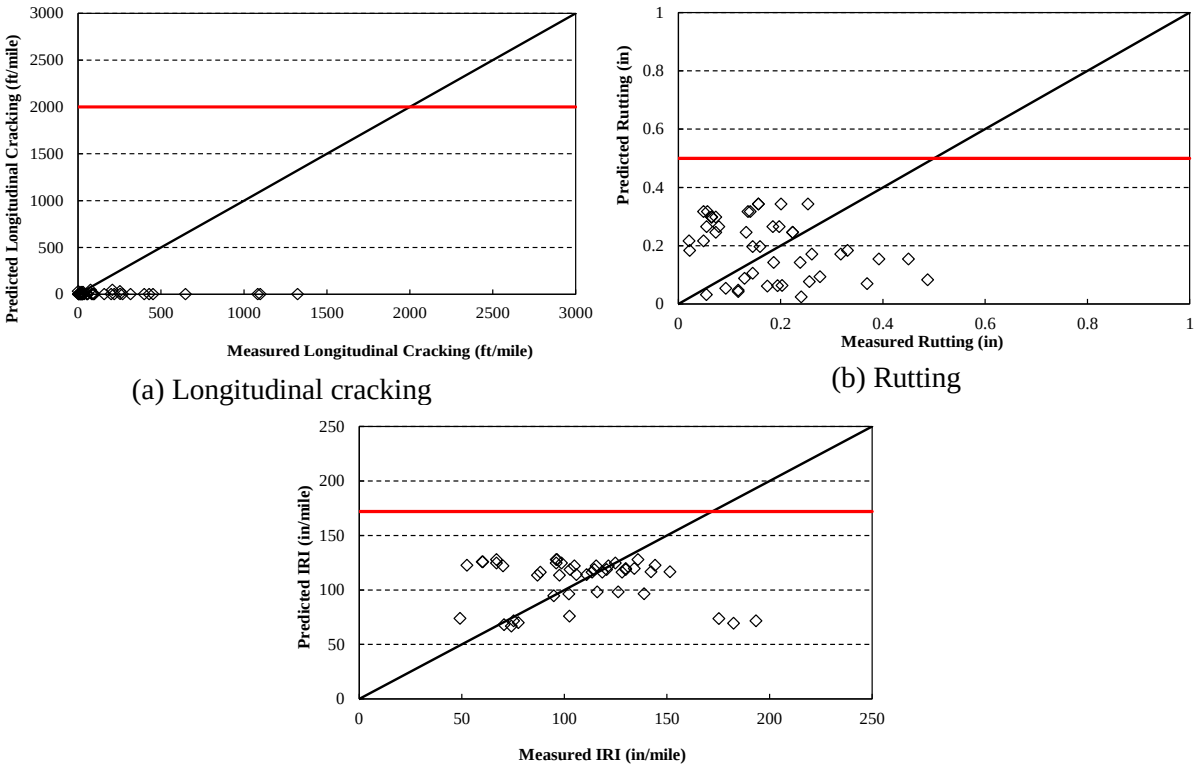

(a) Longitudinal cracking

(b) Rutting

(c) IRI

Figure 5-19 Predicted vs. measured results for all composite overlay projects

5.5.4 HMA over HMA

The verification results for HMA over HMA projects are summarized in this section. As an example, Figure 5-20 shows the measured and predicted distress for the project JN33543. It can be seen that even though a maintenance fix was performed after the 13th year, the propagation of distress is fairly reasonable from year eleven to thirteen for longitudinal cracking. The thermal transverse cracking model under predicts measured thermal transverse cracking. The rutting model over predicts measured rutting. On the other hand, the IRI model predictions are reasonable. Figure 5-21 summarizes the predicted vs. measured performance for all HMA over HMA projects with a poor existing pavement condition rating. Figures5-22 and 5-23 show the results for fair and good existing pavement condition ratings. The DARWin-ME software allows the user to select the condition of the existing HMA pavement layer. Since, the existing HMA pavement condition of the pavement was not known with certainty, the verification of the HMA over HMA performance models was performed using poor, fair, and good conditions. The results in Figure 5-21 also illustrate that the predicted performance is not close to the line of equality. It can be observed that bias exists between the predicted and measured performance for both longitudinal, thermal transverse cracking, rutting and IRI. Therefore, calibration of all the models is necessary to improve the accuracy of DARWin-ME for the Michigan conditions.

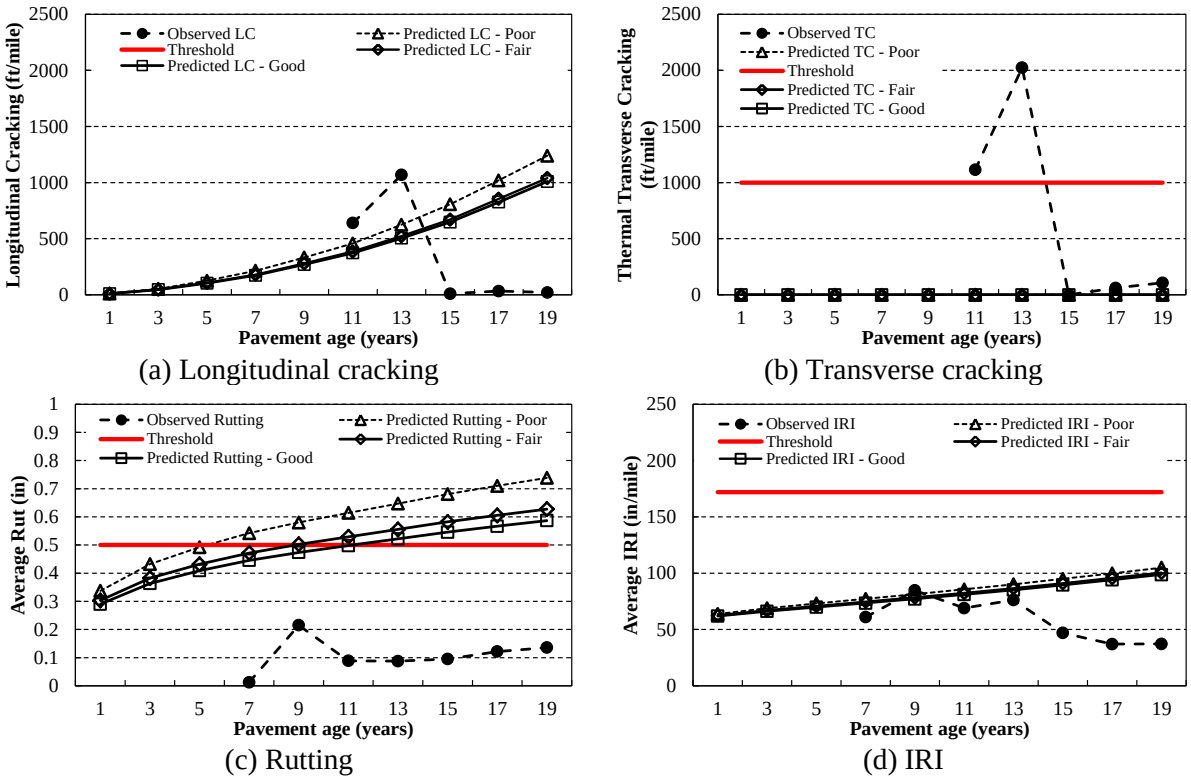

(a) Longitudinal cracking (b) Transverse cracking

(c) Rutting (d) IRI

Figure 5-20 Example of time-series verification results for a HMA over HMA project

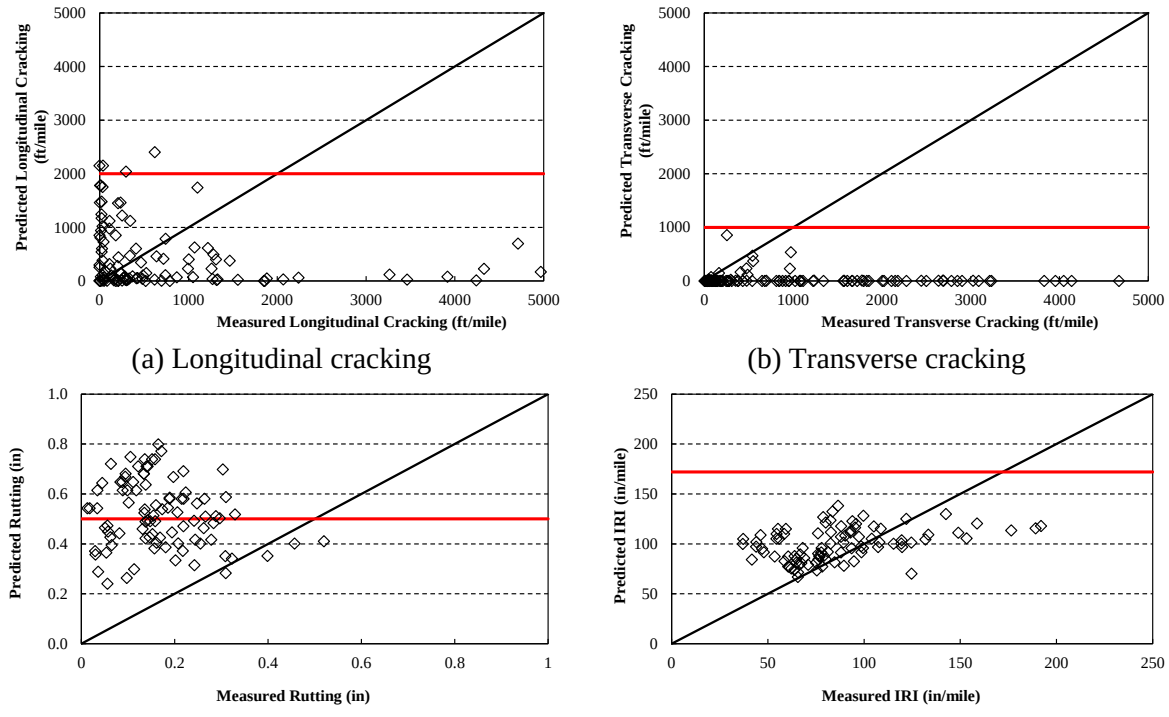

(a) Longitudinal cracking (b) Transverse cracking

(c) Rutting (d) IRI

Figure 5-21 Predicted vs. Measured performance for HMA over HMA with poor existing condition.

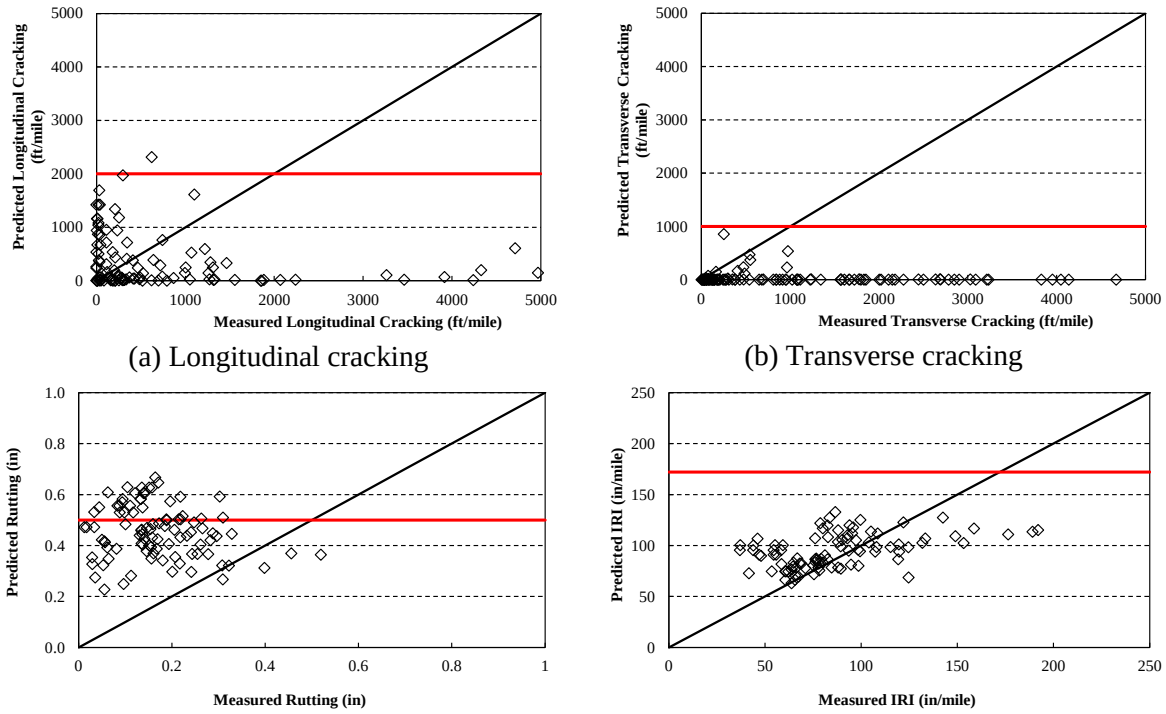

(a) Longitudinal cracking (b) Transverse cracking

(c) Rutting (d) IRI

Figure 22 Predicted vs. Measured performance for HMA over HMA with fair existing condition.

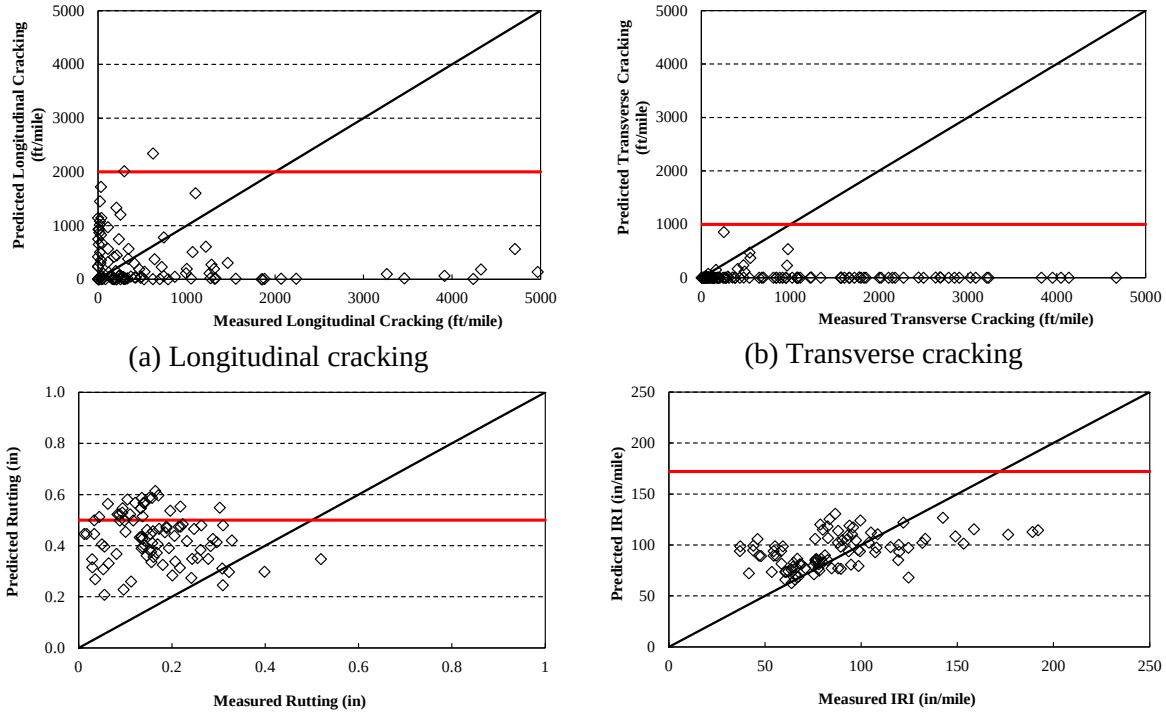

(a) Longitudinal cracking (b) Transverse cracking

(c) Rutting (d) IRI

Figure 23 Predicted vs. Measured performance for HMA over HMA with good existing condition.

5.6 SUMMARY

Verification of the M-E PDG/DARWin-ME performance models are necessary to determine how well the models predict measured pavement performance for Michigan conditions. In this chapter, the following sequential steps for the verification process were presented:

1. Identify projects in different regions in the State based on local pavement design and construction practices.
2. Extract the measured pavement performance data for each project from the MDOT Pavement Management System (PMS) and Sensor database.
3. Obtain all input data related to pavement materials, cross-section, traffic and climatic conditions for the identified projects.
4. Compare the measured and predicted performances for each project to identify the local calibration needs.

The verification of the performance prediction models based on the selected projects for different rehabilitation options show the need for local calibration. This calibration will be executed in Task 3 of the project. It should be noted that work accomplished in this task will facilitate the calibration process due to the following reasons:

- All of the identified projects can be used in the local calibration.
- The custom PMS and sensor databases developed in this task can be used to further identify additional road segments based on distress magnitudes instead of construction records for local calibration (if needed).

CHAPTER 6 - CONCLUSIONS AND RECOMMENDATIONS

6.1 SUMMARY

The main objectives of Part 2 of the project were to determine the impact of various input variables on the predicted pavement performance for the selected rehabilitation design alternatives in the MEPDG/DARWin-ME, and to verify the pavement performance models for MDOT rehabilitation design practice. Therefore, the significant inputs related to material characterization, existing pavement condition, and structural design for the selected rehabilitation options were identified. Subsequently, the accuracy of the rehabilitation performance models was evaluated by comparing measured and predicted performance.

The overarching findings from the sensitivity analyses performed in Part 2 for different rehabilitation options in the MEPDG/DARWin-ME of the study are:

- *HMA over HMA*: the overlay thickness and HMA volumetrics are the most significant inputs for the overlay layer while the existing HMA thickness and pavement condition rating have a significant effect on the predicted pavement performance among the inputs related to the existing pavement structure.
- *Composite pavements*: the overlay thickness and HMA air voids are significant inputs for the overlay layer. In addition, among the inputs related to the existing intact PCC pavement, the existing PCC thickness has a significant effect on the predicted pavement performance.
- *Rubblized pavements*: the HMA thickness, air voids and effective binder content are the most significant inputs for the overlay layer. While none of the inputs related to the existing PCC layer have shown a significant impact on the predicted performance, the results show that the existing PCC layer modulus is important for alligator cracking and IRI.
- *Unbonded overlays*: all overlay (i.e. the new layer) related inputs significantly impact the predicted cracking performance while the modulus of subgrade reaction (*k*-value) is the most important among inputs related to existing layers.

The interaction between overlay air voids and existing pavement thickness significantly impacts all performance measures among HMA rehabilitation options. The interaction between overlay thickness and existing PCC layer modulus has the most significant effect on unbonded overlay predicted performance. It should be noted that all analyses were conducted using input ranges reflecting Michigan practices.

The verification of the performance prediction models based on the selected projects for different rehabilitation options show the need for local calibration. All of the identified projects used for verification will be utilized in Task 3 for local calibration. Based on the results of the analyses, various conclusions and recommendations were made and are presented in the next sections.

6.2 CONCLUSIONS

Based on the results of the analyses performed in Part 2 tasks, various conclusions were drawn. These conclusions can be divided into the following three broad topics:

- Issues related to the MEPDG/DARWin-ME software
- Identification of significant inputs based on sensitivity analyses
- Verification of the MEPDG/DARWin-ME rehabilitation performance models

6.2.1 The MEPDG/DARWin-ME Software Issues

Several issues were encountered while running the MEPDG/DARWin-ME software. These concerns were related to certain structural and material properties. In addition, reasonableness of certain inputs was investigated whenever unusual results were encountered during the analyses. These concerns include:

1. The software internally limits the existing PCC elastic modulus because higher values produce counter intuitive results. Therefore, the recommended value of 3,000,000 psi should be considered as the upper bound limit for elastic modulus.
2. The software reduces the subgrade resilient modulus (MR) value by a fixed factor depending on the soil type; fine or coarse. If the design MR is used as a direct input in the MEPDG/DARWin-ME, the MR values will be reduced internally to reflect laboratory determined MR (for levels 2 and 3). It should be noted that in the DARWin-ME the reduction factor can be specified by the user for level 1 while the software uses an internal reduction factor for unbound layers when using levels 2 & 3.
3. In the MEPDG/DARWin-ME the HMA interlayer modulus and thickness have insignificant impact on the equivalent thickness, especially within the practical range of 1 to 3 inches for interlayer thickness. This implies that the interlayer thickness and stiffness have no significant impact on the predicted performance.

6.2.2 Sensitivity Analyses

The main objective in this task was to evaluate the impact of the inputs specific to various rehabilitation options on the predicted performance. To accomplish this goal, the following types of sensitivity analyses were performed:

1. Preliminary sensitivity
2. Detailed sensitivity
3. Global sensitivity
4. Satellite studies

Each sensitivity analysis has a unique contribution to the overall understanding in determining the impact of design inputs on the predicted pavement performance. The outcome of the preliminary sensitivity resulted in the identification of significant inputs related to the existing pavement layers. Subsequently, these inputs were combined with the

significant inputs for the new pavement layer (overlay) to conduct the detailed sensitivity. The outcome from the detailed sensitivity analyses include the significant main and interactive effects (ANOVA) between the inputs related to the existing and overlay layers. It should be noted that the statistical and practical significant interactive effects were only investigated for the inputs related to the existing layer, overlay layer and a combination of existing and overlay layers.

Finally, the global sensitivity analysis was performed based on the results from the detailed sensitivity analysis. The global sensitivity analysis (GSA) is more robust because of the following reasons:

a. Main and interaction results are based on the entire domain of each input variable.
b. The importance of each input can be quantified using normalized sensitivity index (NSI).
c. Relative importance of each design input can be determined.

In this report, the term "sensitive" implies changes in the output (predicted performance) with respect to change in the input values. On the other hand, the term "significant" implies changes in the design input values that result in substantial changes in the predicted performance.

6.2.2.1 Preliminary sensitivity

Table 6-1summarizes the significant inputs from preliminary sensitivity analyses for the selected rehabilitation options. These inputs only characterize the existing pavement. The results show that existing surface layer thickness and existing pavement structural capacity are the most important inputs for all rehabilitation options.

Table 6-1 List of significant inputs from preliminary sensitivity analysis

Rehabilitation option	Significant inputs
HMA over HMA	• Existing HMA condition rating • Existing HMA thickness
HMA over JPCP (Composite)	• Existing PCC thickness • Existing PCC flexural strength
JPCP over JPCP (Unbonded overlay)	• Existing PCC thickness
CRCP over HMA	• Existing HMA thickness
CRCP over JPCP	• Existing PCC thickness • Existing PCC strength • Subgrade k-value

6.2.2.2 Detailed sensitivity

The detailed sensitivity analyses included the significant variables identified in preliminary analyses in addition to the significant inputs previously identified for new pavement layers.

Full factorials were designed to determine statistically significant main and two-way interaction effects. The results of the sensitivity analyses show that the existing pavement condition rating and existing thickness for HMA over HMA is critical for all performance measures. On the other hand, existing PCC modulus and thickness are important in determining the performance of HMA overlay over intact and rubblized PCC. For a given condition of the existing pavement, HMA overlay volumetric properties, binder type and amount, and thickness play a significant role. In addition, HMA volumetrics, binder type and amount, and thickness should be carefully selected for the overlays to mitigate various distresses whether the existing pavement is intact or rubblized concrete.

For unbonded overlays, the results of the sensitivity analyses show that the existing pavement condition (in terms of *E*) is critical for predicting cracking performance. Higher MOR (within reason) and thickness of overlay will limit the cracking. However, if the existing foundation is weak, a better strategy to reduce the unbonded overlay cracking would be to either increase PCC MOR or thickness, and use concrete with lower CTE. Table 6-2 presents the summary of significant input variable based on the detailed sensitivity analysis.

Table 6-2 List of significant inputs from detailed sensitivity analysis

Rehabilitation option	Significant inputs
HMA over HMA	• Existing HMA condition rating • Existing HMA thickness • Granular base and subgrade modulus • Overlay air voids • Overlay effective binder • Overlay binder PG • Overlay thickness
HMA over JPCP (Composite)	• Existing PCC thickness • Existing PCC flexural strength • Climate • Overlay air voids • Overlay binder PG • Overlay thickness
HMA over JPCP fractured (Rubblized)	• Existing PCC thickness • Existing PCC elastic modulus • Overlay air voids • Overlay effective binder • Overlay binder PG • Overlay thickness
JPCP over JPCP (Unbonded overlay)	• Existing PCC thickness • Existing PCC elastic modulus • Existing modulus of subgrade reaction • Overlay MOR • Overlay thickness • Overlay CTE • Overlay joint spacing

6.2.2.3 Global sensitivity analysis

Four rehabilitation options were considered in global sensitivity analysis (GSA) similar to the preliminary and the detailed sensitivity analyses. First, the relative contributions of the design inputs for various performance measures were identified and discussed. Second, the main effect of design inputs for a base case was investigated. Finally the interactive effect of the design inputs was studied for all performance measures within each rehabilitation option.

The results are summarized based on the main effects determined through the maximum NSI values. The input variables are ranked based on their relative impact on different performance measures. The following are the findings based on the main effects of input variables:

HMA over HMA

- In general, the overlay thickness and HMA volumetrics (air voids and effective binder contents) are the most significant inputs affecting the predicted performance for the overlay layer
- The existing pavement thickness and condition rating have significant effect among the existing pavement related inputs. Table 6-3 shows the list of significant inputs along with the ranking and NSI values.

Table 6-3 List of significant inputs — HMA over HMA

Input variables	Ranking (NSI)
Overlay air voids	1 (6)
Existing thickness	2 (5)
Overlay thickness	3 (4)
Existing pavement condition rating	4 (4)
Overlay effective binder	5 (2)
Subgrade modulus	6 (2)
Subbase modulus	7 (1)

Composite pavement

- The overlay thickness and HMA air voids are the most significant inputs for the overlay layer
- The existing pavement thickness and existing PCC layer modulus have significant effect on predicted performance among the existing pavement related inputs. Table 6-4 shows the list of significant inputs along with the ranking and NSI values.

Table 6-4 List of significant inputs — Composite pavement

Inputs	Ranking (NSI)
Overlay air voids	1 (9)
Overlay thickness	2 (2)
Existing PCC thickness	3 (1)

Rubblized pavement

- The HMA air voids and effective binder content are the most significant inputs for the overlay layer

- For longitudinal cracking and IRI, existing PCC thickness is more important as compared to the existing PCC layer modulus. However, existing PCC layer modulus is more significant for alligator cracking and rutting. Table 6-5 shows the list of significant inputs along with the ranking and NSI values.

Table 6-5 List of significant inputs — Rubblized PCC pavement

Inputs	Ranking (NSI)
Overlay air voids	1 (6)
Overlay effective binder	2 (2)
Overlay thickness	3 (1)

Unbonded overlay

- All overlay related inputs (see Table 6-6) significantly impact the cracking performance
- The existing PCC elastic modulus is the most important input among all inputs related to existing layers. Table 6-6 shows the list of significant inputs along with the ranking and NSI values.

Table 6-6 List of significant inputs — Unbonded PCC overlay

Design inputs	Ranking (NSI)
Overlay PCC thickness (inch)	1 (23)
Overlay PCC CTE (per °F x 10-6)	2 (12)
Overlay PCC MOR (psi)	3 (8)
Overlay joint spacing (ft)	4 (5)
Existing PCC elastic modulus (psi)	6 (1)
Climate	7 (1)

The following are the findings based on the interactive effects of input variables for the selected rehabilitation option:

- The interaction between overlay air voids and existing pavement thickness significantly impacts all performance measures among HMA rehabilitation options. A higher air void in the overlay layers on a thin existing layer thickness seems to be the worst combination for cracking.
- The interaction between overlay thickness and existing PCC layer modulus have the most significant effect on unbonded overlay performance. A thicker overlay may hide the impact of weak existing PCC layer on predicted performance.

All the interactions studied (see Tables 6-7 to 6-10) here are practically and statistically significant. Therefore all of them should be considered in the design and analysis.

Table 6-7 Significant interaction between inputs — HMA over HMA

Interaction	Ranking (NSI)
Overlay air voids and existing thickness	1 (15)
Overlay thickness and existing thickness	2 (10)
Overlay effective binder and existing thickness	3 (7)

Table 6-8 Significant interaction between inputs — Composite pavement

Interaction	Ranking (NSI)
Overlay air voids and existing thickness	1 (44)
Overlay thickness and existing thickness	2 (25)

Table 6-9 Significant interaction between inputs — Rubblized pavement

Interaction	Ranking (NSI)
Overlay air voids and existing thickness	1 (4)
Overlay effective binder and existing thickness	2 (2)
Overlay thickness and existing thickness	3 (1)

Table 6-10 Significant interaction between inputs — Unbonded PCC overlay

Interaction	Ranking (NSI)
Overlay thickness and existing modulus	1 (28)
Overlay MOR and existing modulus	2 (14)
Overlay MOR and existing thickness	3 (6)

6.2.2.4 Satellite studies

Several additional clarification studies were performed to evaluate the sensitivity of input variables in the MEPDG/DARWin-ME. The following are the main findings from the satellite studies:

- HMA base course gradation has a slight effect on the predicted bottom-up alligator cracking while HMA top and leveling course gradations do not significantly impact the predicted performance. Therefore, the average gradation from the specification limits can be used for pavement design.
- The effect of binder rheology (*G** master curve) is important for rutting prediction. Therefore, it is recommended that G* master curve (level 1) should be used if available, especially if rutting is a dominant distress. The variations in *G** master curve could be attributed to different binder sources for the same PG. However, it is anticipated that if a binder from the same source is utilized for mix design at a specific location, the level 1 *G** master curve should not vary significantly. Therefore, an average can be used for multiple *G** master curves. Part 1 of this study addressed this issue in more detail.
- The unbound layer gradations do not have a significant impact on the predicted performance. Based on these results it is recommended that for same material type and climate used in this study, the base and subbase aggregate gradations can be selected within the limits of the specifications.

6.2.3 Verification of the Rehabilitation Performance Models

Verification of the MEPDG/DARWin-ME performance models is necessary to determine how well the models predict the measured pavement performance for Michigan conditions. Results of the verification process support the following conclusions:

- For the unbonded overlay, the MEPDG/DARWin-ME software under-predicts the measured cracking and faulting. The IRI predicted values were closer to the measured performance; however, bias still exists.
- For rubblized pavements, the software under-predicts longitudinal and transverse cracking for most of the pavement sections while it over-predicts the measured distresses for rutting and IRI.
- For composite pavements, the one-to-one plot between the predicted and measured performance for rutting and IRI showed higher variability (i.e., more error). Also, the software under-predicted the longitudinal cracking.
- For HMA over HMA bias exists between the predicted and measured performance for rutting and IRI i.e., the software over predicts the measured performance. While longitudinal cracking showed larger error, thermal transverse cracking was under-predicted.

The validation of the performance prediction models based on the selected projects for different rehabilitation options show the need for local calibration. This calibration will be executed in Part 3 of the research study. It should be noted that work accomplished in this task will facilitate the calibration process due to the following reasons:

- All of the identified projects can be used in the local calibration.
- The custom PMS and sensor databases developed in this task can be used to further identify additional road segments based on distress magnitudes instead of construction records for local calibration (if needed).

6.3 RECOMMENDATIONS

The following are the recommendations based on the findings from Part 2:

1. For unbonded overlays, the existing PCC elastic modulus input should not exceed a value of 3,000,000 psi.
2. An average HMA gradation from the specification limits should be used for pavement design.
3. The average *G** master curve (level 1) should be used if available for a binder from a source, especially if rutting is the dominant distress.
4. For unbound layers, base and subbase aggregate gradations should be selected within the limits of the specifications.
5. It is recommended that the following rehabilitation option in the DARWin-ME should be used for design until local calibration is performed.
    a. HMA over HMA
    b. Composite overlays
    c. Rubblized overlays
    d. Unbonded PCC overlays
6. The use of falling weight deflectometer (FWD) is recommended to characterize the existing pavement, especially for flexible pavements with high traffic volume. The FWD testing guidelines for sensor configuration, number of drops, testing frequency and temperature measurements are outlined in Chapter 3. The guidelines are

recommended in the short-term while modifications should be made in the long-term based on the local experience.

7. The use of ground penetration radar (GPR) for estimating the existing pavement layer thicknesses in conjunction with FWD is recommended to enhance the back-calculation accuracy and testing efficiency.
8. The load pulse of the MDOT FWD equipment should be used to calculate the frequency based on the equation: $f = \frac{1}{2t}$.
9. Further investigation is needed during the local calibration of the performance models (Part 3 of the study) to evaluate the appropriateness of both backcalculated and design subgrade MR values.

6.4 IMPLEMENTATION

Based on the conclusions and recommendations of Part II study, the following are recommendations for the implementation of the DARWin-ME in the state of Michigan:

- Increase the use of FWD for backcalculation of layer moduli to characterize existing pavement conditions for all the rehabilitation options adopted in Michigan is warranted, especially for high traffic volume roads (interstates and freeways).
- PMS distress data and unit conversion is also necessary to ensure compatibility between MDOT measured and DARWin-ME predicted distresses in the long-term for implementation of the new design methodology (see Tables 6-11 and 6-12). The units can be converted by using the equations mentioned in Chapter 5. The results of conversion should be stored separately in the database for the selected PD's listed Chapter 5. Sensor data (IRI, rut depth and faulting) do not need any further conversion because of their compatibility with DARWin-ME.

Table 6-11 Flexible pavement distresses

Flexible pavement distresses	MDOT units	DARWin-ME units	Conversion needed?
IRI	in/mile	in/mile	No
Top-down cracking	miles	ft/mile	Yes
Bottom-up cracking	miles	% area	Yes
Thermal cracking	No. of occurrences	ft/mile	Yes
Rutting	in	in	No
Reflective cracking	None	% area	No

Table 6-12 Rigid pavement distresses

Rigid pavement distresses	MDOT units	DARWin-ME units	Conversion needed?
IRI	in/mile	in/mile	No
Faulting	in	in	No
Transverse cracking	No. of occurrences	% slabs cracked	Yes

- The significant input variables that are related to the various rehabilitation options and summarized in this report should be an integral part of a database for construction and material related information. Such information will be beneficial for future design projects and local calibration of the performance models in the DARWin-ME. Table 6-13 summarizes the testing needs for the significant input variables obtained from the sensitivity analysis performed in Chapter 4.

Table 6-13 Testing needs for significant input variables for rehabilitation

Pavement layer type	Significant input variables	Lab test[1]	Field test
Overlay	HMA air voids	Yes	
	HMA effective binder	Yes	
	PCC CTE (per °F x 10-6)	Yes	
	PCC MOR (psi)	Yes	
Existing	HMA thickness		Extract core
	Pavement condition rating		Distress survey
	Subgrade modulus		FWD testing
	Subbase modulus		FWD testing
	PCC thickness		Extract core
	Existing PCC elastic modulus (psi)		FWD

[1] Either use current practice or AASHTO test methods

REFERENCES

CHAPTER 2

1. Haider, S. W., H. K. Salama, N. Buch, and K. Chatti, "Significant M-E PDG Design Inputs for Jointed Plain Concrete Pavements in Michigan," presented at the Fifth International Conference on Maintenance and Rehabilitation of Pavements and Technological Control, Park City, Utah, USA, 2007, pp. 79-84.
2. Haider, S. W., H. K. Salama, N. Buch, and K. Chatti, "Influence of Traffic Inputs on Rigid Pavement Performance Using M-E PDG in the State of Michigan," presented at the Fifth International Conference on Maintenance and Rehabilitation of Pavements and Technological Control, Park City, Utah, USA, 2007, pp. 85-90.
3. Buch, N., K. Chatti, S. W. Haider, and A. Manik, "Evaluation of the 1-37A Design Process for New and Rehabilitated JPCP and HMA Pavements, Final Report," Michigan Department of Transportation, Construction and Technology Division, P.O. Box 30049, Lansing, MI 48909, Lansing, Research Report RC-1516, 2008.
4. Haider, S. W., N. Buch, and K. Chatti, "Evaluation of M-E PDG for Rigid Pavements—Incorporating the State-of-the-Practice in Michigan," presented at the 9th International Conference on Concrete Pavements San Francisco, California, USA, 2008, pp.
5. Buch, N., S. W. Haider, J. Brown, and K. Chatti, "Characterization of Truck Traffic in Michigan for the New Mechanistic Empirical Pavemnet Design Guide, Final Report," Michigan Department of Transportation, Construction and Technology Division, P.O. Box 30049, Lansing, MI 48909, Lansing, Research Report RC-1537, 2009.
6. Haider, S. W., N. Buch, K. Chatti, and J. Brown, "Development of Traffic Inputs for Mechanistic-Empirical Pavement Design Guide in Michigan," *Transportation Research Record*, vol. 2256, pp. 179-190, 2011.
7. Baladi, G. Y., T. Dawson, and C. Sessions, "Pavement Subgrade MR Design Values for Michigan's Seasonal Changes, Final Report," Michigan Department of Transportation, Construction and Technology Division, P.O. Box 30049, Lansing, MI 48909, Lansing, Research Report RC-1531, 2009.
8. Baladi, G. Y., K. A. Thottempudi, and T. Dawson, "Backcalculation of Unbound Granular Layer Moduli, Final Report," Michigan Department of Transportation, Construction and Technology Division, P.O. Box 30049, Lansing, MI 48909, Lansing, 2010.
9. Schwartz, C. W., R. Li, S. Kim, H. Ceylan, and R. Gopalakrishnan, "Sensitivity Evaluation of MEPDG Performance Prediction," NCHRP 1-47 Final Report, 2011.
10. Zhou, C., B. Huang, X. Shu, and Q. Dong, "Validating MEPDG with Tennessee Pavement Performance Data," *Journal of Transportation Engineering*, vol. 139, pp. 306-312, 2013.
11. NCHRP Project 1-37A, "Guide for Mechanistic-Empirical Design of New and Rehabilitated Pavement structures," National Cooperative Research Program (NCHRP), Washington D.C. Final Report, 2004.

12. NCHRP Project 1-40B, "Local Calibration Guidance for the Recommended Guide for Mechanistic-Empirical Pavement Design of New and Rehabilitated Pavement Structures," Final NCHRP Report 2009.
13. AASHTO, "Mechanistic-Empirical Pavement Design Guide: A Manual of Practice: Interim Edition," American Association of State Highway and Transportation Officials 2008.

CHAPTER 3

1. AASHTO, "Mechanistic-Empirical Pavement Design Guide: A Manual of Practice: Interim Edition," American Association of State Highway and Transportation Officials 2008.
2. NCHRP Project 1-37A, "Guide for Mechanistic-Empirical Design of New and Rehabilitated Pavement structures," National Cooperative Research Program (NCHRP), Washington D.C. Final Report, 2004.
3. Tompkins, D., P. Saxena, A. Gotlif, and L. Khazanovich, "Modification of Mechanistic-Empirical Pavement Design Guide Procedure for Two-Lift Composite Concrete Pavements," 2012.
4. Smith, K. D., J. E. Bruinsma, M. J. Wade, K. Chatti, J. M. Vandenbossche, and H. T. Yu, "Using Falling Weight Deflectometer Data with Mechanistic-Empirical Design and Analysis, Volume 1: Final Report," Federal Highway Administration, 1200 New Jersey Avenue, SE, Washington, DC 20590 2010.
5. Pierce, L. M., K. D. Smith, J. E. Bruinsma, M. J. Wade, K. Chatti, and J. M. Vandenbossche, "Using Falling Weight Deflectometer Data with Mechanistic-Empirical Design and Analysis, Volume 3: Guidelines for Deflection Testing, Analysis, and Interpretation," Federal Highway Administration, 1200 New Jersey Avenue, SE, Washington, DC 20590 2010.
6. Chatti, K., M. Kutay, and L. Lei, "Relationships between Laboratory-Measured and Field-Derived Properties of Pavement Layers," 2011.

CHAPTER 4

1. Buch, N., K. Chatti, S. W. Haider, and A. Manik, "Evaluation of the 1-37A Design Process for New and Rehabilitated JPCP and HMA Pavements, Final Report," Michigan Department of Transportation, Construction and Technology Division, P.O. Box 30049, Lansing, MI 48909, Lansing, Research Report RC-1516, 2008.
2. Haider, S. W., N. Buch, and K. Chatti, "Evaluation of M-E PDG for Rigid Pavements—Incorporating the State-of-the-Practice in Michigan," presented at the 9th International Conference on Concrete Pavements San Francisco, California, USA, 2008, pp.
3. Schwartz, C. W., R. Li, S. Kim, H. Ceylan, and R. Gopalakrishnan, "Sensitivity Evaluation of MEPDG Performance Prediction," NCHRP 1-47 Final Report, 2011.
4. Kutay, E. and A. Jamrah, "Preparation for Implementation of the Mechanistic-Empirical Pavement Design Guide in Michiagn: Part 1 - HMA Mixture Characterization," Michigan Department of Transportation, 425 West Ottawa, P.O. Box 30050 Lansing, MI 48909, Lansing, Research Report ORBP OR10-022, 2012.

5. NCHRP Project 1-37A, "Guide for Mechanistic-Empirical Design of New and Rehabilitated Pavement structures," National Cooperative Research Program (NCHRP), Washington D.C. Final Report, 2004.
6. Rauhut, J. B., A. Eltahan, and A. L. Simpson, "Common Characteristics of Good and Poorly Performing AC Pavements," Federal Highway Administration, FHWA-RD-99-193, December 1999.
7. Khazanovich, L., D. M, B. R, and M. T, "Common Characteristics of Good and Poorly Performing PCC Pavements," Federal Highway Administration, FHWA-RD-97-131, 1998.
8. Haider, S. W., N. Buch, K. Chatti, and J. Brown, "Development of Traffic Inputs for Mechanistic-Empirical Pavement Design Guide in Michigan," *Transportation Research Record*, vol. 2256, pp. 179-190, 2011.
9. Buch, N., S. W. Haider, J. Brown, and K. Chatti, "Characterization of Truck Traffic in Michigan for the New Mechanistic Empirical Pavemnet Design Guide, Final Report," Michigan Department of Transportation, Construction and Technology Division, P.O. Box 30049, Lansing, MI 48909, Lansing, Research Report RC-1537, 2009.
10. AASHTO, "Mechanistic-Empirical Pavement Design Guide: A Manual of Practice: Interim Edition," American Association of State Highway and Transportation Officials 2008.
11. Weckman, G., D. Millie, C. Ganduri, M. Rangwala, W. Young, M. Rinder, and G. Fahnenstiel, "Knowledge extraction from the neural ‘black box’in ecological monitoring," *Journal of Industrial and Systems Engineering*, vol. 3, pp. 38-55, 2009.

APPENDICES

A – PRELIMINARY AND DETAILED SENSITIVITY ANALYSIS RESULTS
B – GLOBAL SENSITIVITY ANALYSIS RESULTS
C – VERIFICATION
D – MDOT PMS DISTRESS MANUAL

TABLE OF CONTENTS

APPENDIX A - PRELIMINARY AND DETAILED SENSITIVITY ANALYSIS RESULTS A.1
A.1 PRELIMINARY SENSITIVITY ANALYSIS A.1
A.2 DETAILED SENSITIVITY ANALYSIS A.1
A.2.1 HMA over HMA A.1
A.2.1.1. Longitudinal cracking A.4
A.2.1.2. Alligator cracking A.8
A.2.1.3. Rutting A.12
A.2.1.4. IRI A.17
A.2.2 Composite Overlays A.22
A.2.2.1. Longitudinal cracking A.23
A.2.2.2. Alligator cracking A.27
A.2.2.3. Rutting A.28
A.2.2.4. IRI A.32
A.2.3 Rubblized Overlays A.34
A.2.3.1. Longitudinal cracking A.35
A.2.3.2. Alligator cracking A.38
A.2.3.3. Rutting A.41
A.2.3.4. IRI A.44
A.2.4 Unbonded Overlay A.47
A.2.4.1. Cracking A.48
A.2.4.2. Faulting A.52
A.2.4.3. IRI A.54

APPENDIX B - GLOBAL SENSITIVITY ANALYSIS RESULTS B.1
B.1 HMA over HMA B.1
B.1.1 Alligator Cracking B.1
B.1.2 Longitudinal Cracking B.7
B.1.3 Rutting B.13
B.1.4 IRI B.19
B.2 Composite Overlays B.25
B.1.5 Longitudinal Cracking B.25
B.1.6 Rutting B.30
B.1.7 IRI B.35
B.3 Rubblized Overlays B.39
B.1.8 Alligator cracking B.39
B.1.9 Longitudinal cracking B.43
B.1.10 Rutting B.48
B.1.11 IRI B.53
B.4 Unbonded Overlays B.58
B.1.12 Cracking B.58
B.1.13 Faulting B.63
B.1.14 IRI B.68

APPENDIX C – VERIFICATION C.1
C.1 INPUT VARIABLE DATA.....C.1
C.1.1 Unbonded Overlays.....C.1
C.1.2 Rubblized Overlays.....C.10
C.1.3 Composite Overlays.....C.21
C.1.4 HMA over HMA.....C.28
C.2 VALIDATION RESULTS.....C.43
C.2.1 Unbonded Overlays.....C.43
C.2.2 Rubblized Overlays.....C.48
C.2.3 Composite Overlays.....C.54
C.2.4 HMA over HMA.....C.58

APPENDIX D – MDOT PMS DISTRESS MANUAL D.1

APPENDIX A - PRELIMINARY AND DETAILED SENSITIVITY ANALYSIS RESULTS

A.1 PRELIMINARY SENSITIVITY ANALYSIS

Tables A-1 and A-2 show the mix types and aggregate gradation details used in preliminary sensitivity analysis.

Table A-1 Binder types used in preliminary sensitivity analysis

Temperature (F)	Binder Type					
	mix 37		Mix 24		Mix 44	
	G*	δ	G*	δ	G*	δ
59	2707405.81	61.47	1669134	51.97	2859351	59.14
114.8	21936.16	77.11	38896.89	56.78	24187.65	75.12
168.8	452.98	87.85	2886.82	63.07	1969.35	83.8

Table A-2 Aggregate gradation used in preliminary sensitivity analysis

	Aggregate gradation		
	Gradation 1	Gradation 2	Gradation 3
% Retained 3/4 in sieve	0	11.62	30
% Retained 3/8 in sieve	1.16	35.3	47
% Retained #4 sieve	27.65	52.64	52.8
% Passing #200 sieve	11.12	7.28	8.38

A.2 DETAILED SENSITIVITY ANALYSIS

In this section, first the factorial matrix for each rehabilitation option is presented. Subsequently, the ANOVA table for each rehabilitation option is presented. The highlighted cells show the statistically significant main and interaction effects. Finally the significant interaction plots for each distress are shown.

A.2.1 HMA over HMA

The tables and figures for HMA overlay are presented below.

Table A-3 Factorial matrix of ANOVA for HMA overlay

Overlay Thickness	Overlay Effective Binder	Overlay PG	Overlay AV	Overlay Agg. Grad.	Existing Cond. Rating	Existing HMA Thickness	Existing Base Mod./Existing Subbase Mod./Subgrade Mod./Climate															
							15000								40000							
							15000				30000				15000				30000			
							2500		25000		2500		25000		2500		25000		2500		25000	
							Pelleston	Detroit	Pelleston	Detroit	Pelleston	Detroit	Pelleston	Detroit	Pelleston	Detroit	Pelleston	Detroit	Pelleston	Detroit	Pelleston	Detroit
2	7%	PG 58-22	5%	Fine	Very Poor	4	1	2	3	4	5	6	7	8	9	10	11	12	13	14	15	16
						12	17	18	19	20	21	22	23	24	25	26	27	28	29	30	31	32
					Excellent	4	33	34	35	36	37	38	39	40	41	42	43	44	45	46	47	48
						12	49	50	51	52	53	54	55	56	57	58	59	60	61	62	63	64
				Coarse	Very Poor	4	65	66	67	68	69	70	71	72	73	74	75	76	77	78	79	80
						12	81	82	83	84	85	86	87	88	89	90	91	92	93	94	95	96
					Excellent	4	97	98	99	100	101	102	103	104	105	106	107	108	109	110	111	112
						12	113	114	115	116	117	118	119	120	121	122	123	124	125	126	127	128
			12%	Fine	Very Poor	4	129	130	131	132	133	134	135	136	137	138	139	140	141	142	143	144
						12	145	146	147	148	149	150	151	152	153	154	155	156	157	158	159	160
					Excellent	4	161	162	163	164	165	166	167	168	169	170	171	172	173	174	175	176
						12	177	178	179	180	181	182	183	184	185	186	187	188	189	190	191	192
				Coarse	Very Poor	4	193	194	195	196	197	198	199	200	201	202	203	204	205	206	207	208
						12	209	210	211	212	213	214	215	216	217	218	219	220	221	222	223	224
					Excellent	4	225	226	227	228	229	230	231	232	233	234	235	236	237	238	239	240
						12	241	242	243	244	245	246	247	248	249	250	251	252	253	254	255	256
		PG 76-28	5%	Fine	Very Poor	4	257	258	259	260	261	262	263	264	265	266	267	268	269	270	271	272
						12	273	274	275	276	277	278	279	280	281	282	283	284	285	286	287	288
					Excellent	4	289	290	291	292	293	294	295	296	297	298	299	300	301	302	303	304
						12	305	306	307	308	309	310	311	312	313	314	315	316	317	318	319	320
				Coarse	Very Poor	4	321	322	323	324	325	326	327	328	329	330	331	332	333	334	335	336
						12	337	338	339	340	341	342	343	344	345	346	347	348	349	350	351	352
					Excellent	4	353	354	355	356	357	358	359	360	361	362	363	364	365	366	367	368
						12	369	370	371	372	373	374	375	376	377	378	379	380	381	382	383	384
			12%	Fine	Very Poor	4	385	386	387	388	389	390	391	392	393	394	395	396	397	398	399	400
						12	401	402	403	404	405	406	407	408	409	410	411	412	413	414	415	416
					Excellent	4	417	418	419	420	421	422	423	424	425	426	427	428	429	430	431	432
						12	433	434	435	436	437	438	439	440	441	442	443	444	445	446	447	448
				Coarse	Very Poor	4	449	450	451	452	453	454	455	456	457	458	459	460	461	462	463	464
						12	465	466	467	468	469	470	471	472	473	474	475	476	477	478	479	480
					Excellent	4	481	482	483	484	485	486	487	488	489	490	491	492	493	494	495	496
						12	497	498	499	500	501	502	503	504	505	506	507	508	509	510	511	512
	14%	PG 58-22	5%	Fine	Very Poor	4	513	514	515	516	517	518	519	520	521	522	523	524	525	526	527	528
						12	529	530	531	532	533	534	535	536	537	538	539	540	541	542	543	544
					Excellent	4	545	546	547	548	549	550	551	552	553	554	555	556	557	558	559	560
						12	561	562	563	564	565	566	567	568	569	570	571	572	573	574	575	576
				Coarse	Very Poor	4	577	578	579	580	581	582	583	584	585	586	587	588	589	590	591	592
						12	593	594	595	596	597	598	599	600	601	602	603	604	605	606	607	608
					Excellent	4	609	610	611	612	613	614	615	616	617	618	619	620	621	622	623	624
						12	625	626	627	628	629	630	631	632	633	634	635	636	637	638	639	640
			12%	Fine	Very Poor	4	641	642	643	644	645	646	647	648	649	650	651	652	653	654	655	656
						12	657	658	659	660	661	662	663	664	665	666	667	668	669	670	671	672
					Excellent	4	673	674	675	676	677	678	679	680	681	682	683	684	685	686	687	688
						12	689	690	691	692	693	694	695	696	697	698	699	700	701	702	703	704
				Coarse	Very Poor	4	705	706	707	708	709	710	711	712	713	714	715	716	717	718	719	720
						12	721	722	723	724	725	726	727	728	729	730	731	732	733	734	735	736
					Excellent	4	737	738	739	740	741	742	743	744	745	746	747	748	749	750	751	752
						12	753	754	755	756	757	758	759	760	761	762	763	764	765	766	767	768
		PG 76-28	5%	Fine	Very Poor	4	769	770	771	772	773	774	775	776	777	778	779	780	781	782	783	784
						12	785	786	787	788	789	790	791	792	793	794	795	796	797	798	799	800
					Excellent	4	801	802	803	804	805	806	807	808	809	810	811	812	813	814	815	816
						12	817	818	819	820	821	822	823	824	825	826	827	828	829	830	831	832
				Coarse	Very Poor	4	833	834	835	836	837	838	839	840	841	842	843	844	845	846	847	848
						12	849	850	851	852	853	854	855	856	857	858	859	860	861	862	863	864
					Excellent	4	865	866	867	868	869	870	871	872	873	874	875	876	877	878	879	880
						12	881	882	883	884	885	886	887	888	889	890	891	892	893	894	895	896
			12%	Fine	Very Poor	4	897	898	899	900	901	902	903	904	905	906	907	908	909	910	911	912
						12	913	914	915	916	917	918	919	920	921	922	923	924	925	926	927	928
					Excellent	4	929	930	931	932	933	934	935	936	937	938	939	940	941	942	943	944
						12	945	946	947	948	949	950	951	952	953	954	955	956	957	958	959	960
				Coarse	Very Poor	4	961	962	963	964	965	966	967	968	969	970	971	972	973	974	975	976
						12	977	978	979	980	981	982	983	984	985	986	987	988	989	990	991	992
					Excellent	4	993	994	995	996	997	998	999	1000	1001	1002	1003	1004	1005	1006	1007	1008
						12	1009	1010	1011	1012	1013	1014	1015	1016	1017	1018	1019	1020	1021	1022	1023	1024

Table A-3 Factorial matrix of ANOVA for HMA overlay (continued)

8	7%	PG 58-22	5%	Fine	Very Poor	4	1025	1026	1027	1028	1029	1030	1031	1032	1033	1034	1035	1036	1037	1038	1039	1040
						12	1041	1042	1043	1044	1045	1046	1047	1048	1049	1050	1051	1052	1053	1054	1055	1056
					Excellent	4	1057	1058	1059	1060	1061	1062	1063	1064	1065	1066	1067	1068	1069	1070	1071	1072
						12	1073	1074	1075	1076	1077	1078	1079	1080	1081	1082	1083	1084	1085	1086	1087	1088
				Coarse	Very Poor	4	1089	1090	1091	1092	1093	1094	1095	1096	1097	1098	1099	1100	1101	1102	1103	1104
						12	1105	1106	1107	1108	1109	1110	1111	1112	1113	1114	1115	1116	1117	1118	1119	1120
					Excellent	4	1121	1122	1123	1124	1125	1126	1127	1128	1129	1130	1131	1132	1133	1134	1135	1136
						12	1137	1138	1139	1140	1141	1142	1143	1144	1145	1146	1147	1148	1149	1150	1151	1152
			12%	Fine	Very Poor	4	1153	1154	1155	1156	1157	1158	1159	1160	1161	1162	1163	1164	1165	1166	1167	1168
						12	1169	1170	1171	1172	1173	1174	1175	1176	1177	1178	1179	1180	1181	1182	1183	1184
					Excellent	4	1185	1186	1187	1188	1189	1190	1191	1192	1193	1194	1195	1196	1197	1198	1199	1200
						12	1201	1202	1203	1204	1205	1206	1207	1208	1209	1210	1211	1212	1213	1214	1215	1216
				Coarse	Very Poor	4	1217	1218	1219	1220	1221	1222	1223	1224	1225	1226	1227	1228	1229	1230	1231	1232
						12	1233	1234	1235	1236	1237	1238	1239	1240	1241	1242	1243	1244	1245	1246	1247	1248
					Excellent	4	1249	1250	1251	1252	1253	1254	1255	1256	1257	1258	1259	1260	1261	1262	1263	1264
						12	1265	1266	1267	1268	1269	1270	1271	1272	1273	1274	1275	1276	1277	1278	1279	1280
		PG 76-28	5%	Fine	Very Poor	4	1281	1282	1283	1284	1285	1286	1287	1288	1289	1290	1291	1292	1293	1294	1295	1296
						12	1297	1298	1299	1300	1301	1302	1303	1304	1305	1306	1307	1308	1309	1310	1311	1312
					Excellent	4	1313	1314	1315	1316	1317	1318	1319	1320	1321	1322	1323	1324	1325	1326	1327	1328
						12	1329	1330	1331	1332	1333	1334	1335	1336	1337	1338	1339	1340	1341	1342	1343	1344
				Coarse	Very Poor	4	1345	1346	1347	1348	1349	1350	1351	1352	1353	1354	1355	1356	1357	1358	1359	1360
						12	1361	1362	1363	1364	1365	1366	1367	1368	1369	1370	1371	1372	1373	1374	1375	1376
					Excellent	4	1377	1378	1379	1380	1381	1382	1383	1384	1385	1386	1387	1388	1389	1390	1391	1392
						12	1393	1394	1395	1396	1397	1398	1399	1400	1401	1402	1403	1404	1405	1406	1407	1408
			12%	Fine	Very Poor	4	1409	1410	1411	1412	1413	1414	1415	1416	1417	1418	1419	1420	1421	1422	1423	1424
						12	1425	1426	1427	1428	1429	1430	1431	1432	1433	1434	1435	1436	1437	1438	1439	1440
					Excellent	4	1441	1442	1443	1444	1445	1446	1447	1448	1449	1450	1451	1452	1453	1454	1455	1456
						12	1457	1458	1459	1460	1461	1462	1463	1464	1465	1466	1467	1468	1469	1470	1471	1472
				Coarse	Very Poor	4	1473	1474	1475	1476	1477	1478	1479	1480	1481	1482	1483	1484	1485	1486	1487	1488
						12	1489	1490	1491	1492	1493	1494	1495	1496	1497	1498	1499	1500	1501	1502	1503	1504
					Excellent	4	1505	1506	1507	1508	1509	1510	1511	1512	1513	1514	1515	1516	1517	1518	1519	1520
						12	1521	1522	1523	1524	1525	1526	1527	1528	1529	1530	1531	1532	1533	1534	1535	1536
	14%	PG 58-22	5%	Fine	Very Poor	4	1537	1538	1539	1540	1541	1542	1543	1544	1545	1546	1547	1548	1549	1550	1551	1552
						12	1553	1554	1555	1556	1557	1558	1559	1560	1561	1562	1563	1564	1565	1566	1567	1568
					Excellent	4	1569	1570	1571	1572	1573	1574	1575	1576	1577	1578	1579	1580	1581	1582	1583	1584
						12	1585	1586	1587	1588	1589	1590	1591	1592	1593	1594	1595	1596	1597	1598	1599	1600
				Coarse	Very Poor	4	1601	1602	1603	1604	1605	1606	1607	1608	1609	1610	1611	1612	1613	1614	1615	1616
						12	1617	1618	1619	1620	1621	1622	1623	1624	1625	1626	1627	1628	1629	1630	1631	1632
					Excellent	4	1633	1634	1635	1636	1637	1638	1639	1640	1641	1642	1643	1644	1645	1646	1647	1648
						12	1649	1650	1651	1652	1653	1654	1655	1656	1657	1658	1659	1660	1661	1662	1663	1664
			12%	Fine	Very Poor	4	1665	1666	1667	1668	1669	1670	1671	1672	1673	1674	1675	1676	1677	1678	1679	1680
						12	1681	1682	1683	1684	1685	1686	1687	1688	1689	1690	1691	1692	1693	1694	1695	1696
					Excellent	4	1697	1698	1699	1700	1701	1702	1703	1704	1705	1706	1707	1708	1709	1710	1711	1712
						12	1713	1714	1715	1716	1717	1718	1719	1720	1721	1722	1723	1724	1725	1726	1727	1728
				Coarse	Very Poor	4	1729	1730	1731	1732	1733	1734	1735	1736	1737	1738	1739	1740	1741	1742	1743	1744
						12	1745	1746	1747	1748	1749	1750	1751	1752	1753	1754	1755	1756	1757	1758	1759	1760
					Excellent	4	1761	1762	1763	1764	1765	1766	1767	1768	1769	1770	1771	1772	1773	1774	1775	1776
						12	1777	1778	1779	1780	1781	1782	1783	1784	1785	1786	1787	1788	1789	1790	1791	1792
		PG 76-28	5%	Fine	Very Poor	4	1793	1794	1795	1796	1797	1798	1799	1800	1801	1802	1803	1804	1805	1806	1807	1808
						12	1809	1810	1811	1812	1813	1814	1815	1816	1817	1818	1819	1820	1821	1822	1823	1824
					Excellent	4	1825	1826	1827	1828	1829	1830	1831	1832	1833	1834	1835	1836	1837	1838	1839	1840
						12	1841	1842	1843	1844	1845	1846	1847	1848	1849	1850	1851	1852	1853	1854	1855	1856
				Coarse	Very Poor	4	1857	1858	1859	1860	1861	1862	1863	1864	1865	1866	1867	1868	1869	1870	1871	1872
						12	1873	1874	1875	1876	1877	1878	1879	1880	1881	1882	1883	1884	1885	1886	1887	1888
					Excellent	4	1889	1890	1891	1892	1893	1894	1895	1896	1897	1898	1899	1900	1901	1902	1903	1904
						12	1905	1906	1907	1908	1909	1910	1911	1912	1913	1914	1915	1916	1917	1918	1919	1920
			12%	Fine	Very Poor	4	1921	1922	1923	1924	1925	1926	1927	1928	1929	1930	1931	1932	1933	1934	1935	1936
						12	1937	1938	1939	1940	1941	1942	1943	1944	1945	1946	1947	1948	1949	1950	1951	1952
					Excellent	4	1953	1954	1955	1956	1957	1958	1959	1960	1961	1962	1963	1964	1965	1966	1967	1968
						12	1969	1970	1971	1972	1973	1974	1975	1976	1977	1978	1979	1980	1981	1982	1983	1984
				Coarse	Very Poor	4	1985	1986	1987	1988	1989	1990	1991	1992	1993	1994	1995	1996	1997	1998	1999	2000
						12	2001	2002	2003	2004	2005	2006	2007	2008	2009	2010	2011	2012	2013	2014	2015	2016
					Excellent	4	2017	2018	2019	2020	2021	2022	2023	2024	2025	2026	2027	2028	2029	2030	2031	2032
						12	2033	2034	2035	2036	2037	2038	2039	2040	2041	2042	2043	2044	2045	2046	2047	2048

A.2.1.1. Longitudinal cracking

Table A-4 ANOVA table for HMA overlay factorial matrix for longitudinal cracking

Source	Type III Sum of Squares	df	Mean Square	F	Sig.
Corrected Model	3.34E+10	56	5.96E+08	221.48	0
Intercept	2.31E+10	1	2.31E+10	8581.25	0
OLTH	1.53E+10	1	1.53E+10	5698.01	0
OLEB	3.69E+08	1	3.69E+08	137.105	0
OLPG	3252647.869	1	3252647.869	1.209	0.27
OLAV	1.98E+09	1	1.98E+09	737.18	0
OLAG	2479152.113	1	2479152.113	0.921	0.34
EXCON	4.48E+09	1	4.48E+09	1663.99	0
EXTH	3.49E+09	1	3.49E+09	1296.21	0
BMOD	1.34E+08	1	1.34E+08	49.735	0
SBMOD	236874.143	1	236874.143	0.088	0.77
SGMOD	8.78E+08	1	8.78E+08	326.336	0
Climate	2752504.654	1	2752504.654	1.023	0.31
EXCON * BMOD	60543223.97	1	60543223.97	22.499	0
EXTH * BMOD	2.73E+08	1	2.73E+08	101.306	0
OLAG * BMOD	474.686	1	474.686	0	0.99
OLAV * BMOD	1224265.29	1	1224265.29	0.455	0.5
OLEB * BMOD	2806218.2	1	2806218.2	1.043	0.31
OLPG * BMOD	425157.258	1	425157.258	0.158	0.69
OLTH * BMOD	20966345.57	1	20966345.57	7.792	0.01
BMOD * SBMOD	87689.129	1	87689.129	0.033	0.86
BMOD * SGMOD	1023030.126	1	1023030.126	0.38	0.54
EXCON * EXTH	5.36E+08	1	5.36E+08	199.073	0
OLAG * EXCON	107406.276	1	107406.276	0.04	0.84
OLAV * EXCON	1.01E+08	1	1.01E+08	37.488	0
OLEB * EXCON	10145350.22	1	10145350.22	3.77	0.05
OLPG * EXCON	80696.258	1	80696.258	0.03	0.86
OLTH * EXCON	2.80E+09	1	2.80E+09	1039.32	0
EXCON * SBMOD	9590125.087	1	9590125.087	3.564	0.06
EXCON * SGMOD	389200.176	1	389200.176	0.145	0.7
OLAG * EXTH	345354.255	1	345354.255	0.128	0.72
OLAV * EXTH	3.24E+08	1	3.24E+08	120.397	0
OLEB * EXTH	21408876.07	1	21408876.07	7.956	0.01
OLPG * EXTH	20016069.52	1	20016069.52	7.438	0.01
OLTH * EXTH	9.62E+08	1	9.62E+08	357.533	0
EXTH * SBMOD	4405402.445	1	4405402.445	1.637	0.2
EXTH * SGMOD	5.03E+08	1	5.03E+08	186.907	0
OLAV * OLAG	32218.166	1	32218.166	0.012	0.91
OLEB * OLAG	1766.817	1	1766.817	0.001	0.98
OLPG * OLAG	26521.348	1	26521.348	0.01	0.92
OLTH * OLAG	231816.235	1	231816.235	0.086	0.77
OLAG * SBMOD	14.841	1	14.841	0	1
OLAG * SGMOD	6690.281	1	6690.281	0.002	0.96
OLEB * OLAV	1.40E+08	1	1.40E+08	52.191	0
OLPG * OLAV	48273651.83	1	48273651.83	17.94	0
OLTH * OLAV	4.20E+08	1	4.20E+08	156.179	0
OLAV * SBMOD	1166039.157	1	1166039.157	0.433	0.51
OLAV * SGMOD	3038505.372	1	3038505.372	1.129	0.29
OLEB * OLPG	36442959.08	1	36442959.08	13.543	0
OLTH * OLEB	3.02E+08	1	3.02E+08	112.356	0
OLEB * SBMOD	1017.653	1	1017.653	0	0.98
OLEB * SGMOD	4593425.563	1	4593425.563	1.707	0.19
OLTH * OLPG	48360207.19	1	48360207.19	17.972	0
OLPG * SBMOD	22047.638	1	22047.638	0.008	0.93
OLPG * SGMOD	15622114.52	1	15622114.52	5.806	0.02
OLTH * SBMOD	73283.472	1	73283.472	0.027	0.87
OLTH * SGMOD	33878122.17	1	33878122.17	12.59	0
SBMOD * SGMOD	16450.146	1	16450.146	0.006	0.94
a. R Squared = .862 (Adjusted R Squared = .858)					

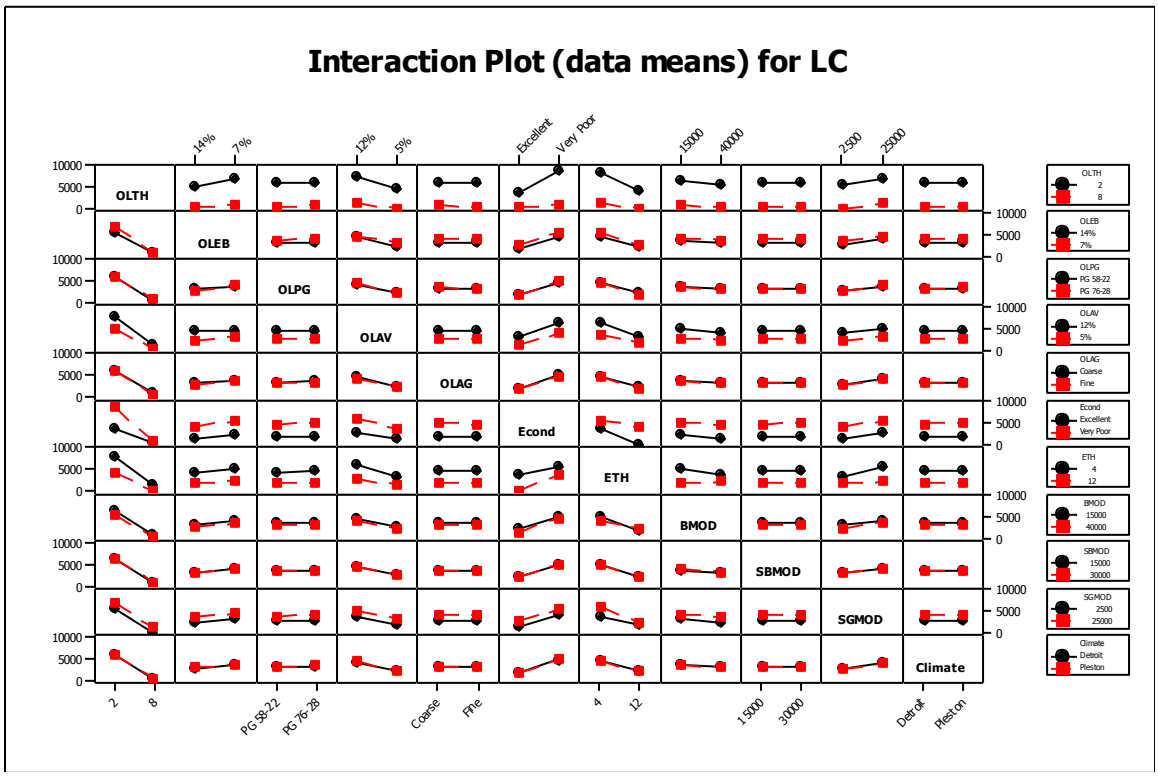

Figure A-1 Summary of interactions

BMOD	OLAV	Mean	Std. Error	95% Confidence Interval	
				Lower Bound	Upper Bound
15000	.05	2604.846	72.496	2462.670	2747.022
	.12	4622.088	72.496	4479.912	4764.264
40000	.05	2142.481	72.496	2000.305	2284.657
	.12	4061.925	72.496	3919.749	4204.101

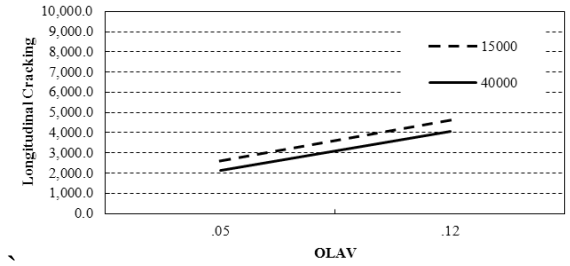

Figure A-2 Overlay air voids vs. base modulus

BMOD	OLTH	Mean	Std. Error	95% Confidence Interval	
				Lower Bound	Upper Bound
15000	2	6450.834	72.496	6308.658	6593.010
	8	776.100	72.496	633.924	918.276
40000	2	5737.209	72.496	55 5.033	5879.385
	8	467.197	72.496	325.021	609.373

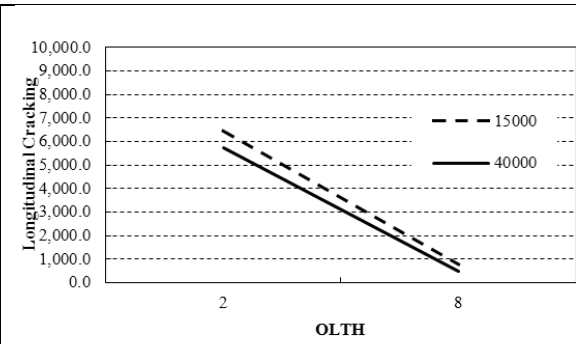

Figure A-3 Overlay thickness vs. base modulus

OLAV	Mean	Std. Error	95% Confidence Interval	
			Lower Bound	Upper Bound
.05	1116.971	72.496	974.795	125 .147
.12	2641.441	72.496	2499.265	2783.617
.05	3630.356	72.496	3488.180	3772.532
.12	6042.572	72.496	5900.395	6184.748

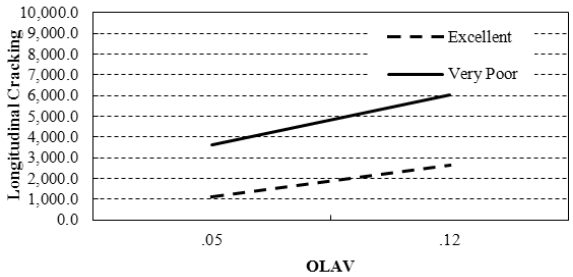

Figure A-4 Overlay air voids vs. existing pavement condition

OLTH	Mean	Std. Er or	95% Confidence Interval	
			Lower Bound	Upper Bound
2	3446.813	72.496	3304.637	3588.989
8	311.599	72.496	169.423	453.775
2	8741.230	72.496	8599.054	8883.406
8	931.697	72.496	789.521	1073.874

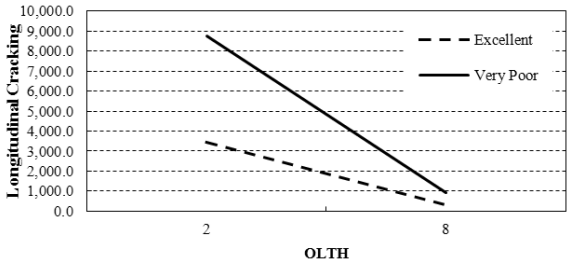

Figure A-5 Overlay thickness vs. existing pavement condition

OLEB	Mean	Std. Error	95% Confidence Interval	
			Lower Bound	Upper Bound
.07	5189.545	72.496	5047.369	5331.721
.14	4136.190	72.496	3994.014	4278.366
.07	2374.995	72.496	2232.819	2517.171
.14	1730.611	72.496	1588.435	1872.787

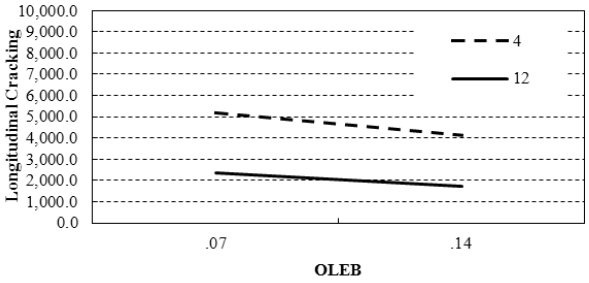

Figure A-6 Overlay effective binder vs. existing pavement thickness

OLPG	Mean	Std. Error	95% Confidence Interval	
			Lower Bound	Upper Bound
PG 58-22	4524.154	72.496	4381.978	4666.330
PG 76-28	4801.580	72.496	4659.404	4943.756
PG 58-22	2111.811	72.496	1969.635	2253.987
PG 76-28	1993.794	72.496	1851.618	2135.970

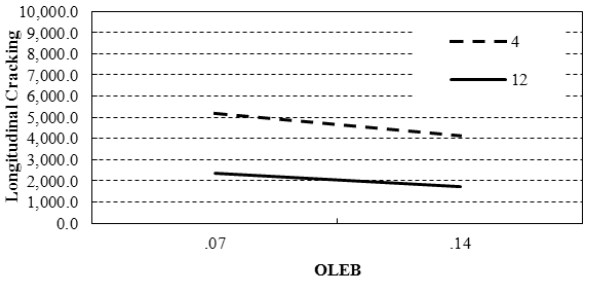

Figure A-7 Overlay effective vs. existing pavement thickness

OLTH	Mean	Std. Error	95% Confidence Interval	
			Low r Bound	Upper Bound
2	8084.451	72.496	7942.275	8226.627
8	1241.283	72.496	1099.107	1383.459
2	4103.592	72.496	3961.416	4245.768
8	2.014	72.496	-140.162	144.190

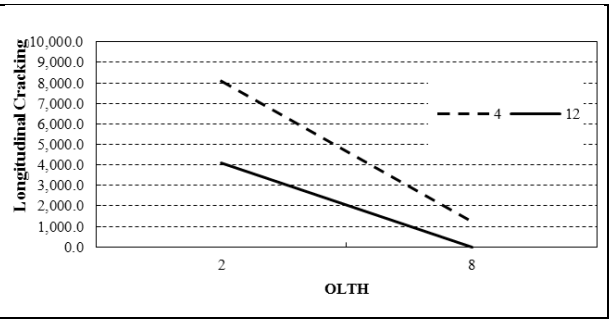

Figure A-8 Overlay Thickness vs. Existing pavement thickness

OLPG	SGMOD	Mean	Std. Error	95% Confidence Interval	
				Lower Bound	Upper Bound
PG 58-22	2500	2750.509	72.496	2608.333	2892.685
	25000	3885.457	72.496	3743.281	4027.633
PG 76-28	2500	2655.537	72.496	2513.361	2797.713
	25000	4139.838	72.496	3997.662	4282.014

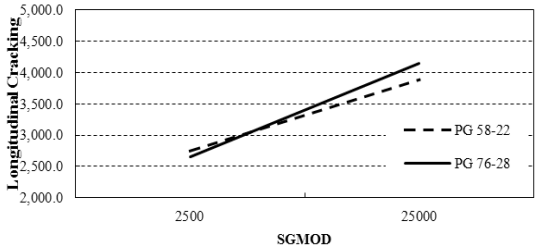

Figure A-9 Overlay PG vs. Subgrade modulus

OLTH	SGMOD	Mean	Std. Error	95% Confidence Interval	
				Lower Bound	Upper Bound
2 in	2500 psi	5310.594	72.496	5168.418	5452.770
	25000 psi	6877.450	72.496	6735.274	7019.626
8 in	2500	95.452	72.496	-46.724	237.628
	25000	1147.845	72.496	1005.669	1290.021

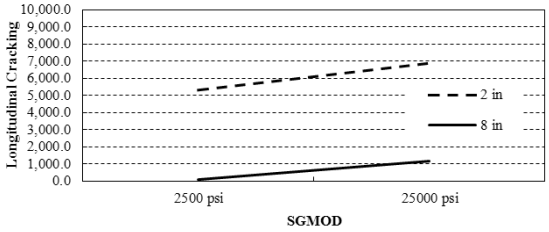

Figure A-10 Overlay Thickness vs. Subgrade modulus

A.2.1.2. Alligator cracking

Table A-5 ANOVA table for HMA overlay factorial matrix for alligator cracking

Source	Type III Sum of Squares	df	Mean Square	F	Sig.
Corrected Model	1074358.925[a]	56	19184.981	365.388	0
Intercept	295690.043	1	295690.04	5631.572	0
OLTH	225836.768	1	225836.77	4301.18	0
OLEB	59573.664	1	59573.664	1134.612	0
OLPG	1058.405	1	1058.405	20.158	0
OLAV	53618.69	1	53618.69	1021.196	0
OLAG	34.018	1	34.018	0.648	0.421
EXCON	286507.442	1	286507.44	5456.684	0
EXTH	9951.749	1	9951.749	189.536	0
BMOD	1612.359	1	1612.359	30.708	0
SBMOD	20.999	1	20.999	0.4	0.527
SGMOD	545.795	1	545.795	10.395	0.001
Climate	527.895	1	527.895	10.054	0.002
EXCON * BMOD	1509.383	1	1509.383	28.747	0
EXTH * BMOD	1316.232	1	1316.232	25.068	0
OLAG * BMOD	0.017	1	0.017	0	0.986
OLAV * BMOD	0.567	1	0.567	0.011	0.917
OLEB * BMOD	9.319	1	9.319	0.177	0.674
OLPG * BMOD	16.659	1	16.659	0.317	0.573
OLTH * BMOD	769.58	1	769.58	14.657	0
BMOD * SBMOD	1.194	1	1.194	0.023	0.88
BMOD * SGMOD	22.673	1	22.673	0.432	0.511
EXCON * EXTH	8992.896	1	8992.896	171.274	0
OLAG * EXCON	25.637	1	25.637	0.488	0.485
OLAV * EXCON	51828.737	1	51828.737	987.105	0
OLEB * EXCON	56240.42	1	56240.42	1071.128	0
OLPG * EXCON	806.104	1	806.104	15.353	0
OLTH * EXCON	227211.141	1	227211.14	4327.355	0
EXCON * SBMOD	17.164	1	17.164	0.327	0.568
EXCON * SGMOD	481.075	1	481.075	9.162	0.003
OLAG * EXTH	1.642	1	1.642	0.031	0.86
OLAV * EXTH	46.18	1	46.18	0.88	0.348
OLEB * EXTH	296.996	1	296.996	5.656	0.017
OLPG * EXTH	64.136	1	64.136	1.222	0.269
OLTH * EXTH	5804.393	1	5804.393	110.548	0
EXTH * SBMOD	18.14	1	18.14	0.345	0.557
EXTH * SGMOD	9.045	1	9.045	0.172	0.678
OLAV * OLAG	3.634	1	3.634	0.069	0.793
OLEB * OLAG	2.358	1	2.358	0.045	0.832
OLPG * OLAG	0.766	1	0.766	0.015	0.904
OLTH * OLAG	52.573	1	52.573	1.001	0.317
OLAG * SBMOD	0.036	1	0.036	0.001	0.979
OLAG * SGMOD	0.145	1	0.145	0.003	0.958
OLEB * OLAV	2542.819	1	2542.819	48.429	0
OLPG * OLAV	662.525	1	662.525	12.618	0
OLTH * OLAV	31206.155	1	31206.155	594.338	0
OLAV * SBMOD	0.096	1	0.096	0.002	0.966
OLAV * SGMOD	5.869	1	5.869	0.112	0.738
OLEB * OLPG	257.973	1	257.973	4.913	0.027
OLTH * OLEB	44650.883	1	44650.883	850.399	0
OLEB * SBMOD	3.311	1	3.311	0.063	0.802
OLEB * SGMOD	34.933	1	34.933	0.665	0.415
OLTH * OLPG	22.883	1	22.883	0.436	0.509
OLPG * SBMOD	2.41	1	2.41	0.046	0.83
OLPG * SGMOD	12.782	1	12.782	0.243	0.622
OLTH * SBMOD	0.285	1	0.285	0.005	0.941
OLTH * SGMOD	114.043	1	114.043	2.172	0.141
SBMOD * SGMOD	5.331	1	5.331	0.102	0.75

a. R Squared = .911 (Adjusted R Squared = .909)

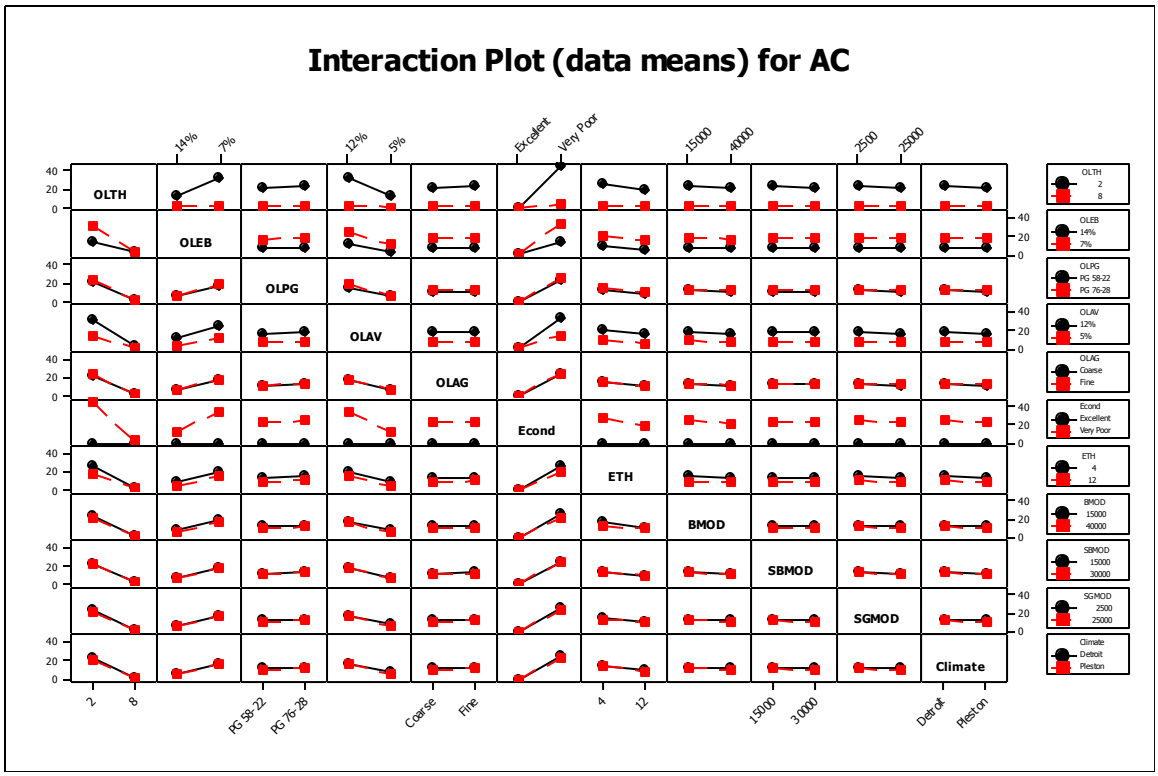

Figure A-11 Summary of interactions

BMOD	OLTH	Mean	Std. Error	95% Confidence Interval	
				Lower Bound	Upper Bound
15000	2	24.017	.320	23.389	24.645
	8	1.789	.320	1.161	2.417
40000	2	21.017	.320	20.389	21.645
	8	1.240	.320	.612	1.869

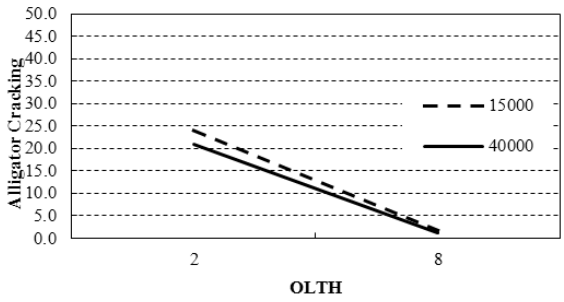

Figure A-12 Overlay thickness vs. base modulus

EXCON	OLAV	Mean	Std. Error	95% Confidence Interval	
				Lower Bound	Upper Bound
Excellent	.05	.102	.320	-.526	.730
	.12	.274	.320	-.354	.902
Very Poor	.05	13.696	.320	13.068	14.324
	.12	33.991	.320	33.363	34.619

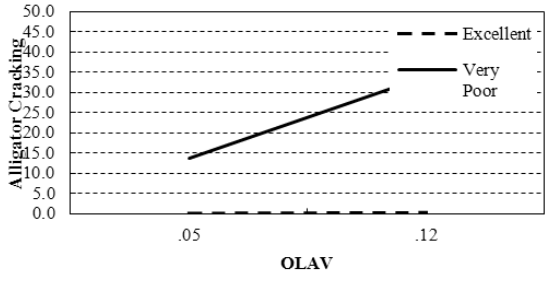

Figure A-13 Overlay air voids vs. existing pavement condition

EXCON	OLEB	Mean	Std. Error	95% Confidence Interval	
				Lower Bound	Upper Bound
Excellent	.07	.341	.320	-.287	.969
	.14	.035	.320	-.593	.663
Very Poor	.07	34.477	. 20	33.849	35.105
	.14	13.210	.320	12.582	13.838

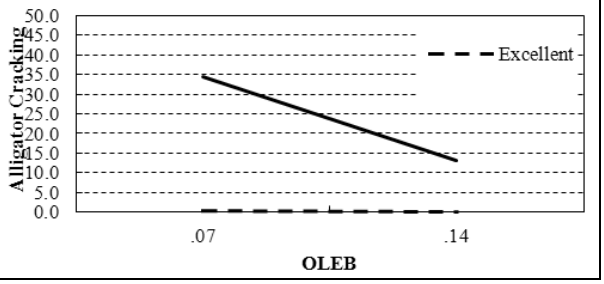

Figure A-14 Overlay effective binder vs. existing pavement condition

EXCON	OLPG	Mean	Std. Error	95% Confidence Interval	
				Lower Bound	Upper Bound
xcellent	PG 58-22	.097	.320	-.531	.725
	PG 76-28	.280	.320	-.348	.908
Very Poor	PG 58-22	22.497	.320	21.869	23.125
	PG 76-28	25.190	.320	24.562	25.818

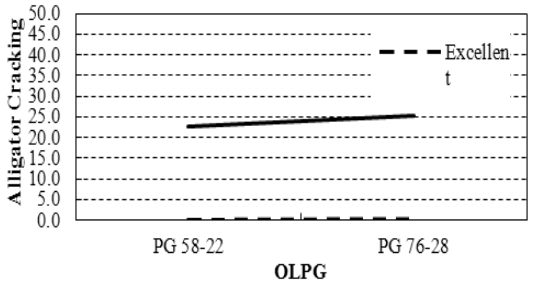

Figure A-15 Overlay PG vs. existing pavement condition

EXCON	OLTH	Mean	Std. Error	95% Confidence Interval	
				Lower Bound	Upper Bound
Excellent	2	.156	.320	-.472	.784
	8	.220	.320	-.408	.848
Very Poor	2	44.878	.320	44.250	45.506
	8	2.810	.320	2.182	3.438

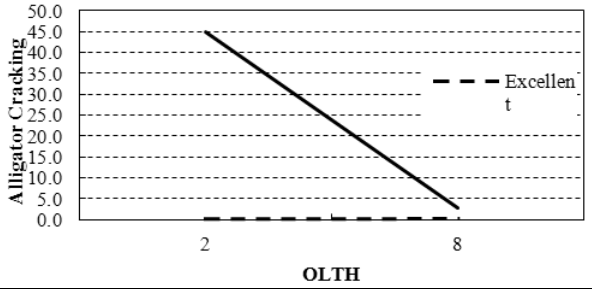

Figure A-16 Overlay thickness vs. existing pavement condition

EXTH	OLEB	Mean	Std. Error	95% Confidence Interval	
				Lower Bound	Upper Bound
4	.07	19.994	.320	19.366	20.622
	.14	8.446	.320	7.818	9.074
12	.07	14.824	.320	14.196	15.452
	.14	4.799	.320	4.171	5.427

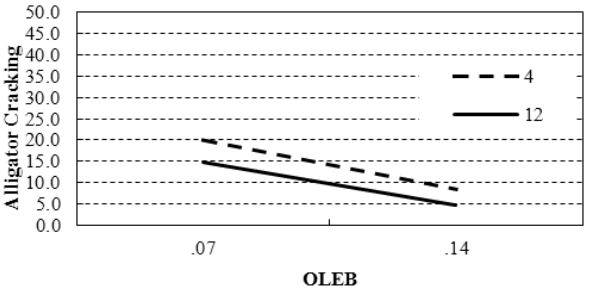

Figure A-17 Overlay effective binder vs. existing pavement thickness

EXTH	OLTH	Mean	Std. Error	95% Confidence Interval	
				Lower Bound	Upper Bound
4	2	26.405	.320	25.777	27.033
	8	2.036	.320	1.408	2.664
12	2	18.629	.320	18.0 1	19.257
	8	.994	.320	.366	1.622

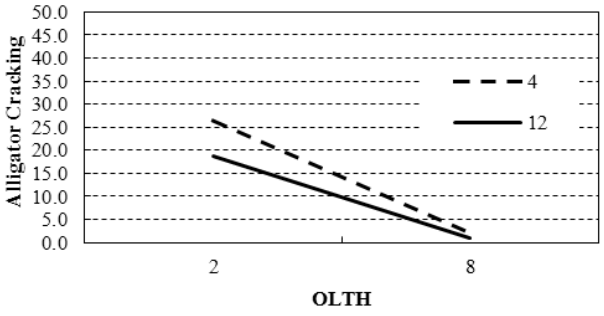

Figure A-18 Overlay thickness vs. existing pavement thickness

A.2.1.3. Rutting

Table A-6 ANOVA table for HMA overlay factorial matrix for rutting

Source	Type III Sum of Squares	df	Mean Square	F	Sig.
Corrected Model	684.888[a]	56	12.23	879.94	0
Intercept	628.29	1	628.29	45204.5	0
OLTH	237.78	1	237.78	17107.91	0
OLEB	2.963	1	2.963	213.195	0
OLPG	1.312	1	1.312	94.371	0
OLAV	4.941	1	4.941	355.461	0
OLAG	0.1	1	0.1	7.181	0.01
EXCON	100.138	1	100.138	7204.788	0
EXTH	128.33	1	128.33	9233.122	0
BMOD	1.565	1	1.565	112.58	0
SBMOD	0.744	1	0.744	53.558	0
SGMOD	0.744	1	0.744	53.519	0
Climate	0.016	1	0.016	1.154	0.28
EXCON * BMOD	0.278	1	0.278	19.995	0
EXTH * BMOD	0.508	1	0.508	36.568	0
OLAG * BMOD	0	1	0	0.007	0.93
OLAV * BMOD	0.003	1	0.003	0.218	0.64
OLEB * BMOD	0.001	1	0.001	0.07	0.79
OLPG * BMOD	0.001	1	0.001	0.082	0.77
OLTH * BMOD	0.717	1	0.717	51.574	0
BMOD * SBMOD	0.006	1	0.006	0.402	0.53
BMOD * SGMOD	0.001	1	0.001	0.081	0.78
EXCON * EXTH	24.594	1	24.594	1769.527	0
OLAG * EXCON	0.004	1	0.004	0.288	0.59
OLAV * EXCON	0.269	1	0.269	19.337	0
OLEB * EXCON	0.073	1	0.073	5.226	0.02
OLPG * EXCON	0.049	1	0.049	3.517	0.06
OLTH * EXCON	96.839	1	96.839	6967.434	0
EXCON * SBMOD	0.028	1	0.028	2.019	0.16
EXCON * SGMOD	0.258	1	0.258	18.538	0
OLAG * EXTH	0.008	1	0.008	0.566	0.45
OLAV * EXTH	0.459	1	0.459	33.014	0
OLEB * EXTH	0.231	1	0.231	16.633	0
OLPG * EXTH	0.13	1	0.13	9.356	0
OLTH * EXTH	80.141	1	80.141	5766.045	0
EXTH * SBMOD	0.086	1	0.086	6.198	0.01
EXTH * SGMOD	0.069	1	0.069	4.939	0.03
OLAV * OLAG	0.004	1	0.004	0.311	0.58
OLEB * OLAG	0.003	1	0.003	0.207	0.65
OLPG * OLAG	0.001	1	0.001	0.068	0.79
OLTH * OLAG	5.55E-05	1	5.55E-05	0.004	0.95
OLAG * SBMOD	1.59E-06	1	1.59E-06	0	0.99
OLAG * SGMOD	0	1	0	0.008	0.93
OLEB * OLAV	0.472	1	0.472	33.973	0
OLPG * OLAV	4.02E-05	1	4.02E-05	0.003	0.96
OLTH * OLAV	0.019	1	0.019	1.399	0.24
OLAV * SBMOD	0	1	0	0.02	0.89
OLAV * SGMOD	0.005	1	0.005	0.341	0.56
OLEB * OLPG	0.251	1	0.251	18.053	0
OLTH * OLEB	0.193	1	0.193	13.919	0
OLEB * SBMOD	8.25E-08	1	8.25E-08	0	1
OLEB * SGMOD	0.001	1	0.001	0.061	0.8
OLTH * OLPG	0.036	1	0.036	2.566	0.11
OLPG * SBMOD	0	1	0	0.024	0.88
OLPG * SGMOD	0.002	1	0.002	0.141	0.71
OLTH * SBMOD	0.107	1	0.107	7.673	0.01
OLTH * SGMOD	0.405	1	0.405	29.117	0
SBMOD * SGMOD	0.004	1	0.004	0.256	0.61

a. R Squared = .961 (Adjusted R Squared = .960)

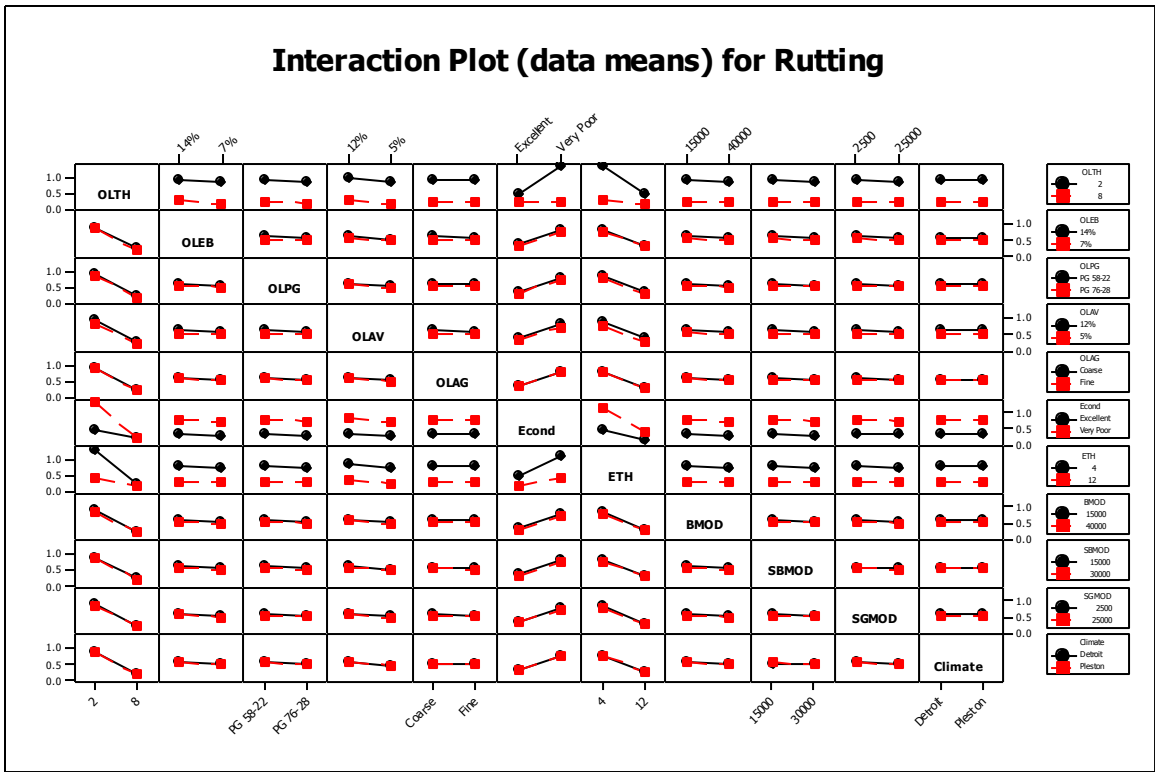

Figure A-19 Summary of interactions

BMOD	OLTH	Mean	Std. Error	95% Confidence Interval	
				Lower Bound	Upper Bound
15000	2	.941	.005	.931	.951
	8	.222	.005	.212	.232
40000	2	.848	.005	.838	.858
	8	.204	.005	.194	.214

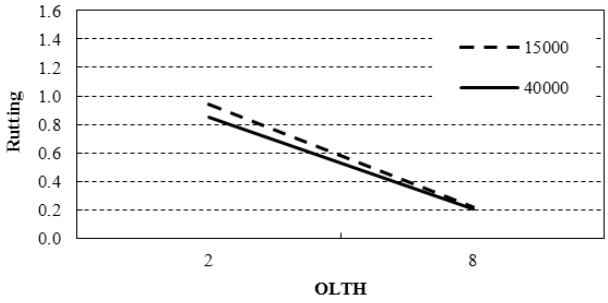

Figure A-20 Overlay thickness vs. overlay thickness vs. Base modulus

EXCON	OLAV	Mean	Std. Error	95% Confidence Interval	
				Lower Bound	Upper Bound
Excellent	.05	.295	.005	.285	.305
	.12	.370	.005	.360	.381
Very Poor	.05	.714	.005	.704	.725
	.12	.836	.005	.825	.846

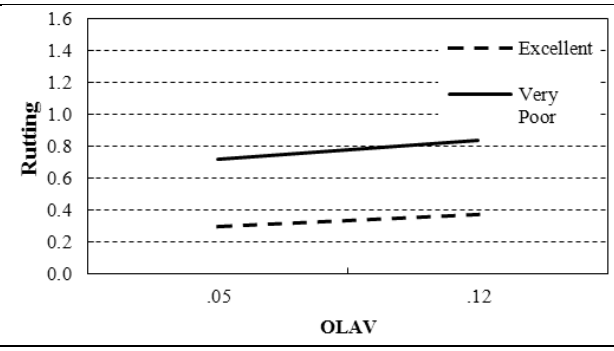

Figure A-21 Overlay air voids vs. existing pavement condition

EXCON	OLEB	Mean	Std. Error	95% Confidence Interval	
				Lower Bound	Upper Bound
Excellent	.07	.301	.005	.290	.311
	.14	.365	.005	.355	.375
Very Poor	.07	.731	.005	.721	.741
	.14	.819	.005	.809	.829

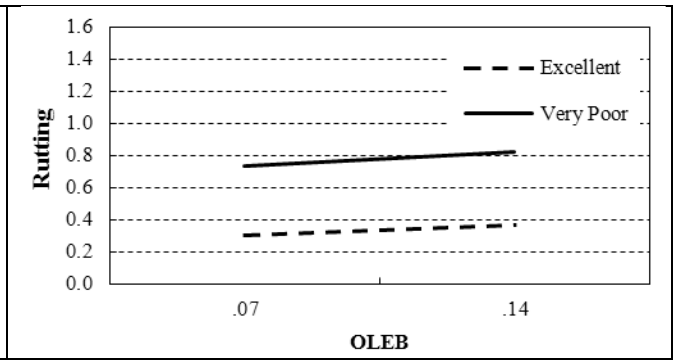

Figure A-22 Overlay effective binder vs. existing pavement condition

EXCON	OLTH	Mean	Std. Error	95% Confidence Interval	
				Lower Bound	Upper Bound
Excellent	2	.456	.005	.446	.466
	8	.209	.005	.199	.220
Very Poor	2	1.333	.005	1.323	1.343
	8	.217	.005	.207	.227

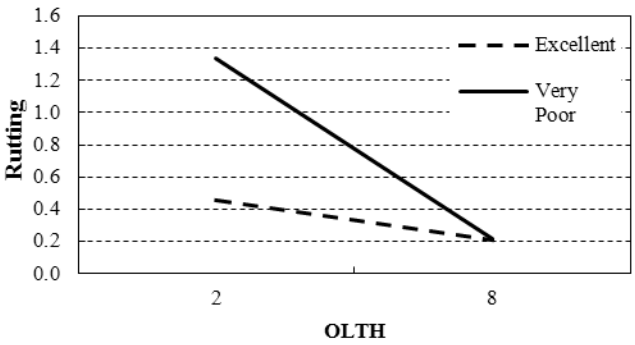

Figure A-23 Overlay thickness vs. existing pavement condition

EXTH	OLAV	Mean	Std. Error	95% Confidence Interval	
				Lower Bound	Upper Bound
4	.05	.740	.005	.730	.750
	.12	.868	.005	.858	.879
12	.05	.269	.005	.259	.280
	.12	.338	.005	.327	.348

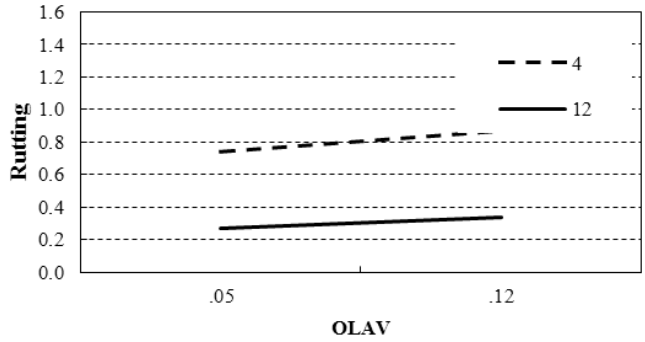

Figure A-24 Overlay air voids vs. existing thickness

EXTH	OLEB	Mean	Std. Error	95% Confidence Interval	
				Lower Bound	Upper Bound
4	.07	.756	.005	.745	.766
	.14	.853	.005	.843	.863
12	.07	.276	.005	.266	.286
	.14	.331	.005	.321	.341

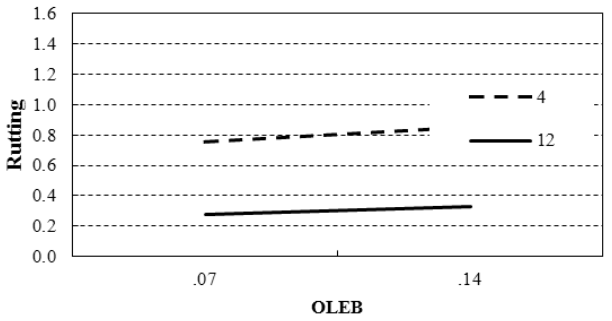

Figure A-25 Overlay effective binder vs. existing pavement thickness

EXTH	OLPG	Mean	Std. Error	95% Confidence Interval	
				Lower Bound	Upper Bound
4	PG 58-22	.837	.005	.827	.848
	PG 76-28	.771	.005	.761	.781
12	PG 58-22	.321	.005	.311	.331
	PG 76-28	.286	.005	.276	.296

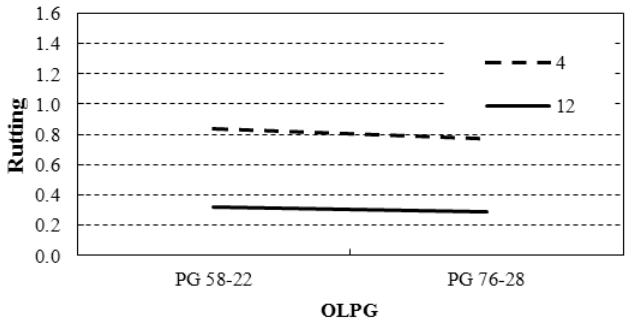

Figure A-26 Overlay PG vs. existing pavement thickness

EXTH	OLTH	Mean	Std. Error	95% Confidence Interval	
				Lower Bound	Upper Bound
4	2	1.343	.005	1.333	1.353
	8	.266	.005	.255	.276
12	2	.446	.005	.436	.457
	8	.161	.005	.150	.171

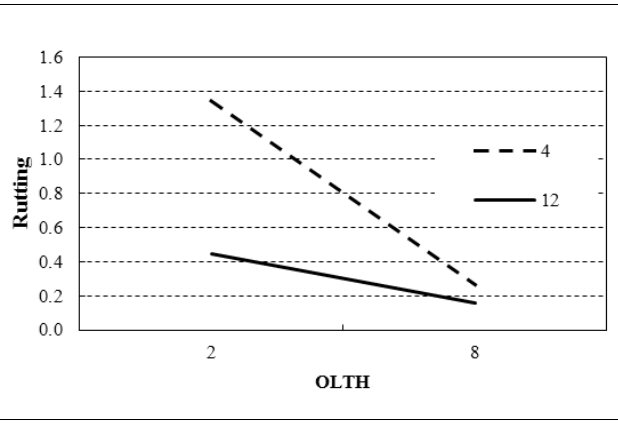

Figure A-27 Overlay thickness vs. existing pavement thickness

OLTH	SBMOD	Mean	Std. Error	95% Confidence Interval	
				Lower Bound	Upper Bound
2	15000	.921	.005	.911	.931
	30000	.868	.005	.858	.879
8	15000	.225	.005	.215	.235
	30000	.201	.005	.191	.212

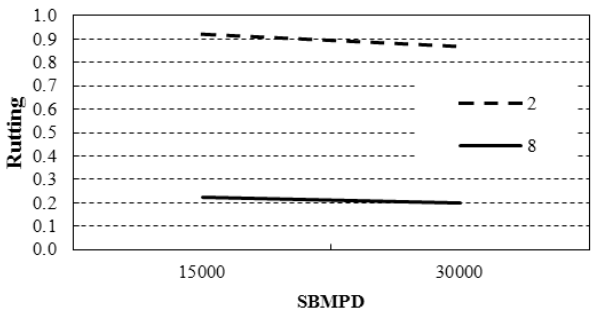

Figure A-28 Overlay thickness vs. subbase modulus

OLTH	SGMOD	Mean	Std. Error	95% Confidence Interval	
				Lower Bound	Upper Bound
2	2500	.928	.005	.918	.938
	25000	.862	.005	.851	.872
8	2500	.218	.005	.208	.228
	25000	.208	.005	.198	.218

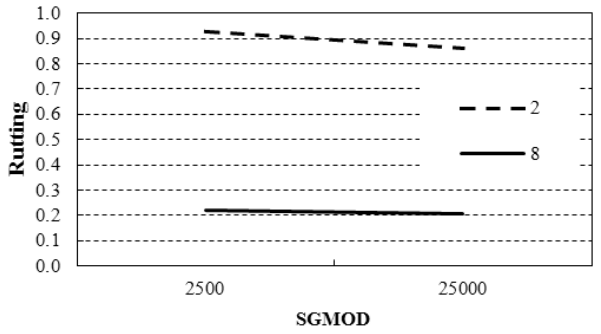

Figure A-29 Overlay thickness vs. subgrade modulus

A.2.1.4. IRI

Table A-7 ANOVA table for HMA overlay factorial matrix for IRI

Source	Type III Sum of Squares	df	Mean Square	F	Sig.
Corrected Model	12658760.342[a]	56	226049.292	97.999	0
Intercept	40029353.5	1	40029353.5	17353.94	0
OLTH	2505182.31	1	2505182.31	1086.073	0
OLEB	525725.784	1	525725.784	227.918	0
OLPG	1370.752	1	1370.752	0.594	0.441
OLAV	726362.745	1	726362.745	314.9	0
OLAG	462.935	1	462.935	0.201	0.654
EXCON	1950491.49	1	1950491.49	845.597	0
EXTH	768300.206	1	768300.206	333.081	0
BMOD	70745.587	1	70745.587	30.67	0
SBMOD	2733.146	1	2733.146	1.185	0.276
SGMOD	15247.491	1	15247.491	6.61	0.01
Climate	6231.117	1	6231.117	2.701	0.1
EXCON * BMOD	55916.905	1	55916.905	24.242	0
EXTH * BMOD	56855.081	1	56855.081	24.648	0
OLAG * BMOD	106.443	1	106.443	0.046	0.83
OLAV * BMOD	24695.448	1	24695.448	10.706	0.001
OLEB * BMOD	31185.19	1	31185.19	13.52	0
OLPG * BMOD	625.143	1	625.143	0.271	0.603
OLTH * BMOD	59046.587	1	59046.587	25.598	0
BMOD * SBMOD	154.385	1	154.385	0.067	0.796
BMOD * SGMOD	1048.391	1	1048.391	0.455	0.5
EXCON * EXTH	382951.966	1	382951.966	166.021	0
OLAG * EXCON	975.853	1	975.853	0.423	0.515
OLAV * EXCON	611704.409	1	611704.409	265.192	0
OLEB * EXCON	607040.155	1	607040.155	263.17	0
OLPG * EXCON	5159.693	1	5159.693	2.237	0.135
OLTH * EXCON	1849319.07	1	1849319.07	801.736	0
EXCON * SBMOD	583.859	1	583.859	0.253	0.615
EXCON * SGMOD	11758.59	1	11758.59	5.098	0.024
OLAG * EXTH	218.34	1	218.34	0.095	0.758
OLAV * EXTH	116945.059	1	116945.059	50.699	0
OLEB * EXTH	103972.275	1	103972.275	45.075	0
OLPG * EXTH	590.928	1	590.928	0.256	0.613
OLTH * EXTH	590529.762	1	590529.762	256.013	0
EXTH * SBMOD	996.951	1	996.951	0.432	0.511
EXTH * SGMOD	2140.011	1	2140.011	0.928	0.336
OLAV * OLAG	709.821	1	709.821	0.308	0.579
OLEB * OLAG	765.505	1	765.505	0.332	0.565
OLPG * OLAG	1.187	1	1.187	0.001	0.982
OLTH * OLAG	1241.732	1	1241.732	0.538	0.463
OLAG * SBMOD	1.235	1	1.235	0.001	0.982
OLAG * SGMOD	22.887	1	22.887	0.01	0.921
OLEB * OLAV	351512.302	1	351512.302	152.391	0
OLPG * OLAV	5613.695	1	5613.695	2.434	0.119
OLTH * OLAV	548664.133	1	548664.133	237.863	0
OLAV * SBMOD	122.217	1	122.217	0.053	0.818
OLAV * SGMOD	3827.305	1	3827.305	1.659	0.198
OLEB * OLPG	7074.18	1	7074.18	3.067	0.08
OLTH * OLEB	630504.842	1	630504.842	273.343	0
OLEB * SBMOD	226.778	1	226.778	0.098	0.754
OLEB * SGMOD	5447.396	1	5447.396	2.362	0.125
OLTH * OLPG	3114.824	1	3114.824	1.35	0.245
OLPG * SBMOD	19.317	1	19.317	0.008	0.927
OLPG * SGMOD	76.068	1	76.068	0.033	0.856
OLTH * SBMOD	777.289	1	777.289	0.337	0.562
OLTH * SGMOD	11547.725	1	11547.725	5.006	0.025
SBMOD * SGMOD	115.853	1	115.853	0.05	0.823
a. R Squared = .734 (Adjusted R Squared = .726)					

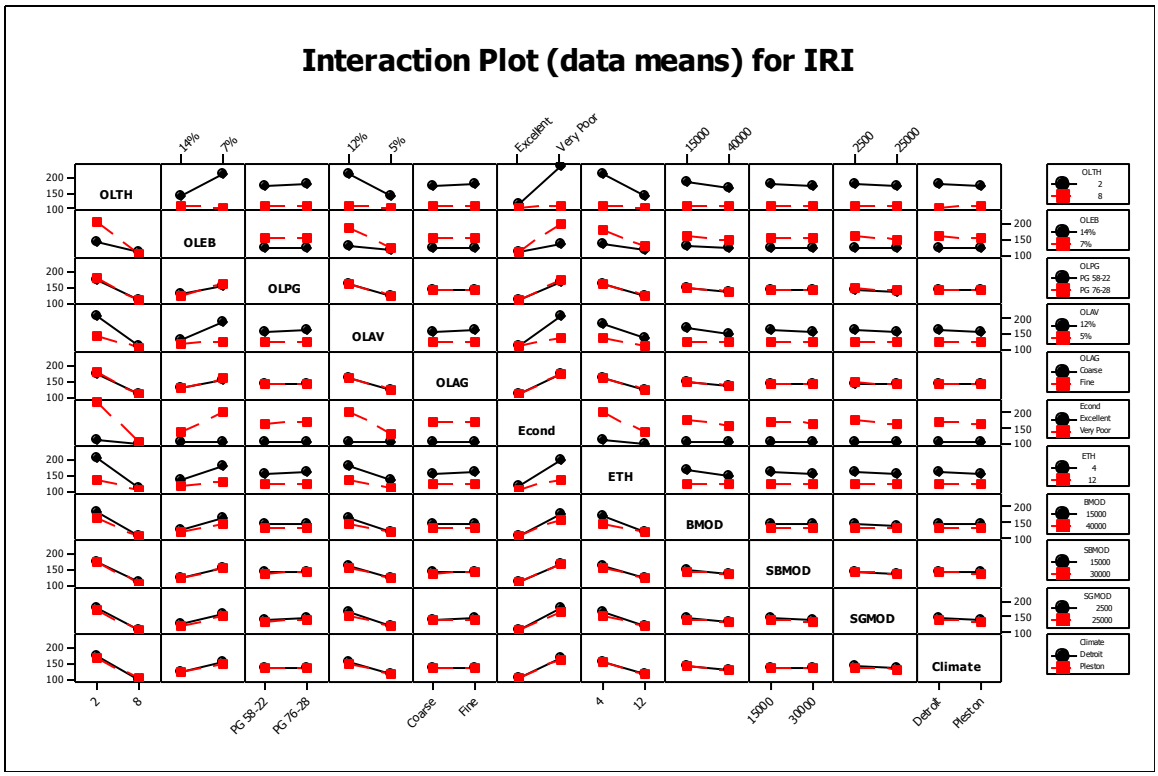

Figure A-30 Summary of interactions

BMOD	OLAV	Mean	Std. Error	95% Confidence Interval	
				Lower Bound	Upper Bound
15000	.05	123.378	2.123	119.215	127.540
	.12	167.988	2.123	163.825	172.151
40000	.05	118.568	2.123	114.405	122.731
	.12	149.288	2.123	145.126	153.451

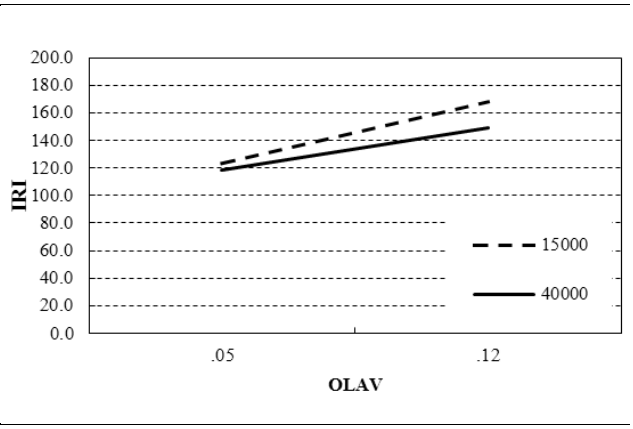

Figure A-31 Overlay air voids vs. base modulus

BMOD	OLEB	Mean	Std. Error	95% Confidence Interval	
				Lower Bound	Upper Bound
15000	.07	165.607	2.123	161.444	169.770
	.14	125.759	2.123	121.596	129.921
40000	.07	146.048	2.123	141.885	150.210
	.14	121.808	2.123	117.646	125.971

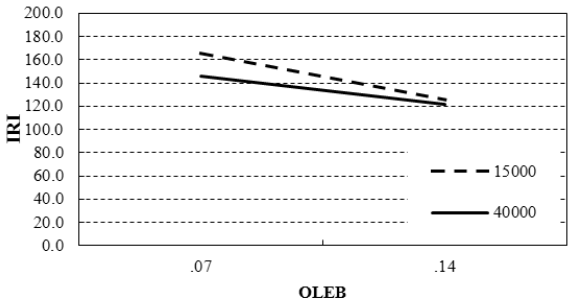

Figure A-32 Overlay Effective binder vs. base modulus

BMOD	OLTH	Mean	Std. Error	95% Confidence Interval	
				Lower Bound	Upper Bound
15000	2	186.027	2.123	181.865	190.190
	8	105.339	2.123	101.176	109.501
40000	2	163.533	2.123	59.371	167.696
	8	104.323	2.123	100.160	108.485

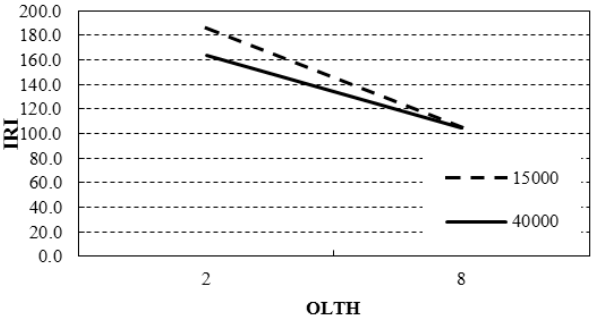

Figure A-33 Overlay thickness vs. base modulus

EXCON	OLAV	Mean	Std. Error	95% Confidence Interval	
				Lower Bound	Upper Bound
Excellent	.05	107.395	2.123	103.232	111.557
	.12	110.495	2.123	106.332	114.658
Very Poor	.05	134.551	2.123	130.389	138.714
	.12	206.781	2.123	202.619	210.944

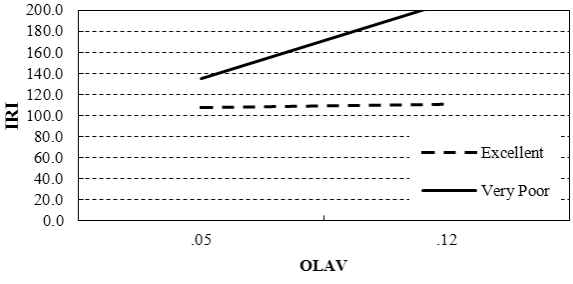

Figure A-34 Overlay air voids vs. existing condition

EXCON	OLB	Mean	Std. Error	95% Confidence Interval	
				Lower Bound	Upper Bound
Excellent	.07	107.750	2.123	103.588	111.913
	.14	110.139	2.123	105.977	114.302
Very Poor	.07	203.905	2.123	199.742	208.067
	.14	137.428	2.123	133.265	141.591

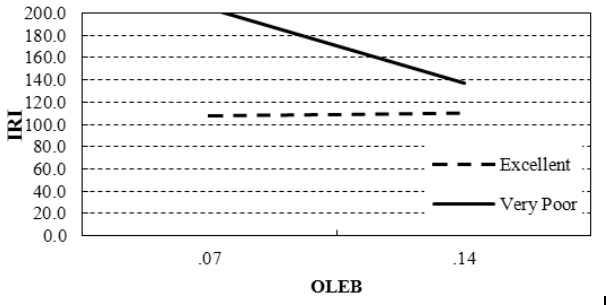

Figure A-35 Overlay effective binder vs. existing condition

EXCON	OLTH	Mean	Std. Error	95% Confidence Interval	
				Lower Bound	Upper Bound
Excellent	2	113.870	2.123	109.707	118.032
	8	104.020	2.123	99.857	108.182
Very Poor	2	235.691	2.123	231.528	239.853
	8	105.642	2.123	101.479	109.804

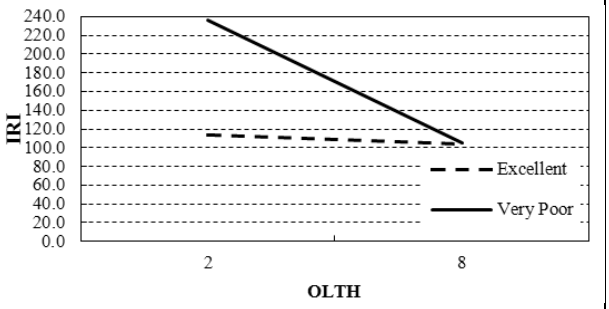

Figure A-36 Overlay thickness vs. Existing condition

EXTH	OLAV	Mean	Std. Error	95% Confidence Interval	
				Lower Bound	Upper Bound
4	.05	132.785	2.123	128.622	136.948
	.12	185.563	2.123	181.401	189.726
12	.05	109.161	2.123	104.998	113.323
	.12	131.713	2.123	127.550	135.876

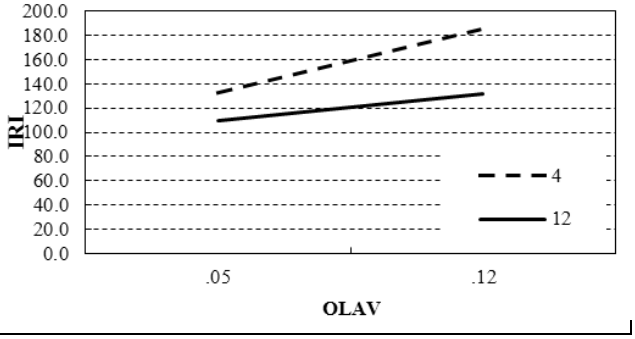

Figure A-37 Overlay air voids vs. existing thickness

EXTH	OLEB	Mean	Std. Error	95% Confidence Interval	
				Lower Bound	Upper Bound
4	.07	182.321	2.123	178.159	186.484
	.14	136.027	2.123	131.865	140.190
12	.07	129.334	2.123	125.171	133.496
	.14	111.540	2.123	107.377	115.703

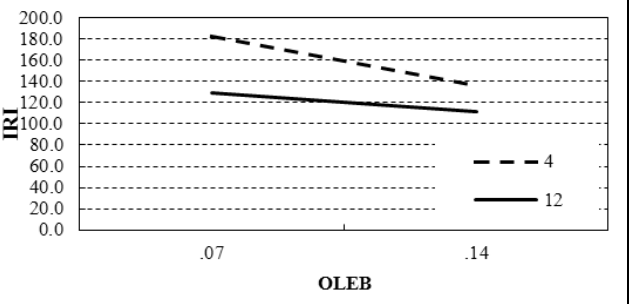

Figure A-38 Overlay Effective binder vs. existing thickness

EXTH	OLTH	Mean	Std. Error	95% Confidence Interval	
				Lower Bound	Upper Bound
4	2	211.130	2.123	206.967	215.292
	8	107.219	2.123	103.056	111.381
12	2	138.431	2.123	134.268	142.593
	8	102.443	2.123	98.280	106.605

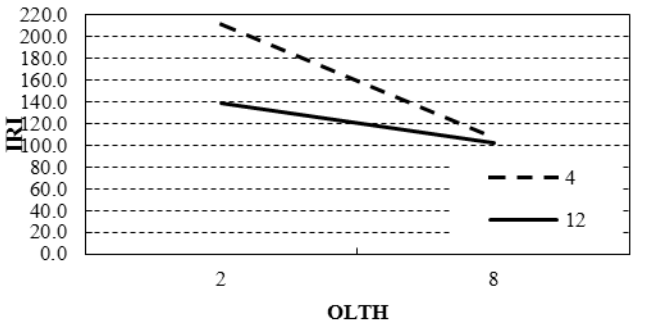

Figure A-39 Overlay thickness vs. existing thickness

OLTH	SGMOD	Mean	Std. Error	95% Confidence Interval	
				Lower Bound	Upper Bound
2	2500	179.883	2.123	175.721	184.046
	25000	169.677	2.123	165.515	173.840
8	2500	105.185	2.123	101.022	109.347
	25000	104.477	2.123	100.314	108.639

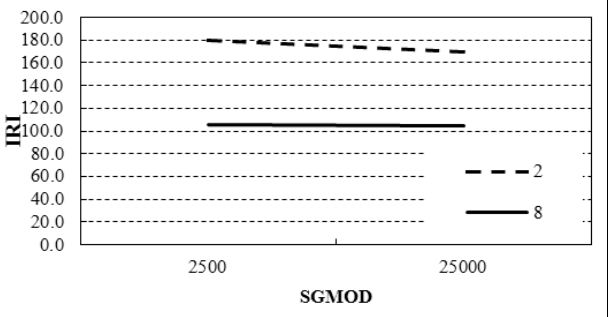

Figure A-40 Overlay thickness vs. subgrade modulus

A.2.2 Composite Overlays

Table A-8 Factorial matrix of ANOVA for composite

OLTH (in)	OLPG	OLGRAD	OLEB (%)	OLAV (%)	EPCCE (psi)/EPCCTH (in)/EK(psi/in)/Climate															
					500000								3000000							
					7				11				7				11			
					50		300		50		300		50		300		50		300	
					Pellston	Detroit	Pellston	Detroit	Pellston	Detroit	Pellston	Detroit	Pellston	Detroit	Pellston	Detroit	Pellston	Detroit	Pellston	Detroit
2	PG 58-22	Coarse	7	5	1	2	3	4	5	6	7	8	9	10	11	12	13	14	15	16
				12	17	18	19	20	21	22	23	24	25	26	27	28	29	30	31	32
			14	5	33	34	35	36	37	38	39	40	41	42	43	44	45	46	47	48
				12	49	50	51	52	53	54	55	56	57	58	59	60	61	62	63	64
		Fine	7	5	65	66	67	68	69	70	71	72	73	74	75	76	77	78	79	80
				12	81	82	83	84	85	86	87	88	89	90	91	92	93	94	95	96
			14	5	97	98	99	100	101	102	103	104	105	106	107	108	109	110	111	112
				12	113	114	115	116	117	118	119	120	121	122	123	124	125	126	127	128
	PG 76-28	Coarse	7	5	129	130	131	132	133	134	135	136	137	138	139	140	141	142	143	144
				12	145	146	147	148	149	150	151	152	153	154	155	156	157	158	159	160
			14	5	161	162	163	164	165	166	167	168	169	170	171	172	173	174	175	176
				12	177	178	179	180	181	182	183	184	185	186	187	188	189	190	191	192
		Fine	7	5	193	194	195	196	197	198	199	200	201	202	203	204	205	206	207	208
				12	209	210	211	212	213	214	215	216	217	218	219	220	221	222	223	224
			14	5	225	226	227	228	229	230	231	232	233	234	235	236	237	238	239	240
				12	241	242	243	244	245	246	247	248	249	250	251	252	253	254	255	256
8	PG 58-22	Coarse	7	5	257	258	259	260	261	262	263	264	265	266	267	268	269	270	271	272
				12	273	274	275	276	277	278	279	280	281	282	283	284	285	286	287	288
			14	5	289	290	291	292	293	294	295	296	297	298	299	300	301	302	303	304
				12	305	306	307	308	309	310	311	312	313	314	315	316	317	318	319	320
		Fine	7	5	321	322	323	324	325	326	327	328	329	330	331	332	333	334	335	336
				12	337	338	339	340	341	342	343	344	345	346	347	348	349	350	351	352
			14	5	353	354	355	356	357	358	359	360	361	362	363	364	365	366	367	368
				12	369	370	371	372	373	374	375	376	377	378	379	380	381	382	383	384
	PG 76-28	Coarse	7	5	385	386	387	388	389	390	391	392	393	394	395	396	397	398	399	400
				12	401	402	403	404	405	406	407	408	409	410	411	412	413	414	415	416
			14	5	417	418	419	420	421	422	423	424	425	426	427	428	429	430	431	432
				12	433	434	435	436	437	438	439	440	441	442	443	444	445	446	447	448
		Fine	7	5	449	450	451	452	453	454	455	456	457	458	459	460	461	462	463	464
				12	465	466	467	468	469	470	471	472	473	474	475	476	477	478	479	480
			14	5	481	482	483	484	485	486	487	488	489	490	491	492	493	494	495	496
				12	497	498	499	500	501	502	503	504	505	506	507	508	509	510	511	512

A.2.2.1. Longitudinal cracking

Table A-9 ANOVA table for composite factorial matrix for longitudinal cracking

Source	Type III Sum of Squares	df	Mean Square	F	Sig.
Corrected Model	7.56E+09	45	1.68E+08	290.86	0
Intercept	2.59E+09	1	2.59E+09	4478.054	0
OLTH	2.57E+09	1	2.57E+09	4453.662	0
OLPG	72471800.4	1	72471800.4	125.487	0
OLGRAD	5270230.13	1	5270230.13	9.126	0.003
OLEB	1989703.29	1	1989703.29	3.445	0.064
OLAV	2.24E+09	1	2.24E+09	3883.855	0
EMOD	15118277	1	15118277	26.178	0
EPCCTH	99276343.9	1	99276343.9	171.899	0
EK	2859.57	1	2859.57	0.005	0.944
Climate	7706531.89	1	7706531.89	13.344	0
EK * Climate	2859.57	1	2859.57	0.005	0.944
EMOD * Climate	19044.689	1	19044.689	0.033	0.856
EPCCTH * Climate	1567547.59	1	1567547.59	2.714	0.1
OLAV * Climate	3413466.43	1	3413466.43	5.91	0.015
OLEB * Climate	36122.016	1	36122.016	0.063	0.803
OLGRAD * Climate	1385.748	1	1385.748	0.002	0.961
OLTH * Climate	7328170.15	1	7328170.15	12.689	0
OLPG * Climate	1062007.38	1	1062007.38	1.839	0.176
EMOD * EK	2859.57	1	2859.57	0.005	0.944
EPCCTH * EK	2859.57	1	2859.57	0.005	0.944
OLAV * EK	2859.57	1	2859.57	0.005	0.944
OLEB * EK	2859.57	1	2859.57	0.005	0.944
OLGRAD * EK	2859.57	1	2859.57	0.005	0.944
OLTH * EK	2859.57	1	2859.57	0.005	0.944
OLPG * EK	2859.57	1	2859.57	0.005	0.944
EMOD * EPCCTH	2476959.27	1	2476959.27	4.289	0.039
OLAV * EMOD	5725355.77	1	5725355.77	9.914	0.002
OLEB * EMOD	41843.629	1	41843.629	0.072	0.788
OLGRAD * EMOD	31022.914	1	31022.914	0.054	0.817
OLTH * EMOD	14578920	1	14578920	25.244	0
OLPG * EMOD	1119314.7	1	1119314.7	1.938	0.165
OLAV * EPCCTH	45218576	1	45218576	78.297	0
OLEB * EPCCTH	161637.344	1	161637.344	0.28	0.597
OLGRAD * EPCCTH	823339.616	1	823339.616	1.426	0.233
OLTH * EPCCTH	97215127.8	1	97215127.8	168.33	0
OLPG * EPCCTH	17200520.1	1	17200520.1	29.783	0
OLEB * OLAV	220512.745	1	220512.745	0.382	0.537
OLGRAD * OLAV	2160579.99	1	2160579.99	3.741	0.054
OLTH * OLAV	2.23E+09	1	2.23E+09	3861.16	0
OLPG * OLAV	33511847.1	1	33511847.1	58.027	0
OLGRAD * OLEB	194.686	1	194.686	0	0.985
OLTH * OLEB	1852124.38	1	1852124.38	3.207	0.074
OLPG * OLEB	54131.193	1	54131.193	0.094	0.76
OLTH * OLGRAD	5103964.58	1	5103964.58	8.838	0.003
OLPG * OLGRAD	304730.631	1	304730.631	0.528	0.468
OLTH * OLPG	70916666	1	70916666	122.794	0
Error	2.69E+08	466	577526.025		
Total	1.04E+10	512			
Corrected Total	7.83E+09	511			
a. R Squared = .966 (Adjusted R Squared = .962)					

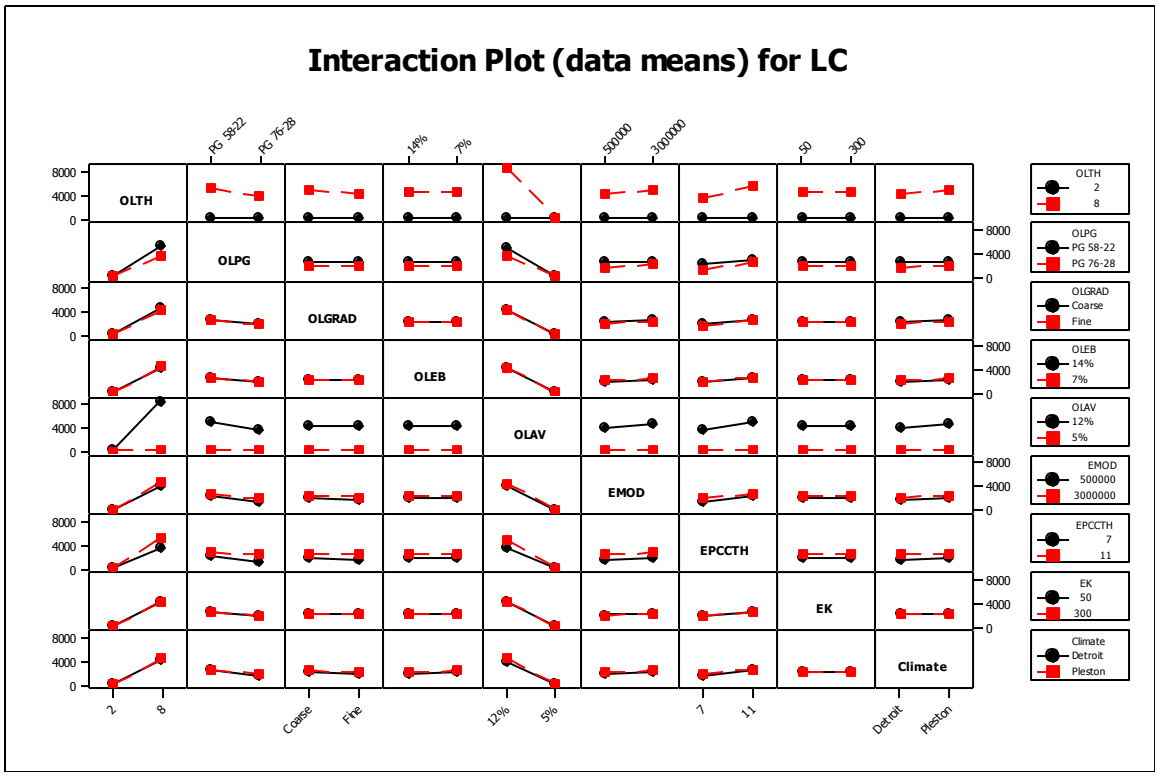

Figure A-41 Summary of interactions

EMOD	OLAV	Mean	Std. Error	95% Confidence Interval	
				Lower Bound	Upper Bound
500000	5.00%	88.325	67.171	-43.670	220.320
	12.00%	4062.957	67.171	3930.962	4194.953
3000000	5.00%	220.505	67.171	88.510	352.501
	12.00%	4618.124	67.171	4486.129	4750.119

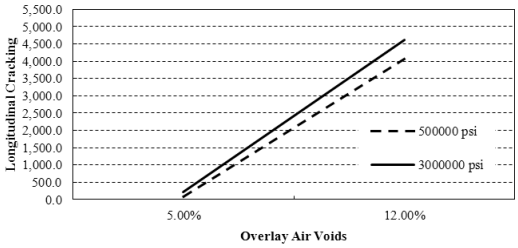

Figure A-42 Overlay air voids vs. existing modulus

EMOD	OLPG	Mean	Std. Error	95% Confidence Interval	
				Lower Bound	Upper Bound
500000 psi	PG 58-22	2498.624	67.171	2366.629	2630.619
	PG 76-28	1652.658	67.171	1520.663	1784.653
3000000 psi	PG 58-22	2748.785	67.171	2616.790	2880.780
	PG 76-28	2089.845	67.171	1957.849	2221.840

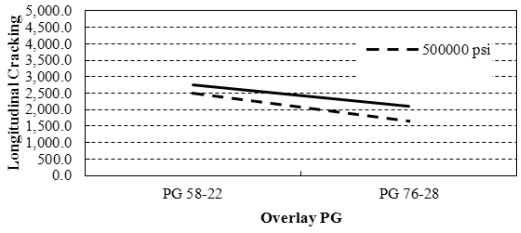

Figure A-43 Overlay PG vs. existing modulus

OLTH	Mean	Std. Error	95% Confidence Interval	
			Lower Bound	Upper Bound
2	3.036	67.171	-128.959	135.032
8	4148.246	67.171	4016.251	4280.241
2	9.222	67.171	-122.773	141.218
8	4829.407	67.171	4697.412	4961.402

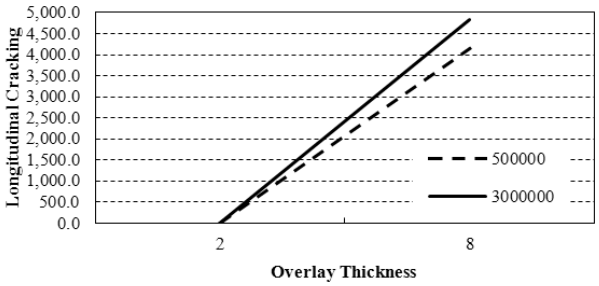

Figure A-44 Overlay thickness vs. existing modulus

OLAV	Mean	Std. Error	95% Confidence Interval	
			Lower Bound	Upper Bound
5.00%	11.258	67.171	-120.737	143.253
12.00%	3603.018	67.171	3471.023	3735.014
5.00%	297.572	67.171	165.577	429.567
12.00%	5078.063	67.171	4946.068	5210.059

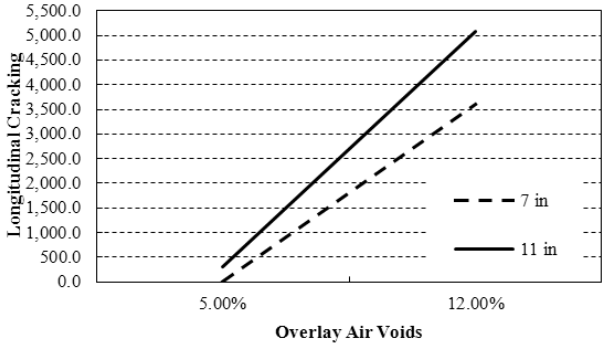

Figure A-45 Overlay air voids vs. existing thickness

OLPG	Mean	Std. Error	95% Confidence Interval	
			Lower Bound	Upper Bound
PG 58-22	2366.654	67.171	2234.658	2498.649
PG 76-28	1247.623	67.171	1115.628	1379.618
PG 58-22	2880.756	67.171	2748.760	3012.751
PG 76-28	2494.880	67.171	2362.885	2626.875

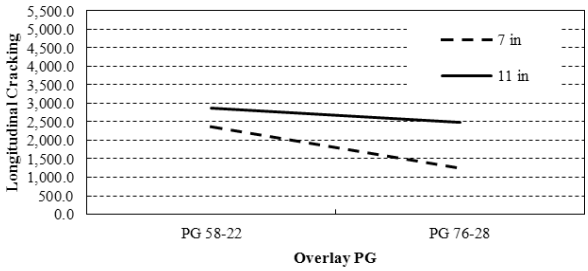

Figure A-46 Overlay PG vs. existing thickness

OLTH	Mean	Std. Error	95% Confidence Interval	
			Lower Bound	Upper Bound
2	1.534	67.171	-130.461	133.529
8	3612.742	67.171	3480.747	3744.738
2	10.725	67.171	-121.271	142.720
8	5364.911	67.171	5232.916	5496.906

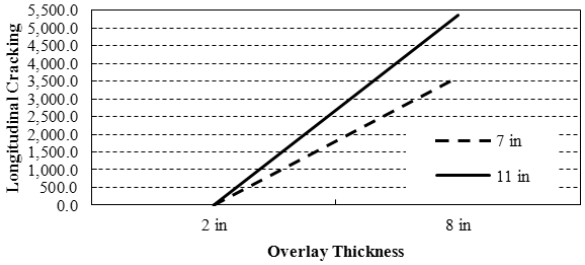

Figure A-47 Overlay thickness vs. existing thickness

A.2.2.2. Alligator cracking

Table A-10 ANOVA table for composite factorial matrix for alligator cracking

Source	Type III Sum of Squares	df	Mean Square	F	Sig.
Corrected Model	2.500E-7[a]	45	5.56E-09	12.328	0
Intercept	2.00E-08	1	2.00E-08	44.381	0
OLTH	2.00E-08	1	2.00E-08	44.381	0
OLPG	0	1	0	0	1
OLGRAD	5.00E-09	1	5.00E-09	11.095	0.001
OLEB	2.00E-08	1	2.00E-08	44.381	0
OLAV	5.00E-09	1	5.00E-09	11.095	0.001
EMOD	2.00E-08	1	2.00E-08	44.381	0
EPCCTH	2.00E-08	1	2.00E-08	44.381	0
EK	0	1	0	0	1
Climate	0	1	0	0	1
EK * Climate	0	1	0	0	1
EMOD * Climate	0	1	0	0	1
EPCCTH * Climate	0	1	0	0	1
OLAV * Climate	0	1	0	0	1
OLEB * Climate	0	1	0	0	1
OLGRAD * Climate	0	1	0	0	1
OLTH * Climate	0	1	0	0	1
OLPG * Climate	0	1	0	0	1
EMOD * EK	0	1	0	0	1
EPCCTH * EK	0	1	0	0	1
OLAV * EK	0	1	0	0	1
OLEB * EK	0	1	0	0	1
OLGRAD * EK	0	1	0	0	1
OLTH * EK	0	1	0	0	1
OLPG * EK	0	1	0	0	1
EMOD * EPCCTH	2.00E-08	1	2.00E-08	44.381	0
OLAV * EMOD	5.00E-09	1	5.00E-09	11.095	0.001
OLEB * EMOD	2.00E-08	1	2.00E-08	44.381	0
OLGRAD * EMOD	5.00E-09	1	5.00E-09	11.095	0.001
OLTH * EMOD	2.00E-08	1	2.00E-08	44.381	0
OLPG * EMOD	0	1	0	0	1
OLAV * EPCCTH	5.00E-09	1	5.00E-09	11.095	0.001
OLEB * EPCCTH	2.00E-08	1	2.00E-08	44.381	0
OLGRAD * EPCCTH	5.00E-09	1	5.00E-09	11.095	0.001
OLTH * EPCCTH	2.00E-08	1	2.00E-08	44.381	0
OLPG * EPCCTH	0	1	0	0	1
OLEB * OLAV	5.00E-09	1	5.00E-09	11.095	0.001
OLGRAD * OLAV	0	1	0	0	1
OLTH * OLAV	5.00E-09	1	5.00E-09	11.095	0.001
OLPG * OLAV	0	1	0	0	1
OLGRAD * OLEB	5.00E-09	1	5.00E-09	11.095	0.001
OLTH * OLEB	2.00E-08	1	2.00E-08	44.381	0
OLPG * OLEB	0	1	0	0	1
OLTH * OLGRAD	5.00E-09	1	5.00E-09	11.095	0.001
OLPG * OLGRAD	0	1	0	0	1
OLTH * OLPG	0	1	0	0	1
Error	2.10E-07	466	4.51E-10		
Total	4.80E-07	512			
Corrected Total	4.60E-07	511			
a. R Squared = .543 (Adjusted R Squared = .499)					

A.2.2.3. Rutting

Table A-11 ANOVA table for composite factorial matrix for rutting

Source	Type III Sum of Squares	df	Mean Square	F	Sig.
Corrected Model	28.040[a]	45	0.623	6612.061	0
Intercept	123.901	1	123.901	1314764.05	0
OLTH	6.347	1	6.347	67346.107	0
OLPG	4.027	1	4.027	42733.315	0
OLGRAD	0.247	1	0.247	2620.255	0
OLEB	3.593	1	3.593	38121.802	0
OLAV	11.727	1	11.727	124443.076	0
EMOD	0.092	1	0.092	981.022	0
EPCCTH	0.367	1	0.367	3896.758	0
EK	5.28E-06	1	5.28E-06	0.056	0.813
Climate	0.148	1	0.148	1567.259	0
EK * Climate	5.28E-06	1	5.28E-06	0.056	0.813
EMOD * Climate	3.40E-05	1	3.40E-05	0.361	0.548
EPCCTH * Climate	3.13E-08	1	3.13E-08	0	0.985
OLAV * Climate	0.011	1	0.011	112.709	0
OLEB * Climate	0.003	1	0.003	31.253	0
OLGRAD * Climate	0	1	0	2.122	0.146
OLTH * Climate	4.51E-05	1	4.51E-05	0.479	0.489
OLPG * Climate	0.002	1	0.002	20.56	0
EMOD * EK	5.28E-06	1	5.28E-06	0.056	0.813
EPCCTH * EK	5.28E-06	1	5.28E-06	0.056	0.813
OLAV * EK	5.28E-06	1	5.28E-06	0.056	0.813
OLEB * EK	5.28E-06	1	5.28E-06	0.056	0.813
OLGRAD * EK	5.28E-06	1	5.28E-06	0.056	0.813
OLTH * EK	5.28E-06	1	5.28E-06	0.056	0.813
OLPG * EK	5.28E-06	1	5.28E-06	0.056	0.813
EMOD * EPCCTH	0.001	1	0.001	7.362	0.007
OLAV * EMOD	0.003	1	0.003	28.468	0
OLEB * EMOD	0.001	1	0.001	8.596	0.004
OLGRAD * EMOD	1.80E-05	1	1.80E-05	0.191	0.662
OLTH * EMOD	0.002	1	0.002	24.896	0
OLPG * EMOD	0.001	1	0.001	5.691	0.017
OLAV * EPCCTH	0.006	1	0.006	68.651	0
OLEB * EPCCTH	0.002	1	0.002	20.891	0
OLGRAD * EPCCTH	6.61E-05	1	6.61E-05	0.702	0.403
OLTH * EPCCTH	0.003	1	0.003	29.054	0
OLPG * EPCCTH	0.001	1	0.001	5.691	0.017
OLEB * OLAV	0.393	1	0.393	4171.999	0
OLGRAD * OLAV	0.021	1	0.021	220.802	0
OLTH * OLAV	0.404	1	0.404	4288.063	0
OLPG * OLAV	0.279	1	0.279	2962.604	0
OLGRAD * OLEB	0.006	1	0.006	67.15	0
OLTH * OLEB	0.125	1	0.125	1323.771	0
OLPG * OLEB	0.085	1	0.085	899.516	0
OLTH * OLGRAD	0.009	1	0.009	94.205	0
OLPG * OLGRAD	0.005	1	0.005	56.836	0
OLTH * OLPG	0.13	1	0.13	1380.01	0
Error	0.044	466	9.42E-05		
Total	151.985	512			
Corrected Total	28.084	511			
a. R Squared = .998 (Adjusted R Squared = .998)					

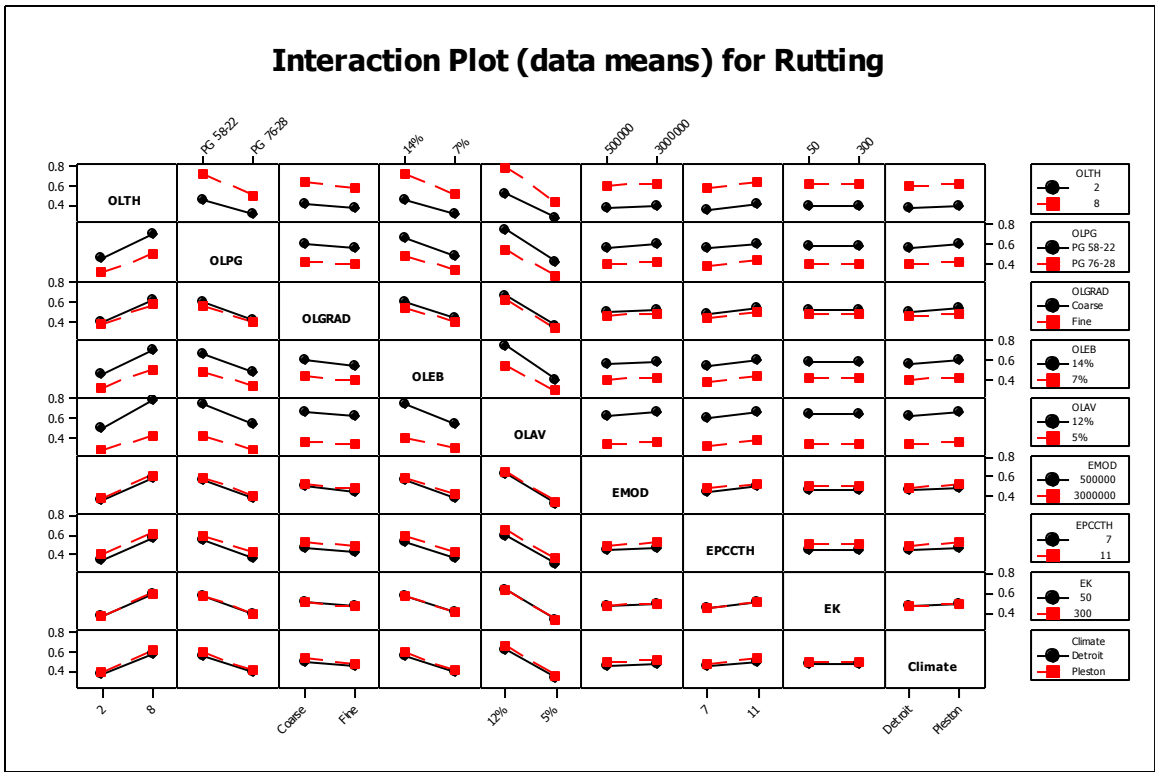

Figure A-48 Summary of interactions

EMOD	OLAV	Mean	Std. Error	95% Confidence Interval	
				Lower Bound	Upper Bound
500000	5.00%	.329	.001	.328	.331
	12.00%	.628	.001	.626	.629
3000000	5.00%	.352	.001	.350	.353
	12.00%	.659	.001	.657	.661

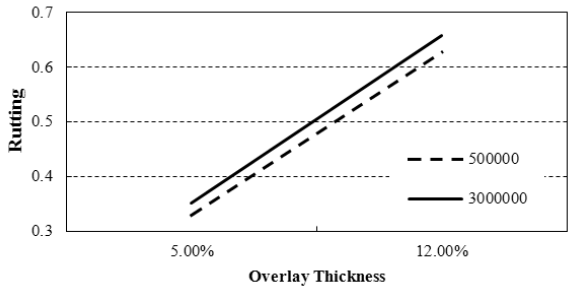

Figure A-49 Overlay air voids vs. existing modulus

EMOD	OLEB	M an	Std. Error	95% Confidence Interval	
				Lower Bound	Upper Bound
500000	7.00%	.396	.001	.394	.398
	14.00 %	.561	.001	.559	.563
3000000	7.00%	.420	.001	.419	.422
	14.00 %	.590	.001	.589	.592

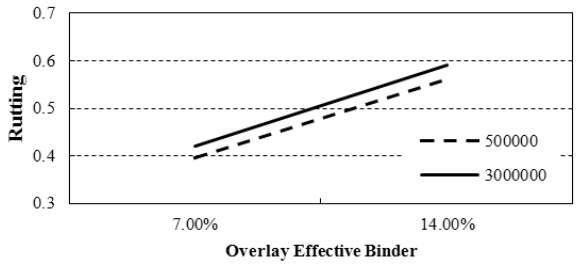

Figure A-50 Overlay effective binder vs. existing modulus

EMOD	OLPG	Mean	Std. Error	95% Confidence Interval	
				Lower Bound	Upper Bound
500000	PG 58-22	.566	.001	.564	.568
	PG 76-28	.391	.001	.389	.393
3000000	PG 58-22	.595	.001	.593	.597
	PG 76-28	.416	.001	.414	.417

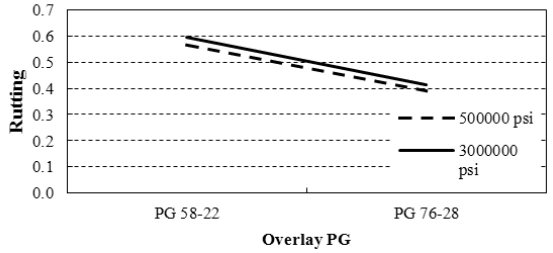

Figure A-51 Overlay PG vs. existing modulus

EMOD	OLTH	Mean	Std. Error	95% Confidence Interval	
				Lower Bound	Upper Bound
500000	2	.365	.001	.363	.367
	8	.592	.001	.590	.594
3000000	2	.396	.001	.394	.398
	8	.615	.001	.613	.616

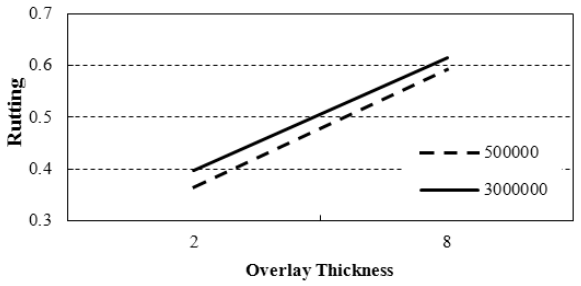

Figure A-52 Overlay thickness vs. existing modulus

EMOD	OLTH	Mean	Std. Error	95% Confidence Interval	
				Lower Bound	Upper Bound
500000	2	.365	.001	.363	.367
	8	.592	.001	.590	.594
3000000	2	.396	.001	.394	.398
	8	.615	.001	.613	.616

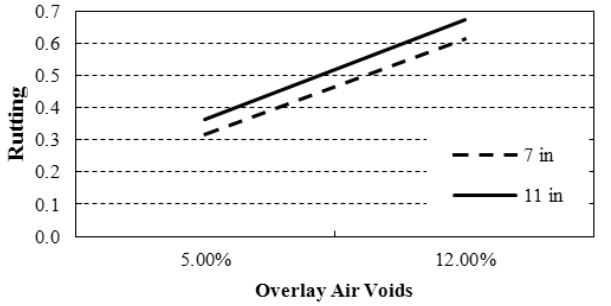

Figure A-53 Overlay air voids vs. existing thickness

ETH	OLEB	Mean	Std. Error	95% Confidence Interval	
				Lower Bound	Upper Bound
7	7.00%	.383	.001	.382	.385
	14.00%	.547	.001	.545	.549
11	7.00%	.433	.001	.431	.435
	14.00%	.604	.001	.603	.606

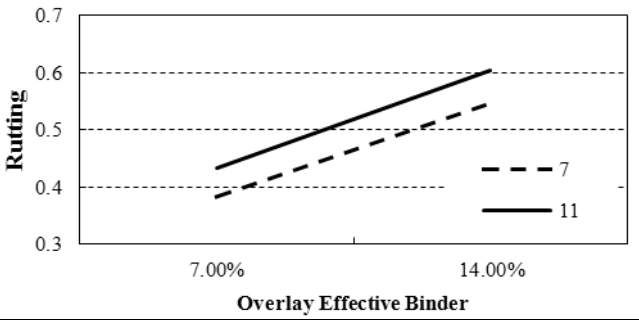

Figure A-54 Overlay effective binder vs. existing thickness

ETH	OLPG	Mean	Std. Error	95% Confidence Interval	
				Lower Bound	Upper Bound
7	PG 58-22	.553	.001	.551	.554
	PG 76-28	.377	.001	.376	.379
11	PG 58-22	.608	.001	.607	.610
	PG 76-28	.429	.001	.427	.431

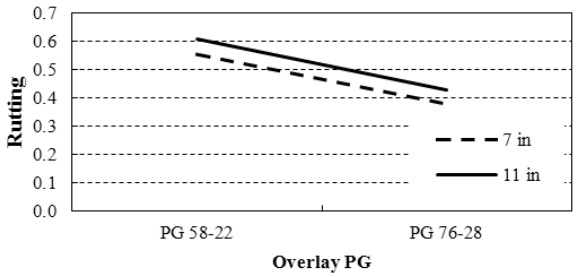

Figure A-55 Overlay PG vs. existing thickness

ETH	OLTH	Mean	Std. Error	95% Confidence Interval	
				Lower Bound	Upper Bound
7	2	.356	.001	.354	.358
	8	.574	.001	.572	.576
11	2	.405	.001	.403	.407
	8	.632	.001	.631	.634

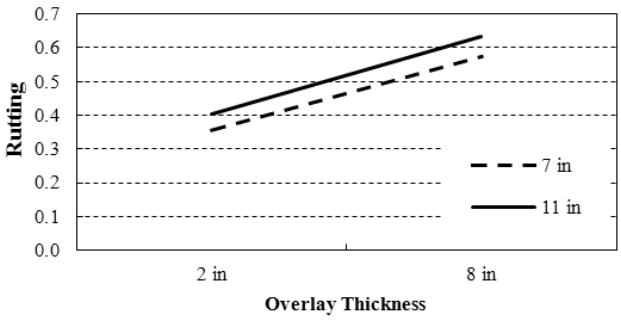

Figure A-56 Overlay thickness vs. existing thickness

A.2.2.4. IRI

Table A-12 ANOVA table for composite factorial matrix for IRI

Source	Type III Sum of Squares	df	Mean Square	F	Sig.
Corrected Model	28.040[a]	45	0.623	6612.061	0
Intercept	123.901	1	123.901	1314764.05	0
OLTH	6.347	1	6.347	67346.107	0
OLPG	4.027	1	4.027	42733.315	0
OLGRAD	0.247	1	0.247	2620.255	0
OLEB	3.593	1	3.593	38121.802	0
OLAV	11.727	1	11.727	124443.076	0
EMOD	0.092	1	0.092	981.022	0
EPCCTH	0.367	1	0.367	3896.758	0
EK	5.28E-06	1	5.28E-06	0.056	0.813
Climate	0.148	1	0.148	1567.259	0
EK * Climate	5.28E-06	1	5.28E-06	0.056	0.813
EMOD * Climate	3.40E-05	1	3.40E-05	0.361	0.548
EPCCTH * Climate	3.13E-08	1	3.13E-08	0	0.985
OLAV * Climate	0.011	1	0.011	112.709	0
OLEB * Climate	0.003	1	0.003	31.253	0
OLGRAD * Climate	0	1	0	2.122	0.146
OLTH * Climate	4.51E-05	1	4.51E-05	0.479	0.489
OLPG * Climate	0.002	1	0.002	20.56	0
EMOD * EK	5.28E-06	1	5.28E-06	0.056	0.813
EPCCTH * EK	5.28E-06	1	5.28E-06	0.056	0.813
OLAV * EK	5.28E-06	1	5.28E-06	0.056	0.813
OLEB * EK	5.28E-06	1	5.28E-06	0.056	0.813
OLGRAD * EK	5.28E-06	1	5.28E-06	0.056	0.813
OLTH * EK	5.28E-06	1	5.28E-06	0.056	0.813
OLPG * EK	5.28E-06	1	5.28E-06	0.056	0.813
EMOD * EPCCTH	0.001	1	0.001	7.362	0.007
OLAV * EMOD	0.003	1	0.003	28.468	0
OLEB * EMOD	0.001	1	0.001	8.596	0.004
OLGRAD * EMOD	1.80E-05	1	1.80E-05	0.191	0.662
OLTH * EMOD	0.002	1	0.002	24.896	0
OLPG * EMOD	0.001	1	0.001	5.691	0.017
OLAV * EPCCTH	0.006	1	0.006	68.651	0
OLEB * EPCCTH	0.002	1	0.002	20.891	0
OLGRAD * EPCCTH	6.61E-05	1	6.61E-05	0.702	0.403
OLTH * EPCCTH	0.003	1	0.003	29.054	0
OLPG * EPCCTH	0.001	1	0.001	5.691	0.017
OLEB * OLAV	0.393	1	0.393	4171.999	0
OLGRAD * OLAV	0.021	1	0.021	220.802	0
OLTH * OLAV	0.404	1	0.404	4288.063	0
OLPG * OLAV	0.279	1	0.279	2962.604	0
OLGRAD * OLEB	0.006	1	0.006	67.15	0
OLTH * OLEB	0.125	1	0.125	1323.771	0
OLPG * OLEB	0.085	1	0.085	899.516	0
OLTH * OLGRAD	0.009	1	0.009	94.205	0
OLPG * OLGRAD	0.005	1	0.005	56.836	0
OLTH * OLPG	0.13	1	0.13	1380.01	0
Error	0.044	466	9.42E-05		
Total	151.985	512			
Corrected Total	28.084	511			
a. R Squared = .998 (Adjusted R Squared = .998)					

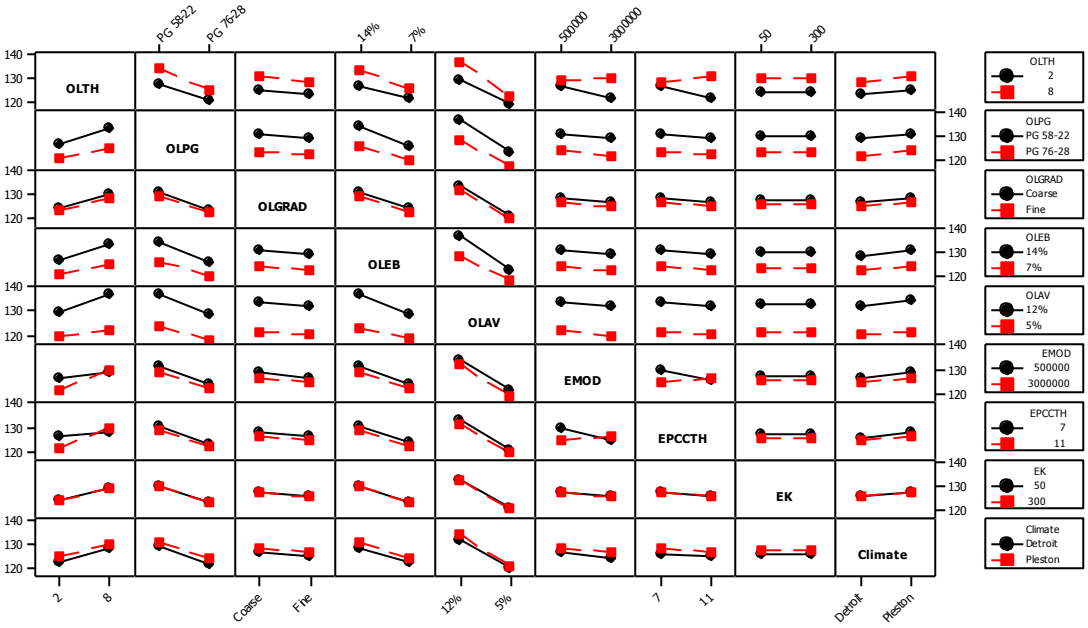

Figure A-57 Summary of interactions

EMOD	OLTH	Mean	Std. Error	95% Confidence Interval	
				Lower Bound	Upper Bound
500000	2	126.40	.153	126.10	126.70
	8	128.77	.153	128.47	129.07
3000000	2	121.31	.153	121.01	121.61
	8	129.78	.153	129.48	130.08

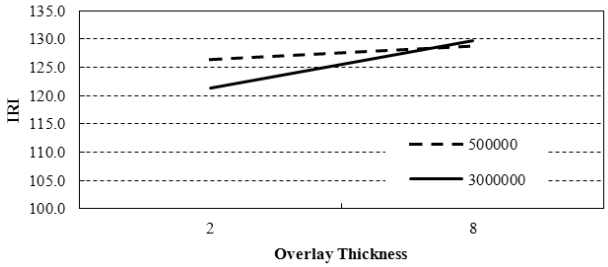

Figure A-58 Overlay thickness vs. existing modulus

ETH	OLTH	Mean	Std. Error	95% Confidence Interval	
				Lower Bound	Upper Bound
7	2	126.510	.153	126.210	126.810
	8	128.082	.153	127.782	128.382
11	2	121.209	.153	120.909	121.510
	8	130.484	.153	130.184	130.785

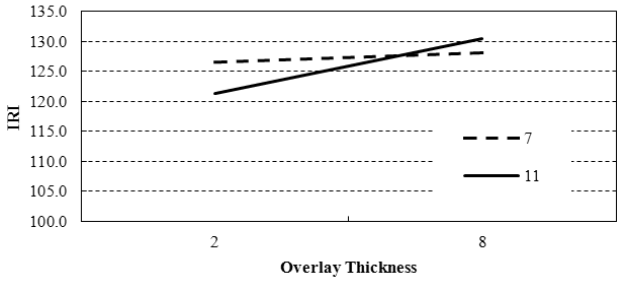

Figure A-59 Overlay thickness vs. existing modulus

A.2.3 Rubblized Overlays

Table A-13 Factorial matrix of ANOVA for rubblized

OLTH (in)	OLPG	OLGRAD	OLEB (%)	OLAV (%)	EPCCE (psi) /EPCCTH (in) /Climate							
					35000				1500000			
					7		11		7		11	
					Pellston	Detroit	Pellston	Detroit	Pellston	Detroit	Pellston	Detroit
2	PG 58-22	Coarse	7	5	1	2	3	4	5	6	7	8
				12	9	10	11	12	13	14	15	16
			14	5	17	18	19	20	21	22	23	24
				12	25	26	27	28	29	30	31	32
		Fine	7	5	33	34	35	36	37	38	39	40
				12	41	42	43	44	45	46	47	48
			14	5	49	50	51	52	53	54	55	56
				12	57	58	59	60	61	62	63	64
	PG 76-28	Coarse	7	5	65	66	67	68	69	70	71	72
				12	73	74	75	76	77	78	79	80
			14	5	81	82	83	84	85	86	87	88
				12	89	90	91	92	93	94	95	96
		Fine	7	5	97	98	99	100	101	102	103	104
				12	105	106	107	108	109	110	111	112
			14	5	113	114	115	116	117	118	119	120
				12	121	122	123	124	125	126	127	128
8	PG 58-22	Coarse	7	5	129	130	131	132	133	134	135	136
				12	137	138	139	140	141	142	143	144
			14	5	145	146	147	148	149	150	151	152
				12	153	154	155	156	157	158	159	160
		Fine	7	5	161	162	163	164	165	166	167	168
				12	169	170	171	172	173	174	175	176
			14	5	177	178	179	180	181	182	183	184
				12	185	186	187	188	189	190	191	192
	PG 76-28	Coarse	7	5	193	194	195	196	197	198	199	200
				12	201	202	203	204	205	206	207	208
			14	5	209	210	211	212	213	214	215	216
				12	217	218	219	220	221	222	223	224
		Fine	7	5	225	226	227	228	229	230	231	232
				12	233	234	235	236	237	238	239	240
			14	5	241	242	243	244	245	246	247	248
				12	249	250	251	252	253	254	255	256

A.2.3.1. Longitudinal cracking

Table A-14 ANOVA table for rubblized factorial matrix for longitudinal cracking

Source	Type III Sum of Squares	df	Mean Square	F	Sig.
Corrected Model	3969060054.148	36	110251668.171	36.716	.000
Intercept	3218734132.697	1	3218734132.697	1071.899	.000
OLTH	160276391.251	1	160276391.251	53.375	.000
OLPG	39788482.766	1	39788482.766	13.250	.000
OLAG	3535767.832	1	3535767.832	1.177	.279
OLEB	38336854.785	1	38336854.785	12.767	.000
OLAV	1966771158.536	1	1966771158.536	654.972	.000
EPCCE	1007816373.150	1	1007816373.150	335.622	.000
EPCCTH	9408068.571	1	9408068.571	3.133	.078
Climate	1827400.415	1	1827400.415	.609	.436
EPCCE * Climate	1625564.438	1	1625564.438	.541	.463
EPCCTH * Climate	24177.918	1	24177.918	.008	.929
OLAG * Climate	57.173	1	57.173	.000	.997
OLAV * Climate	1294108.164	1	1294108.164	.431	.512
OLEB * Climate	16168.076	1	16168.076	.005	.942
OLPG * Climate	249.996	1	249.996	.000	.993
OLTH * Climate	1834084.476	1	1834084.476	.611	.435
EPCCE * EPCCTH	27183136.925	1	27183136.925	9.052	.003
OLAG * EPCCE	7641637.833	1	7641637.833	2.545	.112
OLAV * EPCCE	381702916.485	1	381702916.485	127.114	.000
OLEB * EPCCE	9433106.361	1	9433106.361	3.141	.078
OLPG * EPCCE	16024399.295	1	16024399.295	5.336	.022
OLTH * EPCCE	50588278.596	1	50588278.596	16.847	.000
OLAG * EPCCTH	7281052.247	1	7281052.247	2.425	.121
OLAV * EPCCTH	8057053.865	1	8057053.865	2.683	.103
OLEB * EPCCTH	5445070.574	1	5445070.574	1.813	.180
OLPG * EPCCTH	9850449.024	1	9850449.024	3.280	.071
OLTH * EPCCTH	58460245.565	1	58460245.565	19.468	.000
OLAG * OLAV	445220.894	1	445220.894	.148	.701
OLAG * OLEB	20342.960	1	20342.960	.007	.934
OLPG * OLAG	15421.604	1	15421.604	.005	.943
OLTH * OLAG	1260834.230	1	1260834.230	.420	.518
OLEB * OLAV	1978182.474	1	1978182.474	.659	.418
OLPG * OLAV	5669262.193	1	5669262.193	1.888	.171
OLTH * OLAV	124133830.010	1	124133830.010	41.339	.000
OLPG * OLEB	494970.290	1	494970.290	.165	.685
OLTH * OLEB	20788.233	1	20788.233	.007	.934
OLTH * OLPG	20798946.944	1	20798946.944	6.926	.009
Error	657620703.126	219	3002834.261		
Total	7845414889.972	256			
Corrected Total	4626680757.274	255			

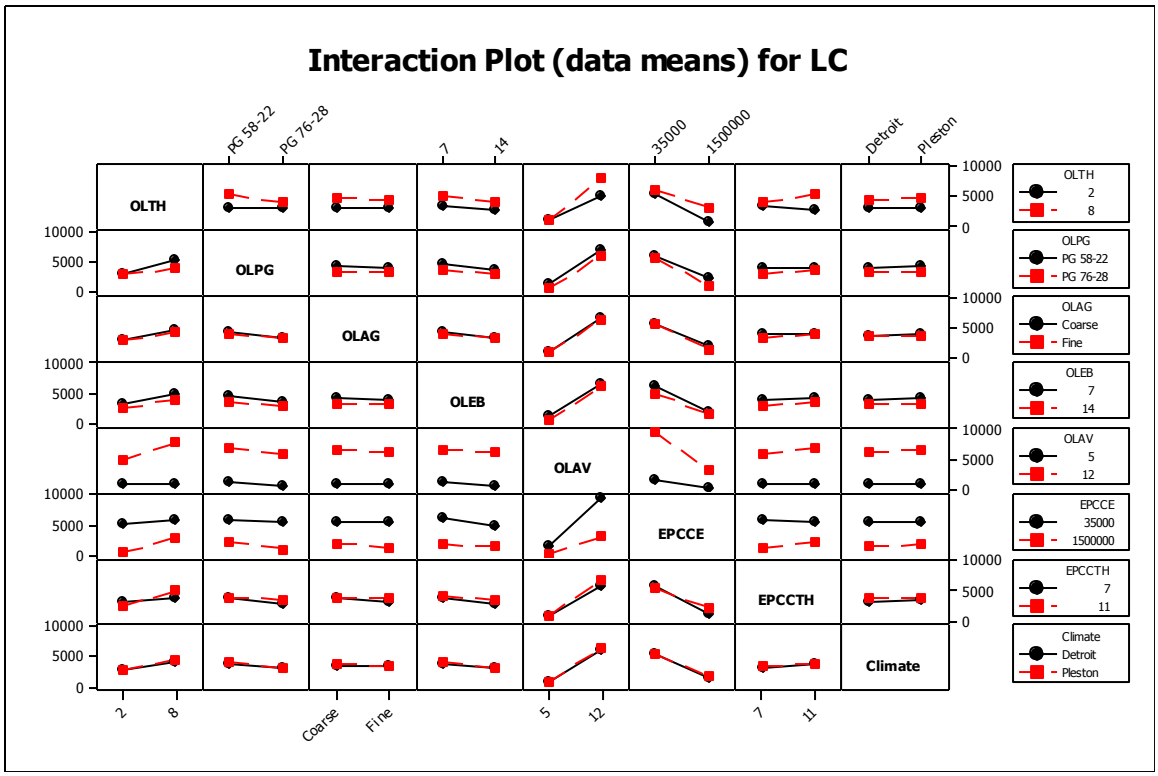

Figure A-60 Summary of interactions

EPCCE	OLAV	Mean	Std. Error	95% Confidence Interval	
				Lower Bound	Upper Bound
35000 psi	5 in	1537.15	216.609	1110.252	1964.060
	12 in	9522.84	216.609	9095.941	9949.750
1500000 psi	5	11.04	216.609	-415.861	437.947
	12	3112.42	216.609	2685.523	3539.332

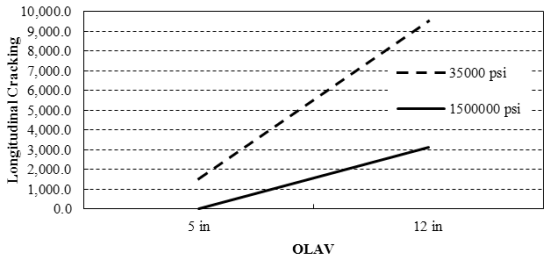

Figure A-61 Overlay air voids vs. existing modulus

EPCCE	OLPG	Mean	Std. Error	95% Confidence Interval	
				Lower Bound	Upper Bound
35000 psi	PG 58-22	5674.04	216.60	5247.14	6100.95
	PG 76-28	5385.95	216.60	4959.04	5812.85
1500000 psi	PG 58-22	2206.16	216.60	1779.26	2633.06
	PG 76-28	917.307	216.60	490.40	1344.21

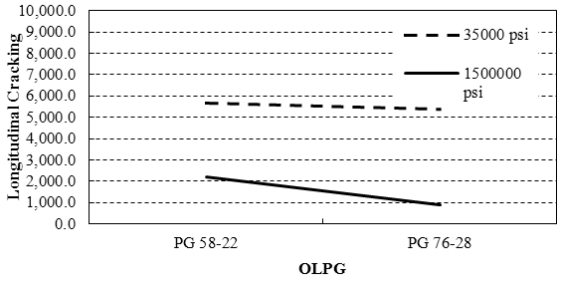

Figure A-62 Overlay PG vs. existing modulus

OLTH	Mean	Std. Error	95% Confidence Interval	
			Lower Bound	Upper Bound
2 in	5183.283	216.609	4756.379	5610.187
8 in	5876.719	216.609	5449.815	6303.623
2	325.949	216.609	-100.955	752.854
8	2797.521	216.609	2370.617	3224.425

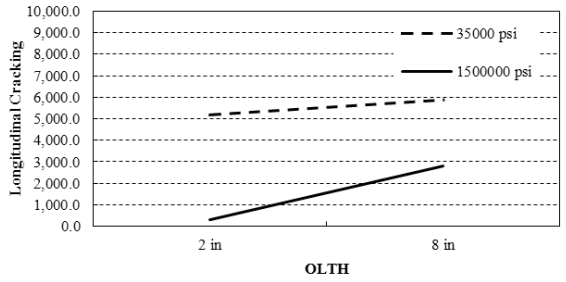

Figure A-63 Overlay thickness vs. existing modulus

OLTH	Mean	Std. Error	95% Confidence Interval	
			Lower Bound	Upper Bound
2 in	3040.783	216.609	2613.879	3467.687
8 in	3667.546	216.609	3240.642	4094.450
2	2468.449	216.609	2041.545	2895.353
8	5006.694	216.609	4579.790	5433.598

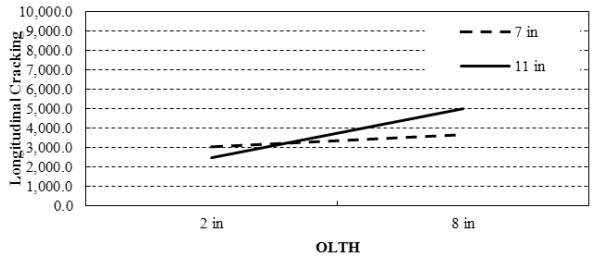

Figure A-64 Overlay thickness vs. existing thickness

A.2.3.2. Alligator cracking

Table A-15 ANOVA table for rubblized factorial matrix for alligator cracking

Source	Type III Sum of Squares	df	Mean Square	F	Sig.
Corrected Model	336962.881	36	9360.080	38.659	.000
Intercept	215796.244	1	215796.244	891.271	.000
OLTH	45357.821	1	45357.821	187.335	.000
OLPG	57.287	1	57.287	.237	.627
OLAG	15.698	1	15.698	.065	.799
OLEB	8815.965	1	8815.965	36.411	.000
OLAV	25024.145	1	25024.145	103.353	.000
EPCCE	193131.689	1	193131.689	797.663	.000
EPCCTH	912.331	1	912.331	3.768	.054
Climate	.030	1	.030	.000	.991
EPCCE * Climate	.032	1	.032	.000	.991
EPCCTH * Climate	.022	1	.022	.000	.992
OLAG * Climate	.000	1	.000	.000	1.000
OLAV * Climate	4.090	1	4.090	.017	.897
OLEB * Climate	1.558	1	1.558	.006	.936
OLPG * Climate	.927	1	.927	.004	.951
OLTH * Climate	9.831	1	9.831	.041	.840
EPCCE * EPCCTH	26.666	1	26.666	.110	.740
OLAG * EPCCE	441.140	1	441.140	1.822	.178
OLAV * EPCCE	17729.863	1	17729.863	73.227	.000
OLEB * EPCCE	4737.966	1	4737.966	19.569	.000
OLPG * EPCCE	302.937	1	302.937	1.251	.265
OLTH * EPCCE	35379.727	1	35379.727	146.124	.000
OLAG * EPCCTH	620.883	1	620.883	2.564	.111
OLAV * EPCCTH	631.254	1	631.254	2.607	.108
OLEB * EPCCTH	586.534	1	586.534	2.422	.121
OLPG * EPCCTH	619.772	1	619.772	2.560	.111
OLTH * EPCCTH	542.083	1	542.083	2.239	.136
OLAG * OLAV	.032	1	.032	.000	.991
OLAG * OLEB	.185	1	.185	.001	.978
OLPG * OLAG	.036	1	.036	.000	.990
OLTH * OLAG	2.174	1	2.174	.009	.925
OLEB * OLAV	215.269	1	215.269	.889	.347
OLPG * OLAV	4.754	1	4.754	.020	.889
OLTH * OLAV	1751.650	1	1751.650	7.235	.008
OLPG * OLEB	.347	1	.347	.001	.970
OLTH * OLEB	4.178	1	4.178	.017	.896
OLTH * OLPG	34.005	1	34.005	.140	.708
Error	53024.698	219	242.122		
Total	605783.823	256			
Corrected Total	389987.579	255			

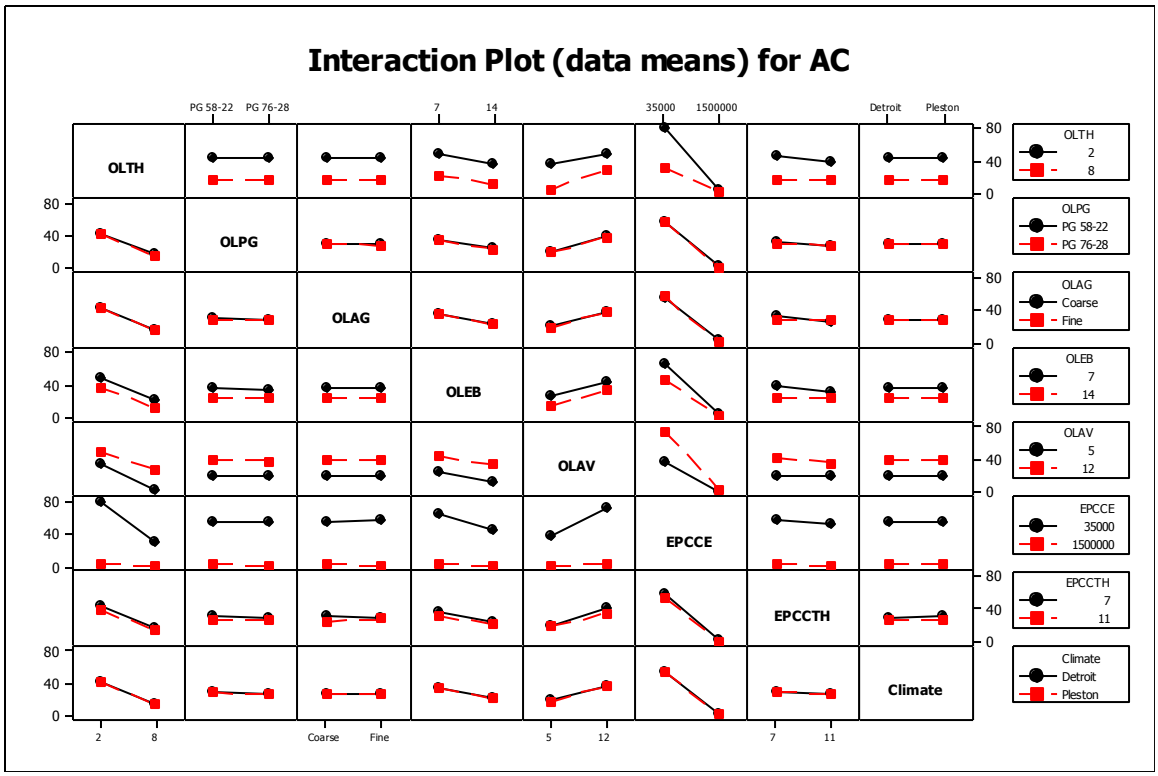

Figure A-65 Summary of interactions

OLAV	Mean	Std. Error	95% Confidence Interval	
			Lower Bound	Upper Bound
5%	38.291	1.945	34.458	42.125
12%	74.709	1.945	70.876	78.543
5	.002	1.945	-3.831	3.836
12	3.132	1.945	-.702	6.965

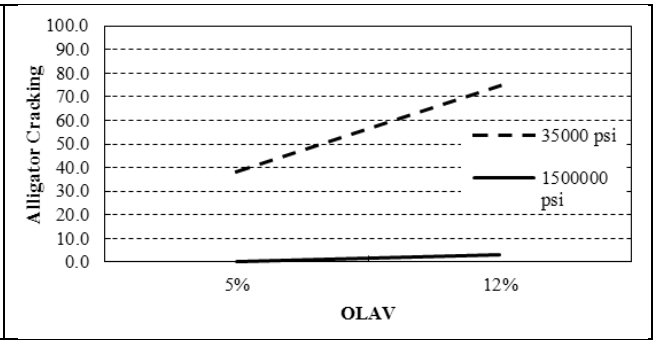

Figure A-66 Overlay air voids vs. Existing modulus

OLEB	Mean	Std. Error	95% Confidence Interval	
			Lower Bound	Upper Bound
7%	66.671	1.945	62.837	70.504
14%	46.330	1.945	42.497	50.163
7	3.133	1.945	-.700	6.967
14	.001	1.945	-3.833	3.834

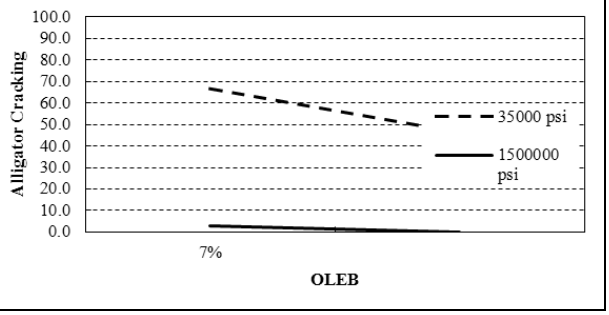

Figure A-67 Overlay effective binder vs. Existing modulus

OLTH	Mean	Std. Error	95% Confidence Interval	
			Lower Bound	Upper Bound
2 in	81.567	1.945	77.734	85.401
8 in	31.434	1.945	27.600	35.267
2	3.122	1.945	-.712	6.955
8	.012	1.945	-3.821	3.845

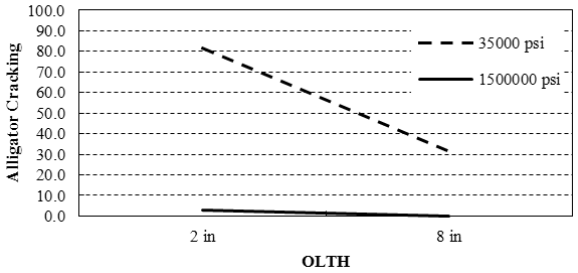

Figure A-68 Overlay thickness vs. Existing modulus

A.2.3.3. Rutting

Table A-16 ANOVA table for rubblized factorial matrix for rutting

Source	Type III Sum of Squares	df	Mean Square	F	Sig.
Corrected Model	41.595	36	1.155	169.152	.000
Intercept	509.137	1	509.137	74537.123	.000
OLTH	.014	1	.014	2.075	.151
OLPG	4.230	1	4.230	619.262	.000
OLAG	.258	1	.258	37.808	.000
OLEB	3.905	1	3.905	571.662	.000
OLAV	12.341	1	12.341	1806.670	.000
EPCCE	4.036	1	4.036	590.915	.000
EPCCTH	.123	1	.123	17.979	.000
Climate	.406	1	.406	59.462	.000
EPCCE * Climate	.001	1	.001	.108	.743
EPCCTH * Climate	.001	1	.001	.118	.731
OLAG * Climate	.000	1	.000	.014	.904
OLAV * Climate	.013	1	.013	1.834	.177
OLEB * Climate	.004	1	.004	.615	.434
OLPG * Climate	.001	1	.001	.171	.680
OLTH * Climate	.001	1	.001	.123	.727
EPCCE * EPCCTH	.149	1	.149	21.806	.000
OLAG * EPCCE	.060	1	.060	8.774	.003
OLAV * EPCCE	1.217	1	1.217	178.211	.000
OLEB * EPCCE	.185	1	.185	27.061	.000
OLPG * EPCCE	.398	1	.398	58.210	.000
OLTH * EPCCE	9.461	1	9.461	1385.025	.000
OLAG * EPCCTH	.009	1	.009	1.282	.259
OLAV * EPCCTH	.000	1	.000	.044	.834
OLEB * EPCCTH	.024	1	.024	3.441	.065
OLPG * EPCCTH	.003	1	.003	.456	.500
OLTH * EPCCTH	.107	1	.107	15.696	.000
OLAG * OLAV	.019	1	.019	2.852	.093
OLAG * OLEB	.004	1	.004	.571	.451
OLPG * OLAG	.004	1	.004	.658	.418
OLTH * OLAG	.044	1	.044	6.475	.012
OLEB * OLAV	.367	1	.367	53.796	.000
OLPG * OLAV	.274	1	.274	40.054	.000
OLTH * OLAV	2.336	1	2.336	341.950	.000
OLPG * OLEB	.077	1	.077	11.309	.001
OLTH * OLEB	.687	1	.687	100.536	.000
OLTH * OLPG	.836	1	.836	122.452	.000
Error	1.496	219	.007		
Total	552.228	256			
Corrected Total	43.091	255			

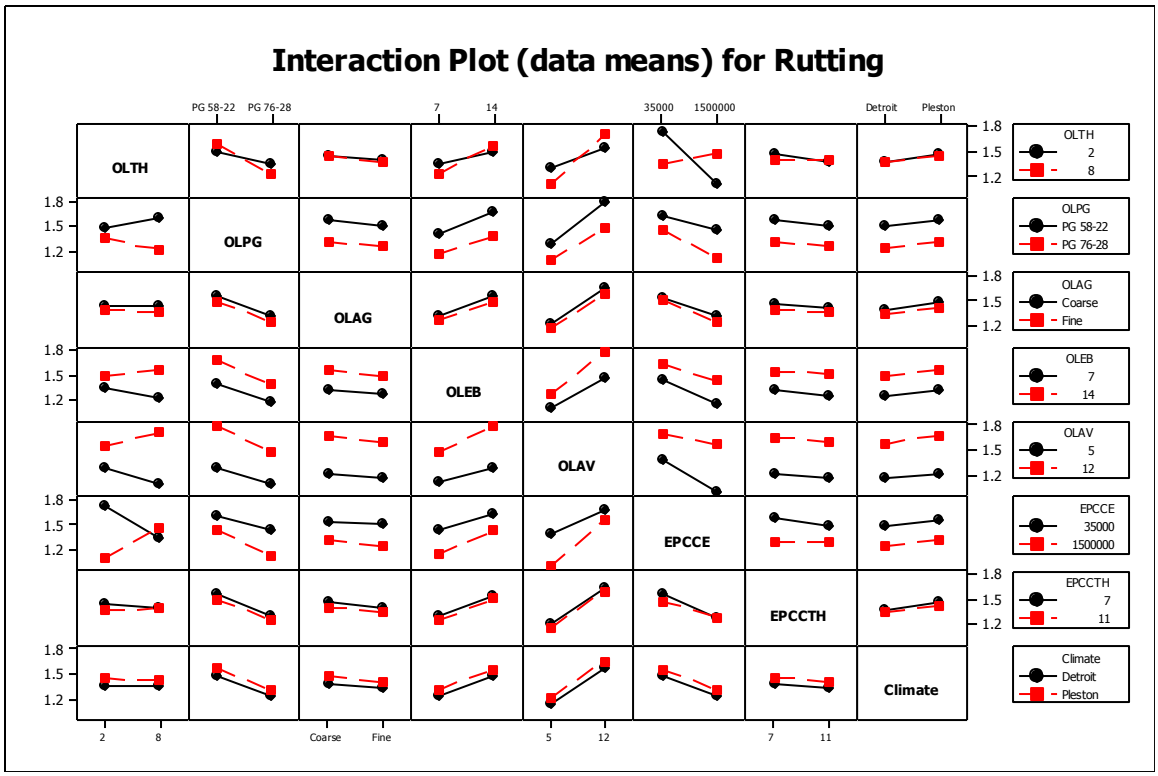

Figure A-69 Summary of interactions

OLAG	Mean	Std. Error	95% Confidence Interval	
			Lower Bound	Upper Bound
Coarse	1.552	.010	1.532	1.573
Fine	1.519	.010	1.499	1.540
Coarse	1.332	.010	1.311	1.352
Fine	1.238	.010	1.217	1.258

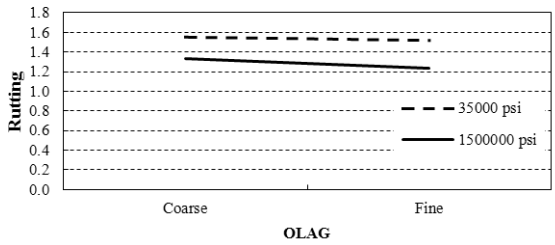

Figure A-70 Overlay aggregate gradation vs. existing modulus

OLAV	Mean	Std. Error	95% Confidence Interval	
			Lower Bound	Upper Bound
5%	1.385	.010	1.365	1.406
12%	1.686	.010	1.666	1.707
5	.996	.010	.976	1.017
12	1.573	.010	1.553	1.594

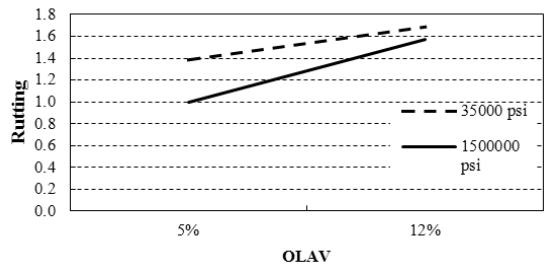

Figure A-71 Overlay air voids vs. existing modulus

OLEB	Mean	Std. Error	95% Confidence Interval	
			Lower Bound	Upper Bound
7%	1.439	.010	1.419	1.460
14%	1.632	.010	1.612	1.653
7	1.134	.010	1.114	1.155
14	1.435	.010	1.415	1.455

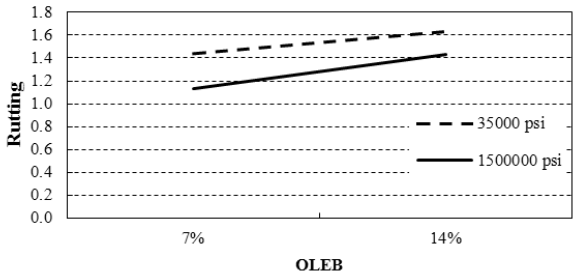

Figure A-72 Overlay effective binder vs. existing modulus

OLPG	Mean	Std. Error	95% Confidence Interval	
			Lower Bound	Upper Bound
PG 58-22	1.625	.010	1.605	1.645
PG 76-28	1.447	.010	1.426	1.467
PG 58-22	1.453	.010	1.432	1.473
PG 76-28	1.117	.010	1.096	1.137

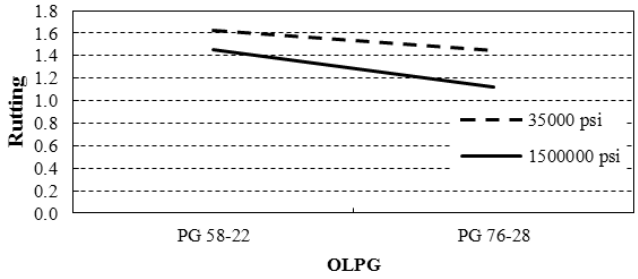

Figure A-73 Overlay PG vs. existing modulus

OLTH	Mean	Std. Error	95% Confidence Interval	
			Lower Bound	Upper Bound
2 in	1.460	.010	1.440	1.480
8 in	1.404	.010	1.384	1.425
2	1.375	.010	1.355	1.396
8	1.401	.010	1.381	1.422

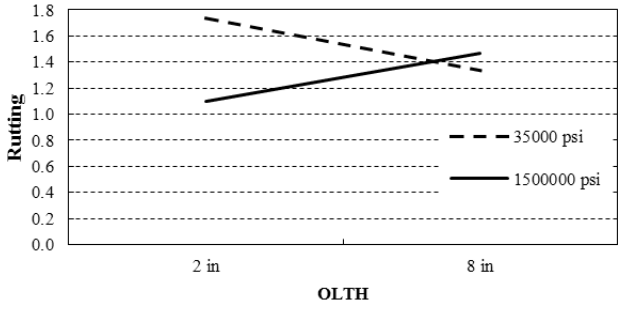

Figure A-74 Overlay thickness vs. existing modulus

A.2.3.4. IRI

Table A-17 ANOVA table for rubblized factorial matrix for IRI

Source	Type III Sum of Squares	df	Mean Square	F	Sig.
Corrected Model	64495565.173	36	1791543.477	11.942	.000
Intercept	33102546.494	1	33102546.494	220.657	.000
OLTH	9196397.409	1	9196397.409	61.302	.000
OLPG	14657.642	1	14657.642	.098	.755
OLAG	6216.337	1	6216.337	.041	.839
OLEB	5153609.399	1	5153609.399	34.353	.000
OLAV	9128971.263	1	9128971.263	60.852	.000
EPCCE	7674943.011	1	7674943.011	51.160	.000
EPCCTH	544616.325	1	544616.325	3.630	.058
Climate	2267.545	1	2267.545	.015	.902
EPCCE * Climate	3979.244	1	3979.244	.027	.871
EPCCTH * Climate	1095.196	1	1095.196	.007	.932
OLAG * Climate	3.353	1	3.353	.000	.996
OLAV * Climate	4379.958	1	4379.958	.029	.864
OLEB * Climate	3551.415	1	3551.415	.024	.878
OLPG * Climate	486.478	1	486.478	.003	.955
OLTH * Climate	8058.428	1	8058.428	.054	.817
EPCCE * EPCCTH	11415.587	1	11415.587	.076	.783
OLAG * EPCCE	340698.394	1	340698.394	2.271	.133
OLAV * EPCCE	4858525.193	1	4858525.193	32.386	.000
OLEB * EPCCE	3006127.458	1	3006127.458	20.038	.000
OLPG * EPCCE	382998.530	1	382998.530	2.553	.112
OLTH * EPCCE	6342433.000	1	6342433.000	42.278	.000
OLAG * EPCCTH	404201.903	1	404201.903	2.694	.102
OLAV * EPCCTH	503168.556	1	503168.556	3.354	.068
OLEB * EPCCTH	499893.188	1	499893.188	3.332	.069
OLPG * EPCCTH	401852.982	1	401852.982	2.679	.103
OLTH * EPCCTH	517437.447	1	517437.447	3.449	.065
OLAG * OLAV	2809.663	1	2809.663	.019	.891
OLAG * OLEB	1880.848	1	1880.848	.013	.911
OLPG * OLAG	.553	1	.553	.000	.998
OLTH * OLAG	1308.178	1	1308.178	.009	.926
OLEB * OLAV	4153826.134	1	4153826.134	27.689	.000
OLPG * OLAV	2360.138	1	2360.138	.016	.900
OLTH * OLAV	6512799.700	1	6512799.700	43.413	.000
OLPG * OLEB	491.453	1	491.453	.003	.954
OLTH * OLEB	4807083.656	1	4807083.656	32.043	.000
OLTH * OLPG	1019.605	1	1019.605	.007	.934
Error	32853973.263	219	150018.143		
Total	130452084.930	256			
Corrected Total	97349538.436	255			

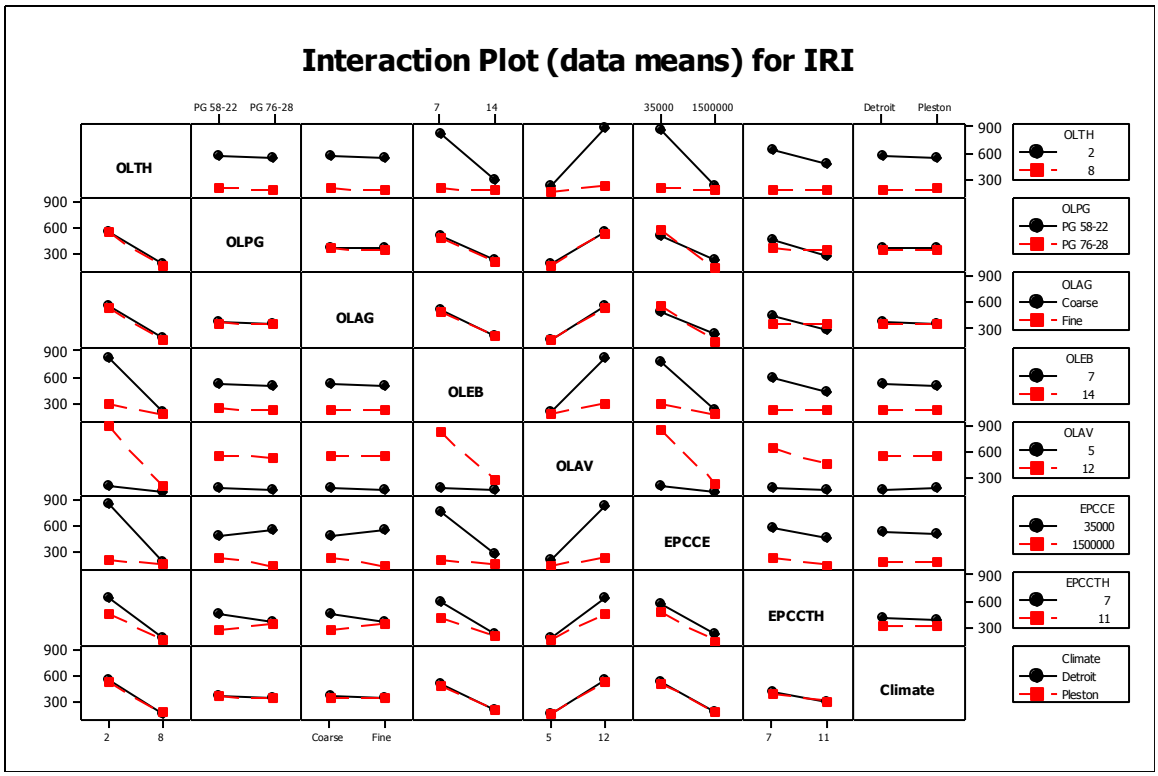

Figure A-75 Summary of interactions

EPCCE	OLAV	Mean	Std. Error	95% Confidence Interval	
				Lower Bound	Upper Bound
35000 psi	5%	206.139	48.415	110.72	301.558
	12%	859.342	48.415	763.92	954.762
1500000 psi	5	135.369	48.415	39.949	230.788
	12	237.520	48.415	142.10	332.940

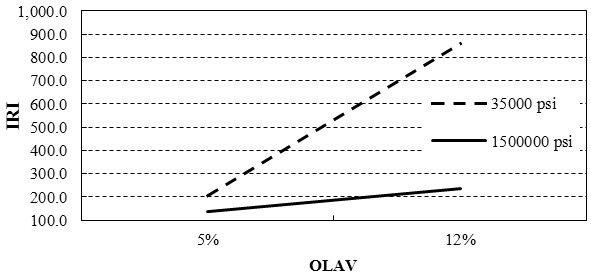

Figure A-76 Overlay air voids vs. existing modulus

EPCCE	OLEB	Mean	Std. Error	95% Confidence Interval	
				Lower Bound	Upper Bound
35000	7	782.989	48.415	687.570	878.408
	14	282.492	48.415	187.073	377.912
1500000	7	219.966	48.415	124.546	315.385
	14	152.923	48.415	57.504	248.343

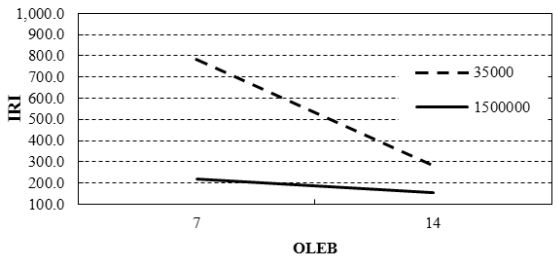

Figure A-77 Overlay effective binder vs. existing modulus

EPCCE	OLTH	Mean	Std. Error	95% Confidence Interval	
				Lower Bound	Upper Bound
35000 psi	2 in	879.677	48.415	784.257	975.096
	8 in	185.805	48.415	90.385	281.224
1500000 psi	2	218.578	48.415	123.159	313.998
	8	154.311	48.415	58.892	249.730

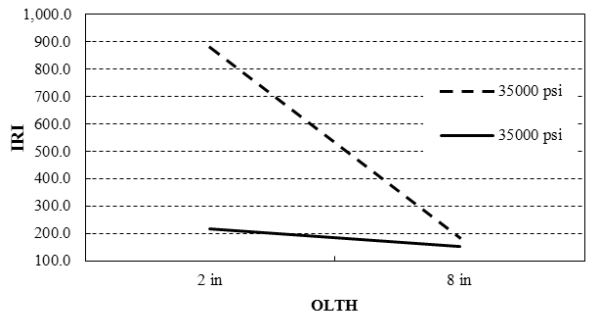

Figure A-78 Overlay thickness vs. existing modulus

A.2.4 Unbonded Overlay

Table A-18 Factorial matrix of ANOVA for unbonded overlay

Overlay PCC Thickness (in)	Overlay PCC CTE	Overlay Joint Spacing (ft)	Overlay PCC MOR (psi)	Subgrade Modulus (psi/in)	Existing PCC Thickness (in) / Existing PCC MOR (psi) / Climate							
					7				11			
					500000		3000000		500000		3000000	
					Pellston	Detroit	Pellston	Detroit	Pellston	Detroit	Pellston	Detroit
7	4	10	450	50	1	2	3	4	5	6	7	8
				300	9	10	11	12	13	14	15	16
			800	50	17	18	19	20	21	22	23	24
				300	25	26	27	28	29	30	31	32
		15	450	50	33	34	35	36	37	38	39	40
				300	41	42	43	44	45	46	47	48
			800	50	49	50	51	52	53	54	55	56
				300	57	58	59	60	61	62	63	64
	7	10	450	50	65	66	67	68	69	70	71	72
				300	73	74	75	76	77	78	79	80
			800	50	81	82	83	84	85	86	87	88
				300	89	90	91	92	93	94	95	96
		15	450	50	97	98	99	100	101	102	103	104
				300	105	106	107	108	109	110	111	112
			800	50	113	114	115	116	117	118	119	120
				300	121	122	123	124	125	126	127	128
9	4	10	450	50	129	130	131	132	133	134	135	136
				300	137	138	139	140	141	142	143	144
			800	50	145	146	147	148	149	150	151	152
				300	153	154	155	156	157	158	159	160
		15	450	50	161	162	163	164	165	166	167	168
				300	169	170	171	172	173	174	175	176
			800	50	177	178	179	180	181	182	183	184
				300	185	186	187	188	189	190	191	192
	7	10	450	50	193	194	195	196	197	198	199	200
				300	201	202	203	204	205	206	207	208
			800	50	209	210	211	212	213	214	215	216
				300	217	218	219	220	221	222	223	224
		15	450	50	225	226	227	228	229	230	231	232
				300	233	234	235	236	237	238	239	240
			800	50	241	242	243	244	245	246	247	248
				300	249	250	251	252	253	254	255	256

A.2.4.1. Cracking

Table A-19 ANOVA table for unbonded overlay factorial matrix for cracking

Source	Type III Sum of Squares	df	Mean Square	F	Sig.
Corrected Model	277700.595	36	7713.905	34.692	.000
Intercept	150597.355	1	150597.355	677.278	.000
OLTH	41817.694	1	41817.694	188.066	.000
OLCTE	23872.181	1	23872.181	107.360	.000
OLJS	29538.867	1	29538.867	132.845	.000
OLMOR	75072.575	1	75072.575	337.622	.000
SGMOD	11322.290	1	11322.290	50.920	.000
EXTH	1457.808	1	1457.808	6.556	.011
EXMOD	17640.820	1	17640.820	79.336	.000
CL	7029.774	1	7029.774	31.615	.000
EXMOD * CL	21.103	1	21.103	.095	.758
EXTH * CL	.110	1	.110	.000	.982
OLCTE * CL	2309.403	1	2309.403	10.386	.001
OLJS * CL	2750.347	1	2750.347	12.369	.001
OLMOR * CL	619.699	1	619.699	2.787	.096
OLTH * CL	402.755	1	402.755	1.811	.180
SGMOD * CL	206.461	1	206.461	.929	.336
EXTH * EXMOD	1006.079	1	1006.079	4.525	.035
OLCTE * EXMOD	63.103	1	63.103	.284	.595
OLJS * EXMOD	71.720	1	71.720	.323	.571
OLMOR * EXMOD	8193.644	1	8193.644	36.849	.000
OLTH * EXMOD	6208.455	1	6208.455	27.921	.000
SGMOD * EXMOD	1107.642	1	1107.642	4.981	.027
OLCTE * EXTH	41.522	1	41.522	.187	.666
OLJS * EXTH	3.827	1	3.827	.017	.896
OLMOR * EXTH	891.396	1	891.396	4.009	.046
OLTH * EXTH	706.563	1	706.563	3.178	.076
SGMOD * EXTH	349.456	1	349.456	1.572	.211
OLCTE * OLJS	9708.407	1	9708.407	43.661	.000
OLCTE * OLMOR	6178.943	1	6178.943	27.788	.000
OLTH * OLCTE	1806.781	1	1806.781	8.126	.005
OLCTE * SGMOD	2066.271	1	2066.271	9.293	.003
OLJS * OLMOR	6032.435	1	6032.435	27.130	.000
OLTH * OLJS	1106.810	1	1106.810	4.978	.027
OLJS * SGMOD	7.528	1	7.528	.034	.854
OLTH * OLMOR	8320.860	1	8320.860	37.421	.000
OLMOR * SGMOD	5667.267	1	5667.267	25.487	.000
OLTH * SGMOD	4100.001	1	4100.001	18.439	.000
Error	48696.100	219	222.357		
Total	476994.050	256			
Corrected Total	326396.695	255			

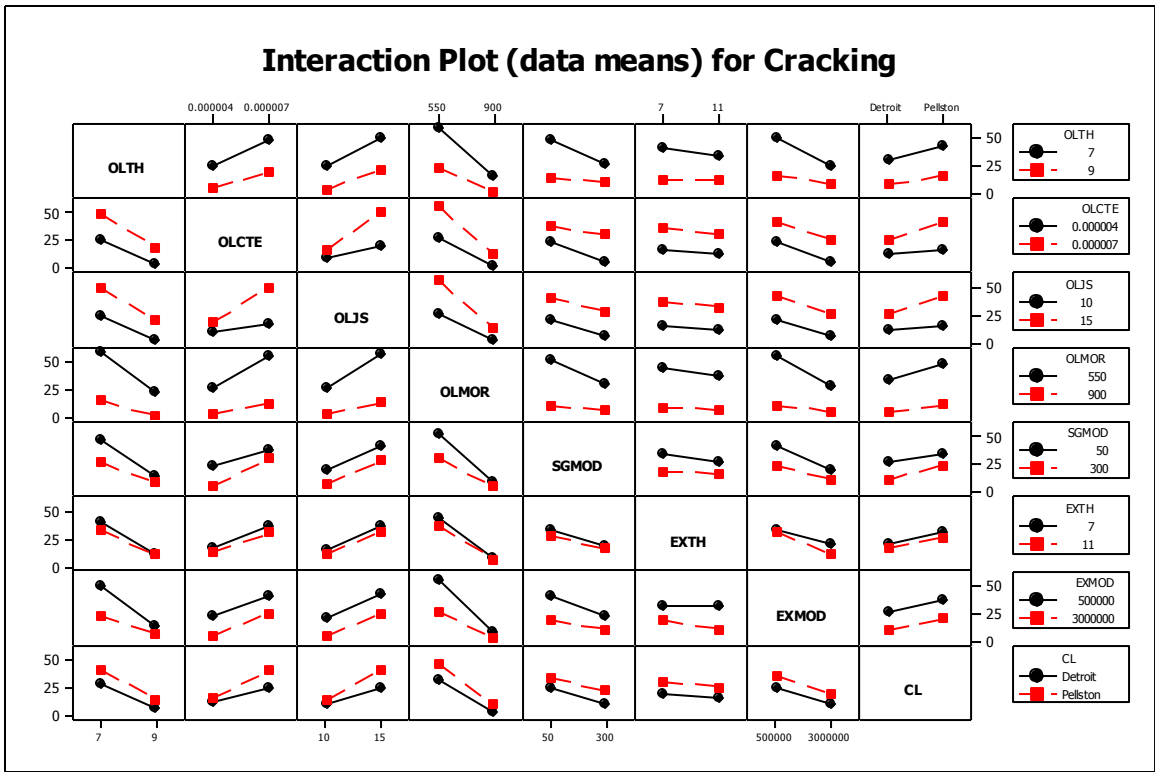

Figure A-79 Summary of Interactions

EXMOD	OLMOR	Mean	Std. Error	95% Confidence Interval	
				Lower Bound	Upper Bound
500,000 psi	550 psi	55.338	1.864	51.664	59.011
	900 psi	9.773	1.864	6.100	13.447
3,000,000 psi	550 psi	27.420	1.864	23.747	31.094
	900 psi	4.486	1.864	.812	8.160

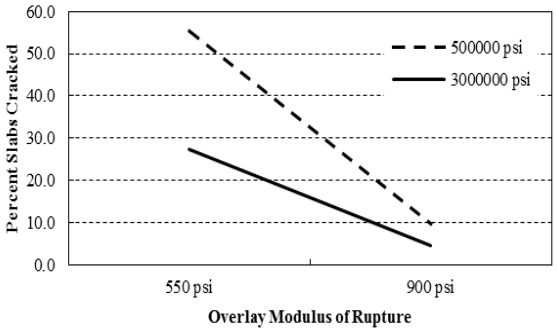

Figure A-80 Existing elastic modulus vs. overlay modulus of rupture

EXMOD	OLTH	Mean	Std. Error	95% Confidence Interval	
				Lower Bound	Upper Bound
500,000 psi	7 in	50.261	1.864	46.587	53.935
	9 in	14.850	1.864	11.176	18.524
3,000,000 psi	7 in	23.809	1.864	20.136	27.483
	9 in	8.097	1.864	4.423	11.770

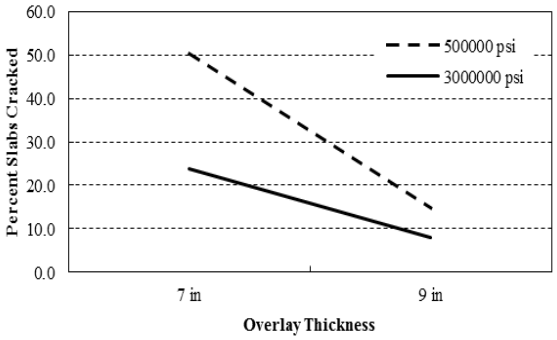

Figure A-81 Existing elastic modulus vs. overlay thickness

EXTH	OLMOR	Mean	Std. Error	95% Confidence Interval	
				Lower Bound	Upper Bound
7 in	550 psi	45.631	1.864	41.958	49.305
	900 psi	7.650	1.864	3.976	11.324
11 in	550 psi	37.127	1.864	33.453	40.800
	900 psi	6.609	1.864	2.936	10.283

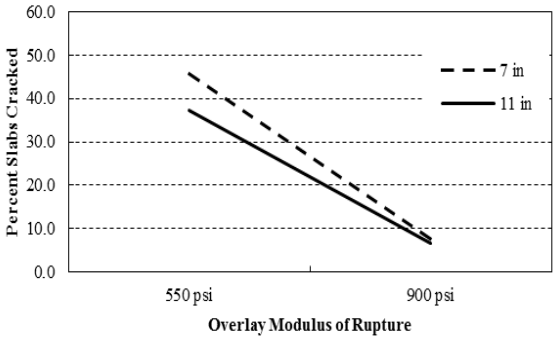

Figure A-82 Existing thickness vs. overlay modulus of rupture

SGMOD	OLCTE	Mean	Std. Error	95% Confidence Interval	
				Lower Bound	Upper Bound
50	4	24.089	1.864	20.415	27.763
	7	37.720	1.864	1.433	8.780
300	4	5.106	1.864	34.047	41.394
	7	30.102	1.864	26.428	33.775

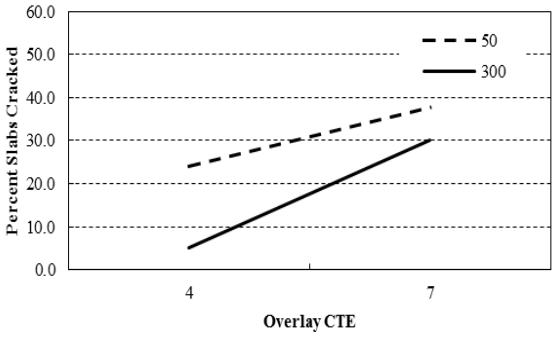

Figure A-83 Modulus of subgrade reaction vs. overlay CTE

SG MOD	OL MOR	Mean	Std. Error	95% Confidence Interval	
				Lower Bound	Upper Bound
50 psi/in	550 psi	52.734	1.864	49.061	56.408
	900 psi	9.075	1.864	26.350	33.697
300 psi/in	550 psi	30.023	1.864	5.401	12.749
	900 psi	5.184	1.864	1.511	8.858

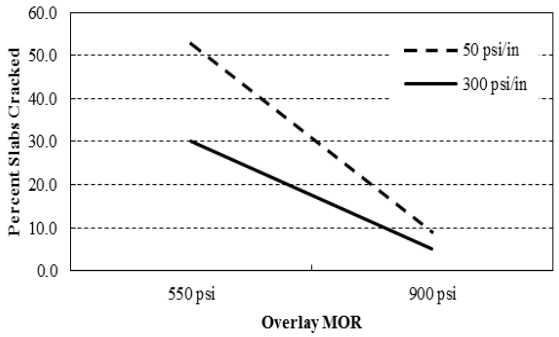

Figure A-84 Modulus of subgrade reaction vs. overlay modulus of rupture

SGMOD	OLTH	Mean	Std. Error	95% Confidence Interval	
				Lower Bound	Upper Bound
50 psi/in	7 in	47.688	1.864	44.014	51.361
	9 in	14.122	1.864	22.709	30.056
300 psi/in	7 in	26.383	1.864	10.448	17.795
	9 in	8.825	1.864	5.151	12.499

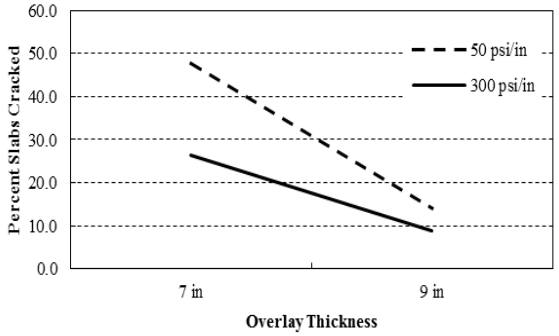

Figure A-85 Modulus of subgrade reaction vs. overlay thickness

A.2.4.2. Faulting

Table A-20 ANOVA table for unbonded overlay factorial matrix for faulting

Source	Type III Sum of Squares	df	Mean Square	F	Sig.
Corrected Model	.938	36	.026	156.797	.000
Intercept	1.746	1	1.746	10511.664	.000
OLTH	.182	1	.182	1095.751	.000
OLCTE	.462	1	.462	2782.771	.000
OLJS	.055	1	.055	333.534	.000
OLMOR	.013	1	.013	77.044	.000
SGMOD	.021	1	.021	123.756	.000
EXTH	.045	1	.045	268.984	.000
EXMOD	.049	1	.049	292.709	.000
CL	.000	1	.000	.003	.954
EXMOD * CL	.000	1	.000	.680	.411
EXTH * CL	.000	1	.000	.054	.816
OLCTE * CL	.000	1	.000	2.592	.109
OLJS * CL	.000	1	.000	2.348	.127
OLMOR * CL	.000	1	.000	.009	.923
OLTH * CL	.000	1	.000	.461	.498
SGMOD * CL	.000	1	.000	2.173	.142
EXTH * EXMOD	.006	1	.006	35.694	.000
OLCTE * EXMOD	.020	1	.020	120.115	.000
OLJS * EXMOD	.003	1	.003	15.353	.000
OLMOR * EXMOD	.000	1	.000	.074	.786
OLTH * EXMOD	.009	1	.009	51.790	.000
SGMOD * EXMOD	.001	1	.001	7.375	.007
OLCTE * EXTH	.014	1	.014	87.235	.000
OLJS * EXTH	.002	1	.002	11.855	.001
OLMOR * EXTH	.000	1	.000	.027	.869
OLTH * EXTH	.006	1	.006	36.276	.000
SGMOD * EXTH	.000	1	.000	1.244	.266
OLCTE * OLJS	.013	1	.013	75.350	.000
OLCTE * OLMOR	.003	1	.003	19.474	.000
OLTH * OLCTE	.022	1	.022	131.202	.000
OLCTE * SGMOD	.003	1	.003	16.045	.000
OLJS * OLMOR	.002	1	.002	11.855	.001
OLTH * OLJS	.001	1	.001	5.195	.024
OLJS * SGMOD	.000	1	.000	.041	.839
OLTH * OLMOR	.002	1	.002	12.670	.000
OLMOR * SGMOD	.003	1	.003	16.357	.000
OLTH * SGMOD	.001	1	.001	6.606	.011
Error	.036	219	.000		
Total	2.720	256			
Corrected Total	.974	255			

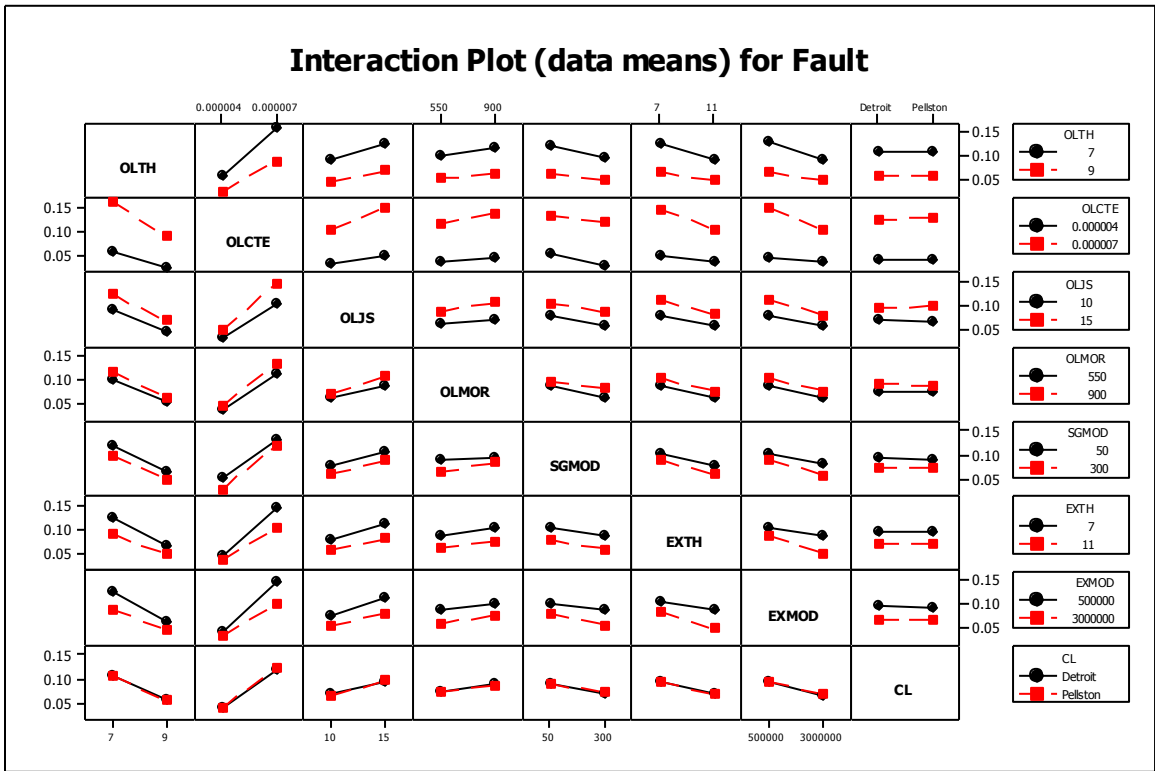

Figure A-86 Summary of interactions

A.2.4.3. IRI

Table A-21 ANOVA table for unbonded overlay factorial matrix for IRI

Source	Type III Sum of Squares	df	Mean Square	F	Sig.
Corrected Model	433282.321	36	12035.620	55.780	.000
Intercept	3113323.428	1	3113323.428	14428.986	.000
OLTH	105558.638	1	105558.638	489.221	.000
OLCTE	157444.661	1	157444.661	729.692	.000
OLJS	6367.561	1	6367.561	29.511	.000
OLMOR	18610.028	1	18610.028	86.250	.000
SGMOD	15975.781	1	15975.781	74.041	.000
EXTH	17307.301	1	17307.301	80.212	.000
EXMOD	33813.001	1	33813.001	156.709	.000
CL	22716.461	1	22716.461	105.282	.000
EXMOD * CL	1.015	1	1.015	.005	.945
EXTH * CL	517.615	1	517.615	2.399	.125
OLCTE * CL	2072.070	1	2072.070	9.603	.003
OLJS * CL	1547.070	1	1547.070	7.170	.009
OLMOR * CL	512.000	1	512.000	2.373	.127
OLTH * CL	444.020	1	444.020	2.058	.155
SGMOD * CL	316.890	1	316.890	1.469	.229
EXTH * EXMOD	1199.275	1	1199.275	5.558	.021
OLCTE * EXMOD	4079.303	1	4079.303	18.906	.000
OLJS * EXMOD	1.088	1	1.088	.005	.944
OLMOR * EXMOD	2726.911	1	2726.911	12.638	.001
OLTH * EXMOD	9241.201	1	9241.201	42.829	.000
SGMOD * EXMOD	17.553	1	17.553	.081	.776
OLCTE * EXTH	3936.063	1	3936.063	18.242	.000
OLJS * EXTH	22.950	1	22.950	.106	.745
OLMOR * EXTH	317.520	1	317.520	1.472	.228
OLTH * EXTH	4324.500	1	4324.500	20.042	.000
SGMOD * EXTH	1.088	1	1.088	.005	.944
OLCTE * OLJS	1819.553	1	1819.553	8.433	.005
OLCTE * OLMOR	205.031	1	205.031	.950	.332
OLTH * OLCTE	9072.045	1	9072.045	42.045	.000
OLCTE * SGMOD	2375.328	1	2375.328	11.009	.001
OLJS * OLMOR	1474.245	1	1474.245	6.833	.010
OLTH * OLJS	174.845	1	174.845	.810	.370
OLJS * SGMOD	79.695	1	79.695	.369	.545
OLTH * OLMOR	1103.325	1	1103.325	5.113	.026
OLMOR * SGMOD	5253.125	1	5253.125	24.346	.000
OLTH * SGMOD	2653.561	1	2653.561	12.298	.001
Error	19634.952	91	215.769		
Total	3566240.700	128			
Corrected Total	452917.272	127			

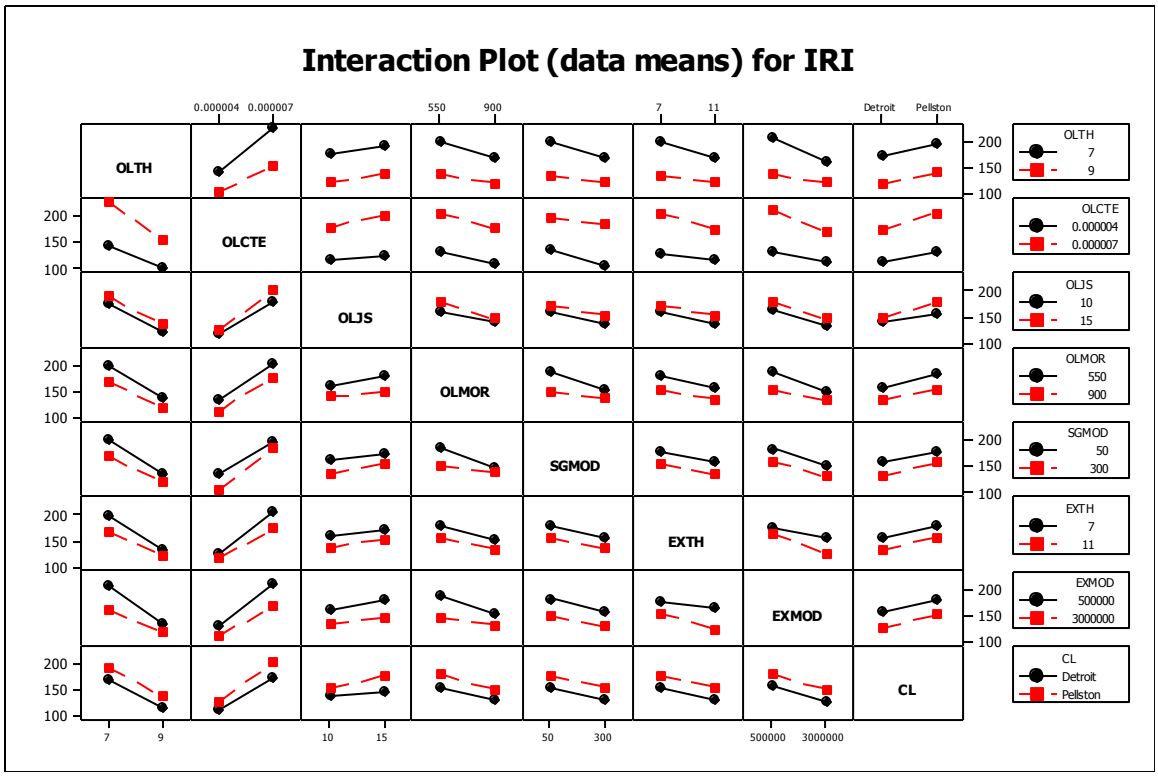

Figure A-87 Summary of interactions

EXMOD	OLCTE	Mean	Std. Error	95% Confidence Interval	
				Lower Bound	Upper Bound
500000 psi	4 CTE	131.41	2.00	127.461	135.355
	7 CTE	211.05	2.00	207.108	215.002
3000000 psi	4	110.81	2.00	106.859	114.753
	7	170.25	2.00	166.303	174.197

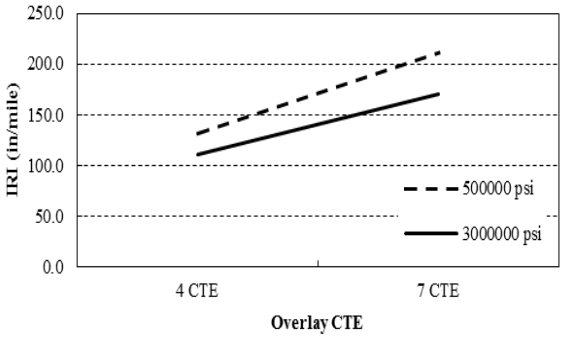

Figure A-88 Overlay CTE vs. existing elastic modulus

EXMOD	OLMOR	Mean	Std. Error	95% Confidence Interval	
				Lower Bound	Upper Bound
500000 psi	550 psi	188.95	2.00	185.002	192.895
	900 psi	153.51	2.00	149.567	157.461
3000000 psi	550	148.32	2.00	144.375	152.269
	900	132.73	2.00	128.787	136.681

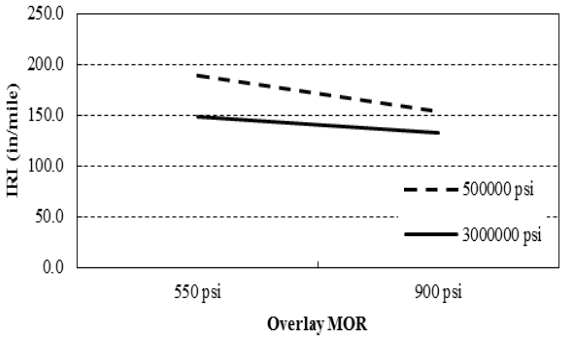

Figure A-89 Overlay MOR vs. existing elastic modulus

EXMOD	OLTH	Mean	Std. Error	95% Confidence Interval	
				Lower Bound	Upper Bound
500000 psi	7 in	207.40	2.00	203.450	211.344
	9 in	135.07	2.00	131.119	139.013
3000000 psi	7	161.44	2.00	157.492	165.386
	9	119.62	2.00	115.670	123.564

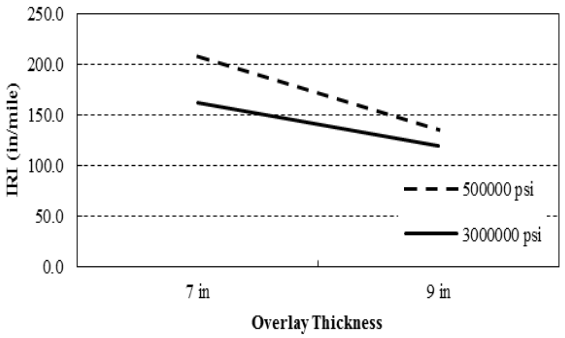

Figure A-90 Overlay thickness vs. existing elastic modulus

EXTH	OLCTE	Mean	Std. Error	95% Confidence Interval	
				Lower Bound	Upper Bound
7 in	4	126.30	2.00	122.358	130.252
	7	206.07	2.00	202.119	210.013
11 in	4	115.91	2.00	111.962	119.856
	7	175.24	2.00	171.292	179.186

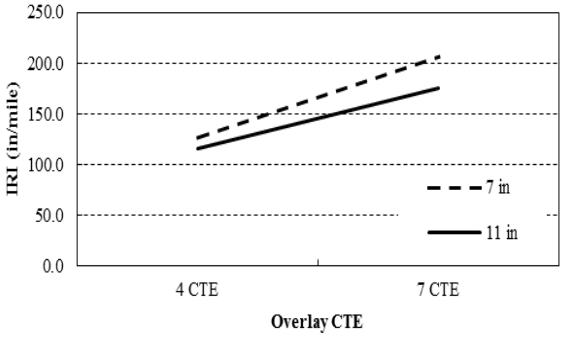

Figure A-91 Overlay CTE vs. existing thickness

EXTH	OLTH	Mean	Std. Error	95% Confidence Interval	
				Lower Bound	Upper Bound
7 in	7 in	199.22	2.00	195.277	203.170
	9 in	133.15	2.00	129.200	137.094
11 in	7	169.61	2.00	165.666	173.559
	9	121.54	2.00	117.589	125.483

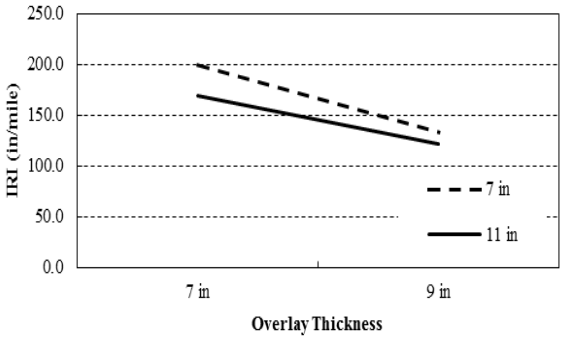

Figure A-92 Overlay thickness vs. existing thickness

OLCTE	SGMOD	Mean	Std. Error	95% Confidence Interval	
				Lower Bound	Upper Bound
4 CTE	50 psi/in	136.96	2.00	133.012	140.906
	300 psi/in	105.25	2.00	101.308	109.202
7 CTE	50	197.69	2.00	193.745	201.639
	300	183.61	2.00	179.666	187.559

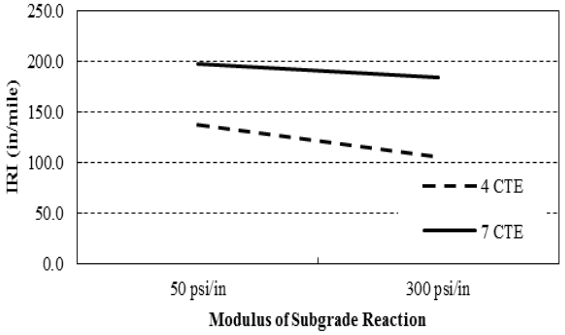

Figure A-93 Overlay CTE vs. modulus of subgrade reaction

OLMOR	SGMOD	Mean	Std. Error	95% Confidence Interval	
				Lower Bound	Upper Bound
550 psi	50 psi/in	186.11	2.00	182.167	190.061
	300 psi/in	151.16	2.00	147.209	155.103
900 psi	50	148.54	2.00	144.591	152.484
	300	137.71	2.00	133.764	141.658

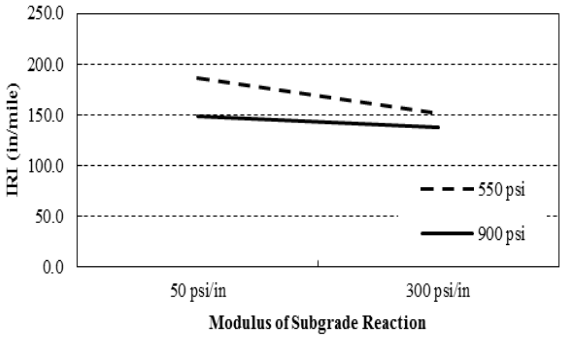

Figure A-94 Overlay MOR vs. modulus of subgrade reaction

OLTH	SGMOD	Mean	Std. Error	95% Confidence Interval	
				Lower Bound	Upper Bound
7 in	50 psi/in	200.65	2.00	196.698	204.592
	300 psi/in	168.19	2.00	164.244	172.138
9 in	50	134.01	2.00	130.059	137.953
	300	120.68	2.00	116.730	124.623

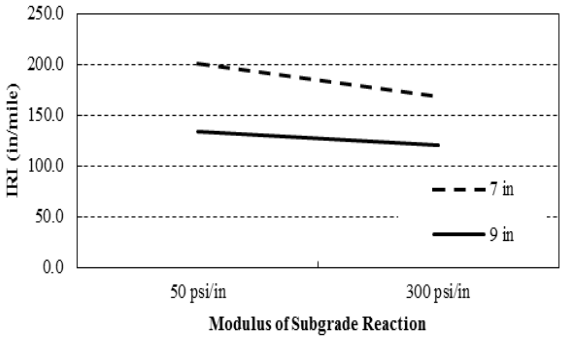

Figure A-95 Overlay thickness vs. modulus of subgrade reaction

TABLE OF CONTENTS

APPENDIX A - PRELIMINARY AND DETAILED SENSITIVITY ANALYSIS RESULTS ... 1
A.1 PRELIMINARY SENSITIVITY ANALYSIS ... 1
A.2 DETAILED SENSITIVITY ANALYSIS ... 1
A.2.1 HMA overlay ... 1
A.2.1.1. Longitudinal cracking ... 4
A.2.1.2. Alligator cracking ... 8
A.2.1.3. Rutting ... 12
A.2.1.4. IRI ... 17
A.2.2 Composite ... 22
A.2.2.1. Longitudinal cracking ... 23
A.2.2.2. Alligator cracking ... 27
A.2.2.3. Rutting ... 28
A.2.2.4. IRI ... 32
A.2.3 Rubblized ... 34
A.2.3.1. Longitudinal cracking ... 35
A.2.3.2. Alligator cracking ... 38
A.2.3.3. Rutting ... 41
A.2.3.4. IRI ... 44
A.2.4 Unbonded Overlay ... 47
A.2.4.1. Cracking ... 48
A.2.4.2. Faulting ... 52
A.2.4.3. IRI ... 54

APPENDIX B - GLOBAL SENSITIVITY ANALYSIS RESULTS

B.1 HMA OVER HMA

B.1.1 Alligator Cracking

Inputs main effect

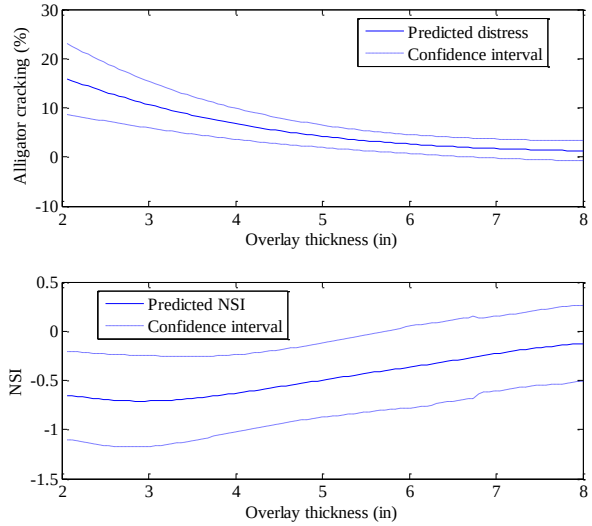

Figure B-1 Predicted alligator cracking and NSI for overlay thickness

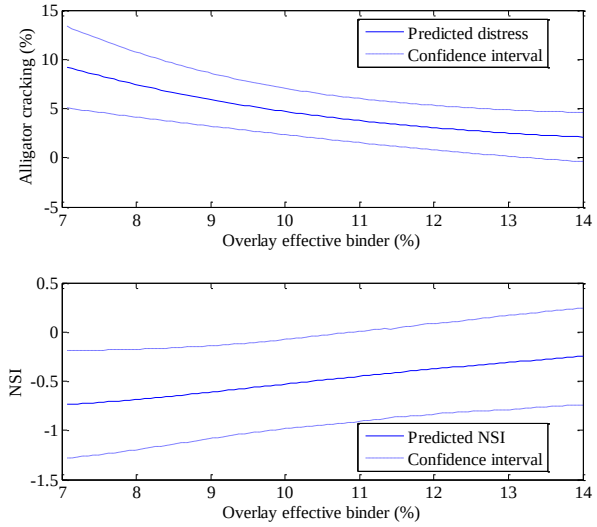

Figure B-2 Predicted alligator cracking and NSI for effective binder

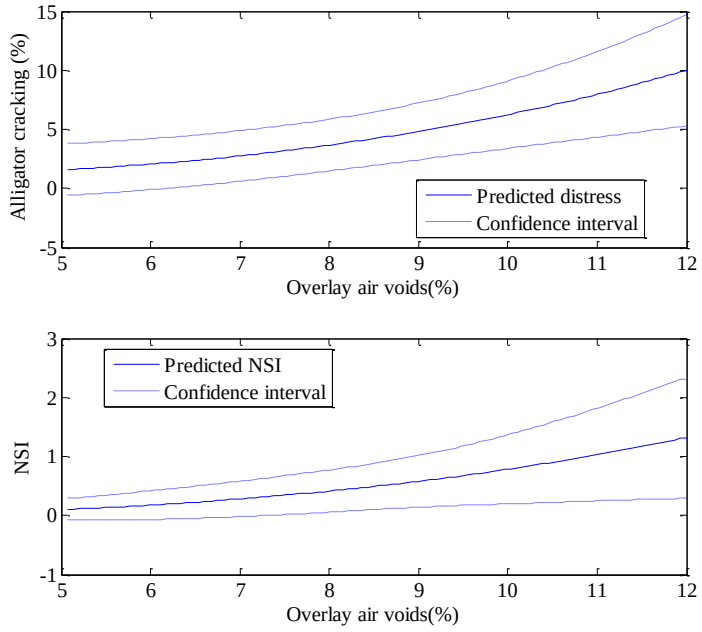

Figure B-3 Predicted alligator cracking and NSI for air voids

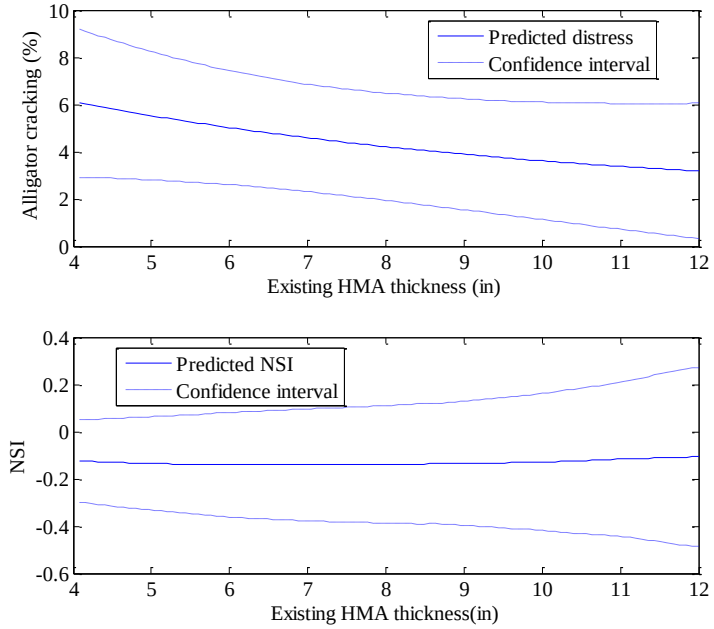

Figure B-4 Predicted alligator cracking and NSI for existing thickness

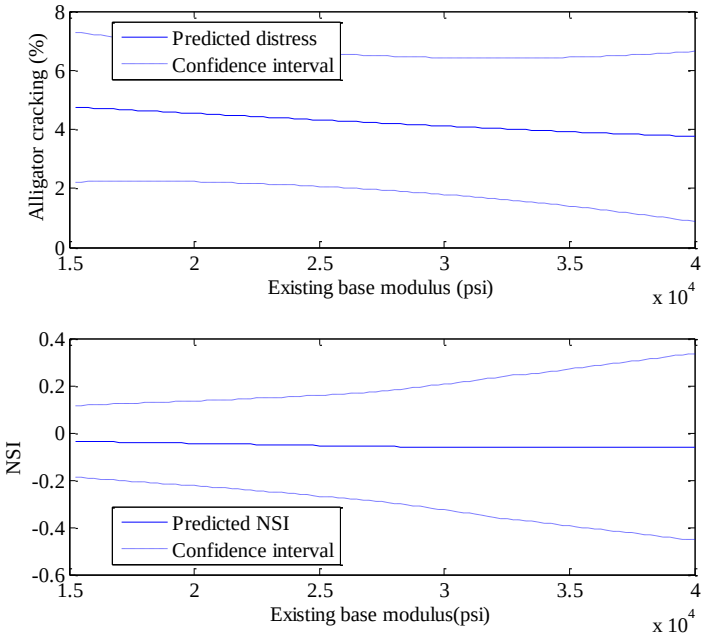

Figure B-5 Predicted alligator cracking and NSI for base modulus

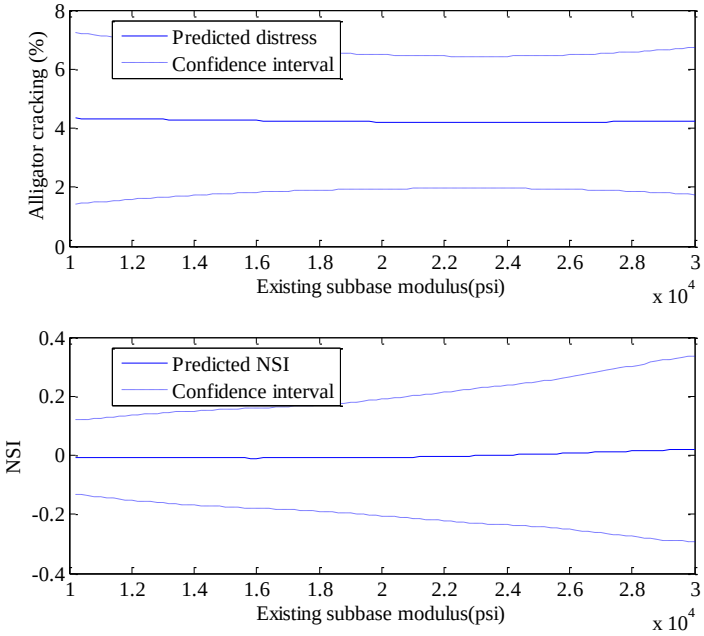

Figure B-6 Predicted alligator cracking and NSI for subbase modulus

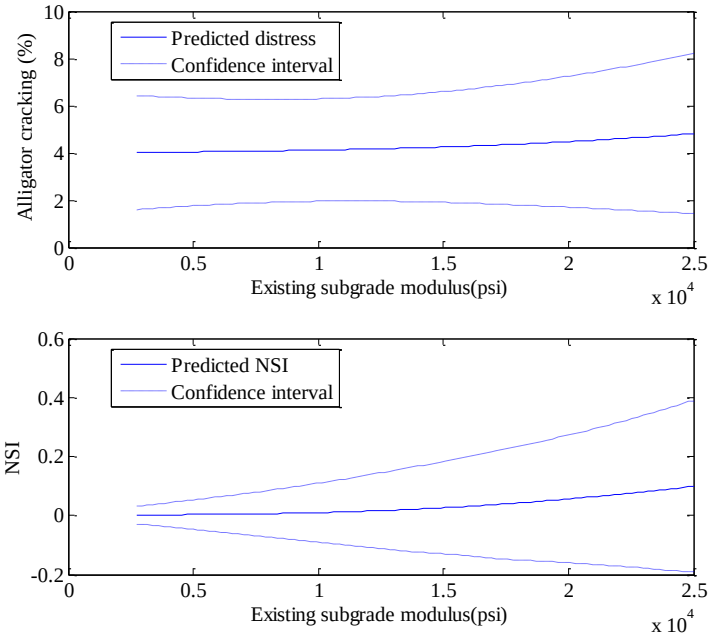

Figure B-7 Predicted alligator cracking and NSI subgrade modulus

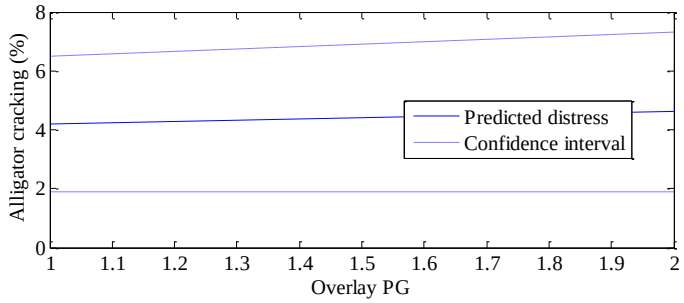

Figure B-8 Predicted alligator cracking for overlay PG

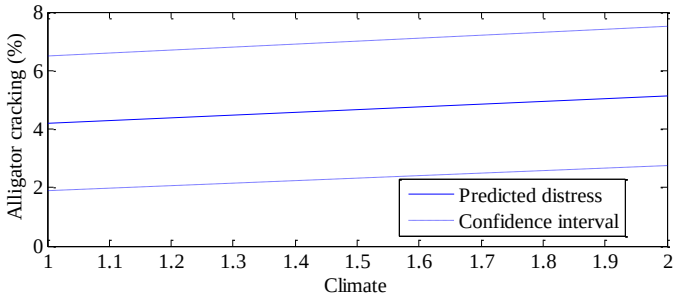

Figure B-9 Predicted alligator cracking for cliamte

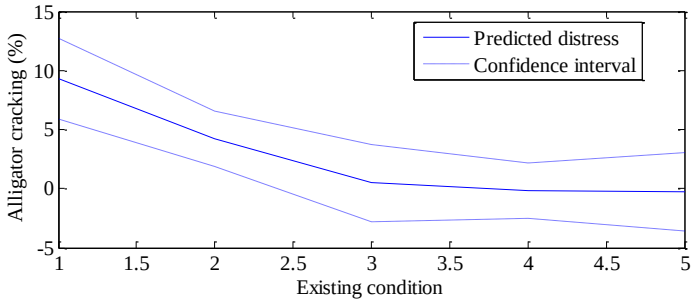

Figure B-10 Predicted alligator cracking for existing condition

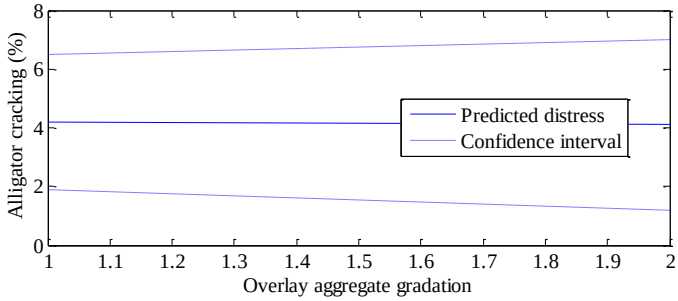

Figure B-11 Predicted alligator cracking for overlay aggregate gradation

Inputs interaction effect

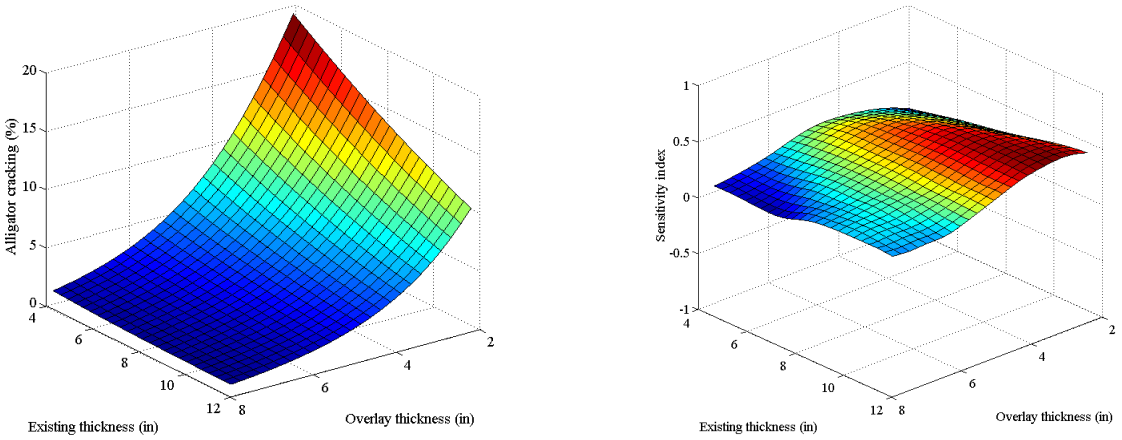

Figure B-12 Predicted interaction and NSI between existing thickness and overlay thickness

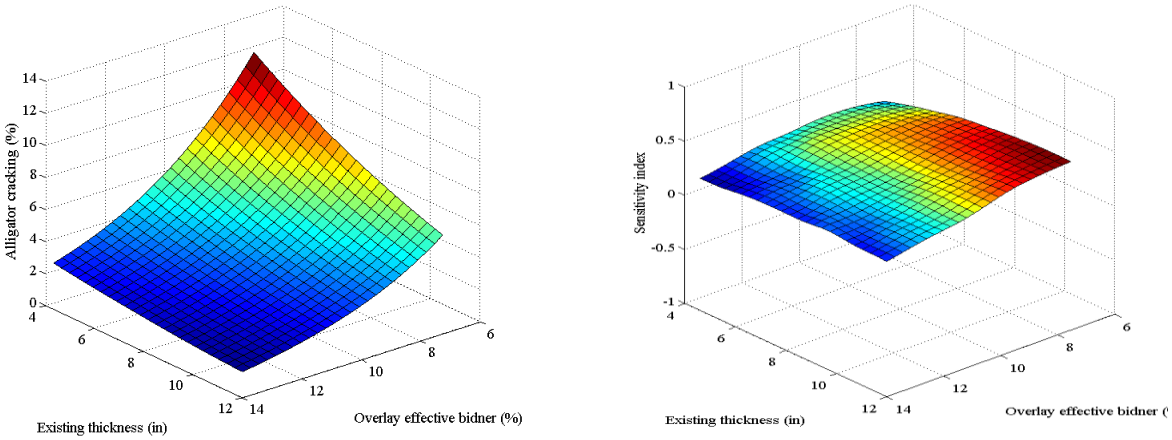

Figure B-13 Predicted interaction and NSI between existing thickness and overlay effective binder

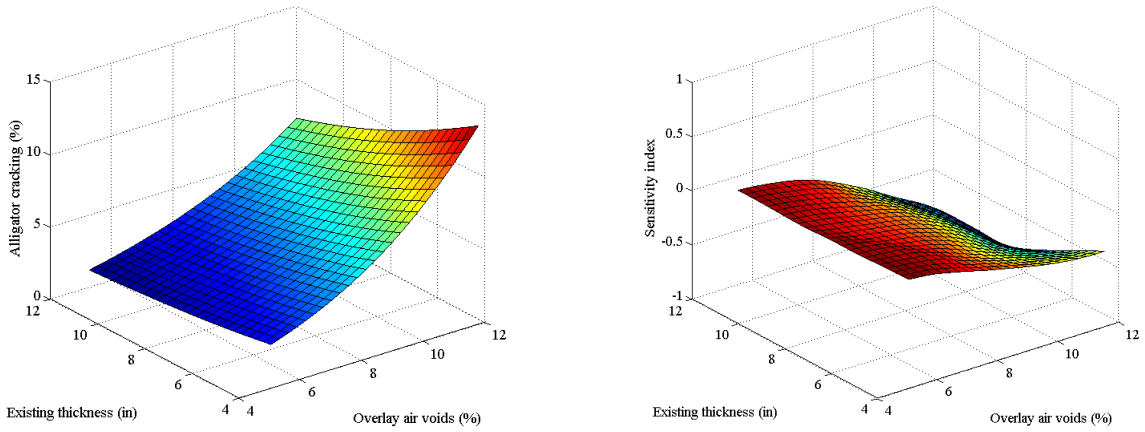

Figure B-14 Predicted interaction and NSI between existing thickness and overlay air voids

B.1.2 Longitudinal Cracking

Inputs main effect

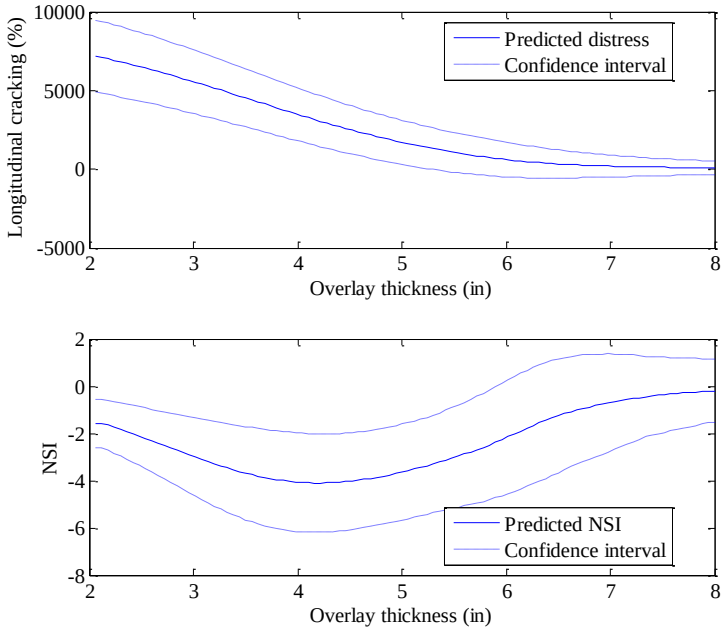

Figure B-15 Predicted longitudinal cracking and NSI for overlay thickness

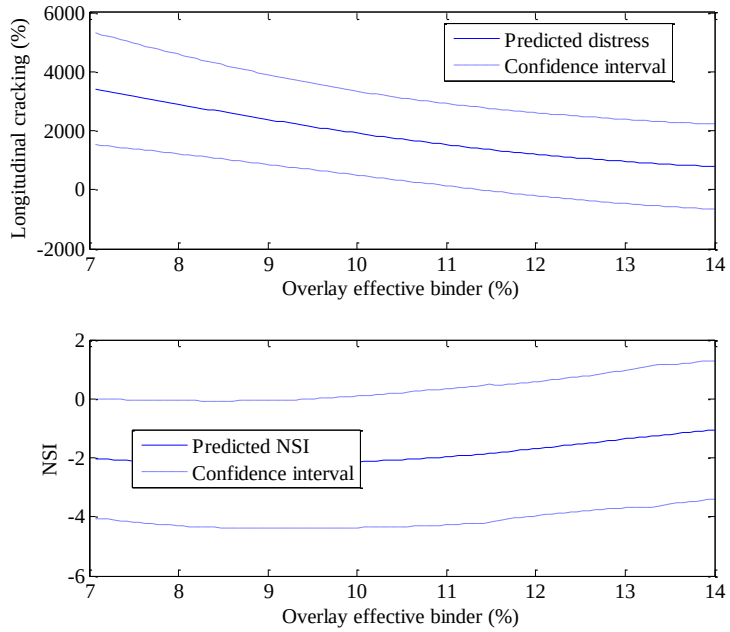

Figure B-16 Predicted longitudinal cracking and NSI for overlay effective binder

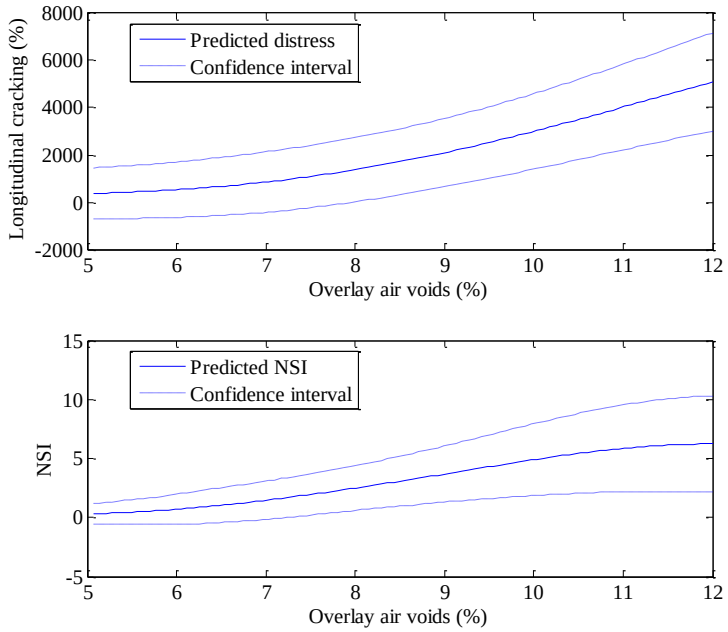

Figure B-17 Predicted longitudinal cracking and NSI for overlay air voids

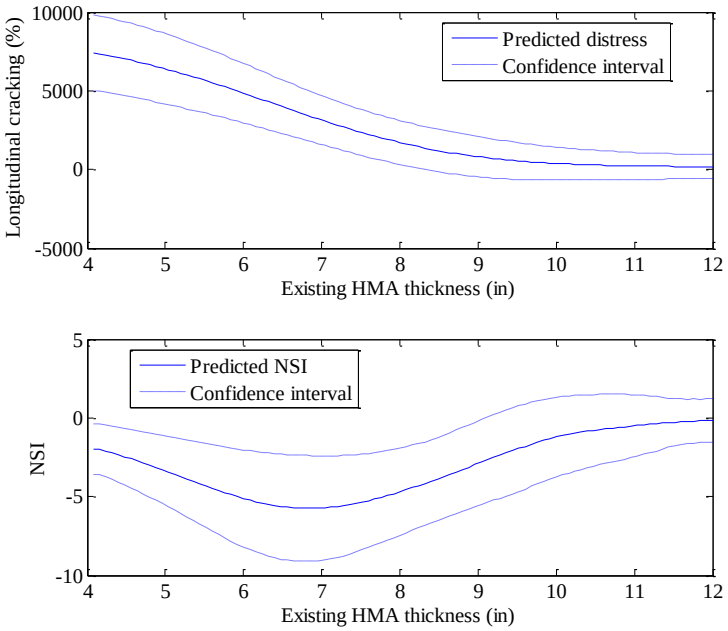

Figure B-18 Predicted longitudinal cracking and NSI for existing thickness

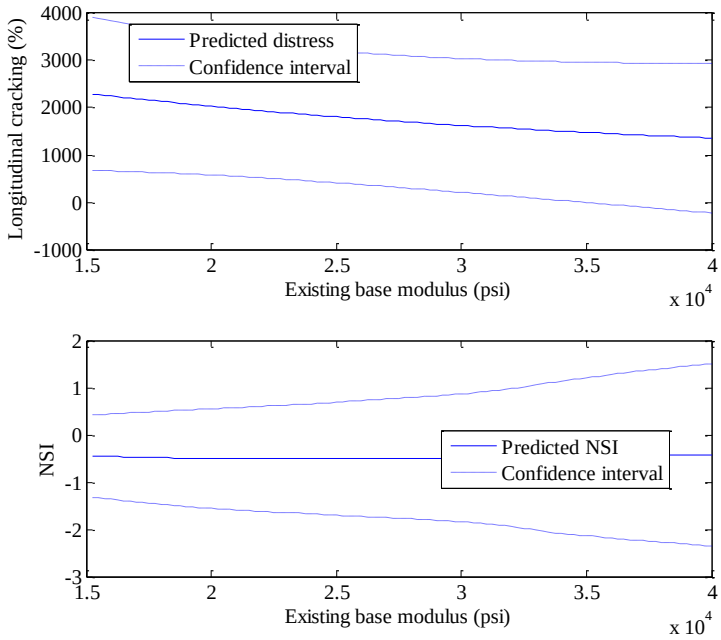

Figure B-19 Predicted longitudinal cracking and NSI for base modulus

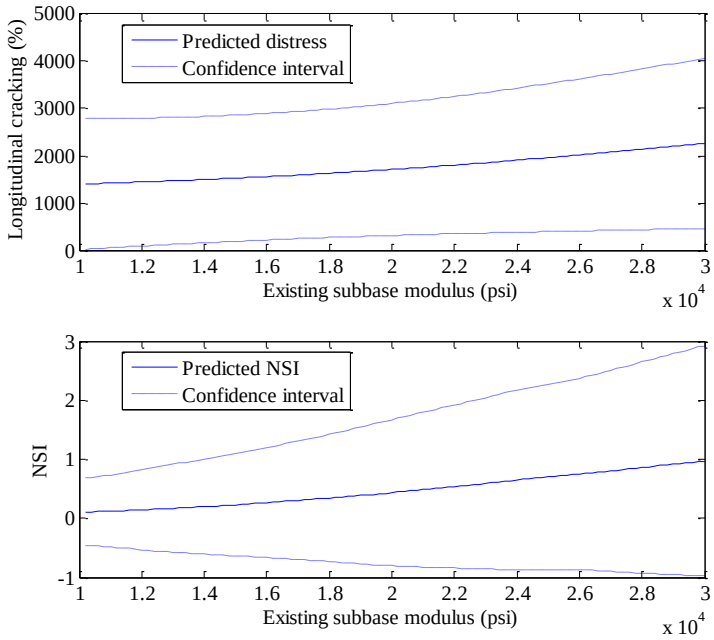

Figure B-20 Predicted longitudinal cracking and NSI for subbase modulus

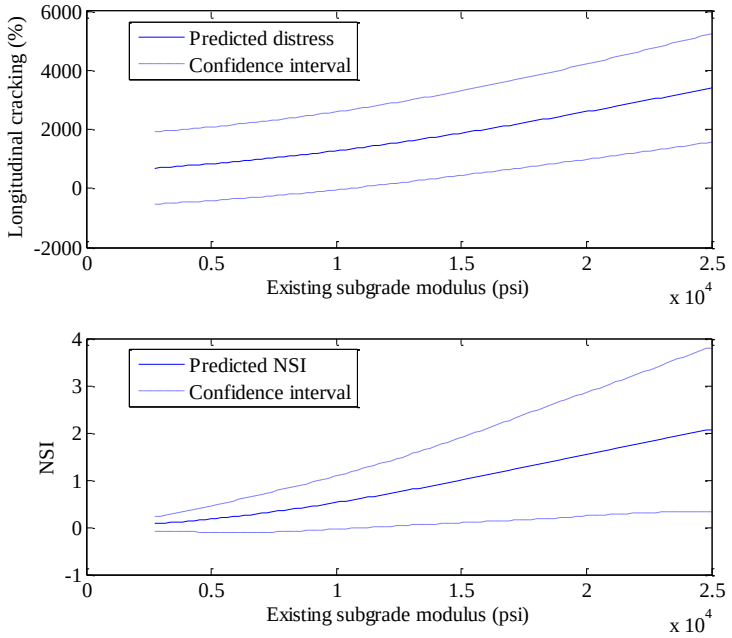

Figure B-21 Predicted longitudinal cracking and NSI for subgrade modulus

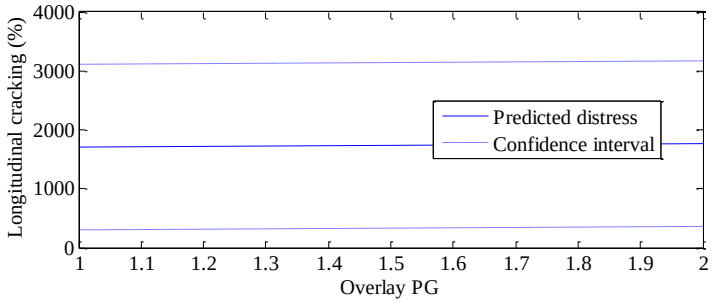

Figure B-22 Predicted longitudinal cracking for overlay PG

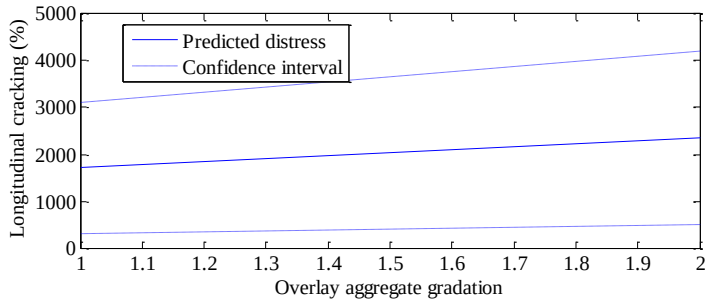

Figure B-23 Predicted longitudinal cracking for overlay aggregate gradation

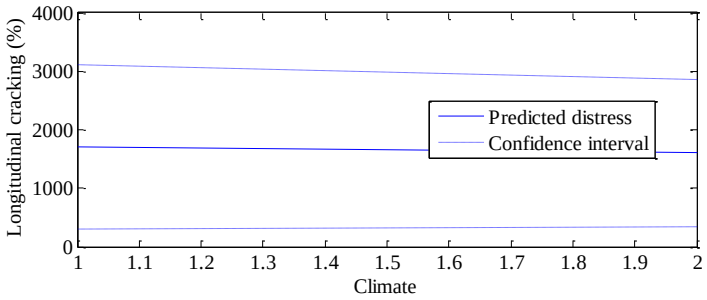

Figure B-24 Predicted longitudinal cracking for cliamte

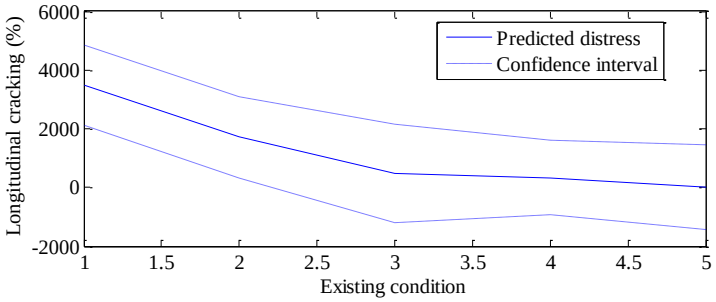

Figure B-25 Predicted longitudinal cracking for existing condition

Inputs interaction effect

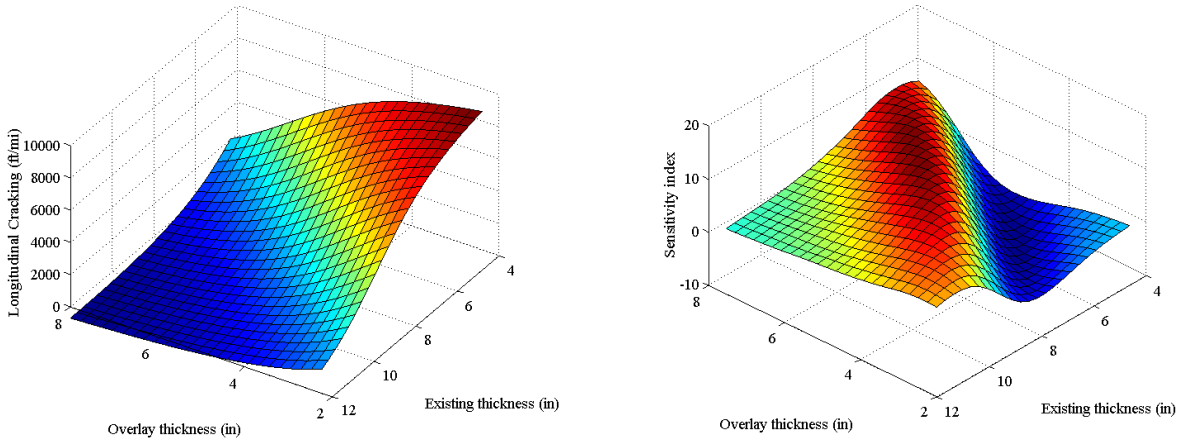

Figure B-26 Predicted interaction and NSI between existing condition and overlay thickness

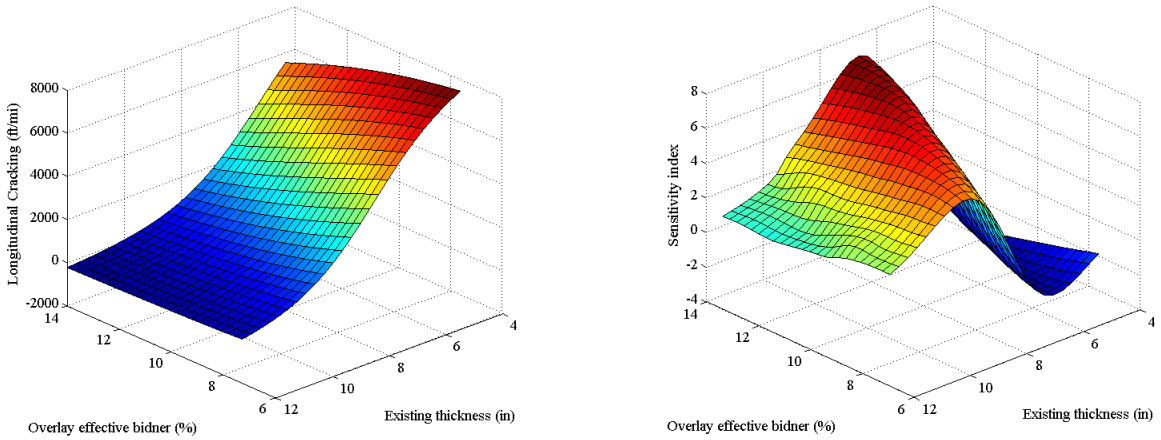

Figure B-27 Predicted interaction and NSI between existing thickness and overlay effective binder

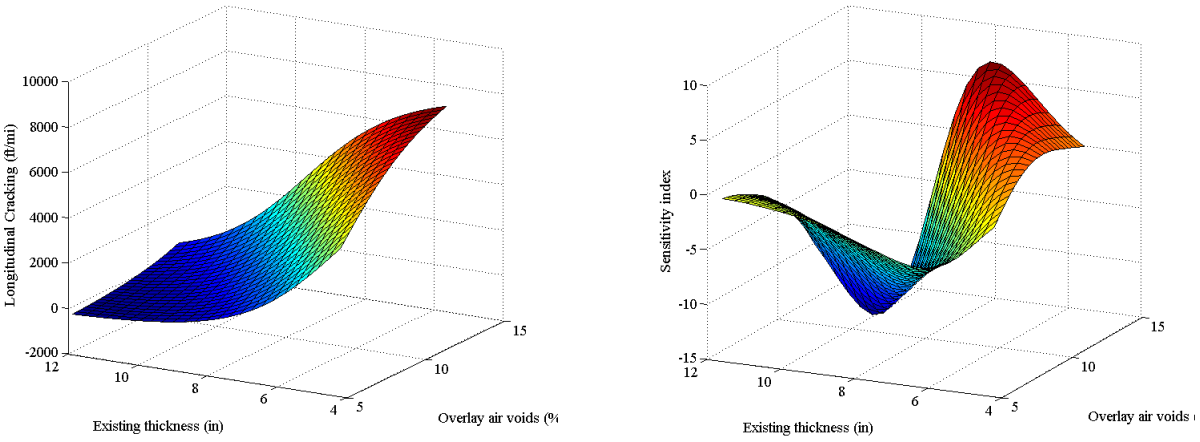

Figure B-28 Predicted interaction and NSI between existing thickness and overlay air voids

B.1.3 Rutting

Inputs main effect

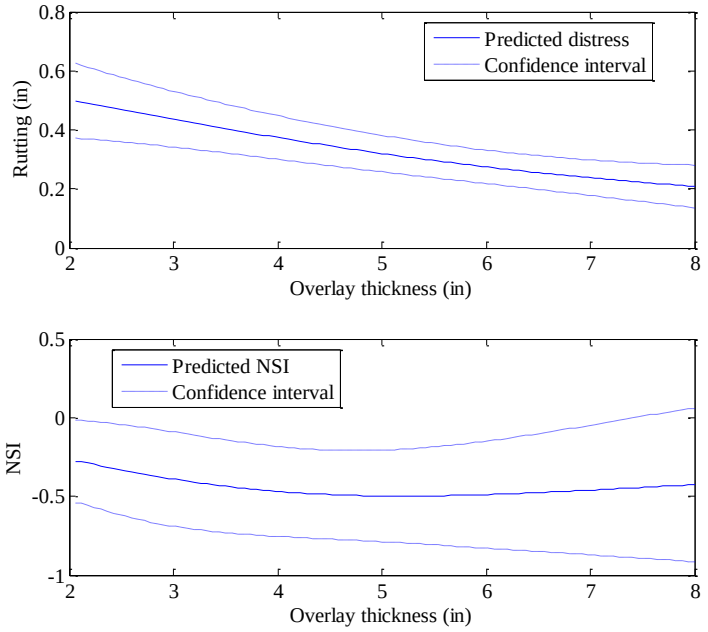

Figure B-29 Predicted rutting and NSI for overlay thickness

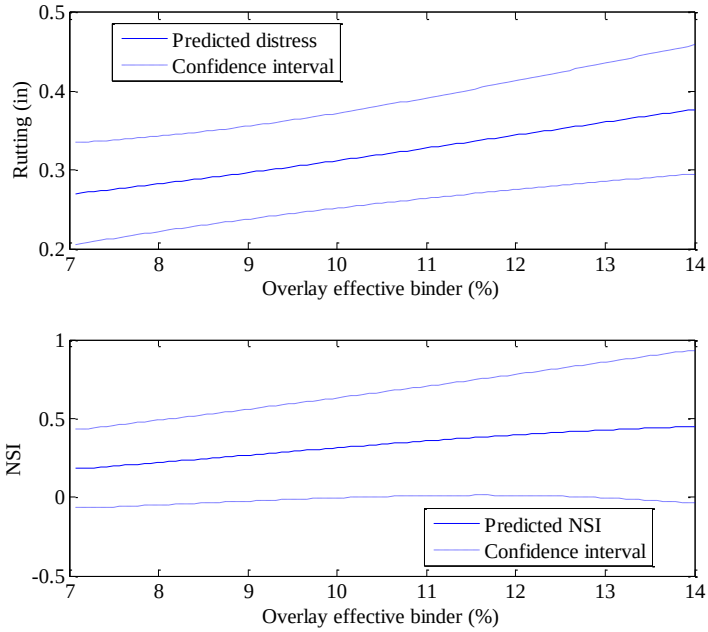

Figure B-30 Predicted rutting and NSI for overlay effective binder

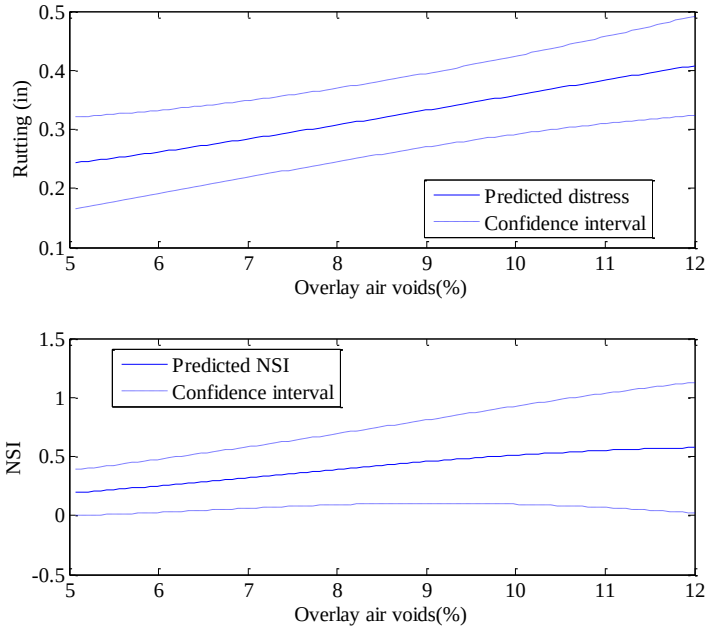

Figure B-31 Predicted rutting and NSI for overlay air voids

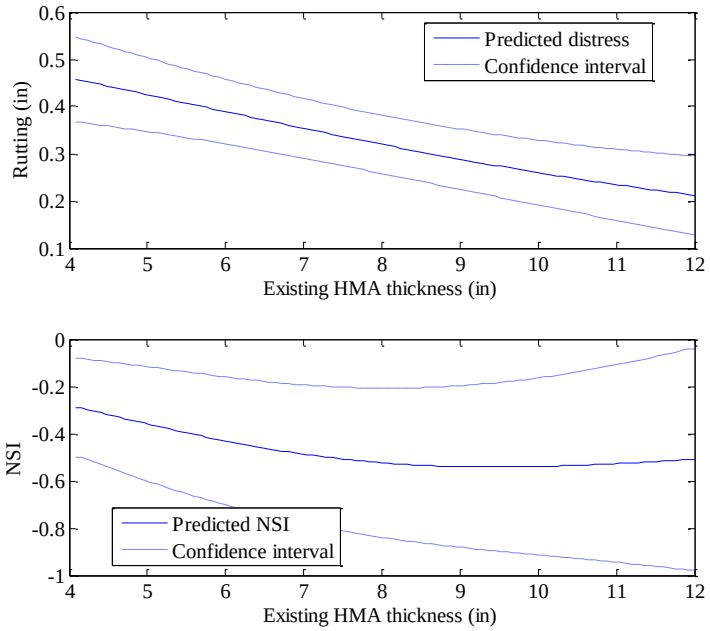

Figure B-32 Predicted rutting and NSI for existing thickness

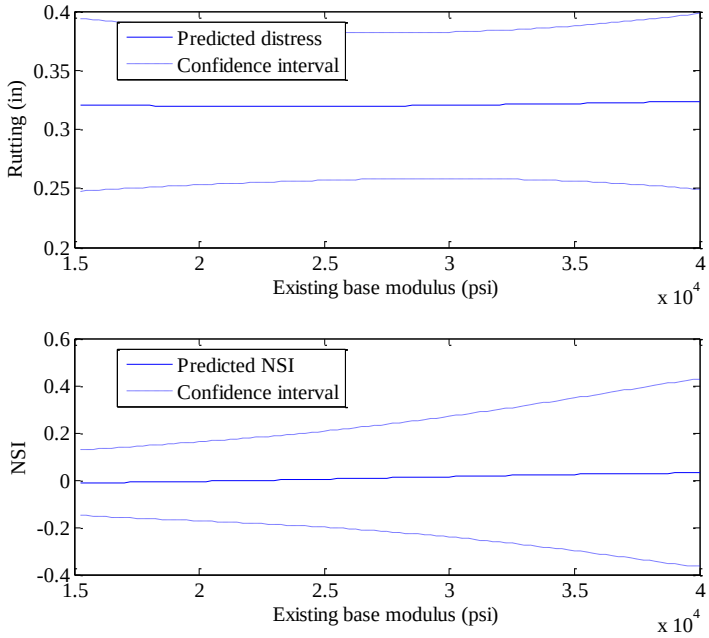

Figure B-33 Predicted rutting and NSI for base modulus

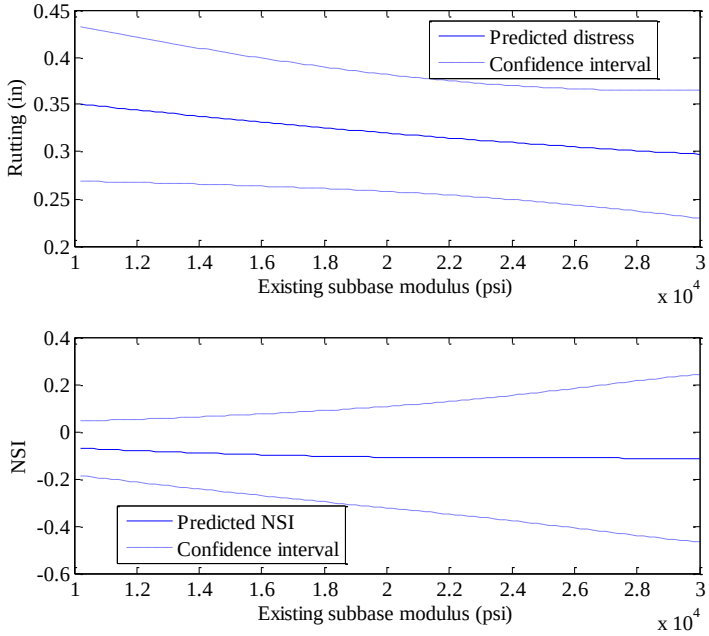

Figure B-34 Predicted rutting and NSI for subbase modulus

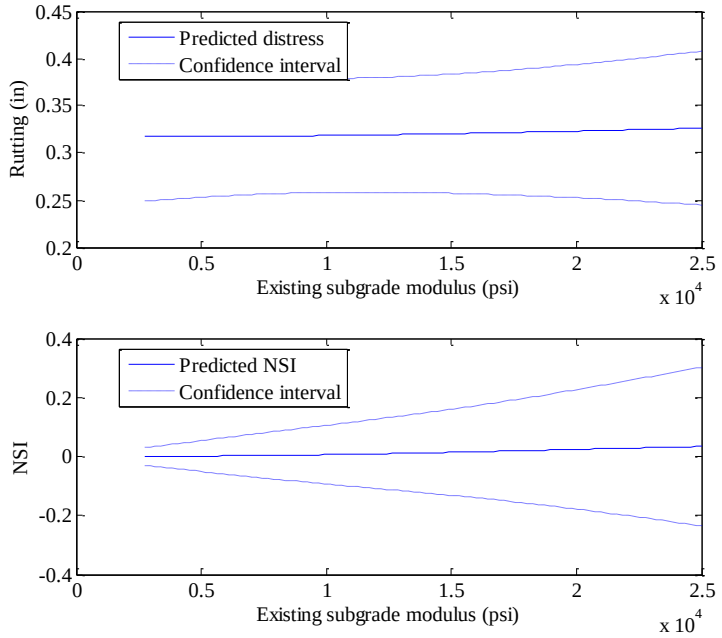

Figure B-35 Predicted rutting and NSI for subgrade modulus

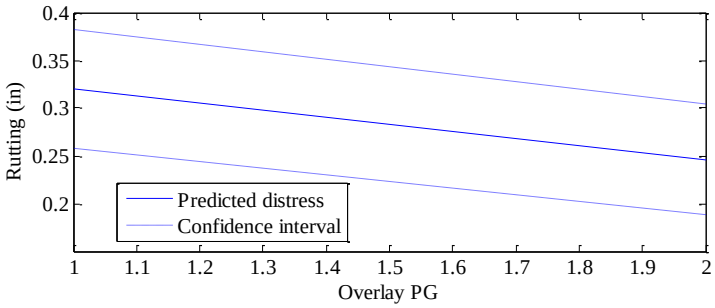

Figure B-36 Predicted rutting for overlay PG

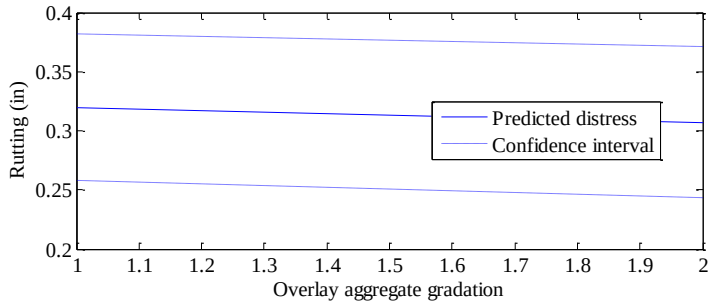

Figure B-37 Predicted rutting for overlay aggregate gradation

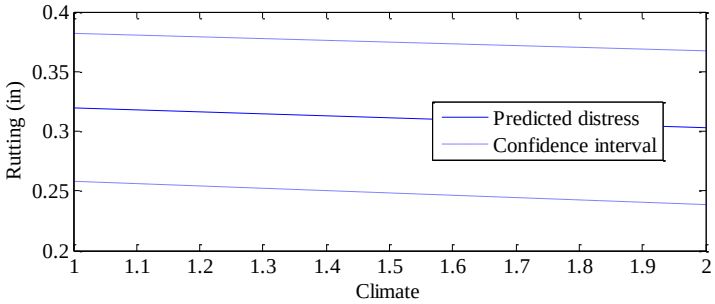

Figure B-38 Predicted rutting for climate

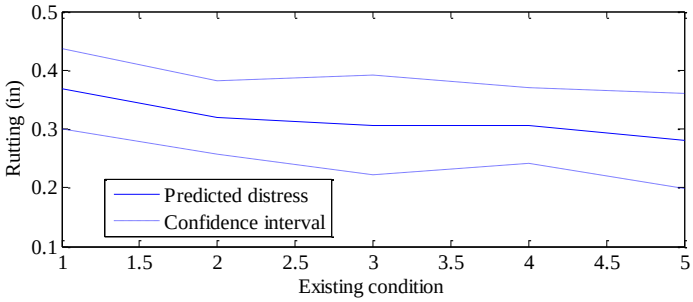

Figure B-39 Predicted rutting existing condition

Inputs interaction effect

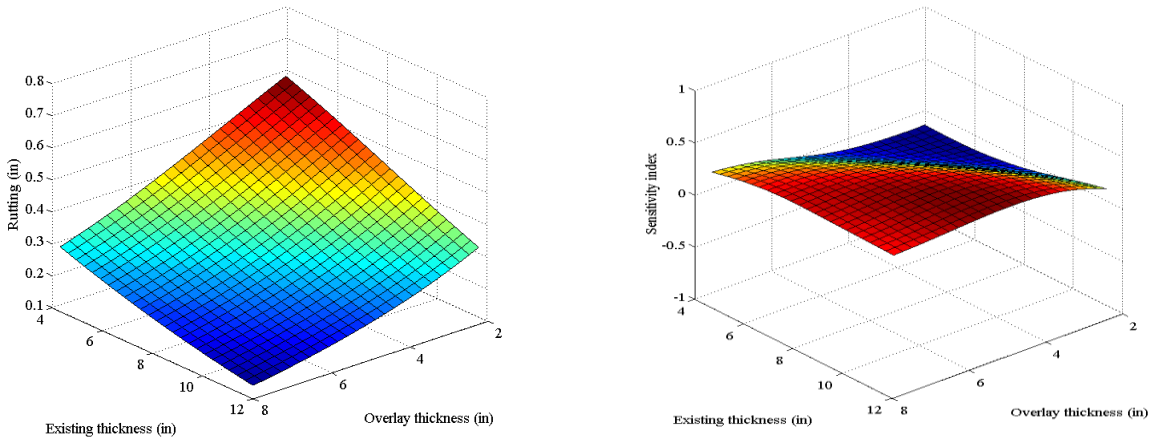

Figure B-40 Predicted interaction and NSI between existing condition and overlay thickness

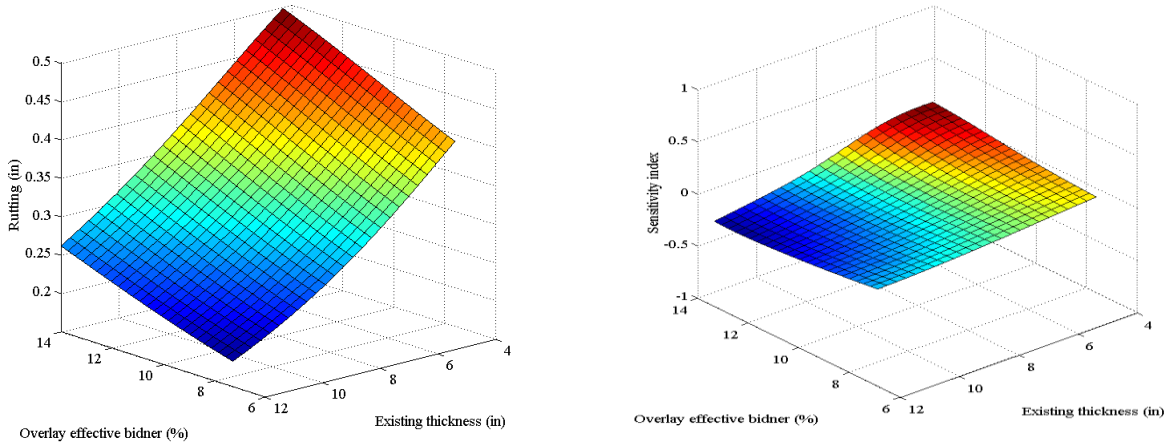

Figure B-41 Predicted interaction and NSI between existing thickness and overlay effective binder

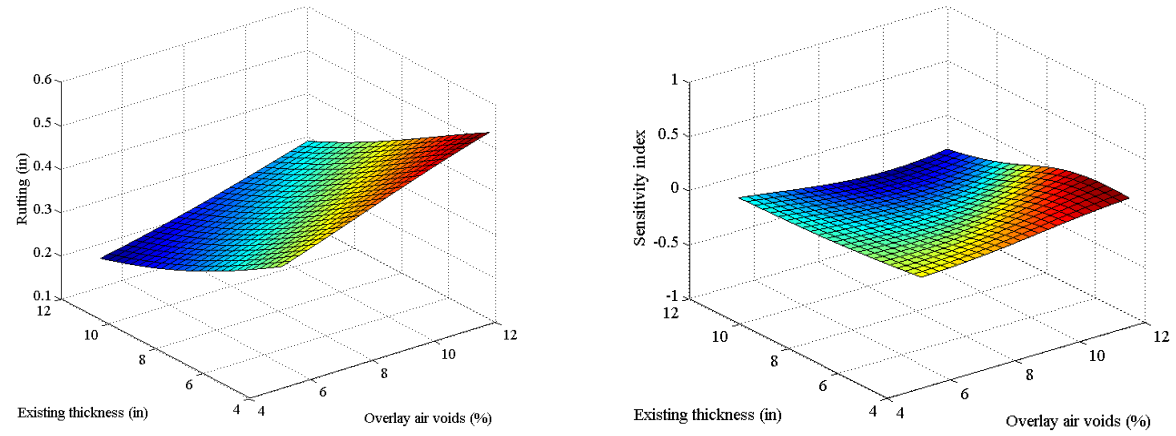

Figure B-42 Predicted interaction and NSI between existing thickness and overlay air voids

B.1.4 IRI

Inputs main effect

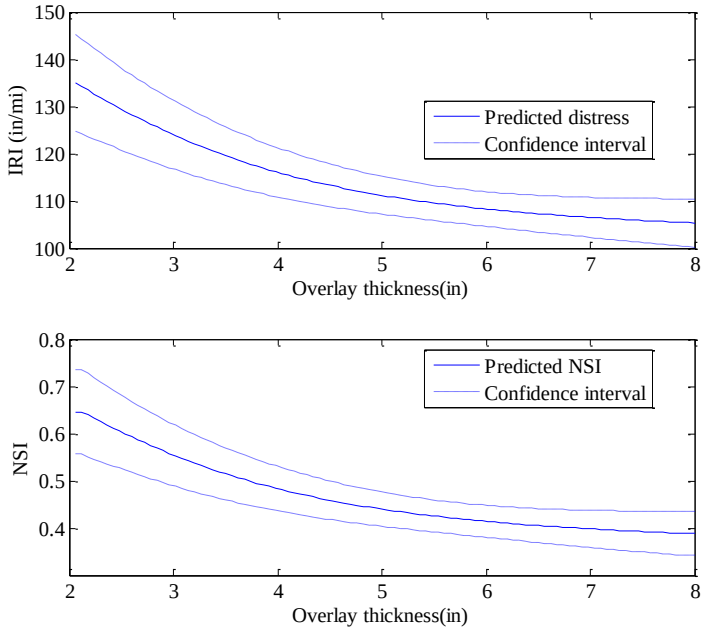

Figure B-43 Predicted IRI and NSI for overlay thickness

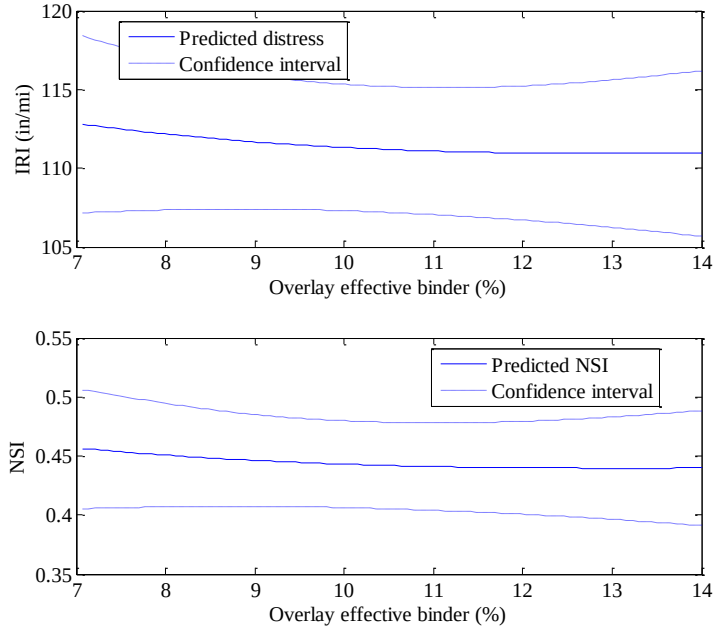

Figure B-44 Predicted IRI and NSI for overlay effective binder

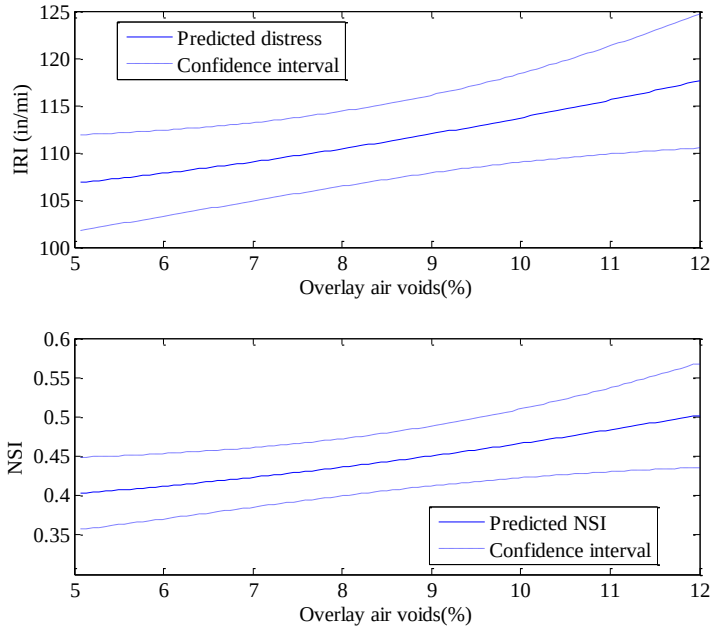

Figure B-45 Predicted IRI and NSI for overlay air voids

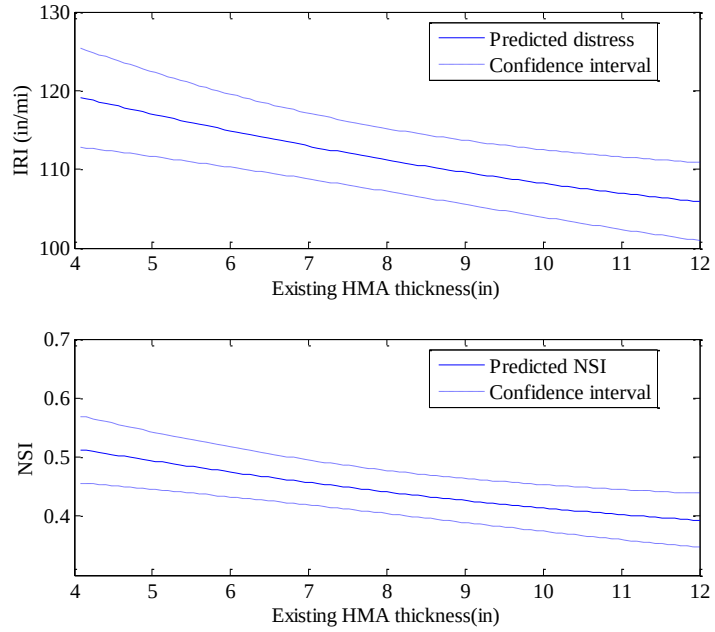

Figure B-46 Predicted IRI and NSI for overlay existing thickness

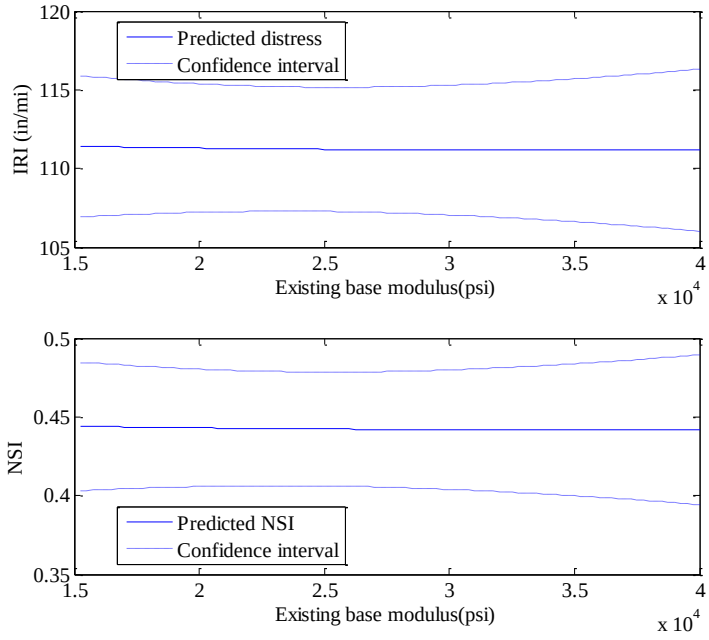

Figure B-47 Predicted IRI and NSI for base modulus

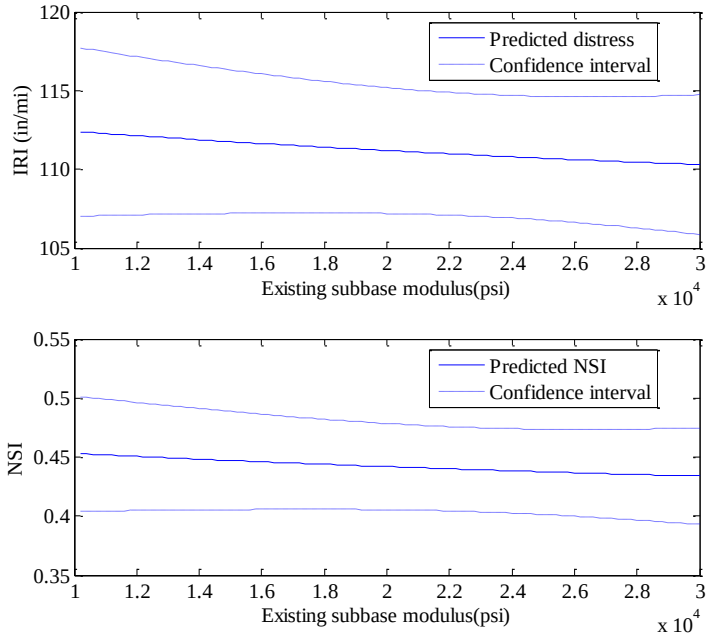

Figure B-48 Predicted IRI and NSI for subbase modulus

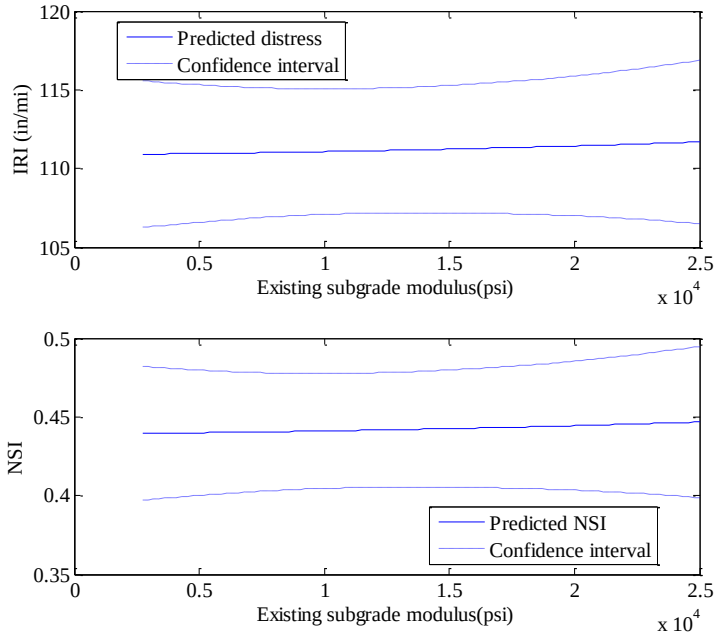

Figure B-49 Predicted IRI and NSI for subgrade modulus

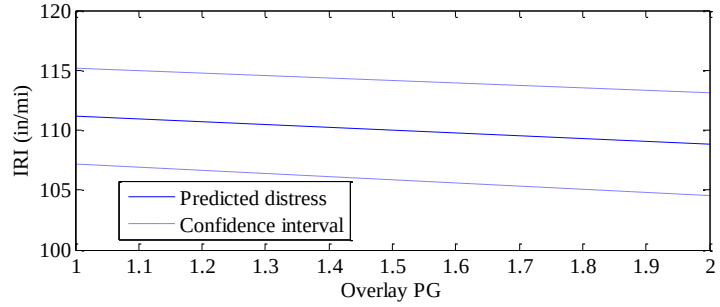

Figure B-50 Predicted IRI for overlay PG

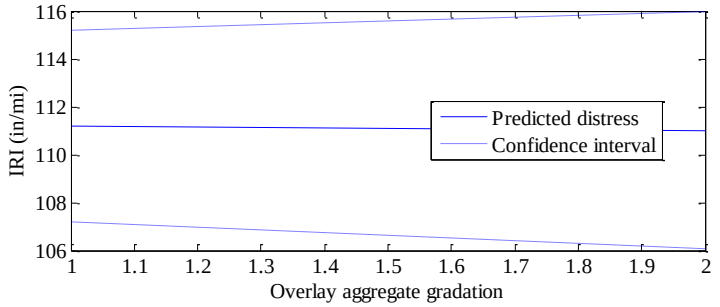

Figure B-51 Predicted IRI for overlay aggregate gradation

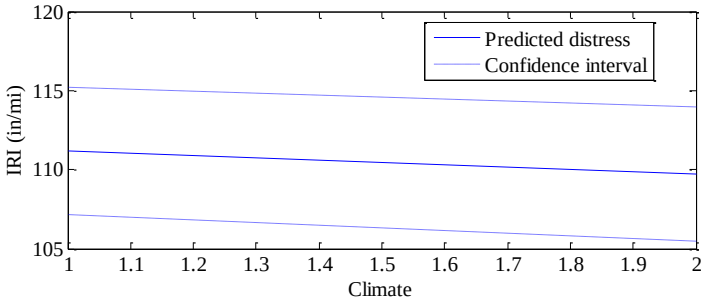

Figure B-52 Predicted IRI for climate

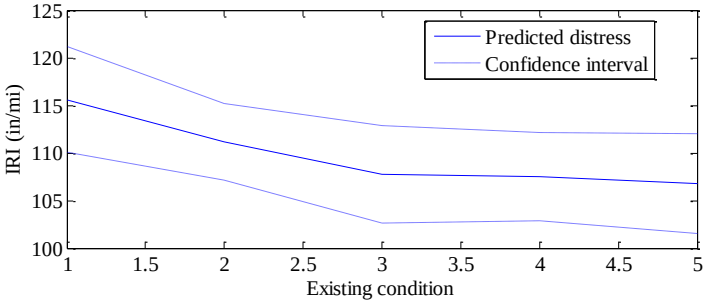

Figure B-53 Predicted IRI for existing condition

Inputs interaction effect

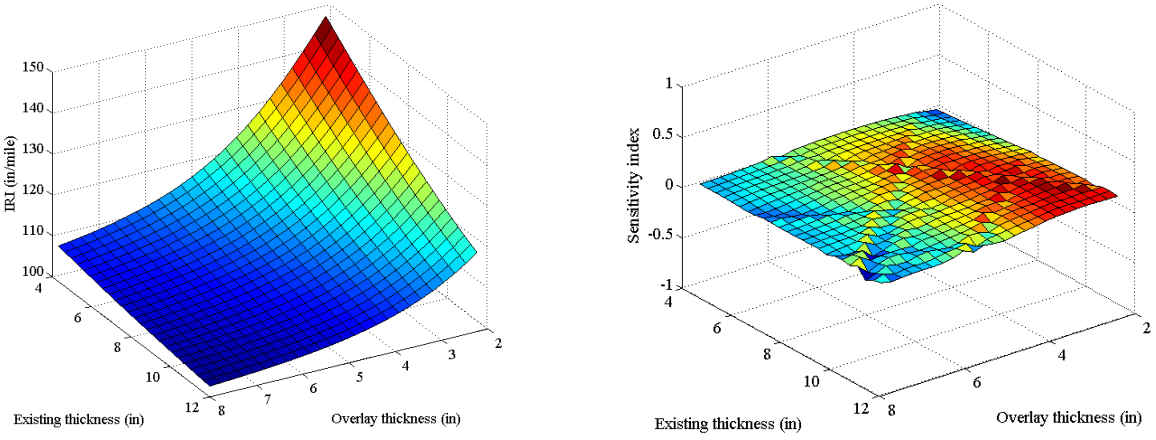

Figure B-54 Predicted interaction and NSI between existing condition and overlay thickness

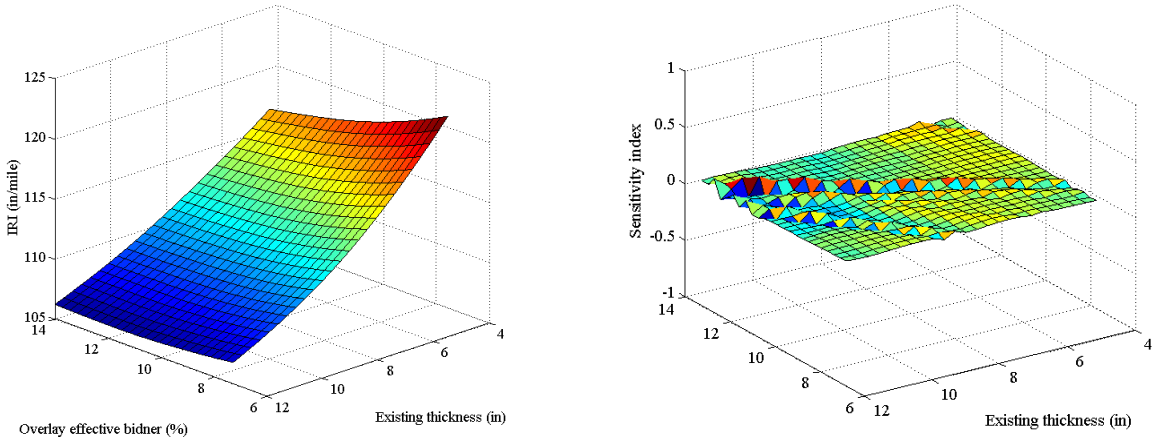

Figure B-55 Predicted interaction and NSI between existing thickness and overlay effective binder

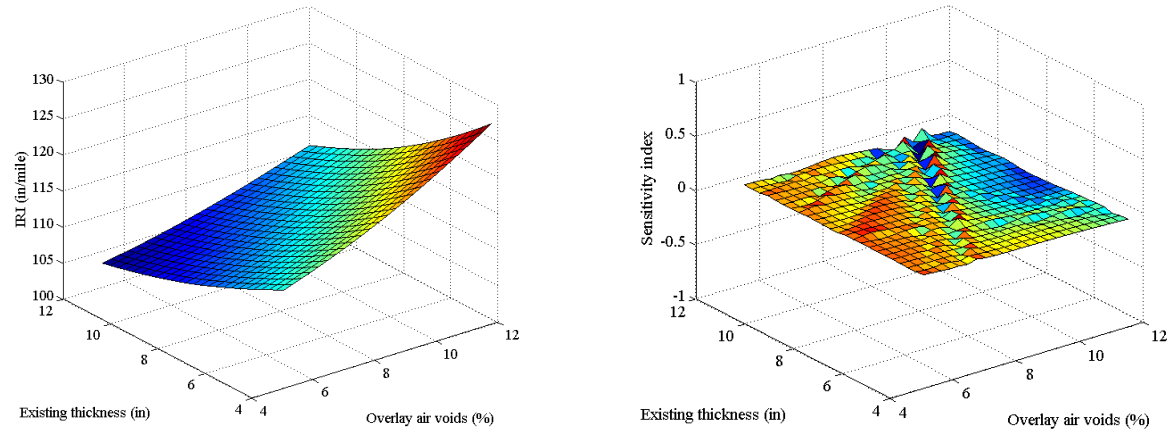

Figure B-56 Predicted interaction and NSI between existing thickness and overlay air voids

B.2 COMPOSITE OVERLAYS

B.1.5 Longitudinal Cracking

Inputs main effect

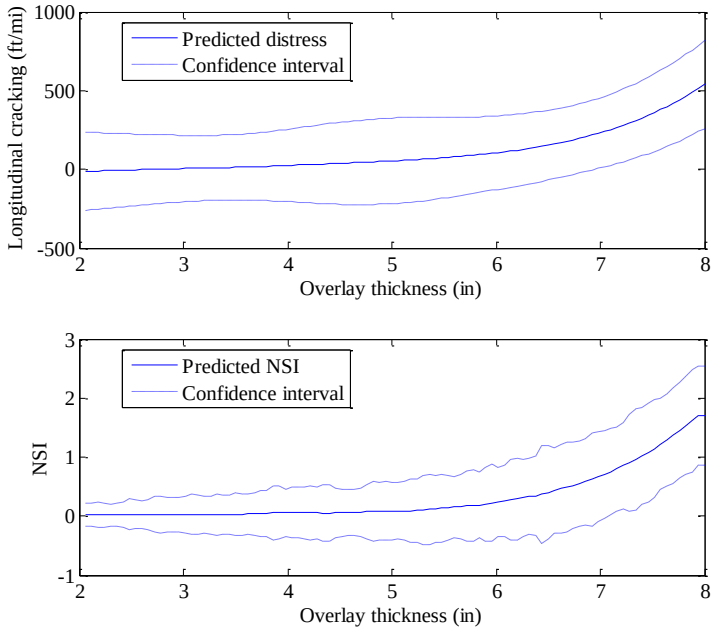

Figure B-57 Predicted longitudinal cracking and NSI for overlay thickness

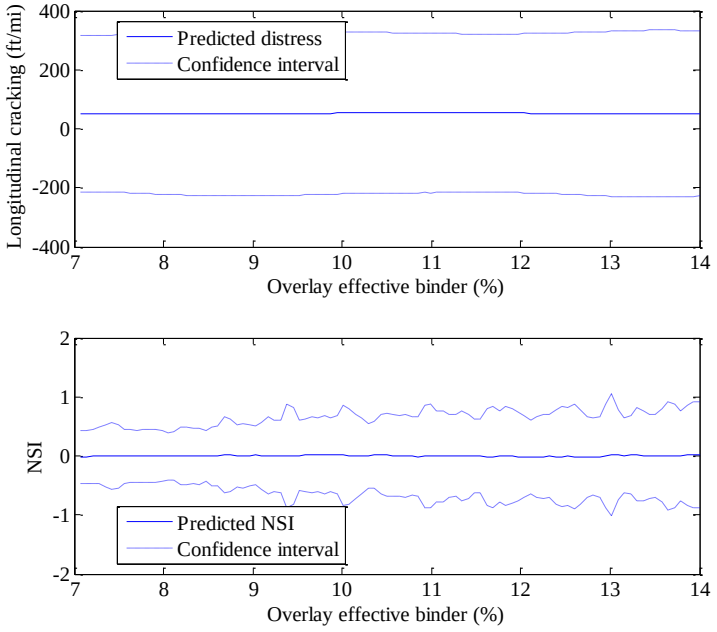

Figure B-58 Predicted longitudinal cracking and NSI for effective binder

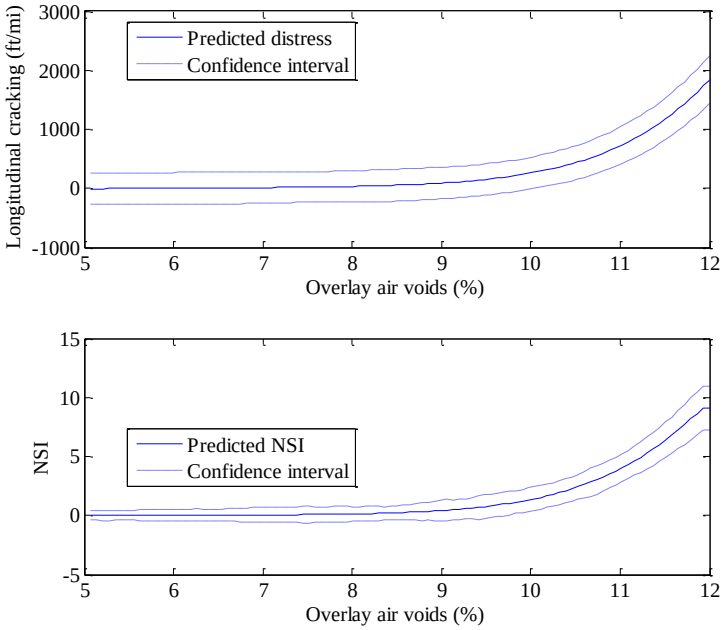

Figure B-59 Predicted longitudinal cracking and NSI for air voids

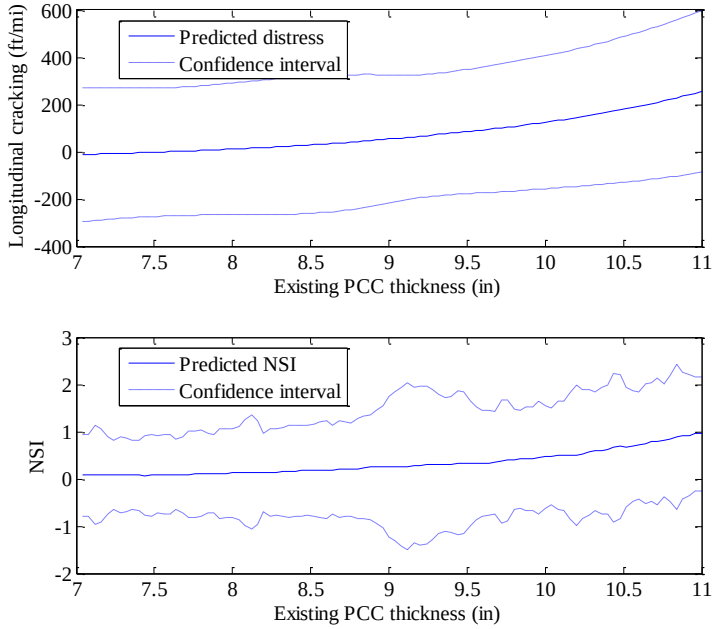

Figure B-60 Predicted longitudinal cracking and NSI for existing PCC thickness

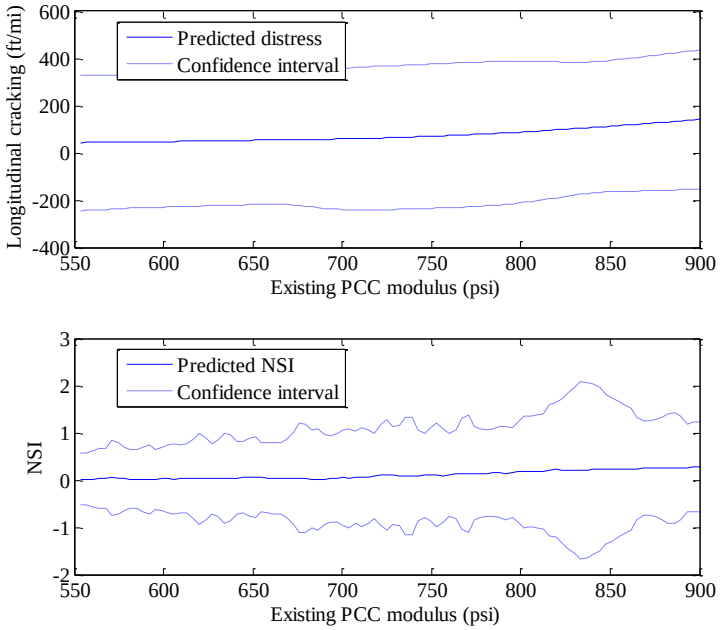

Figure B-61 Predicted longitudinal cracking and NSI for existing PCC modulus

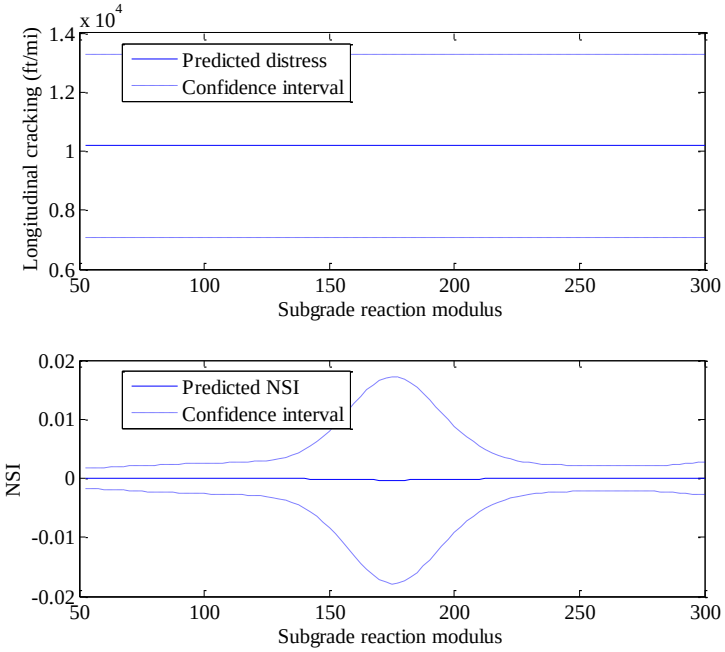

Figure B-62 Predicted longitudinal cracking and NSI for subgrade modulus reaction

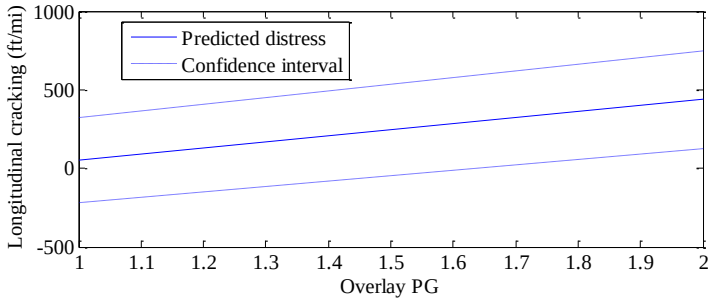

Figure B-63 Predicted longitudinal cracking for overlay PG

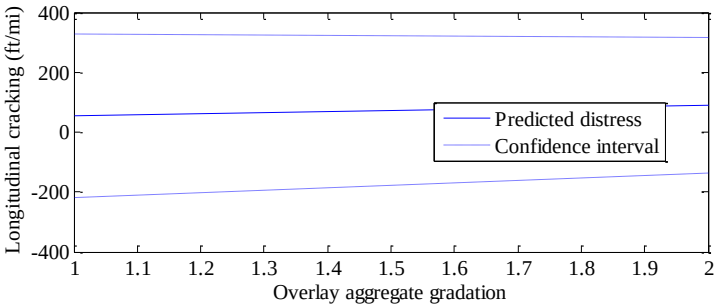

Figure B-64 Predicted longitudinal cracking for overlay aggregate gradation

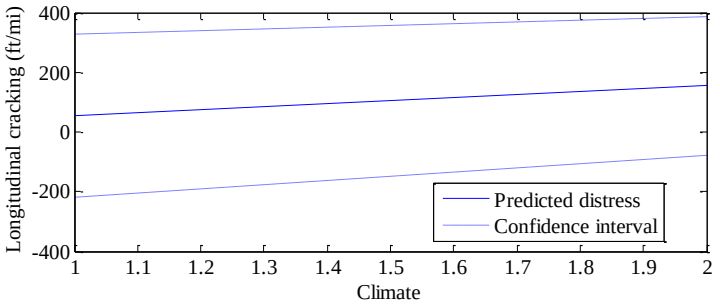

Figure B-65 Predicted longitudinal cracking for climate

Inputs interaction effect

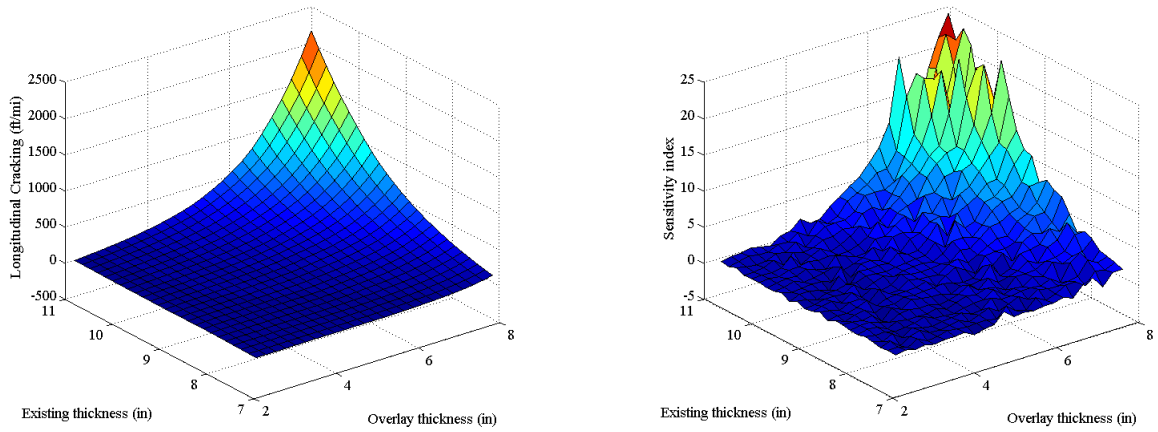

Figure B-66 Predicted interaction and NSI between existing thickness and overlay thickness

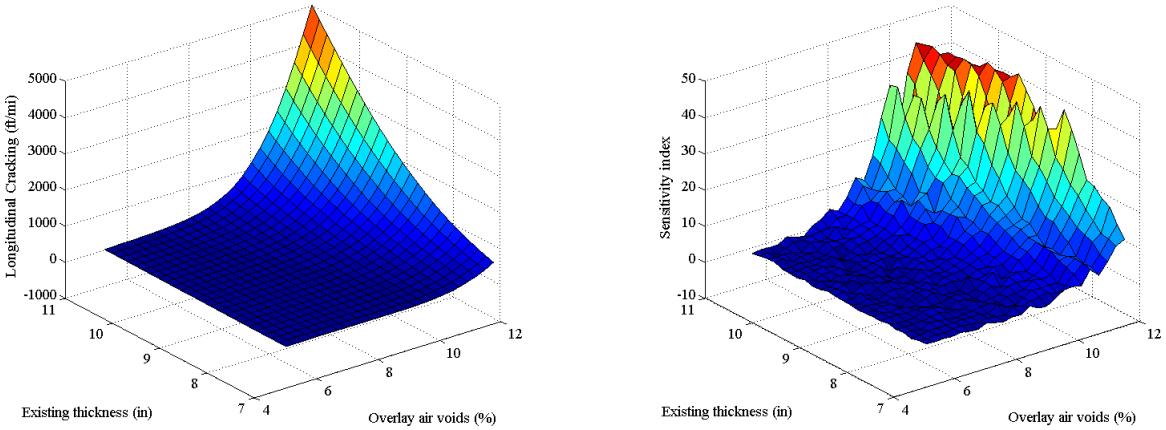

Figure B-67 Predicted interaction and NSI between existing thickness and overlay air voids

B.1.6 Rutting

Inputs interaction effect

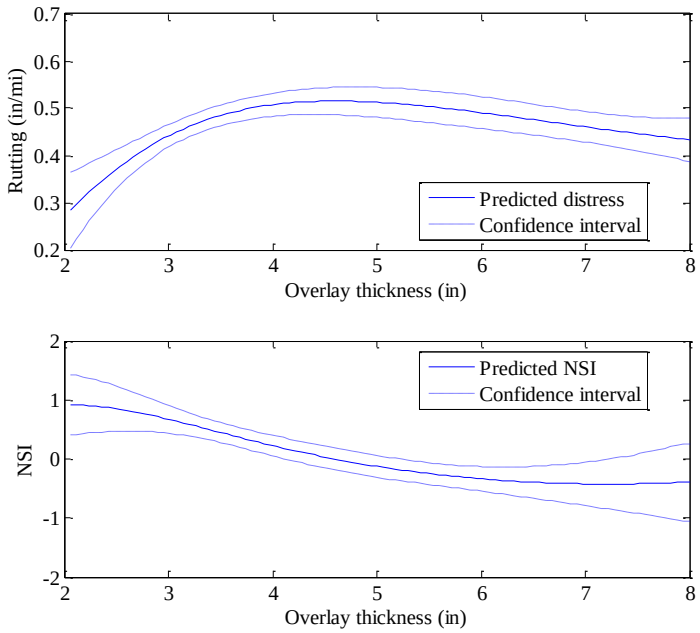

Figure B-68 Predicted rutting and NSI for subgrade overlay thickness

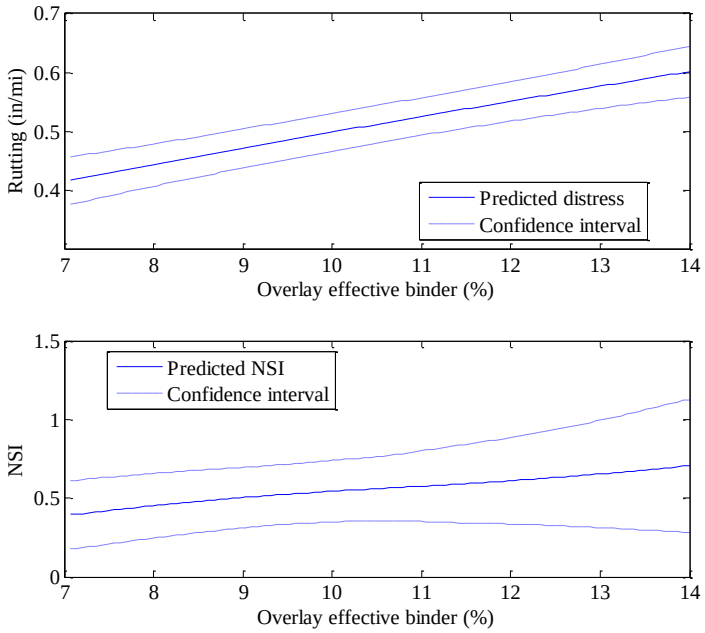

Figure B-69 Predicted rutting and NSI for overlay effective binder

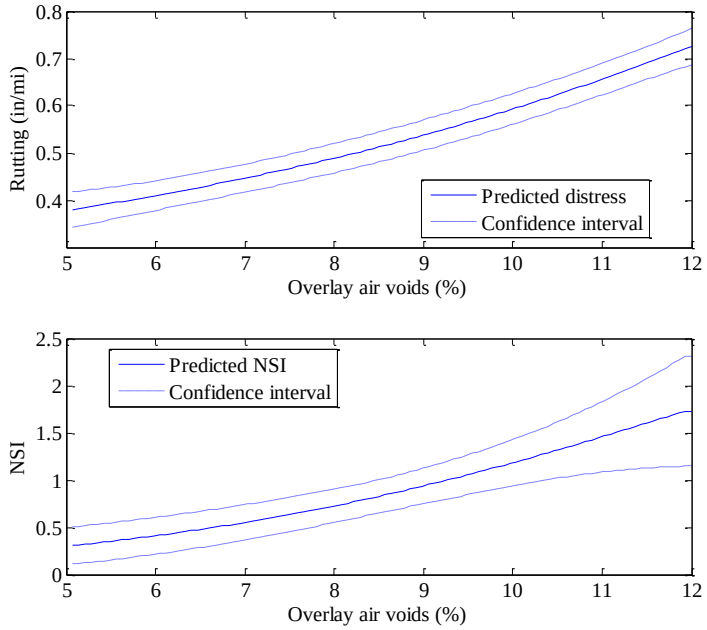

Figure B-70 Predicted rutting and NSI for subgrade overlay air voids

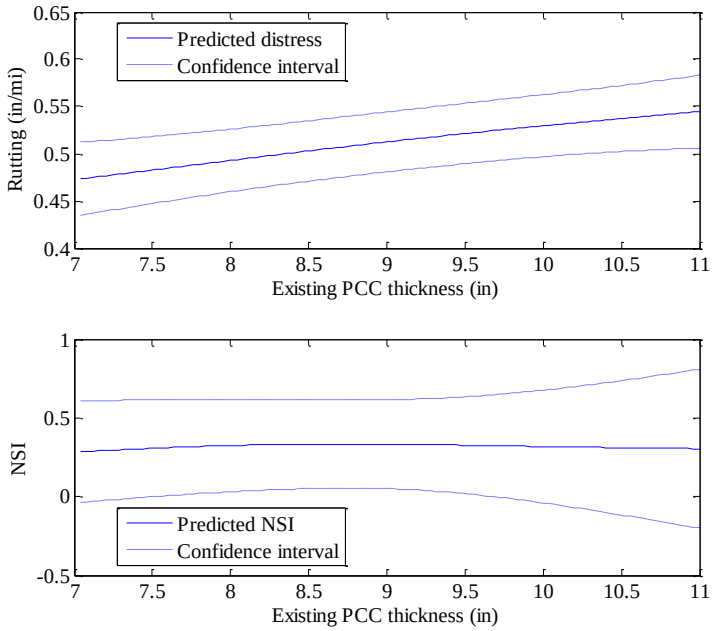

Figure B-71 Predicted rutting and NSI for existing PCC thickness

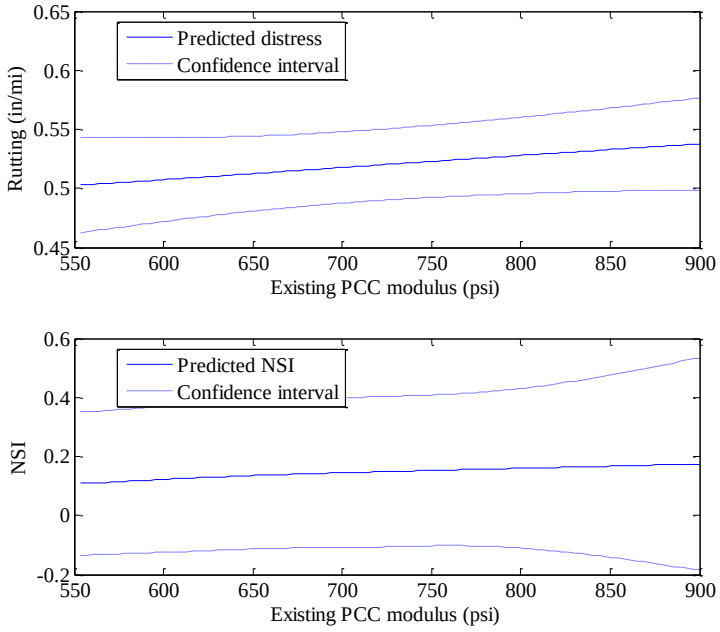

Figure B-72 Predicted rutting and NSI for existing PCC modulus

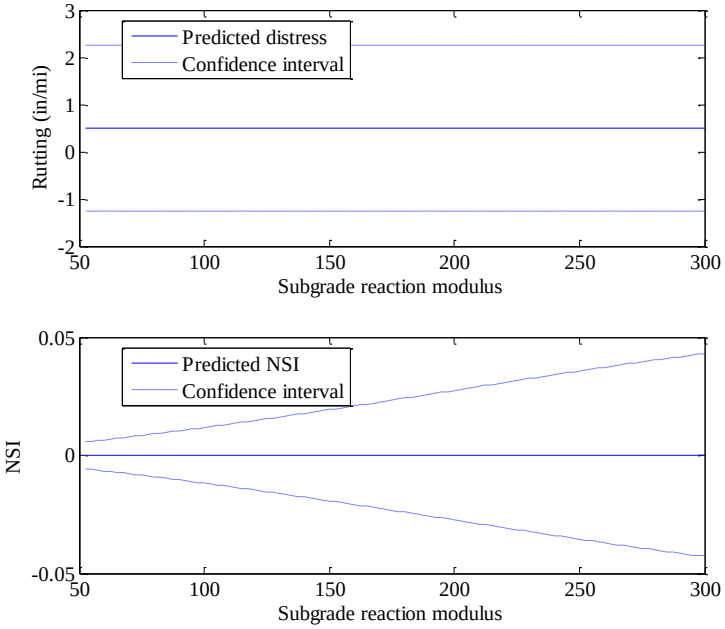

Figure B-73 Predicted rutting and NSI for subgrade reaction modulus

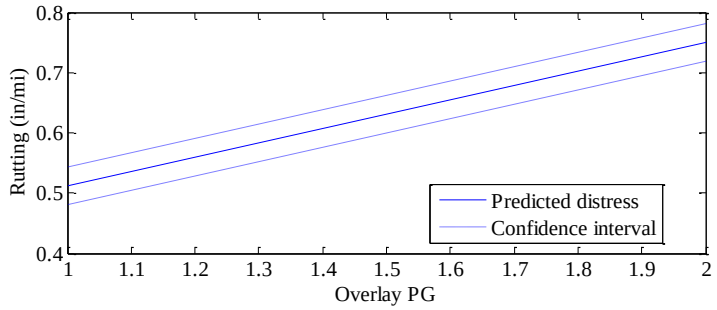

Figure B-74 Predicted rutting for overlay PG

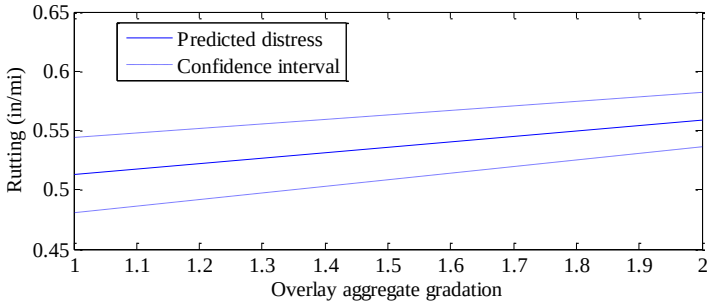

Figure B-75 Predicted rutting for overlay aggregate gradation

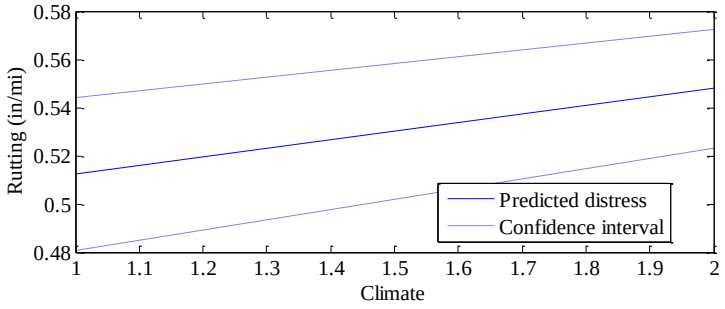

Figure B-76 Predicted rutting for climate

Inputs interaction effect

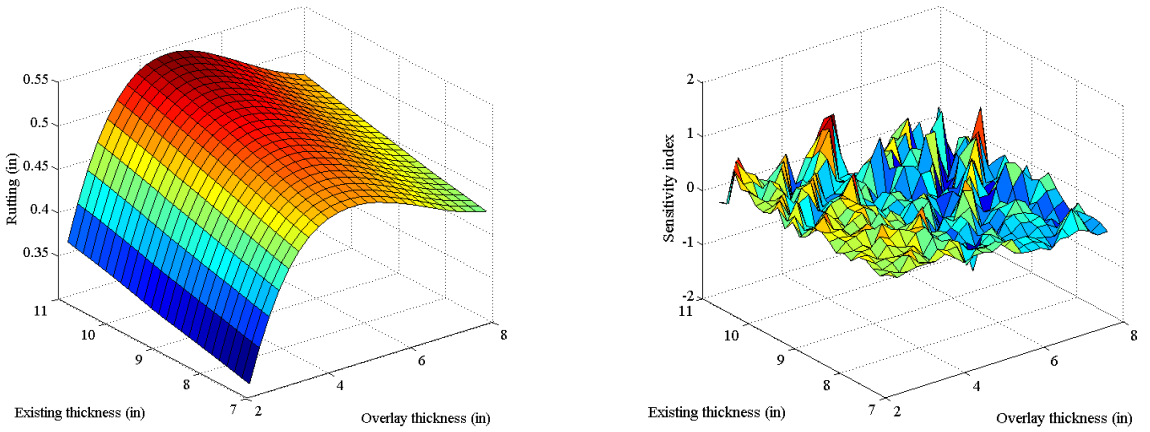

Figure B-77 Predicted interaction and NSI between existing thickness and overlay thickness

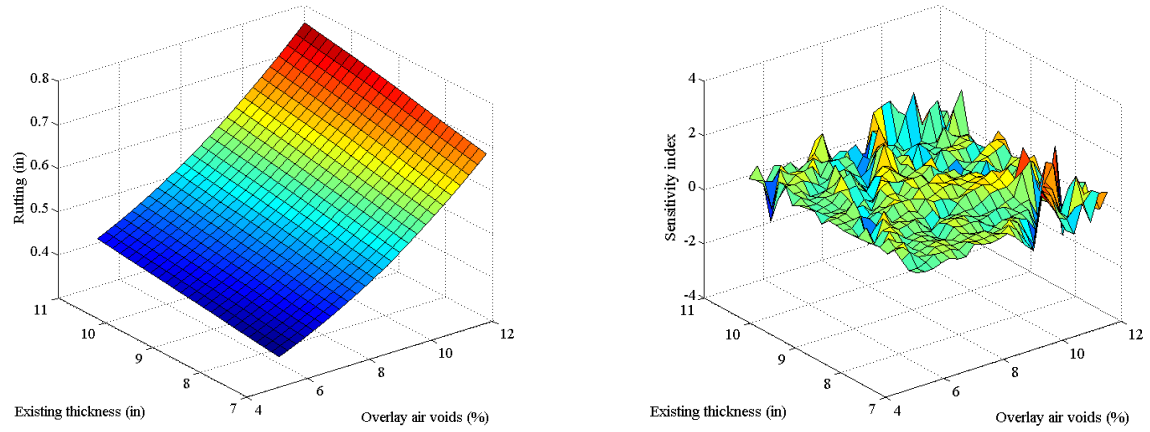

Figure B-78 Predicted interaction and NSI between existing thickness and overlay air voids

B.1.7 IRI

Inputs main effect

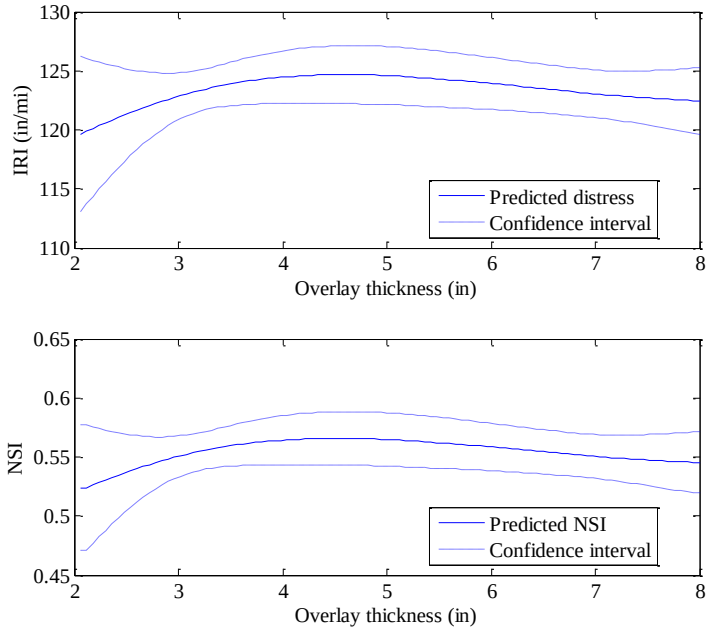

Figure B-79 Predicted IRI and NSI for overlay thickness

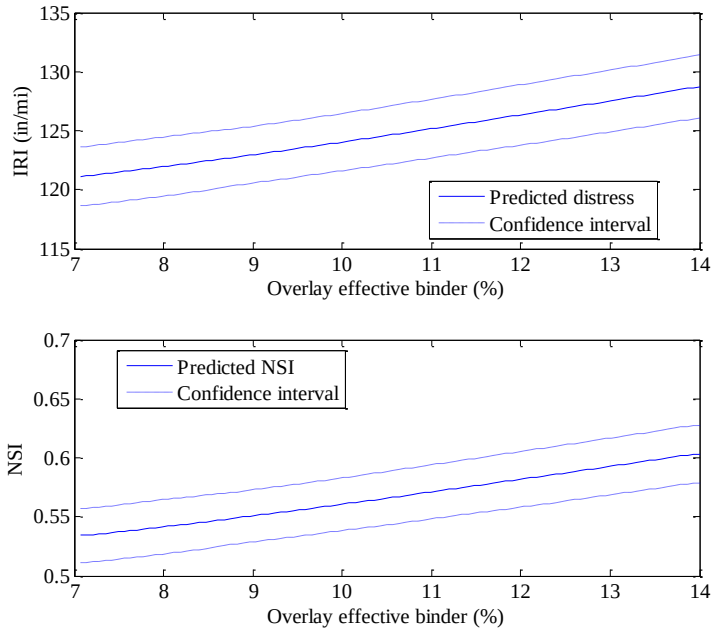

Figure B-80 Predicted IRI and NSI for overlay effective binder

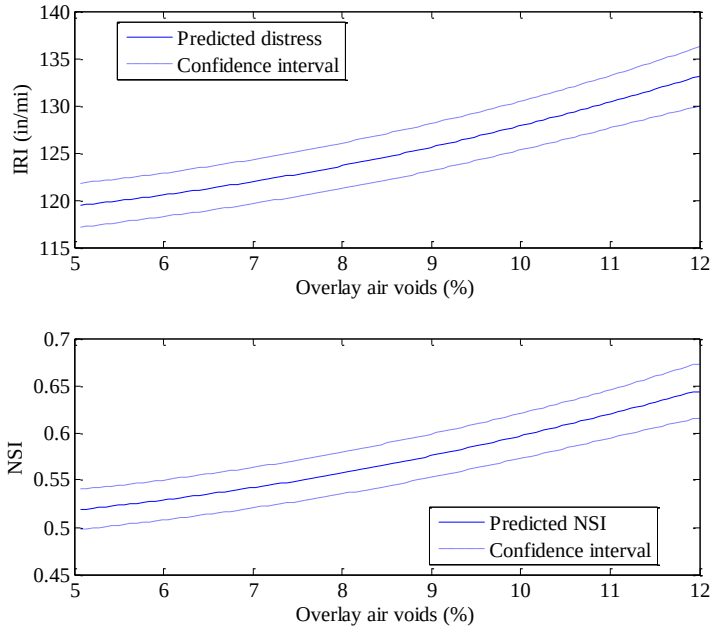

Figure B-81 Predicted IRI and NSI for overlay air voids

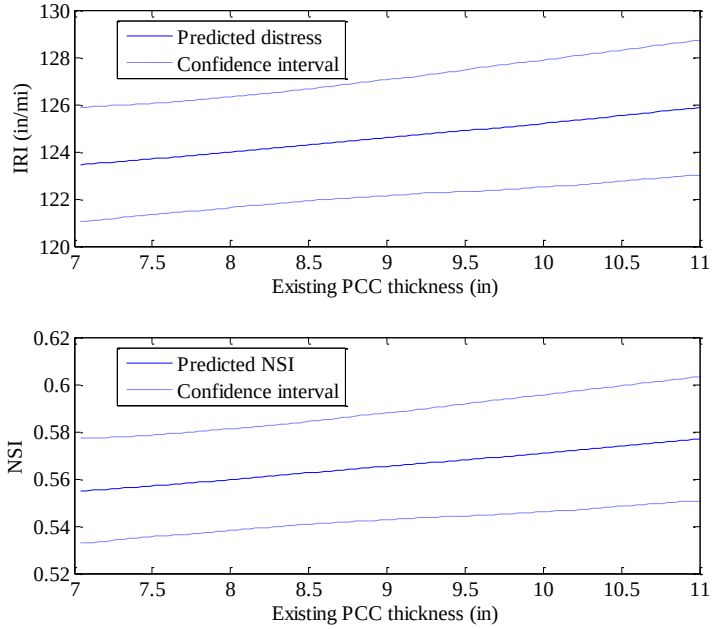

Figure B-82 Predicted IRI and NSI for existing PCC thickness

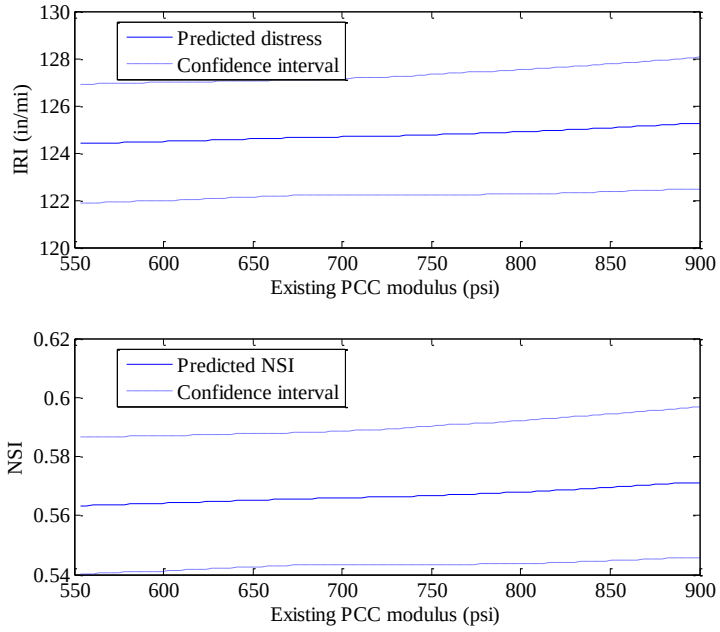

Figure B-83 Predicted IRI and NSI for existing PCC modulus

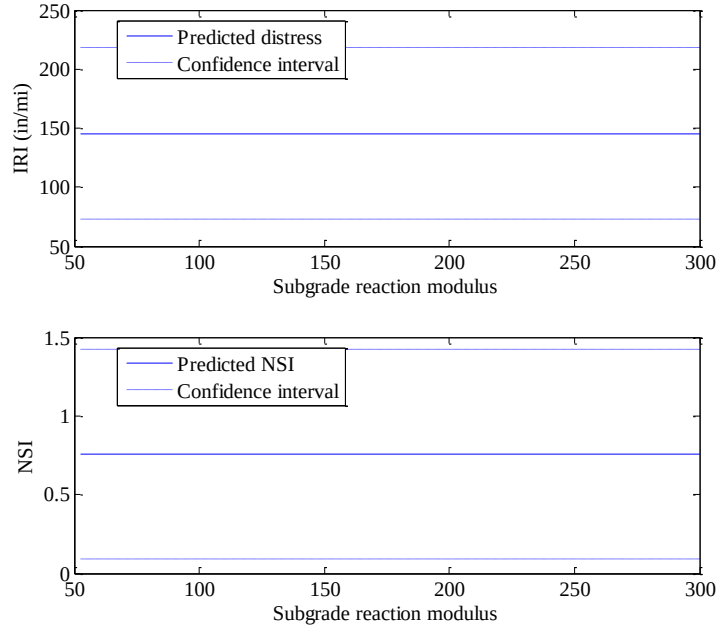

Figure B-84 Predicted IRI and NSI for subgrade reaction modulus

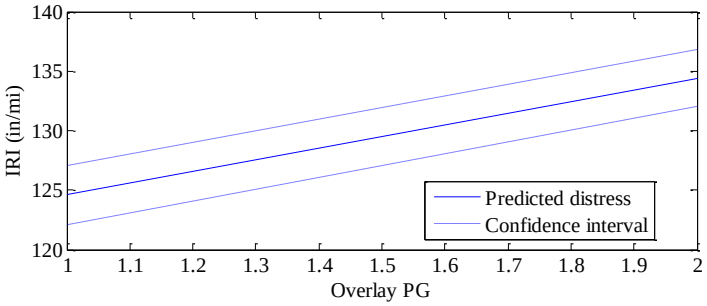

Figure B-85 Predicted IRI for overlay PG

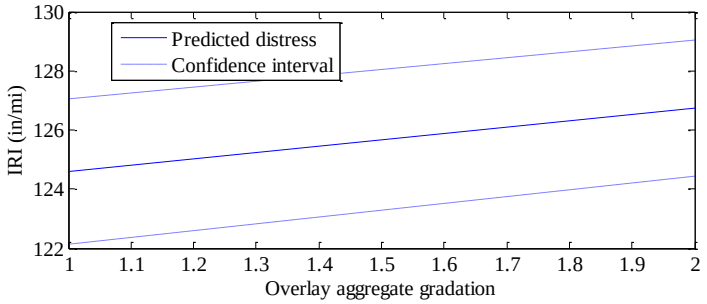

Figure B-86 Predicted IRI for overlay aggregate gradation

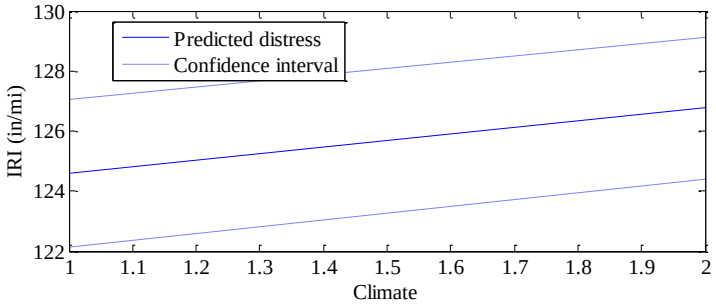

Figure B-87 Predicted IRI for climate

B.3 RUBBLIZED OVERLAYS

B.1.8 Alligator cracking

Inputs main effect

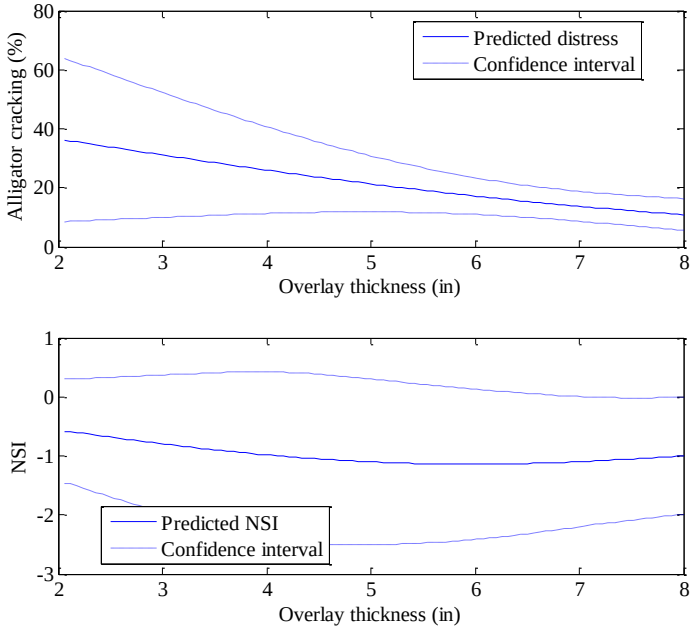

Figure B-88 Predicted alligator cracking and NSI for overlay thickness

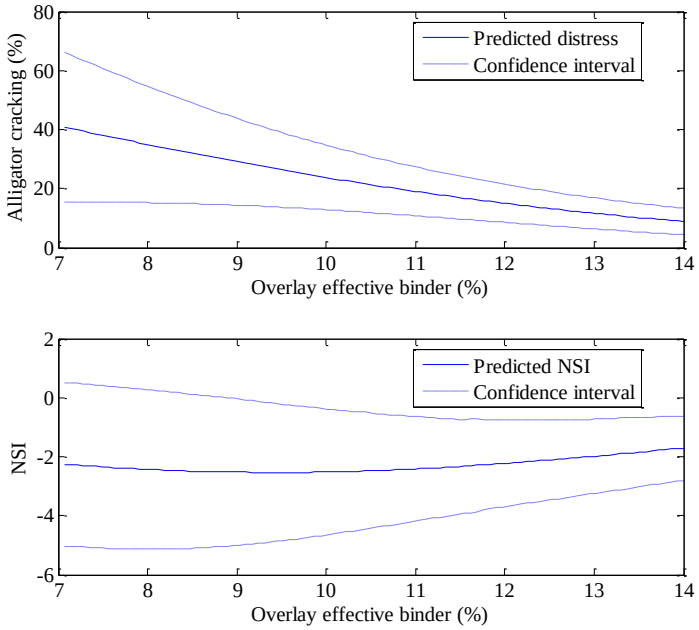

Figure B-89 Predicted alligator cracking and NSI for overlay effective binder

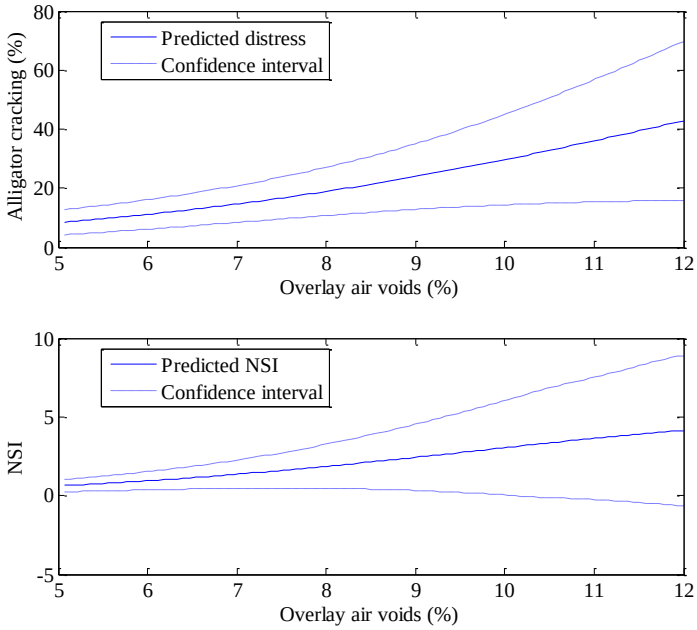

Figure B-90 Predicted alligator cracking and NSI for overlay air voids

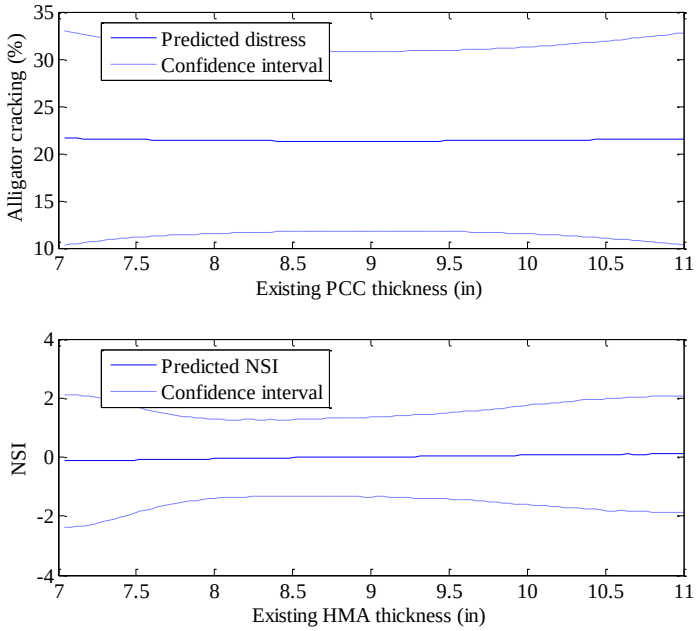

Figure B-91 Predicted alligator cracking and NSI for existing PCC thickness

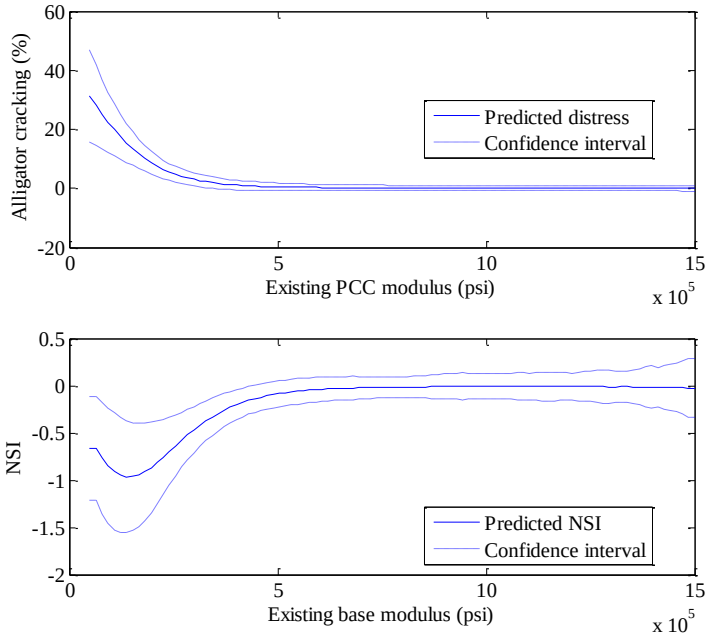

Figure B-92 Predicted alligator cracking and NSI for existing PCC modulus

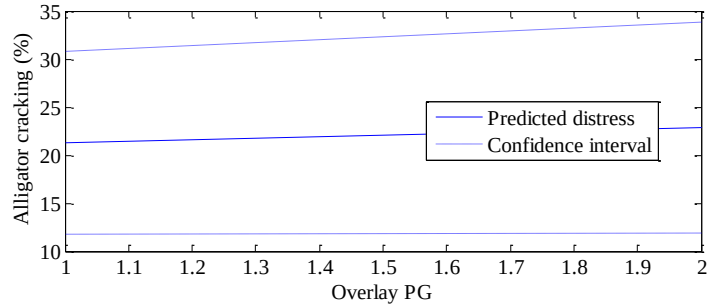

Figure B-93 Predicted alligator cracking for overlay PG

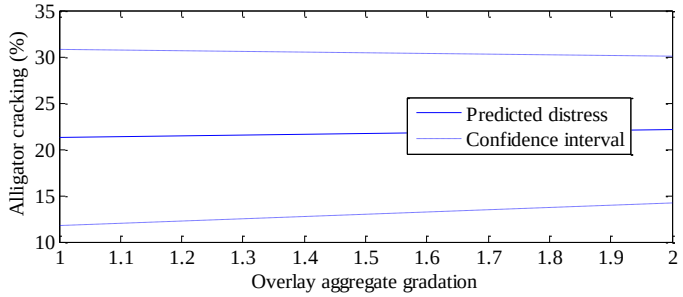

Figure B-94 Predicted alligator cracking for overlay aggregate gradation

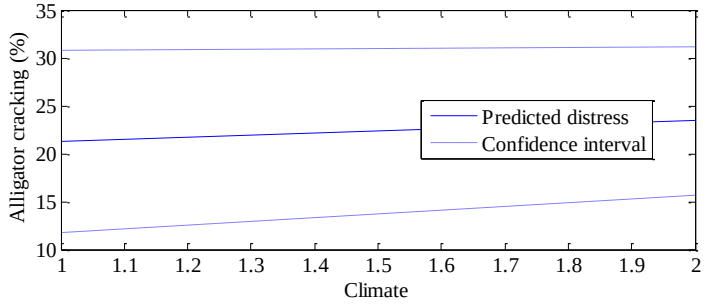

Figure B-95 Predicted alligator cracking for climate

Inputs interaction effect

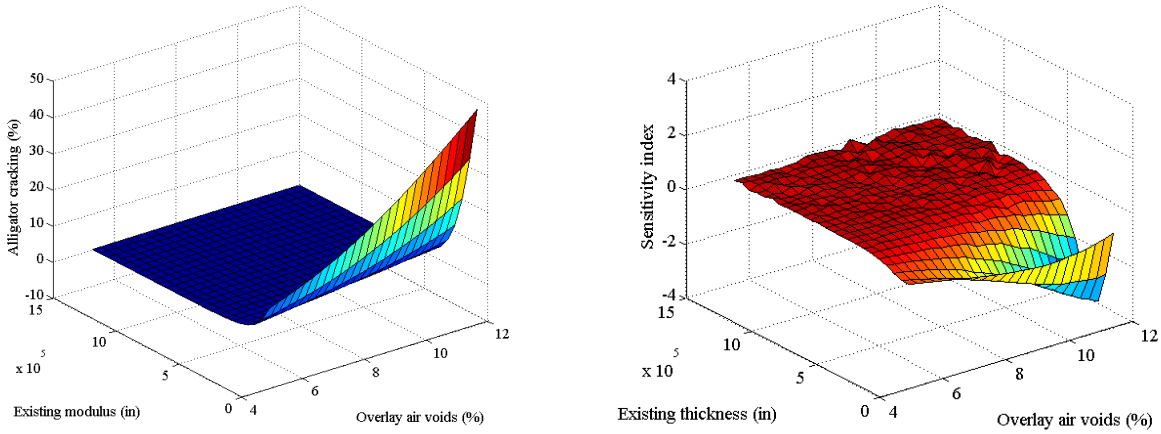

Figure B-96 Predicted interaction and NSI between existing modulus and overlay air voids

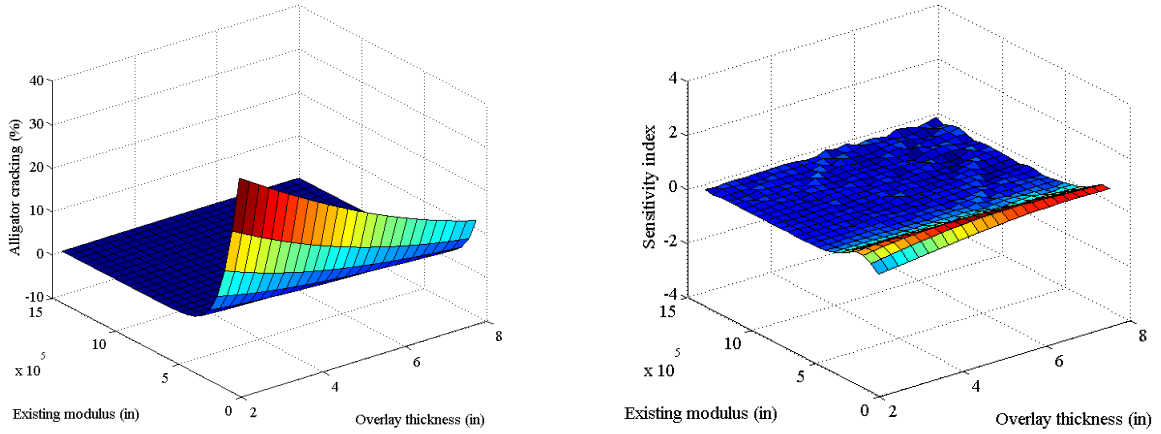

Figure B-97 Predicted interaction and NSI between existing modulus and overlay thickness

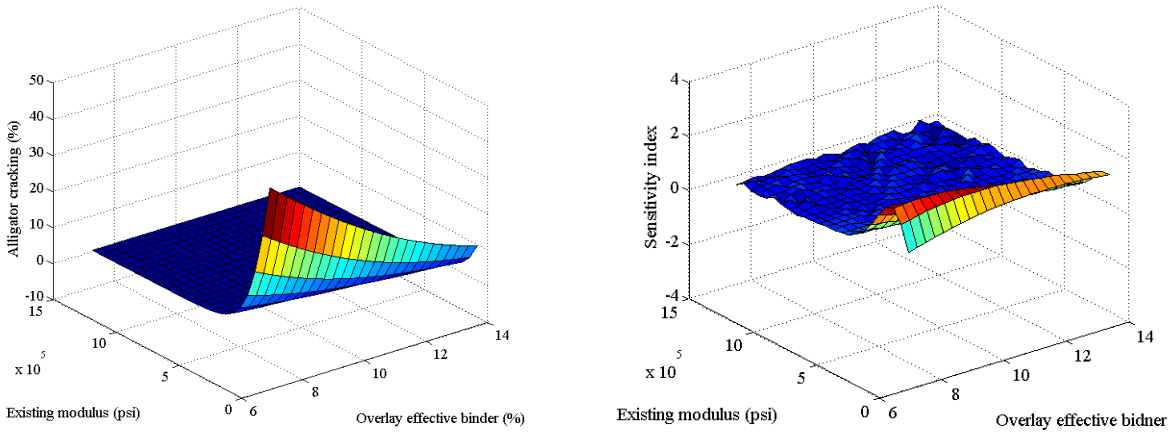

Figure B-98 Predicted interaction and NSI between existing modulus and overlay effective binder

B.1.9 Longitudinal cracking

Inputs main effect

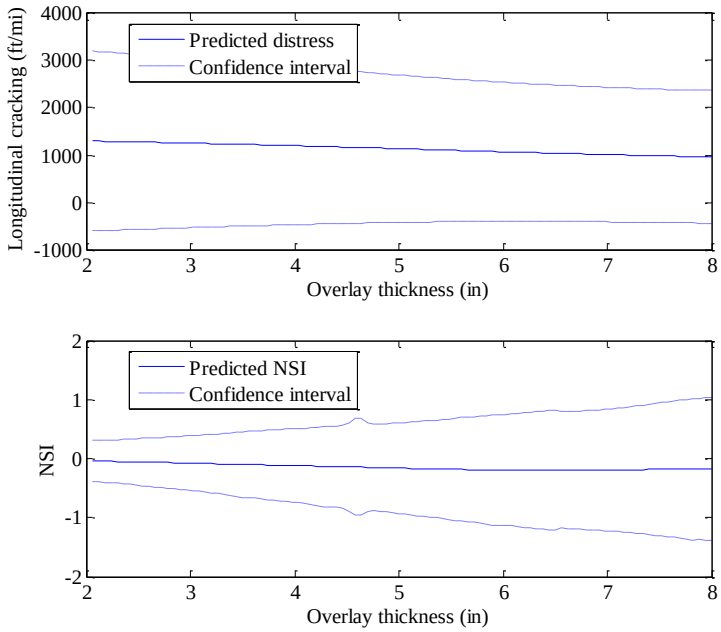

Figure B-99 Predicted longitudinal cracking and NSI for overlay thickness

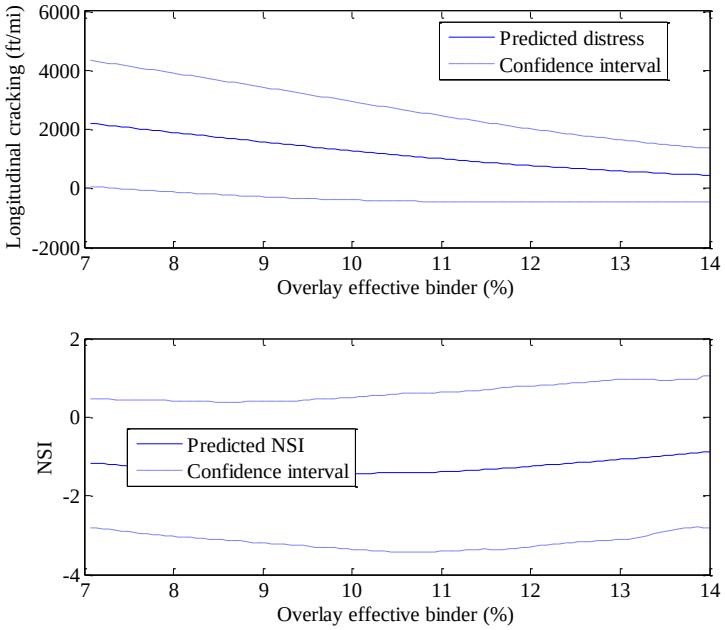

Figure B-100 Predicted longitudinal cracking and NSI for overlay effective binder

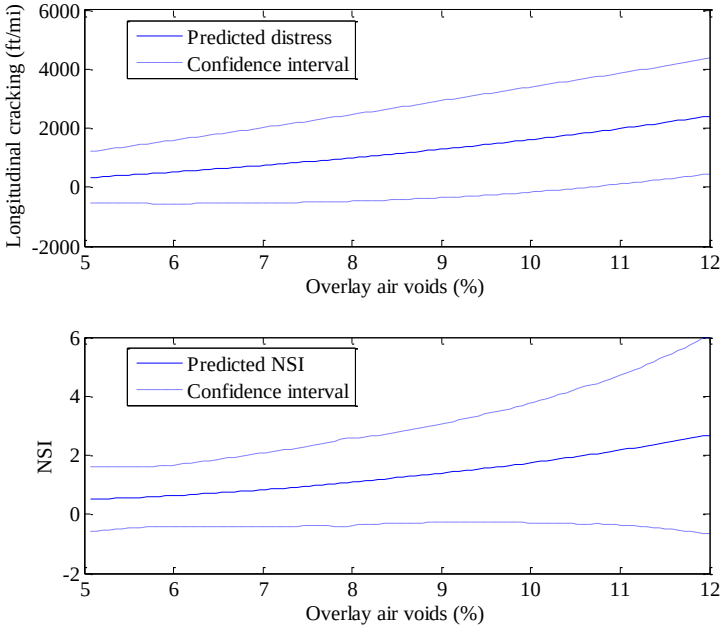

Figure B-101 Predicted longitudinal cracking and NSI for overlay air voids

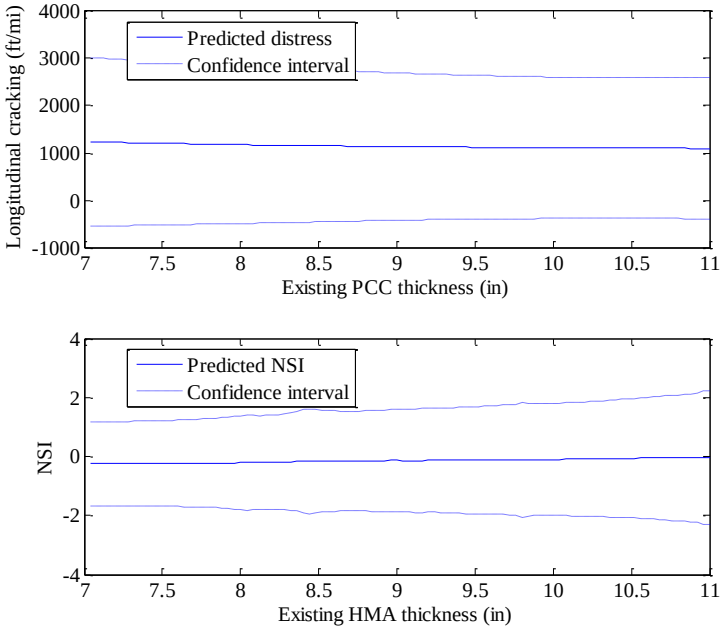

Figure B-102 Predicted longitudinal cracking and NSI for existing PCC thickness

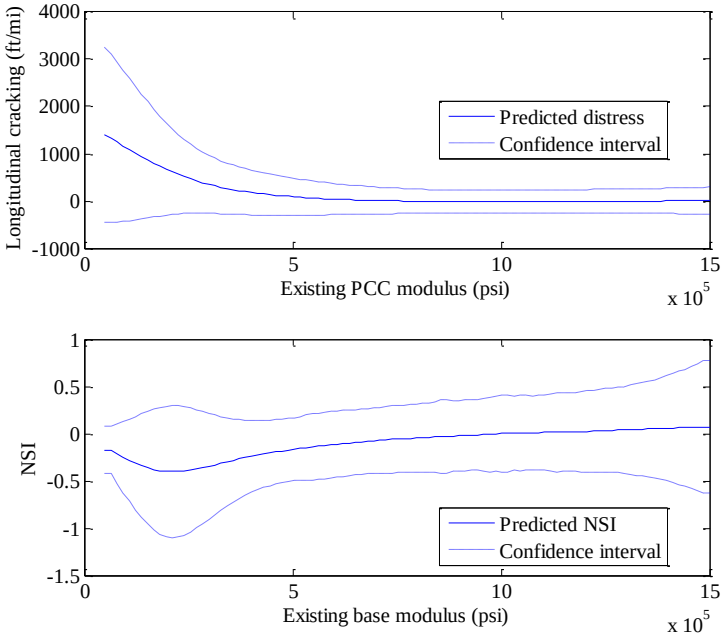

Figure B-103 Predicted longitudinal cracking and NSI for existing PCC modulus

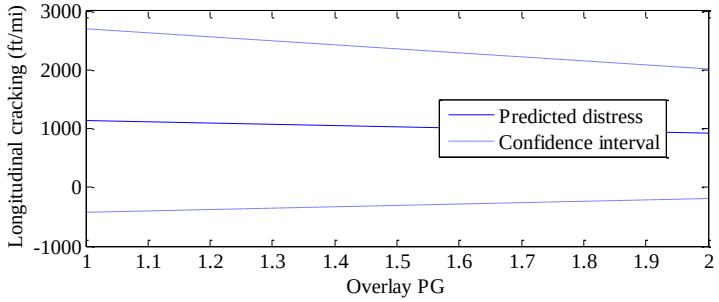

Figure B-104 Predicted longitudinal cracking and NSI for overlay PG

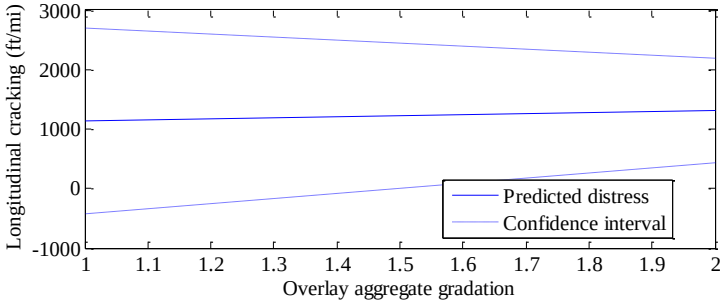

Figure B-105 Predicted longitudinal cracking and NSI for overlay aggregate gradation

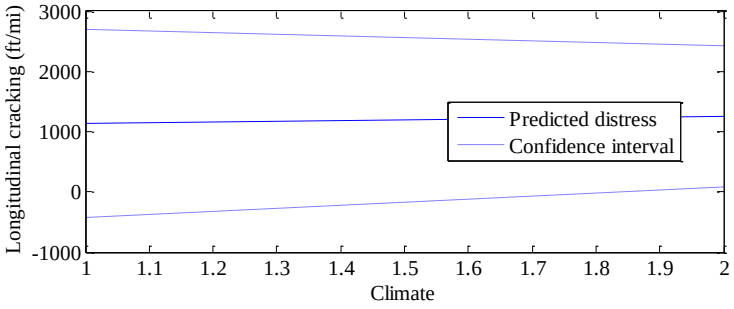

Figure B-106 Predicted longitudinal cracking and NSI for climate

Inputs interaction effect

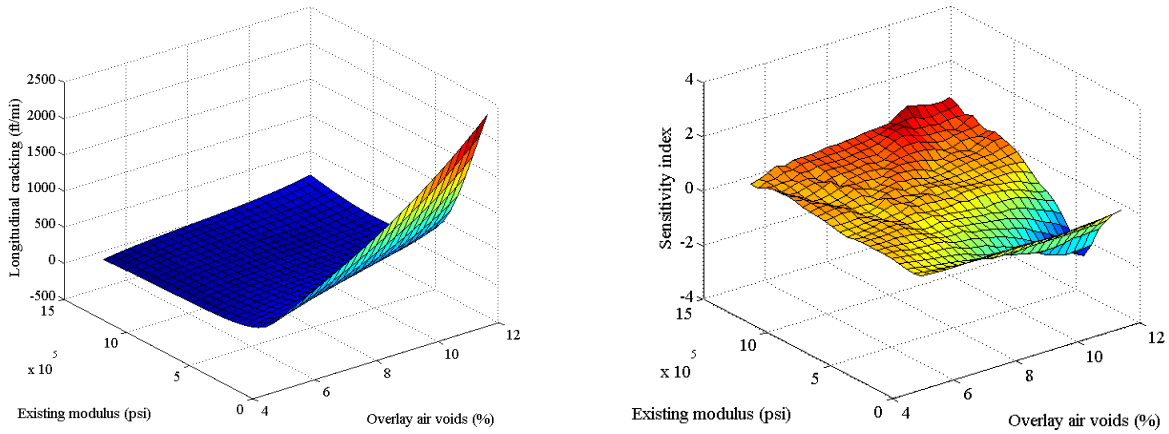

Figure B-107 Predicted interaction and NSI between existing modulus and overlay air voids

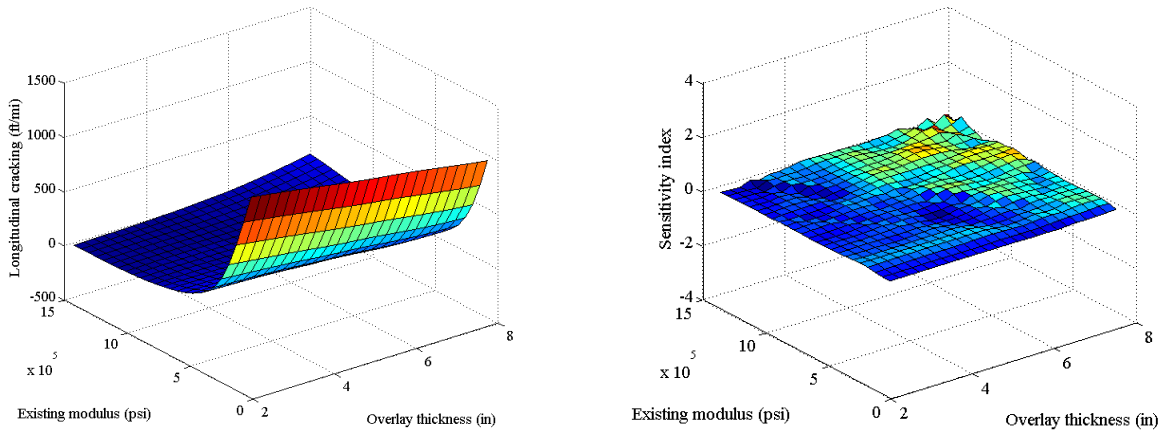

Figure B-108 Predicted interaction and NSI between existing modulus and overlay thickness

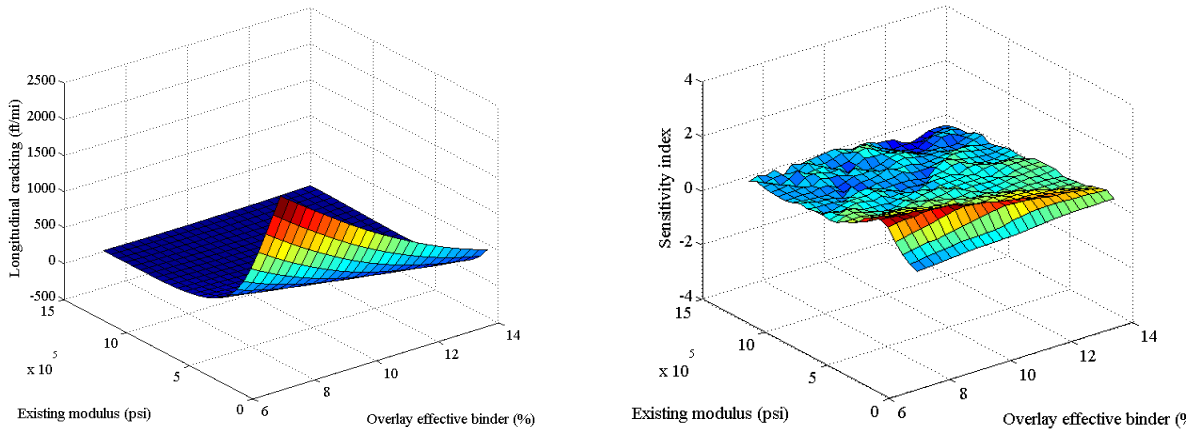

Figure B-109 Predicted interaction and NSI between existing modulus and overlay effective binder

B.1.10 Rutting

Inputs main effect

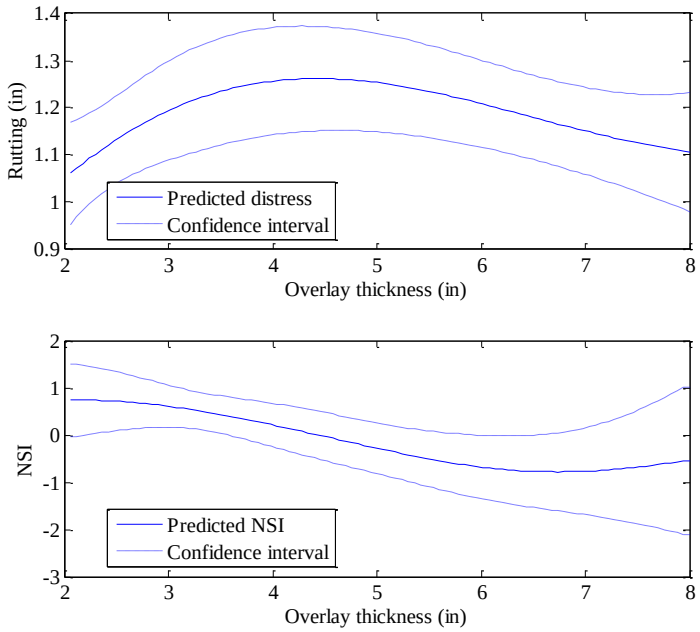

Figure B-110 Predicted rutting and NSI for overlay thickness

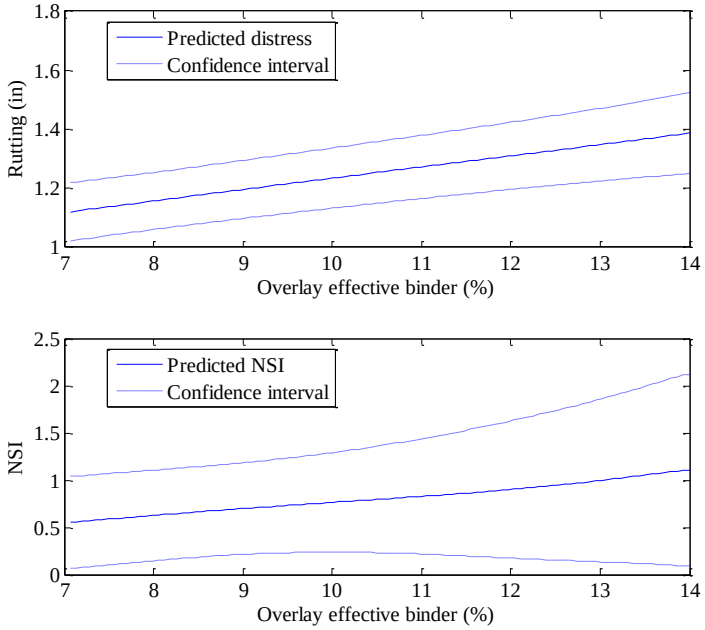

Figure B-111 Predicted rutting and NSI for overlay effective binder

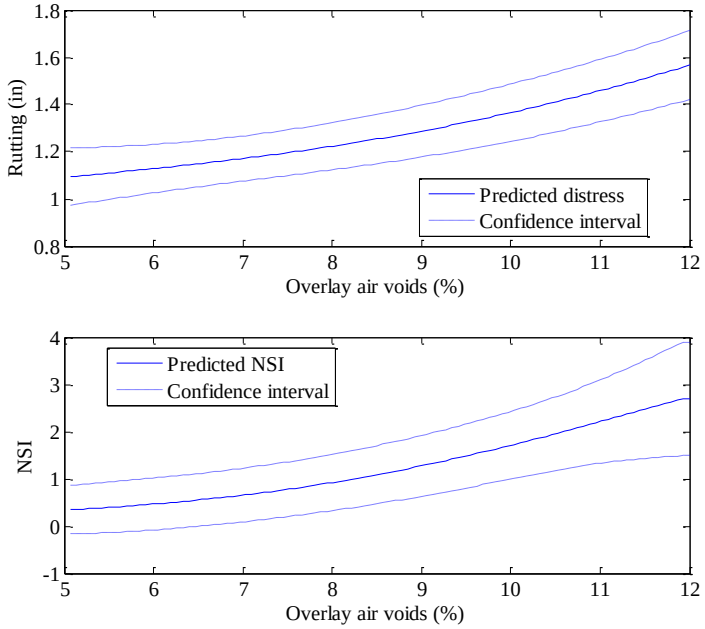

Figure B-112 Predicted rutting and NSI for overlay air voids

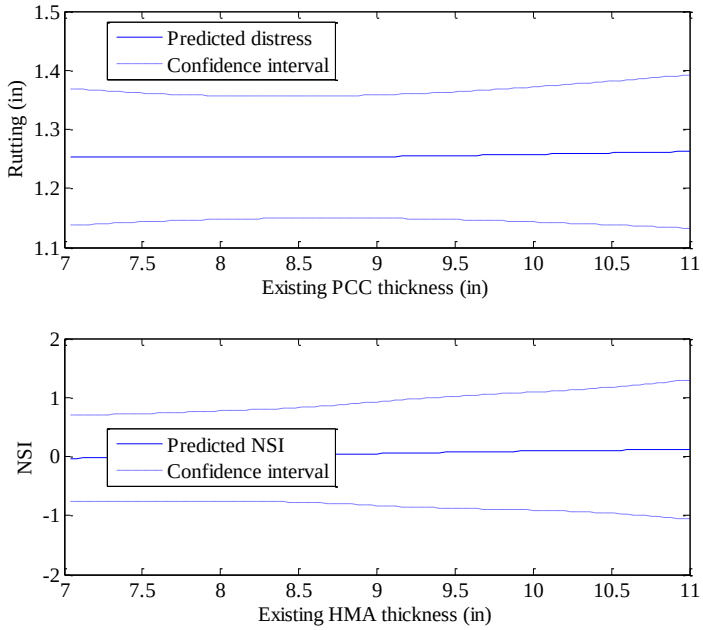

Figure B-113 Predicted rutting and NSI for existing PCC thickness

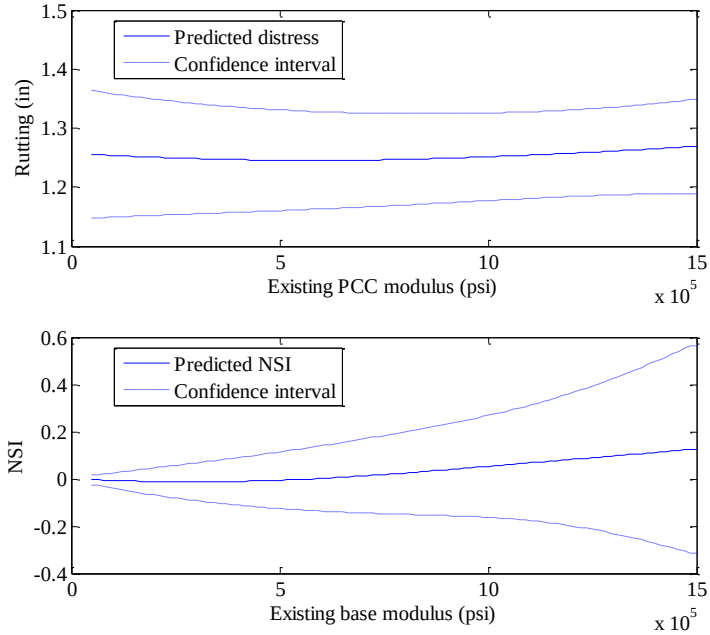

Figure B-114 Predicted rutting and NSI for existing PCC modulus

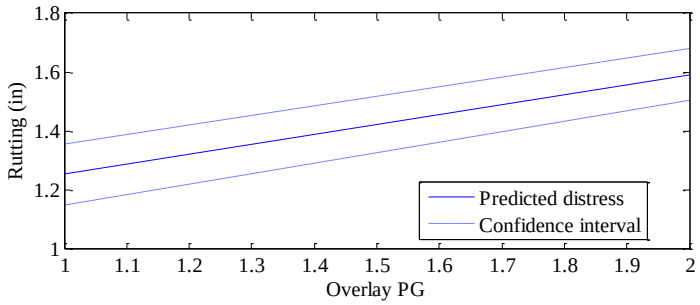

Figure B-115 Predicted rutting for overlay PG

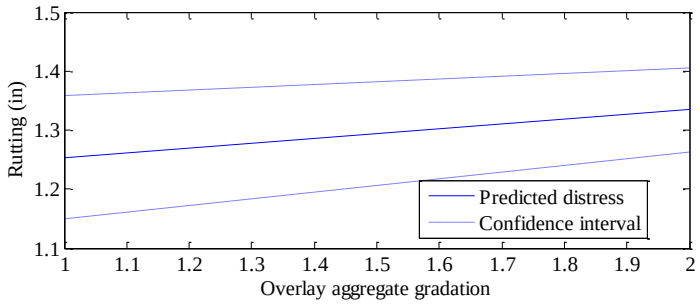

Figure B-116 Predicted rutting for overlay aggregate gradation

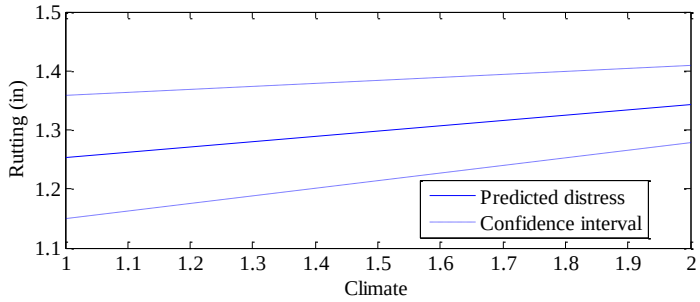

Figure B-117 Predicted rutting for climate

Inputs interaction effect

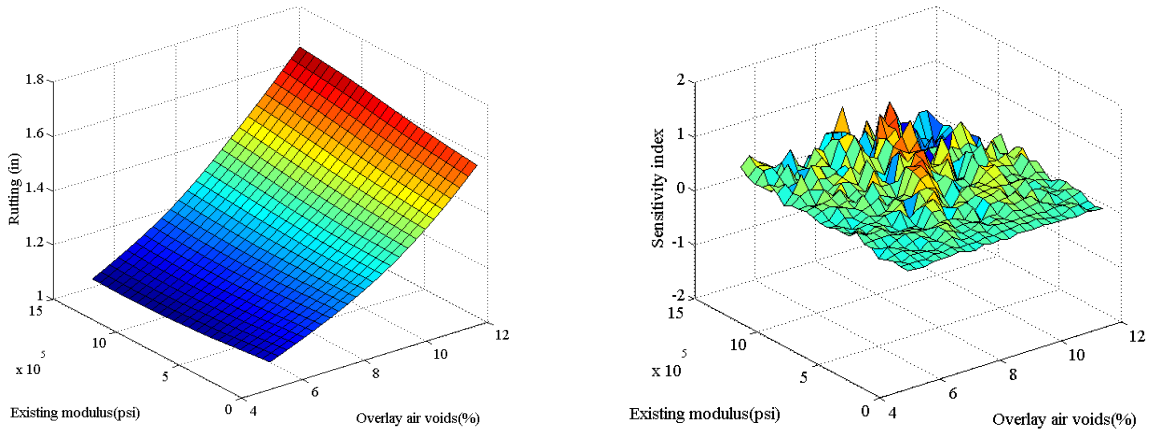

Figure B-118 Predicted interaction and NSI between existing modulus and overlay air voids

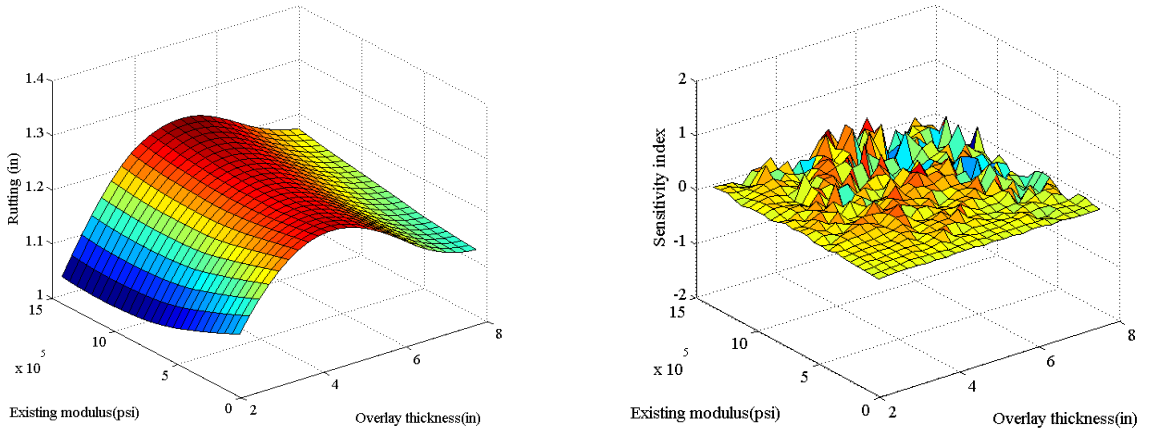

Figure B-119 Predicted interaction and NSI between existing modulus and overlay thickness

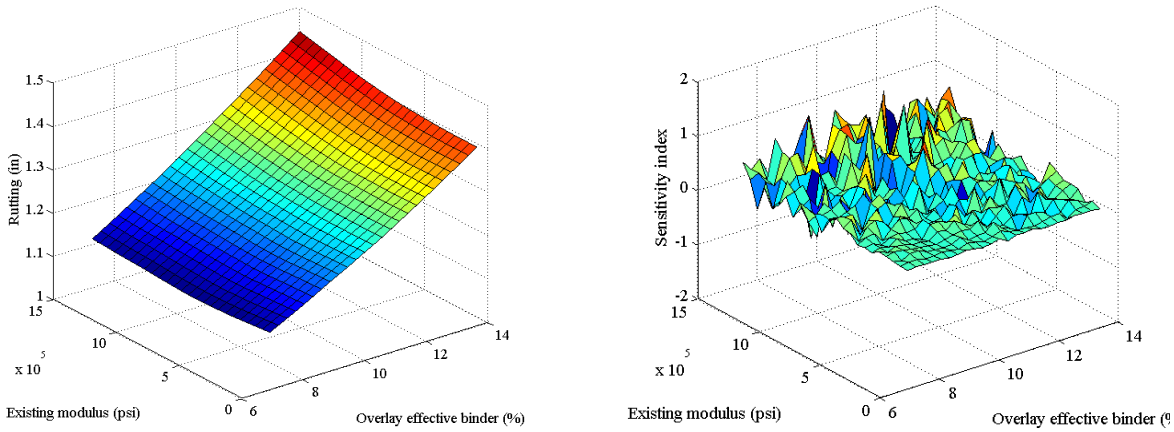

Figure B-120 Predicted interaction and NSI between existing modulus and overlay effective binder

B.1.11 IRI

Inputs main effect

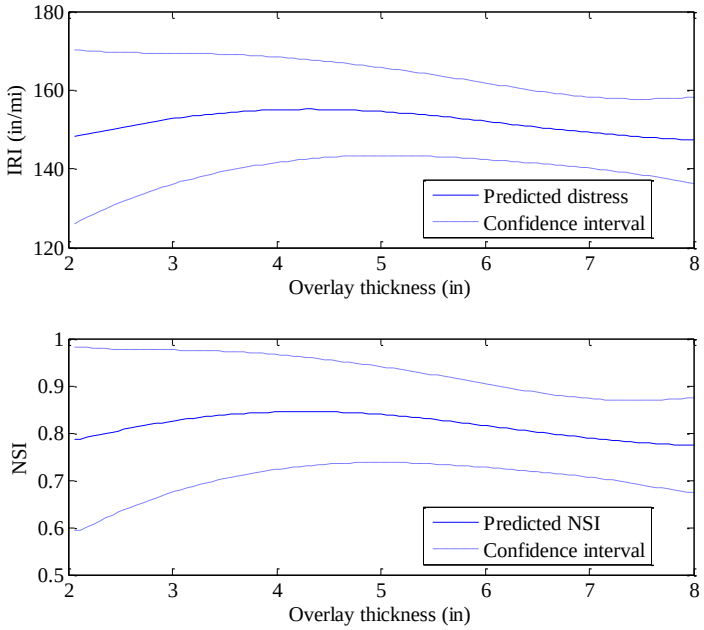

Figure B-121 Predicted IRI and NSI for overlay thickness

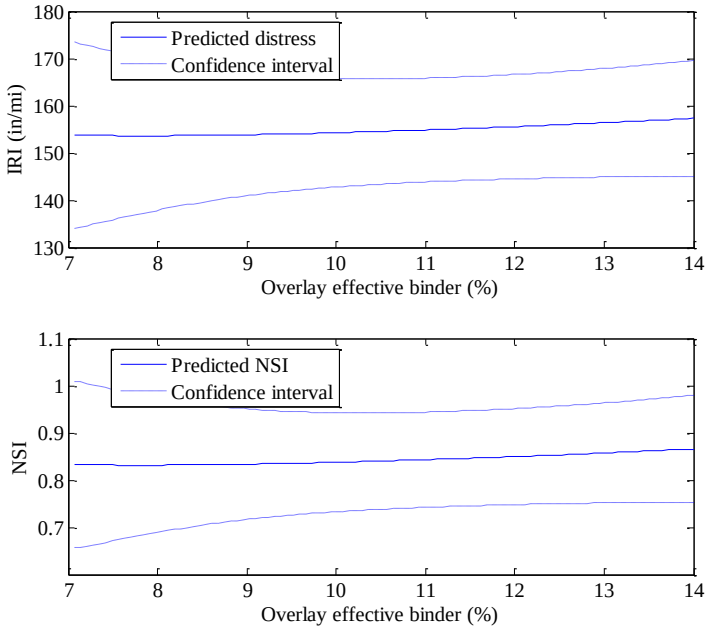

Figure B-122 Predicted IRI and NSI for overlay effective binder

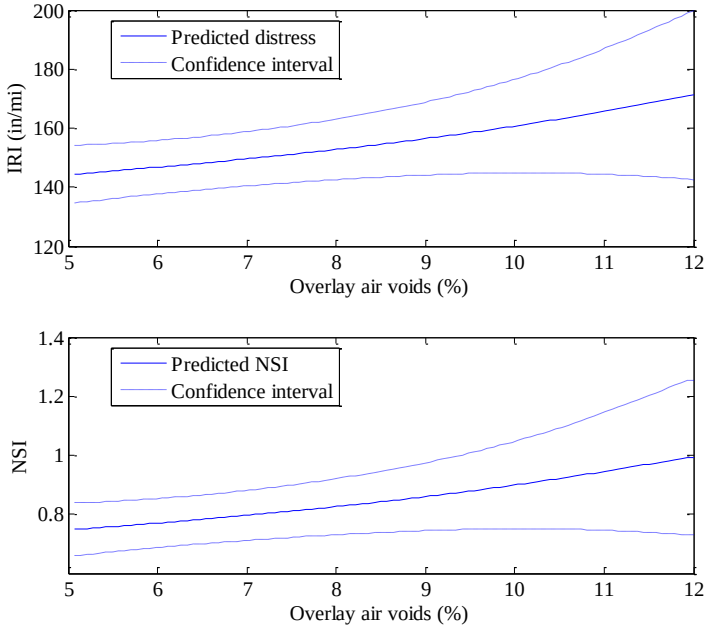

Figure B-123 Predicted IRI and NSI for overlay air voids

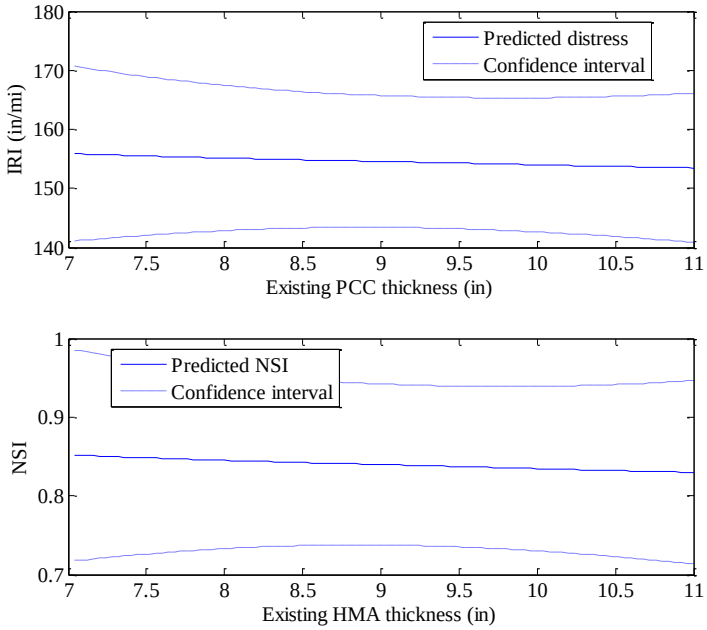

Figure B-124 Predicted IRI and NSI for existing PCC thickness

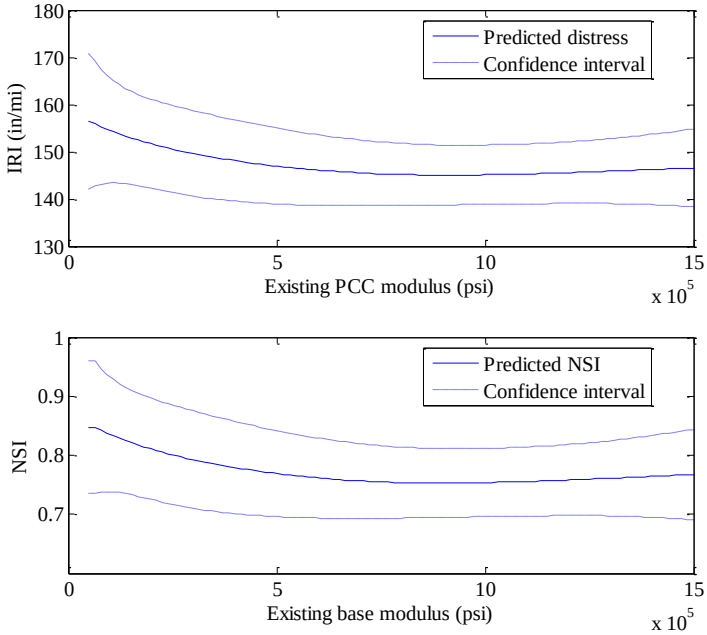

Figure B-125 Predicted IRI and NSI for existing PCC modulus

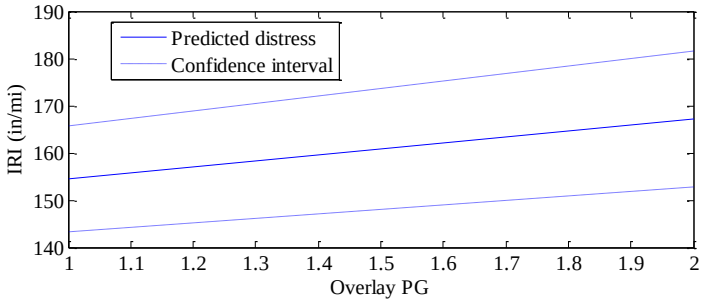

Figure B-126 Predicted IRI and NSI for overlay PG

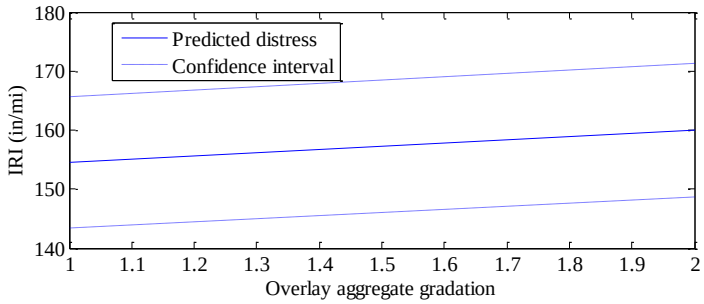

Figure B-127 Predicted IRI and NSI for overlay aggregate gradation

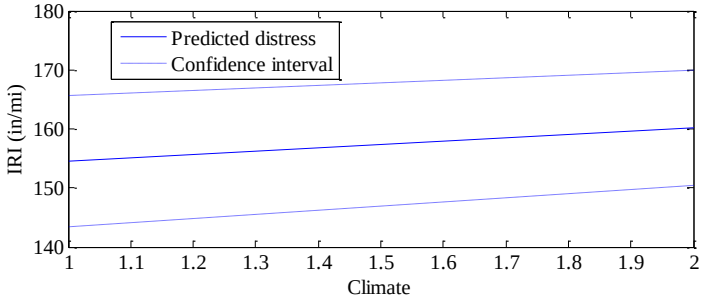

Figure B-128 Predicted IRI and NSI for climate

Inputs interaction effect

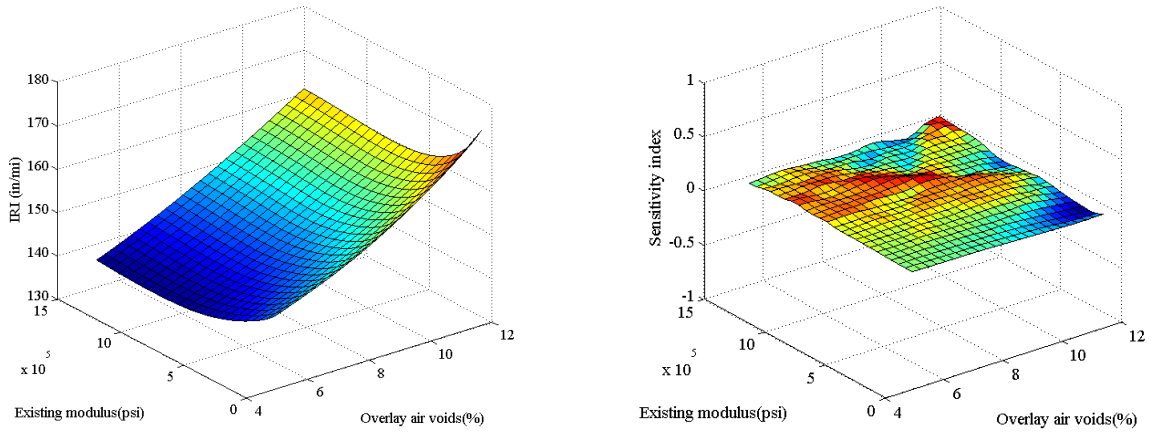

Figure B-129 Predicted interaction and NSI between existing modulus and overlay air voids

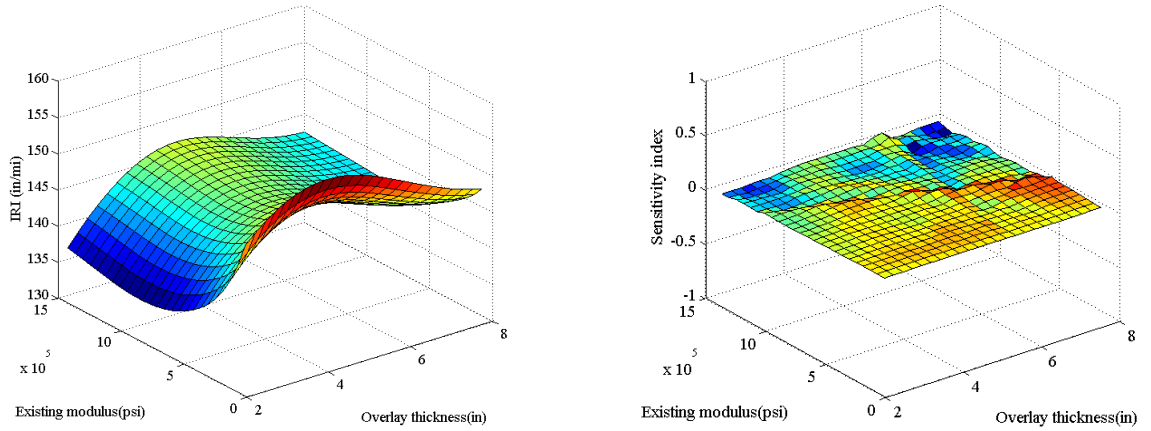

Figure B-130 Predicted interaction and NSI between existing modulus and overlay thickness

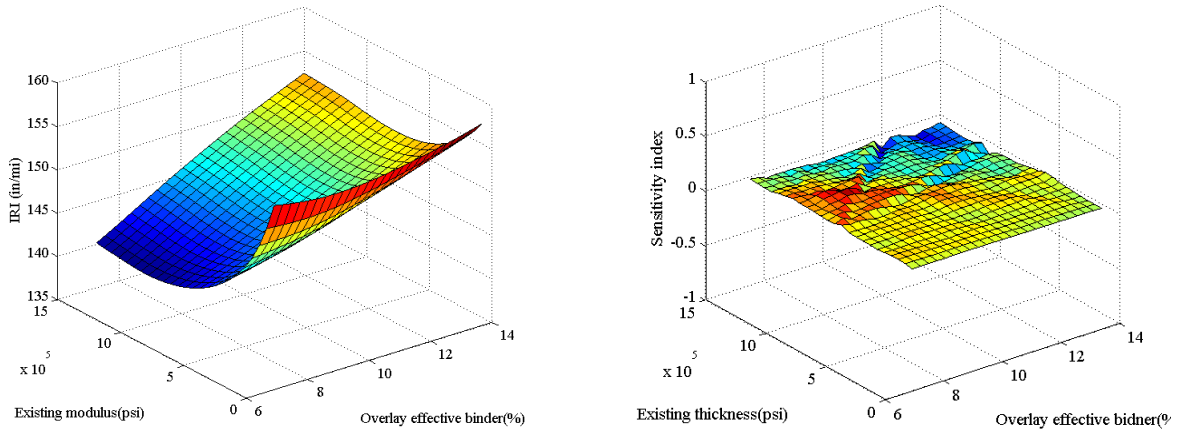

Figure B-131 Predicted interaction and NSI between existing modulus and overlay effective binder

B.4 UNBONDED OVERLAYS

B.1.12 Cracking

Inputs main effect

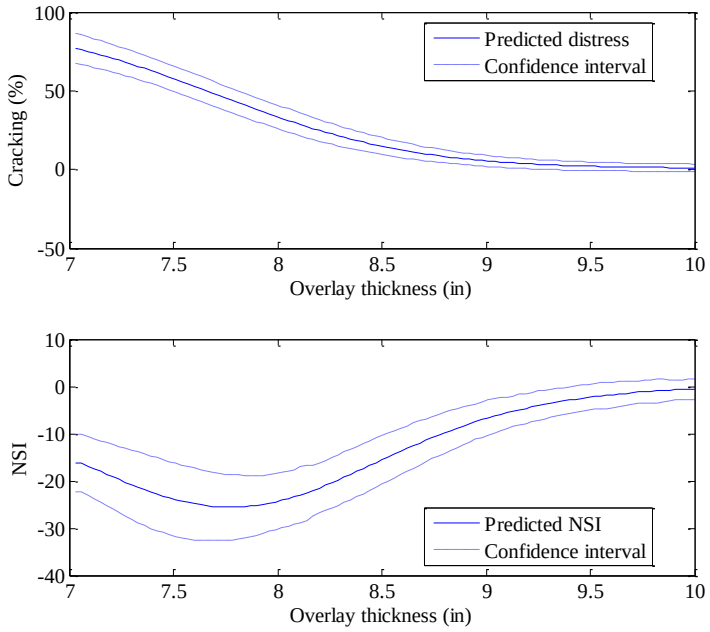

Figure B-132 Predicted cracking and NSI for overlay thickness

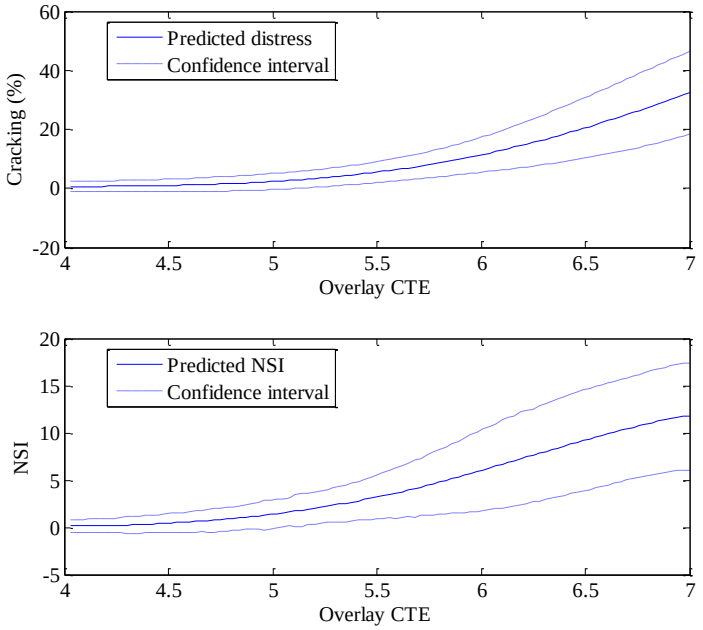

Figure B-133 Predicted cracking and NSI for overlay CTE

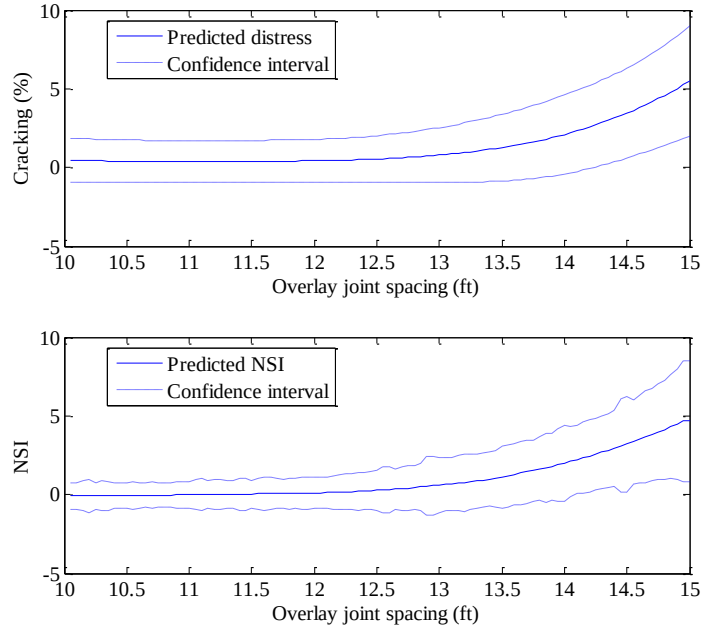

Figure B-134 Predicted cracking and NSI for overlay joint spacing

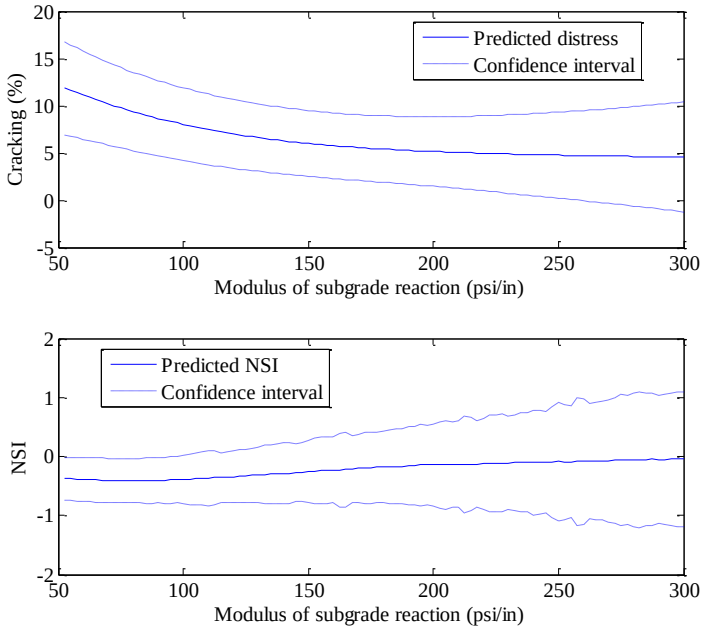

Figure B-135 Predicted cracking and NSI for modulus of subgrade reaction

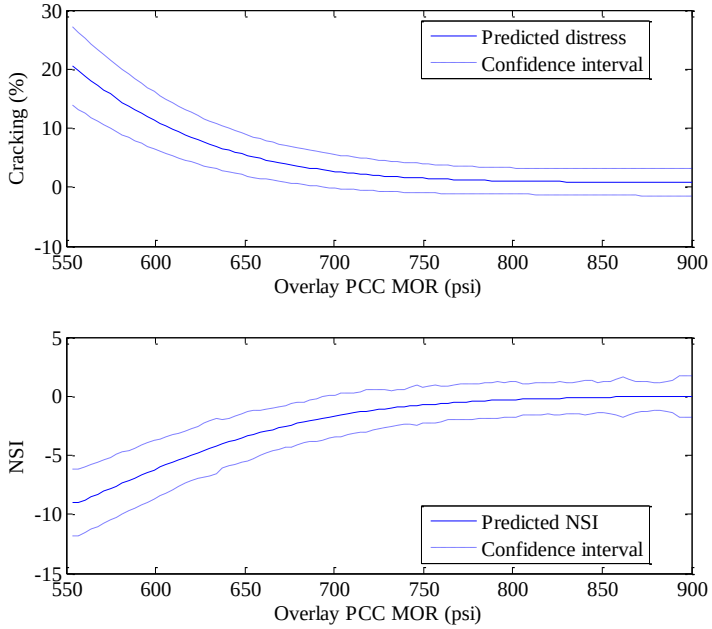

Figure B-136 Predicted cracking and NSI for overlay PCC MOR

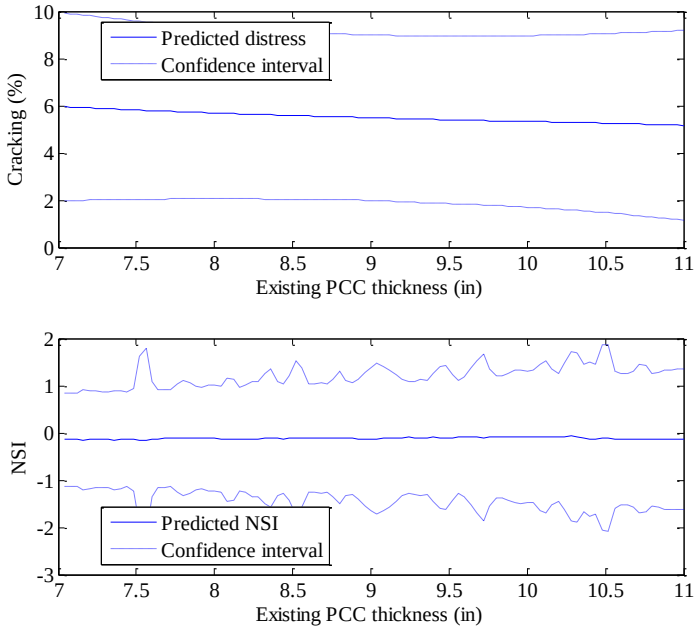

Figure B-137 Predicted cracking and NSI for existing PCC thickness

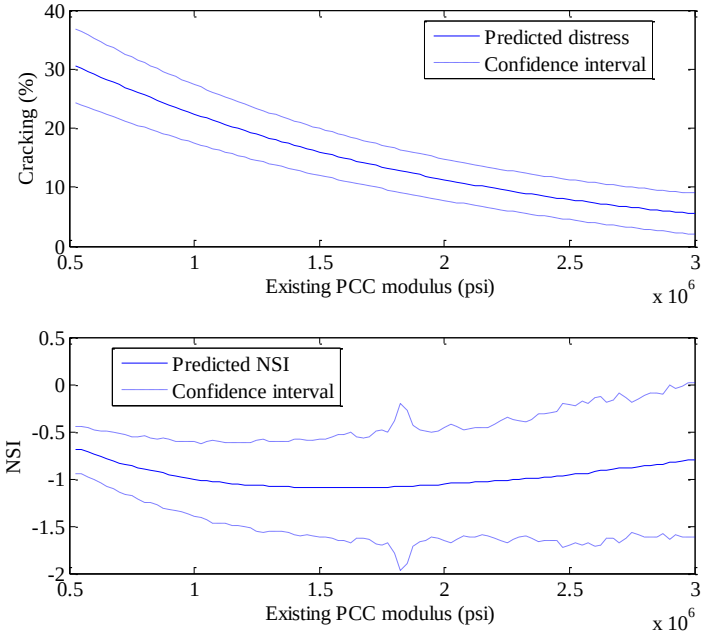

Figure B-138 Predicted cracking and NSI for existing PCC modulus

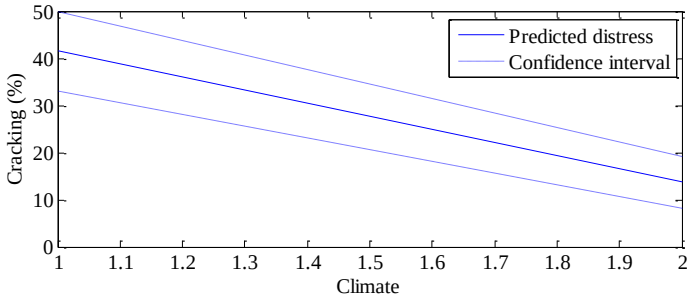

Figure B-139 Predicted cracking for climate

Inputs interaction effect

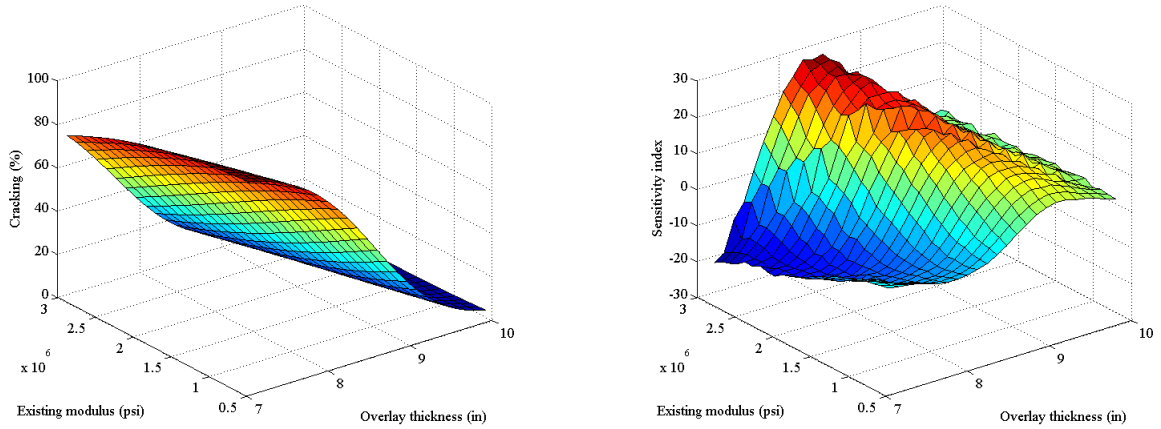

Figure B-140 Predicted interaction and NSI between existing modulus and overlay thickness

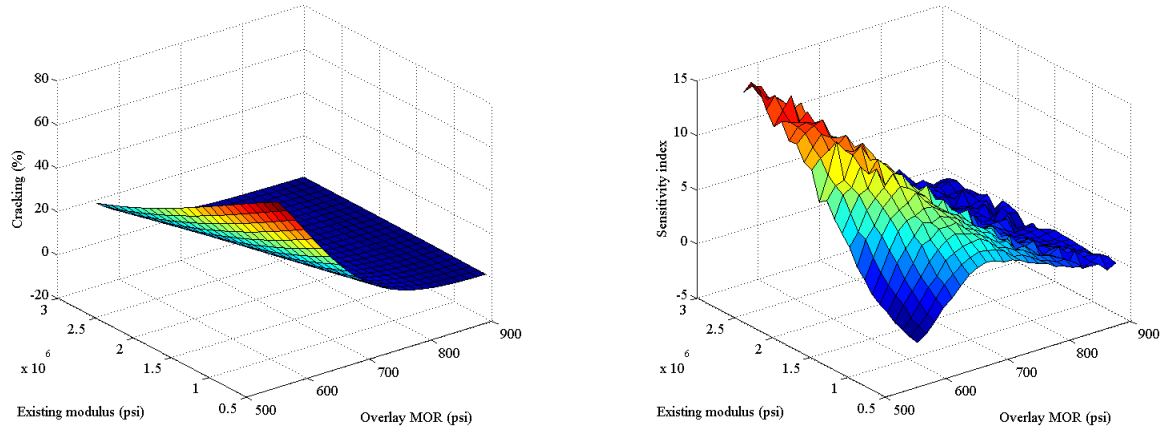

Figure B-141 Predicted interaction and NSI between existing thickness and overlay MOR

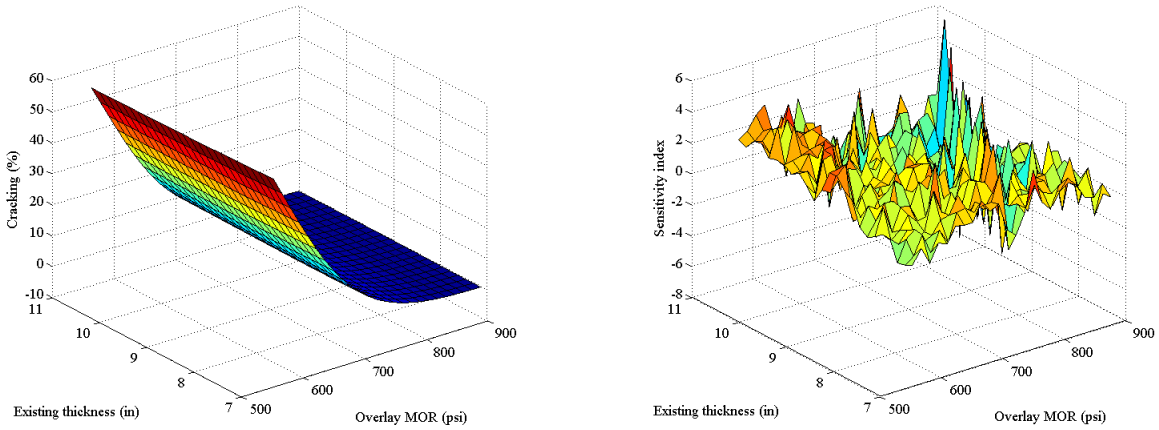

Figure B-142 Predicted interaction and NSI between existing thickness and overlay MOR

B.1.13 Faulting

Inputs main effect

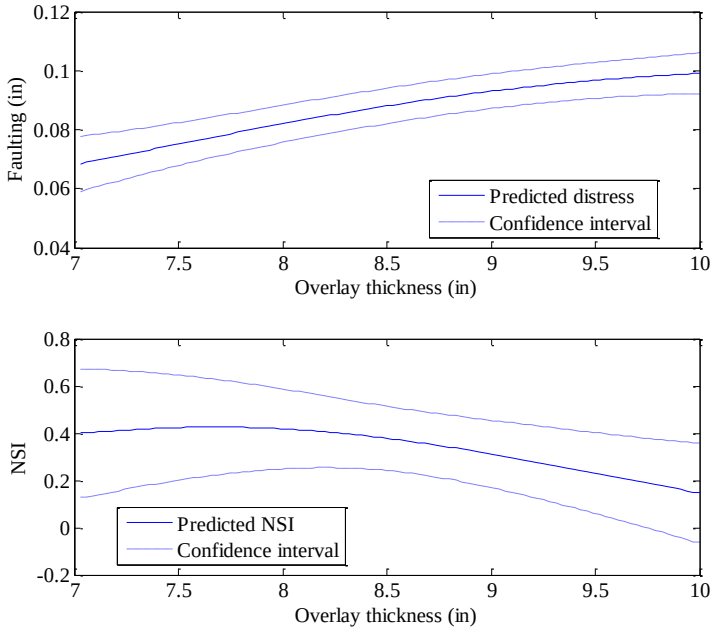

Figure B-143 Predicted faulting and NSI for overlay thickness

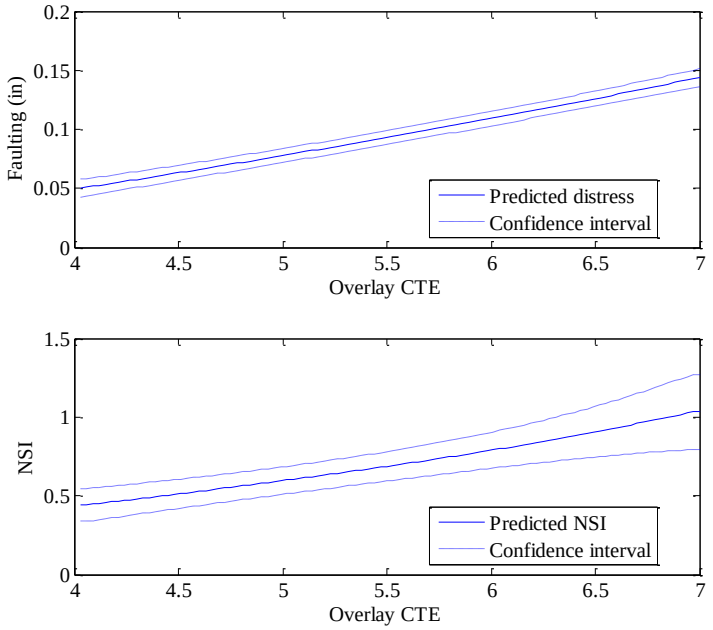

Figure B-144 Predicted faulting and NSI for overlay CTE

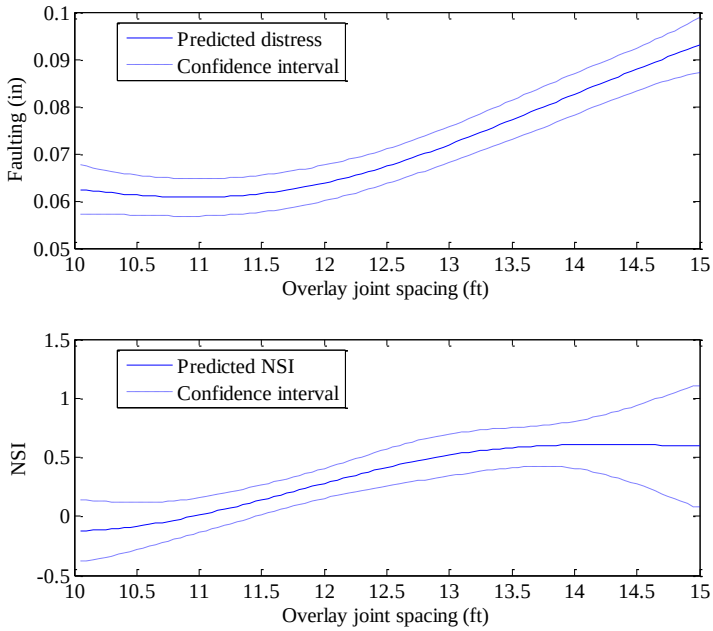

Figure B-145 Predicted faulting and NSI for overlay joint spacing

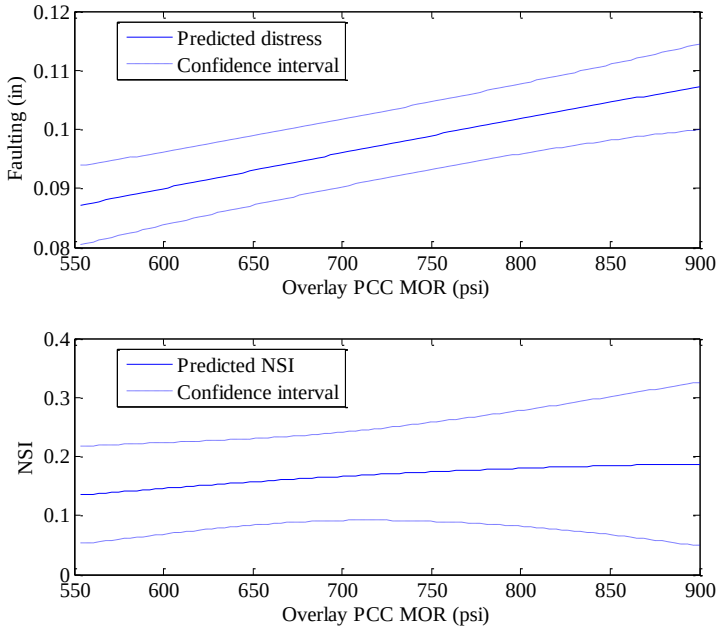

Figure B-146 Predicted faulting and NSI for overlay PCC MOR

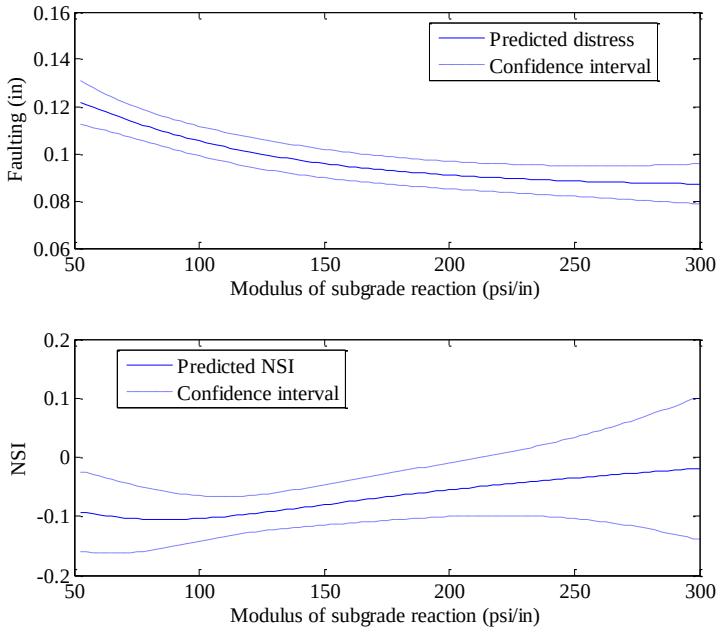

Figure B-147 Predicted faulting and NSI for modulus of subgrade reaction

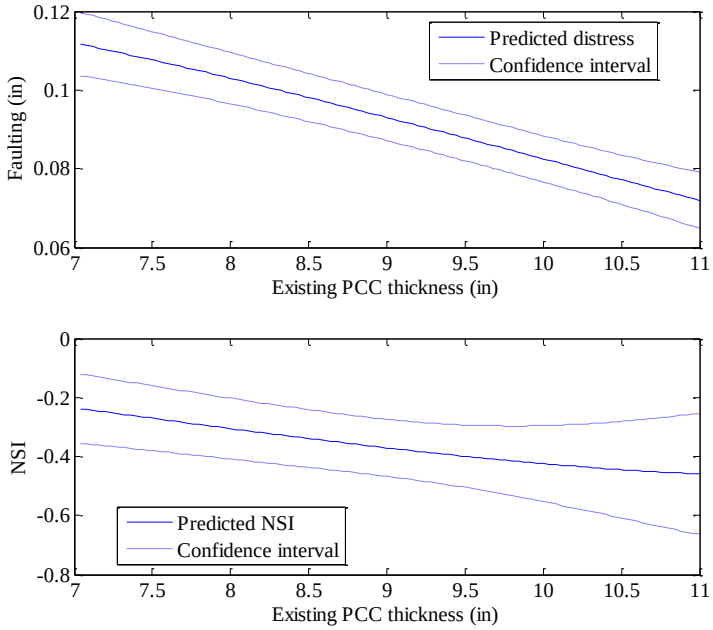

Figure B-148 Predicted faulting and NSI for PCC thickness

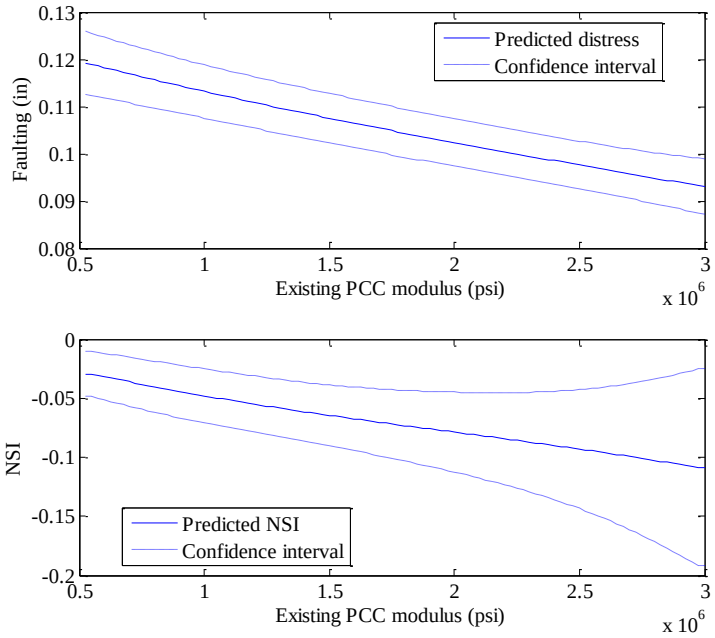

Figure B-149 Predicted faulting and NSI for PCC modulus

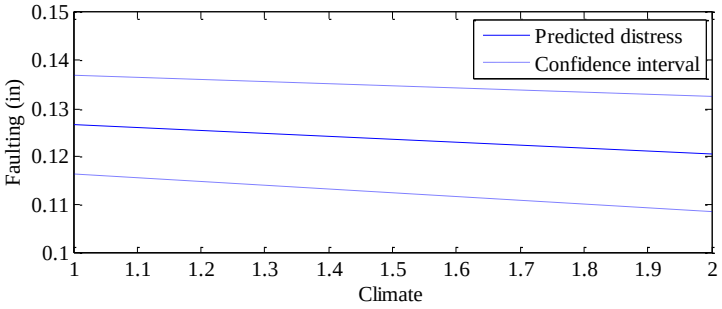

Figure B-150 Predicted faulting for climate

Inputs interaction effect

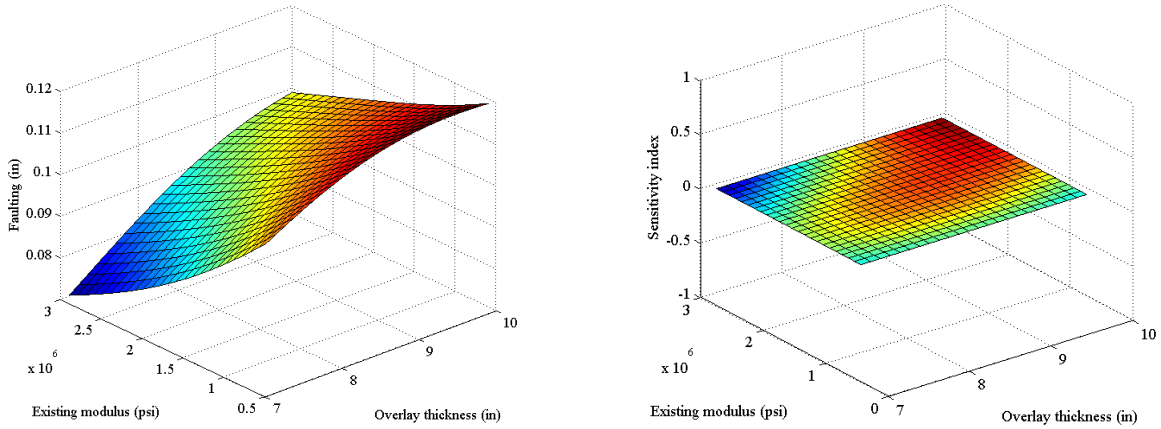

Figure B-151 Predicted interaction and NSI between existing modulus and overlay thickness

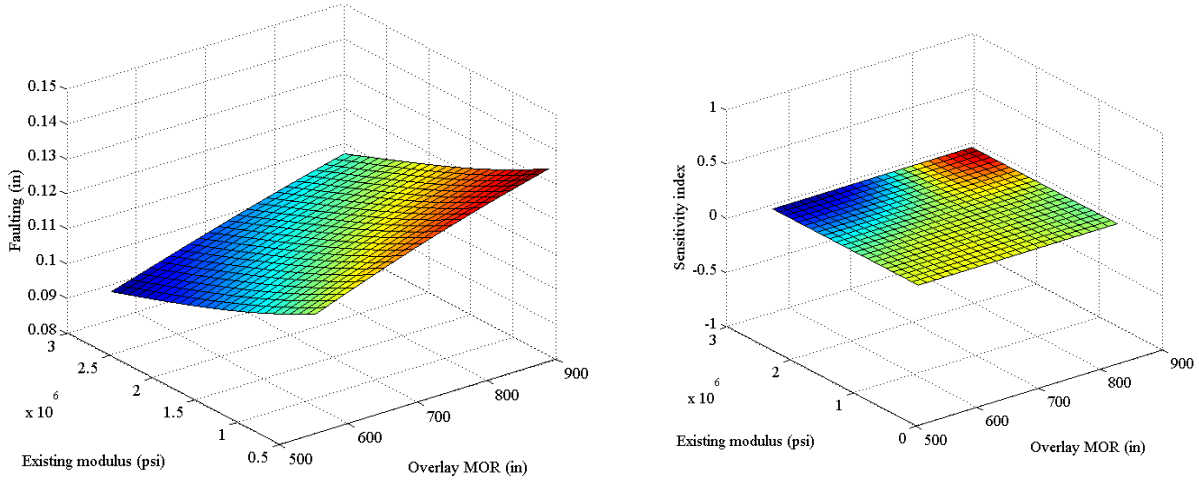

Figure B-152 Predicted interaction and NSI between existing thickness and overlay MOR

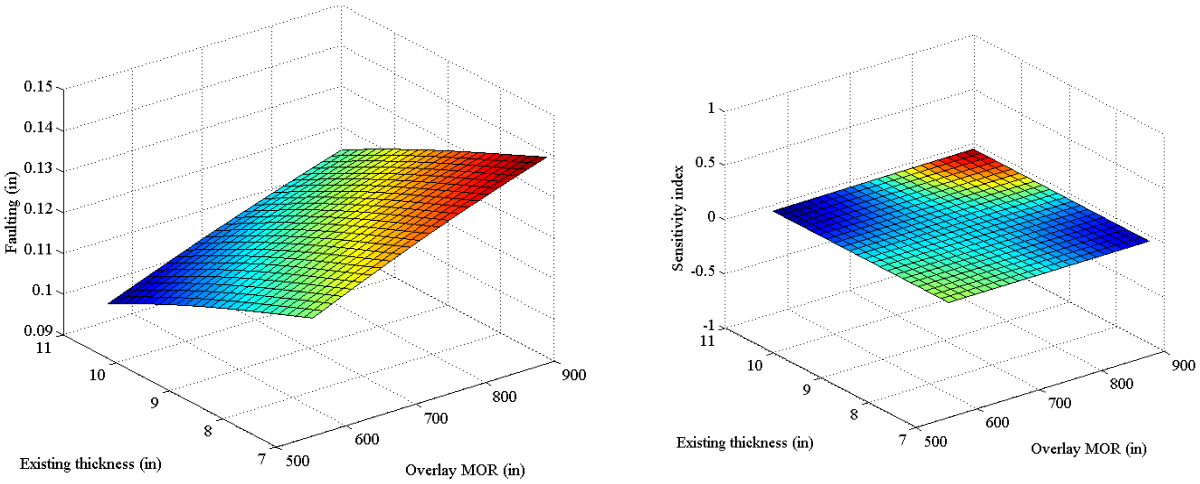

Figure B-153 Predicted interaction and NSI between existing thickness and overlay MOR

B.1.14 IRI

Inputs main effect

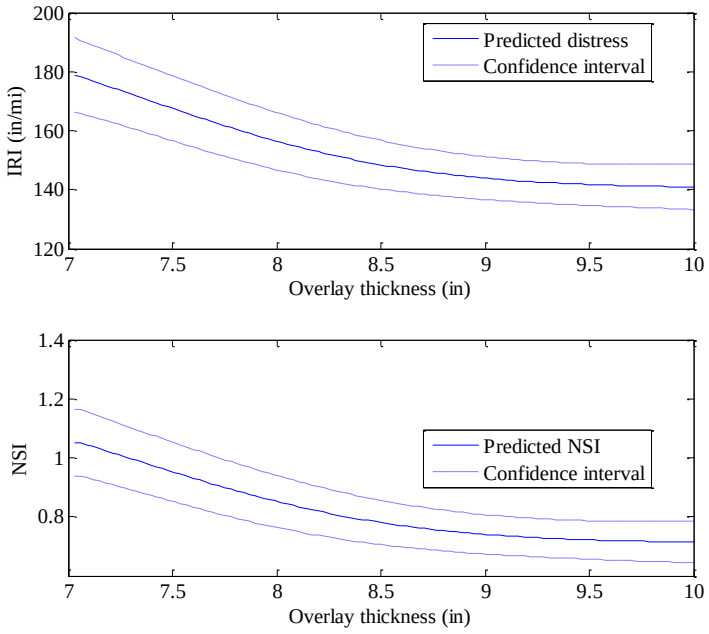

Figure B-154 Predicted IRI and NSI for overlay thickness

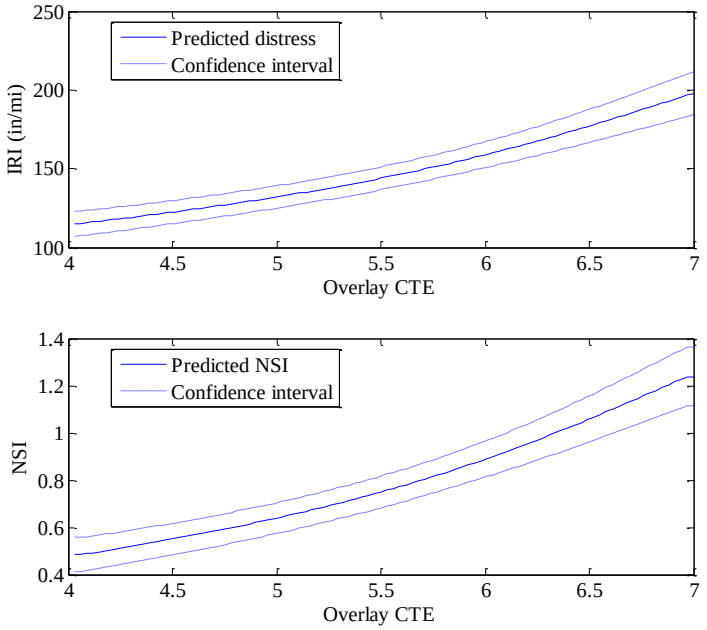

Figure B-155 Predicted IRI and NSI for overlay CTE

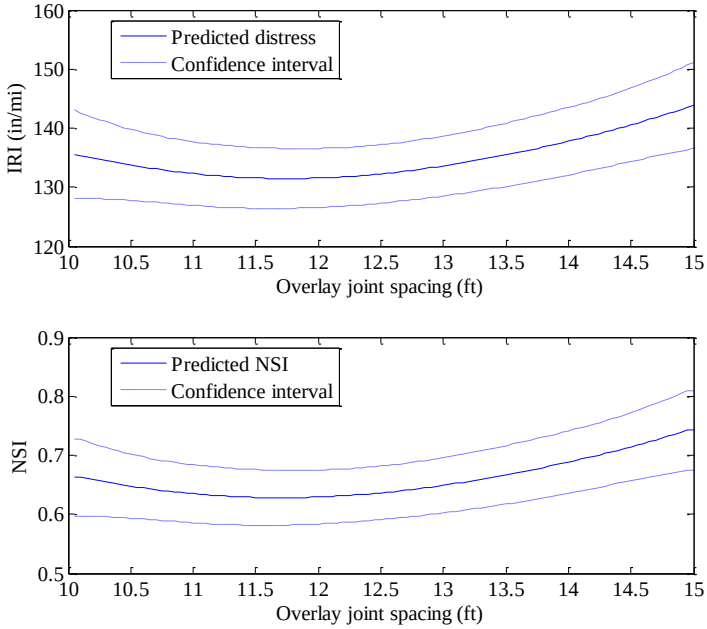

Figure B-156 Predicted IRI and NSI for overlay joint spacing

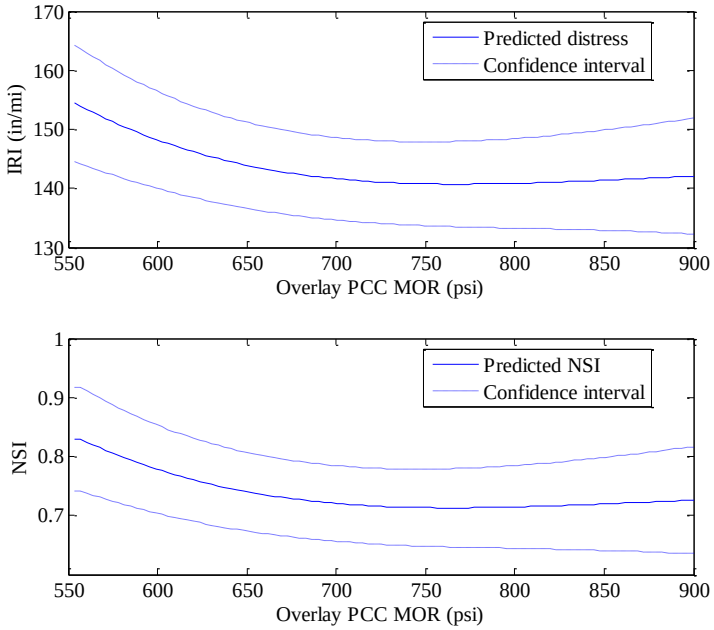

Figure B-157 Predicted IRI and NSI for overlay PCC MOR

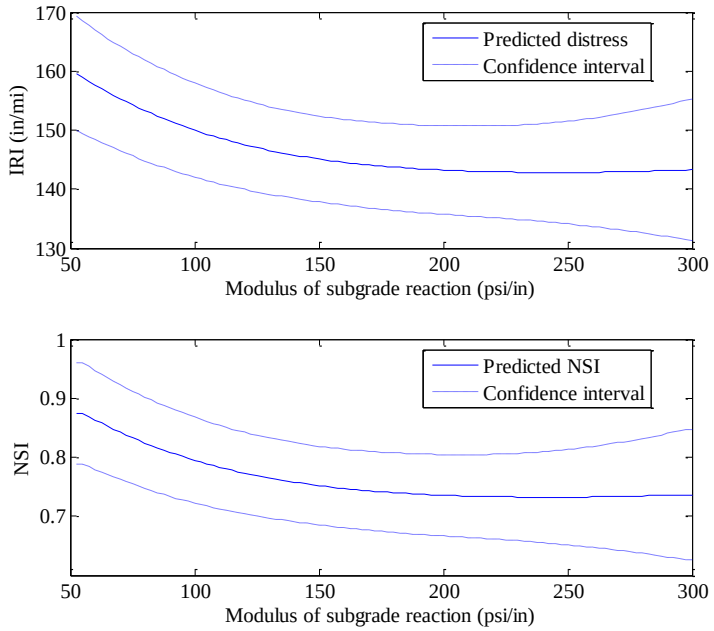

Figure B-158 Predicted IRI and NSI for modulus of subgrade reaction

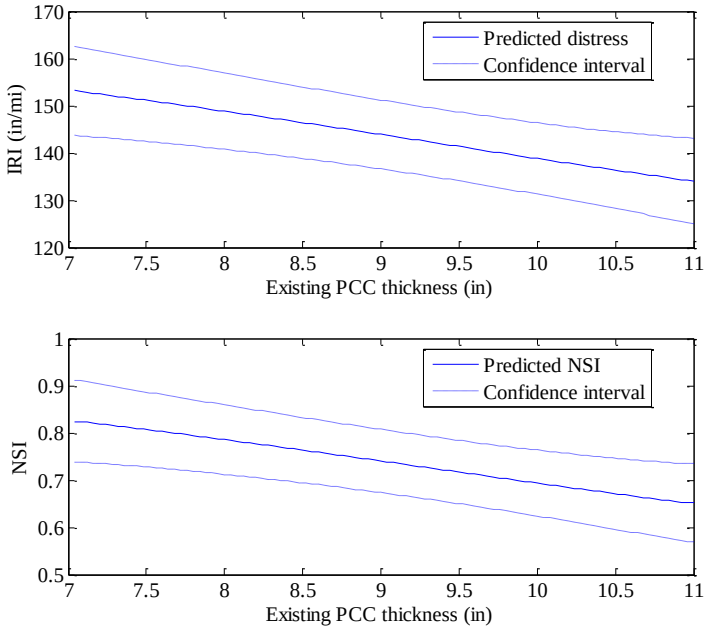

Figure B-159 Predicted IRI and NSI for existing PCC thickness

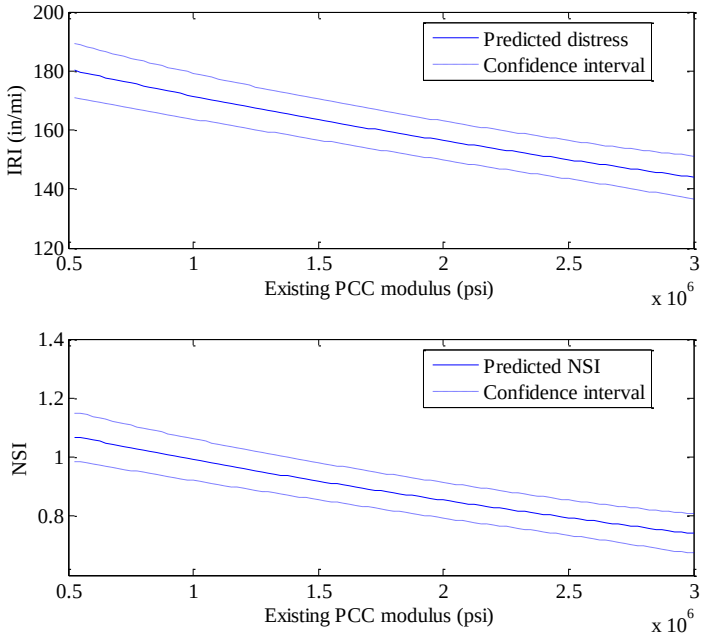

Figure B-160 Predicted IRI and NSI for existing PCC modulus

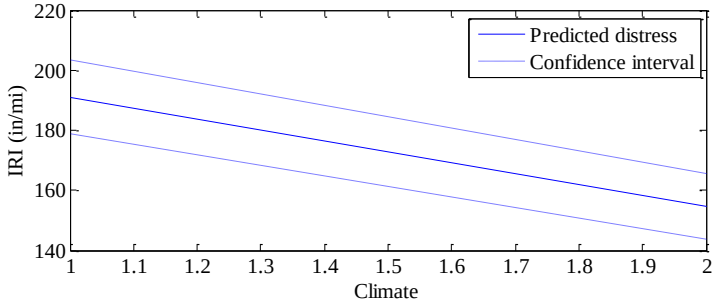

Figure B-161 Predicted IRI for climate

Inputs main effect

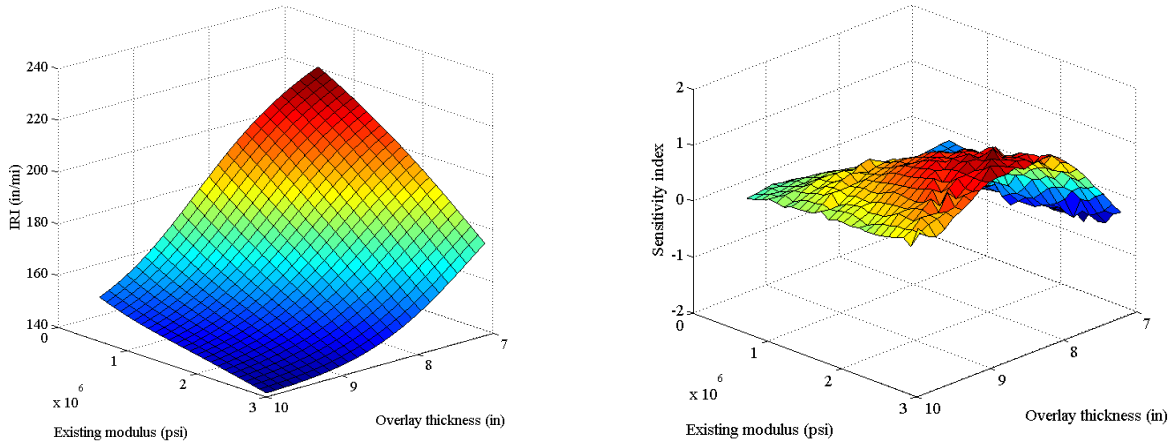

Figure B-162 Predicted interaction and NSI between existing modulus and overlay thickness

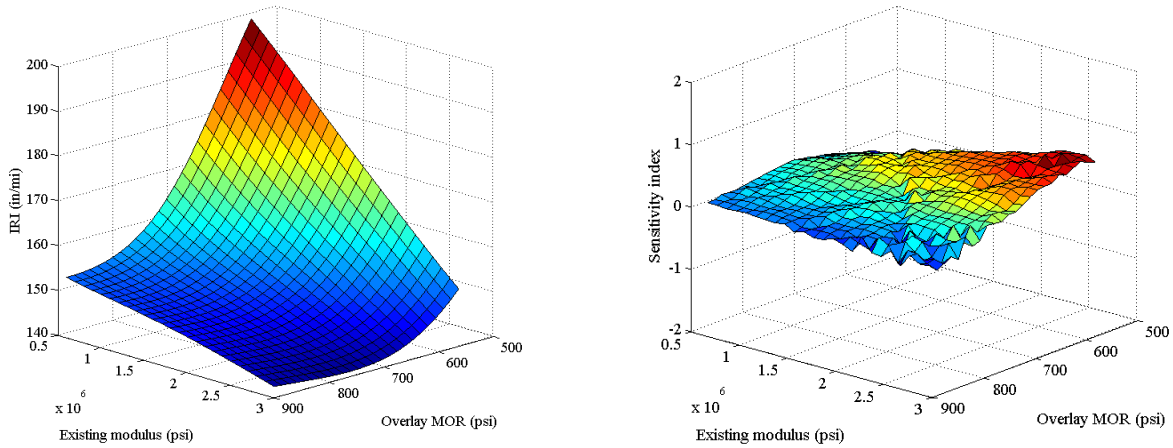

Figure B-163 Predicted interaction and NSI between existing thickness and overlay MOR

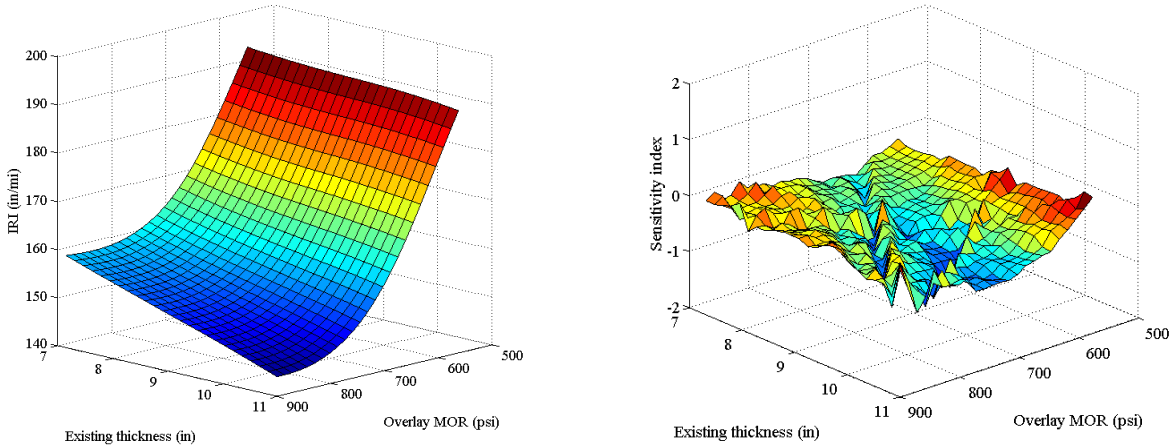

Figure B-164 Predicted interaction and NSI between existing thickness and overlay MOR

APPENDIX C - VERIFICATION

This appendix summarizes the detailed results presented in Chapter 5. The appendix covers the following topics for each selected project:

- Input variable data for each project
- Validation results for each project

C.1 INPUT VARIABLE DATA

The details regarding the input variable values were discussed in Chapter 5.4 of the main report. The values presented here goes into more detail regarding each project.

C.1.1 Unbonded Overlays

The unbonded overlay projects are summarized by project information, pavement cross-section, MEPDG inputs and TTC information if available. The values were used to represent each project in DARWin-ME.

Table C.1.1-1 Unbonded overlay project 37997

Project Information			MEPDG Inputs	
Job number:	37997		**Traffic**	
Project CS:	3111		Two way AADTT	4250
Region:	Southwest		Lanes in design direction	2
Route	US 131 NB, SB		**Climate**	Kalamazoo
Year opened	1998		**Overlay Layer**	
CAADT	4250		PCC Thickness (in)	7.1
Repairs:			PCC MOR (psi)	650
2001	Diamond Grinding		**AC Interlayer**	
2006	Joint Seal & CPR		AC Thickness (in)	1
			AC PG or Penetration Grade	PG 58-28
Pavement Cross Section	Thickness (in)		AC Mixture air voids	3
PCC Overlay	7.1		Design % asphalt	6
AC Interlayer	1		3/4 inch sieve	0
Existing PCC	9		3/8 inch sieve	15.2
Base	3		No. 4	33.3
Subbase	11		No. 200	5.2
			Existing PCC	
TTC Site	7109		PCC Thickness (in)	9
Vehicle Class	Vehicle %		PCC Elastic Modulus (psi)	3,000,000
4	1.17		**Base Layer**	
5	43.69		Thickness (in)	3
6	4.20		Material type	Crushed Stone
7	1.16		Modulus (psi)	30000
8	4.28		**Subbase Layer**	
9	37.28		Thickness (in)	11
10	3.87		Material type	A-3
11	0.47		Modulus (psi)	13500
12	0.24		**Subgrade**	
13	3.64		Material type	SP1-A-3
Sum	100		Modulus (psi)	27739/ 7000

Table C.1.1-2 Unbonded overlay project 34120

Project Information	
Job number:	34120
Project CS:	47014
Region:	University
Route	US-23 NB, SB
Year opened	1999
CAADT	4279
Repairs:	

Pavement Cross Section	
PCC Overlay	7.9
AC Interlayer	1
Existing PCC	9
Base	3
Subbase	14

TTC Site	8229
Vehicle Class	Vehicle %
4	2.46
5	23.46
6	4.32
7	1.40
8	4.07
9	50.08
10	5.78
11	1.65
12	0.56
13	6.22
Sum	100.00

MEPDG Inputs	
Traffic	
Two way AADTT	4279
Lanes in design direction	2
Climate	Ann Arbor
Overlay Layer	
PCC Thickness (in)	7.9
PCC MOR (psi)	650
AC Interlayer	
AC Thickness (in)	1
AC PG or Penetration Grade	PG 58-28
AC Mixture air voids	
Design % asphalt	
3/4 inch sieve	0
3/8 inch sieve	15.2
No. 4	33.3
No. 200	5.2
Existing PCC	
PCC Thickness (in)	9
PCC Elastic Modulus (psi)	3,000,000
Base Layer	
Thickness (in)	3
Material type	Crushed Stone
Modulus (psi)	25000
Subbase Layer	
Thickness (in)	14
Material type	A-3
Modulus (psi)	13500
Subgrade	
Material type	SP2-A-3
Modulus (psi)	25113/ 6500

Table C.1.1-3 Unbonded overlay project 49029

Project Information	
Job number:	49029
Project CS:	13074
Region:	Southwest
Route	I-69 NB, SB
Year opened	1999
CAADT	5700
Repairs:	
2004	Joint Seal and CPR
2007	Joint Seal
2008	CPR
Pavement Cross Section	Thickness (in)
PCC Overlay	7.1
AC Interlayer	1
Existing PCC	9
Base	4
Subbase	10
TTC Site	7269
Vehicle Class	Vehicle %
4	1.30
5	9.14
6	1.65
7	0.09
8	3.02
9	80.54
10	1.11
11	2.34
12	0.52
13	0.28
Sum	100.00

MEPDG Inputs	
Traffic	
Two way AADTT	5700
Lanes in design direction	2
Climate	Kalamazoo
Overlay Layer	
PCC Thickness (in)	7.1
PCC MOR (psi)	650
AC Interlayer	
AC Thickness (in)	1
AC PG or Penetration Grade	PG 58-28
AC Mixture air voids	3
Design % asphalt	6.3
3/4 inch sieve	0
3/8 inch sieve	2.6
No. 4	24.75
No. 200	5.3
Existing PCC	
PCC Thickness (in)	9
PCC Elastic Modulus (psi)	3,000,000
Base Layer	
Thickness (in)	4
Material type	Crushed Stone
Modulus (psi)	30000
Subbase Layer	
Thickness (in)	10
Material type	A-3
Modulus (psi)	13500
Subgrade	
Material type	SP1-A-3
Modulus (psi)	27739/ 7000

Table C.1.1-4 Unbonded overlay project 45591

Project Information	
Job number:	45591
Project CS:	13074-23061
Region:	Southwest, University
Route	I-69 NB, SB
Year opened	2000
CAADT	5595
Repairs:	
2008	CPR

Pavement Cross Section	Thickness (in)
PCC Overlay	7
AC Interlayer	1
Existing PCC	9
Base	4
Subbase	10

TTC Site	7269
Vehicle Class	Vehicle %
4	1.30
5	9.14
6	1.65
7	0.09
8	3.02
9	80.54
10	1.11
11	2.34
12	0.52
13	0.28
Sum	100.00

MEPDG Inputs	
Traffic	
Two way AADTT	5595
Lanes in design direction	2
Climate	Battle Creek
Overlay Layer	
PCC Thickness (in)	7
PCC MOR (psi)	650
AC Interlayer	
AC Thickness (in)	1
AC PG or Penetration Grade	PG 58-28
AC Mixture air voids	
Design % asphalt	
3/4 inch sieve	0
3/8 inch sieve	2.6
No. 4	24.75
No. 200	94.7
Existing PCC	
PCC Thickness (in)	9
PCC Elastic Modulus (psi)	3,000,000
Base Layer	
Thickness (in)	4
Material type	Crushed Stone
Modulus (psi)	30000
Subbase Layer	
Thickness (in)	10
Material type	A-3
Modulus (psi)	13500
Subgrade	
Material type	SP1-A-3
Modulus (psi)	27739/ 7000

Table C.1.1-5 Unbonded overlay project 38209

Project Information	
Job number:	38209
Project CS:	41132-41133
Region:	Grand
Route	US 131 NB, SB
Year opened	2000
CAADT	2744
Repairs:	
2010	Joint Seal

Pavement Cross Section	Thickness (in)
PCC Overlay	7
AC Interlayer	1
Existing PCC	9
Base	4
Subbase	10

TTC Site	5249
Vehicle Class	Vehicle %
4	1.30
5	35.36
6	3.36
7	0.87
8	3.35
9	43.74
10	4.77
11	1.60
12	0.06
13	5.60
Sum	100.00

MEPDG Inputs	
Traffic	
Two way AADTT	2744
Lanes in design direction	2
Climate	Grand Rapids
Overlay Layer	
PCC Thickness (in)	7
PCC MOR (psi)	650
AC Interlayer	
AC Thickness (in)	1
AC PG or Penetration Grade	PG 52-28
AC Mixture air voids	3
Design % asphalt	5.7
3/4 inch sieve	0
3/8 inch sieve	15.2
No. 4	33.3
No. 200	5.2
Existing PCC	
PCC Thickness (in)	9
PCC Elastic Modulus (psi)	3,000,000
Base Layer	
Thickness (in)	4
Material type	Crushed Stone
Modulus (psi)	30000
Subbase Layer	
Thickness (in)	10
Material type	A-3
Modulus (psi)	13500
Subgrade	
Material type	A-4
Modulus (psi)	20314/ 5000

Table C.1.1-6 Unbonded overlay project 43499

Project Information	
Job number:	43499
Project CS:	47014
Region:	University
Route	US-23 NB SB
Year opened	2001
CAADT	5004
Repairs:	

Pavement Cross Section	Thickness (in)
PCC Overlay	7.1
AC Interlayer	1
Existing PCC	9
Base	3
Subbase	14

TTC Site	8229
Vehicle Class	Vehicle %
4	2.46
5	23.46
6	4.32
7	1.40
8	4.07
9	50.08
10	5.78
11	1.65
12	0.56
13	6.22
Sum	100.00

MEPDG Inputs	
Traffic	
Two way AADTT	5004
Lanes in design direction	2
Climate	Ann Arbor
Overlay Layer	
PCC Thickness (in)	7.1
PCC MOR (psi)	650
AC Interlayer	
AC Thickness (in)	1
AC PG or Penetration Grade	PG 70-28
AC Mixture air voids	
Design % asphalt	
3/4 inch sieve	0
3/8 inch sieve	2.6
No. 4	24.75
No. 200	94.7
Existing PCC	
PCC Thickness (in)	9
PCC Elastic Modulus (psi)	3,000,000
Base Layer	
Thickness (in)	3
Material type	Crushed Stone
Modulus (psi)	30000
Subbase Layer	
Thickness (in)	14
Material type	A-3
Modulus (psi)	13500
Subgrade	
Material type	SP2-A-3
Modulus (psi)	25113/ 6500

Table C.1.1-7 Unbonded overlay project 73873

Project Information	
Job number:	73873
Project CS:	65041
Region:	North
Route	I-75 NB
Year opened	2003
CAADT	1458
Repairs:	
2009	Long Joint Seal
2011	Joint Seal
Pavement Cross Section	Thickness (in)
PCC Overlay	7
AC Interlayer	1
Existing PCC	9
Base	4
Subbase	10
TTC Site	4149
Vehicle Class	Vehicle %
4	1.48
5	41.62
6	2.64
7	0.25
8	4.93
9	29.62
10	10.39
11	0.93
12	0.24
13	7.90
Sum	100.00

MEPDG Inputs	
Traffic	
Two way AADTT	1458
Lanes in design direction	2
Climate	Houghton Lake
Overlay Layer	
PCC Thickness (in)	7
PCC MOR (psi)	650
AC Interlayer	
AC Thickness (in)	1
AC PG or Penetration Grade	PG 64-28
AC Mixture air voids	
Design % asphalt	
3/4 inch sieve	0
3/8 inch sieve	15.2
No. 4	33.3
No. 200	5.2
Existing PCC	
PCC Thickness (in)	9
PCC Elastic Modulus (psi)	3,000,000
Base Layer	
Thickness (in)	4
Material type	Crushed Stone
Modulus (psi)	30000
Subbase Layer	
Thickness (in)	10
Material type	A-3
Modulus (psi)	13500
Subgrade	
Material type	SP2-A-3
Modulus (psi)	25113/ 6500

Table C.1.1-8 Unbonded overlay project 50763

Project Information	
Job number:	50763
Project CS:	39014, 3111
Region:	Southwest
Route	US-131 NB, SB
Year opened	2004
CAADT	3185
Repairs:	

Pavement Cross Section	Thickness (in)
PCC Overlay	7
AC Interlayer	1
Existing PCC	9
Base	4
Subbase	10

TTC Site	4149
Vehicle Class	Vehicle %
4	1.17
5	43.69
6	4.20
7	1.16
8	4.28
9	37.28
10	3.87
11	0.47
12	0.24
13	3.64
Sum	100.00

MEPDG Inputs	
Traffic	
Two way AADTT	3185
Lanes in design direction	2
Climate	Kalamzoo
Overlay Layer	
PCC Thickness (in)	7
PCC MOR (psi)	650
AC Interlayer	
AC Thickness (in)	1
AC PG or Penetration Grade	PG 58-28
AC Mixture air voids	4
Design % asphalt	5.5
3/4 inch sieve	0
3/8 inch sieve	20.6
No. 4	36.9
No. 200	4.5
Existing PCC	
PCC Thickness (in)	9
PCC Elastic Modulus (psi)	3,000,000
Base Layer	
Thickness (in)	4
Material type	Crushed Stone
Modulus (psi)	30000
Subbase Layer	
Thickness (in)	10
Material type	A-3
Modulus (psi)	13500
Subgrade	
Material type	SP1-A-3
Modulus (psi)	27739/ 7000

C.1.2 Rubblized Overlays

The rubblized overlay projects are summarized by project information, pavement cross-section, MEPDG inputs and TTC information if available. The values were used to represent each project in DARWin-ME.

Table C.1.2-1 Rubblized overlay project 28115

Project Information	
Job number:	28115
Project CS:	34031-34032
Region:	Grand
Route	M-66 NB SB
Opened	1989
CAADT	490/340
Repairs:	
1998	Chip seal
2000	Overband Crack fill
Pavement Cross Section	Thickness (in)
AC overlay	5
Existing PCC (fractured)	9
Base	3
Subbase	9
TTC Site	State Avg
Vehicle Class	Vehicle %
4	1.50
5	10.00
6	2.00
7	0.80
8	2.50
9	70.00
10	5.50
11	1.10
12	0.20
13	6.40
Sum	100.00

MEPDG Inputs	
Traffic	
Two way AADTT	490/340
Lanes in design direction	2
Climate	Grand Rapids
Overlay Layer	
HMA Thickness (in)	5
HMA binder	Pen 120-150
AC Mixture air voids	7
Design % asphalt	5.4
3/4 inch sieve	20.4
3/8 inch sieve	32.3
No. 4	41
No. 200	3.1
Existing PCC (fractured)	
PCC Thickness (in)	9
PCC Elastic Modulus (psi)	70,000
Base Layer	
Thickness (in)	3
Material type	Crushed Stone
Modulus (psi)	30000
Subbase Layer	
Thickness (in)	9
Material type	A-3
Modulus (psi)	13500
Subgrade	
Material type	A-4
Modulus (psi)	20314/ 5000

Table C.1.2-2 Rubblized overlay project 26755

Project Information	
Job number:	26755
Project CS:	20014
Region:	North
Route	I-75 SB
Opened	1990
CAADT	1550
Repairs:	
1996	CF

Pavement Cross Section	Thickness (in)
AC overlay	4.25
Existing PCC (fractured)	8
Base	0
Subbase	0

TTC Site	4149
Vehicle Class	Vehicle %
4	1.48
5	41.62
6	2.64
7	0.25
8	4.93
9	29.62
10	10.39
11	0.93
12	0.24
13	7.90
Sum	100.00

MEPDG Inputs	
Traffic	
Two way AADTT	1550
Lanes in design direction	2
Climate	Houghton Lake
Overlay Layer	
HMA Thickness (in)	4.25
HMA binder	Pen 120-150
AC Mixture air voids	
Design % asphalt	5.7
3/4 inch sieve	0
3/8 inch sieve	13.9
No. 4	37.2
No. 200	5.1
Existing PCC (fractured)	
PCC Thickness (in)	8
PCC Elastic Modulus (psi)	70,000
Base Layer	
Thickness (in)	0
Material type	Crushed Stone
Modulus (psi)	30000
Subbase Layer	
Thickness (in)	0
Material type	A-3
Modulus (psi)	13500
Subgrade	
Material type	SP2- A-3
Modulus (psi)	25113/ 6500

Table C.1.2-3 Rubblized overlay project 29768

Project Information	
Job number:	29768
Project CS:	47013-47014
Region:	University
Route	US-23 NB, SB
Opened	1992
CAADT	3390
Repairs:	
1999	Minor pothole patching
2000	CM and R
2004	Surface seal
2005	CT
2005	OCF and UT OL

Pavement Cross Section	Thickness (in)
AC overlay	5.0
Existing PCC (fractured)	9.0
Base	3.0
Subbase	14.0

TTC Site	8229
Vehicle Class	Vehicle %
4	2.46
5	23.46
6	4.32
7	1.40
8	4.07
9	50.08
10	5.78
11	1.65
12	0.56
13	6.22
Sum	100.00

MEPDG Inputs	
Traffic	
Two way AADTT	3390
Lanes in design direction	2
Climate	Ann Arbor
Overlay Layer	
HMA Thickness (in)	5.25
HMA binder	Pen 85-100
AC Mixture air voids	3.8
Design % asphalt	5
3/4 inch sieve	0
3/8 inch sieve	13.1
No. 4	40.9
No. 200	7.1
Existing PCC (fractured)	
PCC Thickness (in)	9
PCC Elastic Modulus (psi)	70,000
Base Layer	
Thickness (in)	3
Material type	Crushed Stone
Modulus (psi)	30000
Subbase Layer	
Thickness (in)	14
Material type	A-3
Modulus (psi)	13500
Subgrade	
Material type	SP2- A-3
Modulus (psi)	25113/ 6500

Table C.1.2-4 Rubblized overlay project 29670

Project Information	
Job number:	29670
Project CS:	13033
Region:	Southwest
Route	I-194 NB, SB
Opened	1993
CAADT	856
Repairs:	
1999	Added 1.5" HMA
2003	CT
2007	CM and R
2010	CT
Pavement Cross Section	Thickness (in)
AC overlay	6.25
Existing PCC (fractured)	9
Base	3
Subbase	9
TTC Site	7159
Vehicle Class	Vehicle %
4	1.26
5	13.75
6	2.08
7	0.19
8	2.85
9	73.13
10	2.38
11	1.15
12	0.34
13	2.87
Sum	100.00

MEPDG Inputs	
Traffic	
Two way AADTT	856
Lanes in design direction	2
Climate	Battle Creek
Overlay Layer	
HMA Thickness (in)	6.25
HMA binder	Pen 85-100
AC Mixture air voids	7
Design % asphalt	6.3
3/4 inch sieve	0
3/8 inch sieve	0.3
No. 4	19.9
No. 200	5.8
Existing PCC (fractured)	
PCC Thickness (in)	9
PCC Elastic Modulus (psi)	70,000
Base Layer	
Thickness (in)	3
Material type	Crushed Stone
Modulus (psi)	30000
Subbase Layer	
Thickness (in)	9
Material type	A-3
Modulus (psi)	13500
Subgrade	
Material type	SP1- A-4
Modulus (psi)	27739/ 7000

Table C.1.2-5 Rubblized overlay project 29581

Project Information	
Job number:	29581
Project CS:	33084-33083
Region:	University
Route	I-96 EB WB
Opened	1994
CAADT	3707
Repairs:	
2002	OCF
2006	OCF
Pavement Cross Section	Thickness (in)
AC overlay	7.5
Existing PCC (fractured)	9
Base	4
Subbase	10
TTC Site	8049
Vehicle Class	Vehicle %
4	1.89
5	17.23
6	3.11
7	0.28
8	5.14
9	59.86
10	6.46
11	2.11
12	0.61
13	3.32
Sum	100.00

MEPDG Inputs	
Traffic	
Two way AADTT	3707
Lanes in design direction	2
Climate	Lansing
Overlay Layer	
HMA Thickness (in)	7.5
HMA binder	Pen 85-100
AC Mixture air voids	
Design % asphalt	6.2
3/4 inch sieve	0
3/8 inch sieve	16
No. 4	36.9
No. 200	4.9
Existing PCC (fractured)	
PCC Thickness (in)	9
PCC Elastic Modulus (psi)	70,000
Base Layer	
Thickness (in)	4
Material type	Crushed Stone
Modulus (psi)	30000
Subbase Layer	
Thickness (in)	10
Material type	A-3
Modulus (psi)	13500
Subgrade	
Material type	CL - A-6
Modulus (psi)	17600/ 4400

Table C.1.2-6 Rubblized overlay project 28111

Project Information	
Job number:	28111
Project CS:	24021-16021
Region:	North
Route	M-68
Opened	1990
CAADT	280
Repairs:	
1999	CT
2003	CT
2007	CM and R

Pavement Cross Section	Thickness (in)
AC overlay	4
Existing PCC (fractured)	9
Base	0
Subbase	0

TTC Site	State Avg
Vehicle Class	Vehicle %
4	1.50
5	10.00
6	2.00
7	0.80
8	2.50
9	70.00
10	5.50
11	1.10
12	0.20
13	6.40
Sum	100.00

MEPDG Inputs	
Traffic	
Two way AADTT	280
Lanes in design direction	1
Climate	Pellston
Overlay Layer	
HMA Thickness (in)	4
HMA binder	Pen 200-300
AC Mixture air voids	
Design % asphalt	5.4
3/4 inch sieve	0
3/8 inch sieve	16
No. 4	38.8
No. 200	5.7
Existing PCC (fractured)	
PCC Thickness (in)	9
PCC Elastic Modulus (psi)	70,000
Base Layer	
Thickness (in)	
Material type	
Modulus (psi)	
Subbase Layer	
Thickness (in)	
Material type	
Modulus (psi)	
Subgrade	
Material type	SP1- A-3
Modulus (psi)	27739/ 7000

Table C.1.2-7 Rubblized overlay project 29729

Project Information	
Job number:	29729
Project CS:	74012
Region:	Bay
Route	M-53
Opened	1995
CAADT	370
Repairs:	
2000	CT
2003	CT & UT Overlay

Pavement Cross Section	Thickness (in)
AC overlay	5
Existing PCC (fractured)	9
Base	0
Subbase	18

TTC Site	State Avg
Vehicle Class	Vehicle %
4	1.50
5	10.00
6	2.00
7	0.80
8	2.50
9	70.00
10	5.50
11	1.10
12	0.20
13	6.40
Sum	100.00

MEPDG Inputs	
Traffic	
Two way AADTT	370
Lanes in design direction	1
Climate	Flint
Overlay Layer	
HMA Thickness (in)	5
HMA binder	Pen 120-150
AC Mixture air voids	
Design % asphalt	5.2
3/4 inch sieve	0
3/8 inch sieve	38.3
No. 4	52.2
No. 200	5.6
Existing PCC (fractured)	
PCC Thickness (in)	9
PCC Elastic Modulus (psi)	70,000
Base Layer	
Thickness (in)	0
Material type	
Modulus (psi)	
Subbase Layer	
Thickness (in)	18
Material type	A-3
Modulus (psi)	13500
Subgrade	
Material type	SM - A-4
Modulus (psi)	24764/ 5200

Table C.1.2-8 Rubblized overlay project 45053

Project Information	
Job number:	45053
Project CS:	67021, 67022
Region:	North
Route	US-10
Opened	1999
CAADT	675
Repairs:	
2005	CM and R
2009	OCF and Micro

Pavement Cross Section	Thickness (in)
AC overlay	5.5
Existing PCC (fractured)	9
Base	3
Subbase	12

TTC Site	State Avg
Vehicle Class	Vehicle %
4	1.50
5	10.00
6	2.00
7	0.80
8	2.50
9	70.00
10	5.50
11	1.10
12	0.20
13	6.40
Sum	100.00

MEPDG Inputs	
Traffic	
Two way AADTT	675
Lanes in design direction	1
Climate	Reed City
Overlay Layer	
HMA Thickness (in)	5.5
HMA binder	PG 58-28
AC Mixture air voids	
Design % asphalt	6
3/4 inch sieve	0
3/8 inch sieve	16.7
No. 4	56.2
No. 200	4.1
Existing PCC (fractured)	
PCC Thickness (in)	9
PCC Elastic Modulus (psi)	70,000
Base Layer	
Thickness (in)	3
Material type	Crushed Stone
Modulus (psi)	30000
Subbase Layer	
Thickness (in)	12
Material type	A-3
Modulus (psi)	13500
Subgrade	
Material type	SP1- A-3
Modulus (psi)	27739/ 7000

Table C.1.2-9 Rubblized overlay project 44109

Project Information	
Job number:	44109
Project CS:	5001
Region:	North
Route	US-31
Opened	1999
CAADT	279
Repairs:	
2007	OCF and Micro

Pavement Cross Section	Thickness (in)
AC overlay	7.5
Existing PCC (fractured)	8
Base	0
Subbase	9

TTC Site	State Avg
Vehicle Class	Vehicle %
4	1.50
5	10.00
6	2.00
7	0.80
8	2.50
9	70.00
10	5.50
11	1.10
12	0.20
13	6.40
Sum	100.00

MEPDG Inputs	
Traffic	
Two way AADTT	279
Lanes in design direction	1
Climate	Traverse City
Overlay Layer	
HMA Thickness (in)	7.5
HMA binder	PG 58-28
AC Mixture air voids	8
Design % asphalt	13
3/4 inch sieve	0
3/8 inch sieve	2
No. 4	33.9
No. 200	4.5
Existing PCC (fractured)	
PCC Thickness (in)	8
PCC Elastic Modulus (psi)	70,000
Base Layer	
Thickness (in)	0
Material type	
Modulus (psi)	
Subbase Layer	
Thickness (in)	9
Material type	A-3
Modulus (psi)	13500
Subgrade	
Material type	SP1-A-3
Modulus (psi)	27739/ 7000

Table C.1.2-10 Rubblized overlay project 38190

Project Information	
Job number:	38190
Project CS:	41033, 61171
Region:	Grand
Route	M-37
Opened	2000
CAADT	575
Repairs:	

Pavement Cross Section	Thickness (in)
AC overlay	5.5
Existing PCC (fractured)	9
Base	4
Subbase	14

TTC Site	State Avg
Vehicle Class	Vehicle %
4	1.50
5	10.00
6	2.00
7	0.80
8	2.50
9	70.00
10	5.50
11	1.10
12	0.20
13	6.40
Sum	100.00

MEPDG Inputs	
Traffic	
Two way AADTT	575
Lanes in design direction	1
Climate	Muske-gon
Overlay Layer	
HMA Thickness (in)	5.5
HMA binder	PG 58-28
AC Mixture air voids	8
Design % asphalt	10.4
3/4 inch sieve	0
3/8 inch sieve	16.5
No. 4	33.7
No. 200	4.9
Existing PCC (fractured)	
PCC Thickness (in)	9
PCC Elastic Modulus (psi)	70,000
Base Layer	
Thickness (in)	4
Material type	Crushed Stone
Modulus (psi)	30000
Subbase Layer	
Thickness (in)	14
Material type	A-3
Modulus (psi)	13500
Subgrade	
Material type	SP1-A-3
Modulus (psi)	27739/ 7000

Table C.1.2-11 Rubblized overlay project 32388

Project Information	
Job number:	32388
Project CS:	46082
Region:	University
Route	M-50
Opened	1997
CAADT	455
Repairs:	
2001	CT
2007	CM & R
2008	CT
Pavement Cross Section	Thickness (in)
AC overlay	6
Existing PCC (fractured)	8
Base	0
Subbase	12
TTC Site	State Avg
Vehicle Class	Vehicle %
4	1.50
5	10.00
6	2.00
7	0.80
8	2.50
9	70.00
10	5.50
11	1.10
12	0.20
13	6.40
Sum	100.00

MEPDG Inputs	
Traffic	
Two way AADTT	455
Lanes in design direction	1
Climate	Adrian
Overlay Layer	
HMA Thickness (in)	6
HMA binder	58-28
AC Mixture air voids	3
Design % asphalt	4.9
3/4 inch sieve	12
3/8 inch sieve	46.5
No. 4	51.6
No. 200	5.1
Existing PCC (fractured)	
PCC Thickness (in)	8
PCC Elastic Modulus (psi)	70,000
Base Layer	
Thickness (in)	0
Material type	
Modulus (psi)	
Subbase Layer	
Thickness (in)	12
Material type	A-3
Modulus (psi)	13500
Subgrade	
Material type	CL- A-6
Modulus (psi)	17600/ 4400

C.1.3 Composite Overlays

The composite overlay projects are summarized by project information, pavement cross-section, MEPDG inputs and TTC information if available. The values were used to represent each project in DARWin-ME.

Table C.1.3-1 Composite overlay project 25543

Project Information	
Job number:	25543
Project CS:	25131
Region:	Bay
Route	I-75 NB, SB
Opened	1987
CAADT	2250
Repairs:	None

Pavement Cross Section	Thickness (in)
AC overlay	4
Existing PCC	9
Base	4
Subbase	10

TTC Site	State Avg
Vehicle Class	Vehicle %
4	1.50
5	10.00
6	2.00
7	0.80
8	2.50
9	70.00
10	5.50
11	1.10
12	0.20
13	6.40
Sum	100.00

MEPDG Inputs	
Traffic	
Two way AADTT	2250
Lanes in design direction	2
Climate	Flint
Overlay Layer	
HMA Thickness (in)	4
HMA binder	85-100
AC Mixture air voids	
Design % asphalt	6.1
3/4 inch sieve	0
3/8 inch sieve	11.4
No. 4	31.7
No. 200	6.5
Existing PCC	
PCC Thickness (in)	9
PCC Compressive Strength (psi)	5,000
Base Layer	
Thickness (in)	4
Material type	Crushed Stone
Modulus (psi)	30000
Subbase Layer	
Thickness (in)	10
Material type	A-3
Modulus (psi)	13500
Subgrade	
Material type	SM -
Modulus (psi)	A-4

Table C.1.3-2 Composite overlay project 24252

Project Information	
Job number:	24252
Project CS:	80024, 39024
Region:	Southwest
Route	I-96 EB, WB
Opened	1988
CAADT	6250
Repairs:	
1996	OCF in Decreasing dir.

Pavement Cross Section	Thickness (in)
AC overlay	4.5
Existing PCC	9
Base	3
Subbase	9

TTC Site	State Avg
Vehicle Class	Vehicle %
4	1.50
5	10.00
6	2.00
7	0.80
8	2.50
9	70.00
10	5.50
11	1.10
12	0.20
13	6.40
Sum	100.00

MEPDG Inputs	
Traffic	
Two way AADTT	6250
Lanes in design direction	2
Climate	Kalamazoo
Overlay Layer	
HMA Thickness (in)	4.5
HMA binder	85-100
AC Mixture air voids	
Design % asphalt	5.6
3/4 inch sieve	0
3/8 inch sieve	12
No. 4	31.9
No. 200	5.4
Existing PCC	
PCC Thickness (in)	9
PCC Compressive Strength (psi)	5,000
Base Layer	
Thickness (in)	3
Material type	Crushed Stone
Modulus (psi)	30000
Subbase Layer	
Thickness (in)	9
Material type	A-3
Modulus (psi)	13500
Subgrade	
Material type	SP1-A-3
Modulus (psi)	27739/ 7000

Table C.1.3-3 Composite overlay project 29586

Project Information	
Job number:	29586
Project CS:	41026, 70063
Region:	Grand
Route	I-96 EB, WB
Opened	1990
CAADT	2882
Repairs:	
1999	CM and R

Pavement Cross Section	Thickness (in)
AC overlay	3
Existing PCC	9
Base	3
Subbase	12

TTC Site	State Avg
Vehicle Class	Vehicle %
4	1.50
5	10.00
6	2.00
7	0.80
8	2.50
9	70.00
10	5.50
11	1.10
12	0.20
13	6.40
Sum	100.00

MEPDG Inputs	
Traffic	
Two way AADTT	2882
Lanes in design direction	2
Climate	Grand Rapids
Overlay Layer	
HMA Thickness (in)	3
HMA binder	85-100
AC Mixture air voids	
Design % asphalt	6
3/4 inch sieve	0
3/8 inch sieve	11.6
No. 4	36.2
No. 200	6.5
Existing PCC	
PCC Thickness (in)	9
PCC Compressive Strength (psi)	5,000
Base Layer	
Thickness (in)	3
Material type	Crushed Stone
Modulus (psi)	30000
Subbase Layer	
Thickness (in)	12
Material type	A-3
Modulus (psi)	13500
Subgrade	
Material type	A-4
Modulus (psi)	20314/ 5000

Table C.1.3-4 Composite overlay project 29716

Project Information	
Job number:	29716
Project CS:	67051, 83051
Region:	North
Route	M-115
Opened	1992
CAADT	672
Repairs:	
2000	OCF

Pavement Cross Section	Thickness (in)
AC overlay	3.75
Existing PCC	9
Base	3
Subbase	12

TTC Site	State Avg
Vehicle Class	Vehicle %
4	1.50
5	10.00
6	2.00
7	0.80
8	2.50
9	70.00
10	5.50
11	1.10
12	0.20
13	6.40
Sum	100.00

MEPDG Inputs	
Traffic	
Two way AADTT	672
Lanes in design direction	2
Climate	Reed City
Overlay Layer	
HMA Thickness (in)	3.75
HMA binder	85-100
AC Mixture air voids	
Design % asphalt	
3/4 inch sieve	
3/8 inch sieve	
No. 4	
No. 200	
Existing PCC	
PCC Thickness (in)	9
PCC Compressive Strength (psi)	5,000
Base Layer	
Thickness (in)	3
Material type	Crushed Stone
Modulus (psi)	30000
Subbase Layer	
Thickness (in)	12
Material type	A-3
Modulus (psi)	13500
Subgrade	
Material type	SP1- A-3
Modulus (psi)	27739/7000

Table C.1.3-5 Composite overlay project 33812

Project Information	
Job number:	33812
Project CS:	50031
Region:	Metro
Route	M-97
Opened	1995
CAADT	1380
Repairs:	
1998	Micro
2005	CM and R

Pavement Cross Section	Thickness (in)
AC overlay	3
Existing PCC	9
Base	3
Subbase	14

TTC Site	State Avg
Vehicle Class	Vehicle %
4	1.50
5	10.00
6	2.00
7	0.80
8	2.50
9	70.00
10	5.50
11	1.10
12	0.20
13	6.40
Sum	100.00

MEPDG Inputs	
Traffic	
Two way AADTT	1380
Lanes in design direction	2
Climate	Detroit
Overlay Layer	
HMA Thickness (in)	3
HMA binder	85-100
AC Mixture air voids	3.5
Design % asphalt	5.3
3/4 inch sieve	0
3/8 inch sieve	38.3
No. 4	56
No. 200	5.6
Existing PCC	
PCC Thickness (in)	9
PCC Compressive Strength (psi)	5,000
Base Layer	
Thickness (in)	3
Material type	Crushed Stone
Modulus (psi)	30000
Subbase Layer	
Thickness (in)	14
Material type	A-3
Modulus (psi)	13500
Subgrade	
Material type	SP1-A-3
Modulus (psi)	27739/ 7000

Table C.1.3-6 Composite overlay project 33924

Project Information	
Job number:	33924
Project CS:	9032
Region:	Bay
Route	M-13
Opened	1996
CAADT	1000
Repairs:	
1999	Micro

Pavement Cross Section	Thickness (in)
AC overlay	4
Existing PCC	8
Base	4
Subbase	10

TTC Site	State Avg
Vehicle Class	Vehicle %
4	1.50
5	10.00
6	2.00
7	0.80
8	2.50
9	70.00
10	5.50
11	1.10
12	0.20
13	6.40
Sum	100.00

MEPDG Inputs	
Traffic	
Two way AADTT	1000
Lanes in design direction	2
Climate	Bay City
Overlay Layer	
HMA Thickness (in)	4
HMA binder	85-100
AC Mixture air voids	3.5
Design % asphalt	5
3/4 inch sieve	0
3/8 inch sieve	39
No. 4	61
No. 200	5
Existing PCC	
PCC Thickness (in)	8
PCC Compressive Strength (psi)	5,000
Base Layer	
Thickness (in)	4
Material type	Crushed Stone
Modulus (psi)	30000
Subbase Layer	
Thickness (in)	10
Material type	A-3
Modulus (psi)	13500
Subgrade	
Material type	SC - A-6
Modulus (psi)	17600/ 4400

Table C.1.3-7 Composite overlay project 45443

Project Information	
Job number:	45443
Project CS:	32011
Region:	Bay
Route	M-25
Opened	2000
CAADT	512
Repairs:	
2002	CT

Pavement Cross Section	Thickness (in)
AC overlay	3.5
Existing PCC	8
Base	0
Subbase	15

TTC Site	State Avg
Vehicle Class	Vehicle %
4	1.50
5	10.00
6	2.00
7	0.80
8	2.50
9	70.00
10	5.50
11	1.10
12	0.20
13	6.40
Sum	100.00

MEPDG Inputs	
Traffic	
Two way AADTT	512
Lanes in design direction	2
Climate	Bay City
Overlay Layer	
HMA Thickness (in)	3.5
HMA binder	58-28
AC Mixture air voids	4
Design % asphalt	5
3/4 inch sieve	2.6
3/8 inch sieve	22.9
No. 4	34.2
No. 200	4.5
Existing PCC	
PCC Thickness (in)	8
PCC Compressive Strength (psi)	5,000
Base Layer	
Thickness (in)	0
Material type	Crushed Stone
Modulus (psi)	30000
Subbase Layer	
Thickness (in)	15
Material type	A-3
Modulus (psi)	13500
Subgrade	
Material type	SC - A-6
Modulus (psi)	17600/ 4400

C.1.4 HMA over HMA

The HMA overlay projects are summarized by project information, pavement cross-section, MEPDG inputs and TTC information if available. The values were used to represent each project in DARWin-ME.

Table C.1.4-1 HMA overlay project 33534

Project Information	
Job number:	33534
Project CS:	67015, 83031
Region:	North
Route	US 131
Year opened	1992
CAADT	450
Repairs:	
1998	OCF & Micro
2007	Crush and Shape
Pavement Cross Section	Thickness (in)
HMA overlay	2.5
Existing HMA	3.25
Base	11
Subbase	25
Initial IRI	50
Original construction	1976
TTC Site	State Avg
Vehicle Class	Vehicle %
4	1.50
5	10.00
6	2.00
7	0.80
8	2.50
9	70.00
10	5.50
11	1.10
12	0.20
13	6.40
Sum	100.00

MEPDG Inputs		
Traffic		
Two way AADTT	450	
Lanes in design direction	2	
Climate	Reed City	
Overlay Layer	Top	Leveling
HMA Thickness (in)	1.25	1.25
HMA binder	120-150	
AC Mixture air voids	6	6
Effective Binder Content (%)	9.4	10.4
3/4 inch sieve	0	0
3/8 inch sieve	28.6	14.5
No. 4	50.2	50
No. 200	4.8	5.9
Existing HMA		
HMA Thickness (in)	3.25	
HMA binder	120-150	
AC Mixture air voids	7	
Effective Binder Content (%)	11.6	
3/4 inch sieve	0	
3/8 inch sieve	28.6	
No. 4	50.2	
No. 200	4.8	
Base Layer		
Thickness (in)	11	
Material type	Crushed Stone	
Modulus (psi)	30000	
Subbase Layer		
Thickness (in)	25	
Material type	A-3	
Modulus (psi)	13500	
Subgrade		
Material type	SP-1 A-3	
Modulus (psi)	27739/ 7000	

Table C.1.4-2 HMA overlay project 33550

Project Information	
Job number:	33550
Project CS:	80012
Region:	Southwest
Route	I-196
Year opened	1992
CAADT	1564
Repairs:	
1999	+ 1.5" HMA
2002	CT
2005	CM &R
Pavement Cross Section	Thickness (in)
HMA overlay	3
Existing HMA	4.5
Base	8
Subbase	28
Initial IRI	50
Original construction	1977
TTC Site	State Avg
Vehicle Class	Vehicle %
4	1.50
5	10.00
6	2.00
7	0.80
8	2.50
9	70.00
10	5.50
11	1.10
12	0.20
13	6.40
Sum	100.00

MEPDG Inputs		
Traffic		
Two way AADTT	1564	
Lanes in design direction	2	
Climate	Kalamazoo	
Overlay Layer	Top	Leveling
HMA Thickness (in)	1.5	1.5
HMA binder	85-100	
AC Mixture air voids	6.6	4.8
Effective Binder Content (%)	10	11
3/4 inch sieve	0	0
3/8 inch sieve	36	10.3
No. 4	45.6	41.4
No. 200	6.5	7.5
Existing HMA		
HMA Thickness (in)	4.5	
HMA binder	85-100	
AC Mixture air voids	7	
Effective Binder Content (%)	6	
3/4 inch sieve	0	
3/8 inch sieve	36	
No. 4	45.6	
No. 200	6.5	
Base Layer		
Thickness (in)	8	
Material type	Crushed Stone	
Modulus (psi)	30000	
Subbase Layer		
Thickness (in)	28	
Material type	A-3	
Modulus (psi)	13500	
Subgrade		
Material type	SP-1-A_3	
Modulus (psi)	27739/7000	

Table C.1.4-3 HMA overlay project 28155

Project Information	
Job number:	28155
Project CS:	80111
Region:	Southwest
Route	
Year opened	1991
CAADT	185
Repairs:	

Pavement Cross Section	Thickness (in)
HMA overlay	2.5
Existing HMA	5
Base	7
Subbase	12

Initial IRI	75
Original construction	1975

TTC Site	State Avg
Vehicle Class	Vehicle %
4	1.50
5	10.00
6	2.00
7	0.80
8	2.50
9	70.00
10	5.50
11	1.10
12	0.20
13	6.40
Sum	100.00

MEPDG Inputs		
Traffic		
Two way AADTT	185	
Lanes in design direction	2	
Climate	Kalamazoo	
Overlay Layer	Top	Leveling
HMA Thickness (in)	1.25	1.25
HMA binder	120-150	
AC Mixture air voids	7	7
Effective Binder Content (%)	11.8	11
3/4 inch sieve	0	0
3/8 inch sieve	11	10.6
No. 4	34.1	31.5
No. 200	5.4	5.4
Existing HMA		
HMA Thickness (in)	5.2	
HMA binder	120-150	
AC Mixture air voids	7	
Effective Binder Content (%)	12	
3/4 inch sieve	0	
3/8 inch sieve	10.6	
No. 4	31.5	
No. 200	5.4	
Base Layer		
Thickness (in)	7	
Material type	Crushed Stone	
Modulus (psi)	30000	
Subbase Layer		
Thickness (in)	12	
Material type	A-3	
Modulus (psi)	13500	
Subgrade		
Material type	SP-1-A_3	
Modulus (psi)	27739/7000	

Table C.1.4-4 HMA overlay project 26658

Project Information	
Job number:	26658
Project CS:	28021
Region:	
Route	
Year opened	1992
CAADT	130
Repairs:	

Pavement Cross Section	Thickness (in)
HMA overlay	2.5
Existing HMA	5*
Base	7*
Subbase	12*

Initial IRI	50
Original construction	1975

TTC Site	State Avg
Vehicle Class	Vehicle %
4	1.50
5	10.00
6	2.00
7	0.80
8	2.50
9	70.00
10	5.50
11	1.10
12	0.20
13	6.40
Sum	100.00

MEPDG Inputs		
Traffic		
Two way AADTT	130	
Lanes in design direction	1	
Climate	Traverse city	
Overlay Layer	Top	Leveling
HMA Thickness (in)	1.25	1.25
HMA binder		
AC Mixture air voids	4.8	6
Effective Binder Content (%)	12	11.4
3/4 inch sieve	0	0
3/8 inch sieve	18.6	17.3
No. 4	40.4	37.4
No. 200	5.4	6.4
Existing HMA		
HMA Thickness (in)	5*	
HMA binder	120-150	
AC Mixture air voids	7	
3/4 inch sieve	0	
3/8 inch sieve	17.3	
No. 4	37.4	
No. 200	5.7	
Base Layer		
Thickness (in)	7*	
Material type	Crushed Stone	
Modulus (psi)	30000	
Subbase Layer		
Thickness (in)	12*	
Material type	A-3	
Modulus (psi)	13500	
Subgrade		
Material type	SP-1-A_3	
Modulus (psi)	27739/7000	

Table C.1.4-5 HMA overlay project 29755

Project Information	
Job number:	29755
Project CS:	80072
Region:	North
Route	M-40
Year opened	1994
CAADT	184.3
Repairs:	

Pavement Cross Section	Thickness (in)
HMA overlay	3
Existing HMA	4.75
Base	4
Subbase	0

Initial IRI	63
Original construction	1975

TTC Site	State Avg
Vehicle Class	Vehicle %
4	1.50
5	10.00
6	2.00
7	0.80
8	2.50
9	70.00
10	5.50
11	1.10
12	0.20
13	6.40
Sum	100.00

MEPDG Inputs		
Traffic		
Two way AADTT	184.3	
Lanes in design direction	1	
Climate	Traverse City	
Overlay Layer	Top	Leveling
HMA Thickness (in)	1.5	1.5
HMA binder	120-150	
AC Mixture air voids	4.8	6
Effective Binder Content (%)	12	11.4
3/4 inch sieve	0	0
3/8 inch sieve	18.6	17.3
No. 4	40.4	37.4
No. 200	5.4	5.7
Existing HMA		
HMA Thickness (in)	4.75	
HMA binder	120-150	
AC Mixture air voids	7	
Effective Binder Content (%)	11	
3/4 inch sieve	0	
3/8 inch sieve	17.3	
No. 4	37.4	
No. 200	5.7	
Base Layer		
Thickness (in)	4	
Material type	Stabalized	
Modulus (psi)		
Subbase Layer		
Thickness (in)	0	
Material type		
Modulus (psi)		
Subgrade		
Material type	SP-1 A-3	
Modulus (psi)	27739/ 7000	

Table C.1.4-6 HMA overlay project 30701

Project Information	
Job number:	30701
Project CS:	14041
Region:	Southwest
Route	US-12
Year opened	1994
CAADT	408
Repairs:	

Pavement Cross Section	Thickness (in)
HMA overlay	3
Existing HMA	4.5
Base	7
Subbase	15

Initial IRI	63
Original construction	1959

TTC Site	State Avg
Vehicle Class	Vehicle %
4	1.50
5	10.00
6	2.00
7	0.80
8	2.50
9	70.00
10	5.50
11	1.10
12	0.20
13	6.40
Sum	100.00

MEPDG Inputs		
Traffic		
Two way AADTT	408	
Lanes in design direction	1	
Climate	Kalamazoo	
Overlay Layer	Top	
HMA Thickness (in)	1.5	1.5
HMA binder	85-100	
AC Mixture air voids	6.6	4.8
Effective Binder Content (%)	10	11.8
3/4 inch sieve	0	0
3/8 inch sieve	36	10.3
No. 4	45.6	41.4
No. 200	6.5	5.7
Existing HMA		
HMA Thickness (in)	4.5	
HMA binder	85-100	
AC Mixture air voids	7	
Effective Binder Content (%)	11	
3/4 inch sieve	0	
3/8 inch sieve	36	
No. 4	45.6	
No. 200	6.5	
Base Layer		
Thickness (in)	7	
Material type	Crushed Stone	
Modulus (psi)	30000	
Subbase Layer		
Thickness (in)	15	
Material type	A-3	
Modulus (psi)	13500	
Subgrade		
Material type	SP-1 A-3	
Modulus (psi)	27739/ 7000	

Table C.1.4-7 HMA overlay project 31047

Project Information	
Job number:	31047
Project CS:	2042
Region:	
Route	M-28
Year opened	1996
CAADT	260
Repairs:	

Pavement Cross Section	Thickness (in)
HMA overlay	3
Existing HMA	3
Base	10
Subbase	18

Initial IRI	63
Original construction	1961

TTC Site	State Avg
Vehicle Class	Vehicle %
4	1.50
5	10.00
6	2.00
7	0.80
8	2.50
9	70.00
10	5.50
11	1.10
12	0.20
13	6.40
Sum	100.00

MEPDG Inputs		
Traffic		
Two way AADTT	260	
Lanes in design direction	1	
Climate	Marquette	
Overlay Layer	Top	Leveling
HMA Thickness (in)	1.5	1.5
HMA binder	120-150	
AC Mixture air voids	4.8	6
Effective Binder Content (%)	12	11.4
3/4 inch sieve	0	0
3/8 inch sieve	18.6	17.3
No. 4	40.4	37.4
No. 200	5.4	5.7
Existing HMA		
HMA Thickness (in)	3.3	
HMA binder	120-150	
AC Mixture air voids	7	
Effective Binder Content (%)	11	
3/4 inch sieve	0	
3/8 inch sieve	17.3	
No. 4	37.4	
No. 200	5.7	
Base Layer		
Thickness (in)	10	
Material type	Crushed Stone	
Modulus (psi)	30000	
Subbase Layer		
Thickness (in)	18	
Material type	A-3	
Modulus (psi)	13500	
Subgrade		
Material type	SP-SM	
Modulus (psi)	20400/ 7000	

Table C.1.4-8 HMA overlay project 32361

Project Information	
Job number:	32361
Project CS:	32092
Region:	Bay
Route	M-25
Year opened	1997
CAADT	3900 adt
Repairs:	

Pavement Cross Section	Thickness (in)
HMA overlay	3
Existing HMA	3.3
Base	5-7-5
Subbase	13.7

Initial IRI	50
Original construction	1954

TTC Site	State Avg
Vehicle Class	Vehicle %
4	1.50
5	10.00
6	2.00
7	0.80
8	2.50
9	70.00
10	5.50
11	1.10
12	0.20
13	6.40
Sum	100.00

MEPDG Inputs		
Traffic		
Two way AADTT	3900 adt	
Lanes in design direction	1	
Climate	Flint	
Overlay Layer	Top	Leveling
HMA Thickness (in)	1.5	1.5
HMA binder	120-150	
AC Mixture air voids	4.8	6
Effective Binder Content (%)	12	11.4
3/4 inch sieve	0	0
3/8 inch sieve	18.6	17.3
No. 4	40.4	37.4
No. 200	5.4	5.7
Existing HMA		
HMA Thickness (in)	3.3	
HMA binder	120-150	
AC Mixture air voids	7	
Effective Binder Content (%)	11	
3/4 inch sieve	0	
3/8 inch sieve	17.3	
No. 4	37.4	
No. 200	5.7	
Base Layer		
Thickness (in)	5-7-5	
Material type	Crushed Stone	
Modulus (psi)	30000	
Subbase Layer		
Thickness (in)	13.7	
Material type	A-3	
Modulus (psi)	13500	
Subgrade		
Material type	SM - A-4	
Modulus (psi)	24764/ 5200	

Table C.1.4-9 HMA overlay project 45875

Project Information	
Job number:	45875
Project CS:	14042
Region:	
Route	US-12
Year opened	2002
CAADT	803.4
Repairs:	

Pavement Cross Section	Thickness (in)
HMA overlay	2
Existing HMA	5
Base	11
Subbase	15

Initial IRI	55
Original construction	1968

TTC Site	State Avg
Vehicle Class	Vehicle %
4	1.50
5	10.00
6	2.00
7	0.80
8	2.50
9	70.00
10	5.50
11	1.10
12	0.20
13	6.40
Sum	100.00

MEPDG Inputs		
Traffic		
Two way AADTT	803.4	
Lanes in design direction	1	
Climate	South Bend	
Overlay Layer	Top	Leveling
HMA Thickness (in)	2	2
HMA binder	PG 64-28	
AC Mixture air voids	8	8
Effective Binder Content (%)	12.1	12.42
3/4 inch sieve	0	0
3/8 inch sieve	2.5	13.2
No. 4	32.8	35.1
No. 200	5.4	95.4
Existing HMA		
HMA Thickness (in)	4.5	
HMA binder	PG 64-28	
AC Mixture air voids	7	
Effective Binder Content (%)	11	
3/4 inch sieve	0	
3/8 inch sieve	13.2	
No. 4	35.1	
No. 200	4.6	
Base Layer		
Thickness (in)	11	
Material type	Crushed Stone	
Modulus (psi)	30000	
Subbase Layer		
Thickness (in)	15	
Material type	A-3	
Modulus (psi)	13500	
Subgrade		
Material type	SP-1 A-3	
Modulus (psi)	27739/ 7000	

Table C.1.4-10 HMA overlay project 50715

Project Information	
Job number:	50715
Project CS:	30041
Region:	
Route	M-34
Year opened	2005
CAADT	350
Repairs:	

Pavement Cross Section	Thickness (in)
HMA overlay	3.5
Existing HMA	7.59
Base	6
Subbase	8

Original construction	1951

TTC Site	State Avg
Vehicle Class	Vehicle %
4	1.50
5	10.00
6	2.00
7	0.80
8	2.50
9	70.00
10	5.50
11	1.10
12	0.20
13	6.40
Sum	100.00

MEPDG Inputs			
Traffic			
Two way AADTT	350		
Lanes in design direction	1		
Climate	Jackson		
Overlay Layer	Top	Leveling	Base
HMA Thickness (in)	1	1.25	1.25
HMA binder	PG 64-28	PG 64-28	PG 58-22
AC Mixture air voids	8	8	6
Effective Binder Content (%)	12.1	12.42	11.8
3/4 inch sieve	0	0	1.1
3/8 inch sieve	2.5	13.2	23.8
No. 4	32.8	35.1	37.7
No. 200	5.4	4.6	3.8
Existing HMA			
HMA Thickness (in)	7.59		
HMA binder	PG 64-28		
AC Mixture air voids	7		
Effective Binder Content (%)	11		
3/4 inch sieve	0		
3/8 inch sieve	13.2		
No. 4	35.1		
No. 200	4.6		
Base Layer			
Thickness (in)	6		
Material type	Crushed Stone		
Modulus (psi)	30000		
Subbase Layer			
Thickness (in)	8		
Material type	A-3		
Modulus (psi)	13500		
Subgrade			
Material type	SP-SM		
Modulus (psi)	20400/ 7000		

Table C.1.4-11 HMA overlay project 20313

Project Information	
Job number:	20313
Project CS:	45021
Region:	North
Route	M-72
Year opened	1983
CAADT	300
Repairs:	

Pavement Cross Section	Thickness (in)
HMA overlay	2.25
Existing HMA	1.5
Base	5
Subbase	0

Initial IRI	63
Original construction	1963

TTC Site	State Avg
Vehicle Class	Vehicle %
4	1.50
5	10.00
6	2.00
7	0.80
8	2.50
9	70.00
10	5.50
11	1.10
12	0.20
13	6.40
Sum	100.00

MEPDG Inputs		
Traffic		
Two way AADTT	300	
Lanes in design direction	1	
Climate	Traverse city	
Overlay Layer	Top	Leveling
HMA Thickness (in)	1	1.25
HMA binder	120-150	
AC Mixture air voids	6	7
Effective Binder Content (%)	12	10.4
3/4 inch sieve	0	0
3/8 inch sieve	15.4	13.4
No. 4	32.9	100
No. 200	7.4	5.8
Existing HMA		
HMA Thickness (in)	1.5	
HMA binder	120-150	
AC Mixture air voids	7	
Effective Binder Content (%)	11	
3/4 inch sieve	0	
3/8 inch sieve	13.4	
No. 4	37	
No. 200	5.8	
Base Layer		
Thickness (in)	5	
Material type	Crushed Stone	
Modulus (psi)	30000	
Subbase Layer		
Thickness (in)		
Material type		
Modulus (psi)		
Subgrade		
Material type	SP1-A-3	
Modulus (psi)	27739/ 7000	

Table C.1.4-12 HMA overlay project 12802

Project Information	
Job number:	12802
Project CS:	10041
Region:	
Route	M-115
Year opened	1984
CAADT	3800 ADT
Repairs:	

Pavement Cross Section	Thickness (in)
HMA overlay	2.5
Existing HMA	2.25 or 4.75
Base	7
Subbase	0 or 12

Initial IRI	63
Original construction	1957

TTC Site	State Avg
Vehicle Class	Vehicle %
4	1.50
5	10.00
6	2.00
7	0.80
8	2.50
9	70.00
10	5.50
11	1.10
12	0.20
13	6.40
Sum	100.00

MEPDG Inputs	
Traffic	
Two way AADTT	3800 ADT
Lanes in design direction	1
Climate	Traverse City
Overlay Layer	
HMA Thickness (in)	2.5
HMA binder	120-150
AC Mixture air voids	7
Effective Binder Content (%)	11.2
3/4 inch sieve	0
3/8 inch sieve	15
No. 4	36
No. 200	6.4
Existing HMA	
HMA Thickness (in)	2.25 or 4.75
HMA binder	120-150
AC Mixture air voids	7
Effective Binder Content (%)	11
3/4 inch sieve	0
3/8 inch sieve	15
No. 4	36
No. 200	6.4
Base Layer	
Thickness (in)	7
Material type	Crushed Stone
Modulus (psi)	30000
Subbase Layer	
Thickness (in)	0 or 12
Material type	A-3
Modulus (psi)	13500
Subgrade	
Material type	SP-1 A-3
Modulus (psi)	27739/ 7000

Table C.1.4-13 HMA overlay project 24621

Project Information	
Job number:	24621
Project CS:	13092
Region:	
Route	M-99
Year opened	1987
CAADT	238
Repairs:	

Pavement Cross Section	Thickness (in)
HMA overlay	2.5
Existing HMA	3.75
Base	8
Subbase	0

Initial IRI	63
Original construction	1934

TTC Site	State Avg
Vehicle Class	Vehicle %
4	1.50
5	10.00
6	2.00
7	0.80
8	2.50
9	70.00
10	5.50
11	1.10
12	0.20
13	6.40
Sum	100.00

MEPDG Inputs		
Traffic		
Two way AADTT	238	
Lanes in design direction	1	
Climate	Battle Creek	
Overlay Layer	Top	Leveling
HMA Thickness (in)	1.25	1.25
HMA binder	120-150	
AC Mixture air voids	7	7
Effective Binder Content (%)	11.2	10.4
3/4 inch sieve	0	0
3/8 inch sieve	14.2	13.3
No. 4	36.4	34.1
No. 200	6.9	8.5
Existing HMA		
HMA Thickness (in)	3.75	
HMA binder	120-150	
AC Mixture air voids	7	
Effective Binder Content (%)	11	
3/4 inch sieve	0	
3/8 inch sieve	13.3	
No. 4	34.1	
No. 200	8.5	
Base Layer		
Thickness (in)	8	
Material type	Crushed Stone	
Modulus (psi)	30000	
Subbase Layer		
Thickness (in)		
Material type		
Modulus (psi)		
Subgrade		
Material type	SP-1 A-3	
Modulus (psi)	27739/ 7000	

Table C.1.4-14 HMA overlay project 25515

Project Information	
Job number:	25515
Project CS:	83021
Region:	
Route	M-55 and M-115
Year opened	1989
CAADT	315
Repairs:	

Pavement Cross Section	Thickness (in)
HMA overlay	2.5
Existing HMA	2.25
Base	10
Subbase	0

Initial IRI	63
Original construction	1954

TTC Site	State Avg
Vehicle Class	Vehicle %
4	1.50
5	10.00
6	2.00
7	0.80
8	2.50
9	70.00
10	5.50
11	1.10
12	0.20
13	6.40
Sum	100.00

MEPDG Inputs		
Traffic		
Two way AADTT	315	
Lanes in design direction	1	
Climate	Cadillac	
Overlay Layer	Top	Leveling
HMA Thickness (in)	1.25	1.25
HMA binder	120-150	
AC Mixture air voids	7	7
Effective Binder Content (%)	11	11
3/4 inch sieve	0	0
3/8 inch sieve	10.2	12
No. 4	38.4	35.2
No. 200	5.6	6.6
Existing HMA		
HMA Thickness (in)	2.25	
HMA binder	120-150	
AC Mixture air voids	7	
Effective Binder Content (%)	11	
3/4 inch sieve	0	
3/8 inch sieve	12	
No. 4	35.2	
No. 200	5.6	
Base Layer		
Thickness (in)	10	
Material type	Crushed Stone	
Modulus (psi)	30000	
Subbase Layer		
Thickness (in)		
Material type		
Modulus (psi)		
Subgrade		
Material type	SP-1 A-3	
Modulus (psi)	27739/ 7000	

Table C.1.4-15 HMA overlay project 30702

Project Information	
Job number:	30702
Project CS:	14041
Region:	
Route	
Year opened	1990
CAADT	365
Repairs:	

Pavement Cross Section	Thickness (in)
HMA overlay	2.5
Existing HMA	7.1
Base	5
Subbase	0

Initial IRI	75
Original construction	1959

TTC Site	State Avg
Vehicle Class	Vehicle %
4	1.50
5	10.00
6	2.00
7	0.80
8	2.50
9	70.00
10	5.50
11	1.10
12	0.20
13	6.40
Sum	100.00

MEPDG Inputs	
Traffic	
Two way AADTT	365
Lanes in design direction	1
Climate	South Bend
Overlay Layer	
HMA Thickness (in)	2.5
HMA binder	85-100
AC Mixture air voids	7
Effective Binder Content (%)	11
3/4 inch sieve	0
3/8 inch sieve	11.2
No. 4	32.2
No. 200	6
Existing HMA	
HMA Thickness (in)	7.1
HMA binder	85-100
AC Mixture air voids	7
Effective Binder Content (%)	11
3/4 inch sieve	0
3/8 inch sieve	11.2
No. 4	32.2
No. 200	6
Base Layer	
Thickness (in)	5
Material type	Crushed Stone
Modulus (psi)	30000
Subbase Layer	
Thickness (in)	
Material type	
Modulus (psi)	
Subgrade	
Material type	SP-1 A-3
Modulus (psi)	27739/ 7000

C.2 VALIDATION RESULTS

The validation results include the PMS and Sensor database extracted data. To avoid repetitiveness, only one set of figures are presented to account for both, field performance, and predicted performance. The predicted performance is plotted on the same figure to illustrate how well the software predicts measured performance. For unbonded overlays, each figure is divided into three plots namely:

a) Percent slabs cracked
b) IRI
c) Faulting

For rubblized, composite, and HMA overlay projects, the figures are divided into four plots consisting of:

a) Longitudinal cracking
b) Thermal transverse cracking
c) Rutting
d) IRI

C.2.1 Unbonded Overlays

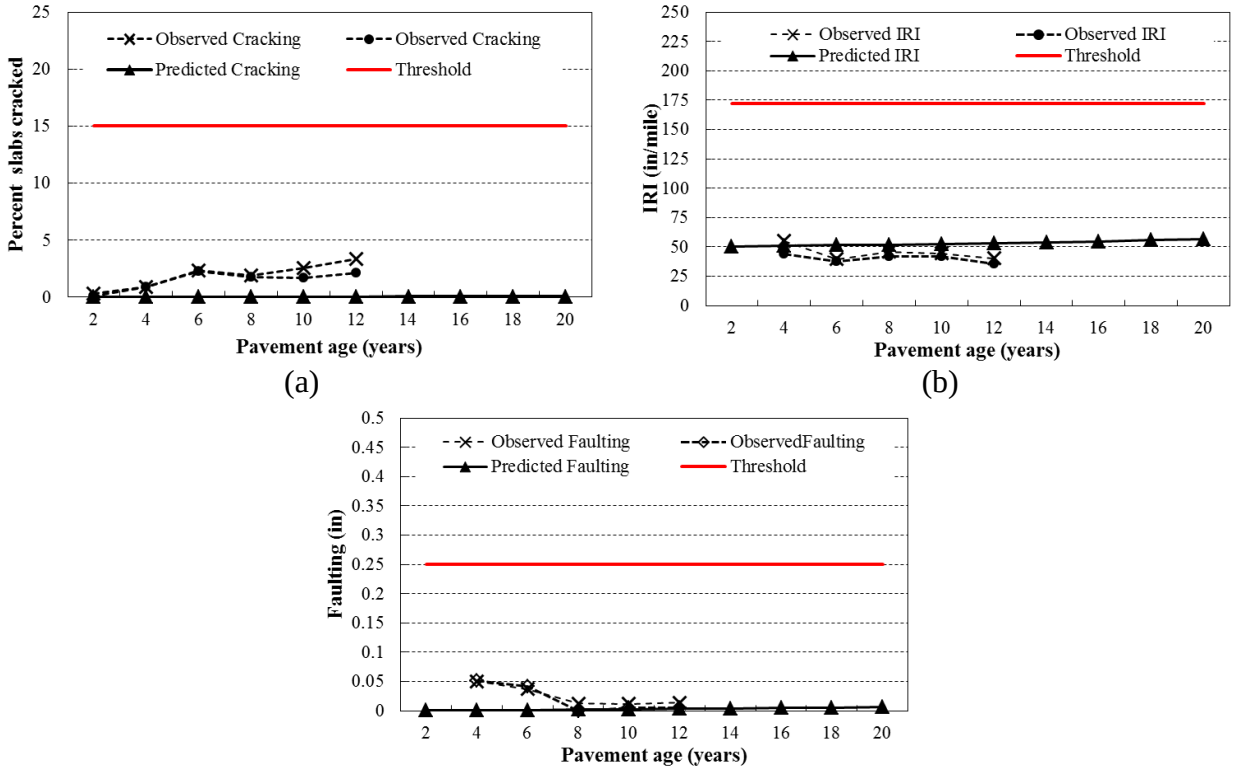

Figure C.2.1-1 Unbonded overlay project 37997

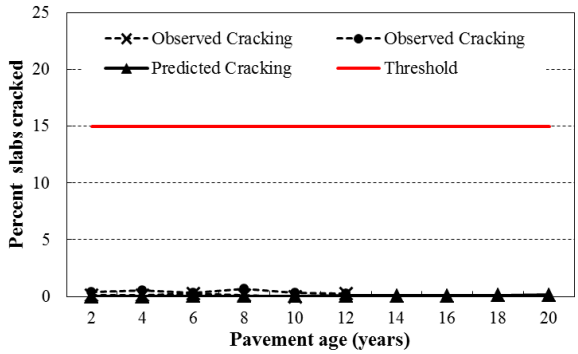

(a)

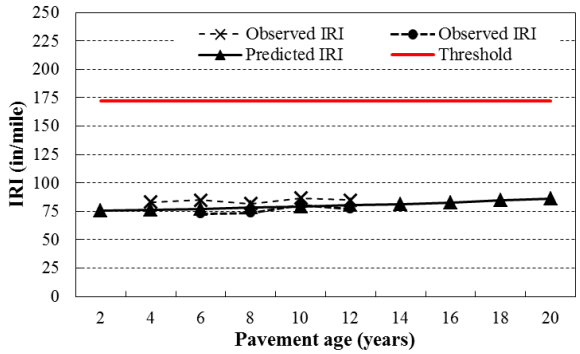

(b)

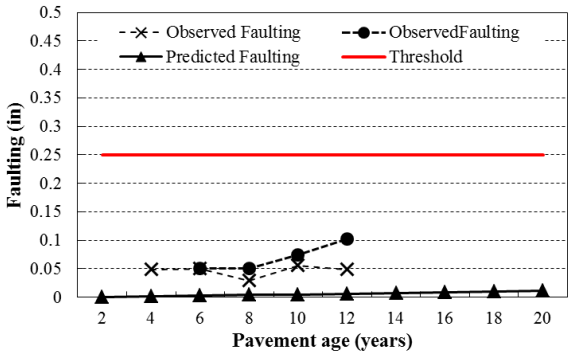

(c)

Figure C.2.1-2 Unbonded overlay project 34120

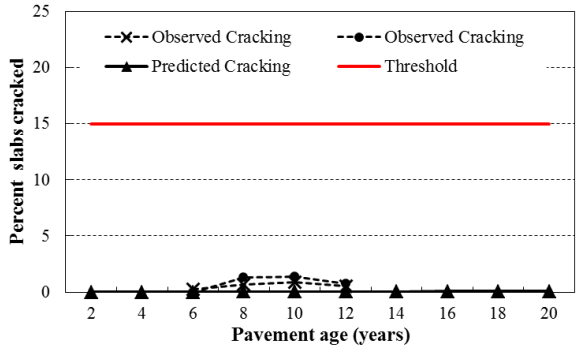

(a)

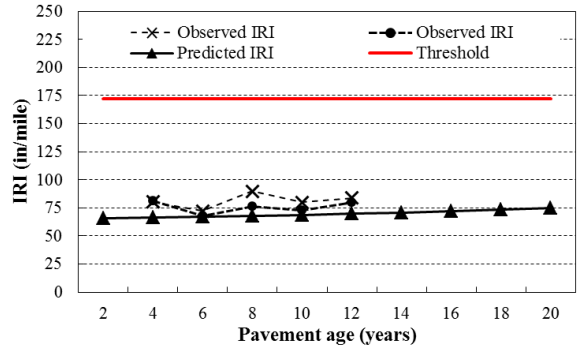

(b)

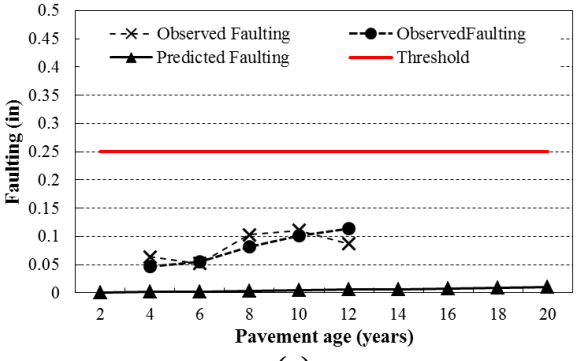

(c)

Figure C.2.1-3 Unbonded overlay project 49029

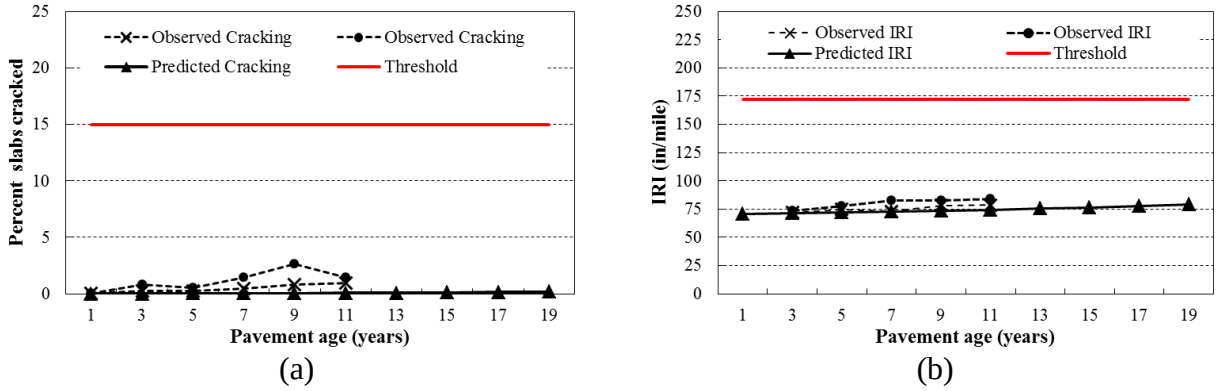

(a) (b)

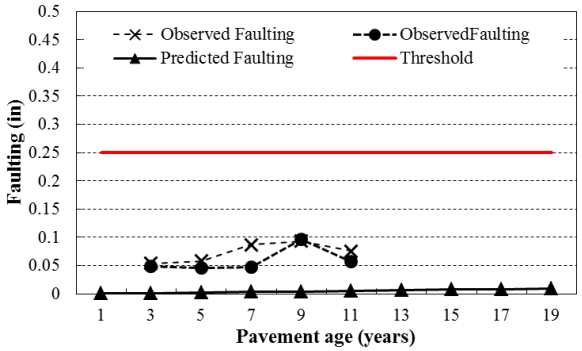

(c)

Figure C.2.1-4 Unbonded overlay project 45591

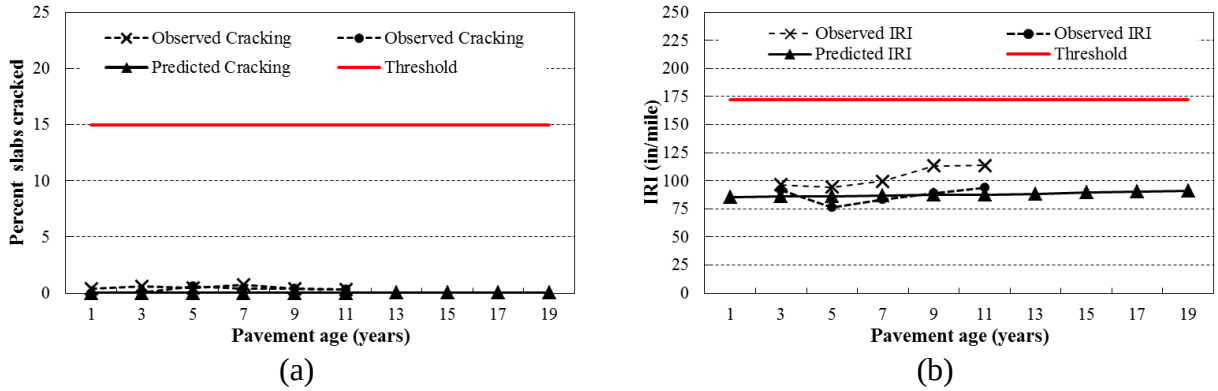

(a) (b)

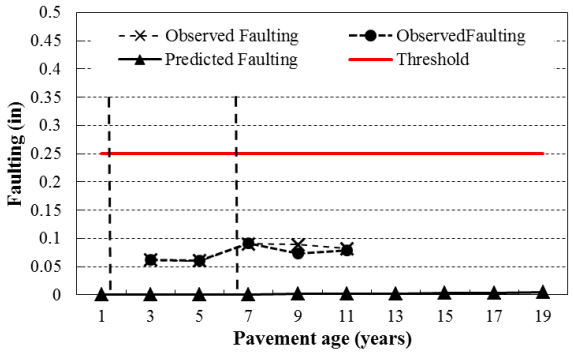

(c)

Figure C.2.1-5 Unbonded overlay project 38209

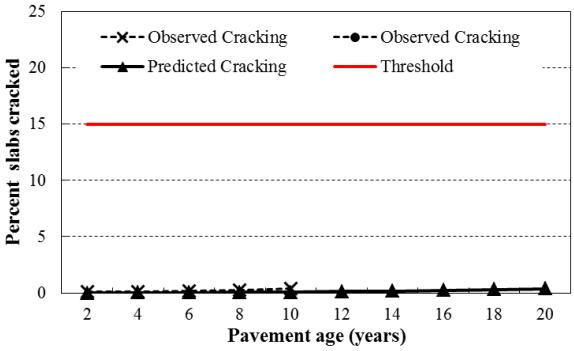

(a)

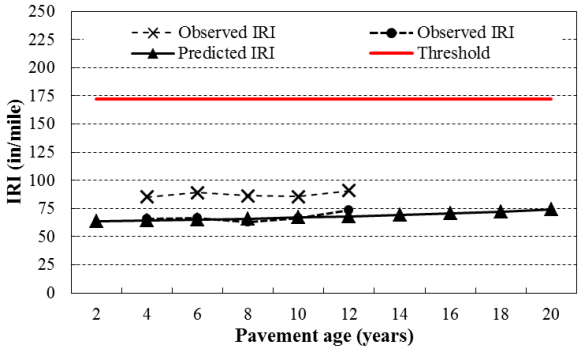

(b)

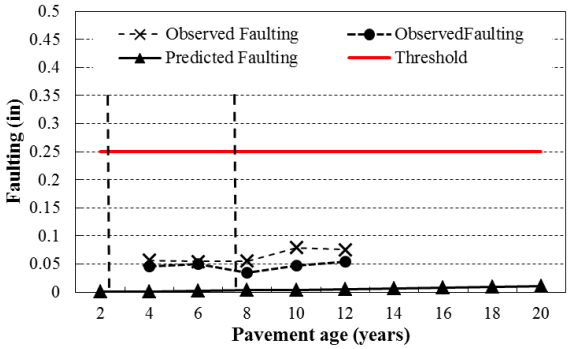

(c)

Figure C.2.1-6 Unbonded overlay project 43499

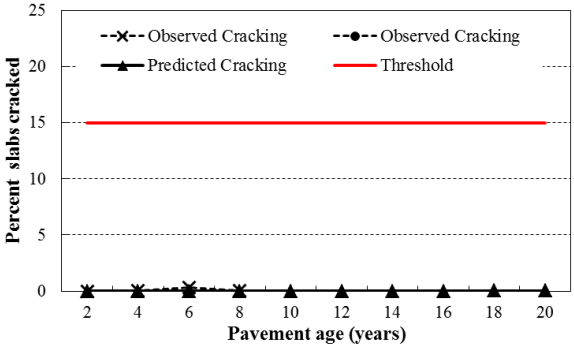

(a)

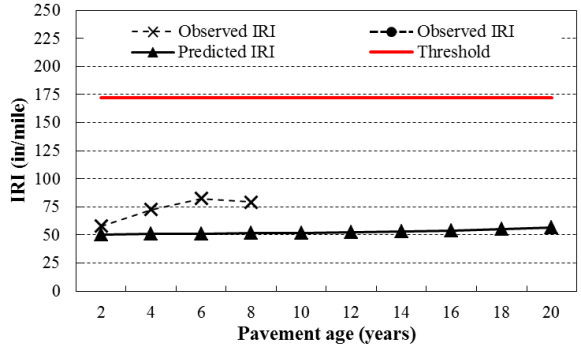

(b)

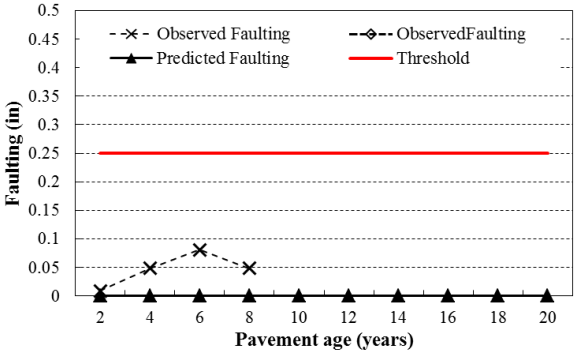

(c)

Figure C.2.1-7 Unbonded overlay project 73873

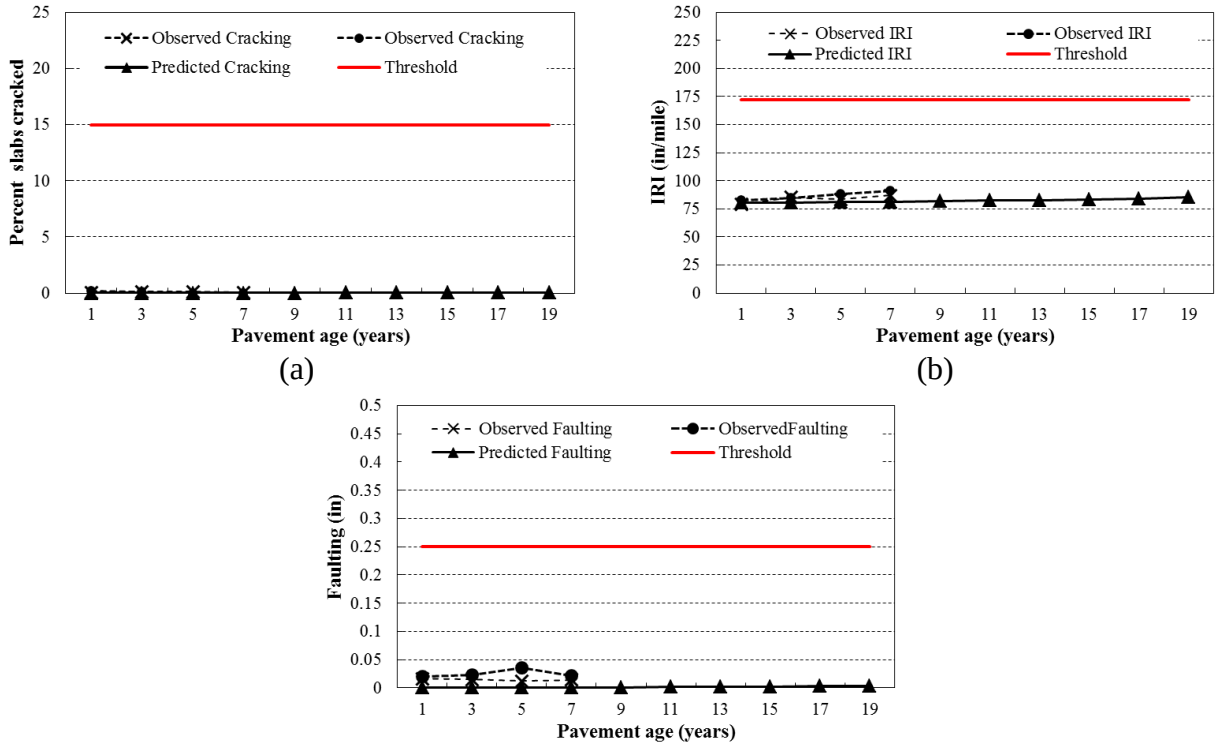

Figure C.2.1-8 Unbonded overlay project 50763

C.2.2 Rubblized Overlays

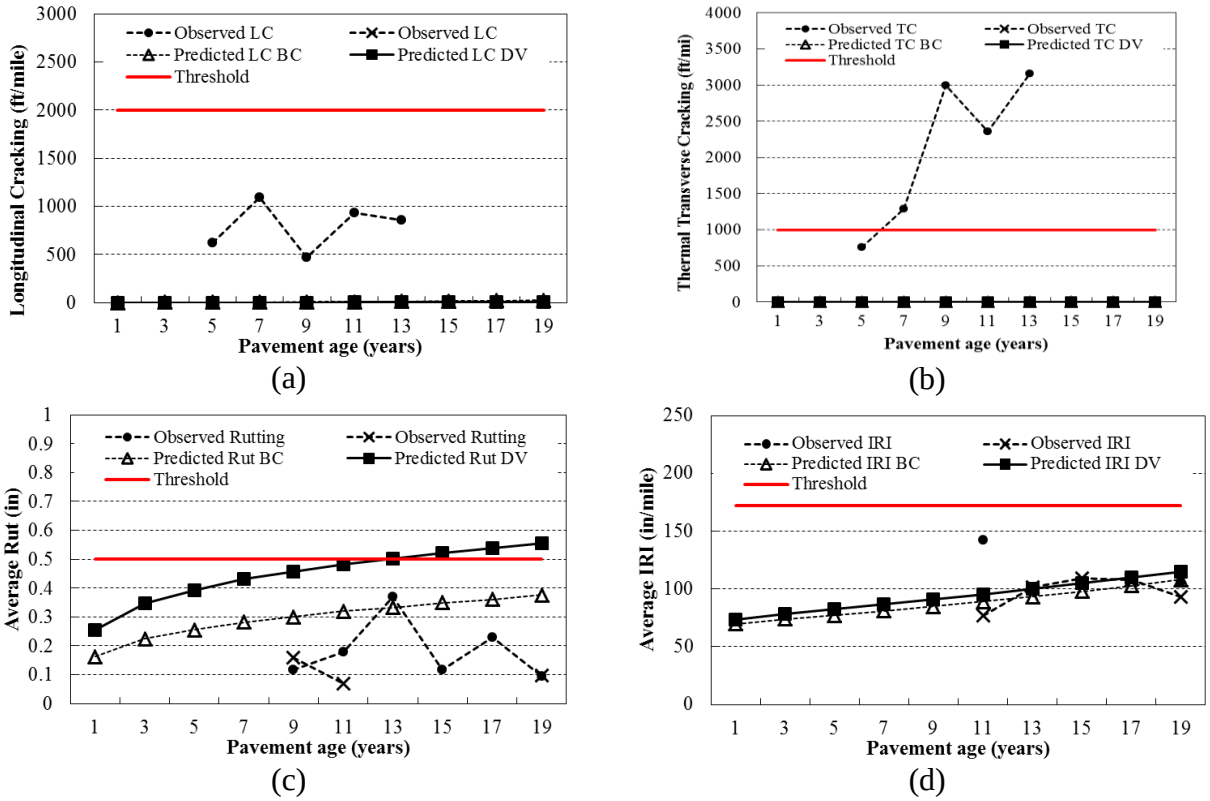

Figure C.2.2-1 Rubblized overlay project 28155

(a) (b)

(c) (d)

Figure C.2.2-2 Rubblized overlay project 26755

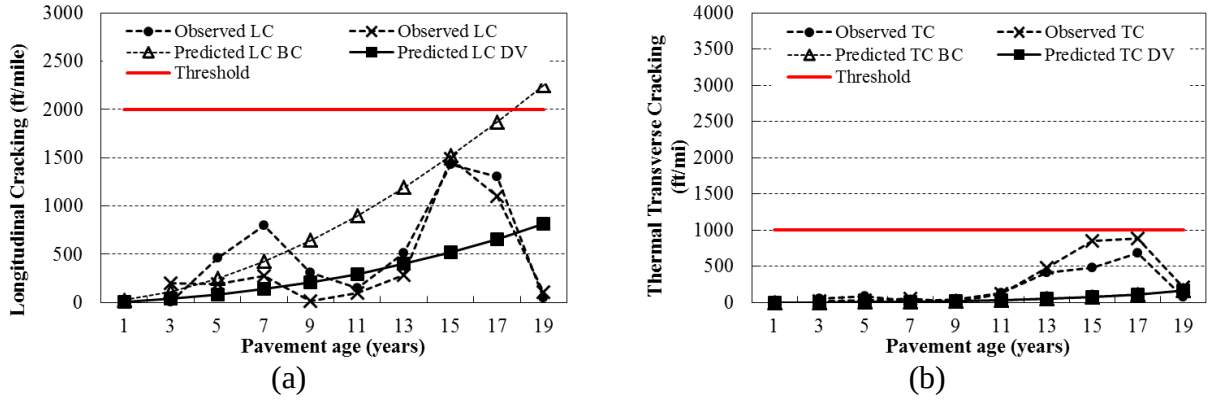

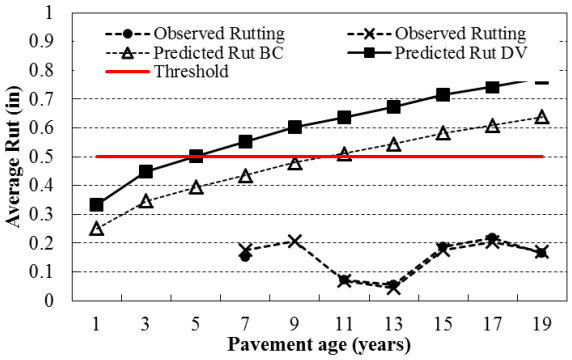

(c)

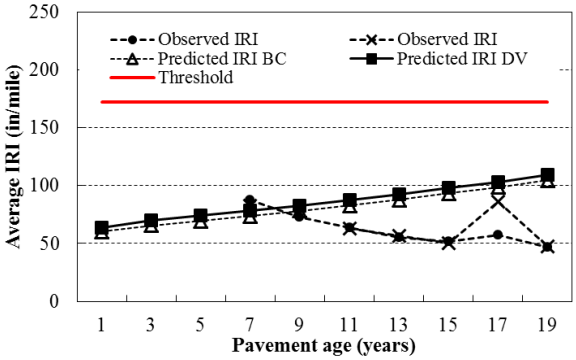

(d)

Figure C.2.2-3 Rubblized overlay project 29768

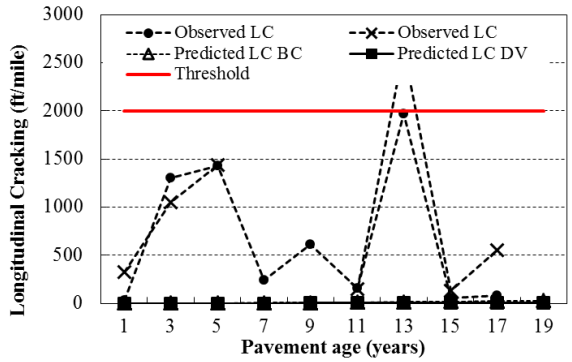

(a)

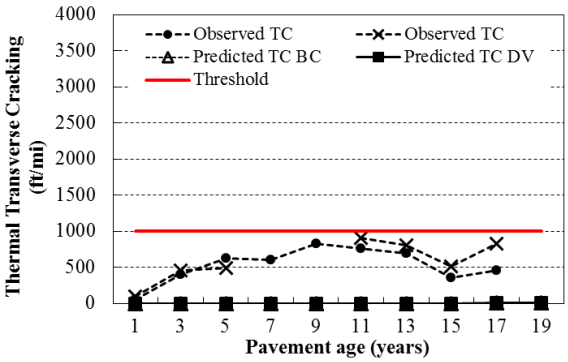

(b)

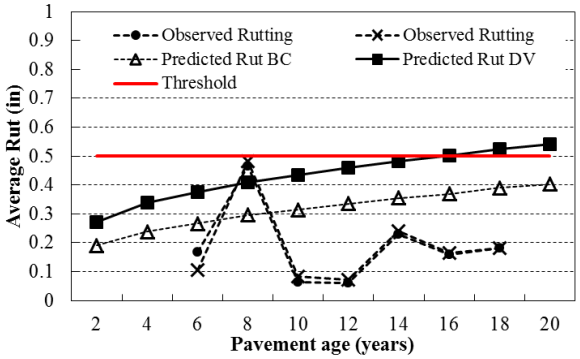

(c)

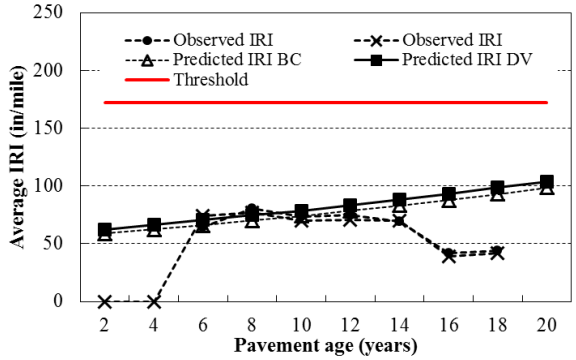

(d)

Figure C.2.2-4 Rubblized overlay project 29670

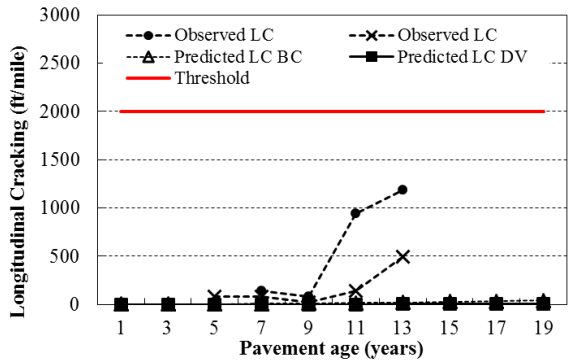

(a)

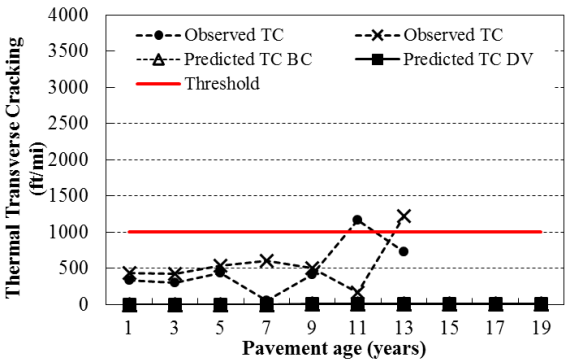

(b)

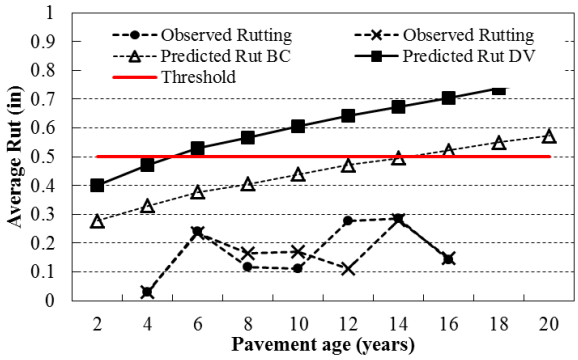

(c)

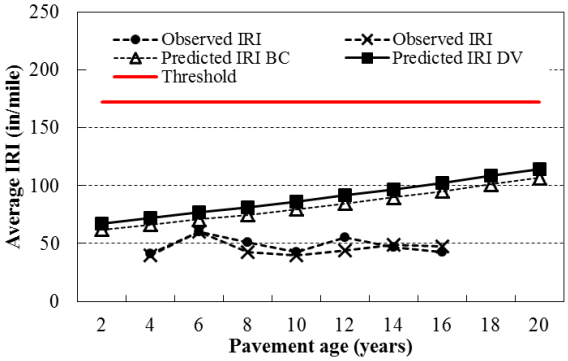

(d)

Figure C.2.2-5 Rubblized overlay project 29581

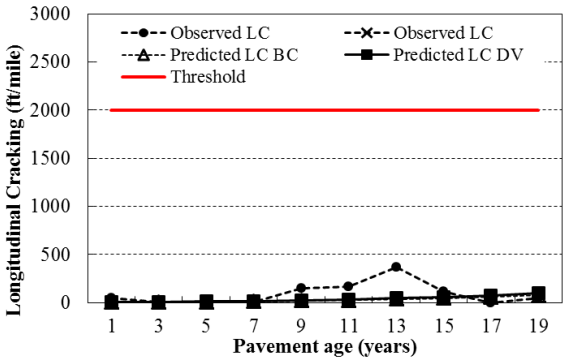

(a)

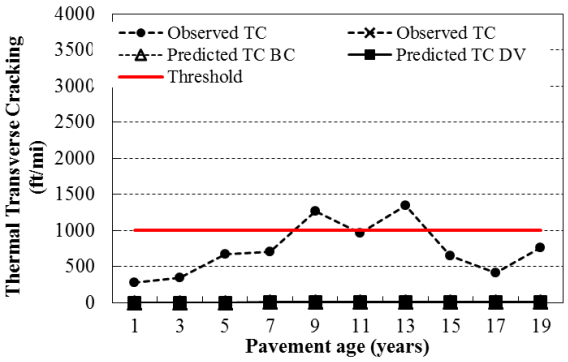

(b)

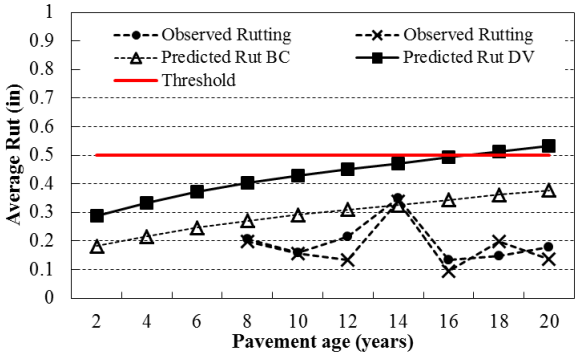

(c)

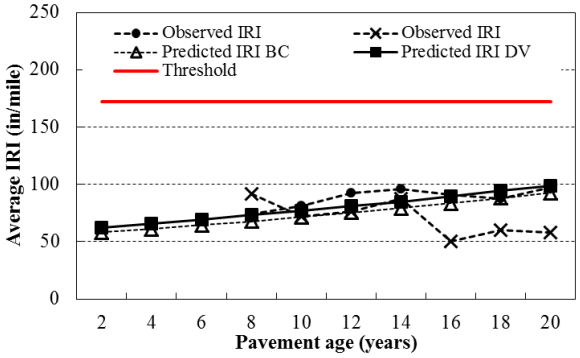

(d)

Figure C.2.2-6 Rubblized overlay project 28111

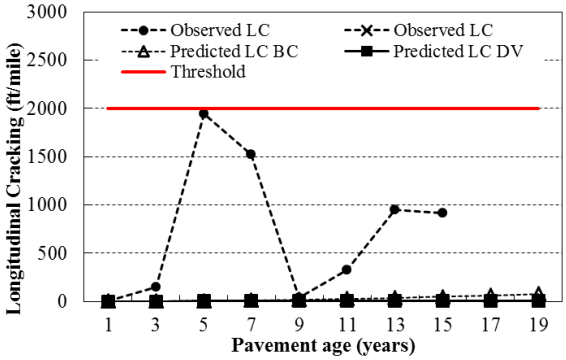

(a)

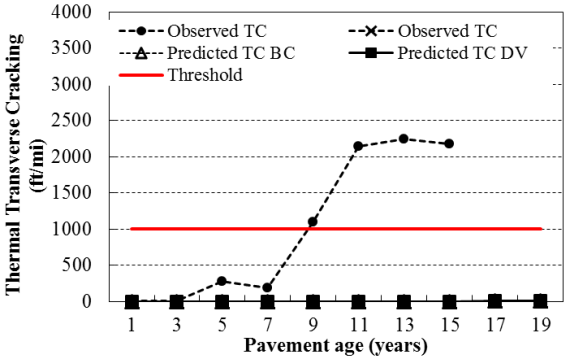

(b)

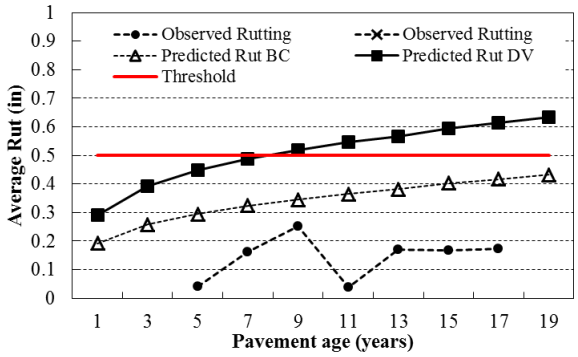

(c)

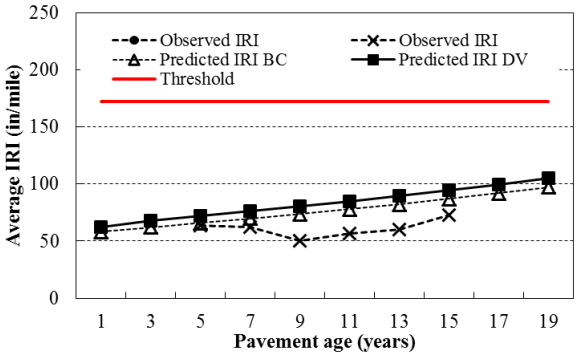

(d)

Figure C.2.2-7 Rubblized overlay project 29729

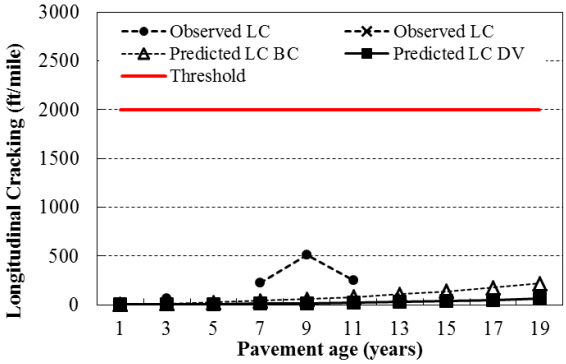

(a)

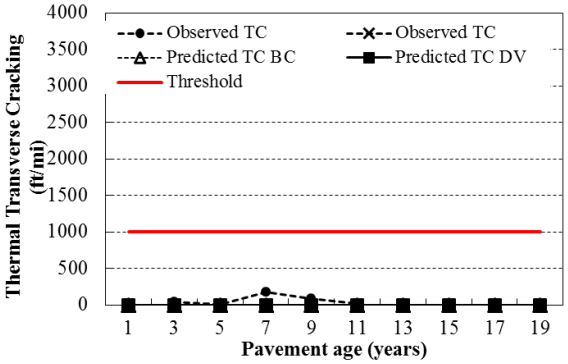

(b)

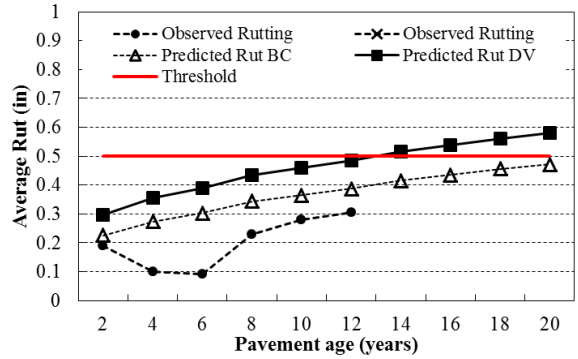

(c)

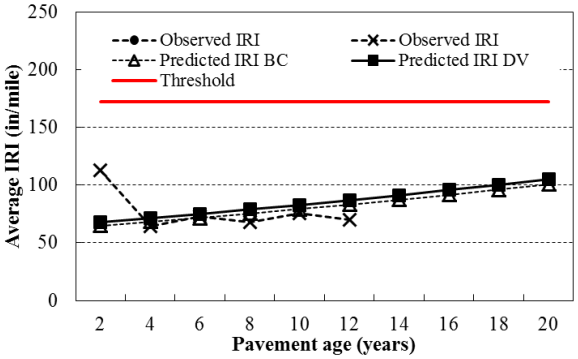

(d)

Figure C.2.2-8 Rubblized overlay project 45053

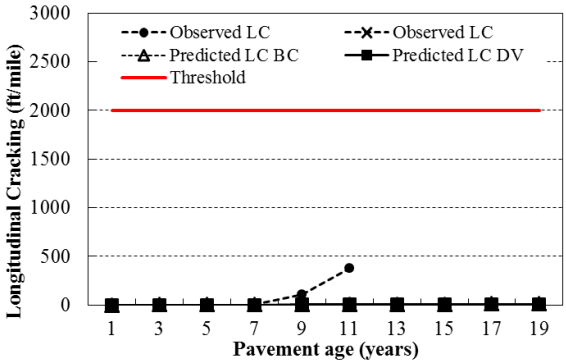

(a)

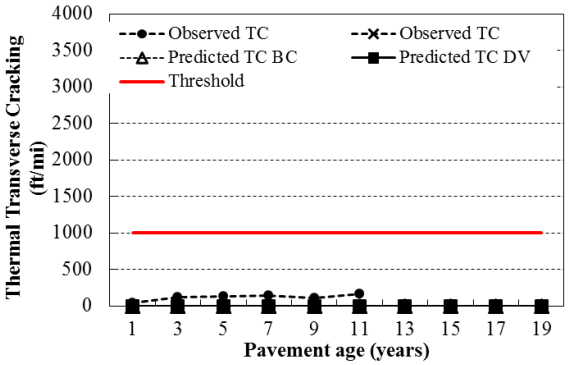

(b)

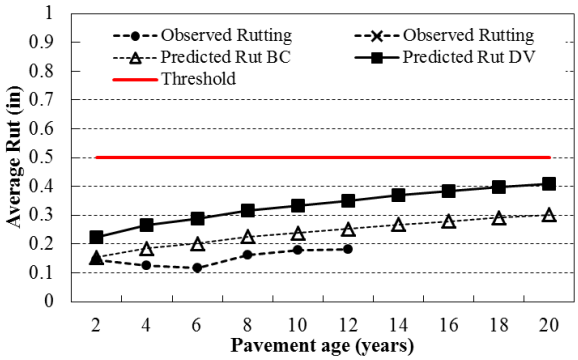

(c)

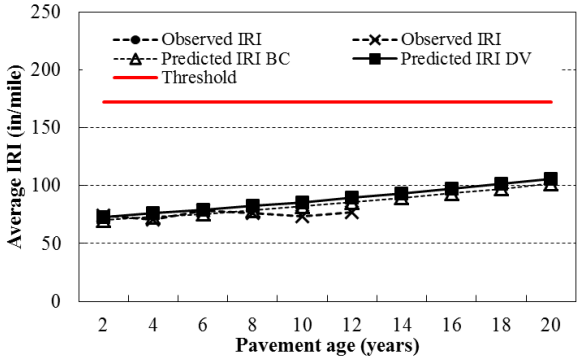

(d)

Figure C.2.2-9 Rubblized overlay project 44109

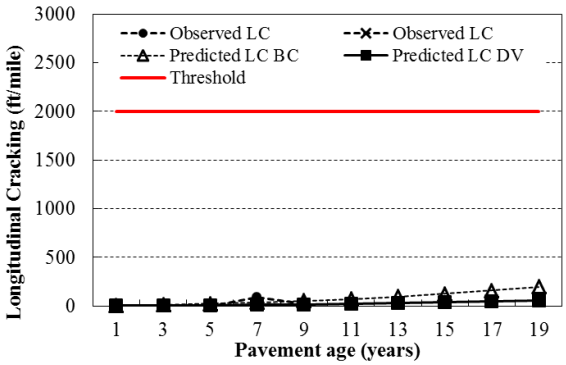

(a)

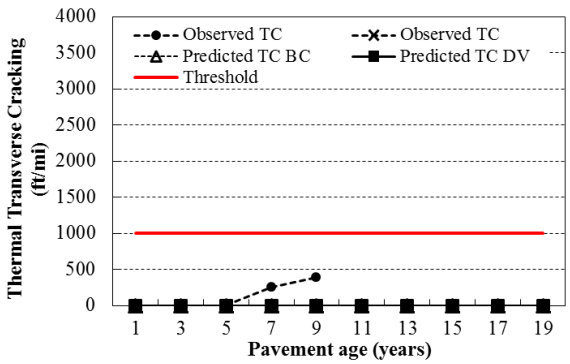

(b)

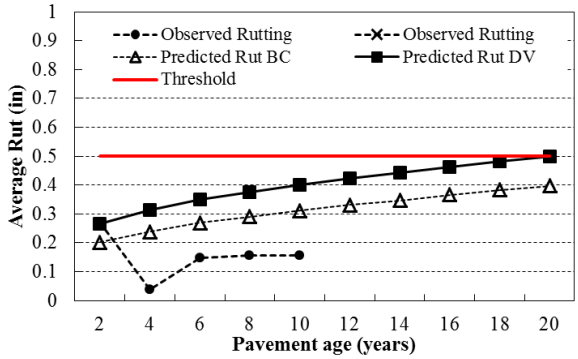

(c)

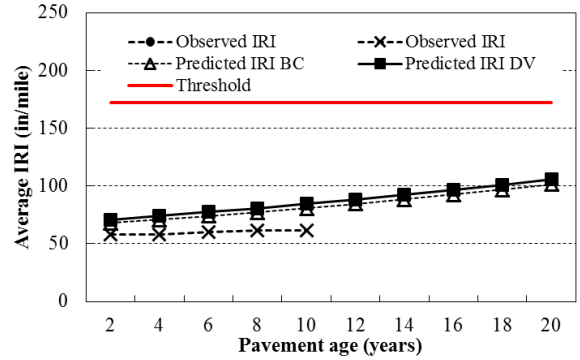

(d)

Figure C.2.2-10 Rubblized overlay project 38190

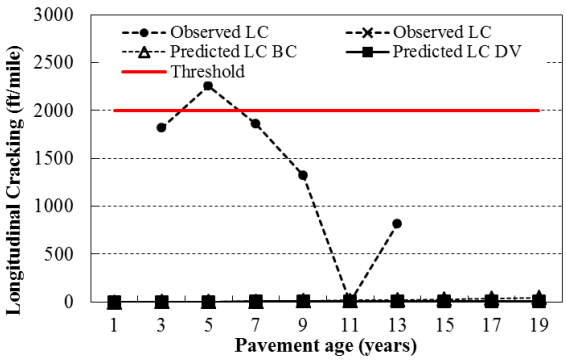

(a)

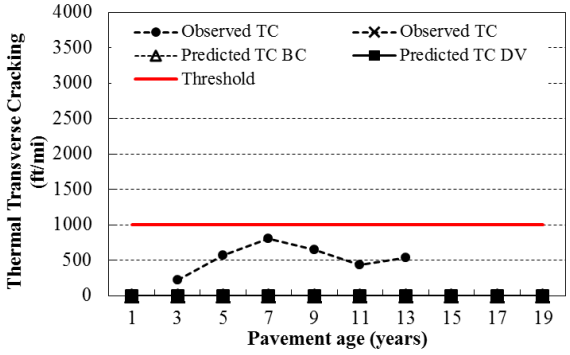

(b)

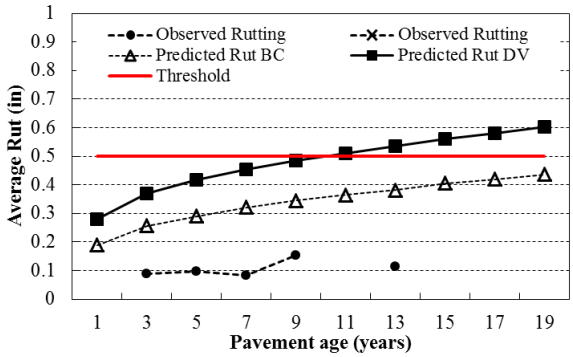

(c)

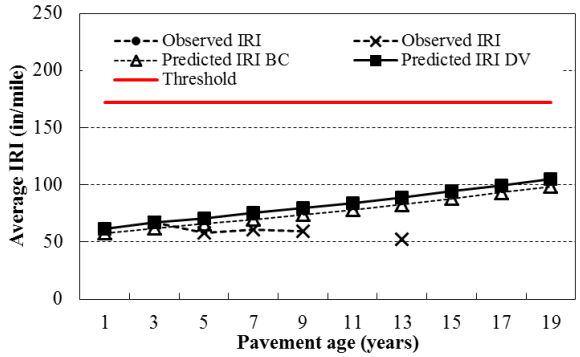

(d)

Figure C.2.2-11 Rubblized overlay project 32388

C.2.3 Composite Overlays

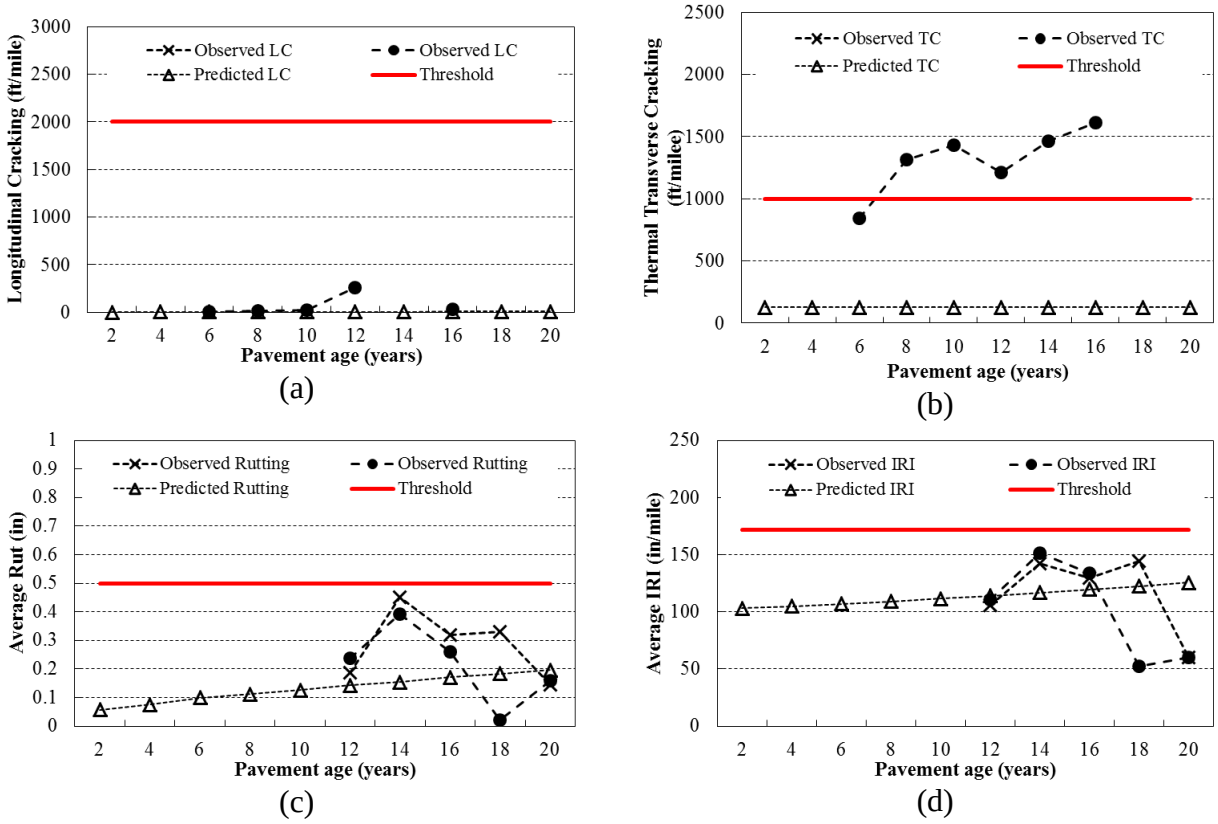

Figure C.2.3-1 Composite overlay project 25543

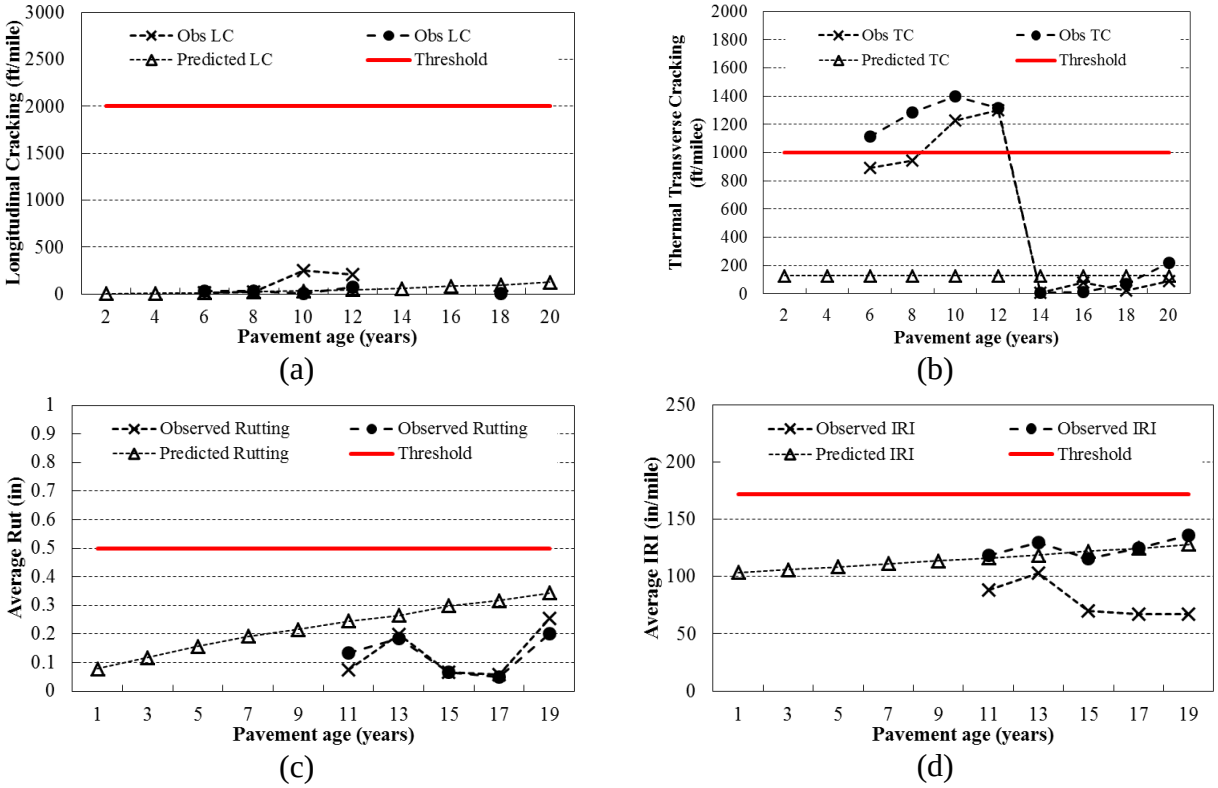

Figure C.2.3-2 Composite overlay project 24252

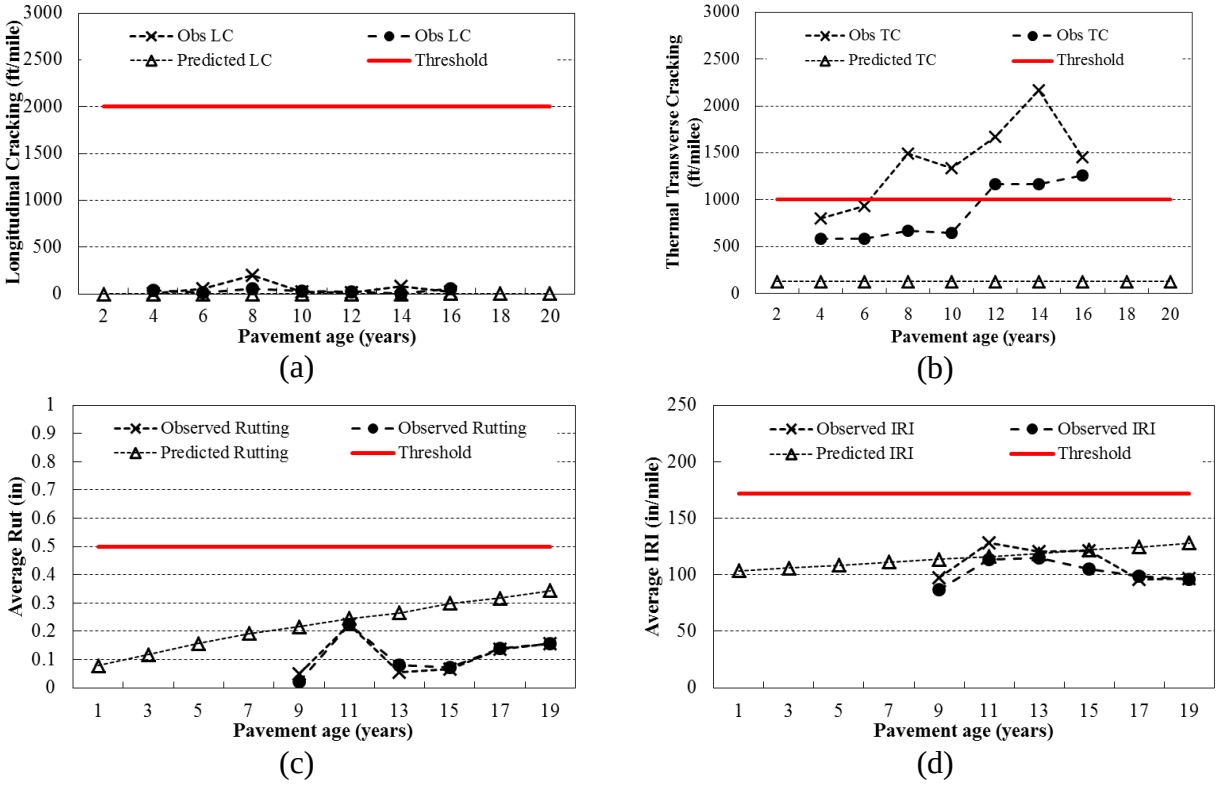

Figure C.2.3-3 Composite overlay project 29586

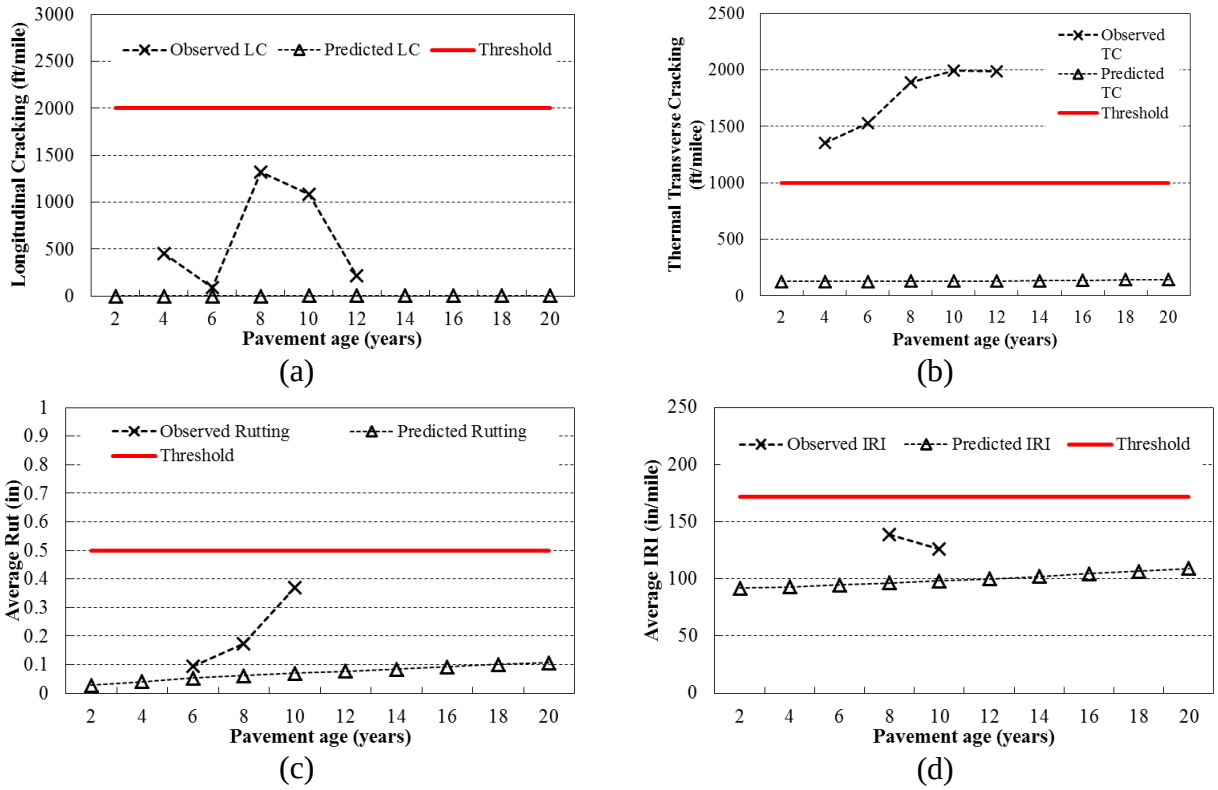

Figure C.2.3-4 Composite overlay project 29716

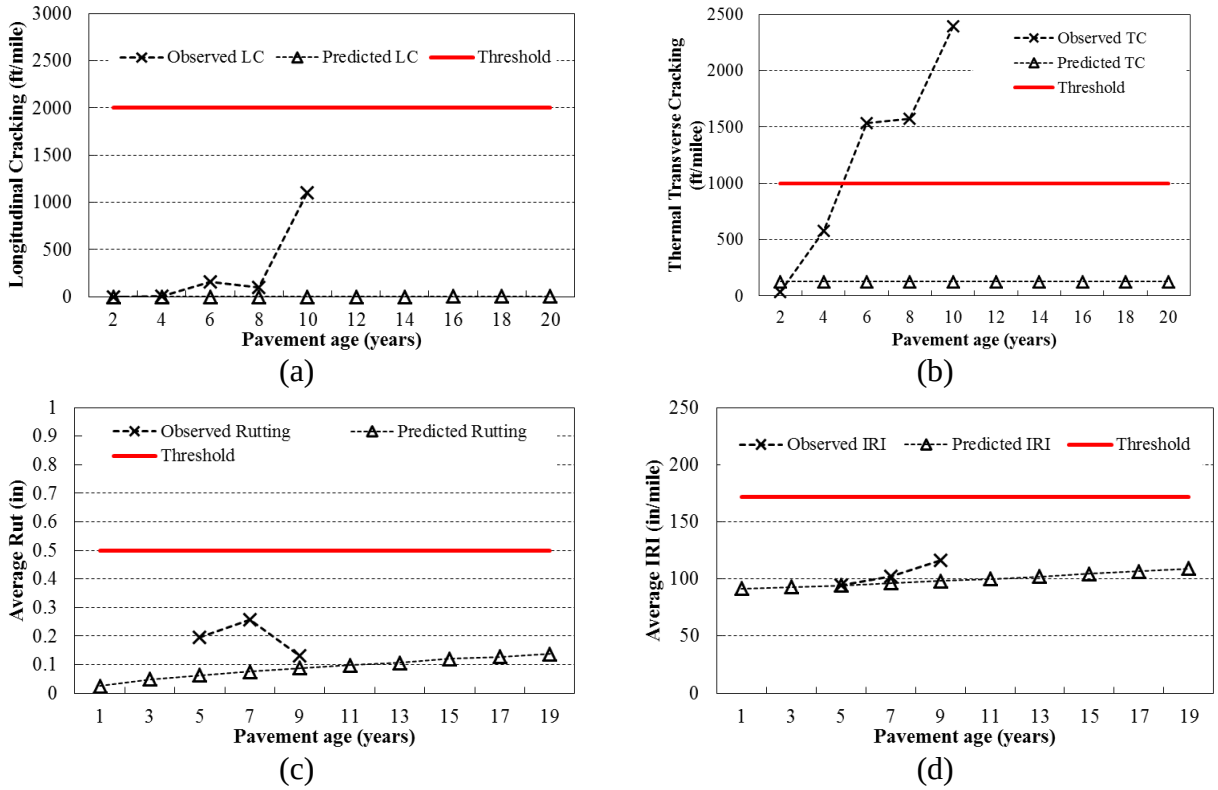

Figure C.2.3-5 Composite overlay project 33812

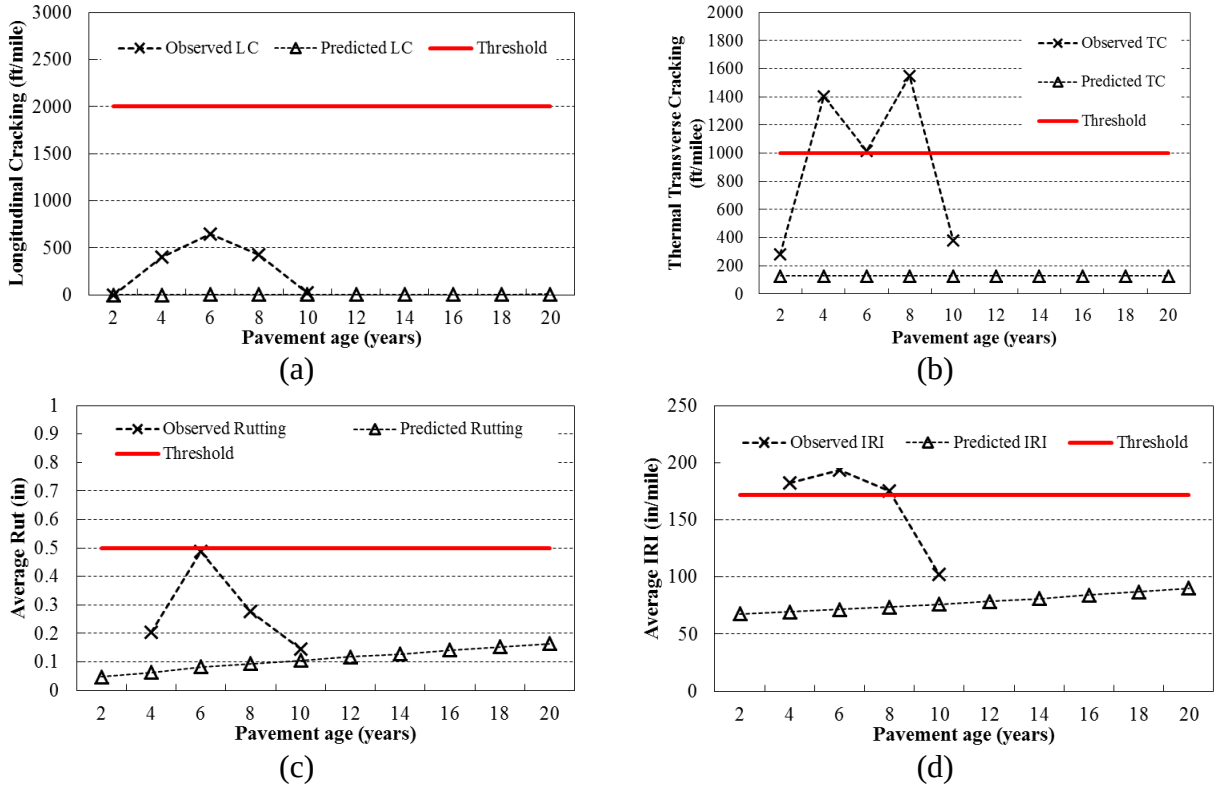

Figure C.2.3-6 Composite overlay project 33924

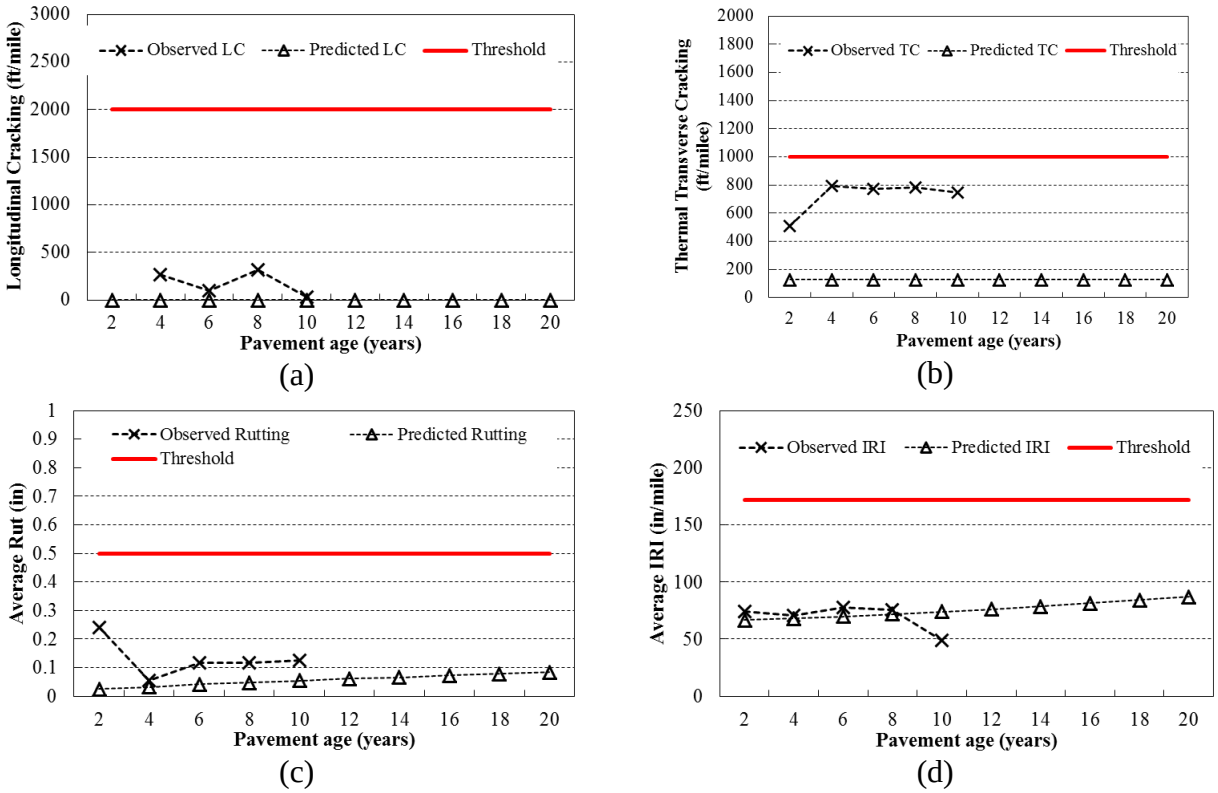

Figure C.2.3-7 Composite overlay project 25443

C.2.4 HMA over HMA

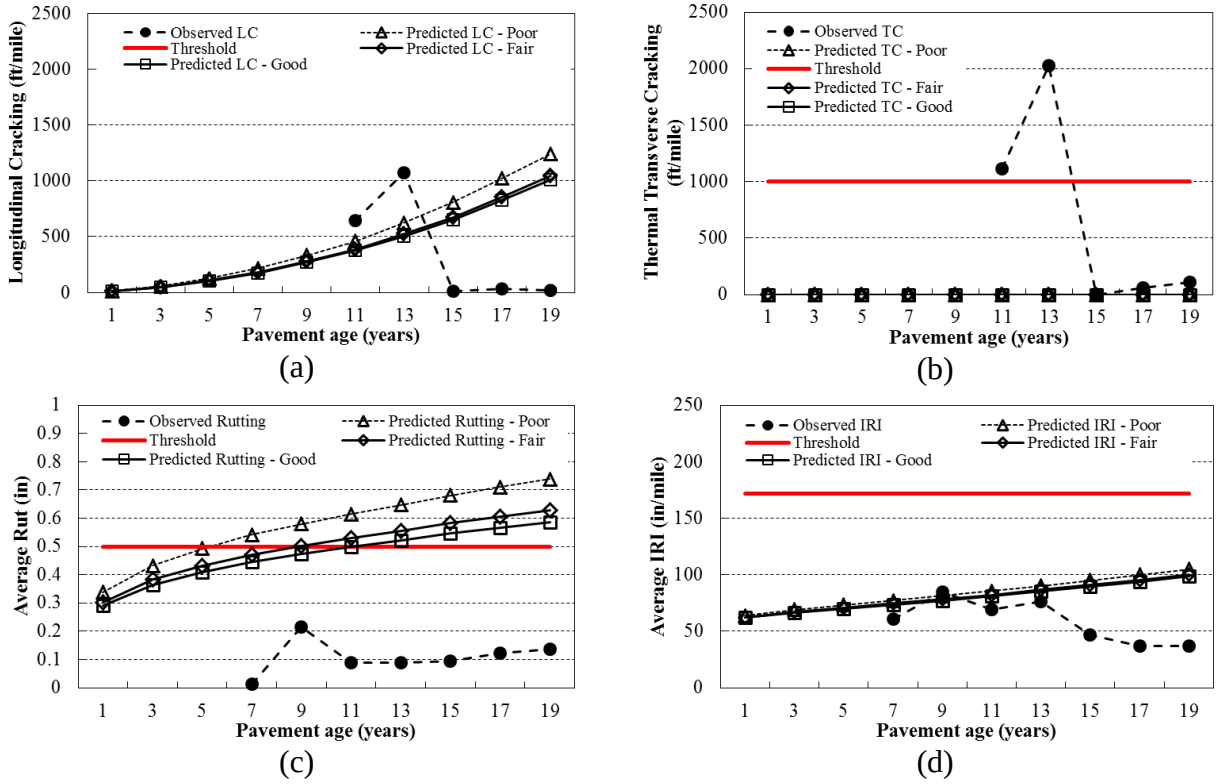

Figure C.2.4-1 HMA overlay project 33534

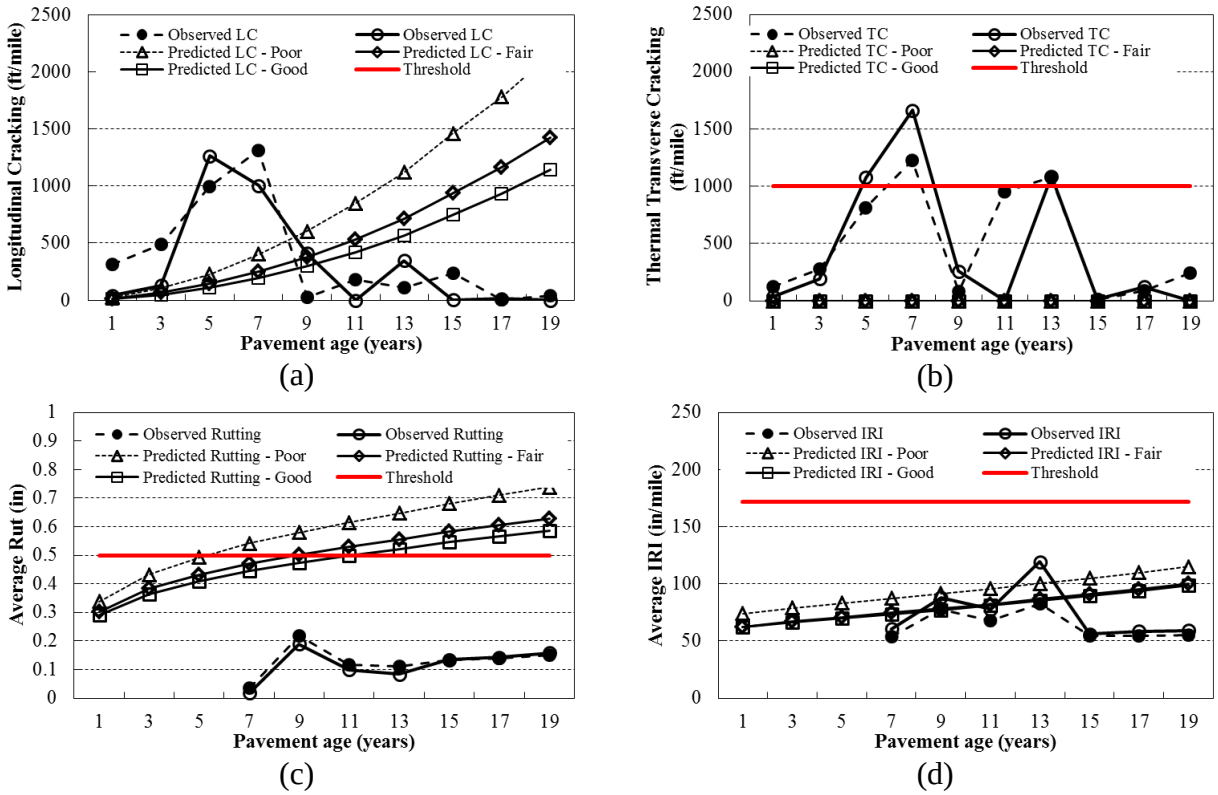

Figure C.2.4-2 HMA overlay project 33550

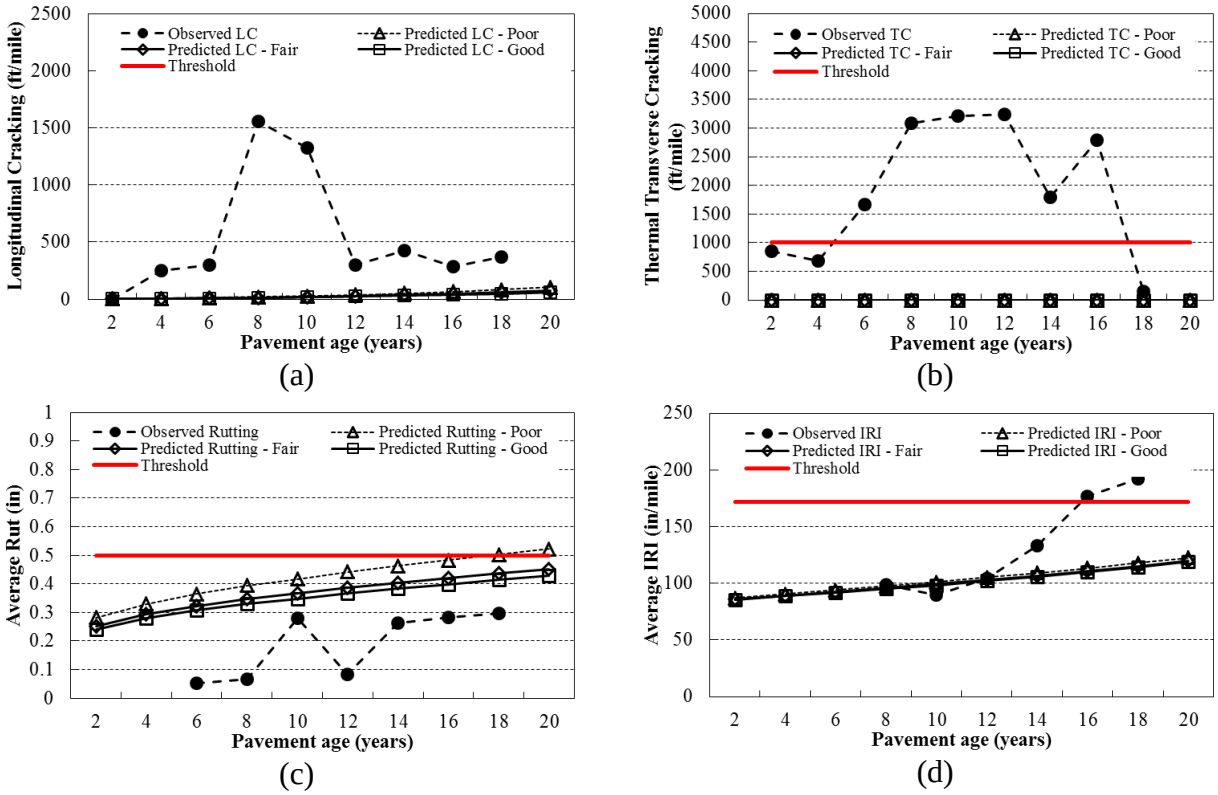

Figure C.2.4-3 HMA overlay project 28155

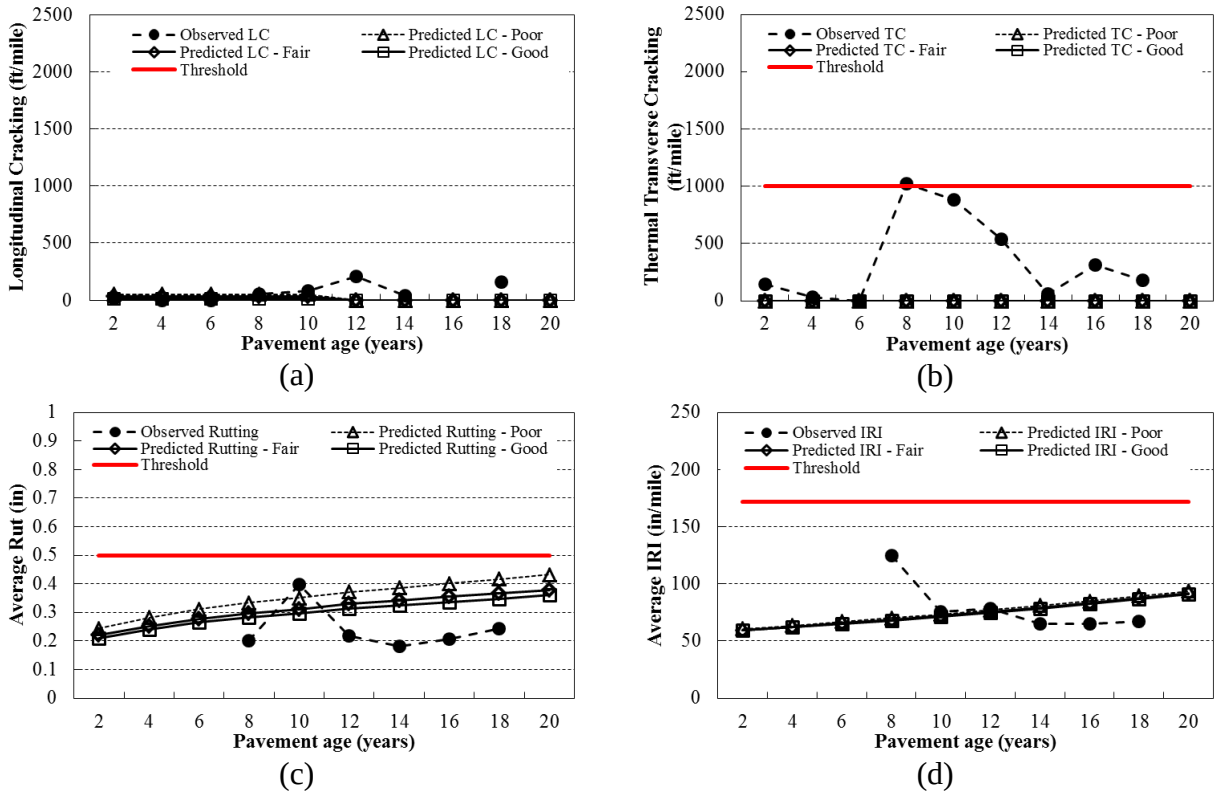

Figure C.2.4-4 HMA overlay project 26658

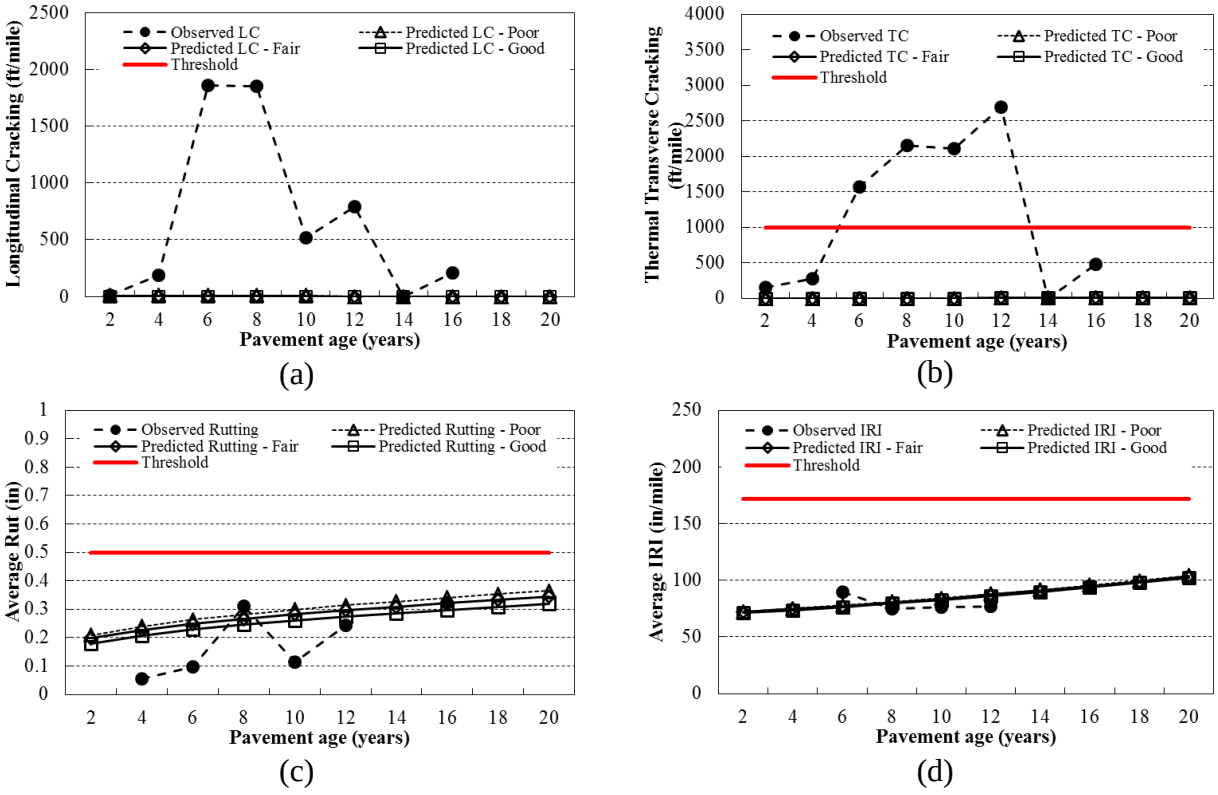

Figure C.2.4-5 HMA overlay project 29755

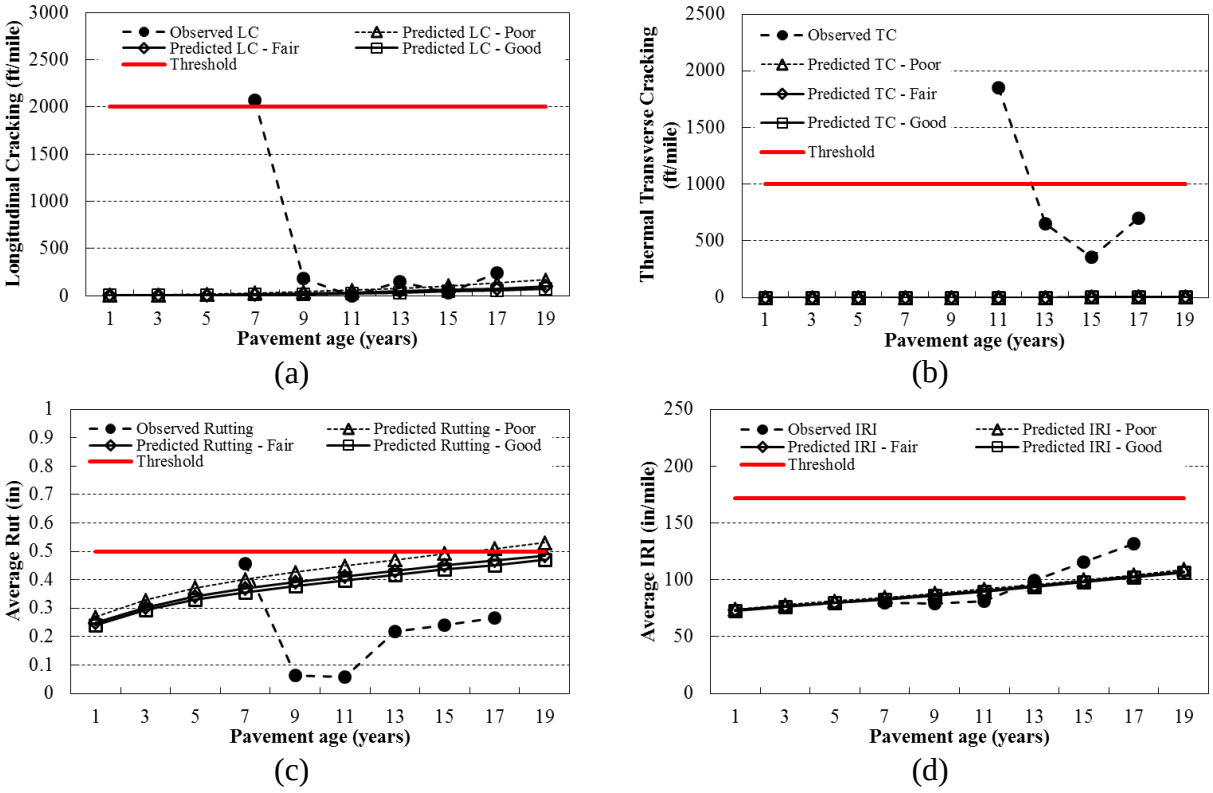

Figure C.2.4-6 HMA overlay project 30701

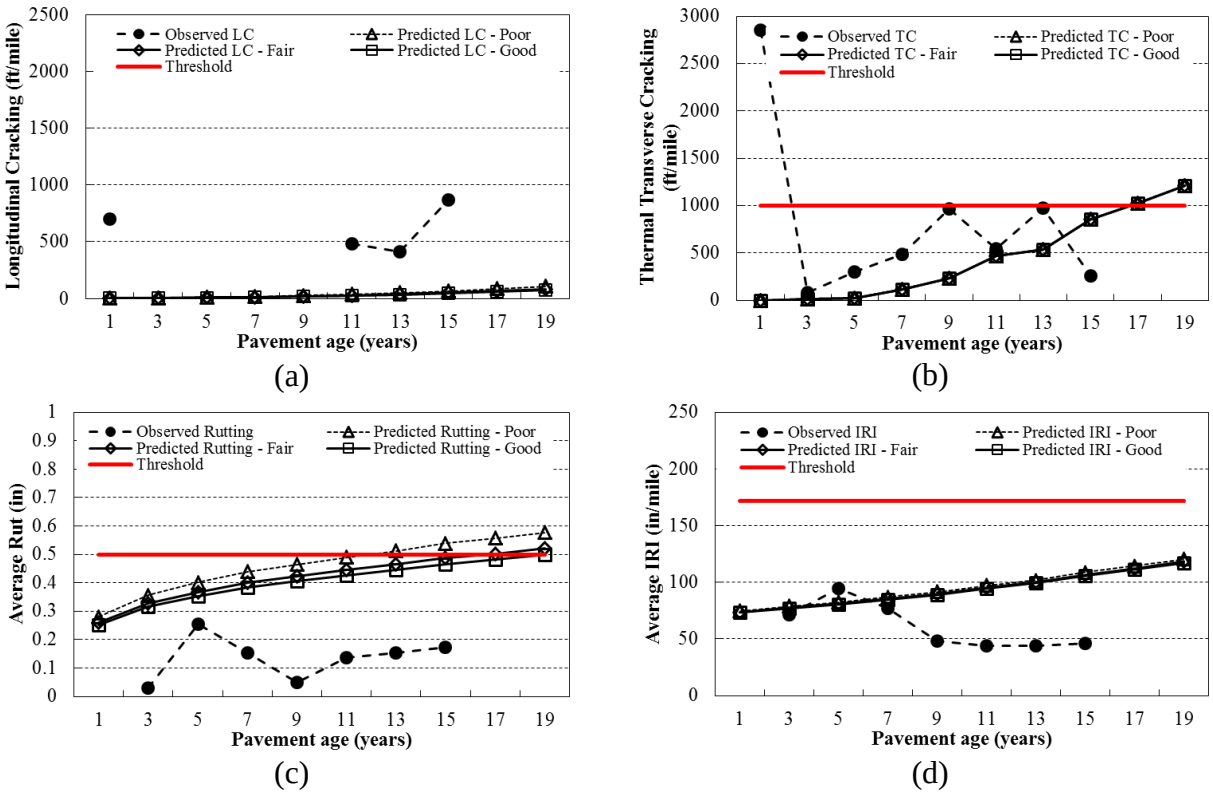

Figure C.2.4-7 HMA overlay project 31047

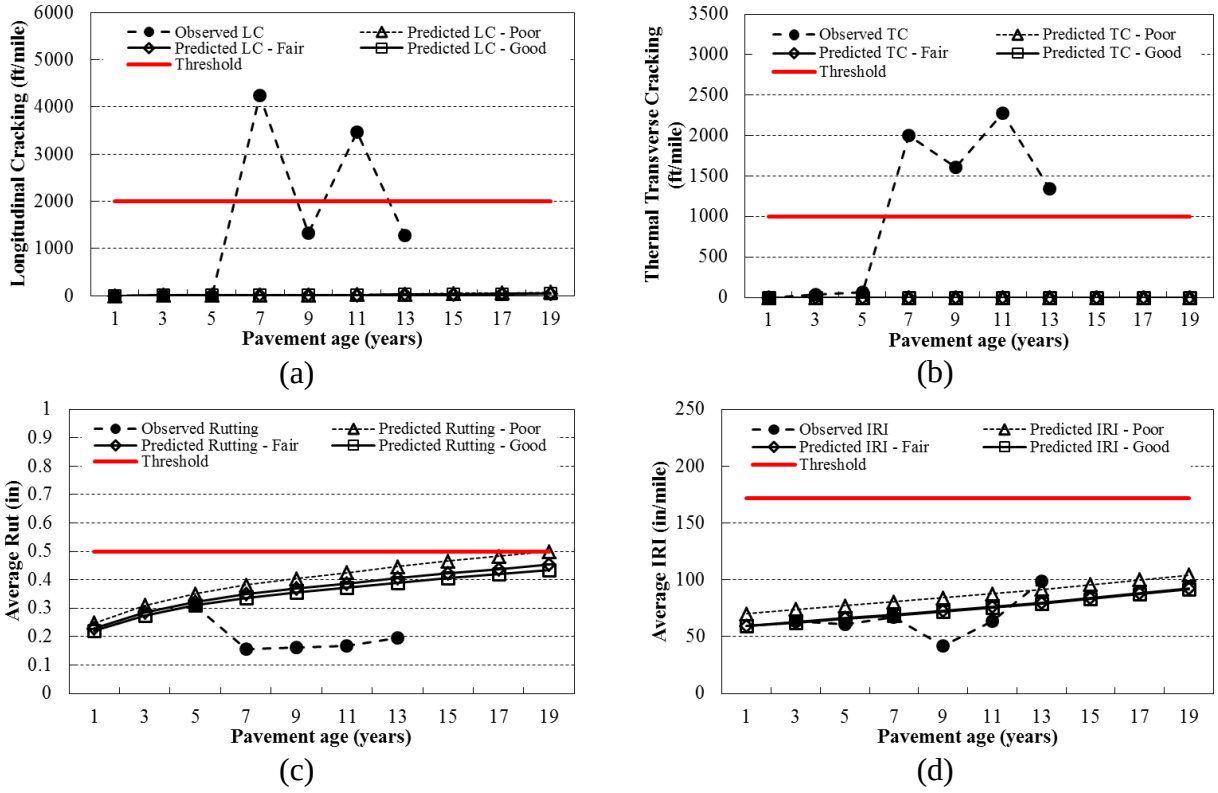

Figure C.2.4-8 HMA overlay project 32361

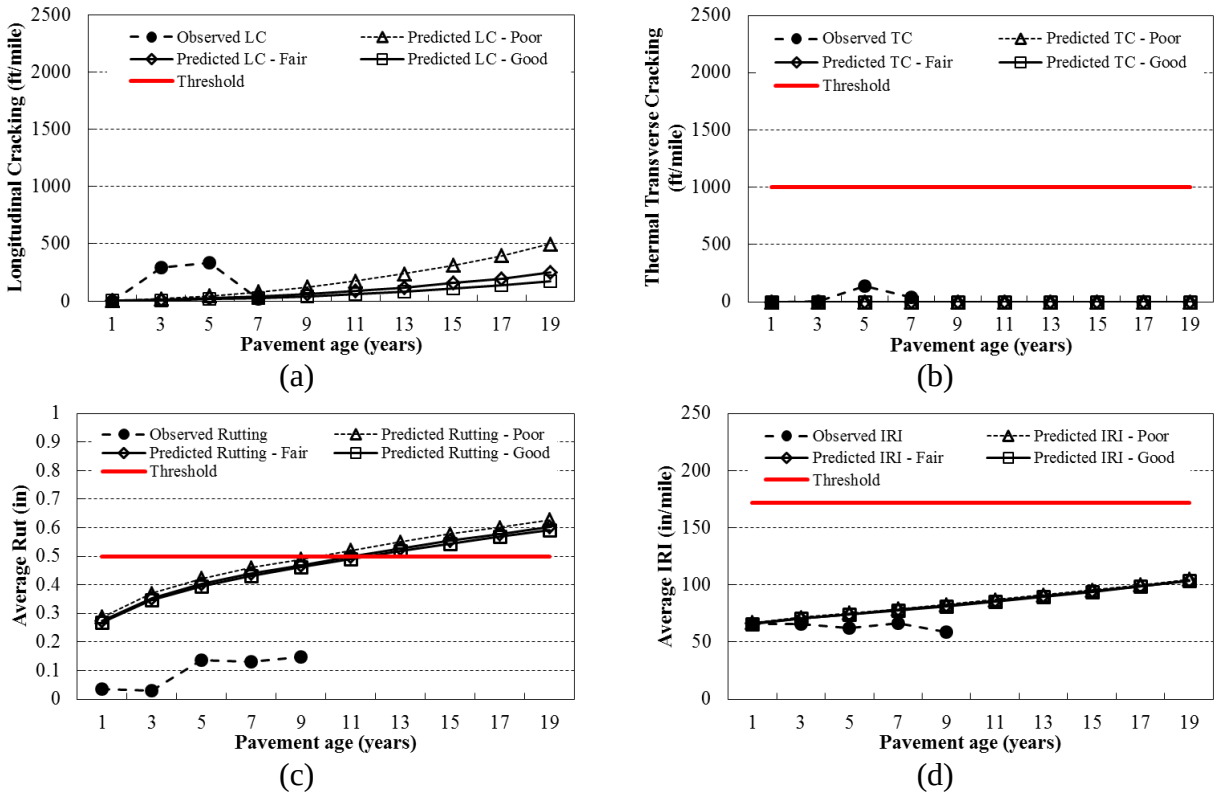

Figure C.2.4-9 HMA overlay project 45875

(a) (b)

(c) (d)

Figure C.2.4-10 HMA overlay project 50715

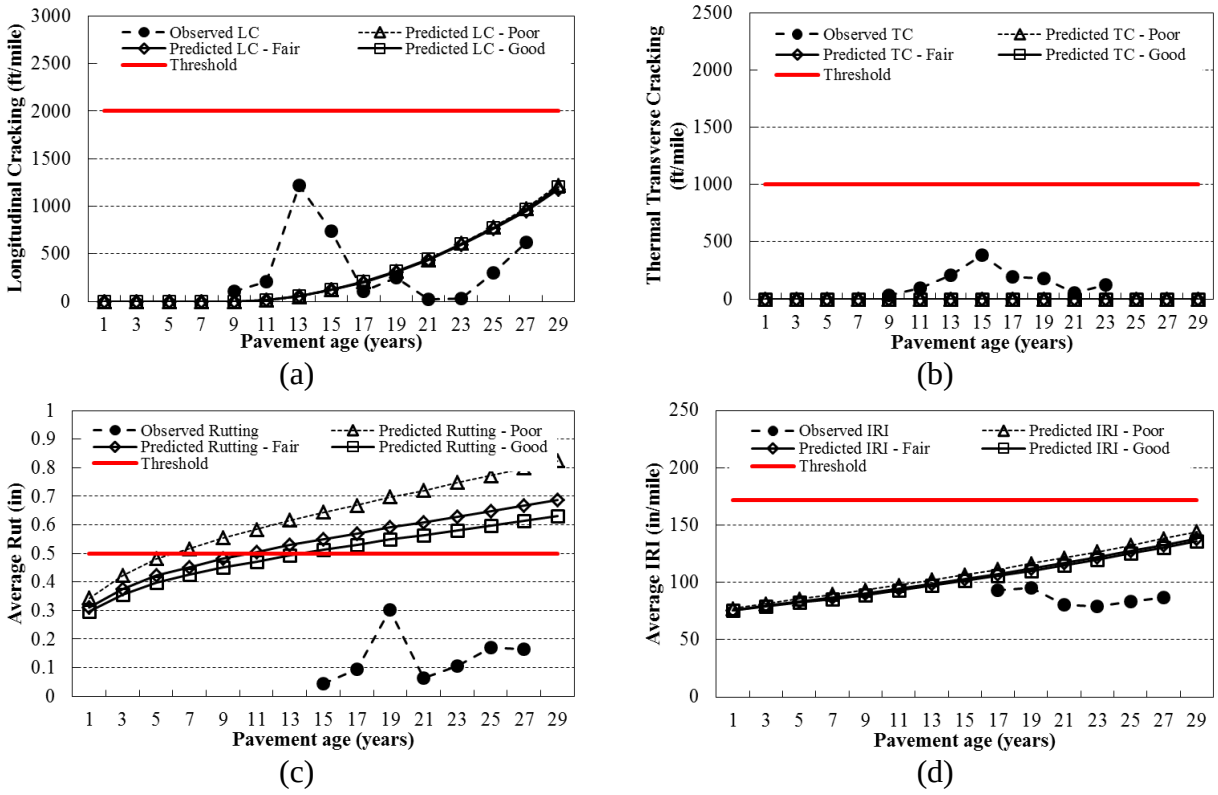

Figure C.2.4-11 HMA overlay project 20313

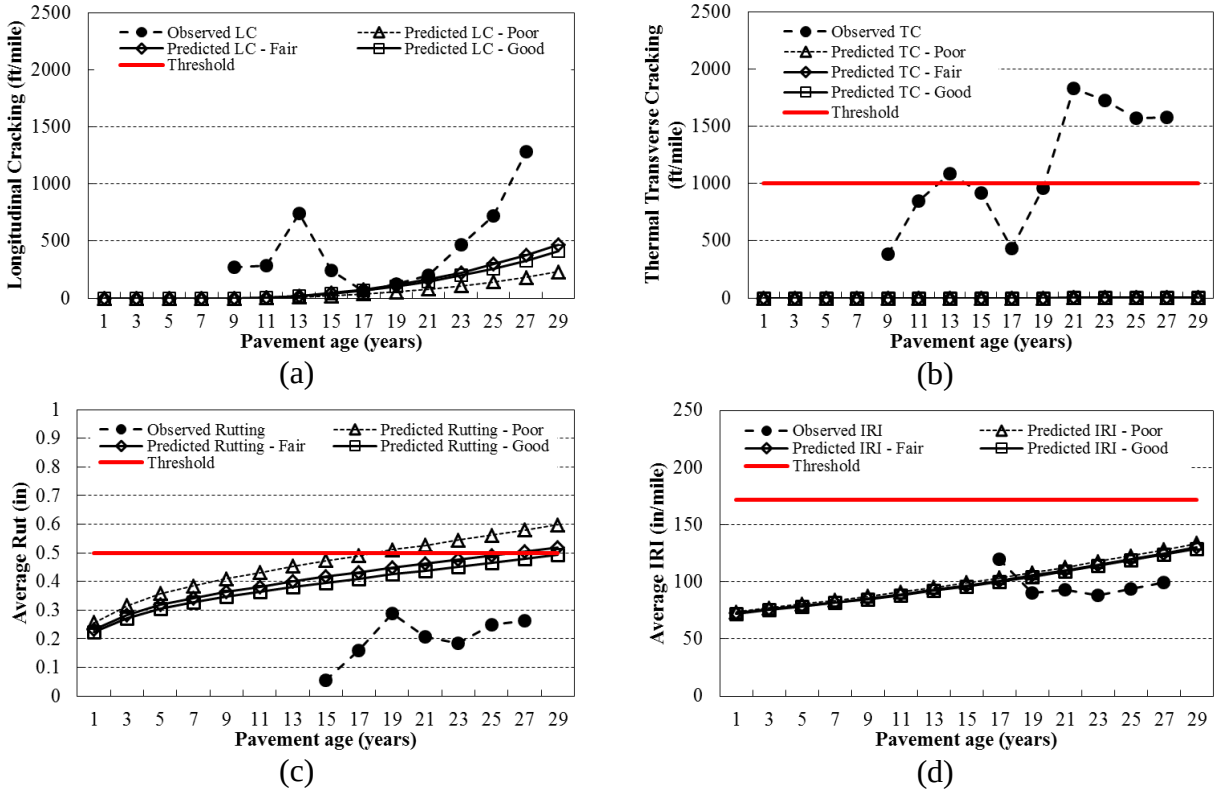

Figure C.2.4-12 HMA overlay project 12802

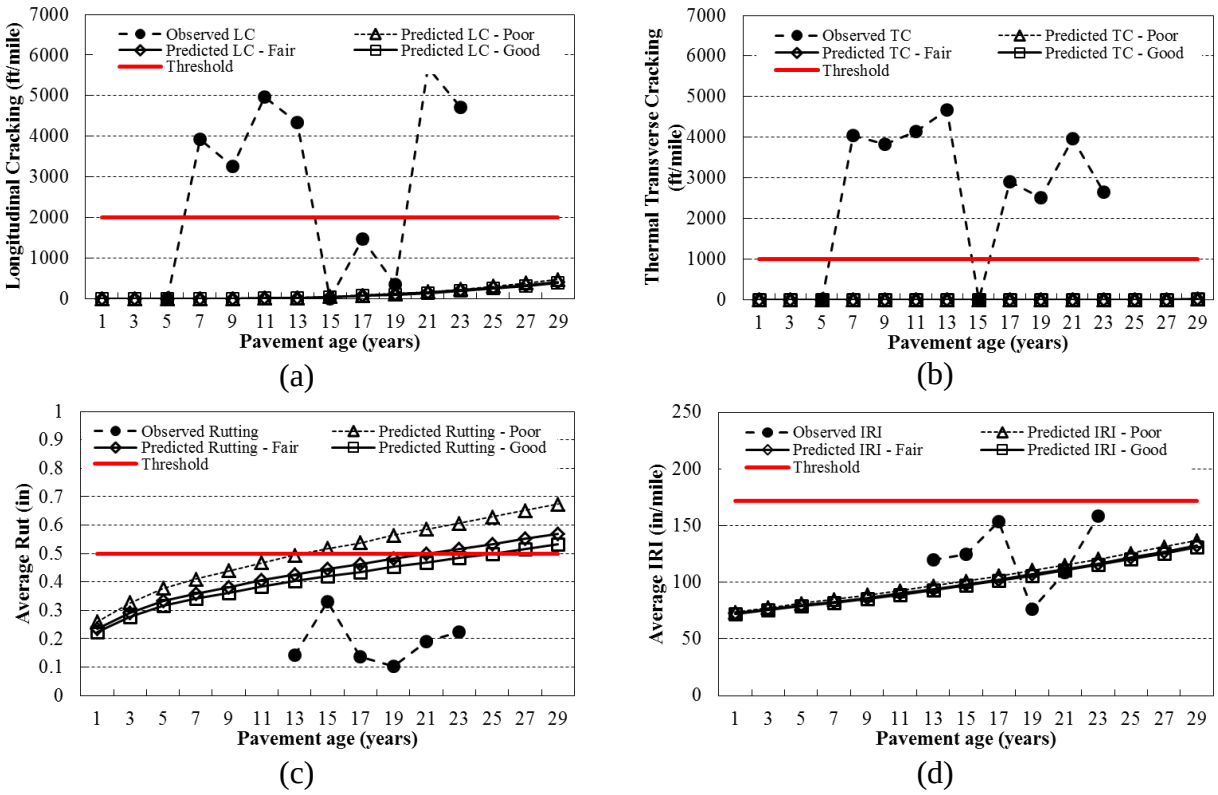

Figure C.2.4-13 HMA overlay project 24621

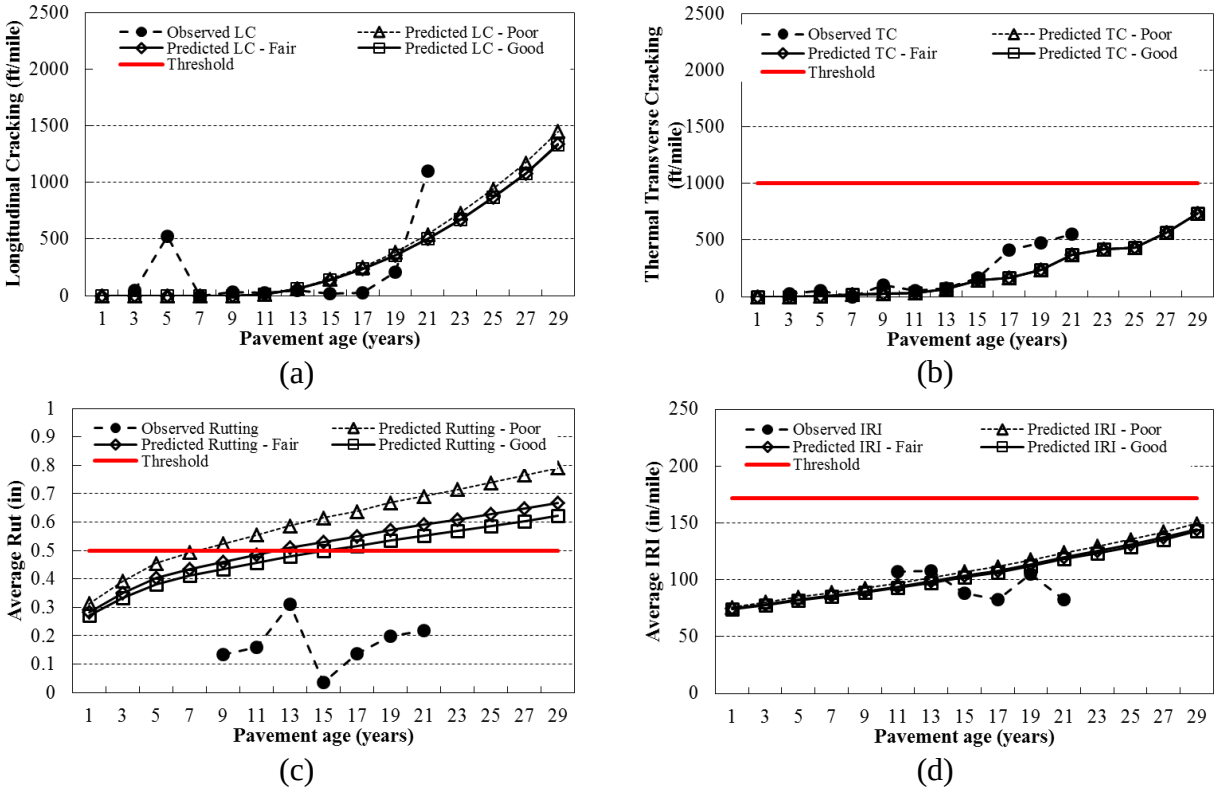

Figure C.2.4-14 HMA overlay project 25515

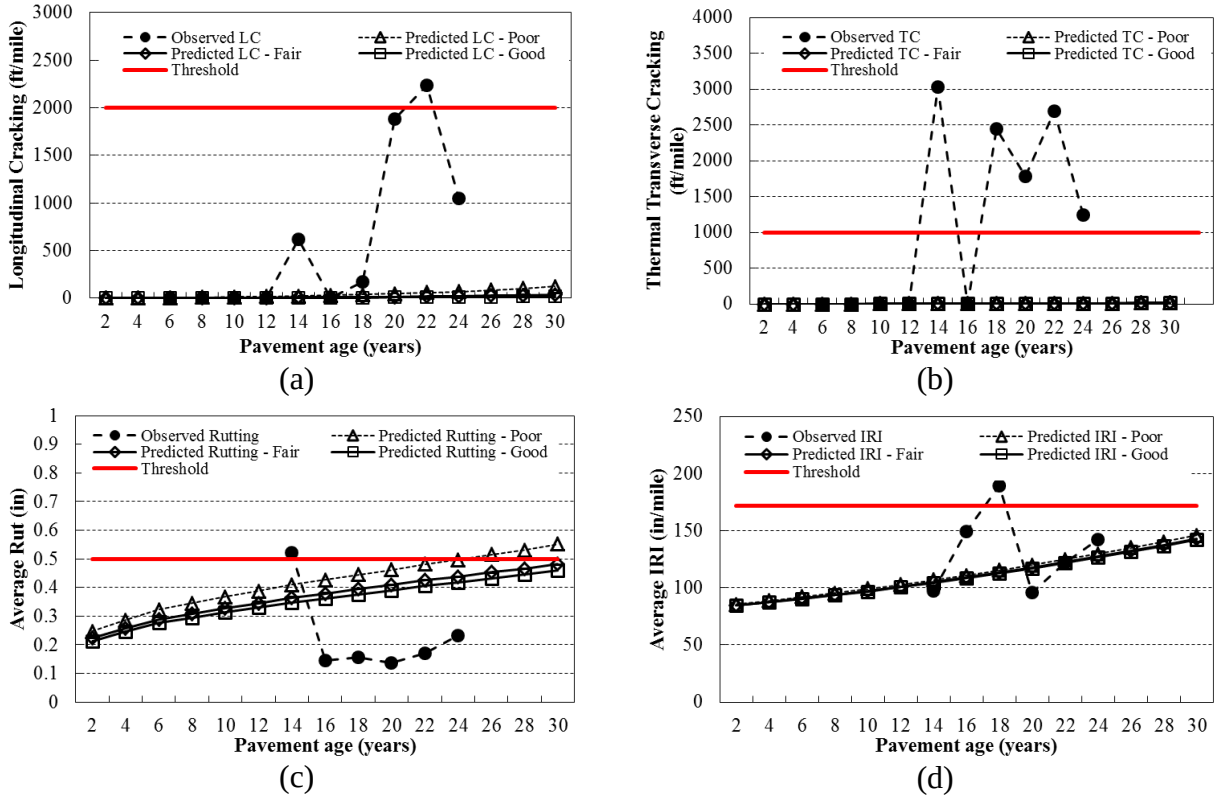

Figure C.2.4-15 HMA overlay project 30702

Table of Contents

APPENDIX C - VERIFICATION 1
C.1 INPUT VARIABLE DATA 1
C.1.1 Unbonded Overlays 1
C.1.2 Rubblized Overlays 10
C.1.3 Composite Overlays 21
C.1.4 HMA Overlays 28
C.2 VALIDATION RESULTS 43
C.2.1 Unbonded Overlays 43
C.2.2 Rubblized Overlays 48
C.2.3 Composite Overlays 54
C.2.4 HMA Overlays 58

ATTACHMENT D

MDOT
PAVEMENT MANAGEMENT SYSTEM

CURRENT DISTRESS MANUAL

FOR SURVEYING
OF
PAVEMENT SURFACE IMAGES

(2006 - 2011 Data Collection Cycle)

Prepared by Pavement Management Unit
Construction & Technology Area

(April, 2010)

This document describes the **Michigan Department of Transportation's (MDOT's)** surface distress type definitions and survey methods. MDOT collects surface images on one half of its trunk-line pavement network every year. The images are displayed on a computer screen by a Distress Survey program. Throughout this document, a computer screen of pavement surface images is referred to as a **Survey Screen**. The pavement surface distresses on a survey screen are observed and recorded by type, extent, and severity through a Distress Survey software. These data are called **Distress Survey Data**.

Distresses can be classified into two categories which are primary and secondary distresses. Throughout this document, a primary distress is called a **Principal Distress**. For most of the **Principal Distresses**, the secondary distresses around a **Principal Distress** are also observed and recorded. The secondary distresses are called the **Associated Distresses** of a **Principal Distress** and are usually measured by the length and width of their surface area. The **Associated Distresses** are used to estimate the severity level and/or extent of a **Principal Distress** and are also used in many applications for estimating fix costs and determining causes of pavement deteriorations. **Associated Distress** type is important information for analyzing causes of pavement deteriorations. Therefore, **Associated Distress** type is also recorded in certain instances.

The following abbreviations are used throughout this document and other PMS documents:

MDOT: Michigan Department of Transportation
PMS : Pavement Management System
PD : Principal Distress
PDs : Principal Distresses
AD : Associated Distress
ADs : Associated Distresses

This document provides a list of **PDs** to be recorded by the **PMS** of **MDOT**. For each **PD**, the following items are defined:

1. Title And Code

Each **PD** has a title and a unique 4-digit code. As an example, **Partial Width Patch (w)** designates the title of a **PD** that is assigned with a code **0326**. Throughout this and other **PMS** documents, the notation **PD<code #>** designates a **PD** identified by code <**code #>**. For the above example, **PD0326** designates **Partial Width Patch (w)**.

2. Definition

This defines the properties or qualifications of a **PD**.

3. Survey

This defines the method used to record a **PD** in a survey screen.

4. Severity / Extent

This defines the criteria for estimating the condition, severity and extent of a **PD** on a survey screen. Extent usually is the width of a distress area in the transverse direction and can be considered as a severity level of a **PD**. Thus, severity and extent are often interchangeable.

For a longitudinal-oriented **PD**, the extent in the longitudinal direction is the PD's length. This length can be computed directly from the location/linear referencing numbers used to identify the survey screens that enclose the **PD**. For this reason, the extent in the longitudinal direction will not be mentioned in this subject.

5. Associated Distress Matrix

This defines what **ADs** of a **PD** are to be recorded.

Each **PD** can have at most two **ADs** that are used to measure the severity level and extent of the **PD**. An **AD** consists of a title and several items for measuring **PD** severity (or extent). These items are referred to as distress severities. Two **ADs** of **PD0326** are presented below for demonstration purposes:

The First AD of PD0326:

This **AD** is shown below in table format. The title of this **AD** is **Transverse Length,** shown as the table header. This **AD** has 5 rows, each is the range of patch width in the transverse direction. Thus, this **AD** measures the extent of this **PD** in the transverse direction. However, the extent in the longitudinal direction can be also considered as severity of this **PD** because it indirectly indicates the range of distress area.

TRANSVERSE LENGTH
0 - 2 ft.
> 2 - 4 ft.
> 4 - 6 ft.
> 6 - 8 ft.
> 8 < 12 ft.

The Second AD of PD0326:

This **AD** is shown below in table format. The title of this **AD** is **CONDITION**, shown as the table header. This **AD** has 3 rows; each is a condition rating of the pavement within a patch. Thus, this **AD** measures the condition level of the **PD**.

CONDITION
GOOD
FAIR
POOR

The above two **ADs** of **PD0326** are combined into the following 2-dimensional table:

	CONDITION		
TRANSVERSE LENGTH	*GOOD*	*FAIR*	*POOR*
0 - 2 ft.			
>2 - 4 ft.			
>4 - 6 ft.			
>6 - 8 ft.			
>8 < 12 ft.			

The above 2-dimensional table is referred to as the **AD Matrix** of **PD0326**. When a **Partial Width Patch (w)** is identified, the surveyor must determine to which cell of the above **AD Matrix** the associated distresses belongs. The **Code** of this **PD** along with the **row** and **column** numbers of the identified cell are recorded into a data file. (For data file format, see both the last section of this document entitled **"Format Layout of Condition-Specific Data Within a Distress Survey File"** and the separate document, **File Formats of Location Referencing, Distress, and Sensor Data**) As an example, for a **Partial Width Patch (w)** that is 5 feet wide (in the transverse direction) and is in fair condition, **0326** is recorded as **PD** and **(3 , 2)** is recorded as its associated distresses. As mentioned previously, the extent of this **PD** in the longitudinal direction is the linear referencing length enclosing this **PD** and, therefore, is not part of the **AD Matrix**. The above explanations are applied to any **PD** that has a 2-dimensional **AD Matrix**.

Not every **PD** has two **ADs**. As an example, **PD0341** (**Delaminated Area**) has only one AD as shown below:

TRANSVERSE LENGTH
>0 - 2 ft.
>2 - 3 ft.
>3 - 6 ft.
>6 - 8 ft.
>8 - 12 ft.

The above **AD** is also referred to as the **AD Matrix** of PD0341**.** This AD Matrix measures the

extent (also severity) of this **PD** in the transverse direction, which is shown as the matrix title.

When a **Delaminated area** is identified, the surveyor must determine to which cell of the above **AD Matrix** the associated distress belongs. The Code of this **PD** along with the row number of the identified cell is recorded into a data file. As an example, for a **Delaminated area** that can be enclosed by a rectangle of width **7** feet in the transverse direction, **0341** is recorded as the **PD<code #>** and **(4, -1)** is recorded as its associated distress. The number **-1** is used to indicate that this **PD** has only one **AD.** The above explanations are applied to any **PD** that has only one **AD.**

Some **PDs** do not have an **AD**. As an example, **PD0405** (**Raveling**) is to have **0405** recorded as its **PD<code #>** and **(-1, -1)** recorded as its associated distress. **(-1,-1)** means that the **PD** does not have an **AD**. The above explanations are applied to any **PD** that does not have an **AD**.

6. ASSOCIATED DISTRESS TYPE

Some **PDs** require that a corresponding associated distress type be recorded. Similar to **AD** matrices, MDOT's system has three distinct **AD Type Tables** (displayed below and identified by unique code numbers – referenced later in this document) with each containing multiple AD Type descriptions from which a single one is selected per each PD.

AD 0083:

ASSOCIATED DISTRESS TYPE
Punched Area
None of Above

AD 0082:

ASSOCIATED DISTRESS TYPE
Associated Cracking
Irregular Surface
None of Above

AD 0081:

ASSOCIATED DISTRESS TYPE
D-Cracked

Map Cracking
Spalled
High Steel
Punch Out
Corner Crack
Delamination
None of Above

Remark: This Table revised from document used for 2000-2005 surveys by replacing "Reactive Aggregate" with "Map Cracking".

If **AD Type** identification is required for a **PD**, the surveyor shall utilize the appropriate **AD Table** above (as specified later in this document) and determine the proper cell of the Table to which the observed **AD Type** description belongs. The row number of the identified cell is recorded as **AD Type**. When multiple types of **AD** are observed, the surveyor shall record only the one that is present in the majority.

The data to be recorded for a **PD** are summarized below:

(1) **PD** Code
(2) Row Number of AD Matrix (-1 for not applicable)
(3) Column Number of AD Matrix (-1 for not applicable)
(4) Row Number of AD Type (-1 for not applicable)
(5) ID used to identify the survey screen that just encloses the beginning point of a **PD** (Or **AD** of a **PD**)
(6a) for a transverse-oriented PD, this is the same as (5).
(6b) for a longitudinal-oriented PD, this is the ID used to identify the survey screen that just misses the end point of a PD.

As previously mentioned, (5) and (6b) are used to compute the extent of a **PD** in the longitudinal direction (longitudinal length) through conversion to linear referencing units.

Before providing the detailed **PD** information, the **PD**s to be recorded are listed in **Table 1** for quick reference. Each row of this table has the following information for a **PD**:

Column 1 : PD Code
Column 2 : PD Title
Column 3 : Applicability of a PD to Rigid Pavement
Column 4 : Applicability of a PD to Flexible Pavement

Column 5 : Applicability of a PD to Composite Pavement
Column 6 : Applicability of a PD to CRC Pavement

TABLE 1
PRINCIPAL DISTRESSES (PD)
PD CODE, PD TITLE, AND APPLICABLE PAVEMENT TYPES

PD CODE	PD TITLE	RIGID	FLEX.	COMP.	CRCP
0103	TC (straight)	—	Yes	---	---
0104	TC (irregular)	—	Yes	---	---
0106	Transverse Joint	Yes	---	---	Yes
0110	TC		---	Yes	
0112	TC (open > 1/4 in.)	Yes	---	---	Yes
0113	TC	Yes	---	---	Yes
0114	Transverse Tear	—	Yes	Yes	---
0201	LC - left edge	---	Yes	Yes	---
0202	LC - center of lane	---	Yes	Yes	---
0203	LC - right edge	---	Yes	Yes	---
0204	LC - right WP	---	Yes	Yes	---
0205	LC - left WP	---	Yes	Yes	---
0208	L. Joint - left	Yes	---	---	Yes
0209	L. Joint - right	Yes	---	---	Yes
~~0220~~0234	Alligator Crack - right WP	---	Yes	---	---
~~0221~~0235	Alligator Crack - left WP	---	Yes	---	---
0227	LC (> 1/4 in.) - right WP	Yes	---	---	Yes
0228	LC (> 1/4 in.) - c. of lane	Yes	---	---	Yes
0229	LC (> 1/4 in.) - left WP	Yes	---	---	Yes
0230	LC - right WP	Yes	---	---	Yes
0231	LC - center of lane	Yes	---	---	Yes
0232	LC - left WP	Yes	—	—	Yes
0326	Partial Width Patch (W)	Yes	Yes	Yes	Yes
0327	Partial Width Patch (b)	Yes	Yes	Yes	Yes
0341	Delaminated Area	Yes	---	---	Yes
0342	Map Cracking	Yes	---	---	Yes
0343	High Steel	Yes	---	---	Yes

PD CODE	PD TITLE	RIGID	FLEX.	COMP.	CRCP
0344	**Shattered Area**	**Yes**	**---**		**Yes**
0345	**Block Cracking**	**---**	**Yes**	**---**	**---**
0346	**Refl. Shattered Area**	**---**	**---**	**Yes**	**---**
0402	**Popouts**	**Yes**	**---**	**---**	**Yes**
0403	**Scaling**	**Yes**	**---**	**---**	**Yes**
0405	**Raveling**	**---**	**Yes**	**Yes**	**---**
0406	**Flushing**	**---**	**Yes**	**Yes**	**---**
0501	**No-Distress Area**	**Yes**	**Yes**	**Yes**	**Yes**
0809	**New Pavement Type or New Survey Lane**	**Yes**	**Yes**	**Yes**	**Yes**
0908	**Not Surveyed**	**Yes**	**Yes**	**Yes**	**Yes**

Remark - This Table revised from document used for 2000-2005 surveys by:

1) Changing Code 0201 title from "LC- centerline" to "LC – left edge".
2) Changing Code 0203 title from "LC- edge" to "LC – right edge".
3) Changing Code 0342 title from "Reactive Aggregate" to "Map Cracking".
4) Changing Code 0809 from "New Pavement Type" to "New Pavement Type or New Survey Lane".

PRINCIPAL DISTRESSES

UNDER

THE CURRENT MDOT SURVEY SYSTEM

TRANSVERSE JOINT - PD0106

(Rigid & CRC Pavements)

DEFINITION:

A **Transverse Joint** (**TJ**) is a regularly spaced saw cut which has been sealed across the slab width.

The usual spacing between two **Transverse Joints** is 15, 27, 44, 72, or 99 feet. Note that **Transverse Joints** in **CRCP** may occur at occasional intervals around bridges.

SURVEY:

A **TJ** that has no associated distress shall not be recorded.

Record every observable **TJ** that has associated distress unless the pavement location can be identified as a **Shattered Area** (**PD0344**). In the case of intersecting transverse and longitudinal cracks and/or joints, an area of associated distress that may be identified with either the longitudinal or transverse PD shall be recorded for only one of PD per location.

SEVERITY / EXTENT:

The severity of a **Transverse Joint** is estimated by **Transverse Length** and **Maximum Width** of the associated distresses that occurs within 4 feet of the joint.

ASSOCIATED DISTRESS MATRIX: AD_{12} 0001 x 0011

	MAXIMUM WIDTH				
TRANSVERSE LENGTH	***No Distress***	***>0 - 1 ft.***	***>1 - 3 ft.***	***>3 - 6 ft.***	***>6 - 8 ft.***
No Distress		**xxxxxxxxx**	**xxxxxxxx**	**Xxxxxxxx**	**xxxxxxxx**
>0 - 1 ft.	**xxxxxxxx**				
>1 - 3 ft.	**xxxxxxxx**				
>3 - 6 ft.	**xxxxxxxx**				
>6 - 12 ft.	**xxxxxxxx**				

Note that cells marked with xxxxx are not applicable.

ASSOCIATED DISTRESS TYPE: AD_4 0081

TRANSVERSE TEAR - PD0114

(Flexible & Composite Pavements)

DEFINITION:

A **Transverse Tear** is a transverse-oriented short crack (4" to ½ of lane width) that appears in any location across the survey lane.

Note that any such short crack shall not be qualified as a **Transverse Tear** if it can be claimed as **AD** of other **PDs** such as **TC**, **LC**, **Alligator Crack**, and **Block Cracking** for flexible pavement or **TC**, **LC**, and **Reflective Shattered Area** for composite pavement.

SURVEY:

A Transverse Tear PD shall be recorded at locations where the above definition and constraints are observed. For a given mile point location (0.001 mile), if multiple unconnected **Transverse Tears** are present across the lane width (without presence of other PDs listed above), there shall be only one **Transverse Tear** record made for the mile point location.

SEVERITY / EXTENT: None

ASSOCIATED DISTRESS MATRIX: None

ASSOCIATED DISTRESS TYPE: None

TC - PD0113 (Rigid & CRC Pavements)
TC - PD0110 (Composite Pavement)

DEFINITION:

TC stands for a **Transverse Crack** that meets the following criteria:
(1) It extends more in the transverse direction than the longitudinal direction. That is, the angle between the overall crack line and the transverse line is less than 45 degrees.
(2) It is visible for at least one half of the lane width.
(3) For **Rigid** and **CRC** pavements, it is not opened up more than 1/4".

SURVEY:

Record every observable **TC** unless the pavement location can be identified as a **Shattered Area** (**PD0344**) for rigid/CRC pavement or **Refl. Shattered Area** (**PD0346**) for composite pavement.

SEVERITY / EXTENT:

The severity of a **TC** is estimated by **Transverse Length** and **Maximum Width** of the associated distresses that occur within 4 feet of the **TC**. In the case of intersecting transverse and longitudinal cracks and/or joints, an area of associated distress that may be identified with either the longitudinal or transverse PD shall be recorded for only one PD per location.

ASSOCIATED DISTRESS MATRIX: AD_{12} 0004 x 0011

	MAXIMUM WIDTH				
TRANSVERSE LENGTH	***No Distress***	***>0 - 1 ft.***	***>1 - 3 ft.***	***>3 - 6 ft.***	***>6 - 8 ft.***
No Distress - No Seal		**xxxxxxxx**	**xxxxxxxx**	**xxxxxxxx**	**xxxxxxxx**
No Distress - Seal (full)		**xxxxxxxx**	**xxxxxxxx**	**xxxxxxxx**	**xxxxxxxx**
No Distress - Seal (part)		**xxxxxxxx**	**xxxxxxxx**	**xxxxxxxx**	**xxxxxxxx**
No Distress - Seal (open)		**xxxxxxxx**	**xxxxxxxx**	**xxxxxxxx**	**xxxxxxxx**
>0 - 1 ft.	**Xxxxxxxx**				
>1 - 3 ft.	**Xxxxxxxx**				
>3 - 6 ft.	**Xxxxxxxx**				
>6 - 12 ft.	**Xxxxxxxx**				

Note that cells marked with xxxxx are not applicable.

ASSOCIATED DISTRESS TYPE: AD_4 0081 for PD0113 (Rigid & CRC pavements)
None for PD0110 (Composite pavement)

TC (straight) - PD0103
TC (irregular) - PD0104
(Flexible Pavement)

DEFINITION:

TC stands for a **Transverse Crack** that meets the following criteria:
(1) It extends more in the transverse direction than the longitudinal direction. That is, the angle between the overall crack line and the transverse line is less than 45 degrees.
(2) It must be visible for at least ½ of the lane width.
(3) For **TC (straight)**, crack must be straight for entire length and not change direction. For **TC (irregular)**, crack must change direction as it progresses across the lane.

SURVEY:

Record every observable **TC** unless the pavement area can be identified as a **Block Cracking** (**PD0345**).

SEVERITY / EXTENT:

The severity of a **TC** is estimated by **Transverse Length** & **Maximum Width** of the **ADs** that occur within 2 feet of the **TC**. In the case of intersecting transverse and longitudinal cracks and/or joints, an area of associated distress that may be identified with either the longitudinal or transverse PD shall be recorded for only one PD per location.

ASSOCIATED DISTRESS MATRIX: AD_{12} 0004 x 0012

	MAXIMUM WIDTH			
TRANSVERSE LENGTH	***No Distress***	***>0 - 1 ft.***	***>1 - 2 ft.***	***>2 - 4 ft.***
No Distress - No Seal		xxxxxxxx	xxxxxxxx	xxxxxxxx
No Distress - Seal (full)		xxxxxxxx	xxxxxxxx	xxxxxxxx
No Distress - Seal (part)		xxxxxxxx	xxxxxxxx	xxxxxxxx
No Distress - Seal (open)		xxxxxxxx	xxxxxxxx	xxxxxxxx
>0 - 1 ft.	xxxxxxxx			
>1 - 3 ft.	xxxxxxxx			
>3 - 6 ft.	xxxxxxxx			
>6 - 12 ft.	xxxxxxxx			

Note that cells marked with xxxxx are not applicable.

ASSOCIATED DISTRESS TYPE: None

TC (open > 1/4 in.) - PD0112

(Rigid & CRC Pavements)

DEFINITION:

TC (open>1/4 in.) stands for a **Transverse Crack** that meets the following criteria:
(1) It extends more in the transverse direction than the longitudinal direction. That is, the angle between the overall crack line and the transverse line is less than 45 degrees.
(2) It is visible for at least one half of the lane width.
(3) It is opened up at least 1/4 in.

SURVEY:

Record every observable **TC (open> ¼ in.)** unless the pavement location can be identified as a **Shattered Area** (**PD0344**).

SEVERITY / EXTENT:

The severity of a **TC (open> ¼ in.)** is estimated by **Transverse Length** and **Maximum Width** of the associated distresses that occur within 4 feet of the TC. In the case of intersecting transverse and longitudinal cracks and/or joints, an area of associated distress that may be identified with either the longitudinal or transverse PD shall be recorded for only one PD per location.

ASSOCIATED DISTRESS MATRIX: AD_{12} 0004 x 0011

	MAXIMUM WIDTH				
TRANSVERSE LENGTH	***No Distress***	***>0 - 1 ft.***	***>1 - 3 ft.***	***>3 - 6 ft.***	***>6 - 8 ft.***
No Distress - No Seal		xxxxxxxx	xxxxxxxx	xxxxxxxx	xxxxxxxx
No Distress - Seal (full)		xxxxxxxx	xxxxxxxx	xxxxxxxx	xxxxxxxx
No Distress - Seal (part)		xxxxxxxx	xxxxxxxx	xxxxxxxx	xxxxxxxx
No Distress - Seal (open)		xxxxxxxx	xxxxxxxx	xxxxxxxx	xxxxxxxx
>0 - 1 ft.	xxxxxxxx				
>1 - 3 ft.	xxxxxxxx				
>3 - 6 ft.	xxxxxxxx				
>6 - 12 ft.	xxxxxxxx				

Note that cells marked with xxxxx are not applicable.

ASSOCIATED DISTRESS TYPE: AD_4 0081

L. JOINT (right) - PD0209
L. JOINT (left) - PD0208
(Rigid & CRC Pavements)

DEFINITION:

L. JOINT stands for **Longitudinal Joint**. The above two **PDs** are the right and left **Longitudinal Joints**, respectively, of the survey lane.

A **Longitudinal Joint** is the sawed or formed joint between two lanes or between the pavement lane and shoulder.

SURVEY:

A **Longitudinal Joint** that has no associated distress shall not be recorded.

Record every observable **Longitudinal Joint** that has associated distress unless the pavement area can be identified as a **Shattered Area** (**PD0344**).

SEVERITY / EXTENT:

The severity of a **Longitudinal Joint** is estimated by **Maximum Width** of the associated distresses that occur within 2 feet of the joint. In the case of intersecting transverse and longitudinal cracks and/or joints, an area of associated distress that may be identified with either the longitudinal or transverse PD shall be recorded for only one PD per location.

ASSOCIATED DISTRESS MATRIX: AD_1 0012

MAXIMUM WIDTH
No Distress
>0 - 1 ft.
>1 - 2 ft.
>2 - 4 ft.

ASSOCIATED DISTRESS TYPE: AD_4 0081

LC (right WP) - PD0230
LC (center of lane) - PD0231
LC (left WP) - PD0232
LC >1/4 in. (Right WP) - PD0227
LC >1/4 in. (C. of lane) - PD0228
LC >1/4 in. (Left WP) - PD0229
(Rigid & CRC Pavements)

DEFINITION:

LC is a **Longitudinal Crack** and (**>1/4 in.)** means (**open > 1/4 in.)**. Each of the above **PDs** is an **LC** in a location across the survey lane that meets the following criteria:

(1) It extends more in the longitudinal direction than the transverse direction. That is, the angle between the overall crack line and the edge line is less than 45 degrees.
(2) The crack is visible and continuous for at least 5 feet.
(3) For **PD0230** - **PD0232**, the crack is opened up **less than** 1/4 in.
(4) For **PD0227** - **PD0229**, the crack is opened up **at least** 1/4 in.

SURVEY:

Record every observable **LC** unless pavement location can be identified as a **Shattered Area** (**PD0344**). Note that each lane location can have at most one **LC** recorded.

SEVERITY / EXTENT:

The severity of a **LC** is estimated by **Maximum Width** of the associated distresses that occur within 2 feet of the **LC**. In the case of intersecting transverse and longitudinal cracks and/or joints, an area of associated distress that may be identified with either the longitudinal or transverse PD shall be recorded for only one PD per location.

ASSOCIATED DISTRESS MATRIX: AD_1 0013

MAXIMUM WIDTH
No Distress - No Seal
No Distress - Seal (full)
No Distress - Seal (part)
No Distress - Seal (open)
>0 - 1 ft.
>1 - 2 ft.
>2 - 4 ft.

ASSOCIATED DISTRESS TYPE: AD_4 0081

LC (left edge) - PD0201
LC (left WP) - PD0205
LC (center of lane) - PD0202
LC (right WP) - PD0204
LC (right edge) - PD0203

(Flexible & Composite Pavements)

DEFINITION:

LC designates **Longitudinal Crack**. Each of the above PDs is an LC for a designated location across the survey lane that meets the following criteria:

(1) It extends more the longitudinally than transversely. That is, the angle between the overall crack line and the edge line is less than 45 degrees.

(2) The crack is visible and continuous for at least 5 feet.

SURVEY:

Record every observable **LC** unless the pavement location can be identified as **Block Cracking (PD0345)** for flexible pavement or **Refl. Shattered Area** (**PD0346**) for composite pavement. Note that each lane location (right WP, left WP and centerline) can have at most one **LC** recorded, including those associated with **Alligator Crack (PD~~0220~~ 0234 and ~~0221~~ 0235),** if it is flexible pavement.

SEVERITY / EXTENT:

The severity of an **LC** is estimated by **Maximum Width** of the associated distresses that occur within 2 feet of the LC. In the case of intersecting transverse and longitudinal cracks and/or joints, an area of associated distress that may be identified with either the longitudinal or transverse PD shall be recorded for only one PD per location.

ASSOCIATED DISTRESS MATRIX: AD_1 0013

MAXIMUM WIDTH
No Distress - No Seal
No Distress - Seal (full)
No Distress - Seal (part)
No Distress - Seal (open)
>0 - 1 ft.
>1 - 2 ft.
>2 - 4 ft.

ASSOCIATED DISTRESS TYPE: None

Remark - This PD description revised from document used for 2000-2005 surveys by:

1) Changing Code 0201 title from “LC- centerline” to “LC – left edge”.
2) Changing Code 0203 title from “LC- edge” to “LC – right edge”.

ALLIGATOR CRACKING (right WP) - PD~~0220~~ 0234
ALLIGATOR CRACKING (left WP) - PD~~0221~~ 0235

(Flexible Pavement)

DEFINITION:

Alligator Cracking is two or more parallel longitudinal cracks (originating in a wheel path – WP) with transverse tears running between them, displaying a pattern similar to an alligator hide. **Alligator Cracking** may extend laterally to other lane locations as severity increases.

SURVEY:

An **Alligator Cracking** PD shall be recorded when the defined condition above is visible for at least 5 feet longitudinally along the pavement unless the location meets the condition definition for **Block Cracking** (**PD0345**). Each lane location (across the lane) may have at most one **LC** or **Alligator Cracking** record per longitudinal pavement location.

SEVERITY / EXTENT:

The severity of **Alligator Cracking** is estimated by the **Maximum Width** of all combined associated distresses occurring within 2 feet from the outermost of the parallel longitudinal cracks. Therefore, **Maximum Width** shall be at least the lateral distance between the two outermost longitudinal cracks (if all visible associated distresses are contained between them).

ASSOCIATED DISTRESS MATRIX: AD_1 ~~0015~~ 0016

MAXIMUM WIDTH
> 1 - 2 ft.
> 2 - 4 ft.
> 4 - 6 ft.

ASSOCIATED DISTRESS TYPE: None

*** Remark: This PD description revised from document used for 2000-2005 surveys:**
The previous matrix structure was 5 rows x 1 column; this new matrix has eliminated the first 2 rows that were in that previous matrix, to become now a 3 row x 1 column structure.

DELAMINATED AREA - PD 0341
MAP CRACKING - PD 0342
HIGH STEEL - PD 0343

(Rigid & CRC Pavements)

DEFINITION:

A **Delaminated Area** is an area that has the following characteristics:

(1) Pieces of concrete are broken out from the surface
(2) The pattern usually begins in a circular shape
(3) The depth must be at least 1" and may reach to the reinforcing steel.

A **Map Cracking** area is typically one with a honeycomb pattern of very tight cracks or intense short (0.5 - 1.0 ft) cracks.

A **High Steel** area shall have at least one of the following characteristics:

(1) Missing concrete observed in the pattern of the reinforcing steel, or
(2) Visible bare steel at the surface.

Note that any of the above PDs shall not be recorded at a given location if some other PD is observed. That is, if there is another observed PD at the same location, the location shall be recorded as that other PD, and the observed delaminated area, map cracked area, or high steel area shall instead be used to measure AD and AD Type (if required) for the other PD.

SURVEY:

A pavement location shall be recorded as a **Delaminated Area**, **Map Cracking** area, or **High Steel** area when the respective definitions above are observed (again, if no other PDs are present).

Note that consecutive, uninterrupted locations observed as any of these three PDs that have the same severity level shall be combined and recorded as one continuous area.

Occasionally, a surveyor may have difficulty judging whether the pavement in a down view survey screen meets the above definitions. The perspective view image must be used in such cases to assist with a decision.

SEVERITY / EXTENT:

The severity of these three **PDs** is estimated by the **Transverse Length** (width of the area in transverse direction) of the qualified area.

DELAMINATED AREA - PD 0341
MAP CRACKING - PD 0342
HIGH STEEL - PD 0343

(Rigid & CRC Pavements)

ASSOCIATED DISTRESS MATRIX: AD_1???? (Undefined yet for internal use)

TRANSVERSE LENGTH
>0 - 2 ft.
>2 - 3 ft.
>3 - 6 ft.
>6 - 8 ft.
>8 - 12 ft.

ASSOCIATED DISTRESS TYPE: None

*** Remark:** This PD description revised from document used for 2000-2005 surveys by changing Code 0342 title from "Reactive Aggregate" to "Map Cracking".

SHATTERED AREA - PD0344

(Rigid & CRC Pavements)

DEFINITION:

A **Shattered Area** typically has a pattern of diagonal and/or looping cracks which may intersect some or all transverse joints/cracks and longitudinal joints/cracks. Typically this distress is caused by a lack of sub-grade support, and is characterized by a broken pattern of multiple individual pavement pieces which may be depressed in relation to the surrounding pavement surface.

SURVEY:

A **Shattered Area** shall be recorded if observation of the pavement location meets the above definition.

Consecutive, uninterrupted pavement locations that meet this definition of a **Shattered Area** shall be combined and recorded as one **Shattered Area**.

Occasionally, a surveyor may have difficulty judging whether the pavement in a pavement down view survey screen meets the above definition. In such a case, the perspective view image must be utilized to assist with a decision.

Note that a pavement location cannot have any other PD recorded when a **Shattered Area** PD is identified.

SEVERITY / EXTENT: None

ASSOCIATED DISTRESS MATRIX: None

ASSOCIATED DISTRESS TYPE: AD_4 0083

BLOCK CRACKING - PD0345

(Flexible Pavement)

DEFINITION:

A **Block Cracking** area is where transverse and longitudinal cracking have progressed to a point where blocks less than 12' by 12' in dimension are visible.

The shape of each block may be irregular because it depends on the form of the initial transverse cracking and later induced longitudinal cracking. Therefore, a pavement location shall also be considered as meeting the above definition if it is covered with long and/or short cracks and broken into irregular blocks.

SURVEY:

A **Block Cracking** area shall be recorded if the pavement location meets the above definition and is broken into at least **6** blocks.

Consecutive, uninterrupted pavement locations identified as **Block Cracking** areas shall be combined and recorded as one continuous **Block Cracking** area.

Occasionally, a surveyor may have difficulty judging whether the pavement in a survey screen meets the above definition. In such a case, the perspective view image must be viewed to assist with a decision.

Note that a pavement location cannot have any other PD recorded when a Block Cracking PD is identified.

SEVERITY: None

ASSOCIATED DISTRESS MATRIX: None

ASSOCIATED DISTRESS TYPE: None

REFL. SHATTERED AREA - PD0346

(Composite Pavement)

DEFINITION:

The above title stands for **REFLECTIVE SHATTERED AREA**.

This is an area of cracking that reflects a deteriorated area in the underlying concrete pavement. This area has a pattern ranging from small "Y" shaped tears to looping cracks that outline large broken pieces.

SURVEY:

A **Reflective Shattered Area** shall be recorded for pavement locations that meet the above definition.

Consecutive, uninterrupted pavement locations that are identified as **Reflective Shattered Areas** shall be combined and recorded as one **Reflective Shattered Area**.

Occasionally, the surveyor may have difficulty judging whether or not a pavement location meets the above definitions from the down view image alone. In such a case, the surveyor must utilize the perspective view image to assist the decision.

Note that a pavement location cannot have any other PD recorded when a Reflective Shattered Area PD is identified.

SEVERITY / EXTENT: None

ASSOCIATED DISTRESS MATRIX: None

ASSOCIATED DISTRESS TYPE: None

POPOUTS - PD0402

(Rigid & CRC Pavements)

DEFINITION:

A **Popout** is a void in the pavement surface caused by soft material or aggregate absorbing water and then "popping" out of the concrete upon freezing. **Popouts** are typically less than 2" in diameter and resemble a small bowl-shaped depression or crater in the pavement surface.

SURVEY:

A **Popouts** PD shall be recorded when an observed pavement location's average number of **Popouts** per linear foot is one or more.

Consecutive, uninterrupted pavement locations that are identified as **Popouts** areas shall be combined and recorded as one continuous **Popouts** area.

Note that other observed PDs are to be recorded regardless of the presence of **Popouts**.

SEVERITY / EXTENT: None

ASSOCIATED DISTRESS MATRIX: None

ASSOCIATED DISTRESS TYPE: None

SCALING - PD0403

(Rigid & CRC Pavements)

DEFINITION:

An area of **Scaling** is one were the top (smooth finish) layer of concrete is separated and displaced from the aggregate, leaving aggregate exposed and creating a rough surface texture. In general, **Scaling** is caused by exposure, wear, over finishing of the mix, or too much water in the mix.

SURVEY:

A **Scaling** PD shall be recorded when a pavement location has more than 50% of its area covered by the condition stated in the above definition.

Consecutive, uninterrupted pavement locations that are identified as **Scaling** areas shall be combined and recorded as one continuous **Scaling** area.

Note that other observed PDs are to be recorded regardless of the presence of **Scaling**.

SEVERITY / EXTENT: None

ASSOCIATED DISTRESS MATRIX: None

ASSOCIATED DISTRESS TYPE: None

RAVELING - PD0405

(Flexible & Composite Pavements)

DEFINITION:

An area of **Raveling** is one where, in more areas than just the wheel paths, the smooth surface has partially or entirely eroded away, leaving the aggregate in the bituminous mixture exposed and creating a rough surface texture.

Raveling may be caused by low asphalt content, mix segregation, or improper placement technique.

SURVEY:

A **Raveling** PD shall be recorded when the condition described in the above definition covers more than 50% of a pavement location's surface area.

Consecutive, uninterrupted pavement locations that are identified as **Raveling** areas shall be combined and recorded as one continuous **Raveling** area.

Note that other observed PDs are to be recorded regardless of the presence of **Raveling**.

SEVERITY / EXTENT: None

ASSOCIATED DISTRESS MATRIX: None

ASSOCIATED DISTRESS TYPE: None

FLUSHING - PD0406

(Flexible & Composite Pavements)

DEFINITION:

A **Flushing** area is one where the pavement is noticeably darker due to asphalt cement being squeezed to the top of the pavement mixture and deposited on the surface. It usually occurs in the wheel paths and may appear shiny in the perspective view.

Flushing may result from too high an asphalt content for the mixture's void volume.

SURVEY:

A **Flushing** PD shall be recorded when more than 50% of a pavement location's surface area meets the above definition.

Consecutive, uninterrupted pavement locations that are identified as **Flushing** areas shall be combined and recorded as one continuous **Flushing** area.

Note that other observed PDs are to be recorded regardless of the presence of **Flushing**.

SEVERITY / EXTENT: None

ASSOCIATED DISTRESS MATRIX: None

ASSOCIATED DISTRESS TYPE: None

PARTIAL WIDTH PATCH (w) - PD 0326
PARTIAL WIDTH PATCH (b) - PD 0327
(All Pavement Types)

DEFINITION:

The **(w)** and **(b)** in the above titles stand for **white patch (concrete)** and **black patch (asphalt)**, respectively.

A **Partial Width Patch** is a repaired section where the original pavement has been removed and replaced.

A **Partial Width Patch** must be narrower than the full-lane width, and can be any length in longitudinal direction.

SURVEY:

A **Partial Width Patch** PD shall be recorded when a pavement location meets the conditions defined above, with the following exception:

If there is another PD crossing through the patched area, the patch shall not be recorded as a **Partial Width Patch** but, instead, the distresses located within and around the patch shall be treated as AD of the other PD.

Otherwise, the distresses within a **Partial Width Patch** shall **exclusively** be used to estimate and record its condition (Good, Fair, or Poor).

Consecutive, uninterrupted pavement locations that are identified as **Partial Width Patch** areas having the same condition level (Good, Fair, or Poor) shall be combined and recorded as one continuous **Partial Width Patch** area.

SEVERITY / EXTENT:

The extent of a **Partial Width Patch** is the **Transverse Length** (width in the transverse direction across the lane) of the patch itself.

PARTIAL WITH PATCH (w) - PD 0326
PARTIAL WITH PATCH (b) - PD 0327
(All Pavement Types)

SEVERITY / EXTENT: continued

The pavement condition (**Good**, **Fair**, or **Poor**) of a **Partial Width Patch** shall be rated as follows:

GOOD: the patch is unbroken and has less than 3 feet of distresses.
FAIR: the patch is broken into 2 pieces by open cracks or has 3' - 6' of distresses.
POOR: the patch is open or broken into 3 or more pieces by open cracks or has more than 6' of distresses.

ASSOCIATED DISTRESS MATRIX: (unspecified yet for internal use)

	CONDITION		
TRANSVERSE LENGTH	*GOOD*	*FAIR*	*POOR*
0 - 2 ft.			
>2 - 4 ft.			
>4 - 6 ft.			
>6 - 8 ft.			
>8 ft.			

ASSOCIATED DISTRESS TYPE: None

*** Remark:** This AD matrix revised from document used for 2000-2005 surveys by changing last Transverse Length range description from ">8 ft. <12 ft." to ">8 ft.".

NOT SURVEYED - PD0908

(All Pavements)

DEFINITION:

A pavement section that cannot be surveyed due to construction, detouring, poor video images, etc.

SURVEY:

A **NOT SURVEYED** PD shall be recorded for pavement locations meeting the above definition.

Consecutive, uninterrupted pavement locations that are identified as **NOT SURVEYED** areas shall be combined and recorded as one continuous **NOT SURVEYED** area.

Other PDs shall not be recorded in **NOT SURVEYED** areas.

SEVERITY / EXTENT: None

ASSOCIATED DISTRESS MATRIX: None

ASSOCIATED DISTRESS TYPE: None

NEW PAVEMENT TYPE or NEW SURVEY LANE - PD0809

(All Pavements)

DEFINITION:

An indicator of pavement location where the pavement type changes or where the image collection vehicle crosses into a different numbered survey lane (resulting from either an actual vehicle lane shift or from the addition or dropping of a thru lane in the pavement cross section that would redefine the vehicle's current lane number designation).

SURVEY:

This PD shall be recorded at the beginning point of either a pavement type or survey lane designation change. For a survey lane designation change caused by a lateral vehicle shift, the beginning point shall be recorded at the point where the pavement down view image is bisected by the lane line between the previous and new survey lanes.

SEVERITY / EXTENT: None

ASSOCIATED DISTRESS MATRIX: None

ASSOCIATED DISTRESS TYPE: None

NO DISTRESS - PD0501

(All Pavements)

DEFINITION:

A pavement section that has no observable distress as defined in this manual shall be recorded as a **NO DISTRESS** area.

SURVEY:

A **No Distress** PD shall be recorded at the beginning point of a pavement section meeting the condition stated above.

SEVERITY / EXTENT: None

ASSOCIATED DISTRESS MATRIX: None

ASSOCIATED DISTRESS TYPE: None